AD_____

CONTRACT NUMBER: DAMD17-94-C-4031

TITLE: Studies on the Molecular Dissection of Human Cholinesterase Variants and Their Genomic Origins

PRINCIPAL INVESTIGATOR: Hermona Soreq, Ph.D.

CONTRACTING ORGANIZATION: Hebrew University of Jerusalem
Jerusalem, 91904, Israel

REPORT DATE: June 1996

TYPE OF REPORT: Final

PREPARED FOR: Commander
U.S. Army Medical Research and Materiel Command
Fort Detrick, Frederick, MD 21702-5012

DISCLAIMER NOTICE

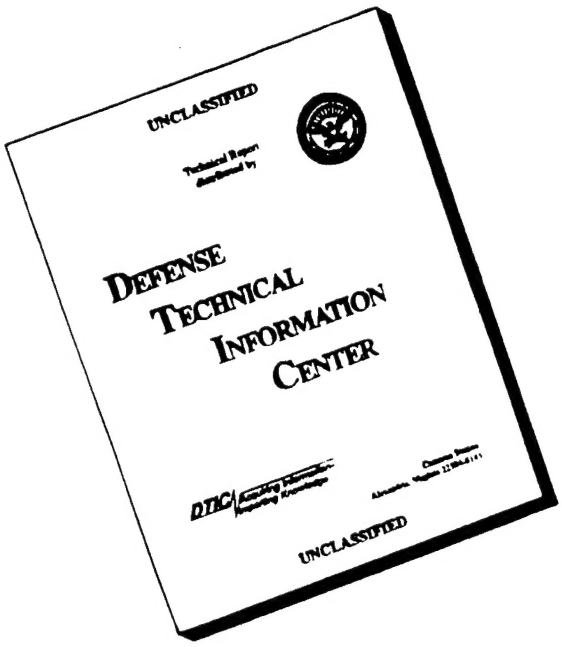

THIS DOCUMENT IS BEST QUALITY AVAILABLE. THE COPY FURNISHED TO DTIC CONTAINED A SIGNIFICANT NUMBER OF PAGES WHICH DO NOT REPRODUCE LEGIBLY.

REPORT DOCUMENTATION PAGE

Form Approved
OMB No. 0704-0188

1. AGENCY USE ONLY *(Leave blank)*	2. REPORT DATE	3. REPORT TYPE AND DATES COVERED
	June 1996	Final (1 Jun 94 - 30 May 96)

4. TITLE AND SUBTITLE
Studies on the Molecular Dissection of Human Cholinesterase Variants and Their Genomic Origins

5. FUNDING NUMBERS
DAMD17-94-C-4031

6. AUTHOR(S)
Hermona Soreq, Ph.D.

7. PERFORMING ORGANIZATION NAME(S) AND ADDRESS(ES)
Hebrew University of Jerusalem
Jerusalem, 91904, Israel

8. PERFORMING ORGANIZATION REPORT NUMBER

9. SPONSORING/MONITORING AGENCY NAME(S) AND ADDRESS(ES)
Commander
U.S. Army Medical Research and Materiel Command
Fort Detrick, MD 21702-5012

10. SPONSORING/MONITORING AGENCY REPORT NUMBER

11. SUPPLEMENTARY NOTES

12a. DISTRIBUTION / AVAILABILITY STATEMENT
Approved for public release; distribution unlimited

12b. DISTRIBUTION CODE

13. ABSTRACT *(Maximum 200*

To evaluate the capacity of overexpressed recombinant human cholinesterases or mutated variants thereof to confer protection against anti-cholinesterase toxicity, we employed transiently transgenic *Xenopus laevis* tadpoles and stably transgenic mice. Normal and mutant variants of butyrylcholinesterase (BuChE) revealed partially overlapping binding sites for several inhibitors and demonstrated the involvement of the oxyanion hole in BuChE catalysis. In the developing tadpoles the isoform of AChE, which terminates with the 3'-exon 6, was efficiently accumulated in neuromuscular junctions and conferred resistance to the organophosphate paraoxon. In transgenic mice, exon 6-terminated AChE, under control of its authentic promoter, accumulated in CNS synapses and conferred resistance to paraoxon and several cholinergic agonists, but caused progressive deterioration in both neuromotor and cognitive functioning. Finally, in a human patient carrying the "atypical" (D70G) gene for BuChE, we observed adverse responses to prophylactic doses of the carbamate pyridostigmine and from this and *in vitro* studies predicted a generalized genetic predisposition to anti-cholinesterase therapies, including that approved for the treatment of Alzheimer's disease.

14. SUBJECT TERMS			15. NUMBER OF PAGES
acetylcholinesterase	butyrylcholinesterase	human	278
natural mutation	OP agent	mouse	16. PRICE CODE
site directed mutagenesis	transgenic	frog	

17. SECURITY CLASSIFICATION OF REPORT	18. SECURITY CLASSIFICATION OF THIS PAGE	19. SECURITY CLASSIFICATION OF ABSTRACT	20. LIMITATION OF ABSTRACT
Unclassified	Unclassified	Unclassified	Unlimited

FOREWORD

Opinions, interpretations, conclusions and recommendations are those of the author and are not necessarily endorsed by the US Army.

____ Where copyrighted material is quoted, permission has been obtained to use such material.

____ Where material from documents designated for limited distribution is quoted, permission has been obtained to use the material.

__X__ Citations of commercial organizations and trade names in this report do not constitute an official Department of Army endorsement or approval of the products or services of these organizations.

__X__ In conducting research using animals, the investigator(s) adhered to the "Guide for the Care and Use of Laboratory Animals," prepared by the Committee on Care and Use of Laboratory Animals of the Institute of Laboratory Resources, National Research Council (NIH Publication No. 86-23, Revised 1985).

__X__ For the protection of human subjects, the investigator(s) adhered to policies of applicable Federal Law 45 CFR 46.

__X__ In conducting research utilizing recombinant DNA technology, the investigator(s) adhered to current guidelines promulgated by the National Institutes of Health.

__X__ In the conduct of research utilizing recombinant DNA, the investigator(s) adhered to the NIH Guidelines for Research Involving Recombinant DNA Molecules.

__X__ In the conduct of research involving hazardous organisms, the investigator(s) adhered to the CDC-NIH Guide for Biosafety in Microbiological and Biomedical Laboratories.

June 25, 96

PI - Signature Date

Table of Contents

	page
Front Cover	1
Report Documentation Page	2
Foreword	3
Table of Contents	4
List of papers published under USAMRDC support	6
Hebrew University of Jerusalem Graduate Theses Supported by USAMRDC Funds	7
Abbreviations	8
Progress Relative to the Statement of Work	9
Introduction	10
Body of the Report	11
1. Transgenic *Xenopus* tadpole	11
Xenopus-expressed AChE is biochemically indistinguishable from native human AChE	11
Transient expression of CMVACHE in *Xenopus* embryos	11
Human acetylcholinesterase remains monomeric in *Xenopus* embryos	12
Subcellular disposition of human acetylcholinesterase in myotomes of CMVACHE injected embryos	12
Ultrastructural consequences of overexpressed acetylcholinesterase in *Xenopus* neuromuscular junctions	12
2. Transgenic mouse	19
Low-level ACHE overexpression is compatible with life	19
Transgenic human ACHE expression is limited to CNS neurons	19
Normally processed transgenic acetylcholinesterase accumulates in cholinergic brain regions	19
Transgenic acetylcholinesterase selectively alters hypothermic drug responses	19
Transgenic acetylcholinesterase induces age-dependent decline in spatial learning capacity	20
Transgenic acetylcholinesterase induces changes at the neuromuscular junction	20
Stress-facilitated changes in electrophysiology induced by pyridostigmine	20
Transgenic BCHE	21
3. *In vitro* studies of OP and carbamate interactions with acetylcholinesterase and butyrylcholinesterase	29
Spatiotemporal dissociation of catalytic steps	29
The gorge lining contributes to enzyme phosphorylation	29
Active site charges hamper reactivation	29
C-terminal variations are innocuous in catalytic terms	30
Effects of variations on kcat	30
Interaction sites on butyrylcholinesterase	30
4. Failure of "atypical" butyrylcholinesterase to protect against anti-cholinesterases	35
Activity of "atypical" butyrylcholinesterase	35
Rate of inhibition of normal and "atypical" butyrylcholinesterase	35
Rate of reactivation of normal and "atypical" butyrylcholinesterase	35
Effective dosage of anti-cholinesterase in carriers of BCHE, the example of tacrine	36
5. Cholinotoxic effects on rodent brain gene expression	38
AF64A modulates cholinergic enzyme activities *in vivo*	38
Differential *in vitro* inhibition of cholinesterases by AF64A	38
Pretreatment of cholinesterase cDNAs with AF64A causes differential damage to *in vitro* transcription	39
AF64A administration modulates cholinesterase mRNA levels *in vivo*	39
AF64A induces region-specific alterations in the differential PCR display of G,C-rich transcripts	39
6. Activation of acetylcholinesterase by phosphorylation	43
Phosphorylation by protein kinase A	43
Acetylcholinesterase is found partially phosphorylated *in vivo*	43
Phosphorylation results in activation of acetylcholinesterase	43

Phosphorylation at non-protein kinase A consensus sites 43
Conclusions 46
References 47

Appendix
Copies of papers published under USAMRDC support
Andres, C., R. Beeri, T. Huberman, M. Shani, H. Soreq, Prog. Brain Res. (in press).
Beeri, R., A. Gnatt, Y. Lapidot-Lifson, D. Ginzberg, M. Shani, H. Soreq, H. Zakut, Human Reprod. 9 (1994) 284-292.
Beeri, R., C. Andres, E. Lev-Lehman, R. Timberg, T. Huberman, M. Shani, H. Soreq, Curr. Biol. 5 (1995) 1063-1071.
Hanin, I., A. Yaron, D. Ginzberg, H. Soreq in *Alzheimer's and Parkinson's Diseases,* I. Hanin et al., eds.; Plenum Press, New York, 1995, pp. 339-345.
Lev-Lehman, E., A. El-Tamer, A. Yaron, M. Grifman, D. Ginzberg, I. Hanin, H. Soreq, Brain. Res. 661 (1994) 75-82.
Loewenstein-Lichtenstein, D. Glick, N. Gluzman, M. Sternfeld, H. Soreq Molec. Pharmacol. (in press)
Loewenstein-Lichtenstein, Y., M. Schwarz, D. Glick, B. Nørgaard-Pedersen, H. Zakut, H. Soreq, Nature Medicine 1 (1995) 1082-1085.
Schwarz, M., D. Glick, Y. Loewenstein, H. Soreq, Pharmacol. Therap. 67 (1995) 283-322.
Schwarz, M., Y. Loewenstein-Lichtenstein, D. Glick, J. Liao, B. Nørgaard-Pedersen, H. Soreq, Molec. Brain Res. 31 (1995) 101-110.
Seidman, R. Ben Aziz-Aloya, R. Timberg, Y. Loewenstein, B. Velan, A. Shafferman, J. Liao, B. Nørgaard-Pedersen, U. Brodbeck, H. Soreq, J. Neurochem. 62 (1994) 167-1681.
Seidman, S., M. Sternfeld, R. Ben Aziz-Aloya, R. Timberg, D. Kaufer-Nachum, H. Soreq", Mol. Cell. Biol. 14 (1995) 459-473.
Soreq, H., G. Ehrlich, M. Schwarz, Y. Loewenstein, D. Glick, Zakut, H., Biomed. Pharmacother. 48 (1994) 253-259.
Andres, C., R. Beeri, A. Friedman, E. Lev-Lehman, R. Timberg, M. Shani, H. Soreq (submitted for publication)
Friedman, A., D. Kaufer-Nachum, J. Shemer, I. Hendler, H. Soreq, I. Tur-Kaspa (submitted for publication)
Grifman, M., A. Arbel, D. Ginzberg, D. Glick, S. Elgavish, B. Shaanan, H. Soreq (submitted for publication)

List of papers published under USAMRDC support

Andres, C., R. Beeri, T. Huberman, M. Shani, H. Soreq, "Cholinergic drug resistance and imparied spatial learning in transgenic mice overexpressing human brain acetylcholinesterase", Prog. Brain Res. (in press).

Beeri, A. Gnatt, Y. Lapidot-Lifson, D. Ginzberg, M. Shani, H. Soreq, H. Zakut, "Testicular amplification and impaired transmission of human butyrylcholinesterase cDNA in transgenic mice", Human Reprod. 9 (1994) 284-292.

Beeri, R., C. Andres, E. Lev-Lehman, R. Timberg, T. Huberman, M. Shani, H. Soreq, "Transgenic expression of human acetylcholinesterase induces progressive cognitive deterioration in mice", Curr. Biol. 5 (1995) 1063-1071.

Hanin, I., A. Yaron, D. Ginzberg, H. Soreq (1995) "The cholinotoxin AF64A differentially attenuates in vitro transcription of the human cholinesterase genes", in *Alzheimer's and Parkinson's Diseases,* I. Hanin et al., eds.; Plenum Press, New York, pp. 339-345.

Lev-Lehman, E., A. El-Tamer, A. Yaron, M. Grifman, D. Ginzberg, I. Hanin, H. Soreq, "Cholinotoxic effects on acetylcholinesterase gene expression are associated with brain-specific alterations in G,C-rich transcripts", Brain. Res. 661 (1994) 75-82.

Loewenstein-Lichtenstein, D. Glick, N. Gluzman, M. Sternfeld, H. Soreq, "Overlapping drug interaction sites of human butyrylcholinesterase dissecteed by site-directed mutagenesis" Molec. Pharmacol. (in press)

Loewenstein-Lichtenstein, Y., M. Schwarz, D. Glick, B. Nørgaard-Pedersen, H. Zakut, H. Soreq, "Genetic predisposition to adverse consequences of anti-cholinesterases in 'atypical' BCHE carriers", Nature Medicine 1 (1995) 1082-1085.

Schwarz, M., D. Glick, Y. Loewenstein, H. Soreq, "Engineering of human cholinesterases explains and predicts diverse consequences of administration of various drugs and poisons", Pharmacol. Therap. 67 (1995) 283-322.

Schwarz, M., Y. Loewenstein-Lichtenstein, D. Glick, J. Liao, B. Nørgaard-Pedersen, H. Soreq, "Successive organophosphate inhibition and oxime reactivation reveals distinct responses of recombinant human cholinesterase variants", Molec. Brain Res. 31 (1995) 101-110.

Seidman, R. Ben Aziz-Aloya, R. Timberg, Y. Loewenstein, B. Velan, A. Shafferman, J. Liao, B. Nørgaard-Pedersen, U. Brodbeck, H. Soreq, "Overexpressed monomeric human acetylcholinesterase induces subtle ultrastructural modifications in developing neuromusclar junctions of *Xenopus laevis* embryos." J. Neurochem. 62 (1994) 167-1681.

Seidman, S., M. Sternfeld, R. Ben Aziz-Aloya, R. Timberg, D. Kaufer-Nachum, H. Soreq, "Synaptic and epidermal accumulation of human acetylcholinesterase are encoded by alternative 3'-terminal exons", Mol. Cell. Biol. 14 (1995) 459-473.

Soreq, H., G. Ehrlich, M. Schwarz, Y. Loewenstein, D. Glick, H. Zakut, "Mutation and impaired expression in the ACHE and BCHE genes: neurological implications", Biomed. Pharmacother. 48 (1994) 253-259.

Andres, C., R. Beeri, A. Firedman, E. Lev-Lehman, R. Timberg, M. Shani, H. Soreq, "Transgenic ACHE induces neuromuscular deterioration in mice" (submitted for publication)

Friedman, A., D. Kaufer-Nachum, J. Shemer, I. Hendler, H. Soreq, I. Tur-Kaspa, "Pyridostimine brain penetration under stress enhances neuronal exclitability and induces early intermediary transcriptional response" (submitted for publication)

Grifman, M., A. Arbel, D. Ginzberg, D. Glick, S. Elgavish, B. Shaanan H. Soreq "Acetylcholinesterase phosphorylation at non-consensus protein kinase A sites enhances the rate of acetylcholine hydrolysis" (submitted for publication)

Hebrew University of Jerusalem graduate theses supported by USAMRDC funds

Doctoral theses

G. Ehrlich, "Congenital and acquired alterations in the human acetyl- and butyrylcholinesterase genes and their expression in healthy and tumor tissues", November 1993

S. Seidman, "A morphogenic role for acetylcholinesterase: heterologous expression studies in microinjected embryos of *Xenopus laevis*", March 1995 (*cum laude*)

Y. Loewenstein-Lichtenstein, "Structural and molecular dissection of biologically active domains in human cholinesterases, August 1995.

Masters thesis

M. Sternfeld, "Biological roles and tissue-specific regulation of alternative human cholinesterase isoforms", June 1996

Abbreviations

ACh	acetylcholine
AChE	acetylcholinesterase enzyme
ACHE	acetylcholinesterase gene
AChR	acetylcholine receptor
AF64A	ethylcholine aziridinium
ASCh	acetylthiocholine
BBB	blood-brain barrier
BCHE	butyrylcholinesterase gene
BuChE	butyrylcholinesterase enzyme
BW284c51	(1,5-bis(4-allyldimethylammoniumphenyl)pentan-3-one dibromide)
ChAT	choline acetyltransferase
ChE	cholinesterase
CMV	cytomegalovirus
CNS	central nervous system
CSF	cerebrospinal fluid
DFP	diisopropylfluorophosphonate
DIP	diisopropylphosphoryl
DTNB	dithionitrobenzoate
E6	human acetylcholinesterase representing exons 2, 3, 4 and 6
EAIA	enzyme-antigen immumoassay
ELISA	enzyme-linked immunosorbant assay
I4/E5	human acetylcholinesterase representing exons 2, 3 and 4, intron 4 and exon 5
ICV	intracerebroventricular
kcat	first-order catalytic rate constant
Km	Michaelis constant
NMJ	neuromuscular junction
OP	organophosphate
PAM	pyridine-2-aldoxime methiodide
PCR	polymerase chain reaction
PF	post-fertilization
PKA	protein kinase A
PSL	post-synaptic membrane length
rHAChE	recombinant human AChE
RT-PCR	reverse transcriptase-PCR

Amino acid residues are indicated by their single-letter code followed by the sequence position. Amino acid replacements are indicated by the single letter code of the original residue, the sequence position, and the single letter code of the new residue. Thus, the replacement of aspartate at position 70 (D70) by glycine, is indicated by D70G.

Progress Relative to the Statement of Work

The wide scope mandate of this contact was defined as follows:

- Does overexpression of cloned ChE genes or mutated variants thereof confer protection against OP toxicity?
- This was planned for experimentation in transiently transgenic *Xenopus laevis* tadpoles and in stably transgenic mice, all with the long-range aim of studying the protective capacities of these proteins in humans. Towards this goal, we have accomplished the following:

Studies in *Xenopus laevis*

We have constructed a novel set of site-directed mutants in the molecularly cloned human BCHE gene and injected the normal and mutated variants into *Xenopus* oocytes for examination of their biochemical characteristics. Our findings revealed partially overlapping binding sites for several inhibitors and demonstrated the involvement of the putative oxyanion hole in BuChE catalysis.

To examine targeting of variant ChEs to NMJs, we employed biochemical, cytochemical and electron microscopy techniques. ACHE and BCHE microinjections followed by electron microscopy and preliminary OP protection studies revealed preferential accumulation of that isoform of ACHE which terminated in exon 6 in synapses and effective protection from paraoxon. Therefore, the ACHE gene was selected as our first lead gene for transgenic mouse studies.

Studies on Transgenic Mice

Under this task, we completed the first thorough analysis of a stable homozygous transgenic mouse line which overexpresses human ACHE in its CNS. These mice displayed resistance to hypothermia induced by paraoxon, as well as by muscarinic, nicotinic and serotonergic agonists. They also developed an age-dependent deterioration of their cognitive and NMJ functions.

Two additional lines which carried variable copy numbers of the human ACHE gene were found to be non-expressing, and thus non-informative for our studies. Whenever the strong viral CMV promoter was employed, we failed to obtain viable progeny. This probably reflects a lethal state of embryos flooded with the transgenic human protein.

Studies *in vitro*

In the course of pursuing these tasks, we fortuitously learned of a family in which a point mutation in the BCHE gene (D70G), one which we discovered and characterized under previous Army support, was associated with adverse responses to anti-ChEs. We were offered blood samples from this family's members and generated the corresponding oocyte-produced recombinant protein. Given the Army Medical Research and Defense Command's goals, as defined in the Broad Agency Announcement, we used this opportunity to examine the interactions of these enzymes with several anti-ChEs. The mutant serum enzyme was thus found to be deficient in its capacity to interact with several carbamate and quaternary ammonium AChE inhibitors, with important implications for the neuropharmacology of Alzheimer's disease.

Phosphorylation of human AChE has been demonstrated and shown to enhance the catalytic efficiency of the enzyme up to ten-fold. There is also evidence that AChE exists *in vivo* in a partially phosphorylated form.

Introduction

Acetylcholinesterase (AChE) has long been recognized as an essential component of nerve conduction and muscular innervation. In a grim recognition of this, was the development of anti-cholinesterases (anti-ChEs) as warfare nerve agents and subsequently of pesticides. The search for an antidote was successful in the development of pyridine-2-aldoxime methiodide (PAM), but the search for prophylactic agents has been more problematical. One approach has been to reversibly block AChE before exposure to the nerve agent in order to compete with and thus prevent the irreversible inactivation of the enzyme. Pyridostigmine was used for this purpose during the 1991 Gulf War. Another more ambitious but not yet developed approach has been to produce alternative targets for the nerve agent that might be injected into an individual at risk. The first such alternative to be proposed as protection of the individual's AChE was exogenous human AChE, to be produced by recombinant molecular biological techniques. Later it was found that human butyrylcholinesterase (BuChE) was also an effective alternative target, and that, indeed, it serves normally, as such a decoy target for anti-ChEs of the natural environment.

There is a fine balance of acetylcholine (ACh) production, presynaptic release upon neural stimulation, binding to and activating the acetylcholine receptor (AChR) and termination of action by hydrolysis of ACh. The shift of this balance in disease states (e.g. autoimmunity to the AChR in myasthenia gravis) or due to poisoning (e.g. OP or carbamate pesticide intoxication) clearly has severe consequences. There is also the potential for severe consequences should the balance of ACh production and destruction be altered by an exogenous synaptic ChE, and we have been evaluating this possibility by several means, chiefly by introducing a human ChE gene into an animal. Selection of a transgenic animal model is constrained by the availability of technology and by experience. We have used the *Xenopus laevis* tadpole because of our experience with *Xenopus* oocytes, the short time for expression of a gene, moderate cost and the ethical imperative to work with a species as phylogenetically remote as possible from the human. We find that alternative forms of human AChE affect the development of the neuromuscular junction (NMJ) and its ultrastructure differently, and that the nature of the mRNA splicing determines tissue targeting. Because of the limitations inherent in using a non-mammalian model, we have also used the mouse, the mammal in which there is the most experience in introducing human genes. We have used the mouse to observe the effect on body temperature regulation of anti-ChEs, and the protection afforded by the human transgene expressed in the mouse's central nervous system (CNS). We find, also, that in this transgenic mouse, the imbalance of ACh production and destruction results in a progressive loss of cognitive function. The NMJs, which represent CNS extensions into muscles, also deteriorate, as seen in morphologically and in junctional dysfunction and amyotrophy.

It had been thought that the blood-brain barrier (BBB) protects the CNS form charged anti-ChEs. However, the reports of CNS symptoms among individuals who had received prophylactic doses of pyridostigmine prompted us to re-examine this assumption in light of reports that stress can increase permeability of the BBB. We have found that the brains of mice which had been subjected to stress-inducing tasks have a drastically increased level of pyridostigmine, with resultant transcriptional and electrophysiological changes.

Parallel with these studies on transgenic animals, we have been studying the chemistry of the interaction of anti-ChEs with human AChE and BuChE and also with the major natural variant of human BuChE, especially as this BuChE, the "atypical" variant appears to offer much less protection against a wide variety of anti-ChEs than normal BuChE. We also evaluated the action of a reactive ACh analog in rat brain, in order to gain some appreciation of the relative vulnerabilities of AChE and BuChE and the dynamics of the brain's recovery from an anti-ChE. That effort also gave us our first experience with differential display PCR, which we continue to exploit.

We have continued our efforts to understand the biological roles of BuChE and its functional interaction with AChE so that this knowledge can be used in the development of more effective prophylaxis against warfare nerve agents.

Body of the Report

1. Transgenic *Xenopus* tadpole

Formation of a functional NMJ requires the targeted deposition of synaptic proteins at the nerve-muscle interface (Froehner, 1991; Ohlendieck *et al.*, 1991; Flucher and Daniels, 1989). Among these proteins is AChE. In the developing *Xenopus* embryo, muscle differentiation, primitive neuromuscular contacts, and spontaneous synaptic activity are observed within 1 day post-fertilization (PF) (Kullberg *et al.*, 1977). During the ensuing 24 h, ultrastructural specializations that characterize synaptic differentiation are observed, followed by the acquisition of spontaneous motor activity and hatching (Cohen, 1980). Fervent embryonic development and ultrastructural maturation of the neuromuscular system continue, giving rise to a free swimming tadpole within 4 to 5 days. From day 2 PF, a steady increase in AChE activity is observed (Gindi and Knowland, 1979), concomitant with a developmentally regulated decrease in the time course of the synaptic potential in *Xenopus* myotomes (Kullberg *et al.*, 1980). We have cloned a DNA sequence encoding human AChE and used it to express catalytically active AChE in microinjected *Xenopus* oocytes (Soreq *et al.*, 1990) and cultured human cells (Velan *et al.*, 1991a). We have presented a biochemical and histochemical characterization of this recombinant human AChE (rHAChE) expressed in *Xenopus*, and have demonstrated the persistence of overexpressed enzyme in NMJs to at least day 3 of embryonic development. Also, we accumulated evidence of subtle alterations in the ultrastructure of NMJs from embryos which overexpress ACHE. Our findings indicate the assignment of catalytically active monomeric AChE to subcellular compartments common to those occupied by native, multimeric *Xenopus* AChE .

***Xenopus*-expressed AChE is biochemically indistinguishable from native human AChE** When microinjected into mature oocytes, 5 ng of *in vitro*-transcribed AChEmRNA directed the production of catalytically active AChE, displayed substrate and inhibitor interactions that were characteristic of the human enzyme (Fig. 1.1A, B). The apparent Km calculated for rAChE towards acetylthiocholine was 0.3 mM, essentially identical to that displayed by AChE expressed in cell lines (Velan *et al.*, 1991b) and native human erythrocyte AChE. In sucrose density centrifugation AChE sedimented primarily as monomers and dimers, although a discernible peak, apparently representing globular tetrameric AChE, was also observed (Fig. 1.1C). When plasmid DNA carrying ACHEcDNA downstream of CMVACHE (Velan et al, 1991b) was microinjected into oocytes, active AChE in yields 10-20 fold higher than that observed following RNA injections was obtained (Fig. 1.1D), demonstrating efficient transcription from this promoter in *Xenopus*.

Transient expression of CMVACHE in *Xenopus* embryos When microinjected into cleaving embryos, CMVACHE directed the biosynthesis of AChE at levels similar to those observed in DNA-injected oocytes, yet, the gross morphology and development of injected embryos appeared normal (Fig. 1.2). Moreover, gross motor function of microinjected embryos was unimpaired. Microinjected tadpoles survived up to 4 weeks and showed no overt developmental handicaps. Following overnight incubation, at which time embryos had reached the late gastrula stage, endogenous AChE levels were negligible and activity represented a 50- to 100-fold excess over normal (Fig. 1.3A). From day 2 PF, endogenous AChE activities increased steadily. Using the irreversible AChE inhibitor echothiophate (Neville *et al.*, 1992) to distinguish endogenous frog AChE from human AChE (Fig. 1.3A, inset), we observed the persistence of receding levels of human AChE for at least 4 days PF. For the first 3 days, human AChE accounted for >50% of the total measured activity in microinjected embryos and resulted in a state of general overexpression. In immunoblot analysis, human AChE was observed to comigrate with native human brain AChE, yielding a clearly visible doublet band at around 68 kD (Fig. 1.3B). The doublet may reflect differences in glycosylation (Kronman *et al.*, 1992).

Human acetylcholinesterase remains monomeric in *Xenopus* embryos To examine the possibility that heterologous human AChE undergoes homomeric oligomeric assembly or interacts with either catalytic or non-catalytic subunits of *Xenopus* AChE to produce hybrid oligomers, sucrose density centrifugation and EAIA were performed. At all time points examined, we observed human AChE exclusively as non-assembled monomers which sedimented at approximately 3.2 S, despite the concomitant accumulation of various multimeric forms of the endogenous frog enzyme (Fig. 1.4). When oligomeric AChE which had been purified from CMVACHE-transfected cell cultures (Velan *et al.*, 1991a) or from human brain (Liao *et al.*, 1992) was preincubated with extracts of day 3 uninjected embryos and similarly analyzed, monomers, dimers, and tetramers were detected, and the distribution of oligomeric forms was observed to be identical to that of controls (data not shown).

Subcellular disposition of human acetylcholinesterase in myotomes of CMVACHE-injected embryos Whole mount cytochemical staining of CMVACHE-injected embryos indicated accumulation of AChE in myotomes 2 days PF (not shown). We therefore undertook an ultrastructural analysis. Longitudinal and transverse sections from rostral trunk somites revealed clearly discernible myofibers 2 days PF in both injected and uninjected embryos (Fig. 1.5). By day 3 PF, both groups displayed significant increases in their numbers of myofibrillar elements and in maturation of the sarcoplasmic reticulum (SR; Fig. 1.6). To examine the subcellular localization of nascent AChE in transgenic and control embryos we employed cytochemical activity staining (Karnovsky, 1964). Crystalline deposits were observed primarily in association with myofibrils, among the myofilaments and within the SR (Figs. 1.5 and 1.6). Various organelles, including the nuclear membrane, free and bound polyribosomes, Golgi apparatus, and sometimes mitochondria were also observed to be stained (Figs. 1.5 and 1.6 and data not shown). At day 2 PF, staining in CMVACHE-injected embryos was more pronounced, both in the quantity and intensity of reaction product (Fig. 1.5). However, variability was observed between tissue blocks which probably reflected mosaic expression of the injected DNA and/or variability in the efficiency of expression between embryos. Staining appeared to be concentrated at the I band of myofibers, particularly around the triad marking the intersection of the SR and T-tubule systems. Cross sections revealed especially prominent staining within the SR (Fig. 1.6A,B). Strong staining was now observed at both the A and I bands, and for the first time, within the T-tubules (Fig. 1.6C,D). Overall, day 2 CMVACHE-injected myotomes resembled day 3 uninjected control myotomes in staining incidence and intensity (Figs. 1.5A,C and 1.6B,D).

Ultrastructural consequences of overexpressed acetylcholinesterase in *Xenopus* neuromuscular junctions To examine the persistence of overexpression and its implications for synaptic ultrastructure, we studied both cytochemically stained and closely appositioned unstained NMJs from 3 day-old injected embryos (Fig. 1.7 and Table 1.1). Seventy-two percent of the post-synaptic membrane length, on average, stained for active AChE (SL/PSL, Table 1.1). Moreover, the total area covered by reaction product was approximately 4-fold greater than controls in NMJs from CMVACHE-injected embryos (SA, Table 1.1). In addition, the staining observed in NMJs from injected embryos was considerably more intense, forming large black accumulations of reaction product (Fig. 1.7A-B,D-E). Ultrastructural features of NMJs from injected embryos were best discerned in unstained synapses. NMJs from CMVACHE-injected embryos displayed more secondary folds and discrete contacts between pre- and post-synaptic membranes (Fig. 1.7F). Furthermore, the average post-synaptic membrane length in NMJs from CMVACHE-injected embryos was 30% larger and considerably less variable (SL, Table 1.1), yet, the distance across the synaptic cleft was both larger and more variable. NMJs which overexpress human AChE thus appeared more developed in their structural buildup.

Despite their lack of MyoD elements, some constructs which carry the CMV promoter were shown to be expressed in myotomes of transgenic mouse embryos (Kothary *et al.*, 1991). Therefore, the characteristic subcellular segregation of overexpressed human AChE in muscle may reflect either tissue-specific biosynthesis or post-translational processing of nascent enzyme present in myotomal progenitor cells at the onset of myogenesis. The high levels of human AChE present in gastrula stage embryos may argue for the latter possibility. In that case,

the cytochemical data indicate the existence of an intrinsic, evolutionarily conserved property which directs the subcellular trafficking of AChE in muscle, and thus explain the accumulation of human AChE in NMJs of ACHEDNA-injected embryos. Furthermore, these results may imply that cotranslational processes are not required for the correct compartmentalization of AChE in muscle cells.

The general state of myotomal overexpression induced by microinjection of CMVACHE persisted at least 3 days. The area covered by reaction product in cytochemically stained NMJs from day 3 CMVACHE-injected embryos was 4-5 fold greater than that observed in controls. The apparent reduction in the level of synaptic overexpression from day 2 to day 3 PF may reflect the overall decline in total human AChE activity. However, since this calculation does not consider the higher density of staining observed in NMJs from CMVACHE-injected embryos, it represents an underestimate of the actual synaptic AChE content. Therefore, our data indicate enhanced stability of human AChE at the NMJ compared to the total pool, a conclusion consistent with the observation that extracellular matrix-associated AChE persists *in situ* long after denervation of adult frog skeletal muscle (Anglister and McMahan, 1985).

Table 1.1 *Overexpression of AChE in NMJs of 3-day-old CMVACHE-injected* Xenopus *embryos*

Experiment	PSL (μm)	SL (μm)	SL/PSL ratio	SA (μm²)
Uninjected	2.57	0.79	0.004	0.156
	3.95	0.79	0.200	0.126
	1.54	0.80	0.060	0.080
	2.35	0.73	0.310	0.082
	1.17	0.44	0.085	0.063
	1.60	0.29	0.180	0.056
	1.02	0.29	0.280	0.040
	0.88	0.58	0.650	0.075
Average ± SD	1.88 ± 0.93	0.58 ± 0.22	0.22 ± 0.19	0.084 ± 0.038
+ CMVACHE	1.76	1.17	0.660	0.284
	2.50	2.05	0.820	0.331
	2.64	1.91	0.720	0.285
	2.50	2.40	0.960	0.476
	3.50	2.03	0.580	0.396
	1.85	1.66	0.900	0.333
	3.10	1.85	0.600	0.535
	3.23	1.76	0.540	0.289
Average ± SD	2.64 ± 0.58	1.85 ± 0.33	0.72 ± 0.15	0.37 ± 0.09
p	<0.01	<0.002	<0.002	<0.002

Eight representative synapses from CMVACHE-injected or control uninjected embryos were assessed for postsynaptic membrane length (PSL), the sum total length covered by reaction product (SL), the fraction of nerve–muscle contact distance displaying reaction product (SL/PSL), and the total stained area (SA). Average ± SD values are given. Measurements were performed on electron micrographs using a hand-held mapping device.

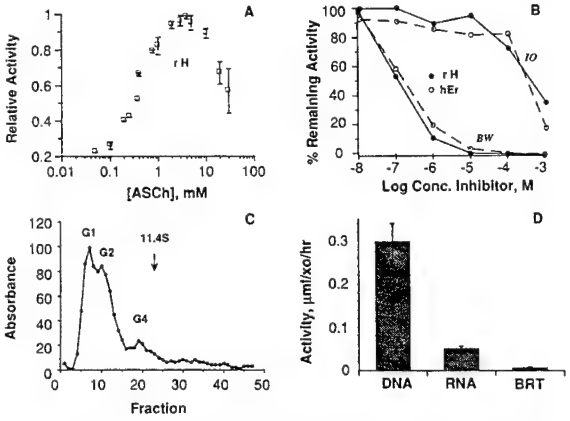

Fig. 1.1 *Xenopus* oocytes express catalytically active rHAChE. **A:** Inhibition by excess substrate. Mature *Xenopus* oocytes were injected with 5 ng of in vitro-transcribed AChE mRNA (Soreq et al., 1990) and incubated overnight at 17°C. Homogenates corresponding to one-third oocyte were assayed for AChE activity in the presence of various concentrations of acetylthiocholine (ASCh) substrate [average of three experiments ± SEM (bars)]. **B:** Sensitivity to selective inhibitors. Oocyte homogenates were preincubated for 30 min in assay buffer containing the AChE-specific, reversible inhibitor 1,5-bis(4-allyldimethylammoniumphenyl)-pentan-3-one dibromide [BW284C51 (BW)] or the butyrylcholinesterase-specific inhibitor tetraisopropylpyrophosphoramide (IO) at the indicated concentrations and assayed for remaining activity following addition of 2 m*M* ASCh. Data are averages of duplicate assays from two independent microinjection experiments. AChE extracted from human erythrocytes (hEr) served as control. rH, rHAChE. **C:** Oligomeric assembly. Homogenates from ACHE mRNA-injected oocytes were subjected to sucrose density centrifugation. Data are averages of three experiments. Note that in addition to the free monomer (3.2S; G1), the oocyte appears to generate dimers (5.6S; G2) and to a lesser extent tetramers (10.2S; G4) of human AChE. Endogenous oocyte AChE activity is undetectable under these conditions. The arrow marks the position of bovine liver catalase (11.4S). **D:** Expression of ACHE DNA in *Xenopus*. Oocytes were injected with 5 ng of synthetic ACHE mRNA or CMVACHE (Velan et al., 1991a) and incubated for 1 (RNA) to 3 (DNA) days. Oocytes injected with incubation medium (BRT) or uninjected oocytes served as control. Activity is expressed as micromoles of substrate hydrolyzed per hour per oocyte, in mean ± SEM (bars) values for three independent microinjection experiments.

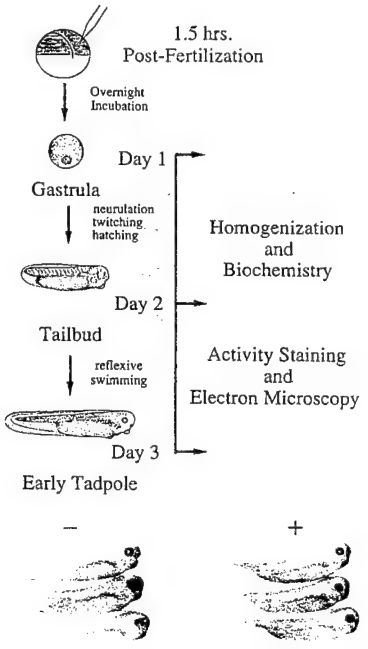

Fig. 1.2 Normal development of CMVACHE-injected embryos. A schematic representation of a microinjection experiment depicting the principal developmental stages and analytical approaches used in this work is shown together with photographs displaying the normal gross development of unstained microinjected embryos (+) compared with control uninjected embryos (–) 3 days PF. In vitro fertilized eggs of *Xenopus laevis* were injected with 1 ng of CMVACHE and cultured for 1–4 days as described in Materials and Methods. Sketches are modeled after those of Deuchar (1966).

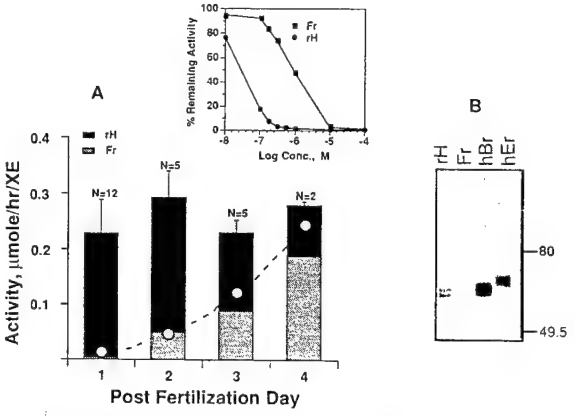

Fig. 1.3 CMVACHE-injected *Xenopus* embryos express and maintain biochemically distinct heterologous human AChE for at least 4 days. **A:** Overexpression of rHAChE in developing embryos. High-salt/detergent extracts of CMVACHE-injected and uninjected embryos were prepared and assayed for AChE activity in the presence and absence of the selective inhibitor echothiophate (3.3×10^{-7} *M*; **inset**). Endogenous AChE activity was calculated according to an algorithm assuming 90% inhibition of rHAChE and 20% inhibition of frog AChE at this concentration of inhibitor. The bar graph represents the total AChE activity measured per microinjected embryo at various time points following microinjection and the calculated activities attributable to rHAChE (dark shading) and endogenous frog AChE (light shading). The total AChE activity measured in uninjected control embryos at the same time points is indicated by open circles. Data represent average ± SEM (bars) values from four to six embryos from the indicated number (N) of independent microinjection experiments. Inset: Selective inhibition of rHAChE by echothiophate. Homogenates representing endogenous frog (Fr) or recombinant human (rH) AChE were assayed for activity following a 40-min preincubation with the indicated concentrations of echothiophate. Data are averages of three experiments. **B:** Immunochemical discrimination between rHAChE and embryonic *Xenopus* AChE. Affinity-purified AChE from CMVACHE-injected *Xenopus* embryos (rH), control uninjected embryos (Fr), human brain (hBr), and erythrocytes (hEr) was subjected to denaturing gel electrophoresis and protein blot analysis Each lane represents ~20 ng of protein, except rH, which contained only 6 ng. Note the complete absence of immunoreactivity with embryonic *Xenopus* AChE, although silver staining of a parallel gel demonstrated detectable protein at the corresponding position (data not shown). The faint upper bands (140–160 kDa) in the lanes displaying native human AChEs represent dimeric forms resulting from incomplete reduction of the intersubunit disulfide bonds (see Liao et al., 1992). Prestained molecular weight markers indicated on the right were from Bio-Rad, U.S.A..

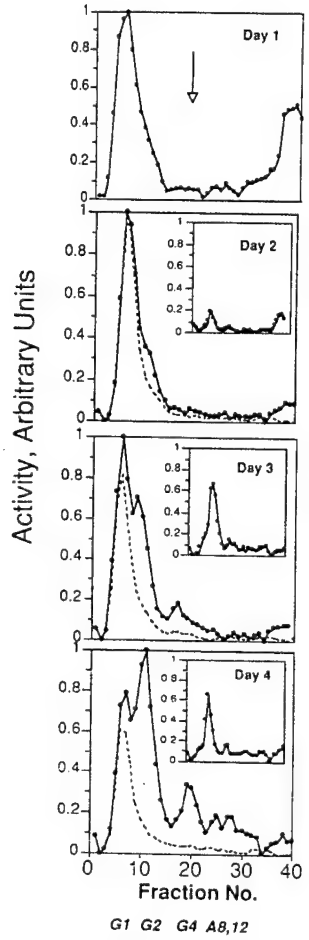

Fig. 1.4 rHAChE in microinjected *Xenopus* embryos remains monomeric. High-salt/detergent extracts representing two embryos were subjected to sucrose density centrifugation. Shown are total AChE (solid line) and immunoreactive rHAChE (dotted line) from CMVACHE-injected embryos 1–4 days PF. rHAChE appeared exclusively as a peak representing monomeric AChE (~3.2S) at all time points. The arrow marks the position of bovine liver catalase (11.4S). **Insets:** AChE molecular forms in control uninjected embryos scaled to the total activity levels observed in DNA-injected embryos Peak analysis demonstrated that the distribution of oligomeric forms was identical to that observed in CMVACHE-injected embryos. Note that monomeric AChE is essentially undetectable in control embryos. G1, G2, and G4 indicate the expected positions of the globular monomer, dimer, and tetramer in the gradient; A8 and 12 indicate the positions of "tailed" asymmetric forms. Fraction 0 represents the top of the gradient.

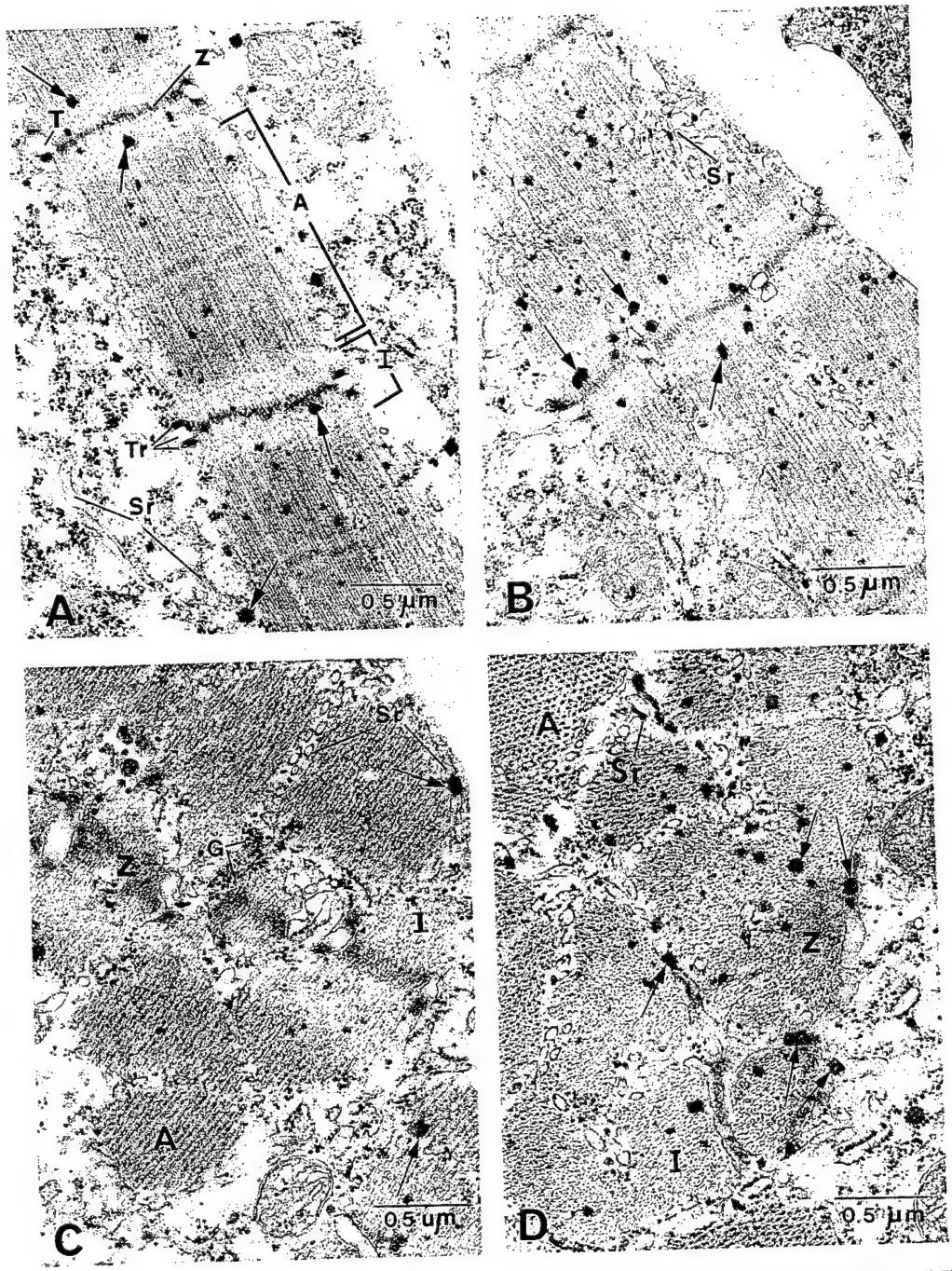

Fig. 1.5 Disposition of rHAChE in myotomes from 2-day-old microinjected *Xenopus* embryos. Fertilized *Xenopus* eggs were microinjected with 1 ng of CMVACHE, incubated for 2 days at 17°C, fixed, stained, and prepared for electron microscopy.

Uninjected embryos from the same fertilization served as controls and were similarly treated. Arrows mark accumulations of reaction product indicating sites of catalytically active AChE. **A:** Uninjected control myotome in longitudinal section following activity staining for AChE. **B:** Myotome section from CMVACHE-injected embryo. **C:** Uninjected control myotome in transverse section. **D:** Transverse section from CMVACHE-injected embryo. Note the increased intensity of staining in sections from injected embryos versus uninjected controls within the same subcellular compartments, especially within the sarcoplasmic reticulum (Sr). A, A band; I, I band; Z, Z disc; Tr, triad; T, T tubules; G, glycogen particles. Bar = 0.5 μm.

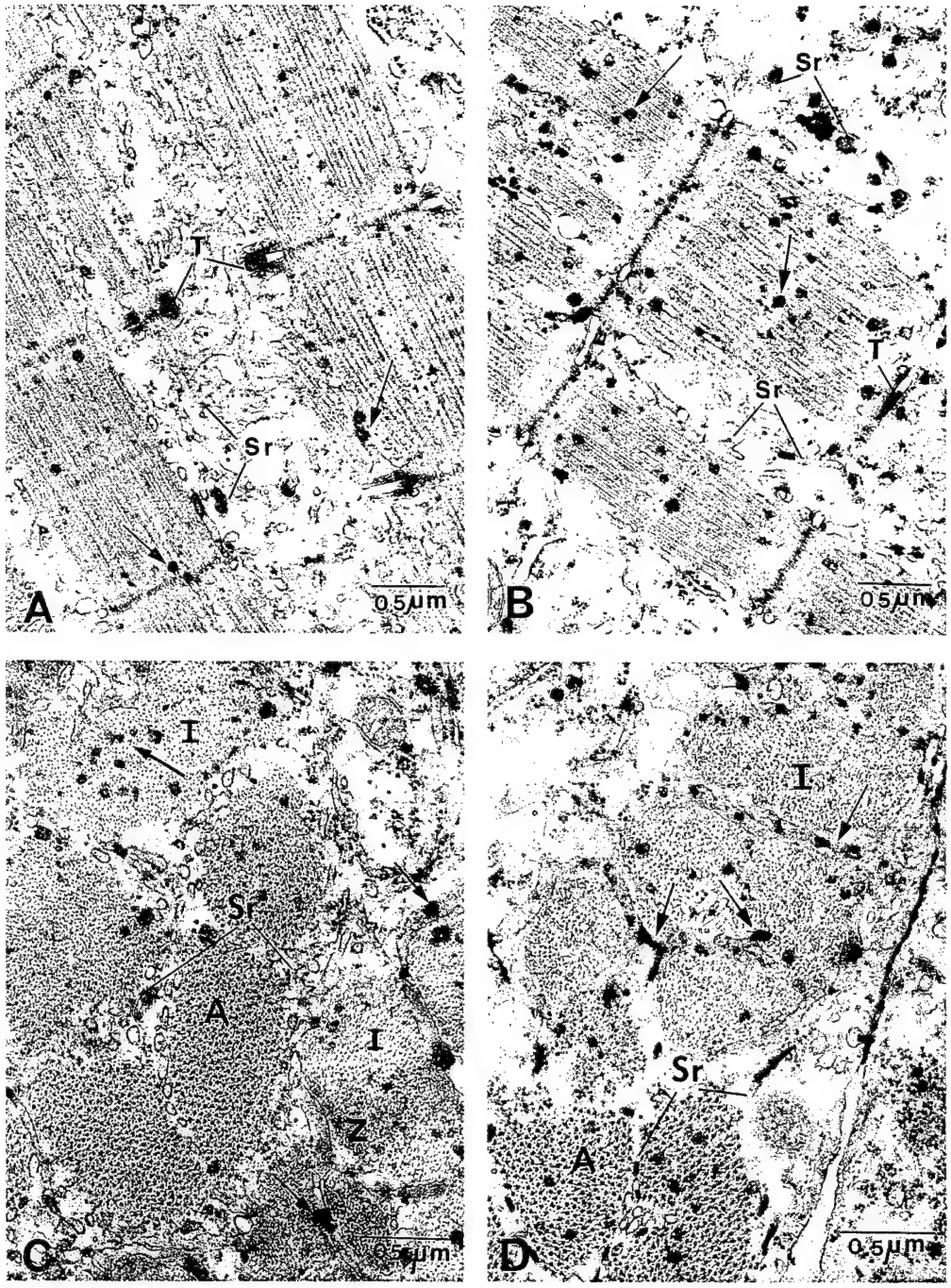

Fig. 1.6 Overexpression of AChE in myotomes of CMVACHE-injected embryos persists to day 3. Analyses were as in Fig. 5 except that embryos were analyzed after incubation for 3 days. Note the developmental increases in myotomal AChE in both control uninjected (**A** and **C**) and CMVACHE-injected sections (**B** and **D**), especially within the sarcoplasmic reticulum (Sr) and T-tubules (T). Bar = 0.5 μm.

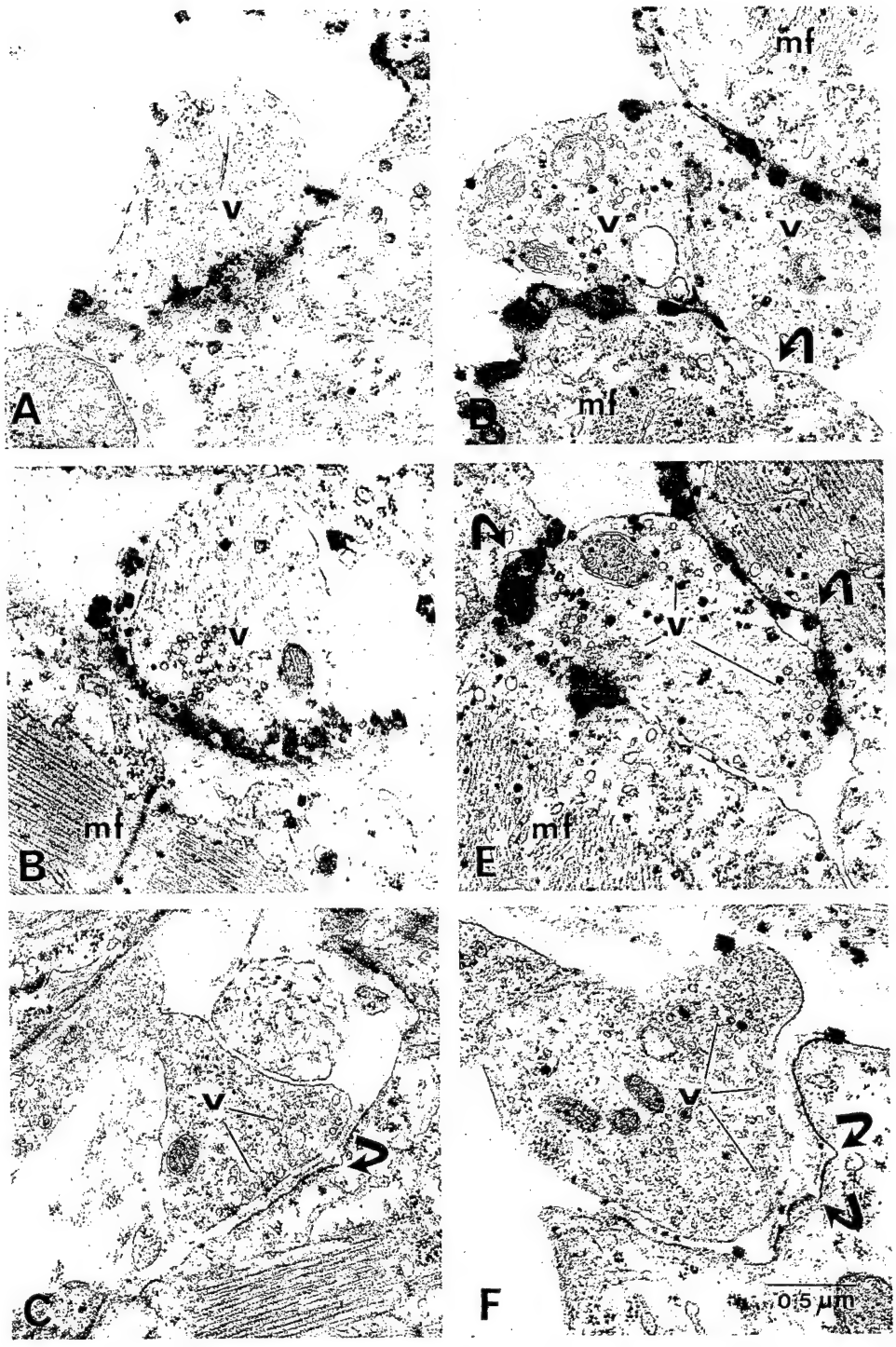

Fig. 1.7. Structural features in NMJs of 3-day-old CMVACHE-injected *Xenopus* embryos overexpressing AChE. *Xenopus* embryos were cultured for 3 days, fixed, stained for AChE catalytic activity, and examined by transmission electron microscopy as described in Materials and Methods. Two cytochemically stained synapses are presented from uninjected control (**A** and **B**) and CMVACHE-injected (**D** and **E**) embryos. Note the particularly high-density staining in areas directly opposite nerve terminal zones enriched in presynaptic neurotransmitter vesicles (v). **C** and **F:** Representative unstained NMJs from a control and a CMVACHE-injected embryo, respectively. The synapse shown in B represents the highest degree of staining observed in a control section. mf, myofibril. Arrows indicate postsynaptic folds.

2. Transgenic mouse

Low level ACHE overexpression is compatible with life The exceedingly low success rates that we found for obtaining viable AChE-transgenic mice suggests that only at low levels is AChE overexpression compatible with life. Seven generations of transgenic mice were raised, all of which presented grossly normal development, activity and behavior.

The limited neuronal expression and the low copy number of the ACHE transgene ensured that it could cause only a subtle cholinergic imbalance. Thanks to the extremely high homology between the human and the mouse enzymes, the transgenic protein was processed and assembled normally. It therefore accumulated in all of the relevant sites, with its highest excess levels found in basal forebrain.

Transgenic human ACHE expression is limited to central nervous system neurons Reverse transcription and quantitative PCR amplification (Beeri *et al.*, 1994) revealed both human and mouse ACHEmRNA transcripts in brain regions of the homozygous transgenic mice, as is demonstrated in Fig. 2.1A. Bone marrow and adrenal glands displayed only mouse ACHEmRNAs, with apparently unmodified concentrations of the principal alternative products. The transgene was not expressed in muscle. To associate human ACHEmRNA transcripts with specific brain cell types, we performed *in situ* hybridization experiments. Cholinoceptive hippocampal neurons were intensively labeled, especially in the CA1-CA2 region (Fig. 2.1B). Thus, expression of the transgene was apparently confined to host CNS neurons that normally express the mouse ACHE gene.

Normally processed transgenic acetylcholinesterase accumulates in cholinergic brain regions AChE from the brain demonstrated unmodified assembly into multimeric enzyme forms (Fig. 2.1C). Up to 50% of the active enzyme in basal forebrain (Fig. 2.1C), but none in bone marrow (Table 2.1), interacted with monoclonal antibodies specific to human AChE (Seidman *et al.*, 1995). Catalytic activity measurements in tissue homogenates revealed a 100% increase over control in the detergent-extractable amphiphilic AChE fraction from basal forebrain and more limited increments in cortex, brainstem, cerebellum and spinal cord extracts (Table 2.1). There were no age-dependent changes in this pattern and no differences in the cell type composition of bone marrow of transgenic as compared with control mice. Intensified cytochemical staining of AChE activity was observed in brain sections from transgenic mice in all of the areas that stain for AChE activity in normal mice (Kitt *et al.*, 1994), particularly in the neo-striatum and pallidum (Fig. 2.2A) as well as in hippocampus (Fig. 2.2B), the latter two areas associated with learning and memory (Eichenbaum *et al.*, 1990; Yu et al, 1989). Moreover, there were more conspicuous depositions of the electron-dense product of AChE cytochemical staining within synapse-forming dendrites in the anterior hypothalamus from transgenic mice than from control brain sections (Table 2.2). However, synapses which interacted with these stained dendrites were of similar length in transgenic mice and in controls (Table 2.2), demonstrating that unlike *Xenopus laevis* NMJs (Shapira *et al.*, 1994; Seidman *et al.*, 1995) AChE overexpression in the mouse brain did not modify the post-synaptic length of at least some of the cholinergic synapses. In addition, there was no sign of neurofibrillary tangles or amyloid plaques in the analyzed brain sections from mice up to 6 months of age.

Transgenic acetylcholinesterase selectively alters hypothermic drug responses We desired a parameter that measured the physiological involvement of transgenic AChE, and since cholinergic synapses in the anterior hypothalamus, where we had noted AChE overexpression, are involved in thermoregulation (Simpson et al, 1994), we examined hypothermic responses of these transgenic mice to the OP AChE inhibitor paraoxon, the toxic metabolite of the insecticide parathion. Both young and adult transgenic mice were more resistant to paraoxon-induced hypothermia than controls (Fig. 2.3A, B). The transgenic mice were almost totally resistant to a low paraoxon dose (Fig. 2.3A). With higher doses, they displayed limited reduction in body temperature and shorter duration of response, as compared with controls. Most importantly, transgenic mice exposed to 1 mg/kg dose of paraoxon (Fig.

2.3B) retained apparently normal physical activity, while control mice under this dose experienced myoclonia and muscle stiffening, symptoms characteristic of cholinergic overstimulation.

The resistance of these mice with the human ACHE gene to the induction of hypothermia by different agents demonstrated modified functioning of cholinergic synapses which overexpress human AChE. Resistance to paraoxon could be expected, as the amount of its target protein, AChE, was significantly increased in the brain of these mice. However, the resistance to muscarinic, nicotinic and serotonergic agonists reflected secondary changes which affected both cholinergic and serotonergic synapses. These changes were caused, either directly or indirectly, by the transgenic enzyme. Yet, no general alterations occurred in the network of neurons which control thermoregulation, as these transgenic mice retained normal responses to noradrenergic agents and to cold exposure. This suggests loss of specific synapses and/or receptor desensitization as possible causes and indicates the use of cholinergic and serotonergic agonists for early diagnosis of imbalanced cholinergic neurotransmission in human patients.

Transgenic acetylcholinesterase induces an age-dependent decline in spatial learning capacity To examine their cognitive functioning, transgenic and control mice were subjected to several behavioral tests. When compared to sex-matched groups of non-transgenic control mice at the age of 1, 2 to 3 and 5 to 7 months, the AChE-transgenic mice retained normal locomotor and explorative behavior, covering the same space and distance in an open field as did their control counterparts. At the same time the open field anxiety of these mice remained unchanged, as evaluated in the frequency of defecation incidents and grooming behavior (Table 2.3). In contrast, conspicuous behavioral differences were observed in these mice in two versions of the Morris water maze (Morris *et al.*, 1981). A different, age-independent defect was observed in the visible platform version of the Morris water maze, in which mice are trained to escape the swimming task by using short-distance cues to climb on a visible platform decorated by a flag and a paper cone (Morris *et al.*, 1981). The transgenics could not improve their performance in this test through training, regardless of their age (Table 2.3). In either case, the early occurrence of this defect at the age of 4 weeks, when the hidden platform task was still correctly performed by these transgenic mice, demonstrates that the defects in the visual and the hidden platform test were unrelated.

Transgenic acetylcholinesterase induces changes at the neuromuscular junction The long-term contribution of balanced cholinergic neurotransmission toward neuromuscular properties was studied by expressing human acetylcholinesterase (hAChE) in motoneurons, but not muscle, of transgenic mice (Figs. 2.4, 2.5). Spinal cord cholinergic axodendritic synapses in transgenic mice were morphologically normal despite 7-fold higher cytochemical AChE activity as compared with control synapses. In contrast, although muscle extracts included only ca. 6% of hAChE of motoneuron origin, transgenic NMJs were 60% larger than controls and displayed either exaggerated or shortened post-synaptic folds (Fig. 2.6, Table 2.4). Neuromuscular impairment was evident in grip tests at the age of 4 weeks (Fig. 2.7), worsened with age and was accompanied by progressive amyotrophy (Fig. 2.8) and abnormal electrical motor response (Fig. 2.9) which reflected enlarged motor units and junctional dysfunction (Fig. 2.10). The vulnerability of vertebrate NMJs to alterations in cholinergic neurotransmission highlights the morphogenic role of AChE and outlines the cascade of NMJ transformations which lead to neuromotor impairments.

Stress-facilitated changes in electrophysiology induced by pyridostigmine When prophylactically administered during the Gulf War under the threat of chemical warfare, use of the peripherally-acting AChE inhibitor pyridostigmine was unexpectedly associated CNS symptoms. Therefore, we examined pyridostigmine access to brain AChE under stress and investigated the outcome of such access. We found that stress-induced increase in BBB permeability reduces by >100 fold the pyridostigmine dose required to inhibit mouse brain AChE activity by 50% (Fig. 2.11). Furthermore, pyridostigmine directly enhanced electrical excitability and induced transcription of the c-fos oncogene in hippocampal slices *in vitro* (Fig. 2.12). These findings suggest that peripherally acting drugs administered under stress may reach the brain and directly affect centrally controlled functions (Fig. 2.13).

Transgenic BCHE Gene amplification occurs frequently in tumor tissues yet is, in general, non-heritable. To study the molecular mechanisms which confers this restraint, we created transgenic mice carrying a human BCHE coding sequence, previously found to be amplified in a father and a son. Blot hybridization of tail DNA samples revealed somatic transgene amplifications with variable restriction patterns and intensities, suggesting the occurrence of independent amplification events in 31% of mice from the FII generation but only 3.5% of the FIII and FIV generations. In contrast, >10-fold amplifications of the BCHE transgene and the endogenous ACHE and c-raf genes appeared in both testis and epididymis DNA for >80% of FIII mice. Drastic, selective reductions in testis BCHEmRNA were detected by PCR amplification of testis cDNA from transgenic mice, and apparently resulted in the limited transmission of amplified genes.

Table 2.1 Activity of human AChE in mouse tissues.

Tissue	AChE activity* Transgenic Total	Transgenic Anti-AChE†	Control Total	Control Anti-AChE†
Central nervous system				
Basal forebrain	402 ± 25	201	187 ± 30	0
Cortex	283 ± 18	119	235 ± 12	0
Brainstem/cerebellum	95 ± 36	30	88 ± 25	0
Spinal cord	255	82	208	0
Other				
Adrenal gland	25	0	24.6	0
Bone marrow	13.4 ± 0.3	0	17.1 ± 2.3	0

*Catalytic activities (nmol acetylthiocholine hydrolyzed min^{-1} mg $protein^{-1}$) were determined for detergent-solubilized homogenates. Values are averages of three experiments ± standard deviation, except for spinal cord and adrenal gland where single experiments are presented. †Activity after binding to monoclonal antibodies specific for human AChE.

Table 2.2 AChE overexpression does not modify the length of axo-dendritic synapses in the anterior hypothalamus of transgenic mice.

Parameters	Control	Transgenic	p*
Number of synapses	32	12	–
Electron-dense deposits‡	3.4 ± 3.2	6.5 ± 4.0	$p < 0.02$
Post-synaptic length§	0.8 ± 0.3	0.7 ± 0.2	NS

*Significance was verified by the Student's t test. NS = not significant.

Average values ± standard deviations are presented. ‡Number of dendritic electron-dense deposits per μm^2. Only deposits with rigid limits, reflecting crystal structures, were counted. §Post-synaptic length was measured, in µm, only for those synapses associated with AChE reaction products (that is, cholinergic synapses).

Table 2.3. Selective behavioural deficits in AChE-transgenic mice.

Behavioural parameter	Age (months) One Transgenic	One Control	Two Transgenic	Two Control	Five to eleven Transgenic	Five to eleven Control
Water maze*						
Visual test	33.8 ± 25.0	6.7 ± 1.8	22.5 ± 14.8	5.3 ± 2.2	33.3 ± 12.2	7.3 ± 3.9
Hidden platform test	17.3 ± 12.5	8.7 ± 3.5	26.4 ± 21.3	14.0 ± 3.5	49.1 ± 27.8	20.5 ± 18.2
Explorative behaviour						
Space explored	51.4 ± 19.7	40.3 ± 29.8	62.5 ± 33.6	43.7 ± 21.7	51.5 ± 17.2	54.1 ± 19.4
Distance walked	11.2 ± 5.1	10.4 ± 8.5	15.9 ± 9.6	11.0 ± 5.4	13.0 ± 5.0	12.2 ± 3.5
Open field anxiety‡						
Defecation	1.0 ± 0.6	0.6 ± 0.5	0.1 ± 0.4	0.5 ± 0.8	0.8 ± 0.4	0.4 ± 0.5
Grooming	1.7 ± 1.0	0.6 ± 1.0	1.7 ± 1.0	1.0 ± 0.9	1.3 ± 1.0	1.2 ± 1.3

*Average escape latencies (seconds) ± standard deviations at day 4 of a Morris water maze test. Explorative behaviour in the open field test was evaluated by measuring the percentage of open field space explored out of 0.36 m^2 and the distance covered (metres) in 5 minutes. Note that there is no significant difference for both parameters between transgenics and controls. ‡In the same 5 minute period, the number of defecation and grooming events, accepted signs of open field anxiety, were noted.

Table 2.4 Morphometric parameters of hAChE-expressing cholinergic synapses[a]

A. Anterior spinal cord axo-dendritic synapses				
Parameter	**Control**		**Transgenic**	
axon minimal diameter, μm	0.93 ± 0.34	(40)	0.74 ± 0.28	(44)
axonic mitochondria area, μm²	0.23 ± 0.13	(37)	0.19 ± 0.1	(31)
dendrite minimal diameter, μm	2.44 ± 2.3	(20)	1.61 ± 0.9	(15)
dendritic mitochondria area, μm	0.52 ± 0.52	(19)	0.35 ± 0.21	(13)
AChE stained area, μm⁻	0.05 ± 0.04	(43)	0.34 ± 0.90 P<0.03	(47)
space occupied by vesicles, μm²	0.47 ± 0.3	(37)	0.39 ± 0.29	(44)
vesicles No/μ⁻	95.8 ± 33.9	(16)	107.9 ± 27.9	(16)

B. Neuromuscular junctions				
Parameter	**Control**		**Transgenic**	
AChE stained area, μm⁻	398 ± 136.4	(90)	625.6 ± 227.7 P<0.001	(100)
End plate methylene blue stained area, μm²	301 ± 92.1	(38)	723.7 ± 495.3 P< 0.001	(33)
Vesicles, number/μ⁻	122.5±30.7	(12)	161.4±41.8 P< 0.02	(9)
Mean length of post-synaptic folds/μm NMJ	0.56 ± 0.12	(14)	0.65 ± 0.37	(16)
Muscle fiber diameter, μm	30.8 ± 7.45	(69)	35.6 ± 5.17	(7.5)

[a]Morphometric parameters were determined under visual or electron microscopy for the numbers noted in parentheses of axo-dendritic cholinergic synapses from the anterior spinal cord of at least 5 adult control and transgenic mice (A) and of the noted numbers of NMJs (B1-3) or analysed folds (B4-6) from the gastronemius muscle of control and transgenic mice. Statistical significance (Student's test) is noted wherever relevant.

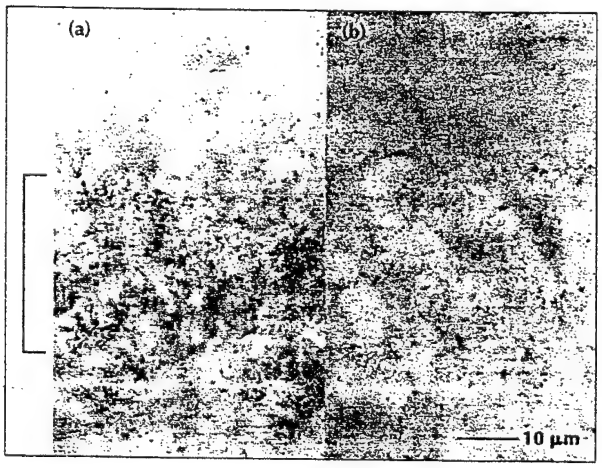

Fig. 2.2 . Expression of transgenic *Hp-ACHE* mRNA in mouse brain neurons. Whole-mount *in situ* hybridizations were performed on fixed brain sections from (a) transgenic and (b) control mice. CA1 hippocampal neurons (bracketed) were intensely labelled in the transgenic, but not the control, section.

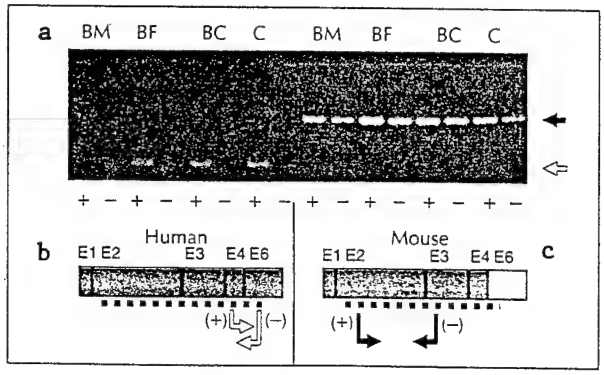

Fig. 2.1 Identification of human *ACHE* mRNA. RNA was extracted and amplified from transgenic (+) and control (–) mouse cortex (C), brainstem and cerebellum (BC), basal forebrain (BF) and bone marrow (BM). Species-specific PCR primers were designed for the indicated positions within the open reading frame (dotted underline) on the schemes above.
Resultant PCR products (276 and 786 bp, respectively) were electrophoresed on agarose gels. Note that expression of human *ACHE* mRNA was limited to the central nervous system.

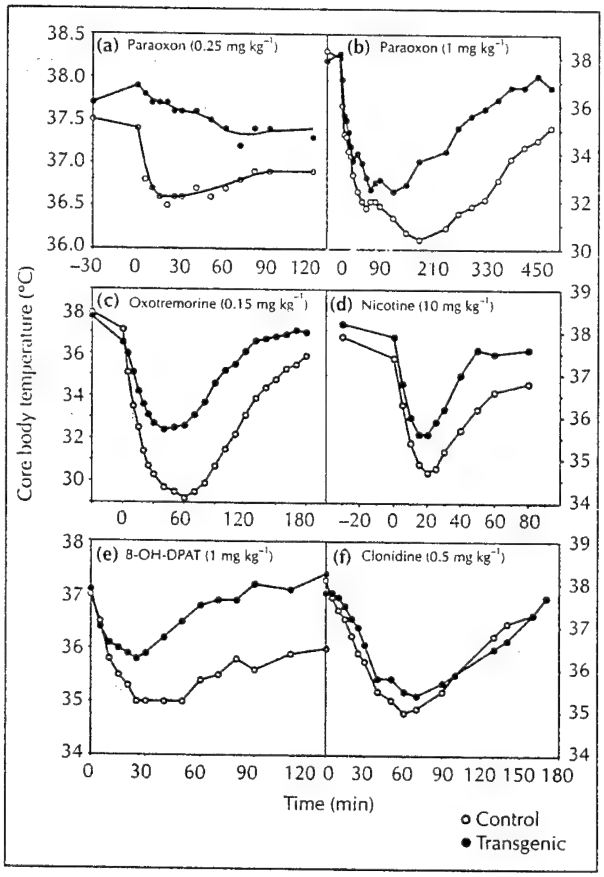

Fig. 2.3 Transgenic mice display reduced hypothermic responses to cholinergic and serotonergic, but not adrenergic, agonists. Core body temperature was measured in control and transgenic mice, five–seven months old, at the noted times, after intraperitoneal injections of the marked doses of (a,b) paraoxon, (c) oxotremorine, (d) nicotine, (e) tetralin (8-OH-DPAT) or (f) clonidine. Presented are average data for (a,f) five or (c–e) four male and female mice, or (b) one representative pair out of three tested. Note different time and temperature scales. Temperatures of transgenic mice at all time points after 10 min from injection were statistically different from those of controls for oxotremorine, nicotine and 8-OH-DPAT (Student's t test, $p < 0.05$).

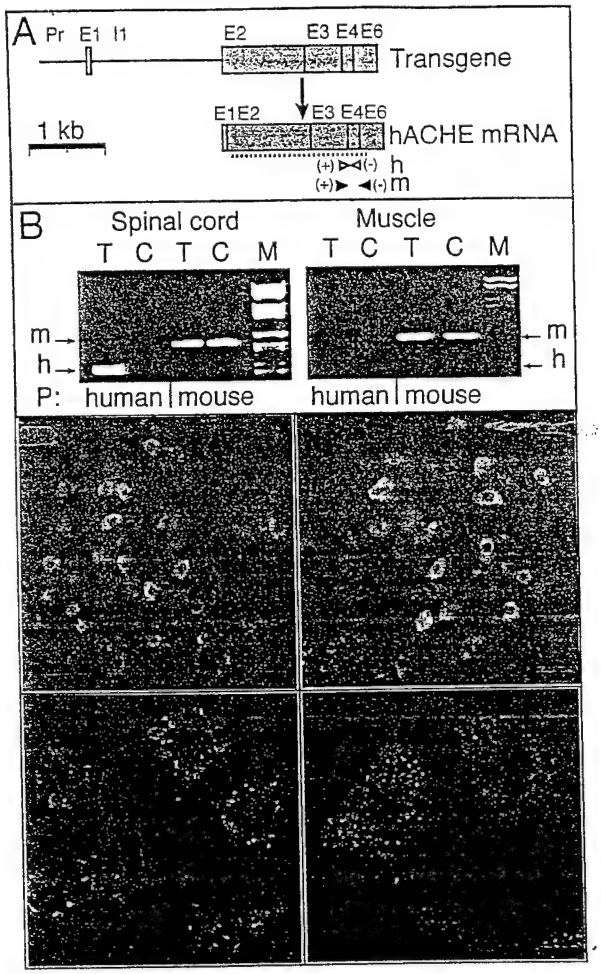

Figure 2.4: The hACHE DNA transgene is expressed in spinal cord neurons but not in muscle.
A: Scheme of the human ACHE transgene. Exons (E) are represented by boxes. I=Intron, Pr=Promoter. Open reading frame (dotted underline) initiates at exon 2. Because of species differences, it was possible to distinguish between human and mouse ACHEmRNA by RT-PCR. Species-specific primers between the regions noted by arrows yielded the following expected RT-PCR products: h, human-specific, m, mouse-specific. + and - signs denote primer orientations.
B: PCR products. RT-PCR products of the sizes expected for human (h) and mouse-specific (m) ACHEcDNA were obtained from spinal cord (left) and striated muscle (right) RNA and were electrophoresed on agarose gels. T = transgenic, C = control, M = molecular weight marker. P=primer type. Note that no expression of hACHE mRNA could be detected in muscle.
C-F: ACHE mRNA expression in both control and transgenic spinal cord is limited to neurons. Wholemount *in situ* hybridization was performed on sections of cervical spinal cords from transgenic and control animals, using a 5í-biotinylated 2-0-methylated 50-mer ACHEcRNA probe. Detection was with a fluorogenic substrate for streptavidin-conjugated alkaline phosphatase. Presented are low magnification micrographs of transgenic (C) and control (D) anterior cervical spinal cord sections, as well as high magnification of ACHEmRNA labeling in motorneurons (E) and smaller, presumably interneurons (F) from the spinal cord of control mice. Size bars equal 100 and 10 µm, respectively for C,D and E,F.

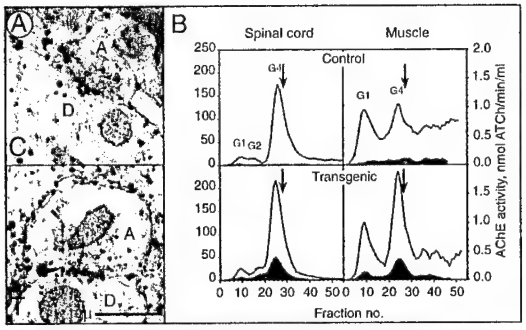

Figure 2.5: Transgenic AChE accumulates in spinal cord synapses and reaches muscle.
A: AChE overexpression in axo-dendritic synapses from anterior spinal cord of transgenic mice. Electron micrographs are presented for 80 nm sections of paraformaldehyde-glutaraldehyde fixed spinal cord from transgenic (T) and control (C) mice. Acetylthiocholine hydrolysis products appear as dark crystals, particularly conspicuous in the synaptic cleft between axons (A) and dendrites (D). Size bar equals 10 µm.
B: Transgenic spinal cord human AChE is found in muscle homogenates. Detergent-soluble homogenates of spinal cord and muscle were fractionated by sucrose gradient centrifugation and AChE activity determined prior to (line) or after binding to a specific anti-human AChE monoclonal antibody (shaded area) (Seidman et al., 1995). Note the different activity scales for spinal cord and muscle. Arrows denote sedimentation of an internal marker, bovine catalase (11.4 S). Activity peaks reflecting globular monomers, dimers and tetramers are labeled G1, G2 and G4, respectively with the top of each tube at the left handside.

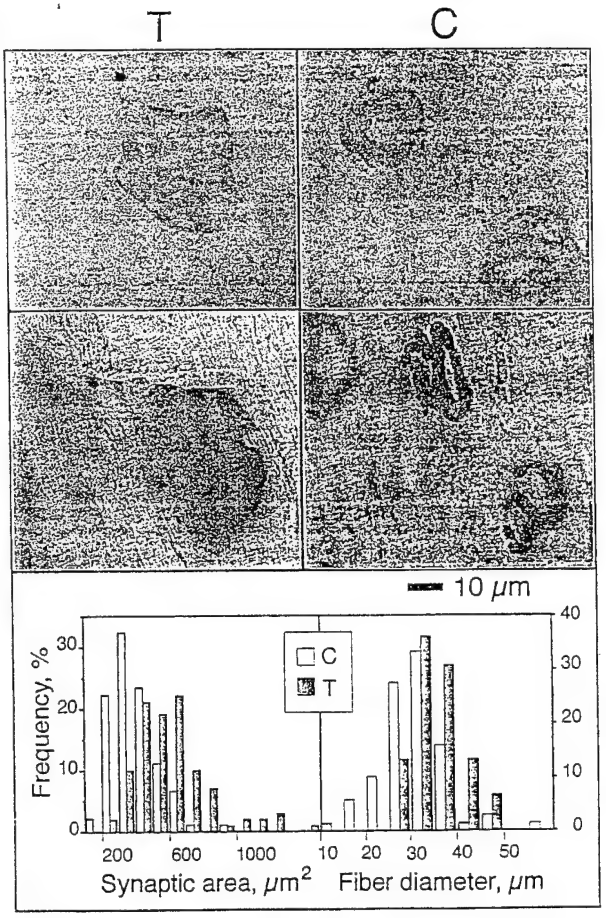

Fig. 2.6: Enlargement and shape modifications in diaphragm neuromuscular junctions of transgenic animals.
Top: Synapse stainings. Wholemount cytochemical staining of AChE activity was performed on fixed diaphragms of 4 month old control (C) and transgenic (T) animals. Note weaker AChE staining and larger circumference and elipsoid, fading boundaries of transgenic NMJs as compared with the complex, sharp contours in controls. Two representative diaphragms out of 12 control and 12 transgenic ones.
Center: Similarly fixed diaphragms stained with 0.1% methylene blue to reveal protein density.
Bottom: Distribution analyses. Left: Area stained by AChE reaction product, in μm^2 (for 90 control, 100 transgenic terminals). Right: Muscle fiber diameter, in μm (for 69 control, 75 transgenic fibers). Note the upward shift in distribution of both parameters for transgenic as compared with control mice.

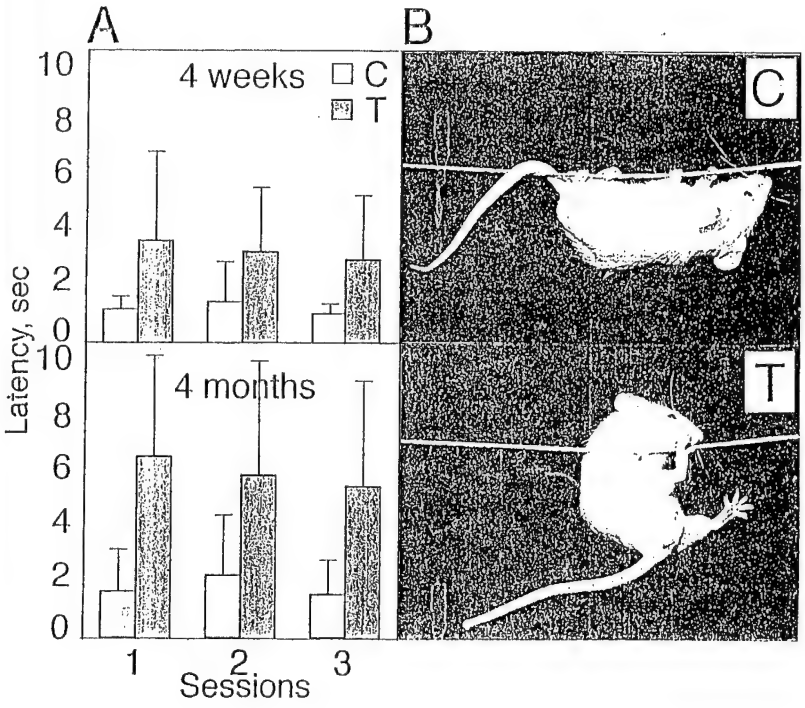

Figure 2.7: Motor function impairments appear early and worsen with age.
A: Muscle strength impairment. Rope-grip tests were performed thrice at 1 min intervals for groups of 4 week (top) and 4 month (bottom) old transgenic (T, n = 5 & 7 for top and bottom figures respectively) and control (C, n = 5 & 10) mice. Noted are escape latency values in sec. ± SD. Note the slower performance of transgenics as compared with controls at both age groups and the worsening of this phenotype with age.
B: Trunk and hindlegs weakening. Mice were suspended with their forelegs on a 3 mm diameter rope and their ability to grip the rope with their hindlegs was noted. Presented are a 4 months old control mouse, 3 sec following test initiation (C), and a matched transgenic mouse (T), whose hindlegs, trunk and tail postures are clearly abnormal. This mouse fell off the rope 5 sec after this photograph was taken.

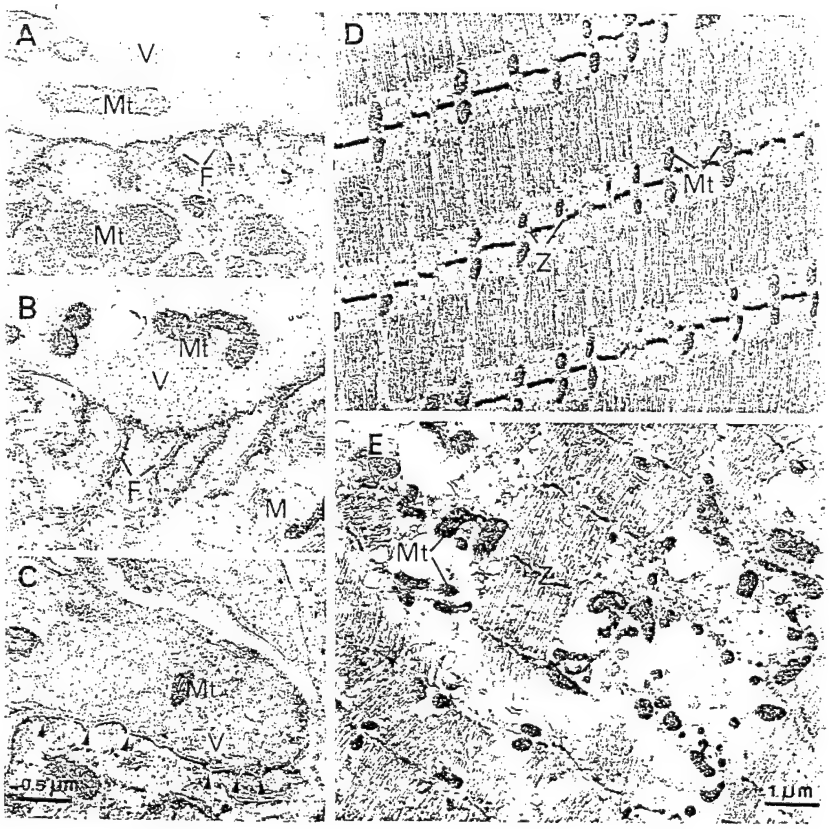

Figure 2.8: Various NMJ deformities and amyotrophy in transgenic mice.
Electron microscopy of 80 nm sections of terminal diaphragm zones was performed following AChE activity staining for 10 min. Note the exaggerated post-synaptic folds (F, panels A,B) as well as the short, undeveloped folds marked by arrowheads (C) in transgenic NMJs as compared with controls (A). V = vesicles. Muscle fiber amyotrophy, loss of muscle fiber organization and swelling of mitochondria (Mt) at disrupted Z bands (Z) is shown for transgenic (E) as compared with control muscle (D).

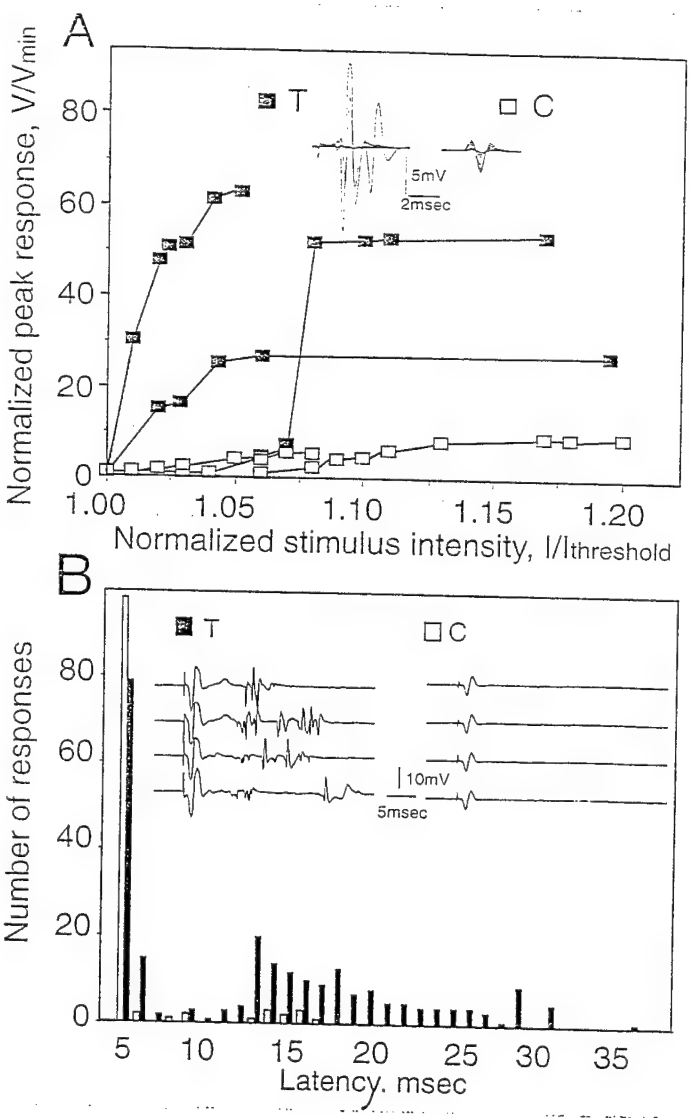

Figure 2.9: Transgene-induced electromyographic abnormalities.
Electromyographic recordings were taken from the gastrocremius muscle in response to stimulation of the sciatic nerve.
A: Motor units enlargement. Evoked muscle fiber potentials following sciatic nerve stimulation were recorded by a microelectrode placed on the surface of the gastrocnemius muscle in 3 transgenic (filled squares) and 3 control (empty squares) mice. In control animals, a small increase in stimulus intensity induced small and gradual increases in the amplitude of the muscleís compound action potential. Supramaximal response amplitudes were up to 10-fold greater than the threshold response. In transgenic animals, parallel increases in stimulus intensity triggered considerably larger jumps in the amplitude of the action potentials.
Inset. Superposition of responses evoked by increasing stimulus intensity up to 1.0 mA at 1 Hz as in the enclosed scale. Saturation of response occurred only at high stimulus intensities and required more stimuli in transgenics than in controls. Note that in the transgenic muscle several negative peaks were observed in response to a single stimulus.
B: Latencies of evoked spikes. Delayed repetitive firing of action potentials was frequently recorded in 4 transgenic muscles but only rarely in 4 controls. Following 100 supramaximal stimulations at 1 Hz, abnormal late potentials (filled bars) appeared in transgenic animals for up to 40 msec post-stimulation as compared with a few signals in control animals (empty bars). Presented are numbers of response spikes as a function of latency time for 10 different measurements.

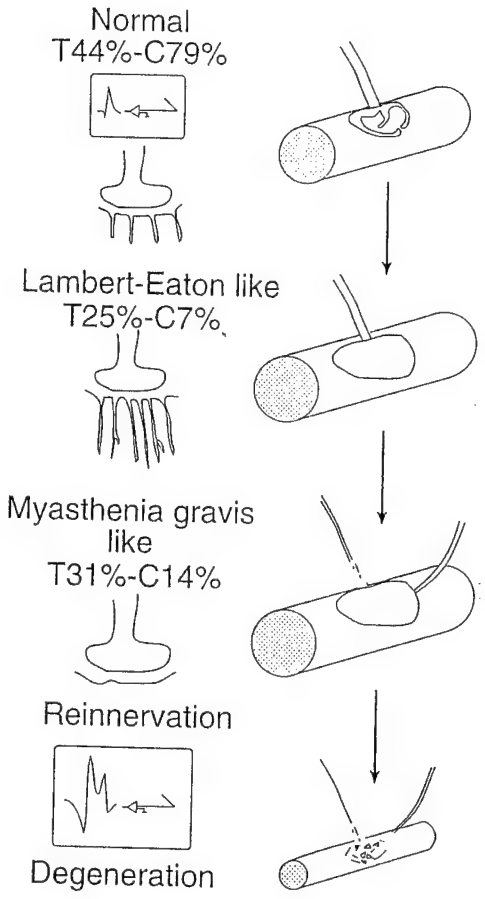

Fig. 2.10: Transgenic hAChE induces two distinct phenotypes in neuromuscular junctions.
The putative course of events which results from AChE overexpression in motorneurons is presented schematically for a series of single muscle fibers (right-hand side) and a series of NMJs (left-hand side). Normal NMJs (top panel) should be pretzel-shaped, create a characteristic electromyographical pattern, presented in the top inset, and possess average size, non-branched post-synaptic folds. Abnormal NMJs with exaggerated folds, similar to those occurring in the Eaton-Lambert syndrome (second panel) as well as NMJs with degenerated folds, ressembling those characteristic of myasthenia gravis (third panel) appeared more frequently in transgenic than in control mice. The percent of analyzed NMJs which presented distinct types of post-synaptic folds in transgenic (T) and control (C) mice are shown for each category. Reinnervation created the abnormal electromyographic response observed in transgenic mice (bottom inset). Finally, degeneration occurred.

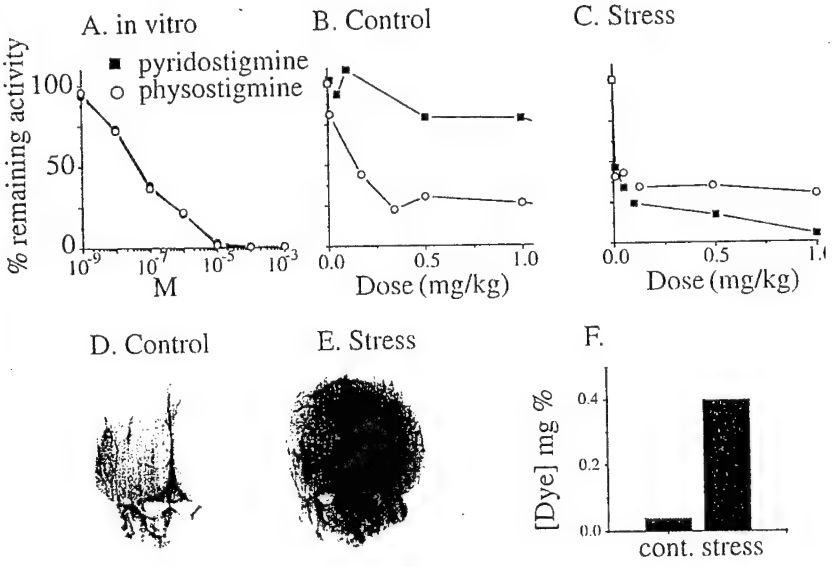

Fig. 2.11: Stress intensifies AChE inhibition by pyridostigmine due to increased BBB permeability.
A: AChE inhibition in brain homogenates. Acetylthiocholine hydrolysis was measured following addition of increasing concentrations of pyridostigmine (filled squares) or physostigmine (empty circles) to brain homogenates from control animals. Presented are percent activities as compared with those of brain homogenates with no added drug.
B: Inhibiting brain AChE activity by drug injection. Percent of normal specific cortical AChE activity was measured in brain homogenates prepared from non-stressed animals sacrificed 10 min following injection of the noted doses of physostigmine (n=9) or pyridostigmine (n=11) in non-stressed animals. Presented are percent activities as compared with those of brain homogenates from non-stressed, 0.9% NaCl injected animals (n=12).
C: Pyridostigmine inhibition of brain AChE following stress. Swim forced test was followed 10 min later by injection of either 0.1 mg/kg pyridostigmine (n=8), or physostigmine (n=5). AChE activity measurments were as under B. Presented are percent activities as compared with those of brain homogenates from similarly stressed, 0.9% NaCl injected animals (n=6).
D-E: BBB permeability following stress, shown are representative brains dissected from anaesthetized animals, 10 min following the intracardial injection of Evans-blue. D: control animal, E: 10 min following stress session.
F: Spectrophotometric evaluation of dye concentration in brain homogenates.

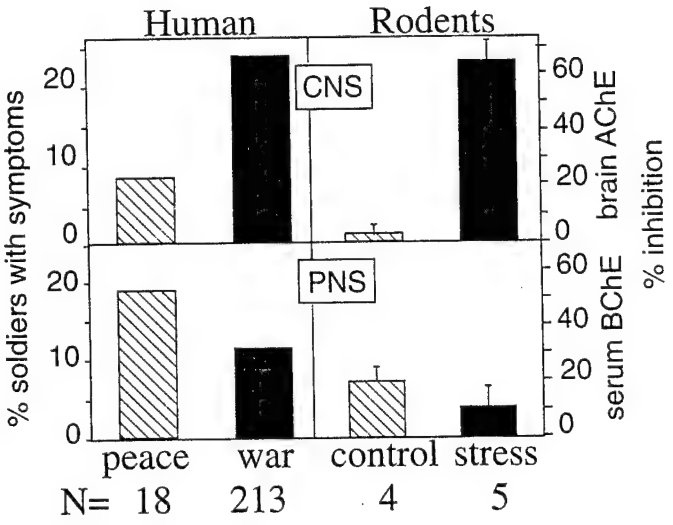

Fig. 2.12: Pyridostigmine enhances neuronal excitability and increases oncogene mRNA levels.
A: The kinetics of brain c-fos cDNA accumulation during RT-PCR amplification. Total RNA from hippocampus dissected from mice was extracted using RNAclean (AGS, Heidelberg, Germany), its integrity verified by gel elctrophoresis (ratio of 2.0 between between 28 S and 18 S ribosomal RNA) and its quantity and purity from proteins evaluated by a ratio of 1.8-2.0 of A_{260} to A_{280} nm. c-fos cDNA was amplified following reverse transcription of similar RNA samples from the brain of control or stressed animals. PCR product samples were withdrawn every third cycle, which allows for 8-fold increases between samples. The earlier appearance in PCR cycle number of amplified c-fos-cDNA 20 min following injection of 2 mg/kg pyridostigmine (+) as compared to 0.9% NaCl (-) indicates >100-fold increases in the amount of c-fos mRNA under stress.
B: Extracellular evoked potentials. Cortico-hippocampal slices (400 mm thick) were cut using a vibratome (Vibroslice, Campden Instruments, Loughborough, UK.), and were placed in a humidified holding chamber, continuously perfused with oxygenated (95% O_2, 5% CO_2) artificial cerebrospinal fluid (aCSF). Schaffer collateral fibers were stimulated with a bipolar tungsten stimulating electrode and extracellular evoked potentials were recorded in the cell-body layer of the CA1 area of the hippocampus. Single response to supramaximal stimulus intensity (1.5 times stimulus the intensity of which caused maximal response) is drawn before (-) and 30 min following (+) addition of pyridostigmine (1 mM) to the perfusing solution.

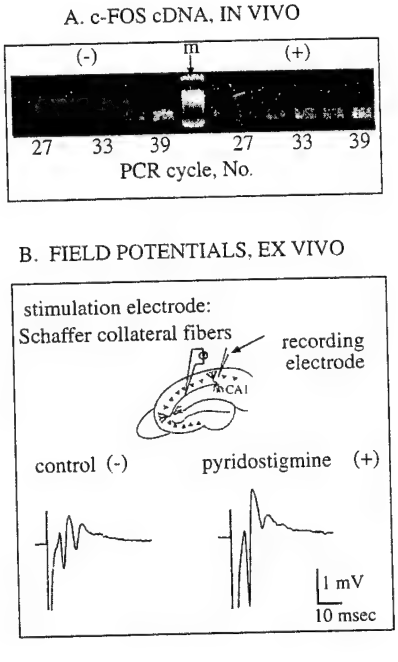

Fig. 2.13: Pyridostigmine effects in humans during peace and war time and in non-stressed and stressed rodents
Left panels (humans): Results of a double blind, placebo controlled study (extension of Glickson et al., 1991) (dashed bars, "peace"). Pyridostigmine (n=18) or placebo (n=17) were administered to young healthy males volunteers. Symptoms were reported at the end of the study. Presented are percentages of soldiers reporting pyridostigmine-induced symptoms related to CNS (top) or PNS (bottom panel). During the Gulf war 213 male soldiers aged 18-22 years were questioned, 24 h after initiation of pyridostigmine treatment (filled bars). Mean values for human data are marked by horizontal lines across the relevant bars.
Right panels (rodents): summary of measured brain AChE inhibition (top) and serum BChE inhibition in mice (bottom) 10 min following injection of 0.1 mg/kg pyridostigmine in non-stressed (control, n=4), and stressed (n=5) mice. Percent inhibition and standard deviation was calculated in comparison to the average activity calculated in non-injected, not-stressed (n=12) and stressed (n=6) animals.

3. *In vitro* studies of organophosphorus and carbamate interactions with acetylcholinesterase and butyrylcholinesterase

Detailed dissection of catalysis by any natural or recombinant ChE variant (Neville *et al.*, 1992; Ordentlich *et al.*, 1993; Soreq and Zakut, 1993; Vellom et al, 1993) should attempt to discriminate among effects on one or another of the several stages of catalysis. As the slowest stage has a half-time on the order of 100 μs (Gilson et al, 1994; Quinn, 1987; Rosenberry, 1975), we have recruited the inactivation of ChEs by an OP (Taylor, 1990) as an analogous reaction in order to study in isolation each of the first two stages (Fig. 3.1A). Cleavage of the phosphoryl-ChE bond is extremely slow, making OPs hemi-substrate inhibitors, but the rate of dephosphorylation can be enhanced by PAM (Fig. 3.1B) (Wilson, 1954), a rigid zwitterionic molecule that juxtaposes its nucleophilic group precisely against the phosphoryl bond, which it displaces. To analyze catalysis on a micro scale and to avoid interference with rate measurements by inactivating or reactivating reagents, we immobilized recombinant *Xenopus* oocyte-produced variant ChEs on selective monoclonal antibodies in multi-well plates and subjected the bound enzymes to successive OP inactivation and oxime-promoted reactivation. By this approach we measured major changes in rates of the reaction with DFP and PAM (Fig. 3.1B) for a large series of human ChE variants which differed within the gorge lining, the acyl-binding site or the C-terminus, always by comparison to the wild-type enzyme forms.

Spatiotemporal dissociation of catalytic steps We collected rate constants for each of the two recombinant human enzymes as produced in microinjected *Xenopus* oocytes from the corresponding cloned *in vitro*-transcribed mRNA (Neville *et al.*, 1992) or cDNA (Seidman *et al.*, 1994). We also examined a chimera in which the gorge rim, the gorge lining, the conserved oxyanion hole and the choline-binding site of BuChE were substituted with the homologous peptide of AChE (Loewenstein *et al.*, 1993). To test whether variations in the C-terminus (Soreq and Zakut, 1993) would affect catalytic properties of isolated, immobilized ChEs, we used ACHEcDNA vectors, including a vector which encoded the major form of human AChE expressed in brain and muscle (Soreq *et al.*, 1990), and designated E6, and an alternative vector, differing in the 3'-terminus and which represented the variant ACHEmRNA species expressed in hematopoietic and tumor cells (E5) (Karpel *et al.*, 1994). Several natural and site-directed mutants of recombinant human BuChE completed this series. Each of the recombinant, immobilized enzyme variants was reacted with DFP, followed by regeneration of activity by PAM. The enzymes were enriched by adsorption onto an immobilized antibody (Liao et al, 1993; Seidman *et al.*, 1994). ELISA measurements provided determinations of the amounts of recombinant proteins for evaluation of k_{cat} values.

The gorge lining contributes to enzyme phosphorylation Rates of DFP inactivation were determined for normal BuChE, the chimera and a series of site-directed and natural mutants, as compared with the two alternative forms of AChE (Fig. 3.2A, Table 3.1). The second order rate constant for inactivation of AChE by DFP was found to be 160-fold lower than that of BuChE. Introduction of a positive charge into the acyl-binding site of the L286K mutant slowed the inactivation rate of BuChE approximately 8-fold (Table 3.1). In contrast, substitution of the gorge lining by the corresponding AChE peptide, reduced this rate 60-fold. In general, inactivation rates of natural BuChE mutants were not severely affected.

Active site charges hamper reactivation The same series of enzymes was further assessed for rates of reactivation. The Kd for DIP-BuChE, 0.3 mM, was close to the value of 0.2 mM found for purified diethylphosphoryl-BuChE (Vellom *et al.*, 1993). The pseudo-first order rate constant for reactivation of DFP-inhibited BuChE (Table 3.1) was 25-fold higher than for either form of AChE (Fig. 3.2B and Table 3.1). The chimera displayed a reactivation constant only moderately lower than that of native BuChE. This lower rate for AChE and the chimera was due to a lower true first-order rate constant, as the affinity for PAM remained unchanged (Table 3.2). In contrast, the BuChE L286K mutant displayed a 40-fold reduction in the pseudo-first order rate constant for reactivation, reflecting a reduction in both reactivation rate and affinity for PAM. This emphasizes the importance of the acyl-binding site in the

reactivation process. We further substituted an acidic, a basic, a sulfhydryl and a polar group for F329. Of these, only the sulfhydryl and acidic groups disrupted the reactivation (Table 3.1). For the natural BuChE variants, effects of D70G and Y144H on reactivation were cumulative.

C-terminal variations are innocuous in catalytic terms Both alternative ACHE DNA forms led to enzymes with similar inactivation rates (Fig. 3.2A and Table 3.1), which demonstrates that the natural variability in the C-terminus of AChE contributes to the inactivation rate far less than differences in the acyl-binding site and gorge lining of ChEs.

Effects of variations on kcat The consequences of each variation were further evaluated by determining turnover numbers (kcat, Table 3.2). Effects on kcat in the various mutants were not cumulations of effects on inactivation rate constant and reactivation rate constant, nor are they expected to be, as only the slowest step will be reflected in the catalytic rate. Thus, substitution of L286 with a basic residue reduced reactivation 40-fold but led to only a 5-fold reduction in kcat (Table 3.1). Other replacements at this position, and substitution of the gorge lining in the chimera, had considerably smaller effects on this value.

We chose to focus on three peptide regions of the human ChE molecules: (a) the gorge lining, (b) the acyl-binding site, and (c) the C-terminal peptide in AChE. We found the reactivity of AChE toward DFP to be remarkably lower than that of BuChE, in spite of the close similarity of these two enzymes; our use of the "atypical" and the chimeric enzyme suggested that aromatic gorge-lining residues, especially residues Y72 and Y124, which participate in the peripheral anionic site (Shafferman *et al.*, 1992) contribute significantly to this difference. Even OP agents that are, unlike DFP, designed as anti-AChE poisons, inactivate BuChE and AChE at similar rates (Raveh *et al.*, 1993), suggesting a special vulnerability of BuChE to OPs. Even in the case of those anti-AChEs, BuChE, with a larger binding site, acts as a scavenger to protect AChE (Raveh *et al.*, 1993). The strikingly lower inactivation rate of the chimera than that of BuChE may be attributable to its having its active site gorge narrowed by numerous aromatic residues. (The chimera's acyl binding site is unchanged.) For the L286K mutation, both inactivation and reactivation are affected. Introduction of a positive charge at the acyl biding site, and possibly also tightly bound water molecules, may disrupt both phases of the reaction. The capacity of AChE to hydrolyze the disfavored substrate, butyrylthiocholine, is reduced to 1/30th the rate of BuChE. The accessibility of BuChE as a serum enzyme raises the possibility that PAM acts by regenerating BuChE and allowing it to react with more of the OP before the OP has a chance to inactivate neuromuscular AChE, in effect turning serum BuChE into an OPase. A finding with important consequences for dealing with OP poisoning is that D70G, by far the most common of the phenotypically different BuChE variants (Whittaker, 1986) reacts with DFP as fast as the normal enzyme, but is reactivated by PAM at only one-fifth the rate. Since D70G also has a 4-fold lower specific activity, than the wild type enzyme (Neville *et al.*, 1990 and unpublished observations), D70G BuChE will have less detoxifying capacity to protect OP-poisoned individuals than its normal counterpart. Moreover, when intravenous PAM administration, in conjunction with other therapies, is used to treat OP intoxication (Taylor, 1990), carriers of D70G BuChE will have a genetic predisposition to poor responses to such therapy. This applies to "atypical" homozygotes, as well as heterozygotes, who together compose up to 7.5% of some populations (Ehrlich *et al.*, 1994). Thus, the recently reported variable efficacy of PAM treatment (Willems *et al.*, 1993) may be due to genetic diversity in the treated patients. Individual differences may further be expected in the sensitivity to poisoning by therapeutic anti-ChEs, such as those used in Alzheimer's disease (Knapp et al;, 1994). Natural anti-ChEs, such as glyco-alkaloids in *Solanum* plants (Neville *et al.*, 1992) and neurotoxins excreted by cyanobacteria (Carmichael, 1994) may also have anomalous effects on these individuals.

Interaction sites on butyrylcholinesterase BuChE limits the access of drugs, including tacrine, to other proteins. The "atypical" BuChE variant, in which aspartate 70 at the rim of the active site gorge is substituted by glycine, displayed a more drastically weakened interaction with tacrine than with cocaine, dibucaine, succinylcholine, BW284c51 (1,5-bis(4-allyldimethylammoniumphenyl)pentan-3-one dibromide) or α-solanine. To delineate the protein

domains that are responsible for this phenomenon, we mutated residues within the rim of the active site gorge, the region parallel to the peripheral site in the homologous enzyme AChE, the oxyanion hole and the choline-binding site. When expressed in microinjected *Xenopus* oocytes, all mutant DNAs yielded comparable amounts of immunoreactive protein products. Most mutants retained catalytic activity close to that of wild-type BuChE and were capable of binding ligands (Fig. 3.3, Table 3.3). However, certain modifications in and around the oxyanion hole caused dramatic loss in activity. The affinities for tacrine were reduced more dramatically than for all other ligands, including cocaine, in both oxyanion hole and choline-binding site mutants. Modified ligand affinities further demonstrated a peripheral site in residues homologous with those of AChE. BuChE mutations which prevented tacrine interactions also hampered its ability to bind other drugs and inhibitors, which suggests a partial overlap of the binding sites (Fig. 3.4). This predicts that in addition to their genetic predisposition to adverse responses to tacrine, homozygous carriers of "atypical" BuChE will be overly sensitive to additional anti-ChEs, and especially so when exposed to several anti-ChEs in combination.

Table 3.1
Kinetic rate constants for DFP-inactivation, PAM-reactivation and catalysis of cholinesterases [a]

Variant	$k_i \times 10^{-4}$ (M^{-1} min^{-1})	$k'_r \times 10^3$ (min^{-1})	$k_{cat} 10^{-3}$ (min^{-1})
BuChE	1220 ± 4 (3)	150 ± 30 (11)	96 ± 22 (6)
Chimera	19 ± 8 (2)	40 ± 18 (6)	36 ± 14 (5)
AChE (E6)	7 ± 1 (4)	6 ± 2 (3)	7.5 [c]
AChE (E5)	5 (1)	8 ± 3 (2)	
$L^{286}D$	188 ± 24 (3)	120 ± 30 (3)	38 ± 15 (5)
$L^{286}Q$	166 ± 40 (3)	120 ± 20 (4)	42 ± 24 (5)
$L^{286}R$	268 ± 164 (3)	6 ± 3 (3)	13 ± 7 (5)
$L^{286}K$	138 ± 4 (3)	4 ± 1 (3)	13 ± 5 (4)
$F^{329}R$		43 (1)	
$F^{329}Q$	1398 ± 532 (3)	44 ± 15 (5)	
$F^{329}C$	552 ± 408 (2)	14 ± 2 (4)	
$F^{329}D$	442 ± 190 (3)	8 ± 1 (4)	
$S^{425}P$ [b]	1054 ± 408 (3)	134 ± 8 (4)	
$D^{70}G$ [b]	1008 ± 418 (3)	32 ± 4 (4)	
$D^{70}G + Y^{114}H$ [b]	2112 ± 1074 (3)	12 ± 5 (3)	
$D^{70}G + S^{425}P$ [b]	260 ± 12 (2)	11 (1)	
$D^{70}G + Y^{114}H + S^{425}P$ [b]	1598 ± 294 (3)	4 ± 1 (3)	

[a] Second order rate constants for inhibition (k_i) were calculated for each of the noted variants of human ChEs from rates observed between 1 nM and 1 μM DFP. Pseudo-first order rate constants for reactivation (k'_r) were calculated from rates observed at 1 mM PAM. k_{cat} values were calculated from the rates of reaction with 30 mM butyrylthiocholine and the quantity of enzyme evaluated by ELISA assay of the enzyme, using known amounts of human serum BuChE to construct a standard curve. Numbers of experiments, in parentheses, and standard deviations are shown.

[b] Natural variant of BuChE.

Table 3.2
Constants for PAM reactivation of DIP-ChEs [a]

Variant	$k_r \times 10^3$ (min^{-1})	K_d (mM)
BuChE	220 ± 60 (4)	0.30 ± 0.08
Chimera	48 ± 20 (3)	0.34 ± 0.13
AChE (E6)	7 ± 3 (3)	0.27 ± 0.04
AChE (E5)	10 ± 5 (2)	0.19 ± 0.07
$L^{286}K$	35 ± 27 (3)	> 5

[a] True first order rate constants for reactivation (k_r) and dissociation constants for the DIP-enzyme/PAM complex (K_d) were evaluated from a plot of the reciprocals of the pseudo-first order rate constants vs. the reciprocals of PAM concentrations between 0.1 and 0.6 mM. Numbers of experiments, in parentheses, and standard deviations are shown.

Table 3.3. Kinetic properties of variant butyrylcholinesterases: Km and Ki values[a]

		Km	Ki					
variant/mutation		(mM)	tacrine (μM)	succinylcholine (mM)	dibucaine (μM)	α-solanine (μM)	BW284c51 (μM)	cocaine (mM)
normal	BuChE	2.8± 0.7	0.06± 0.03	4.0 ± 2.6	6.9± 4.6	3.3 ± 2.8	480 ± 110	0.39± 0.03
"atypical"	D70G	3.8± 0.4	9.1 ± 2.4	52 ± 13	182 ± 100	78.0 ± 2.5	2540	3.2 ± 0.1
peripheral site	N68D	1.1± 0.4	0.03± 0.01	0.26± 0.05	10.0± 0.2	1.26± 0.05	18	n.d.
	" K	2.5± 1.1	0.01± 0.005	4.3 ± 0.6	17 ± 6	3.7 ± 1.3	>700	0.43± 0.0
	" R	4.6± 1.	0.06± 0.03	11.2 ± 0.7	4.3± 0.9	6.5 ± 3.3	>800	0.20± 0.07
	" Y	3.4± 2.	0.04± 0.02	2.9 ± 0.9	39 ± 2	0.5 ± 0.3	112 ± 50	n.d.
	" A	1.1± 0.6	0.04± 0 03	0.7 ± 0.3	10 ± 6	0.7 ± 0.2	179 ± 91	n.d.
	Q119A	1.2± 0.6	0.02± 0.01	0.6 ± 0.2	20 ± 9	0.4 ± 0.1	68 ± 10	n.d.
	" E	0.6± 0.2	0.03± 0.03	0.12± 0.06	28.5± 5.0	0.28± 0.11	25.9± 4.6	n.d.
	" G	1. ± 0.1	0.04± 0.03	0.7 ± 0.3	26.2± 2.3	0.23± 0.18	95 ± 16	n.d.
	" H	0.7± 0.1	0.01± 0.003	0.5 ± 0.1	11.5± 4.7	0.3 ± 0.1	65	n.d.
	" K	0.8± 0.1	0.02± 0.004	30 ± 5.6	54.6± 5.7	9.0 ± 7.1	>450	0.20± 0.08
	" R	1.5± 0.6	0.05± 0.006	42 ± 16	115 ± 6	6.5 ± 3.7	>600	0.24± 0.16
	" Y	5.9± 0.6	0.09± 0.01	5.1 ± 0.3	107 ± 12	1.8 ± 0.9	78 ± 5	n.d.
	T120E	2.2± 0.4	0.12± 0.07	1.5 ± 0.1	1.1± 0.8	5.6 ± 1.3	128 ± 49	n.d.
	" G	2.6± 0.6	0.15± 0.08	4.6 ± 1.6	32 ± 5	0.65± 0.0	>400	n.d.
	" H	2.6± 0.3	1.20± 0.05	19 ± 3	80 ± 46	17 ± 6	>700	n.d.
	" K	6.1± 1.1	>85	78 ± 24	>900	>200	>800	12.6
choline site	W82Y	76 ± 28	3.2 ± 3.	61 ± 14	140 ± 6	78 ± 37	>1000	3.6 ± 0.1
	" F	31 ± 20	1.7 ± 1.1	86 ± 4	149 ± 39	77 ± 18	>1000	1.7 ± 1.3
oxyanion hole	G115A	1.7± 0.6	9.5 ± 1.6	33 ± 10	33 ± 9	157	460	0.9 ± 0.1
	" S	0.9± 0.1	0.83	24.3	74 ± 36	27	>500	1.1
	G117E	1.5± 0.3	0.2 ± 0.2	0.09± 0.05	19 ± 3	12.3 ± 9.9	330 ± 140	8.7 ± 5.3
back door	V127D	4.9± 1.	0.06± 0.03	2.5 ± 0.8	18 ± 5	4.6 ± 0.7	644 ± 32	n.d.
acetylcholinesterase		2.5	0.21	1.0	710	n.d.	0.13	3.9

[a]The first column identifies the natural or site-directed mutant. Assays were performed in 0.1 to 25 mM BTCh (in the case of AChE, acetylthiocholine), pH 7.4, and Km values were extracted using GraFit 3.0 (Erithacus Software Ltd., Staines, UK). Note that the assays were all conducted at 22 °C, which may account for differences in the kinetic constants from data collected by other laboratories. IC50 values were determined in 1 mM substrate over the indicated range of inhibitor concentrations (GraFit), and from them Ki values were calculated. Standard deviations are shown for 2 or 3 determinations; where no standard deviation is shown, only one determination was performed. The "atypical" natural BuChE mutant is also included. Mutants G115 D, G116E, G116A/G117D, G117C and D and G118E and D are not included in the Table because they had no detectable activity. n.d., not determined.

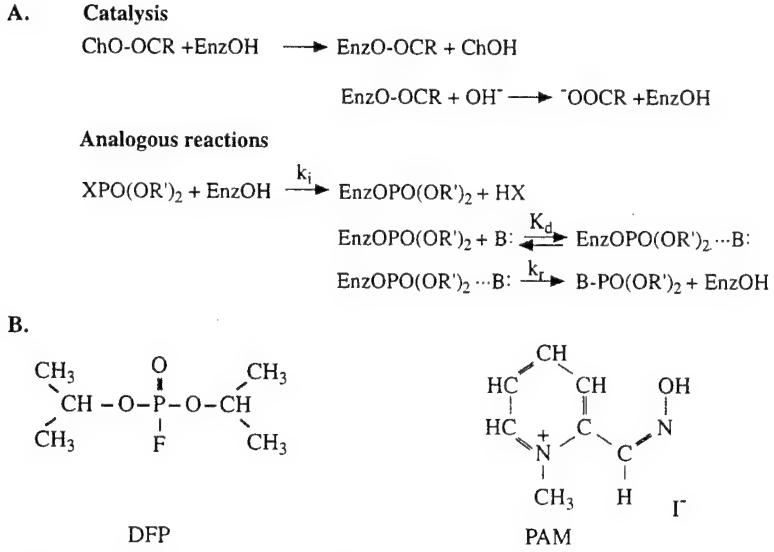

Fig. 3.1 The experimental paradigm. A: catalysis and analogous reactions. In the catalytic cycle the enzyme's active site serine (Enz-OH) displaces the choline moiety of the substrate, forming an acyl-enzyme (covalent) intermediate. The OP agents, being hemi-substrates, act analogously: serine displaces the leaving group (X), forming a dialkylphosphoryl-enzyme [30]. Catalysis continues with the hydrolysis of the acyl enzyme, whereas hydrolysis of the phosphoryl-ChE bond is extremely slow. The reactivation rate, however, can be enhanced by nucleophiles (B) such as choline and PAM, which actively displace the phosphoryl group. B: structure of DFP and PAM.

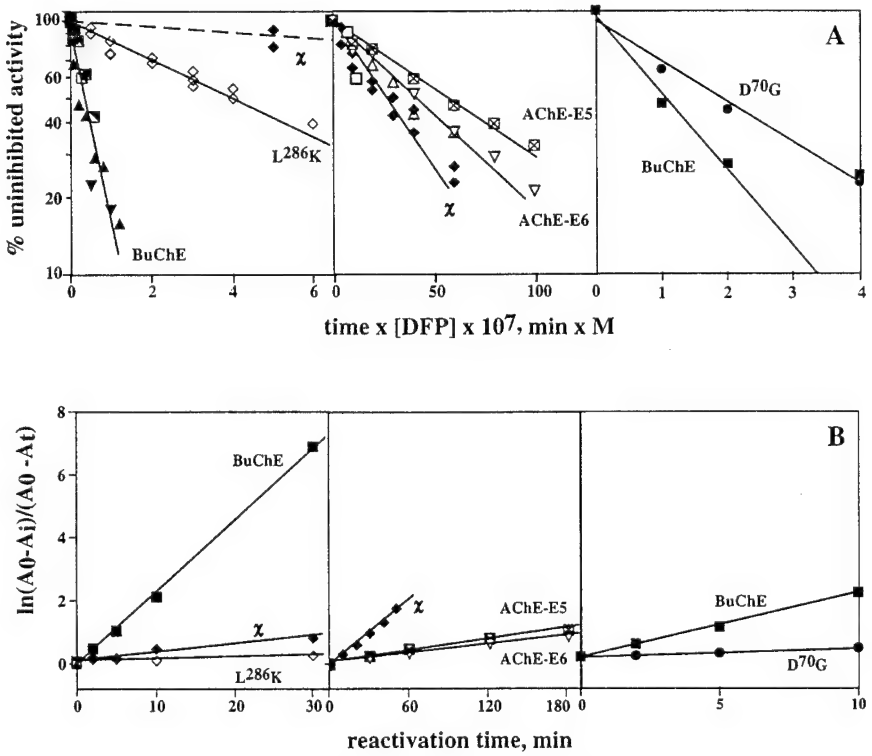

Fig. 3.2 Inactivation of ChEs and reactivation by PAM. A: data are presented as percent original activity vs. duration of exposure to DFP times the DFP concentration (k_i [DFP]). In the left panel, a comparison of BuChE and its $L^{286}K$ mutant and the BuChE/AChE chimera (χ). In the center panel, a comparison of the natural alternatives of AChE (E6) and AChE (E5), and the chimera. In the right panel, a comparison of representative data for the $D^{70}G$ variant and BuChE. The chimera is presented in the left panel and BuChE in the right panel to assist correlation of the rates of $L^{286}K$ and $D^{70}G$. BuChE inactivations: ■ 1 nM, ◥ 5 nM, ▲ 10 nM, ▼ 50 nM DFP. AChE (E6) inactivations: □ 0.1 μM, △ 0.5 μM, ▽ 1 μM DFP; AChE (E5) ⊠ 1 μM DFP. $L^{286}K$ BuChE inactivation: ◇ 50 nM DFP. $D^{70}G$ inactivation: ●, 5 nM DFP. B: a logarithmic function of the regain in activity vs. time is presented in the left panel for BuChE ■, the BuChE/AChE chimera ◆, and the $L^{286}K$ mutant ◇ in 1 mM PAM; in the center panel for AChE (E6) ▽, AChE (E5) ⊠, and the chimera ◆, in 0.6 mM; and in the right panel, representative data for BuChE, ●. and the $D^{70}G$ variant, ■, in 1 mM PAM.

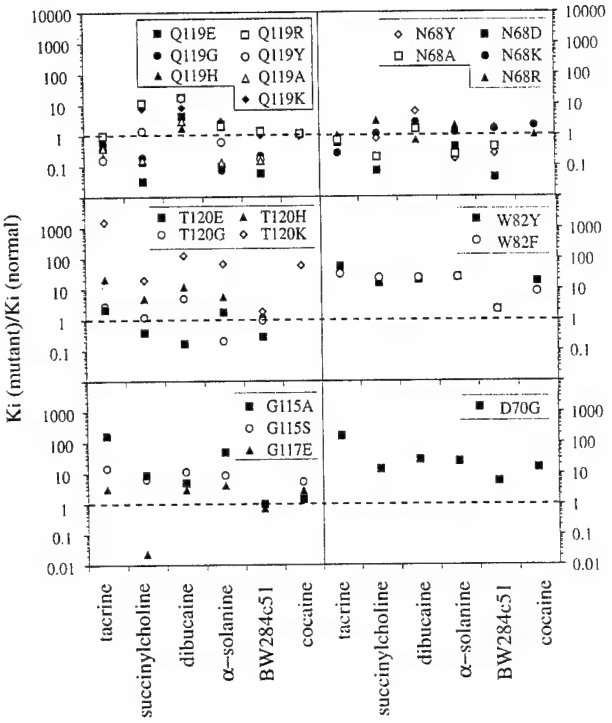

Fig. 3.3: Relative inhibition constants of BuChE mutants.
The Ki values of inhibitors for the mutant enzymes (from Table) are shown relative to normal BuChE for mutations of three residues at the peripheral site (N68, Q119 and T120), the choline-binding site (W82), two at the oxyanion hole (G115 and G117) and the "atypical" variant (D70G). Where only a minimum value is known, that value has been used in calculation the relative constant.

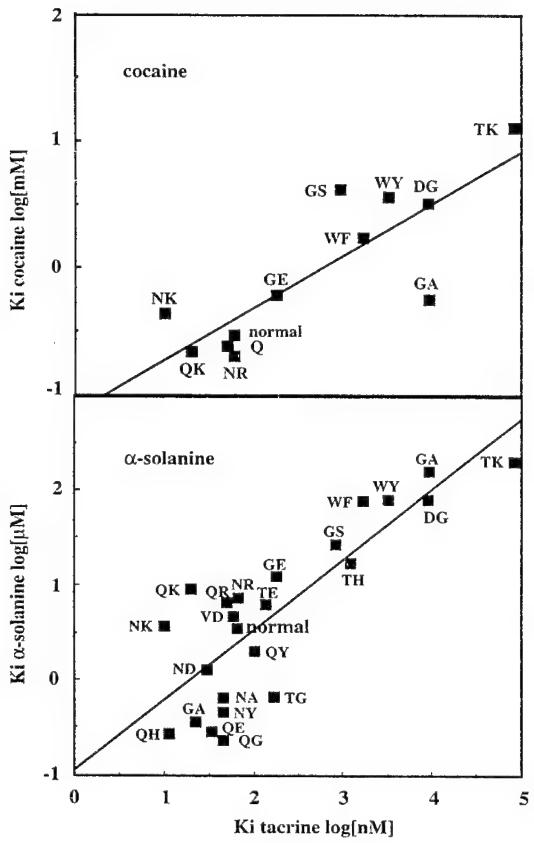

Fig. 3.4: Correlation of tacrine's affinity for BuChE variants with affinities for cocaine and α-solanine.
Upper panel: A plot of the logarithms of the dissociation constants for tacrine vs. those for cocaine and the least squares linecorrelating them.
Lower panel: the corresponding plot for tacrine vs. α-solanine. the data are taken from Table . and the identification of the mutations is as in the Table. lacking only the sequence number of each residue.

4. Failure of "atypical" butyrylcholinesterase to protect against anti-cholinesterases

"Atypical" BCHE, which causes the D70G substitution, is the most common allele of the BCHE gene that causes a clinically variant phenotype. "Atypical" BuChE is incapable of hydrolyzing succinylcholine administered at surgery (Kalow and Davis, 1958; Lockridge, 1990), and is much less sensitive than the normal enzyme to several inhibitors (Neville *et al.*, 1992; McGuire *et al.*, 1989; Kalow and Davis, 1958; Lockridge, 1990). Homozygous carriers of this variant allele -- under 0.04% in Europe but up to 0.6% in certain middle-Eastern populations (Ehrlich *et al.*, 1994) -- suffer post-anesthesia apnea (Lockridge, 1990) and hypersensitivity to the anti-ChE insecticide parathion (Soreq and Zakut, 1993). Recently, we learned of an individual who had experienced succinylcholine-induced apnea and, during the Gulf War under treatment with pyridostigmine, cholinergic symptoms. Therefore, we initiated a study of the interaction of ChE inhibitors in clinical use or testing (Schwarz *et al.*, 1995a) with serum ChEs from members of this subject's family, as compared to the enzyme from serum and with recombinantly produced variant ChEs (Neville *et al.*, 1992).

BuChE from sera of the subject and his father, homozygous and heterozygous carriers of the "atypical" BCHE allele, respectively (Ehrlich *et al.*, 1994), were compared to BuChE from individuals homozygous for the normal allele. To analyze inhibitors that covalently interact with ChEs, we immobilized native human BuChEs through monoclonal antibodies to multiwell microtiter plates (Schwarz *et al.*, 1995b). Recombinant *Xenopus* oocyte-produced variant ChEs, including normal and "atypical" BuChEs and brain- and blood cell-characteristic AChEs (Seidman *et al.*, 1995) were also subjected to inactivation by anti-ChEs and to subsequent spontaneous reactivation (Schwarz *et al.*, 1995b).

Activity of "atypical" butyrylcholinesterase The activity of "atypical" BuChE was found to be about 3-fold lower than normal in the subject's serum, which contained a normal amount of enzyme protein. Heterozygotes presented intermediate specific activities. "Atypical" BuChE reacts much slower than does normal with four carbamates, pyridostigmine (Keeler *et al.*, 1991), physostigmine (Giacobini, 1991), heptyl physostigmine (Iversen, 1993) and SDZ-ENA 713 (Enz *et al.*, 1993) (Table 4.1A).

Rate of inhibition of normal and "atypical" butyrylcholinesterase Inhibition by the reversible Alzheimer's disease drug tacrine (Knapp *et al.*, 1994) was examined (Table 4.1B). To mimic the heterozygous state, we tested 1:1 mixtures of oocyte homogenates which expressed recombinant normal and "atypical" enzyme (Fig. 4.1B). In both cases, we observed a drastic reduction in the capacity of "atypical" BuChE to interact with tacrine. Analysis of the relevant site in the enzyme's three-dimensional structure (Harel *et al.*, 1993), further revealed that the distance from the Asp70 carboxyl group to the tacrine anilinic nitrogen in BuChE is only 5.2 Å indicating the possibility of a salt bridge. This interaction is removed in "atypical" BuChE, reflected in a two orders of magnitude increase in tacrine's IC_{50}.

Rate of reactivation of normal and "atypical" butyrylcholinesterase The reactivation rates of AChE and BuChE differed for several drugs, with the decreasing order SDZ-ENA 713, heptyl physostigmine, pyridostigmine and physostigmine (Table 4.1C). However, for no drug was there a dramatic difference between the blood and brain forms of AChE or between normal and "atypical" BuChE (Table 4.1C), which indicates that the differential drug responses of "atypical" BuChE occur at the initial scavenging step.

The possibility that anti-ChE therapies may cause adverse reactions in individuals with variant BCHE genotypes, becomes a pertinent issue in view of the administration of pyridostigmine bromide to over 400,000 Gulf War soldiers. In homozygotes and possibly in heterozygous carriers of the "atypical" BCHE allele, the lower capacity of blood BuChE to interact with and detoxify some of the drug should result in larger effective doses. "Atypical" homozygotes with

practically none of the normal protective detoxifier, would hence become most vulnerable to AChE inhibition under treatment by any anti-ChE drug. Several Alzheimer's disease drugs emerged in this study as much faster inactivators of BuChE than of AChE, suggesting that when administered to patients, these drugs will interact primarily with plasma BuChE.

Effective dosage of anti-cholinesterase in carriers of BCHE, the example of tacrine In order to determine whether there are enough binding sites to effect a significant depletion in the level of the reversible inhibitor, tacrine, to which the cholinergic system is exposed, we have calculated the levels of ChE sites in the blood. The concentration of ChE in blood is approximately 50 nM, 75% due to soluble BuChE (Chatonnet and Lockridge, 1989) 25% due to erythrocyte membrane AChE (Ott et al., 1982). This may be compared with plasma tacrine levels of 21 nM in patients under therapy (Johansson and Nordberg, 1993). Dissociation constants of 40 nM for normal BuChE (Berman and Leonard, 1992) and 8,000 nM for "atypical" BuChE (calculated from the data of Table 4.1), indicate that about 40% of plasma tacrine is bound to BuChE in individuals with the normal allele. In contrast, only 1% is bound to BuChE in "atypical" homozygotes, heterozygotes falling in between. The clinically effective dose reaching the CNS depends heavily, therefore, on the BCHE genotype. Even without the complication of BCHE polymorphism, BuChE levels can vary with the general state of health (Soreq and Zakut, 1993). Since Alzheimer's disease patients are far from being as healthy as the pyridostigmine-treated soldiers, they may present yet more drastic symptoms in response to inappropriate dosage of anti-ChEs. The reported high percentage of cholinergic symptoms under tacrine treatment (up to 15%) (Winker, 1994) may reflect BCHE heterozygotes and, in addition, patients with liver malfunctions and consequently with low serum BuChE levels.

Table 4.1 **Deficient interaction of 'atypical' butyrylcholinesterase with various inhibitors**

	BuChE		*AChE*	
	Normal	Atypical	Brain-type (E6)	Blood cell-type (E5)
(*a*) second order inactivation rate constants[a] (M^{-1} min^{-1}) × 10^{-3}				
Pyridostigmine (10^{-5} M)	1.4 ± 0.5	0.2 ± 0.3	22 ± 9	25 ± 7
Physostigmine (10^{-6} M)	380 ± 160	26 ± 9	ND	ND
Heptyl physostigmine (10^{-8} M)	11000 ± 3000	770 ± 440	1600 ± 700	1400 ± 400
SDZ-ENA 713 (10^{-5} M)	14 ± 3	0.47 ± 0.46	4.3 ± 1.8	3.3 ± 0.6
(*b*) IC_{50} values[b] (μM)				
Tacrine (recombinant)	0.054 ± 0.036	11.4 ± 1.4	0.15 ± 0.08	0.15 ± 0.04
Tacrine (serum)	0.082 ± 0.009	8.9 ± 2.5	–	–
(*c*) Time dependent reactivation[c] (percent original activity after 30 min)				
Pyridostigmine	9	8	32	24
Physostigmine	17	12	67	54
Heptyl physostigmine	13	13	3	3
SDZ-ENA 713	2	1	8	4

[a]Pseudo-first-order rate constants were extracted from data such as those in Fig.4.1but for the recombinant enzymes, and with the reagent concentrations indicated in parentheses, and were fit to a first-order decay model using the least-squares approach. Averages and standard deviations of at least four determinations are presented. ND, not determined because of the exceedingly high reactivation rates.

[b]IC_{50} values of tacrine were measured for recombinant human ChEs and for sera in the presence of 1 mM BTCh for BuChE or 1 mM acetylthiocholine for AChE. Values are calculated by GraFit 3.0 (Erithacus Software, Staines, UK). The data shown are averages and standard deviations of two serum samples or three recombinant enzyme samples.

[c]Spontaneous reactivation of recombinant human ChEs was examined after complete inhibition of the immobilized enzymes, followed by removal of unreacted inhibitor. Values of percent regained activity after 30 min are shown (average of two experiments).

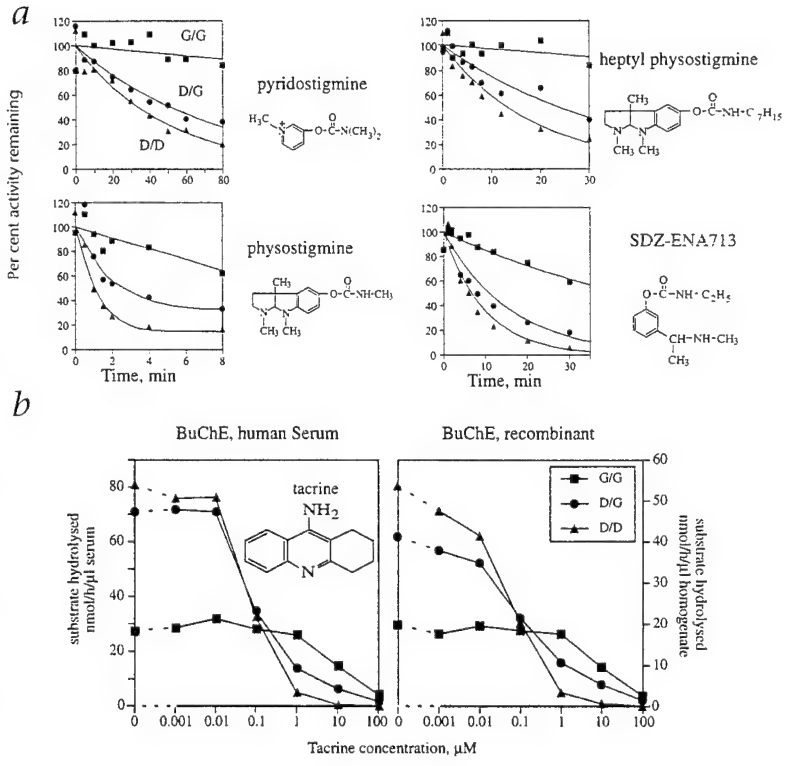

Fig. 4.1 Inhibition of BuChE variants by anti-ChEs. *a*, Differential inactivation kinetics of variant human sera BuChEs with carbamate inhibitors. Percent original activity as a function of time of exposure to four carbamates is presented for a representative experiment. Activities of immobilized ChEs were determined in 10 mM BTCh following incubation for the noted times with the covalent inhibitors pyridostigmine (10 μM), physostigmine (1 μM), heptyl physostigmine (0.01 μM), and SDZ-ENA 713 (10 μM). The lines are best fits of the data to pseudo-first-order conditions. ▲, normal, Asp70, BuChE homozygote (D/D); ■, atypical, Gly70, homozygote (G/G); ●, BuChE heterozygote (G/D). Lines are drawn for the inactivation by pyridostigmine using the pseudo-first-order rate constants 0.0014 min^{-1} (G/G), 0.0135 min^{-1} (G/D) and 0.0205 min^{-1} (D/D). *b*, Inhibition of serum and recombinant BuChE by tacrine. In the left panel, data for 3 representative serum types inhibited by tacrine: serum of the propositus, A.B., a homozygote for the atypical, Gly70, BuChE variant (G/G); of his father, a heterozygote for this variant (G/D); and of a normal homozygote with Asp70 (D/D). In the right panel, tacrine inhibition is observed on equivalent total amounts of recombinant normal (D/D) and atypical (G/G) enzymes produced in microinjected *Xenopus* oocytes[6].

5. Cholinotoxic effects on rodent brain gene expression

Cholinergic deficits have been associated with several neurodegenerative disorders such as Alzheimer and Huntington's diseases (Wurtman, 1992), suggesting that finely balanced cholinergic metabolism contributes to the maintenance of CNS circuits. An animal model in which a selective cholinergic deficit has been induced is the ethylcholine aziridinium (AF64A) treated rat (Fisher *et al.*, 1982). AF64A is structurally similar to choline, with the distinction that it possesses an ethyl moiety and the highly reactive aziridinium ion. It is taken up by cholinergic neurons via the high affinity choline transport system (Manitone *et al.*, 1981) and causes a specific and long-lasting reduction in the concentration and the activity of cholinergic pre-synaptic biochemical markers (Manitone *et al.*, 1981; Sandberg *et al.*, 1984), including ACh, AChE, ChAT (Leventer *et al.*, 1987), and the high affinity transport system for choline, which is the rate limiting step in ACh synthesis (Murrin, 1980). In addition, rats treated with AF64A also show behavioral cognitive deficits, suggesting that loss of synapses has occurred (Chrobak *et al.*, 1988). Like other aziridinium compounds, AF64A was also found to react also with DNA, to induce DNA damage and to cause premature termination of RNA transcription *in vitro*. Thus, the cholinotoxic effects of AF64A could be attributed to its inhibitory action on cholinergic enzymes activities, to interference with the synthesis of such enzymes, to its DNA damaging activity on G,C-rich genes or to all of these actions together.

AChE and the closely related enzyme BuChE are highly similar in their amino acid sequence and in their computer-modeled three dimensional structure, yet vary in their substrate specificity and in their interaction with inhibitors. In addition, the rat ACHE gene is G,C-rich (Legay *et al.*, 1993) like its human homolog (Soreq *et al.*, 1990), with high predicted sensitivity to guanine-binding agents, whereas the BCHE gene is A,T-rich (Prody *et al.*, 1987) and may be expected to be less sensitive to such agents. This difference made the two ChE genes appropriate models for *in vitro* studies on the effectiveness of AF64A on cholinergic gene expression and/or enzymatic activities. In parallel, we further examined the effects of ICV administration of AF64A on cholinergic enzyme activities and determined the *in vivo* effect of AF64A on ChEmRNA levels by reverse transcription coupled with DNA amplification (RT-PCR) in different rat brain areas. To compare the pattern of expression of G,C-rich genes in brains from AF64A treated and control rats, differential PCR-displays (Liang and Pardee, 1992) were prepared with an arbitrary G,C-rich primer (Welsh *et al.*, 1992). Our findings suggested a consistent correlation between the cholinotoxic effects of AF64A on G,C-rich sequences *in vitro* and *in vivo* and the use of this approach for identifying the target genes to cholinotoxic agents.

AF64A modulates cholinergic enzyme activities *in vivo* AF64A effects on different cholinergic markers *in vivo* were measured in a time-dependence study. To address the cholinergic deficits following ICV administration of 2 nmol AF64A, we determined the enzymatic activities of AChE and ChAT in different brain regions. Septal AChE showed a slight but significant reduction which occurred late, while striatal AChE activity remained apparently unchanged until day 60. In contrast, AChE activity in hippocampus was reduced at day 7 through 60 post-AF64A administration (Fig. 5.1). The enzymatic activity of ChAT showed a different pattern: septal ChAT activity was significantly increased on day 7, returned to normal level by day 14 and decreased by day 60 post-AF64A treatment. In the striatum, ChAT activities remained normal after 0.5, 1.0 and 2 nmol/side AF64A at all of these time points (Fig. 5.1, and El-Tamer *et al.*, unpublished data). However, hippocampal ChAT activity was significantly decreased at day 7 through 60. The biochemical measurements thus revealed a particular long-term vulnerability to AF64A effects for cholinergic enzyme activities in the hippocampus.

Differential *in vitro* inhibition of cholinesterases by AF64A We analyzed enzyme activity following preincubation of AF64A. Our measurements fully reflected the interaction of the released thiocholine product with DTNB, and the color reduction under these experimental

conditions was due to enzyme inhibition alone (Hanin *et al.*, 1994). Following incubation of AChE and BuChE with AF64A a reduction of the activity of these enzymes was observed (Fig. 5.2, top). At the high concentration of AF64A used *in vitro*, one would expect susceptibility to nucleophilic attack by ChE activities. Moreover, at the physiologically-effective average AF64A concentration of 5 to 20 mM, neither of the enzymes should be inhibited. Therefore, we next focused our investigation on measurements at the mRNA level.

Pretreatment of cholinesterase cDNAs with AF64A causes differential damage to *in vitro* transcription To compare the sensitivity of the ACHE and BCHE genes to AF64A, plasmid DNAs carrying each of these ChE coding sequences were subjected to *in vitro* transcription following pre-incubation with AF64A. Reductions were observed in the yields of RNA transcripts from both ACHE and BCHEcDNA, however to different extents. The ACHE gene therefore displayed differential sensitivity over that of the BCHE gene toward AF64A toxicity *in vitro*, which predicted that physiologically effective concentrations of this cholinotoxin may modulate transcriptional activities of the corresponding genes in cholinergic and/or cholinoceptive cells.

AF64A administration modulates cholinesterase mRNA levels *in vivo* To assess the *in vivo* levels of CHEmRNAs, total RNA extracts from septum, hippocampus and striatum from AF64A-treated rats were subjected to reverse transcription followed by kinetic follow-up of PCR amplification using primers specific to each of the ChE genes (RT-PCR). This analysis revealed that the amounts of septal and striatal ACHEmRNA were reduced, while BCHEmRNA levels remained unchanged (not shown). In contrast, hippocampal ACHEmRNA was higher in treated rats at day 7 post-injection and returned to apparently normal levels at day 60. In this same region, BCHEmRNA was reduced by 70% on day 7 and remained as low as 50% of control on day 60 (Fig. 5.3). Although AChE activity was significantly reduced in the hippocampus, the RT-PCR analysis revealed a concomitant and pronounced increase in ACHEmRNA, unique to this brain region.

AF64A induces region-specific alterations in the differential PCR display of G,C-rich transcripts To examine whether the increased levels of ACHEmRNA in hippocampus reflected a general change in transcription of G,C-rich genes, we employed the approach of differential PCR display. The general pattern of displayed products did not change in the AF64A-treated rats as compared to control rats (Fig. 5.4). While no AF64A-dependent changes could be observed in striatal mRNA, we were able to detect several quantitative changes in PCR products displayed from hippocampus and septum following AF64A administration. In the septum the levels of 3 transcripts were decreased on day 7 and remained low at day 60 (Fig. 5.4). At least three other PCR fragments appeared to be stronger in the treated hippocampus 60 days post-AF64A. This implies that the increase of ACHEmRNA in the hippocampus was consistent with an increase in multiple G,C-rich transcripts which was particular to this cholinoceptive brain region.

The *in vivo* experiments were complemented by a series of *in vitro* tests. *In vitro* inhibition of transcription of G,C-rich ACHEcDNA was achieved at concentrations of AF64A that were 2 times lower than those required to inhibit the A,T-rich BCHEcDNA, attributing at least part of the *in vivo* changes in ACHE gene expression to its G,C-rich composition. *In vitro* studies further revealed that AChE activity was more sensitive to this alkylating agent than that of BuChE, and that this inhibition required higher AF64A concentrations than those generally administered ICV. Moreover, access of such compounds to intracellular enzymes in the CNS parenchyma in the *in vivo* situation is very limited. Therefore, our *in vitro* tests suggest that to achieve direct inhibition of enzyme activities, the intracellular concentration of AF64A should be higher than those present in the CSF. The *in vivo* inhibition of AChE activity thus suggested that ICV-administered AF64A actively accumulated in cholinergic synapses and entered into cholinergic and/or cholinoceptive cell bodies, where it could reach higher local concentrations. Our findings therefore support the theory of active uptake into cholinergic cell bodies via the choline transport system, which was previously suggested as a mechanism of action for AF64A (Manitone *et al.*, 1981; Sandberg *et al.*, 1985). Once in these cell bodies, AF64A is likely to

interact with G,C-rich genes such as ACHE and interfere with their transcription (Futscher *et al.*, 1992). Moreover, the theory of active uptake further explains the apparent direct reduction of protein activities. Altogether, these findings imply that penetration of this alkylating agent into the brain can induce multileveled cholinergic damage. This includes mechanisms of nucleophilic attack and blocking of guanines in the DNA at cholinergic cell bodies on the one hand, and interference with specific protein subsets at cell bodies and nerve terminals on the other hand.

At the level of mRNA, the main damage induced *in vivo* by AF64A appeared to be region-specific and partially transient. At the protein level we could discriminate between the vulnerable hippocampus and the more resistant septum and striatum. Injection of 2 nmol AF64A/ventricle did not affect the activities of cholinergic markers measured in the striatum, which was previously found to be sensitive to higher doses of this cholinotoxin (Sandberg *et al.*, 1984). In contrast, the mRNA levels of both ACHE, b-actin and other unidentified G,C-rich genes were significantly increased in the hippocampus by 7 days post AF64A administration. This indicated that the *in vivo* decrease in AChE activities in the hippocampus was secondary to the reduction in ACHEmRNA in the septum, projecting to the hippocampus, and that this change caused a feedback increase of transcription of several genes, including ACHE and b-actin, in this cholinoceptive and vulnerable area.

To evaluate the general transcriptional damage caused by AF64A, we employed differential PCR display. Differentially expressed mRNAs were indeed observed in septum, striatum and hippocampus, and some of those particular to the hippocampus were modulated following AF64A administration. The long term changes in gene expression detected by the PCR display suggest the use of this approach to clone and identify the modulated transcripts. That both the protein activities and the PCR display changes were long-term can further indicate damage to the machinery of mRNA translation. This would reduce AChE activities even under conditions where ACHEmRNA levels returned to normal, as was the case by day 60 post AF64A treatment. The transcriptional changes in AF64A-treated hippocampus are in line with the behavioral effects induced by this cholinotoxin.

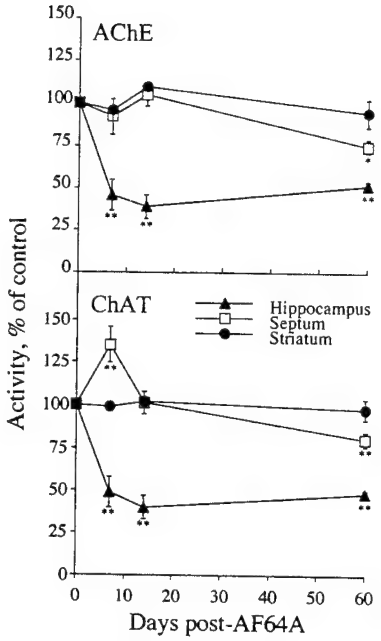

Fig. 5.1 In vivo effects of AF64A on cholinergic markers. Time-dependent effects of AF64A (2.0 nmol/side) on AChE and ChAT activities are presented for septum, hippocampus and striatum. Animals were sacrificed by decapitation at the indicated time after i.c.v. injection of AF64A. Enzymatic assays were performed in duplicate on tissue homogenates.

Data represent the average (mean ± S.E.M., $n = 3$ rats per group) of enzymatic activity expressed as percent of control. AChE activity in control group: mean ± S.E.M., 3476 ± 228, 9214 ± 281 and 20876 ± 474 nmol/mg/h in hippocampus, septum and striatum, respectively. ChAT activity in control group: mean ± S.E.M., 42.1 ± 3.5, 66.5 ± 5.2 and 209.7 ± 7.54 nmol/mg/h in hippocampus, septum and striatum, respectively. * $P < 0.05$; ** $P < 0.01$, compared to vehicle treated group.

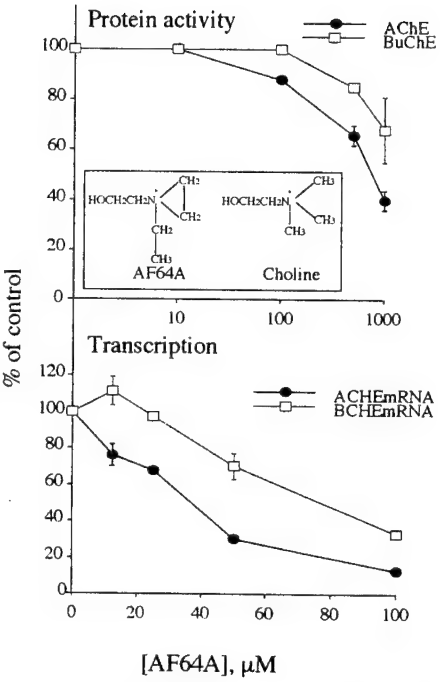

Fig. 5.2 In vitro effects of AF64A on mammalian CHE genes and their enzyme products. Top: direct AF64A induced inhibition of cholinesterase activities. Inhibition was measured following incubation with increasing concentrations of AF64A by determining remaining activities of AChE and BChE, all as detailed under methods. Inset: chemical structures of the cholinotoxin AF64A (a) and the native choline molecule (b), after Fisher et al. Bottom: differential sensitivity of the AChE and BChE genes for transcriptional damage induced by AF64A. Equal amounts of the noted plasmids incubated with the noted concentrations of AF64A were used for in vitro transcription in the presence of [^{32}P] nucleotides followed by agarose gel electrophoresis and autoradiogrephy of the ^{32}P-labeled reaction products. Note the relative resistance to AF64A of BChE – as compared with AChEcDNA. The same results were obtained for BChE mRNA transcribed from two transcription plasmids containing the human BChE coding sequences with two distinct RNA polymerases (not shown), demonstrating that the AF64A effects were due to the cDNA seqence and not to the type of RNA polymerase.

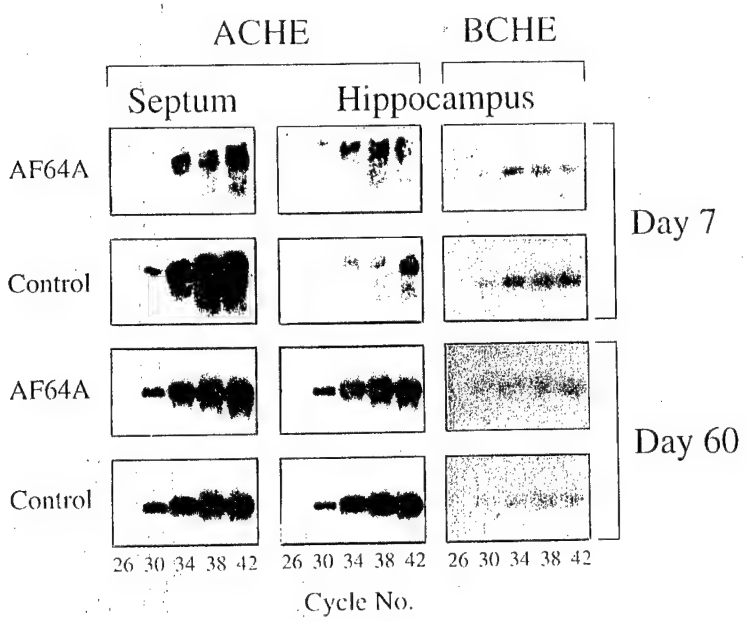

Fig. 5.3 In vivo modifications in cholinesterase mRNA levels following AF64A treatment. RNA was extracted from septum, hippocampus and striatum of 3 pooled animals 7 and 60 days post AF64A treatment and was subjected to RT-PCR procedure. PCR products were detected as dark bands after hybridization followed by autoradiography.

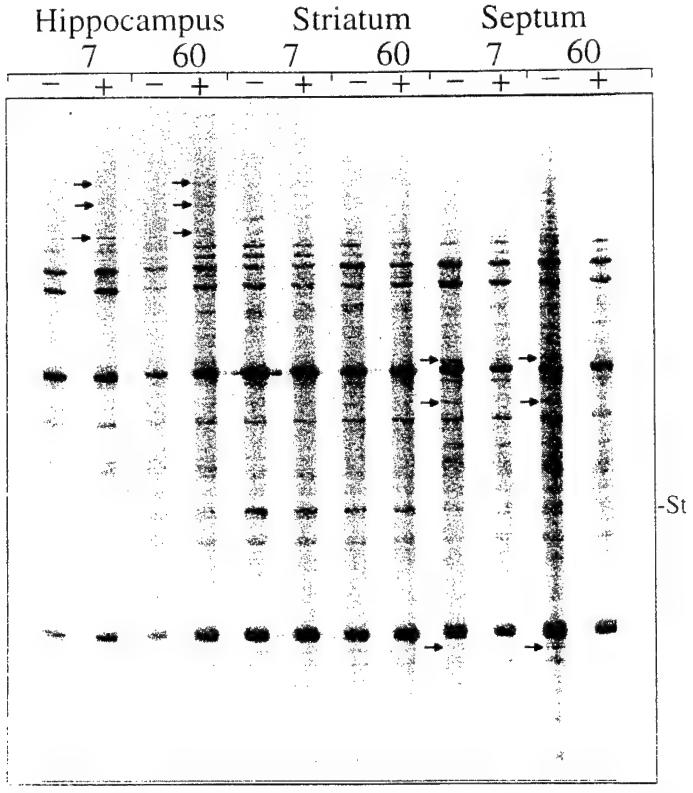

Fig. 5.4 PCR display. Differential PCR display of 1 μg total RNA extracted from hippocampus, striatum and septum pooled regions (from 3 animals/sample) of saline (−) and AF64A (+) injected rat brains, 7 and 60 days post treatment. Exposure was for 1 day at room temperature, for 10% of reaction mixture per lane. PCR fragments size was between 200 and 400 bp. Altogether most of the PCR products were common to the different brain regions; some were specific for either striatum (St) or hippocampus (not shown in this part of the gel). Arrows indicate PCR products whose intensity changed following AF64A injection.

6. Activation of acetylcholinesterase by phosphorylation

We have demonstrated that human AChE from several sources can all be phosphorylated, that AChE from these sources is partially phosphorylated *in vivo*, that this phosphorylation enhances the catalytic rate and that this phosphorylation must occur at a non-consensus site.

Phosphorylation by protein kinase A The catalytic subunit of protein kinase A (PKA) , but not casein kinase II or protein kinase C, incorporates ^{33}P from labeled ATP into human AChE that had been expressed in 293 kidney cells or *E. coli*, or purified from human erythrocytes (Fig. 6.1). The homologous enzyme, human BuChE, failed to become phosphorylated.

Acetylcholinesterase is found partially phosphorylated *in vivo* Recombinant human AChE isolated from 293 cells or *E . coli* or from human erythrocytes were treated with alkaline phosphatase, then compared with the untreated enzymes on isoelectric focusing gels (Fig. 6.2). The treatment created a new subtype of AChE, with a high isoelectric point, indicating that some phosphorylated AChE had been present.

Phosphorylation results in activation of acetylcholinesterase The treatment with PKA resulted in activation of human AChE from the various sources (Table 6.1). *Torpedo* AChE was also activated, but not human BuChE. However, inhibition of human AChE by several reversible and irreversible inhibitors was not affected by the phosphorylation (Table 6.2).

Phosphorylation at non-protein kinase A consensus sites Human AChE contains one PKA phosphorylation consensus site, T249. Because *Torpedo* AChE does not contain this potential phosphorylation site, yet becomes activated by PKA, the possibility of phosphorylation at a non-PKA phosphorylation consensus site was tested. T249 was changed to an alanine residue by site-directed mutagenesis. Activation of T249A by PKA-treatment confirmed that phosphorylation must be occurring at a non-consensus phosphorylation site (Table 6.3).

Table 6.1. Effect of protein kinase A on the activity of cholinesterases from various sources[a]

	catalytic activity (µmol/min/ml)		+kinase / - kinase	consensus site[d]
	- kinase	+ kinase		
AChE				
recombinant human, from 293 cells	8.3	76.9	9.3	+
recombinant human, from *E. coli*	0.3	2.4	8.0	+
human erythrocyte	3.2	12.8	4.0	+
human brain	4.5	11.3	2.5	+
Torpedo electroplax[b]	4.2	17.7	4.2	-
COS cells transfected with normal E6-ACHEDNA[c]	0.9	1.8	2.0	+
COS cells transfected with T249A E6-ACHEDNA[c]	1.0	2.2	2.2	-
BuChE				
human serum	1.1	1.2	1.1	+

[a]The data shown are from one out of three experiments with standard deviations below 30%. For BuChE activity determinations, 5 mM butyrylthiocholine was used as a substrate. All enzyme preparations were highly purified except for [b] which was partially purified and for [c] which was tested in medium secreted from transfected cells with no further purification. [d]The existence of a PKA consensus site on each of the examined sequences is noted.

Table 6.2. Kinetic constants of human acetyl-cholinesterase purified from embryonic kidney 293 cells.[a]

	- kinase	+ kinase
Km (µM) [a]	50	50
Ki values (µM)		
tacrine	0.007	0.006
fasciculin 02	0.0002	0.0003
BW284c51	0.3	0.3
IC50 (µM)		
physostigmine	0.01	0.01
echothiophate	0.01	0.01

[a] Kinetic constants of recombinant AChE purified from 293 cells with no further treatment (-kinase) or treated with PKA (+kinase) were determined.

Table 6.3. Abolition of the PKA consensus site does not modify AChE properties.

	E6-ACHEDNA-transfected[a]	T249A E6-ACHEDNA-transfected[b]
Ki values (µM)		
succinylcholine	290	290
dibucaine	720	730
BW284c51	0.007	0.007
tacrine	0.058	0.072
fasciculin 02	0.000,000,1	0.000,000,1
fasciculin 03	0.000,000,2	0.000,000,2
IC50 value (µM)		
pyridostigmine	0.50	0.55

[a] COS cells were tansfected with E6-ACHEDNA and the biochemical properties of AChE secreted into the medium were determined as in Tables 6.1 and 6.2.
[b] Site-directed mutagenesis was employed to substitute T249 into A. Tests were similar to for "T249A E6-ACHEDNA-transfected".

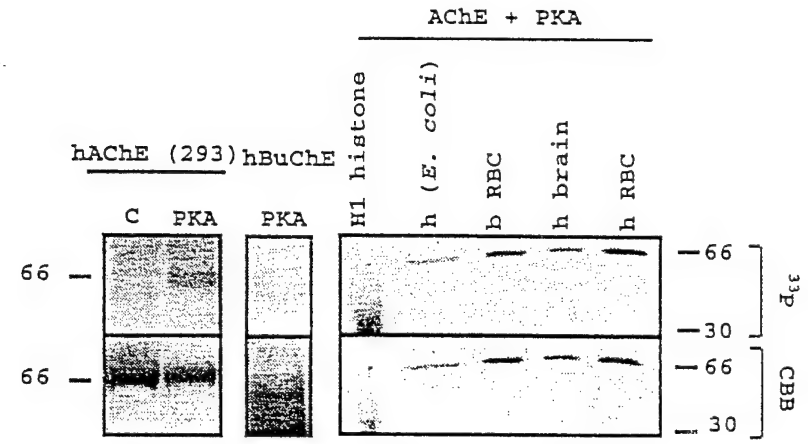

Fig. 6.1: *In vitro* phosphorylation of AChEs. Phosphorylation reactions were performed on 5 µg purified recombinant AChE expressed in 293 kidney cells (hAChE (293)), 2 µg purified recombinant AChE expressed in *E coli* (h (E. coli)), 5, 3 and 5 µg of native AChE purified from human erythrocytes (hRBC), human brain (hbrain) and bovine erythrocytes respectively, 0.2 mU human BuChE (hBuChE) and 5 µg histone (H1). One fifth of each of the phosphorylation reactions , was separated by SDS-PAGE followed by either protein staining with Commassie brilliant blue (CBB) or by 48 h autoradiography (^{33}P). A reaction without PKA served as a control (C). Note that all proteins except BuChE were phosphorylated by PKA. Numbers on both sides of the figure indicate molecular weight in kD.

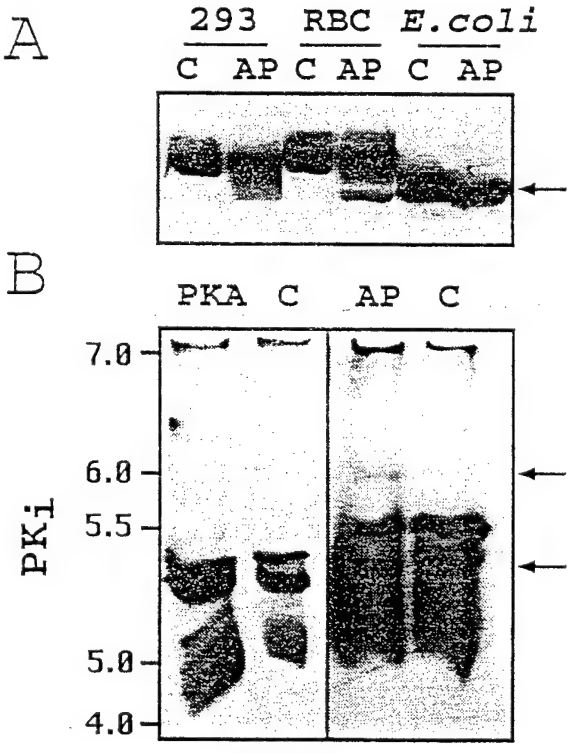

Fig. 6.2: Dephosphorylation of AChE modifies its electrophoretic and isoelectric properties.
A. Alkaline phosphatase enhances the electrophoretic migration of AChE. Alkaline phosphatase (AP) treated and control untreated (C) recombinant human AChE from 293 cells (293, 3 µg), from human erythrocytes (hRBC, 5 µg) or human AChE produced in *E coli* (*E. coli*, 3 µg) were electrophoretically separated under denaturing conditions and immunochemically detected.
The arrow indicates the position of that fraction of these proteins that migrated faster after dephosphorylation.
B. Alkaline phosphatase induces the appearance of a novel AChE subtype with high isoelectric point. 3 µg hAChE (293) in a final volume of 20 µl was treated either with PKA or with AP and was subjected to isoelectric focusing gel electrophoresis followed by activity staining of the gels. Similarly treated AChEs served as a control (C). The arrow indicates an additional band at a higher isoelectric point, which could only be observed after dephosphorylation.

Conclusions

In conducting this research, we employed transgenic *Xenopus* tadpoles to reveal the molecular mechanisms leading to the accumulation of AChE in synapses. We have found that the 40 amino acid-long C-terminal peptide of the brain form of AChE is an essential requirement for this accumulation. In contrast, the 42 amino acids of the "readthrough" form of this enzyme, which so far has been demonstrated only at the level of the ACHE gene and its mRNA products, supports epidermal expression and excretion of a more hydrophilic monomeric form of this enzyme.

The *Xenopus* data implied that to obtain synaptic protection against OP poisons, one needs the brain cDNA. Therefore, we constructed transgenic mice expressing such DNA in their CNS neurons. These mice indeed became resistant to the hypothermia-inducing effects of OPs. However, they also developed progressive deterioration of learning and memory and of neuromuscular junction anatomy and function, suggesting that for safer protection one needs to confer expression of the transgenic enzyme in tissues other than brain.

OP and carbamate interactions of AChE and BuChE and their natural variants were studied in *Xenopus* oocyte-produced recombinant proteins, following their partial purification and enrichment onto selective monoclonal antibodies in microtiter plates. These tests demonstrated that BuChE interacts faster and more efficiently than AChE with a number of these anti-ChEs, and suggested that it operates *in vivo* as a scavenger of these inhibitors and drugs of these categories.

Interestingly, the relatively common "atypical" allelic variant of BuChE was found to differ from its normal counterpart by being incapable of scavenging carbamate and quaternary amine inhibitors, including pyridostigmine and tacrine. This, in turn, implies that in individuals who carry this allelic variant, the effective dose of anti-ChEs would be higher than in others. This may lead to adverse responses to such drugs.

To test the effects of cholinotoxic damage in the mammalian brain, we adapted the use of differential PCR display to dissected brain regions. Using this method, we demonstrated long-lasting (months long) changes in gene expression in brain regions of rats that were subjected to mild intoxication of cholinergic neurons.

The fact that AChE activity may be enhanced by phosphorylation, opens the possibility that modulation of this control mechanism may provide a means of minimizing the effects on the cholinergic system of exposure to anti-ChEs, such as warfare nerve agents.

References

Anglister L and McMahan UJ (1985) *J. Cell Biol.* 101:735-743.

Beeri R, Gnatt A, Lapidot-Lifson Y, Ginzberg D, Shani M, Soreq H and Zakut H (1994) *Human Reprod.* 9:284-292.

Berman HA and Leonard E (1992) *Molec. Pharmacol.* 41:412-418.

Carmichael M (1994) *Sci. Am.* 270:64-72.

Chatonnet A and Lockridge O (1989) *Biochem J.* 260:625-634.

Chrobak JJ, Hanin I, Schmechel DE and Walsh TJ (1988) *Brain Res.* 4632:107-117.

Cohen MW (1980) J. Exp. Biol. 89:43-56.

Ehrlich G, Ginzberg D, Loewenstein Y, Glick D, Kerem B, Ben-Ari S, Zakut H and Soreq H (1994) *Genomics* 22:288-245.

Eichenbaum H, Steward C and Morris RGM (1990) *J. Neurosci.* 10: 3531-3542.

Enz A, Amstutz R, Boddeke H, Gmelin G, Malonowski J (1993) *Brain Res.* 98-431-437.

Fisher A, Manitone CR, Abraham DJ and Hanin I (1982) *J. Pharm. Exp. Ther.* 222: 140-145.

Flucher BE and Daniels MD (1989) *Neuron* 3:163-175.

Froehner SC (1991) *J. Cell Biol.* 114:1-7.

Futscher BW, Pieper O, Barnes DM, Hanin I and Erickson LC (1992) *J. Neurochem.* 58:1504-1509.

Giacobini E (1991) In R Becker and E Giacobini (eds.) *Cholinergic Basis for Alzheimer Therapy*, Birkhauser, Boston , 247-262.

Gilson MK, Straatsma TP, McCammon JA, Ripoll DR, Faerman CH, Axelsen PH, Silman I and Sussman JL (1994) *Science* 263:1276-1278.

Gindi T and Knowland J (1979) *Exp. Morphol.* 51:209-215.

Hanin I, Yaron, A, Ginzberg D and Soreq H (1994). In: I Hanin, A Fisher and M Yoshida (eds.) *Alzheimer's and Parkinson's Diseases:Recent Advances*, Plenum Press, New York.

Harel M, Sussman JL, Krejci E, Bon S, Chanal P, Massoulie J and Silman I (1992) *Proc. Natl. Acad. Sci. USA 89*:10827-10831.

Iversen LL (1993) *Brain Res.* 98:423-426.

Johansson IM and Nordberg A (1993) *Acta Neurol. Scand. Suppl* 149:22-25.

Kalow W and Davis RO (1958) *Biochem. Pharmacol.* 1:183-192.

Karnovsky MJ (1964) *J. Cell Biol.* 23:217-232.

Karpel R, Ben Aziz-Aloya R, Sternfeld M, Ehrlich G, Ginzberg D, Tarroni P, Clementi F, Zakut H and Soreq H (1994) *Exp. Cell Res.* 210:268-277.

Keeler JR, Hurst CG, Dunn MA (1991) *J. Am. Med. Assn.* 266:6903-695.

Kitt CA, Höhmann C, Coyle JT and Price DL (1994) *J. Comp. Neurol.* 341:117-129.

Knapp MJ, Knopman DS, Solomon PR, Pendlebury WW, Davis CS, Gracon SI (1994) *J. Am. Med. Assn.* 271:985-991.

Kothary R, Barton SC, Franz T, Norris ML, Hettle S and Surani AMH (1991) *Mech. Develop.* 35: 25-31.

Kronman C, Velan B, Gozes Y, Leitner M, Flashner Y, Lazar A, Marcus D, Sery T, Papier A, Grosfeld H, Cohen S and Shafferman A (1992) *Gene* 121:295-304.

Kullberg RW, Lentz TL and Cohen MW (1977) *Devel. Biol.* 60: 101-129.

Kullberg RW, Mikelberg FS and Cohen MW (1980) *Devel. Biol.* 75:255-267.

Legay C, Bon S, Vernier P, Coussens F and Massoulie J (1993) *J. Neurochem.* 60:337-346.

Leventer SM, Wulfert E and Hanin I (1987) *Neuropharmacol.* 26:361-365.

Liang P and Pardee AB (1992) *Science* 257:967-971.

Liao J, Mortensen V, Nørgaard-Pedersen B, Koch C and Brodbeck U (1993) *Eur. J. Biochem.* 215:333-340.

Liao J. Heider H, Sun MC and Brodbeck U (1992) *J. Neurochem.* 58:1230-1238.

Lockridge O (1990) *Pharmacol. Ther.* 47:35-60.

Loewenstein Y, Gnatt A, Neville LF and Soreq H (1993) *J. Mol. Biol.* 234:289-296.

Manitone CR, Fisher A and Hanin I (1981) *Science* 213:579-580.

McGuire MC, Nogueira CP, Bartels CF, Lightstone H, Hajra A, van der Spek AFL, Lockridge O and La Du BN (1989) *Proc. Natl. Acad. Sci USA* 86:953-957.
Morris RGM, Garrud P, Rawlins JNP and O'Keefe J (1981) *Nature* 297: 681-682.
Murrin, LC et al. (1980) *Pharmacol.* 21:132-140.
Neville LF, Gnatt A, Loewenstein Y and Soreq H (1990) *J. Neurosci Res.* 27:452-460.
Neville LF, Gnatt, Loewenstein Y, Seidman S, Ehrlich G and Soreq H (1992) *EMBO J.* 11:1641-1649.
Ohlendieck K, Ervasti JM, Matsumura K, Kahl SD, Levelille CJ and Campbell KP (1991) *Neuron* 7:499-508.
Ordentlich A, Barak D, Kronman C, Flashner Y, Leitner M, Ariel N, Cohen S, Velan B and Shafferman A (1993) *J. Biol. Chem.* 268:17083-17095.
Ott P, Lustig A, Brodbeck U and Rosenbusch JP (1982) *FEBS Lett.* 138:187-189.
Prody CA, Zevin-Sonkin D, Gnatt A, Goldberg O and Soreq H (1987) *Proc. Natl. Acad. Sci USA* 84:3555-3559.
Quinn D (1987) Chem. Rev. 87:955-979.
Raveh L, Grunwald J, Marcus D, Papier Y, Cohen E and Ashani Y (1993) *Biochem. Pharmacol.* 45:2465-2474.
Rosenberry TL (1975) *Adv. Enzymol.* 43:1-4-210.
Sandberg K, Hanin I, Fisher A and Coyle JT (1984) *Brain Res.* 293:49-55.
Schwarz, M, D Glick, Y Loewenstein, H Soreq (1995a) *Pharmacol. Therap.* 67:283-322.
Schwarz, M, Y Loewenstein-Lichtenstein, D Glick, J Liao, B Nørgaard-Pedersen, H Soreq (1995b) *Molec. Brain Res.* 31:101-110.
Seidman S, Ben Aziz-Aloya R, Timberg R, Loewenstein Y, Velan B, Shafferman A, Liao J, Nørgaard-Pedersen B and Soreq H (1994) *J. Neurochem.* 62:1670-1681.
Seidman, S, M Sternfeld, R Ben Aziz-Aloya, R Timberg, D Kaufer-Nachum, H Soreq, (1995) *Mol. Cell. Biol.* 14:459-473.
Shafferman A, Velan B, Ordentlich A, Kornman C, Grosfeld H, Leitner M, Flashner Y, Cohen S, Barak D and Ariel N (1992) *EMBO J.* 11:3561-3568.
Shapira M, Seidman, S, Sternfeld M. Timberg R, Kaufer D, Patrick J and Soreq H (1994) *Proc. Natl. Acad. Sci. USA* 91:9072-9076.
Simpson CV, Ruwe WD and Myers RD (1994) *Neurosci. Behavior. Rev.* 18:1-20.
Soreq H and Zakut H (1993) *Human Cholinesterases and Anticholinesterases*, Academic Press, San Diego.
Soreq H, Ben-Aziz R, Prody CA, Seidman S, Gnatt A, Neville L, Lieman-Hurwitz J, Lev-Lehman E, Ginzberg D, Lapidot-Lifson Y and Zakut H (1990) *Proc. Natl. Acad. Sci. USA* 87:9688-9692.
Taylor P (1990) In LS Goodman, AG Gilman, TW Rall, AS Nies and P Taylor (eds.) *Pharmacological Basis of Therapeutics*, Macmillan Publishing Co., New York, 131-147.
Velan B, Grosfeld H, Kronman C, Leitner M, Gozes Y, Lazar A, Flashner Y, Marcus D, Cohen S and Sharfferman A (1991a) *J. Biol. Chem.* 266:23977-23984.
Velan B, Kronman C, Grosfeld H, Lietner M, Gozes Y, Flashner Y, Sery T, Cohen S, Ben-Aziz R, S Seidman S, Shafferman A and Soreq H (1991b) *Cell. Mol. Neurobiol.* 11:143-156.
Vellom DC, Radic Z, Li Y, Pickering NA, Camp S and Taylor P (1993) *Biochemistry* 32:12-17.
Welsh J, Chada K, Dalal S, Cheng R, Ralph D and McClelland M (1992) *Nucl. Acids Res.* 20:4965-4970.
Whittaker M (1986) *Cholinesterase*, Karger, Basel.
Willems JL, DeBisschop HC, Verstraete AG, Declerck C, Christiaens Y, Vanscheeuwyck P, Buylaert WA, Vogelaers D and Colardyn F (1993) *Arch. Toxicol.* 67:79-84.
Wilson IB (1954) In WD McElroy and B Glass (eds.) *The Mechanism of Enzyme Catalysis,* Johns Hopkins Press, Baltimore.
Winker MA (1994) *J. Am. Med. Assn.* 271:1023-1024.
Wurtman RJ (1992) *Trends Neurosci.* 15:117-122.
Yu J, Thomson R, Huestis PW, Bjelajac VM and Crinella FM (1989) *Physiol. Behav.* 45:133-144.

CHOLINERGIC DRUG RESISTANCE AND IMPAIRED SPATIAL LEARNING IN TRANSGENIC MICE OVEREXPRESSING HUMAN BRAIN ACETYLCHOLINESTERASE

Christian Andres, Rachel Beeri, Tamir Huberman, Moshe Shani and Hermona Soreq

Introduction

Appropriate functioning of the cholinergic synapse requires a precise balance of its elements. Important contributors towards this balance are the acetylcholine (ACh) synthesizing enzyme choline acetyltransferase, the hydrolyzing enzyme acetylcholinesterase (AChE) and ACh receptors (Taylor, 1990). Balanced cholinergic neurotransmission is disrupted in several pathological situations. For example, organophosphorus (OP) AChE inhibitors like agricultural insecticides or chemical warfare agents lead to increased ACh levels which cause hypothermia, tremor and muscle paralysis (Soreq and Zakut, 1993; Schwarz et al., 1995). Inversely, the level of muscle nicotinic ACh receptor decreases in myasthenia gravis, due to autoimmune antibodies blocking these receptors (Drachman, 1987). Moreover, death of cholinergic neurons and subsequent cholinergic imbalance appears and worsens progressively in the most common cause of human dementia, Alzheimer's disease, as well as in humans with Down's syndrome (Katzman, 1986; Coyle et al., 1988). This explains the efforts invested in creating animal models with cholinergic neurotransmission deficits: surgical lesions (Cuello et al., 1990), chemical lesions (Mantione et al., 1981; Lev-Lehman et al., 1995), selection of animal strains (Bentivoglio et al., 1994), genetic manipulation of chromosome 16, the equivalent of human trisomy 21 in mouse (Holtzman et al., 1992) or knock-out of specific acetylcholine receptor subtypes (Picciotto et al., 1995). While all of these models display transient or continuous defects in cholinergic neurotransmission, none combines cholinergic imbalance with progressive cognitive impairments, which are the hallmarks of Alzheimer's disease.

The experimental approach

To examine the in vivo consequences of synaptic cholinergic imbalance we chose to overexpress AChE in transgenic animals. First, we expressed human AChE in transiently transgenic embryos of the South-African frog Xenopus laevis (Ben Aziz-Aloya et al., 1993). The recombinant human enzyme accumulated in frog neuromuscular junctions, increased their post-synaptic length and deepened their synaptic cleft (Shapira et al., 1994; Seidman et al., 1995). The structural alterations observed in frog neuromuscular junctions resembled those reported for cholinergic brain synapses in patients at the early stages of Alzheimer's disease (DeKosky et al., 1990). This, in turn, raised the possibility that the latter changes as well could perhaps be caused by imbalanced cholinergic neurotransmission. To examine the consequences of congenital cholinergic imbalance onto mammalian brain functioning, we created transgenic mice expressing human AChE in brain neurons and examined pharmacological responses and cognitive functions in these animals. Our findings demonstrate that AChE overexpressing mice acquire

resistance to cholinergic drugs and undergo selective progressive decline in their capacity for spatial learning and memory. This, in turn, suggests the use of these mice to search for the regulatory genes whose functioning is modified in conjunction with the cognitive deterioration characteristic of diseases associated with cholinergic imbalance.

Results and discussion

Efficient expression and/or high copy numbers of the ACHE transgene may be lethal

Two DNA constructs encoding the brain and muscle form of human AChE (Ben Aziz-Aloya et al., 1993) were employed for microinjecting mouse eggs. One of these included the potent ubiquitous promoter of cytomegalovirus (CMV) (Schmitt et al., 1990) and the other a 596 nucleotide long fragment from the authentic promoter of the human ACHE gene, followed by its first intron and the same coding sequence (HpACHE). Figure 1 presents these two DNA sequences and the transcription factor binding sites identified in them. Interestingly, all of the transcription factor binding sites in the CMV promoter-enhancer sequence also exist in the human ACHE promoter, although not necessarily in the same copy numbers and positions within each promoter. Moreover, the ACHE promoter includes at least 4 additional sequence motifs for binding transcription factors that are not recognized by the CMV promoter. These include nervous system, muscle and embryonically active factors (Fig. 1); however, myogenic factors were recently found to be ineffective with the closely homologous promoter of the mouse ACHE gene (Mutero et al., 1995), suggesting that at least part of the transcription factor binding sites in HpACHE are inactive.

Both HpACHE and the CMV promoter were previously found to direct human AChE production in Xenopus oocytes and embryos, however, the CMV promoter was ca. 10-fold more efficient in its capacity to direct production of the AChE protein than the HpACHE human promoter (Ben Aziz-Aloya et al., 1993; Seidman et al., 1994). When injected into fertilized eggs of FZB/N mice as previously described (Shani, 1985), integration of the transgene into the host genome of founder mice and their progeny was only observed in 4 cases out of 110 microinjections (Table I). One viable founder mouse carried the CMVACHE transgene, whereas microinjection of HpACHE DNA yielded 3 viable pedigrees with 2, 10 and 15 copies of the transgene (Beeri et al., 1995).

Expression of the transgene was examined in mouse tissues by RNA extraction followed by PCR amplification (Beeri et al., 1994). Species-specific PCR primers were designed to distinguish between human and mouse ACHEmRNA transcripts. Transgenic mRNA was only expressed in that pedigree with the lowest amount (2 copies) of HpACHE DNA. The limited number of viable AChE-transgenic mice and the yet lower success in obtaining ACHEmRNA expression suggest that AChE overexpression may be lethal above certain levels. Moreover, these findings suggest that the additional

consensus motifs present in the HpACHE DNA have negative roles, suppressing AChE production. However, the mouse pedigree with ACHEmRNA transcription developed and proliferated normally, pertaining HpACHE DNA with unmodified organization and copy number. All subsequent experiments were carried out with apparently homozygous mice from this pedigree.

Transgenic HpACHE is not expressed outside the CNS

Reverse transcription and PCR amplification (Beeri et al., 1994) revealed that unlike the normal ACHE gene, the transgene is not expressed in muscle, adrenal and bone marrow. In contrast, both human and mouse ACHEmRNA transcripts were observed in dissected brain regions of the transgenic mice. There was no interference with the levels and alternative splicing patterns of host ACHEmRNAs, both remained apparently similar to those observed by others (Rachinsky et al., 1990).

When fixed brain sections from the mice were subjected to in situ hybridization with digoxigenin ACHEcRNA, followed by detection with alkaline phosphatase-conjugated anti-digoxigenin antibody (Boehringer/ Mannheim), ACHEcRNA labeling was seen in the same brain neurons in transgenics and controls (Beeri et al., 1995). Particularly intense labeling was observed in cell bodies in the basal forebrain and brainstem nuclei of the transgenic mice and in the cholinoceptive hippocampal neurons, especially in the CA1-CA2 region. Thus, the HpACHE transgene was expressed in the central nervous system neurons but not in the peripheral tissues normally expressing this gene in mammals. This is consistent with findings of others, who observed that separable promoter elements control neurogenic expression of pan-neural genes (i.e. Drosophila, snail) in the central and peripheral nervous system (Ip et al., 1994).

Multimeric transgenic AChE reaches cholinergic brain synapses

To search for multimeric assembly of the transgenic enzyme, brain region homogenates were subjected to sucrose gradient centrifugation followed by adhesion to immobilized human-selective anti-AChE monoclonal antibodies and measurements of acetylthiocholine hydrolysis levels. AChE from the brain of control and transgenic mice displayed similar sedimentation profiles, demonstrating unmodified assembly into multimeric enzyme forms. Up to 50% of the active enzyme in basal forebrain (Fig. 2) adhered to monoclonal antibodies specific to human AChE. Moreover, catalytic activity measurements of antibody-immobilized AChE from tissue homogenates revealed that the transgenic enzyme was present in higher levels within the basal forebrain, whereas more limited amounts of this protein were detected in cortex, brainstem, cerebellum and spinal cord extracts. There were no age-dependent changes in this pattern. Gel electrophoresis followed by cytochemical staining of enzyme activity (Seidman et al., 1995) revealed similar migration for AChE from the brain of transgenic and control mice, indicating comparable glycosylation patterns (Fig. 3).

Cytochemical staining of AChE activity was observed in 50 μm brain sections from transgenic mice in all of the areas that showed high AChE activity in homogenate assays. Intense staining was detected in the neostriatum, pallidum and hippocampus. Thus, the extent of excess AChE reflected the brain region distribution characteristic of the primate brain, suggesting that the transgenic mice retained the initial species-specific capacity to regulate human AChE production.

Transgenic AChE selectively alters thermoregulatory responses to cholinergic and serotonergic agonists

Among other functions, cholinergic neurotransmission is involved in controlling body temperature in mammals (Simpson et al., 1994). We ascertained that thermoregulation was properly retained in the transgenic mice by checking their cold adaptation, which remained unchanged. We then examined hypothermic responses of these transgenic mice to intraperitoneally-injected hypothermia-inducing cholinergic drugs. Core body temperature was reduced by a limited extent and for shorter duration in the transgenic as compared with control mice. This was first examined with the potent AChE inhibitor diethyl p-nitrophenyl phosphate (paraoxon), the toxic metabolite of the agricultural insecticide parathion (Table II). Most importantly, transgenic mice exposed to 1 mg/kg dose of paraoxon retained apparently normal locomotor activity and behavior, while control mice subjected to this dose presented symptoms characteristic of cholinergic overstimulation.

In addition to their improved, yet predictable, capacity for scavenging of the anti-AChE paraoxon, the transgenic mice also displayed resistance to the hypothermic effects of oxotremorine, an effective agonist of muscarinic receptors (Clement, 1991). They were also resistant to the less potent effect of nicotine, and to the serotonergic agonist 8-hydroxy-2-(di-*n*-propylamino) tetralin (8-OH-DPAT), but not to the α_2-adrenergic agonist clonidine (Table II). Serotonergic agonists may act directly on serotonin receptors, involved in thermoregulation (Simpson et al., 1994). However, they may also interact with ACh receptors (Garcia-Colunga and Miledi, 1995). Therefore, the altered drug responses may reflect either transcriptional or post-transcriptional changes in ACh (and perhaps serotonin) receptors within the brain of transgenic mice.

Transgenic AChE does not affect open-field behavior but induces progressive decline in spatial learning

When compared to matched groups of non-transgenic control mice at the age of 1, 2-3 and 5-7 months, AChE-transgenic mice retained normal behavior in an open field. They covered the same space and distance as their control counterparts (Fig. 4). In addition, these mice did not display more anxiety than controls, as evaluated in the frequency of defecation incidents and grooming behavior.

In contrast, memory and learning tests revealed clear differences between transgenic and control mice. We first used the hidden platform version of the Morris water maze (Morris et al., 1981), in which mice are

expected to use their spatial orientation to find a platform submerged under opaque water and escape a swimming task. The transgenics' performance in this test was apparently normal at the age of 4 weeks, when they needed a similar time (defined as the escape latency) to reach the platform as age-matched control mice. At the age of 2-3 months, transgenics already needed more time at the 4th day of training compared to controls. Finally, at the age of 6 months, the escape latency of the transgenic mice was significantly longer than that of controls, showing that they failed to find the platform even after 16 training sessions (Fig. 4). That this deterioration pattern was not caused by locomotion deficiencies was clear from the normal performance of these mice in the open field test (Fig. 4). Moreover, the progressive decline of these transgenic mice in spatial learning and memory was more pronounced than the defects observed in mice with knocked-out glutamate receptor 1 (Conquet et al., 1994), NMDA receptor ε1 (Sakimura et al., 1995), fyn (Grant et al., 1992), calcium calmodulin kinase II (Silva et al., 1992) or CREB-binding protein (Bourtchuladze et al., 1994). This, in turn, suggests that a more substantial, yet delayed, and progressive perturbation in learning and memory occurred in our mice than in any of these knock-out strains. Interestingly, the defects observed in our mice resembled those reported in mice treated with blockers of central muscarinic or nicotinic acetylcholine receptors (i. e. atropine, scopolamine or mecamylamine) (McNamara and Skelton, 1993).

An earlier, persistent defect was observed in the visible platform version of the Morris water maze. In this test, mice are trained to escape the swimming task by using short-distance cues. They can then climb on a visible platform decorated by a flag and a paper cone. The transgenics' performance in this test was poor from the age of 4 weeks onward (Fig. 4). This could perhaps be due to early-onset difficulties in short-distance vision or reflect abnormal avoidance behavior. That the defect in this visual memory test occurred in these transgenic mice when they still succeeded in the hidden platform test, demonstrates a dissociation between the visual and the hidden platform test performances.

Implications for future research

The transgenic mice expressing human AChE can serve as a novel appropriate model system for several lines of research. First and foremost, they can be used as a model to unravel the exact contribution of cholinergic neurotransmission toward learning and memory processes, using electrophysiological tools and behavioral tests. In addition, these mice should be of major assistance for identifying the molecular regulatory mechanisms involved in maintenance of normal cholinergic neurotransmission. These two lines of investigation can therefore lead to development of new physiological concepts involved in control over body temperature as well as in memory impairments in mammals. At the clinical level, such new concepts should be of primary importance toward the development of new strategies for diagnosis and treatment of diseases associated with cholinergic deficits, like Alzheimer disease.

Conclusion

Expression of human AChE under control of the authentic human promoter and first intron was limited to central nervous system neurons of transgenic mice. This expression changed responses to hypothermia-inducing drugs acting on cholinergic and probably serotonergic receptors. In addition, it created a progressive spatial learning and memory impairment. In contrast, the open field behavior of these transgenic animals remained normal. These findings suggest that subtle alterations in the cholinergic balance may cause physiologically-observable changes and contribute by itself to the memory deterioration in at least part of the patients with cholinergic deficits.

Acknowledgments: We thank Drs. T. Bartfai (Stockholm), J. Crawley (Washington, DC), A. Ungerer (Strasbourg) and H. Zakut (Tel Aviv) for helpful discussions and Dr. B. Nørgaard-Pedersen (Copenhagen) for antibodies. This work was supported by USARMRDC grant 17-94-C-4031 and the Israel Academy of Sciences and Humanities (to H. S.). C. A. was a recipient of an INSERM, France fellowship, and an INSERM-NCRD exchange fellowship with the Israel Ministry of Science and Arts. The behavioural experiments were performed in the Smith Foundation Institute for Psychobiology at the Life Sciences Institute in the Hebrew University.

References

Beeri, R., Andres, C., Lev-Lehman, E., Timberg, R., Huberman, T., Shani, M. And Soreq (1995) Transgenic expression of human acetylcholinesterase induces progressive cognitive deterioration in mice. Current Biology, in press.

Beeri, R., Gnatt, A., Lapidot-Lifson, Y., Ginzberg, D., Shani, M., Soreq, H. and Zakut, H. (1994) Testicular amplification and impaired transmission of human butyrylcholinesterase cDNA in transgenic mice. Human Reprod., 9: 284-292.

Ben Aziz-Aloya, R., Seidman, S., Timberg, R., Sternfeld, M., Zakut, H. and Soreq, H. (1993) Expression of a human acetylcholinesterase promoter-reporter construct in developing neuromuscular junctions of Xenopus embryos. Proc Natl Acad Sci USA, 90:2471-2475.

Bentivoglio, A.R., Altavista, M.C., Granata, R. and Albanese, A. (1994) Genetically determined cholinergic deficiency in the forebrain of C57BL/6 mice. Brain Res., 637:181-189.

Bourtchuladze, R., Frenguelli, B., Blendy, J., Cioffi, D., Schutz, G. and Silva, A. J. (1994) Deficient long-term memory in mice with a targeted mutation of the cAMP-responsive element-binding protein. Cell, 79: 59-68.

Clement, J.G. (1991) Effect of a single dose of an acetylcholinesterase inhibitor on oxotremorine- and nicotine-induced hypothermia in mice. Pharmacol. Biochem. Behav., 39:929-934.

Conquet, F., Bashir, Z.I., Davies, C.H., Daniel, H., Ferraguti, F., Bordi, F. *et al.* (1994) Motor deficit and impairment of synaptic plasticity in mice lacking mGluR1. Nature, 372:237-243.

Coyle, J. T., Oster-Granite, M. L., Reeves, R. H. and Gearhart, J. D. (1988) Down syndrome, Alzheimer's disease and the trisomy 16 mouse. Trends in Neurosci., 11:390-394.

Cuello, A.C., Garofalo, L., Maysinger, D., Pioro, E.P. and Da Silva, A.R. (1990) Injury and repair of central cholinergic neurons. Prog. Brain Res., 84:301-311.

DeKosky, S.T. and Scheff, S.W. (1990) Synapse loss in frontal cortex biopsies in Alzheimer's disease: correlation with cognitive severity. Ann. Neurol. 27:457-464.

Drachman, D.B. (1987) Myasthenia Gravis: Biology and Treatment. Annals of the New York Academy of Sciences, Vol. 505.

Garcia-Colunga, J. and Miledi, R. (1995) Effects of serotonergic agents on neuronal nicotinic acetylcholine receptors. Proc. Natl. Acad. Sci. USA, 92: 2919-2923.

Grant, S.G.N., O'Dell, T.J., Karl, K.A., Stein ,P.L., Soriano, P. and Kandel, E.R. (1992) Impaired long-term potentiation, spatial learning, and hippocampal development in fyn mutant mice. Science, 258:1903-1909.

Holtzman, D.M., Li, Y., DeArmond, S.J., McKinley, M.P., Gage, F.H., Epstein, C.J. and Mobley, W.C. (1992) Mouse model of neurodegeneration: atrophy of basal forebrain cholinergic neurons in trisomy 16 transplants. Proc Natl Acad Sci USA, 89:1383-1387.

Ip, Y.T., Levine, M. and, Bier E. (1994) Neurogenic expression of *snail* is controlled by separable CNS and PNS promoter elements. Development, 120:199-207.

Katzman, R. (1986) Alzheimer's disease. N. Engl. J. Med., 314:962-973.

Lev-Lehman, E., El-Tamer, A., Yaron, A., Grifman, M., Ginzberg, D., Hanin, I. and Soreq, M. (1994) Cholinotoxic effects on acetylcholinesterase gene expression are associated with brain-region specific alterations in G,C-rich transcripts. Brain Res., 661:75-82.

McNamara, R. K. and Skelton, R. W. (1993) The neuropharmacological and neurochemical basis of place learning in the Morris water maze. Brain Res. Reviews 18:33-49.

Mantione, C.R., Fisher, A. and Hanin, I. (1981) The AF64A-treated mouse: possible model for central cholinergic hypofunction. Science, 213:579-580.

Morris, R.G.M., Garrud, P., Rawlins, J.N.P. and O'Keefe, J. (1981) Place navigation impaired in rats with hippocampal lesions. Nature, 297:681-682.

Mutero, A., Camp, S. and Taylor, P. (1995) Promoter elements of the mouse acetylcholinesterase gene. J. Biol. Chem., 270:1866-1872.

Picciotto, M.R., Zoli, M., Léna, C., Bessis, A., Lallemand, Y., LeNovère, N. *et al.* (1995) Abnormal avoidance learning in mice lacking functional high-affinity nicotine receptor in the brain. Nature, 374:65-67.

Rachinsky, T.L., Camp, S., Li, Y., Ekström, T.J., Newton, M. and Taylor, P. (1990) Molecular cloning of mouse acetylcholinesterase: tissue distribution of alternatively spliced mRNA species. Neuron, 5:317-327.

Sakimura, K., Kutsuwada, T., Ito, I., Manabe, T., Takayama, C., Kushiya, E., Yagi, T. et al. (1995) Reduced hippocampal LTP and spatial learning in mice lacking NMDA receptor ε1 subunit. Nature 373:151-155.

Schmitt, E.V., Christoph, G., Zeller, R. and Leder, P. (1990) The cytomegalovirus enhancer: a pan-active control element in transgenic mice. Mol. Cell Biol., 10:4406-4411.

Schwarz, M., Glick, D., Loewenstein, Y. and Soreq, H. (1995) Engineering of human cholinesterases explains and predicts diverse consequences of

administration of various drugs and poisons. Pharmacol. Therap. (in press).

Seidman, S., Ben Aziz-Aloya, R., Timberg, R., Loewenstein, Y., Velan, B., Shafferman, A., Liao, J., Nørgaard-Pedersen, B., Brodbeck, U. and Soreq, H. (1994) Overexpressed monomeric human acetylcholinesterase induces subtle ultrastructural modifications in developing neuromuscular junctions of Xenopus laevis embryos. J. Neurochem., 62:1670-1681.

Seidman, S., Sternfeld, M., Ben Aziz-Aloya, R., Timberg, R., Kaufer-Nachum, D. and Soreq, H. (1995) Synaptic and epidermal accumulations of human acetylcholinesterase are encoded by alternative 3'-terminal exons. Mol. Cell Biol., 14:459-473.

Shani, M. (1985) Tissue-specific expression of rat myosin light-chain 2 gene in transgenic mice. Nature, 314:283-286.

Shapira, M., Seidman, S., Sternfeld, M., Timberg, R., Kaufer, D., Patrick, J. and Soreq, H. (1994) Transgenic engineering of neuromuscular junctions in Xenopus laevis embryos transiently overexpressing key cholinergic proteins. Proc. Natl. Acad. Sci. USA, 91:9072-9076.

Silva, A.J., Paylor, R., Wehner, J.M. and Tonegawa, S. (1992) Impaired spatial learning in α–calcium-calmodulin kinase II mutant mice. Science, 257:206-211.

Simpson, C.V., Ruwe, W.D. and Myers, R.D. (1994) Prostaglandins and hypothalamic neurotransmitter receptors involved in hypothermia: a critical evaluation. Neurosci. Behavior Rev., 18:1-20.

Soreq, H. and Zakut, H. (1993) Human Cholinesterases and Anticholinesterases. Academic Press, San Diego.

Taylor, P. (1990) Anticholnesterase agents. In: L.S. Goodman, A.G. Gilman, T.W. Rall, A.S. Nies and P. Taylor (Eds.), Pharmacological Basis of Therapeutics, Macmillan Publishing Co., New York, 1990, pp. 131-147.

Promoters	CMV	HpACHE
Number of microinjections	70	40
Number of pedigrees carrying the transgene	1	3
Number of DNA copies in each pedigree	3	2-10-15
Pedigrees expressing the transgene	0	1- 0 - 0

Table I: Effect of promoter selection and transgene copy numbers on the creation of human AChE transgenic mice (CMV: cytomegalovirus promoter, HpACHE: human AChE promoter). See text for details.

Drugs	Dose (mg/kg)	Minimum temperature in ° C			Area under baseline in ° C x min			Number of animals	
		C	T	Signif	C	T	Signif	C	T
Paraoxon	1	30.4	32.4	-	2868	1505	-	1	1
Oxotremorine	0.15	29.2 ± 0.9	32.3 ± 0.3	0.02	909 ± 211	392 ± 91	0.04	3	3
Nicotine	10	33.8 ± 0.6	35.5 ± 0.2	0.006	160 ± 57	93 ± 14	ns	4	4
8OH-DPAT	1	34.8 ± 0.5	35.5 ± 0.3	ns	273 ± 97	78 ± 25	0.02	4	3
Clonidine	0.5	31.4 ± 1.2	31.6 ± 0.8	ns	1338 ± 207	1696 ± 296	ns	3	3

Table II: Effects of different hypothermia-inducing drugs administered intra-peritoneally to control (C) and transgenic (T) 6 months old mice. The baseline for the area above the curve of experimental points is a horizontal line drawn through the temperature of the animals before the injection. Results are expressed in means ± standard deviations, except for the high dose paraoxon experiment, which was performed only once. Statistical significance (signif) was tested with Student's t-test.

LEGENDS TO FIGURES

Fig. 1 Comparison of the human ACHE and the CMV sequences used to direct AChE production in transgenic mice.

Sequences of the two promoters are presented with schematic localizations of consensus sequence motifs for binding transcription factors. Sites common to both promoters are presented in the middle, sequences unique to HpACHE are shown on top. For details of each of these motifs, see Ben Aziz-Aloya et al., (1993).

The transcribed sequence of the human ACHE gene is presented on the right side and was linked (arrows) to each of these promoters. Exons are noted E1 to E6. Note that E1 and intron 1 (I1) were only included in the HpACHE construct with the human ACHE promoter. Open reading frame is noted by a dashed underline. Length of each of the promoter sequences is noted in base pairs. For the transcribed regions of HpACHE, a single bar in kb is included.

Fig. 2. AChE activity in brain and different organs.

AChE activities were measured with acetylthiocholine as substrate (Seidman et al., 1994). AChE of human origin was quantified by binding extracts from the noted tissues and brain regions to specific anti-human AChE monoclonal antibodies.

Fig. 3. Non denaturing gel electrophoresis of AChE.

Brain homogenates from the noted sources were prepared in the presence of Triton X-100 and were run on a non-denaturing 7% polyacrylamide gel. AChE activity was revealed by an acetylthiocholine precipitating method as described elsewhere (Seidman et al., 1995).

Fig. 4. Behavioural tests

A. Open field

Mice spent 5 minutes in a void 60 X 60 cm box and their walkpath was traced. The walked distance and the explored fraction of the box floor were calculated thereafter.

B. Water maze

Mice were tested in a water maze with a hidden platform in a fixed location (top) or with a visible platform in alternate location for each test (bottom). They were introduced into alternating corners of the maze in 4 daily sessions during 4 consecutive days. Means of daily escape latencies are presented for the 4th day of transgenic ($n = 6$ to 10) and age-matched controls. Stars note statistically significant different latencies (ANOVA followed by Neuman Keuls test, $p<0.05$).

Human ACHE Promoter

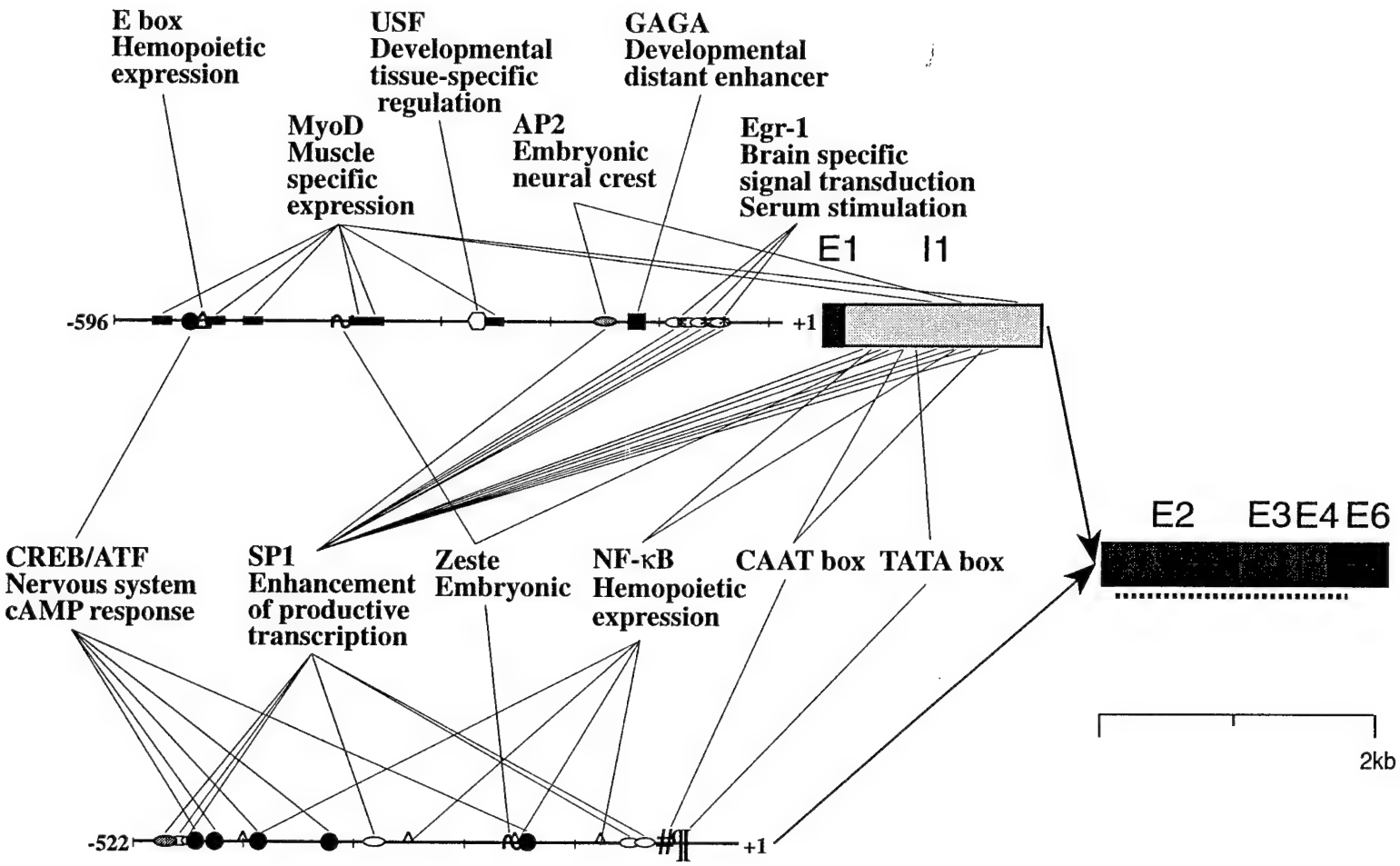

CMV Enhancer-Promoter

Fig 1

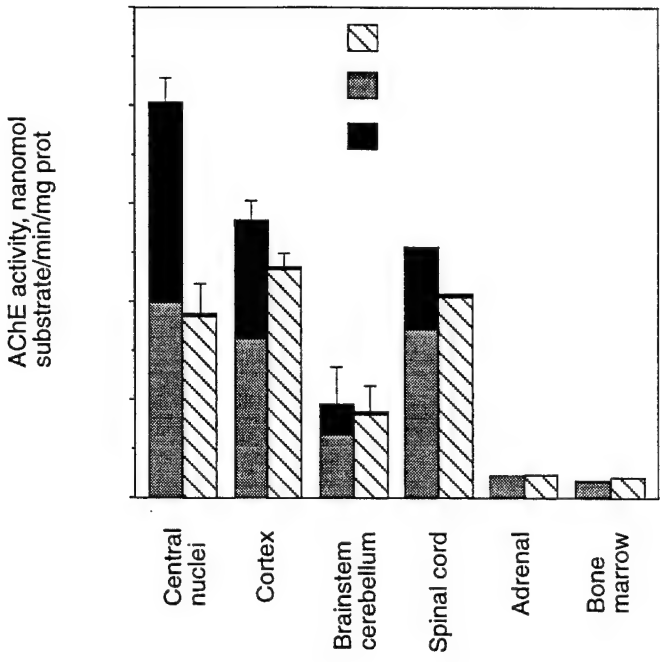
AChE activity, nanomol substrate/min/mg prot
Central nuclei
Cortex
Brainstem cerebellum
Spinal cord
Adrenal
Bone marrow

Fig 2

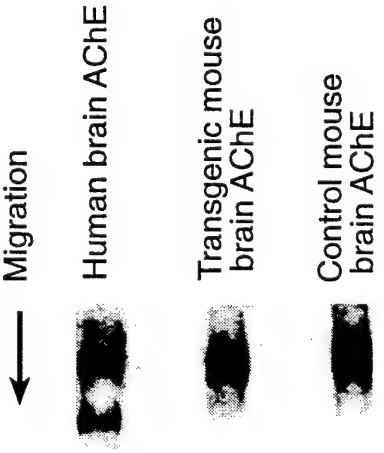
Migration
Human brain AChE
Transgenic mouse brain AChE
Control mouse brain AChE

Fig 3

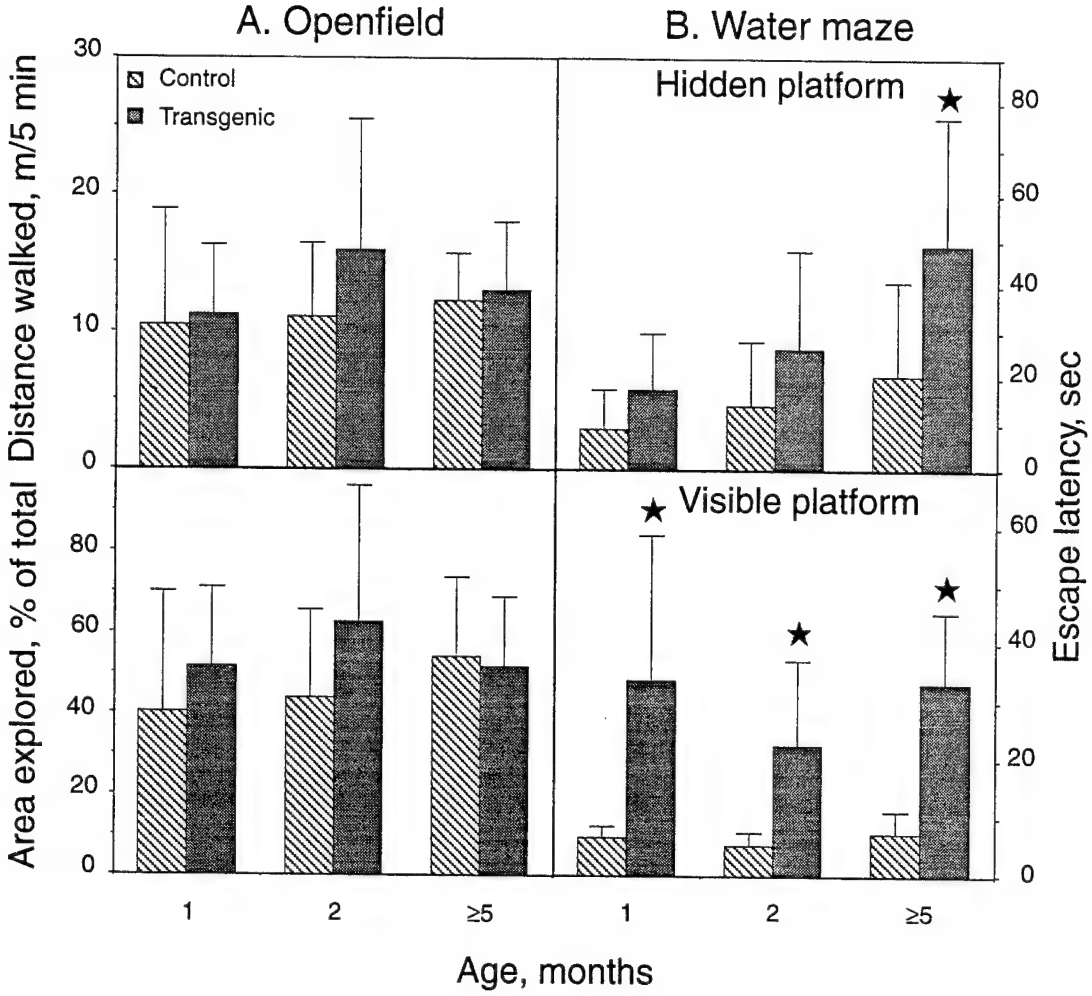
A. Openfield
B. Water maze
Control
Transgenic
Hidden platform
Visible platform
Area explored, % of total Distance walked, m/5 min
Escape latency, sec
Age, months
1
2
≥5
0
10
20
30
40
60
80

Fig 4

Human Reproduction vol.9 no.2 pp.284–292, 1994

Testicular amplification and impaired transmission of human butyrylcholinesterase cDNA in transgenic mice

Rachel Beeri[1], Averell Gnatt[1,4], Yaron Lapidot-Lifson[1,3], Dalia Ginzberg[1], Moshe Shani[2], Hermona Soreq[1] and Haim Zakut[3,5]

[1]Department of Biological Chemistry, The Life Sciences Institute, The Hebrew University, Jerusalem 91904, [2]Department of Genetic Engineering, The Institute of Animal Science, Agricultural Research, 906, Beit Dagan 50250, [3]Department of Obstetrics and Gynaecology, The Sackler Faculty of Medicine, Tel-Aviv University, The Edith Wolfson Medical Centre, Holon (58100), Israel

[4]Present address: Department of Cell Biology, Stanford University School of Medicine, Stanford, CA 94305–5400, USA

[5]To whom correspondence should be addressed

Gene amplification occurs frequently in tumour tissues yet is, in general, non-inheritable. To study the molecular mechanisms conferring this restraint, we created transgenic mice carrying a human butyrylcholinesterase (BCHE) coding sequence, previously found to be amplified in a father and son. Blot hybridization of tail DNA samples revealed somatic transgene amplifications with variable restriction patterns and intensities, suggesting the occurrence of independent amplification events, in 31% (11/35) of mice from the FII generation but in only 3.5% (2/58) of the FIII and FIV generations. In contrast, >10-fold amplifications of the BCHE transgene and the endogenous acetylcholinesterase and c-*raf* genes appeared in both testis and epididymis DNA from >80% of FIII mice. Drastic, selective reductions in testis BCHEmRNA but not in actin mRNA were detected by the PCR amplification of testis cDNA from the transgenic mice, and apparently resulted in the limited transmission of amplified genes. The testicular amplification of the BCHE transgene may potentially represent a general phenomenon with clinical implications in human infertility.

Key words: cholinesterase/fertility/human/polymerase chain reaction/testicular gene amplification

Introduction

Gene amplification is common in eukaryotic chromosomes of tumour tissues and transfected cells (Delidakis *et al.*, 1989; Stark *et al.*, 1989). Amplification often provides cells in which it occurs with resistance to toxic ligands which bind to the over-expressed protein products of the amplified genes (Schimke, 1990). Alternatively, over-expressed proteins may support proliferation as in the case of oncogene products (Bishop, 1991) or, as found in amphibia and insects, they may be necessary for essential processes during development (Laat *et al.*, 1986). The inheritance of amplified sequences at a specific gene locus has been assessed in the present work.

Both novel point mutations (Cooper and Schmidtke, 1987) and the expansion of CGG and CTG repeats within the fragile X (Oberle *et al.*, 1991; Kremer *et al.*, 1991) and the myotonic dystrophy domains (Brook *et al.*, 1992; Harley *et al.*, 1992), are successfully transmitted to subsequent generations. In contrast, gene amplifications are, in general, non-inheritable. One exception is the heritable esterase gene amplification which provides resistance to insecticides in mosquitoes (Mouches *et al.*, 1986). In humans, the BCHE gene encoding butyrylcholinesterase (acylcholine acyl hydrolase, BCHE, EC. 3.1.1.8) was observed to be amplified in a father and son exposed to the Pro-insecticide *N*-methyl parathion, which functions through cholinesterase inhibition (Prody *et al.*, 1989). However, there was some doubt as to whether the amplified DNA was actually inherited, or whether a similar propensity for amplification in two genetically similar individuals was inherited. Subsequently, the BCHE gene, together with the related ACHE gene encoding acetylcholinesterase (acetylcholine acetyl hydrolase, ACHE, EC, 3.1.1.7) and several oncogenes were found to amplify in leukaemias (Lapidot-Lifson *et al.*, 1989) and ovarian tumours (Zakut *et al.*, 1990) and in non-cancerous disorders of haemopoietic development, such as the impaired megakaryocytopoiesis in the autoimmune disease lupus erythematosus (Zakut *et al.*, 1992). These observations make the BCHE gene particularly attractive for studies of the amplification phenomenon. Here, we describe a transgenic model for a germline BCHE gene amplification, and the developmental mechanism by which this potentially stable amplification event was selectively precluded from the pool of inherited genetic material.

Material and methods

Mouse strains and microinjection

The pSVL-CHE sequence (see Figure 1 for details) was employed for microinjection into fertilized mouse eggs which had been flushed from the oviduct of (C57BL/6J × BALB/C) FI females mated with (C57BL/6J × DBA) FI males. Manipulations of the mice and eggs, and the microinjection techniques, were as previously described (Shani, 1985).

Probes

Purified, electro-eluted probes included a 1.5 kb long *Eco*RI fragment of ACHEcDNA (Lapidot-Lifson *et al.*, 1989) and a

2.4 kb long *Pst*I−*Sac*I fragment of BCHEcDNA (Prody *et al.*, 1987). C-*raf* DNA was obtained from Amersham (Buckinghamshire, UK). SV-40 DNA was gratefully received from Professor S.Lavi (Tel-Aviv), haptoglobin cDNA-from Dr E.Zerial (Heidelberg) and the 1.4 kb *Eco*RI repetitive DNA fragment was eluted from a gel following electrophoresis of total mouse genomic DNA after digestion with *Eco*RI. All probes were labelled with [^{32}P]dATP by the random primed technique using the relevant kit from Boehringer (Mannheim, Germany).

Quantification of amplification by slot blot hybridization

Denatured genomic DNA from tail, testis or epididymis was diluted and spotted onto Gene Screen filters (NEN, Boston, MA, USA). Slot blot hybridization and wash stringency were as previously detailed (Prody *et al.*, 1989), using genomic or electro-eluted insert DNA supplemented with denatured herring testis DNA to yield a total of 2 μg DNA per slot. Signals were totally abolished following DNAse treatment but were unaffected by 0.4 N NaOH, excluding the possibility of non-specific binding due to RNA contamination. Exposure was carried out for 3 days at −70°C with an intensifying screen. DNA copy numbers were calculated as described (Lapidot-Lifson *et al.*, 1989) by using densitometric comparisons to the signals obtained with serial dilutions of the purified cDNA.

DNA blot hybridization

Genomic DNA samples digested with restriction enzymes were electrophoresed on 1.0% agarose gels, transferred to filters and subjected to hybridization under the same conditions used for the slot blot analyses. Lambda and QX174 phage DNAs cut with *Hin*dIII served for molecular weight markers. Exposure was carried out overnight.

Evaluation of sperm motility

Mouse spermatozoa extruded from dissected epididymis were placed in 50 μl drops on microscope slides and motility evaluated at 23°C, essentially as detailed elsewhere (Makler, 1991).

Results

BCHE coding sequences amplify in transgenic mice

Three out of 17 founder transgenic mice created as previously detailed (Shani, 1985) with the BCHE coding sequence, the late SV-40 promoter and late polyadenylation site (pSVL-CHE DNA, Figure 1) were shown by tail DNA hybridization to carry a single transgenic sequence hybridizing with BCHEcDNA. Two of these founders were mated with C57B1/6J mice. The FI offspring examined still carried single copies of BCHE DNA.

Two independent FII pedigrees were subsequently established (nos 12 and 40). Slot blot hybridization tail DNA demonstrated the appearance of gene amplification characterized by a wide variability in BCHE DNA copy number among FII mice (Figure 2). All mice appeared to be healthy, and no tumours could be detected in any of their tissues. Altogether 31% of the tail DNA samples from FII mice carried multiple (5−200) copies of the BCHE DNA sequence (Figure 3).

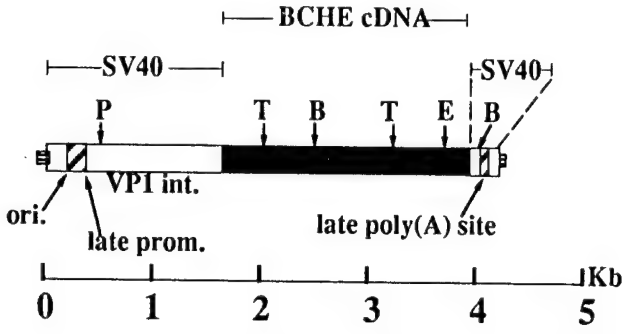

Fig. 1. The pSVL-CHE DNA construct. The 4.7 kb pSVL-CHE construct was created by ligating the 2.3 kb long human BCHE cDNA insert (Prody *et al.*, 1987), bordered by *Pst*I and *Sac*I sites, into the pSVL plasmid (Pharmacia, Sweden) constructed with parts of pBR and the SV-40 genome. The 7.2 kb circular DNA product was cut with the enzymes *Aht*II and *Nar*I to yield the linear pSVL-CHE transgene which includes CHE cDNA with upstream SV-40 origin of replication (ori.), late promoter (prom.) and VP-1 intron (int.), and with the SV-40 late polyadenylation site downstream. Short (30−70 bp) sequences from the pBR plasmid remained at both ends of this construct (hatched boxes). Restriction sites for the enzymes *Taq*I (T), *Bam*HI (B), *Pvu*II (P) and *Eco*RI (E) are noted.

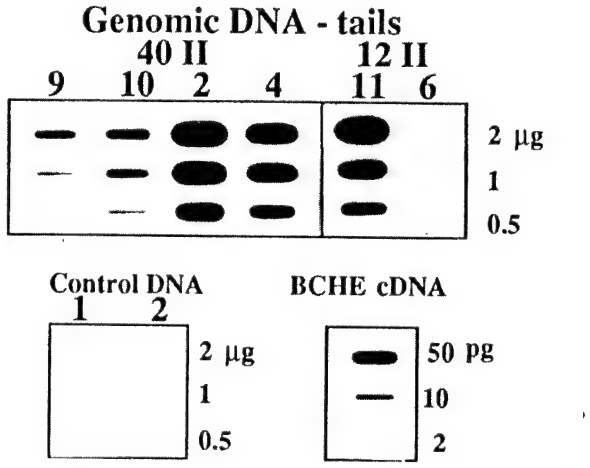

Fig. 2. Quantification of BCHE DNA amplification levels in tail DNA samples. The autoradiogram of a slot blot DNA hybridization experiment with tail DNA from six representative transgenic mice (40 II-2, 4, 9, 10 and 12 II-6, 11) and two control non-transgenic mice is shown. DNA quantities are noted. BCHE sequence copy numbers were calculated (Lapidot-Lifson *et al.*, 1989) to be ~20 and 100 for mice 40 II-10 and 12 II-11, respectively.

Variable litter sizes

Litter sizes were highly variable in the transgenic mice, with a range of 3−13 mice per litter within 11 such litters of the FI−FIV generations (Figure 3). For comparison with other transgenic mice having no DNA amplification, we recently observed a far less variable range of 10−12 mice per litter among seven litters. Thus, the mere introduction of an exogenous transgene was not sufficient to induce this variability in litter sizes. This, in turn, suggests that the amplification phenomenon may be correlated with reduced fertility. However, because of these small sample sizes, further analyses will be required to establish statistically significant causal relationships between the observed

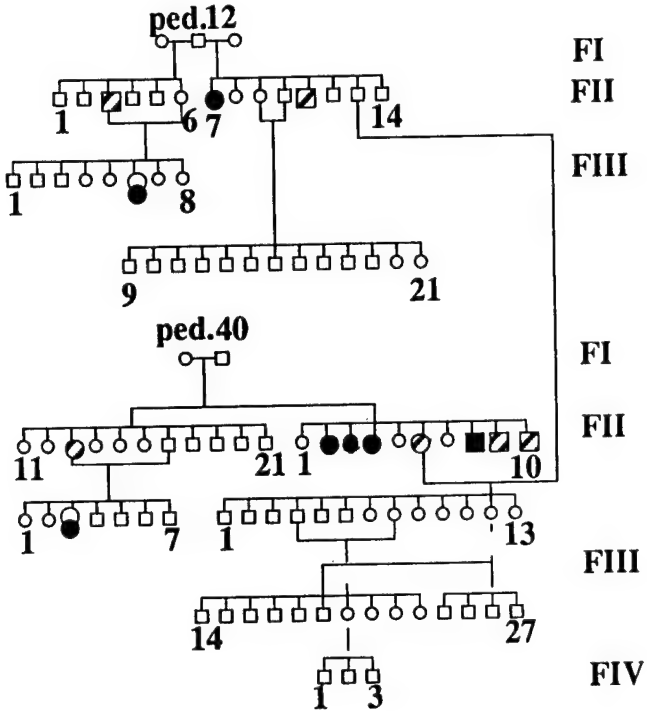

Fig. 3. Somatic amplification of CHE coding sequences in pSVL-CHE pedigrees. Tail DNA from four generations of the pSVL-CHE pedigrees 12 and 40 was examined for copy numbers of DNA sequences from the coding regions of the BCHE and ACHE genes. Generations (F) are noted by roman numerals. Squares = males, circles = females. Dashed and black signs = >20 and 100 copies of BCHE DNA, respectively. Double circle signs = co-amplified ACHE DNA, >100 copies. Open symbols = non-transgenic and low copy transgenic mice.

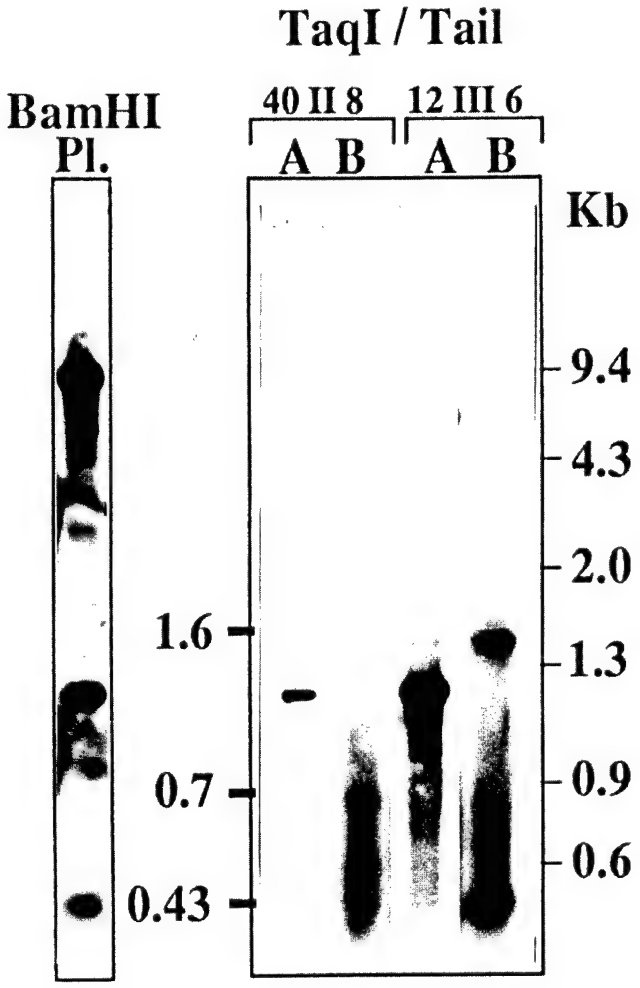

Fig. 4. Restriction fragment analysis of somatic ACHE and BCHE DNA. **Right**: 10 μg tail DNA samples from mice 40 II-8 and 12 III-6 were digested with *Taq*I, electrophoresed and subjected to DNA blot hybridization with BCHE (B) and then with ACHEcDNA (A) probes, followed by autoradiography. **Left**: 1 ng plasmid DNA which contains the human ACHE DNA was cut by *Bam*HI, electrophoresed and hybridized with the 1.5 kb ACHE cDNA probe, to reveal hybridization standard equivalent to 100 copies of the ACHE sequence.

DNA amplification and the apparently reduced fertility in these transgenic mice.

Limited transmission of the amplification and appearance of amplified ACHE gene

Only 3.6% of FIII generation mice (2/55) in six different litters displayed somatically amplified BCHE DNA sequences (Figure 3). Blot hybridization revealed major *Taq*I-digested BCHE DNA fragments of different sizes and confirmed the amplification levels in tail DNA from various mice (Figure 4). Since BCHE coding sequences co-amplify with the ACHE coding region in leukaemias (Lapidot-Lifson *et al.*, 1989), ovarian carcinomas (Zakut *et al.*, 1990) and lupus erythematosus (Zakut *et al.*, 1992), the endogenous ACHE DNA coding sequence was also examined in the pSVL CHE transgenic mice. None of the FII mice displayed somatic ACHE DNA amplification. In contrast, tail DNA from the two FIII mice carrying amplified BCHE DNA, but not other FIII mice, also carried co-amplified ACHE DNA (Figures 3 and 4). A unique *Taq*I restriction pattern was observed for the endogenous amplified DNA which displayed short DNA fragments hybridizing with the G,C-rich human [^{32}P]ACHEcDNA (Soreq *et al.*, 1990), easily distinguishable from the pattern derived from the BCHE probe (Figure 4).

Characterization of somatically amplified transgenic BCHE DNA

Variability in intensities and length of the amplified restriction fragment were observed for BCHE DNA fragments in different members of single FII litters (Figure 5A), suggesting that indepenent amplification events had occurred. Amplified BCHE DNA generally presented major BamHI fragments, possibly due to repeated arrangements of the amplification units. These fragments, sized between 4.2 and 6.5 kb each, were all larger than those expected to be derived from the transgene. Rehybridization with SV-40 DNA revealed fragments having the same sizes as the major BCHE DNA-labelled fragments (Figure 5B). The strong hybridization signal with the viral SV-40 probe implied that the amplified sequence was of exogenous origin. In addition, the non-similar intensities of signals with the BCHE and SV-40 probes imply, at least in one case, variable copy numbers of the corresponding regions in the transgene.

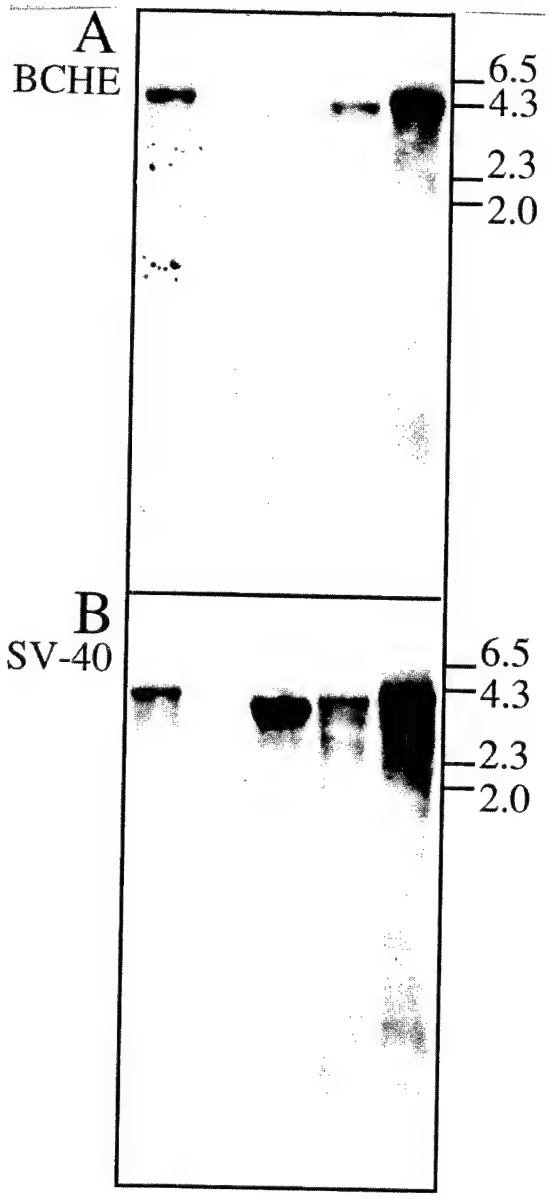

Fig. 5. *Bam*HI analysis of BCHE and SV-40 amplified sequences in tail DNA. 10 μg tail DNA samples of five females, all belonging to a single 40 FII litter were digested by *Bam*HI and subjected to blot hybridization with the BCHE cDNA probe (**A**) and the SV-40 probe (**B**). Exposure: **A** overnight, **B** over 2 days. Samples, in the following order from left to right, were derived from mice 3, 5, 6, 4 and 2 (Ped 40, FII generation). These DNA samples plus additional controls were further subjected to hybridization with *Eco*RI repetitive DNA fragment which revealed similar, multiband restriction patterns and similar labelling intensities with all the examined DNA samples (not shown), implying that the amplified sequences were limited in size and that no gross changes occurred in the host genome.

Part of the restriction sites included in the original transgene were lost in the amplified pSVL-CHE sequences [i.e. a *Bam*HI site missing in pedigree 40 FII DNAs; (Figure 5A,B)]. This could reflect rearrangements within the amplification unit, a common event in other amplified genes (Libermann *et al.*, 1985).

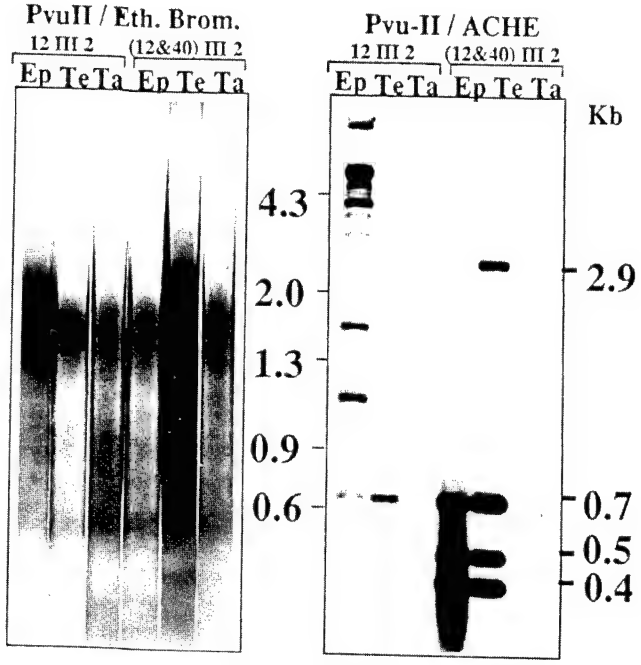

Fig. 6. Restriction fragment analysis of amplified ACHE DNA in testis and epididymis of pSVL-CHE transgenic mice. 10 μg DNA samples from tail (Ta), testis (Te) and epididymis (Ep) of mice 12 III-2 and 12/40 III-2 were digested with the restriction enzyme *Pvu*II, electrophoresed and subjected to DNA blot hybridization with the ACHE cDNA probe followed by autoradiography (**right**). Ethidium bromide staining of the digested samples (**left**) demonstrates similar amounts of DNA in all lanes. Digestion of EpDNA from sample 12 FII-2 was apparently incomplete.

Amplification of CHE genes and oncogenes in testis and epididymis

To monitor the fate of the amplified DNA between generations, we hybridized DNA from somatic and germline tissues with cDNA probes for ACHE, BCHE, the ubiquitous amplifiable oncogene c-*raf*, and the tissue-specific haptoglobin gene. Whereas neither tail (Figures 6 and 7) nor liver DNA (not shown) from any of the selected FII or FIII mice carried somatically amplified genes, all of these mice displayed BCHE, c-*raf* and SV-40 amplifications in DNA from testis and epididymis (Figure 7 and data not shown). Most of these samples also carried amplified ACHE DNA (Figures 6 and 7), and c-*fes*(*fps*) DNA (not shown). The extent of gene amplification observed with the various probes appeared similar within particular mice. In contrast, haptoglobin DNA was found in equally low copy numbers (1–3) in all tissues examined (Figure 7). The *Pvu*II restriction pattern observed for the amplified endogenous ACHE gene in the testis and epididymis of the transgenic mice (Figure 6) confirmed the enhancement in hybridization signals observed by DNA slot hybridization and resembled, in all respects, the pattern observed previously for this gene when amplified in human peripheral blood cells (Lapidot-Lifson *et al.*, 1989; Zakut *et al.*, 1992).

DNA blot hybridization following *Eco*RI and *Pvu*II digestions of epididymis and testis DNA revealed labelled fragments of similar sizes using SV-40 and BCHE cDNA probes (Figure 8). This observation demonstrated their transgenic origin, in a manner similar to the somatic amplifications. The observed single

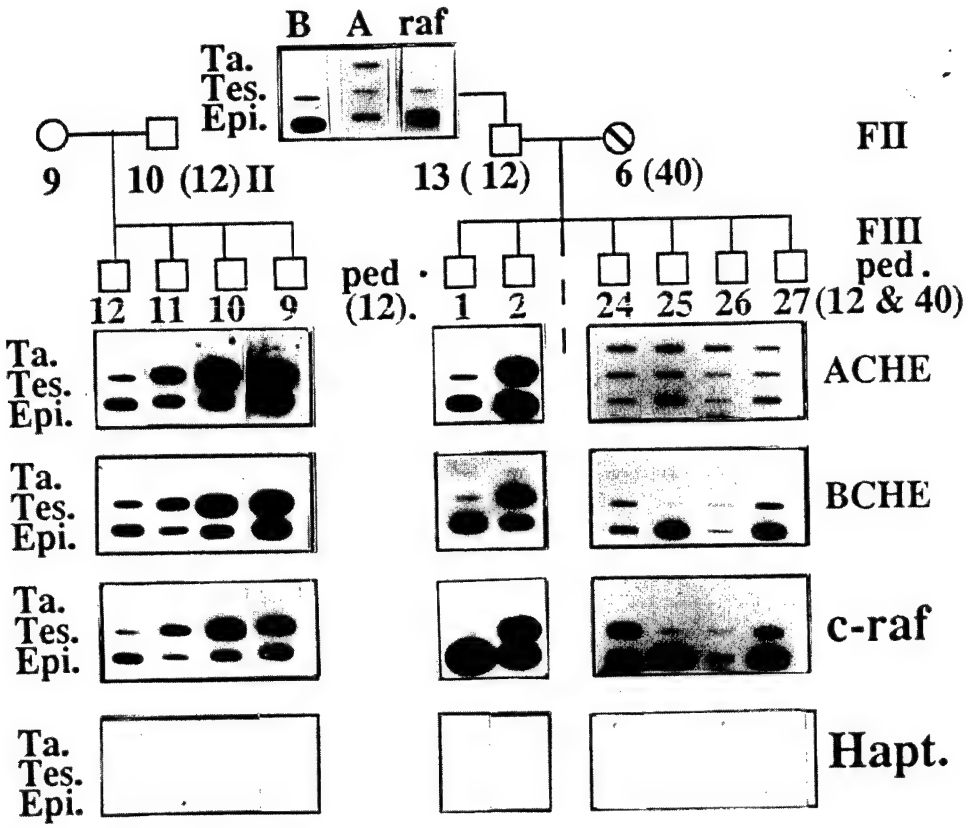

Fig. 7. Selective amplification of ACHE, BCHE and c-*raf* DNA in testis and epididymis of transgenic mice. Hybridization with the ACHE, BCHE, c-*raf* and haptoglobin (Hapt.) DNA probes were performed (as in Figure 2) with tail, testis and epididymis DNA from one adult FII male and 10 FIII males. These were 3 months old (no. 9–12, pedigree 12 and no. 1, 2, pedigree 12/40) or 4 weeks old (no. 24–27, pedigree 12/40). Dashed circles: ~20 copies of BCHE DNA in tail DNA. Five non-transgenic control mice were found to carry single copies of each of the analysed sequences in all tissues (not shown). Quantification was done as described (Lapidot-Lifson *et al.*, 1989).

fragments, however, appeared to be shorter than the complete transgene (Figure 8). This suggested the occurrence of deletions within the rearranged, amplified testicular transgenic sequences.

Selective BCHEmRNA reductions in testis of transgenic mice

To search for putative correlations between the testicular gene amplifications and spermatogenesis, developmental alterations were pursued. There were no clear differences in BCHE, ACHE and c-*raf* copy numbers between testis and epididymis DNA from adult mice. However, in 4-week-old mice the hybridization signals with DNA from testis, which at this age is poorer in mature sperm cells, were significantly lower than those observed with epididymis DNA (Figure 7). This observation potentially correlated the amplification phenomenon with sperm cell maturation. Interestingly, similar increases occur in copy numbers of the CGG and CTG repeats in the fragile X and myotonic dystrophy genes during germ cell development (Oberle *et al.*, 1991; Kremer *et al.*, 1991; Brook *et al.*, 1992; Harley *et al.*, 1992). The loss of amplification from subsequent generations could hence be due to the defective properties of germ cells in which the amplification occurred.

Further experiments were initiated to examine transcription in testis tissue from the transgenic mice. Gene expression in mammalian spermatogenic tissue is considered to be confined to the limited number of transcripts essential for germ cell development and/or function (Richler *et al.*, 1992; Willison and Ashworth, 1987). Cholinesterase and choline acetyltransferase activities were observed in mammalian sperm cells (Rama Sastry and Sadavongvivad, 1979; Rama Sastry *et al.*, 1981), and several reports have implicated acetylcholine with sperm motility (Ibanez *et al.*, 1991). The presence of BCHEmRNA transcripts was therefore examined in testis of control and transgenic mice by the use of direct reverse transcription coupled with PCR amplification (RNA–PCR). Parallel RNA–PCR amplification was performed with primers from the mouse gene encoding smooth muscle γ-actin (SMGA), which is one of the few transcripts known to be expressed during spermiogenesis (Kim *et al.*, 1989).

Total RNA from testis of two control mice and six transgenic mice carrying between five and 15 copies of the amplified genes in their testis DNA displayed apparently similar levels of actin mRNA (Figure 9). In addition, testis smears from adult transgenic mice showed normal density and a regular morphology of sperm cells. An apparently normal motility was observed in sperm cells extruded from epididymal preparations of these mice. In contrast, the results of RNA–PCR using BCHE primers reflected drastic reductions in BCHEmRNA levels in the testis of transgenic mice carrying pSVL-CHE amplifications versus control mice (Figure 10). In two of the transgenic mice, the BCHE PCR product could not be observed at all. This result implies that testis RNA from

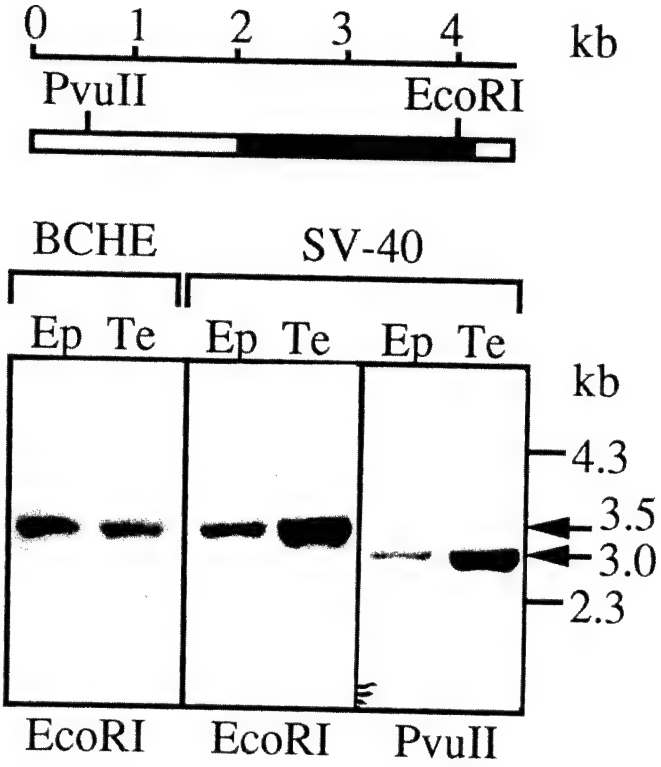

Fig. 8. *Eco*RI and *Pvu*II analysis of BCHE and SV-40 amplified sequences in testis and epididymis DNA. 10 μg testis (Te) and epididymis (Ep) DNA samples from mice 12/40 FIII nos 2 and 1, respectively (see Figure 7), were cut separately by *Eco*RI and *Pvu*II and were hybridized with BCHE and SV-40 probes. Restriction sites for *Pvu*II and *Eco*RI within the pSVL-CHE are shown above. Rehybridization with isolated 300 bp long SV-40 origin probe demonstrated that this sequence is included in the amplified DNA, indicating a tandem organization.

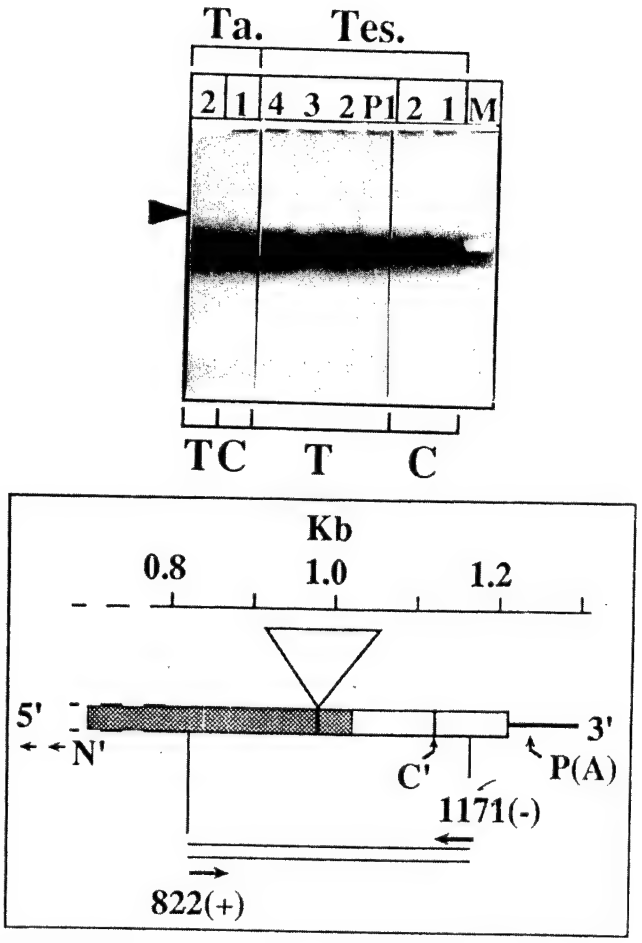

Fig. 9. Maintenance of actin mRNA levels in testis of transgenic mice. Testis (Tes) and tail (Ta) RNA was extracted from control (C) mice and from six adult transgenic (T) mice: 2, 3, 4 = 12/40 FIV-1, 2, 3, P1 = pooled RNA from mice 12 FIII-11, 12 and 12/40 FIII-1 (Figure 3). Reverse transcription was performed using the RNA−PCR kit (Perkin Elmer Cetus, Norwalk, CT, USA) following the manufacturer's recommendations, except that incubation with MuLV reverse transcriptase was extended for 25 min. PCR amplification of the resultant Actin cDNA (35 cycles) was performed using oligodeoxynucleotide primer pairs from two different exons in the mouse smooth muscle actin γ-actin (SMGA) (Kim *et al.*, 1989), primers mACT 822(+), 5′TGAAACAACATA-CAATTCCATCATGAAGTGTGAC-3′ and 1171(−), 5′-TGGCT-GGTGACCAAGTCTTGTGGGGAT-3′. See Nakqjima-Iijima *et al.* (1985) and Veyama *et al.* (1984) for details on actin gene structure. Upstream and downstream orientations are noted by (+) and (−) signs, respectively. Numbers indicate the 5′ end position in each of these primers within the relevant cDNA sequence. The positions of the primers within different exons are shown (down). RNA−PCR products (20%) were electrophoresed on 3% nussieve−1% agarose gels, in Tris−acetate buffer. Ethidium bromide staining of the RNA−PCR products is shown. M = DNA size marker. (+) = reactions carried out in the presence of reverse transcriptase. (−) = control reactions, without the enzyme, demonstrating the absence of contaminating DNA (one of two independent experiments).

the transgenic mice included $<10^4$ molecules/μg based on the kinetic follow-up of this PCR amplification using in-vitro transcribed deleted BCHE RNA (G.Ehrlich *et al.*, unpublished observations). In contrast, the levels of the BCHE PCR product from somatic tail RNA were $>10^5$ molecules/μg and indistinguishable in control and transgenic mice presenting no somatic amplifications (Figure 10). This evidence showed that the BCHE gene structure and its transcriptional ability in somatic tissues of the transgenic mice were normal, and focused the transcriptional damage to the testis tissue.

Discussion

We have observed in transgenic mice the occurrence of testicular gene amplification, the somatic amplification of the BCHE cDNA transgene which was limited to two generations and a concomitant variability in litter sizes which could reflect reduced fertility. The finding of somatic and testicular gene amplifications presented in this report demonstrates that in-vivo DNA amplifications may occur during germ cell development and are not limited to cancerous tissues and cultured cells. This extends recent observations of heritable CGG repeat expansion related with the X-linked mental retardation syndrome (Oberle *et al.*, 1991; Kremer *et al.*, 1991; Sutherland *et al.*, 1991) and CTG repeat expansion related to myotonic dystrophy (Brook *et al.*, 1992; Harley *et al.*, 1992).

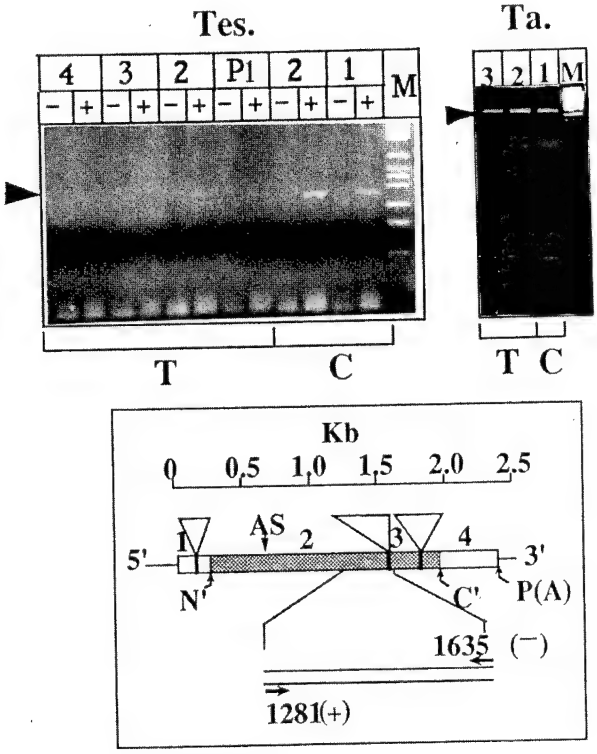

Fig. 10. Selective reduction in RNA−PCR-measured BCHE mRNA levels in testis of transgenic mice carrying amplified sequences. Experimental details were as in the legend to Figure 9, except that the following BCHE primers from exons 2 and 3 were employed: BCHE 1281(+), 5′-AGACTGGGTAGATGATCAGAG-ACCTGAAAACTACCG-3′ and 1635(−), 5′-GACAGGCCAGCTT GTGCTATTGTTCTGAGTCTCAT-3′, complementary to human BCHE cDNA (Prody *et al.*, 1987). Cycle numbers were 35 for tail BCHE mRNA (**right**), 42 for testis BCHE (**left**). See Arpagaus *et al.* (1990) for details on BCHE gene structure. One of two independent experiments.

The stable integration of the pSVL-CHE transgenic DNA into the mouse genome may be assumed to reflect a random event (Jaenisch, 1988). Yet, its amplification in two different pedigrees could have occurred by several mechanisms, independent of the insertion sites and thereby of sequences flanking the foreign DNA. SV-40 replication generally depends on the presence of the large T-antigen (Fiers *et al.*, 1978). Therefore, it is unlikely that this amplification was due to the SV-40 origin alone. Nevertheless, the unique transmission pattern of the amplified sequences is noteworthy, regardless of the initial cause for this phenomenon. The BCHE DNA sequence could have *cis*-activated randomly localized origins of replication in the host DNA adjacent to the transgene insertion sites. Alternatively, it could contain an intrinsic signal capable of directing its own amplification *in vivo*. If so, it could have replicated independently from the mouse genomic DNA during sperm development, when the host DNA is densely packed (Huret, 1986) and so less available for the incorporation of a foreign DNA into its chromatin structure. Interestingly, the 3q26 chromosomal site where the human BCHE gene resides (Gnatt *et al.*, 1990) carries an integration site for retroviruses (Soreq and Zakut, 1993). This site could hence be directly involved in the first amplification event of this gene in humans as well (Prody *et al.*, 1989).

Our findings raise the possibility that certain gene loci would be particularly vulnerable for germ cell gene amplification following viral infection. Initial changes in gene dosage by chromosome non-disjunction may trigger a general loss of accuracy in DNA replication (Holliday, 1989), and the co-amplification of several genes frequently occurs in cultured cells (Pauw *et al.*, 1986). Therefore, we consider that additional unexamined genes may also have undergone amplification in our model system. To the best of our knowledge, there are no previous examples of human DNA sequences undergoing amplification in transgenic mice; neither are there any indications that the amplification of a particular gene in transgenic mice may initiate a chain reaction resulting in the amplification of otherwise unlinked DNA sequences.

In view of our previous findings of ACHE, BCHE and c-*raf* co-amplifications in human cancers (Soreq and Zakut, 1990), one might suggest that the ACHE and BCHE genes, which are positioned on separate chromosomes in humans (Gnatt *et al.*, 1990; Ehrlich *et al.*, 1992), belong to an interrelated family of autosomal genes which co-amplify in various biosystems. Above a threshold copy number of one of these genes, the initial amplification event may have disrupted a natural equilibrium which under normal conditions prevents the uncontrolled amplification of multiple genes. This process could, for example, operate by the removal of an inhibitory protein element from the relevant DNA sites, explaining the similar extents of amplification among various dispersed endogenous amplifiable mouse genes, in FIII testis.

Our present observations imply that developing spermatozoa may be particularly vulnerable for cascade reactions of gene amplification, consistent with the variable litter sizes in the transgenic mice. The BCHE DNA amplifications observed in tail DNA from FII mice, and which presumably occurred in FI testis, do not appear to have imposed an impediment to their heritability. In contrast, the selective decrease in BCHE gene expression in the testis of the transgenic mice carrying multiple amplified genes apparently accompanied reduced fertilizing capacity of sperm cells carrying the amplifications. This could potentially be due to the amplification of additional genes, and particularly the endogenous ACHE gene. Interestingly, the ACHE and BCHE genes are co-regulated in multiple systems (Layer, 1991), perhaps indicating competition for common transcription factors, or direct or indirect feedback interactions involving the protein products. Either of these possibilities could implicate ACHE gene amplifications with reduced BCHE transcription.

The litter size variability observed in our transgenic mice reflects an apparent defect in fertility. Although qualitative evaluation failed to detect differences in sperm motility, we cannot exclude the possibility that minor yet effective changes in sperm motility did indeed occur. Parallel phenomena may hence occur in humans as well, particularly following viral infections and/or gene amplification events. This calls for further refinement of sperm motility measurements. Defects in human sperm motility, which are probably associated with cholinergic signalling (Rama Sastry *et al.*, 1981), constitute one of the primary factors in human male infertility (Chandley, 1988). The recently cloned promoter of the human ACHE gene (Ben Aziz-Aloya *et al.*,

1993) resembles promoters of other testicularly expressed genes in its contents of consensus motifs for binding transcription factors. If, indeed, CHE gene amplifications also occur in human sperm cells, they could induce defects in fertility and remain unnoticed. In contrast with mice, where the observed reduction in fertility was rather limited, parallel amplifications in humans may affect fertility more drastically because of the smaller size progeny. Other gene amplifications may similarly affect additional yet undefined vital processes in sperm development. The gonadal amplification phenomena observed in this study may potentially represent a case study of a general phenomenon which calls for clinical investigation in infertile humans.

Acknowledgements

We are grateful to Dr S.Lavi (Tel Aviv) for helpful discussions and the SV-40 DNA probes and to Dr J.Wahrmann, Ms C.Richler and Mr S.Seidman (Jerusalem) for helpful discussions. Supported, in part, by the Medical Research and Development Command, the US Army (grant DAMD-17-90-Z-0038), the American Israel Binational Science Foundation (grant No. 89-00205) and the Chief Scientist of the Israeli Health Ministry (to H.S. and H.Z.), and by the British Research Trust E.Wolfson Hosp., London (to H.Z. and H.S).

References

Arpagaus,M., Kott,M., Vatsis,K.P., Bartels,C.F., LaDu,B.N. and Lockridge,O. (1990) Structure of the gene for human butyrylcholinesterase. Evidence for a single copy. *Biochemistry*, **29**, 124–131.

Ben Aziz-Aloya,R., Seidman,S., Timberg,R., Sternfeld,M., Zakut,H. and Soreq,H. (1993) Expression of a human acetylcholinesterase promoter-reporter construct in developing neuromuscular junctions of *Xenopus* embryos. *Proc. Natl. Acad. Sci. USA*, **90**, 2471–2475.

Bishop,J.M. (1991) Molecular themes in oncogenesis. *Cell*, **64**, 235–248.

Brook,J.D., McCurrach,M.E., Harley,H.G., Buckler,A.J., Church,D., Aburatani,H., Hunter,K., Stanton,V.P., Thirion,J.P., Hudson,T., Sohn,R., Zemelman,B., Snell,R.G., Rundle,S.A., Crow,S., Davies,J., Shelbourne,P., Buxton,J., Jones,C., Juvonen,V., Johonson,K., Harper,P.S., Shaw,D.J. and Housman,D.E. (1992) Molecular basis of myotonic dystrophy: expansion of a trinucleotide (CTG) repeat at the 3′ end of a transcript encoding a protein kinase family member. *Cell*, **68**, 799–808.

Chandley,A.C. (1988) Meiosis in man. *Trends Genet.*, **4**, 79–84.

Cooper,D.N. and Schmidtke,J. (1987) Human gene cloning and disease analysis. *Lancet*, **i**, 273.

Delidakis,C., Swimmer,C. and Kafatos,F.C. (1989) Gene amplification: an example of genome rearrangement. *Curr. Opin. Cell Biol.*, **1**, 488–449.

Ehrlich,G., Viegas-Pequignot,E., Ginzberg,D., Sindel,L., Soreq,H. and Zakut,H. (1992) Mapping the human acetylcholinesterase gene to chromosome 7q22 by fluorescent *in situ* hybridization coupled with selective PCR amplification from a somatic hybrid cell panel and chromosome-sorted DNA libraries. *Genomics*, **13**, 1192–1197.

Fiers,W., Contreras,R., Haegeman,G., Rogiers,R., Van De Voora,A., Van Hauverswyn,H., Van Herreweghe,J., Volckaert,G. and Ysebaert,M. (1978) Complete nucleotide sequence of SV-40 DNA. *Nature*, **273**, 113–120.

Gnatt,A., Prody,C.A., Zamir,R., Lieman-Hurwitz,J., Zakut,H. and Soreq,H. (1990) Expression of alternatively terminated unusual CHEmRNA transcripts mapping to chromosome 3q26-ter in nervous system tumours. *Cancer Res.*, **50**, 1983–1987.

Harley,H.G., Brook,J.D., Rundle,S.A., Crow,S., Reardon,W., Buckler,A.J., Harper,P.S., Housman,D.E. and Shaw,D.J. (1992) Expansion of an unstable DNA region and phenotypic variation in myotonic dystrophy. *Nature*, **355**, 545–546.

Holliday,R. (1989) Chromosome error propagation and cancer. *Trends Genetics*, **5**, 42–45.

Huret,J.L. (1986) Nuclear chromatin decondensation of human sperm. *Arch. Androl.*, **16**, 97–109.

Ibanez,C.F., Petto-Huikko,M., Soder,O., Ritzen,E.M., Hersh,L.B., Hokfelt,T. and Persson,H. (1991) Expression of cholineacetyl transferase mRNA in spermatogenic cells results in an accumulation of the enzyme in the postacrosomal region of mature spermatozoa. *Proc. Natl. Acad. Sci. USA*, **88**, 3676–3680.

Jaenisch,R. (1988) Transgenic animals. *Science*, **240**, 1468–1474.

Kim,E., Waters,S.H., Hake,L.E. and Hech,N.B. (1989) Identification and developmental expression of a smooth-muscle actin in postmeiotic male germ cells in mice. *Mol. Cell Biol.*, **9**, 1875–1881.

Kremer,E.J., Pritchard,M., Lynch,M., Holman,Y.K., Baker,E., Warren,S.T., Schlessinger,D., Sutherland,G.R. and Richards,R.I. (1991) Mapping of DNA instability at the fragile X domain to a trinucleotide repeat sequence P(CCG)n. *Science*, **252**, 1711–1714.

Laat,S.A., LaLande,M. and Donlon,T. (1986) DNA-based detection of chromosome deletion and amplification: Diagnostic and mechanistic significance. *Cold Spring Harbor Symp. Quant. Biol.*, **LI**, 299–307.

Lapidot-Lifson,Y., Prody,C.A., Ginzberg,D., Maytes,D., Zakut,H. and Soreq,H. (1989) Co-amplification of human acetylcholinesterase and butyrylcholinesterase genes in blood cells: Correlation with various leukemias and abnormal megakaryocytopoiesis. *Proc. Natl. Acad. Sci. USA*, **6**, 4715–4719.

Lapidot-Lifson,Y., Patinkin,D., Prody,C.A., Ehrlich,G., Seidman,S., Ben-Aziz,R., Benseler,F., Eckstein,F., Zakut,H. and Soreq,H. (1992) Cloning and antisense oligodeoxynucleotide inhibition of a human homolog of cdc2 required in hematopoiesis. *Proc. Natl. Acad. Sci. USA*, **89**, 579–583.

Layer,P.G. (1991) Cholinesterases during development of the avian nervous system. *Cell. Mol. Neurobiol.*, **11**, 7–33.

Libermann,T.A., Nusbaum,H.R., Razon,N., Kirs,R., Lax,I., Soreq,H., Whitle,N., Waterfield,M.D. and Ullrich,A. (1985) Amplification, enhanced expression and possible rearrangement of EGF receptor gene in primary human tumours of glial origin. *Nature*, **313**, 144–147.

Makler,A. (1991) Sealed mini-chamber of variable depth for direct observation and extended evaluation of sperm motility under the influence of various genes. *Hum. Reprod.*, **6**, 1275–1278.

Mouches,C., Pasteur,N., Berge,J.B., Hyrien,O., Raymond,M., de Saint Vincent,B.R., de Silvestry,M. and Georghiou,G.P. (1986) Amplification of an esterase gene is responsible for insecticide resistance in a California Culex mosquito. *Science*, **233**, 778–780.

Nakqjima-Iijima,S., Hamada,H., Reddy,P. and Kakunaga,T. (1985) Molecular structure of the cytoplasmic ϒ-actin gene: Interspecies homology of sequences in the introns. *Proc. Natl. Acad. Sci. USA*, **82**, 6133–6137.

Oberle,I., Rousseau,F., Heitz,D., Kretz,C., Devys,D., Hanauer,A., Boue,J., Bertheas,M.F. and Mandel,J.L. (1991) Instability of a 550-base pair DNA segment and abnormal methylation in fragile X syndrome. *Science*, **252**, 1097–1102.

Pauw,P.G., Johnson,M.D., Moore,P., Morgan,MN., Finemon,R.M., Kalka,T. and Ash,J.F. (1986) Stable gene amplification and overexpression of sodium- and potassium-activated ATPase in Hela cells. *Mol. Cell Biol.*, **6**, 1164–1171.

Prody,C.A., Zevin-Zonkin,D., Gnatt,A., Goldberg,O. and Soreq,H. (1987) Isolation and characterization of full-length cDNA clones coding for cholinesterase from fetal human tissues. *Proc. Natl. Acad. Sci. USA*, **84**, 3555–3559.

Prody,C.A., Dreyfus,P., Zamir,R., Zakut,H. and Soreq,H. (1989) De novo amplification within a 'silent' human cholinesterase gene in a family subjected to prolonged exposure to organophosphorous insecticides. *Proc. Natl. Acad. Sci. USA*, **6**, 690–694.

Rama Sastry,B.V. and Sadavongvivad,C. (1979) Cholinergic systems

in non nervous tissues. *Pharmacol. Rev.*, **30**, 65–132.

Rama Sastry,B.V., Janson,V.E. and Chaturvedi,A.K. (1981) Inhibition of human sperm motility by inhibitors of cholineacetyl transferase. *J. Pharmacol. Exp. Ther.*, **216**, 378–384.

Richler,C., Soreq,H. and Wahrman,J. (1992) X inactivation in mammalian spermiogenesis is correlated with inactive X specific transcription. *Nature*, **2**, 192–195.

Schimke,R.T. (1990) The search for early genetic events in tumourigenesis: an amplification paradigm. *Cancer Cells*, **2**, 149–151.

Shani,M. (1985) Tissue specific expression of rat myosin light chain 3 gene in transgenic mice. *Nature*, **314**, 283–286.

Soreq,H. and Zakut,H. (1993) *Human Cholinesterases and Anti-Cholinesterases*. Academic Press, New York, 300 pp.

Soreq,H., Ben-Aziz,R., Prody,C.A., Seidman,S., Gnatt,A., Neville,L., Lieman-Hurwitz,J., Lev-Lehman,E., Ginzberg,D., Lapidot-Lifson,Y. and Zakut,H. (1990) Molecular cloning and construction of the coding region for human acetylcholinesterase reveals a G,C rich attenuating structure. *Proc. Natl. Acad. Sci. USA*, **87**, 9688–9692.

Stark,G.R., Dabatisse,M., Giulotto,E. and Wahl,G.M. (1989) Recent progress in understanding mechanisms of mammalian DNA amplification. *Cell*, **57**, 901–908.

Sutherland,R., Haan,E.A., Kremer,E., Lynch,M., Pritchard,M., Yu,S. and Richard,R.I. (1991) Hereditary unstable DNA: a new explanation for some old genetic questions? *Lancet*, **338**, 289–292.

Veyama,H., Hamada,H., Battula,N. and Kakunaga (1984) Structure of the human smooth muscle actin gene (aortic type) with a unique intron site. *Mol. Cell. Biol.*, **4**, 1073–1078.

Willison,K. and Ashworth,A. (1987) Mammalian spermatogenic gene expression. *Trends Genet.*, **3**, 351–355.

Zakut,H., Ehrlich,G., Ayalon,A., Prody,C.A., Malinger,G., Seidman,S., Ginzberg,D., Kehlenbach,R. and Soreq,H. (1990) Acetylcholinesterase and butyrylcholinesterase genes coamplify in primary ovarian carcinomas. *J. Clin. Invest.*, **6**, 900–908.

Zakut,H., Lapidot-Lifson,Y., Beeri,R., Ballin,A. and Soreq,H. (1992) In vivo gene amplification in non-cancerous cells: cholinesterase genes and oncogenes amplify in thrombocytopenia associated with lupus erythematosus. *Mutat. Res.*, **276**, 275–284.

Received on April 27, 1993; accepted on October 15, 1993

Transgenic expression of human acetylcholinesterase induces progressive cognitive deterioration in mice

Rachel Beeri*†, Christian Andres*†, Efrat Lev-Lehman†, Rina Timberg†, Tamir Huberman†, Moshe Shani‡ and Hermona Soreq†

†Department of Biological Chemistry, The Hebrew University of Jerusalem, 91904 Israel.
‡Institute of Animal Science, ARO, The Volcani Center, Bet Dagan, 50250 Israel.

Background: Cognitive deterioration is a characteristic symptom of Alzheimer's disease. This deterioration is notably associated with structural changes and subsequent cell death which occur, primarily, in acetylcholine-producing neurons, progressively damaging cholinergic neurotransmission. We have reported previously that excess acetylcholinesterase (AChE) alters structural features of neuromuscular junctions in transgenic *Xenopus* tadpoles. However, the potential of cholinergic imbalance to induce progressive decline of memory and learning in mammals has not been explored.

Results: To approach the molecular mechanisms underlying the progressive memory deficiencies associated with impaired cholinergic neurotransmission, we created transgenic mice that express human AChE in brain neurons. With enzyme levels up to two-fold higher than in control mice, transgenic mice displayed an age-independent resistance to the hypothermic effects of the AChE inhibitor, paraoxon. In addition to this improved scavenging capacity for anti-AChEs, however, these transgenic mice also resisted muscarinic, nicotinic and serotonergic agonists, indicating that secondary pharmacological changes had occurred. The transgenic mice also developed progressive learning and memory impairments, although their locomotor activities and open-field behaviour remained similar to those of matched control mice. By six months of age, transgenic mice lost their ability to respond to training in a spatial learning water maze test, whereas they performed normally in this test at the age of four weeks. This animal model is therefore suitable for investigating the transcriptional changes associated with cognitive deterioration and for testing drugs that may attenuate progressive damage.

Conclusion: We conclude that upsetting cholinergic balance may by itself cause progressive memory decline in mammals, suggesting that congenital and/or acquired changes in this vulnerable balance may contribute to the physiopathology of Alzheimer's disease.

Current Biology 1995, **5**:1063–1071

Background

Progressive deterioration of memory and learning is a characteristic manifestation of Alzheimer's disease [1]. The molecular mechanisms that underlie this phenomenon are still obscure, as the vast majority (> 90 %) of Alzheimer's disease cases originate sporadically — presumably as a result of multigenic contributions combined with environmental causes [2]. There is therefore a need to search for potential reasons to explain the progressive cognitive decline in Alzheimer's disease.

At the neuropathological level, the neuritic plaques and neurofibrillary tangles which are defining features of this disease are particularly concentrated in brain regions where cholinergic circuits operate [3]. Moreover, the progression of disease symptoms is primarily associated with structural changes in cholinergic synapses [4], the loss of particular acetylcholine (ACh) receptor subtypes [5], the death of ACh-producing neurons [6] and the consequent damage to cholinergic neurotransmission [7]. These factors result in a relative excess of the ACh-hydrolyzing enzyme, acetylcholinesterase (AChE). This spatio-temporal correlation led to the cholinergic theory of Alzheimer's disease [7] and promoted the development of cholinergic therapies [8].

The first of the cholinergic drugs to be approved for clinical use is tacrine (tetrahydroaminoacridine, THA, Cognex®), an AChE inhibitor which temporarily attenuates the worsening of certain clinical symptoms in patients at the early stages of Alzheimer's disease [8]. The concept behind the use of tacrine is to restore the cholinergic balance, at least for a while, by elevating ACh levels and augmenting the function of the remaining ACh receptors [9]. That tacrine administration has some therapeutic value emphasizes the importance of balanced cholinergic neurotransmission for satisfactory steady-state cognitive function. However, whether imbalanced cholinergic neurotransmission can, by itself, contribute to the progressive decline in Alzheimer's disease has not been addressed.

To examine the consequences of synaptic cholinergic imbalance *in vivo*, we have recently expressed human AChE in transiently transgenic embryos of *Xenopus laevis* frogs [10]. The recombinant human enzyme accumulated in neuromuscular junctions and altered their structural features [11]. Moreover, transgenic expression of the mouse

*The first two authors contributed equally to this research. Correspondence to: Hermona Soreq. E-mail address: soreq@vms.huji.ac.il

muscle nicotinic ACh receptor induced similar structural changes at *Xenopus* neuromuscular junctions, enlarging their post-synaptic length and deepening their synaptic cleft [11]. These alterations resembled those reported for cholinergic brain synapses in patients at the early stages of Alzheimer's disease [4], suggesting that these changes could also be caused by imbalanced cholinergic neurotransmission. This, in turn, initiated our interest in creating transgenic mice with congenital AChE overexpression and examining cognitive function in such animals.

The construction of our transgenic mice was conceptually different from other recent models designed to recreate the neuropathological features of Alzheimer's disease. Transgenic mice expressing normal or mutant forms of the β-amyloid protein died prematurely [12] or developed amyloid plaques rich in β-amyloid peptides [13]. This shed new light on the histopathological changes that are characteristic of Alzheimer's disease, particularly in carriers of β-amyloid mutations, but not on the relevant mental deficiencies. The elimination of several key brain proteins by homologous recombination (gene knockout) caused no histopathological changes, but damaged spatial learning [14–16] or avoidance learning [17]. However, neither the β-amyloid transgenic mice nor any of these knockout mice were reported to display the neurochemical changes particular to Alzheimer's disease, one of which is cholinergic imbalance. Furthermore, none of the reported cognitive changes appeared to involve progressive deterioration.

In contrast with the above studies, our efforts were devoted to creating a subtle change in the normal balance of cholinergic neurotransmission within the mammalian brain, mimicking conditions that might exist in patients with no hereditary tendency for Alzheimer's disease. We further limited this change to those cell types in which it naturally takes place, and studied its neurochemical, physiopathological and cognitive consequences in an age-dependent manner. Our findings demonstrate that AChE-overexpressing mice with inheritable cholinergic imbalance undergo selective progressive decline in their capacity for spatial learning and memory, and indicate the usefulness of these mice for exploring the detailed molecular mechanisms that underlie cognitive deterioration in Alzheimer's disease.

Results

Low-level AChE overexpression is compatible with life

To produce transgenic mice overexpressing AChE, we used two DNA constructs that included the *ACHE* coding sequence for the brain and muscle form of human AChE [10]. In the first construct, this gene was preceded by the potent ubiquitous promoter from cytomegalovirus (*CMV-ACHE* construct) [18]. In the second construct, this gene was preceded by a 596 base-pair fragment from the authentic promoter of the human *ACHE* gene, followed by its first intron (*Hp-ACHE* construct) [10]. Both promoters were shown previously to direct human AChE accumulation in *Xenopus* neuromuscular junctions [10,11], although the *CMV* promoter was approximately ten-fold more efficient in its capacity to direct production of the AChE protein in *Xenopus* [10].

We carried out parallel experiments with both constructs to produce transgenic mice. In the first experiment, we microinjected *CMV-ACHE* DNA into 70 mouse eggs, but obtained only one viable founder mouse carrying the *CMV-ACHE* transgene. However, the transgenic DNA was not expressed in the progeny of that mouse. In the second experiment, 40 microinjections of *Hp-ACHE* DNA yielded three viable pedigrees with 2, 10 and 15 copies of the transgene, respectively. Of these, no enzyme production was observed in the two pedigrees with higher copy numbers of the transgene, but AChE was expressed in the pedigree with two copies of the *Hp-ACHE* DNA.

The rate of success in obtaining viable AChE-transgenic mice was considerably lower than we have observed previously with other microinjected DNAs [19,20], suggesting that AChE overexpression was compatible with life only at low levels. Seven generations of transgenic mice with unmodified *Hp-ACHE* DNA were thereafter raised from the successful pedigree, and all of them presented grossly normal development, activity and behaviour.

Transgenic *Hp-ACHE* expression is limited to neurons of the central nervous system

Reverse transcription and quantitative polymerase chain reaction (PCR) amplification [20] revealed both human and mouse *ACHE* mRNA transcripts in dissected brain regions of the apparently homozygous transgenic mice from the fifth and subsequent generations (Fig. 1). Host *ACHE* mRNA levels and alternative splicing patterns remained apparently unchanged [21]. Bone marrow and adrenal glands expressed only mouse *ACHE* mRNAs,

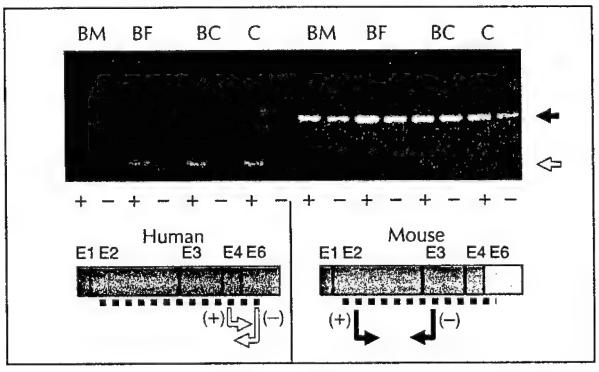

Fig. 1. Identification of human *ACHE* mRNA. RNA was extracted and amplified from transgenic (+) and control (–) mouse cortex (C), brainstem and cerebellum (BC), basal forebrain (BF) and bone marrow (BM). Species-specific PCR primers were designed for the indicated positions within the open reading frame (dotted underline) on the schemes above (see Materials and methods). Resultant PCR products (276 and 786 bp, respectively) were electrophoresed on agarose gels. Note that expression of human *ACHE* mRNA was limited to the central nervous system.

with apparently unmodified concentrations of the principal alternative products. Although the *Hp-ACHE* promoter includes several MyoD-binding elements [10], the transgene was not expressed in muscle.

To locate human *Hp-ACHE* mRNA transcripts in specific mouse brain cell types, we performed *in situ* hybridization experiments. Labelling was observed in essentially similar brain neurons to those observed in other mammals [22,23]; these included cell bodies in the basal forebrain, brainstem and cortex of the transgenic mice. Cholinoceptive hippocampal neurons were intensively labelled, especially in the CA1-CA2 region (Fig. 2). Thus, expression of the *Hp-ACHE* transgene was apparently confined to neurons of the host central nervous system (CNS) that normally express the mouse *ACHE* gene.

Normally processed transgenic AChE accumulates in cholinergic brain regions

AChE from the brains of control and transgenic mice displayed similar sedimentation profiles in sucrose gradient centrifugation, demonstrating unmodified assembly into multimeric enzyme forms (Fig. 3). Up to 50 % of the active enzyme in basal forebrain, but none in bone marrow, interacted with monoclonal antibodies specific to human AChE (Fig. 3 and Table 1) [24]. Catalytic activity measurements in tissue homogenates revealed a 100 % increase over control levels in the detergent-extractable amphiphilic AChE fraction from basal forebrain, and more limited increments in cortex, brainstem, cerebellum and spinal cord extracts (Table 1). There were no age-dependent changes in this pattern and no differences in the cell-type composition of the bone marrows of transgenic and control mice. Gel electrophoresis followed by chemical staining for enzyme activity [24] revealed similar migration patterns for AChE fromthe brains of transgenic and control mice, indicating comparable glycosylation patterns.

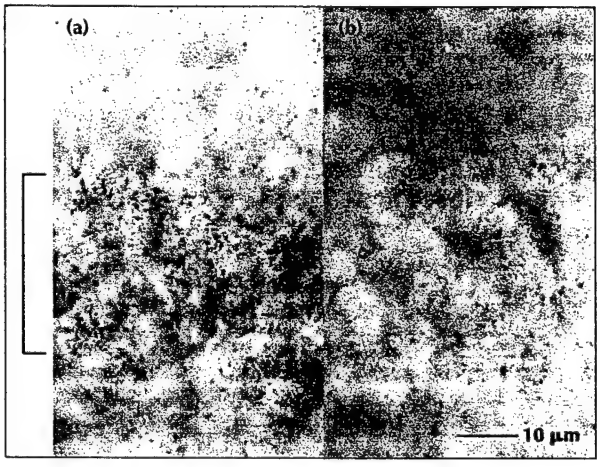

Fig. 2. Expression of transgenic *Hp-ACHE* mRNA in mouse brain neurons. Whole-mount *in situ* hybridizations were performed on fixed brain sections from **(a)** transgenic and **(b)** control mice. CA1 hippocampal neurons (bracketed) were intensely labelled in the transgenic, but not the control, section.

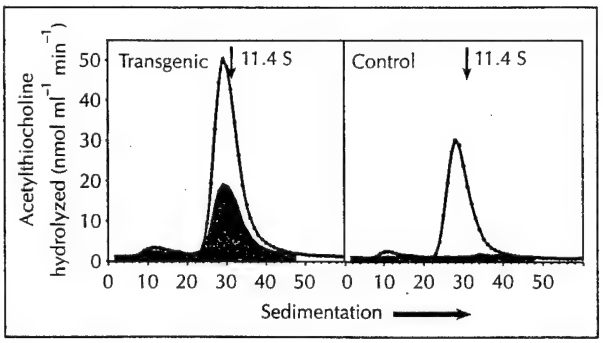

Fig. 3. Multimeric assembly of transgenic human AChE activity. Acetylthiocholine hydrolysis levels were determined for basal forebrain homogenates from transgenic and control mice after sucrose gradient centrifugation prior to (clear areas), or following (blue area), adhesion to human-selective anti-AChE monoclonal antibodies. Vertical arrows denote sedimentation of an internal marker, bovine catalase (11.4 S).

Intensified cytochemical staining of AChE activity was observed in brain sections from transgenic mice in all of the areas that stain for AChE activity in normal mice [25]. Staining was particularly intense in the neo-striatum and pallidum (Fig. 4a,b) as well as in the hippocampus (Fig. 4c,d); the latter two areas are associated with learning and memory [26,27]. Moreover, depositions of the electron-dense product of AChE-cytochemical staining were more conspicuous within synapse-forming dendrites in the anterior hypothalamus from transgenic mice than in control brain sections (Fig. 4e,f and Table 2). However, synapses interacting with these stained dendrites were of similar lengths in transgenic mice and in controls (Table 2), demonstrating that, unlike the situation in *Xenopus laevis* neuromuscular junctions [11,24], AChE overexpression in the mouse brain did not modify the post-synaptic length of (at least part of) the cholinergic synapses. In addition, there was no indication of

Table 1. Activity of human AChE in mouse tissues.

	AChE activity*			
	Transgenic		Control	
Tissue	Total	Anti-AChE†	Total	Anti-AChE†
Central nervous system				
Basal forebrain	402 ± 25	201	187 ± 30	0
Cortex	283 ± 18	119	235 ± 12	0
Brainstem/cerebellum	95 ± 36	30	88 ± 25	0
Spinal cord	255	82	208	0
Other				
Adrenal gland	25	0	24.6	0
Bone marrow	13.4 ± 0.3	0	17.1 ± 2.3	0

*Catalytic activities (nmol acetylthiocholine hydrolyzed min^{-1} mg protein^{-1}) were determined for detergent-solubilized homogenates as detailed [24]. Values are averages of three experiments ± standard deviation, except for spinal cord and adrenal gland where single experiments are presented. †Activity after binding to monoclonal antibodies specific for human AChE [24].

neurofibrillary tangles or amyloid plaques in the analyzed brain sections from mice up to six months of age.

Transgenic AChE selectively alters hypothermic drug responses

To investigate the physiological effects of overexpressing transgenic AChE, and because cholinergic synapses in the anterior hypothalamus (where we noted AChE overexpression) are known to be involved in thermoregulation [28], we examined the responses of transgenic mice to drugs causing hypothermia. The potent AChE inhibitor diethyl *p*-nitrophenyl phosphate (paraoxon) is the toxic metabolite of the agricultural insecticide parathion; both young (4–5 weeks) and adult (5–7 months) transgenic mice were considerably more resistant to paraoxon-induced hypothermia than non-transgenic controls (Fig. 5a,b). The transgenic mice were almost totally resistant to a low paraoxon dose (0.25 mg kg^{-1}, Fig. 5a). With higher doses, they displayed limited reduction in body temperature and shorter duration of response than controls (Fig. 5b). Most importantly, transgenic mice exposed to a 1 mg kg^{-1} dose of paraoxon retained apparently normal physical activity, whereas control mice experienced myoclonia and muscle stiffening, symptoms characteristic of cholinergic over-stimulation.

In addition to their improved capacity for scavenging paraoxon, the transgenic mice also displayed resistance to the hypothermic effects of the muscarinic agonist oxotremorine (Fig. 5c), to the less potent effect of nicotine (Fig. 5d), and to the serotonergic agonist 8-hydroxy-2-(di-*n*-propylamino) tetralin (8-OH-DPAT) (Fig. 5e), but not to the α_2-adrenergic agonist clonidine (Fig. 5f). However, the thermal response to cold exposure remained unchanged in both transgenic and control mice: after 60 minutes of exposure to 5 °C, the body temperature of all mice had decreased to 35.5 °C, indicating that no changes had occurred in their peripherally induced control over body temperature (data not shown).

Transgenic AChE induces an age-dependent decline in spatial learning capacity

To examine their cognitive functioning, transgenic and control mice were subjected to several behavioural tests. At the ages of one, two–three and five–seven months, transgenic mice retained normal locomotor and exploratory behaviour, covering the same space and distance in an open field as sex-matched groups of non-transgenic control mice. The open field anxiety of the mice also

Table 2. AChE overexpression does not modify the length of axo-dendritic synapses in the anterior hypothalamus of transgenic mice.

Parameters	Control	Transgenic	p^*
Number of synapses†	32	12	–
Electron-dense deposits‡	3.4 ± 3.2	6.5 ± 4.0	$p < 0.02$
Post-synaptic length§	0.8 ± 0.3	0.7 ± 0.2	NS

*Significance was verified by the Student's *t* test. NS = not significant. †Electron microscopy and cytochemical staining of anterior hypothalamus tissue were as described previously [24], with modifications as detailed in Materials and methods. Average values ± standard deviations are presented. ‡Number of dendritic electron-dense deposits per μm^2. Only deposits with rigid limits, reflecting crystal structures, were counted. §Post-synaptic length was measured, in μm, only for those synapses associated with AChE reaction products (that is, cholinergic synapses). For a representative example, see Fig. 4e,f.

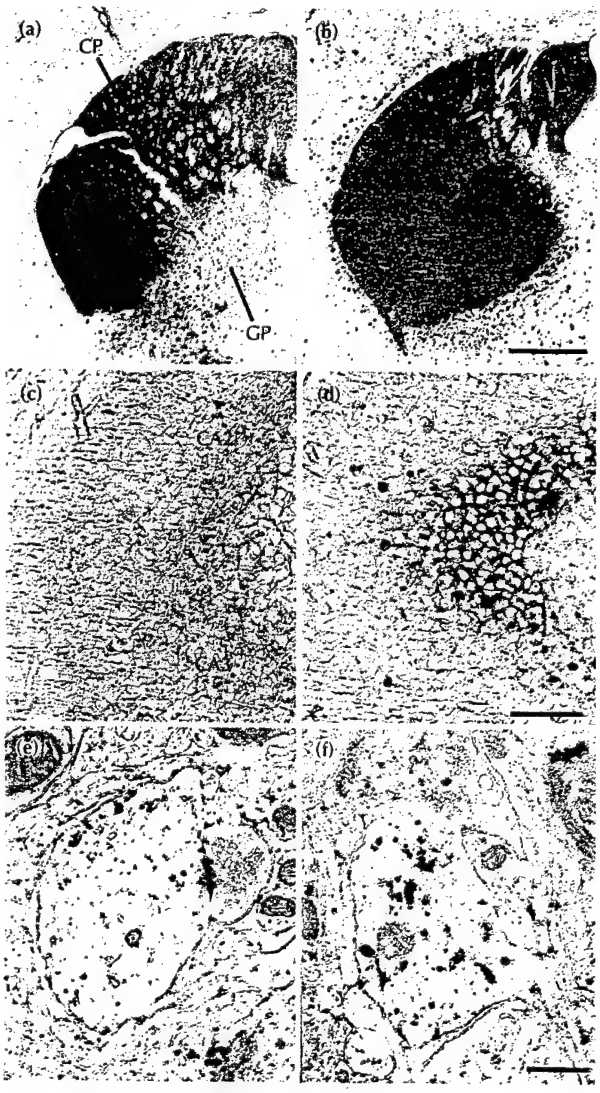

Fig. 4. Neuronal localization of AChE. **(a–d)** Cells that express AChE. Wholemount cytochemical staining of AChE activity was performed on fixed sections of (a,c) control and (b,d) transgenic brains. Neuronal cell bodies in (a,b) caudate-putamen (CP), globus pallidus (GP) and (c,d) hippocampal regions CA2 and CA3 were stained more intensely in transgenic than in control brain. Scale bars: (a,b) = 1mm; (c,d) 100 μm. **(e,f)** Dendritic accumulation of AChE. Cytochemical staining of AChE activity and electron microscopy were performed on fixed brain sections including axo-dendritic terminals from the anterior hypothalamus. Excess electron-dense reaction products appeared as dark grains within dendrites (centre of field) in (f) transgenic brain as compared with low-density labelling in (e) control brain. Scale bar = 0.5 μm.

remained similar, as evaluated in the frequency of defecation incidents and grooming behaviour (Table 3).

Conspicuous behavioural differences between the transgenic and control mice were observed, however, in two versions of the Morris water maze [29]. In the hidden platform version of this test, mice are expected to use long-distance cues to orient themselves, to find a platform submerged under opaque water and to escape a swimming task [29]. The performance of the transgenic mice was apparently normal in this test at the young age of four weeks — they needed a similar number of training sessions as compared to control mice in order to reach the platform within a significantly shorter time (defined as the escape latency) than untrained mice (Fig. 6a and Table 3). At the age of two or three months, transgenic mice needed eight more training sessions than control mice to improve their performance; the variation between animals also increased, and their shortest escape latency was significantly longer than that of control mice of the same age (Fig. 6b and Table 3). At the age of six months, naive transgenic mice, but not control mice, became totally incapable of improving their performance

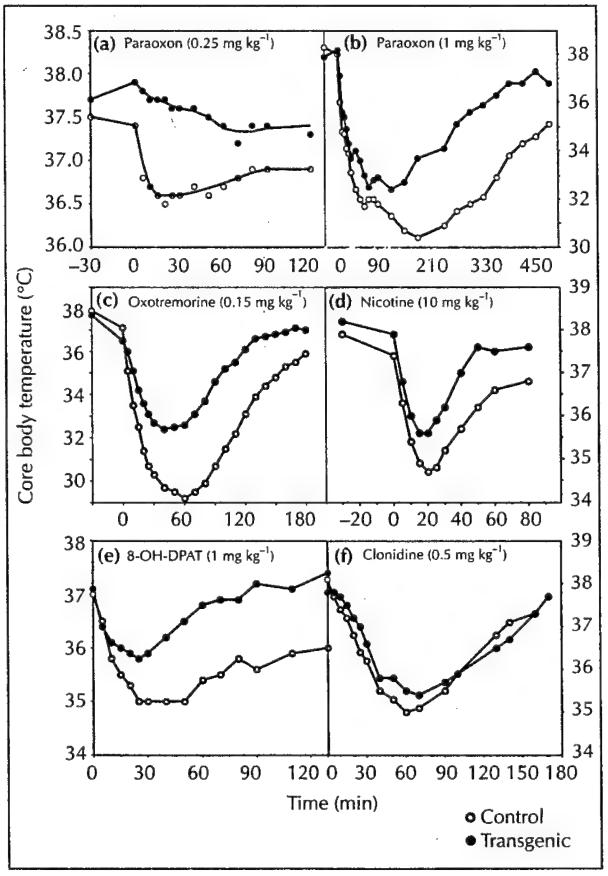

Fig. 5. Transgenic mice display reduced hypothermic responses to cholinergic and serotonergic, but not adrenergic, agonists. Core body temperature was measured in control and transgenic mice, five–seven months old, at the noted times, after intraperitoneal injections of the marked doses of **(a,b)** paraoxon, **(c)** oxotremorine, **(d)** nicotine, **(e)** tetralin (8-OH-DPAT) or **(f)** clonidine. Presented are average data for (a,f) five or (c–e) four male and female mice, or (b) one representative pair out of three tested. Note different time and temperature scales. Temperatures of transgenic mice at all time points after 10 min from injection were statistically different from those of controls for oxotremorine, nicotine and 8-OH-DPAT (Student's t test, $p < 0.05$).

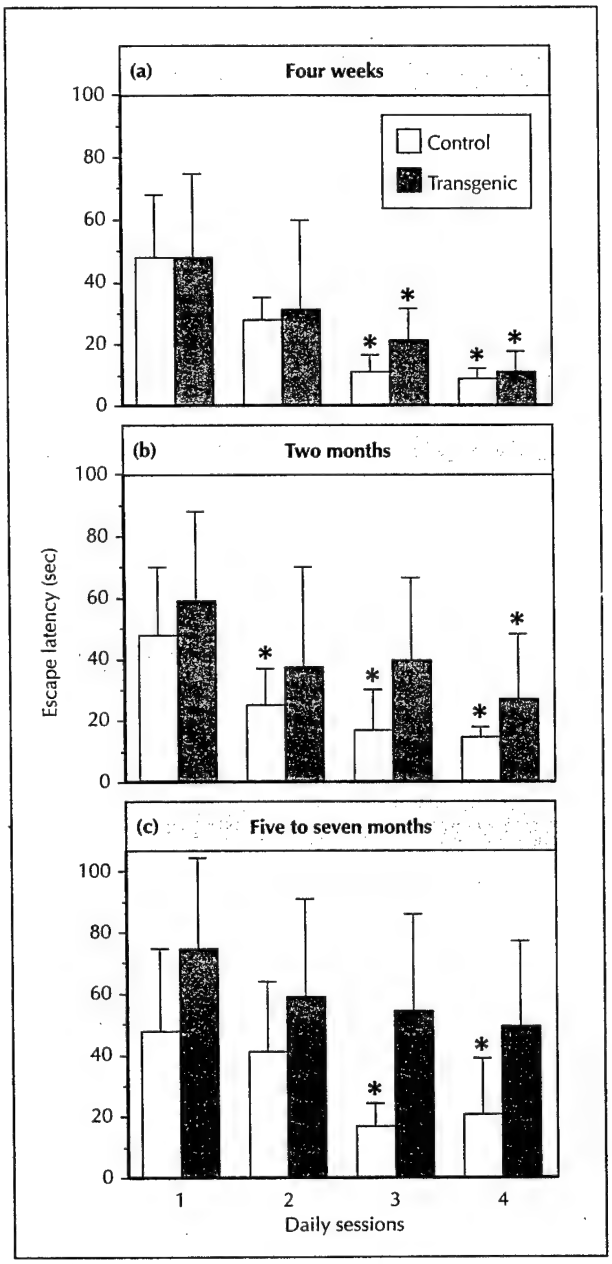

Fig. 6. Progressive impairment in spatial learning and memory of *Hp-ACHE* transgenic mice. Mice were tested in a water maze with a hidden platform in a fixed location. Averages of daily mean escape latencies are presented for **(a)** four-weeks-old transgenic ($n = 10$) and control ($n = 5$) mice, **(b)** two-months-old transgenic ($n = 10$) and control ($n = 10$) mice and **(c)** five–seven-months-old transgenic ($n = 9$) and control ($n = 11$) mice. Stars mark statistically significant reductions of latencies, as compared with the first day values in each section (one-way ANOVA, followed by Neuman Keuls test, $p < 0.02$).

Table 3. Selective behavioural deficits in AChE-transgenic mice.

	Age (months)					
	One		Two		Five to eleven	
Behavioural parameter	**Transgenic**	**Control**	**Transgenic**	**Control**	**Transgenic**	**Control**
Water maze*						
Visual test	33.8 ± 25.0	6.7 ± 1.8	22.5 ± 14.8	5.3 ± 2.2	33.3 ± 12.2	7.3 ± 3.9
Hidden platform test	17.3 ± 12.5	8.7 ± 3.5	26.4 ± 21.3	14.0 ± 3.5	49.1 ± 27.8	20.5 ± 18.2
Explorative behaviour†						
Space explored	51.4 ± 19.7	40.3 ± 29.8	62.5 ± 33.6	43.7 ± 21.7	51.5 ± 17.2	54.1 ± 19.4
Distance walked	11.2 ± 5.1	10.4 ± 8.5	15.9 ± 9.6	11.0 ± 5.4	13.0 ± 5.0	12.2 ± 3.5
Open field anxiety‡						
Defecation	1.0 ± 0.6	0.6 ± 0.5	0.1 ± 0.4	0.5 ± 0.8	0.8 ± 0.4	0.4 ± 0.5
Grooming	1.7 ± 1.0	0.6 ± 1.0	1.7 ± 1.0	1.0 ± 0.9	1.3 ± 1.0	1.2 ± 1.3

*Average escape latencies (seconds) ± standard deviations at day 4 of a Morris water maze test. †Open field tests were performed as described in Materials and methods. Explorative behaviour in the open field test was evaluated by measuring the percentage of open field space explored out of 0.36 m^2 and the distance covered (metres) in 5 minutes. Note that there is no significant difference for both parameters between transgenics and controls. ‡In the same 5 minute period, the number of defecation and grooming events, accepted signs of open field anxiety, were noted.

in this test through training, such that their escape latency remained the same as that of untrained mice (Fig. 6c and Table 3).

This pattern of deterioration was not caused by locomotor deficiencies, as was clear when the two groups of mice were compared in the open field test (see above). It could, therefore, reflect changes in memory. Alternatively, or in addition, changes in the acquisition of learning could be involved, which might be affected by motivational factors. It should be noted that the progressive behavioural decline of these transgenic mice was more pronounced than that observed in mice with targetted mutations in the glutamate receptor 1 [14], the kinase Fyn [15] or calcium calmoduline kinase II [16], suggesting a more substantial perturbation than in any of these cases.

A different, age-independent defect was observed in the visible platform version of the Morris water maze, in which mice are trained to escape the swimming task by using short-distance cues to climb on a visible platform decorated by a flag and a paper cone [29]. Interestingly, the transgenic mice could not improve their performance in this test through training, regardless of their age (Table 3), perhaps due to early-onset difficulties in short-distance vision or because of abnormal avoidance behaviour. In either case, the early occurrence of this defect at the age of four weeks, when the hidden platform test was still correctly performed by the transgenic mice, demonstrates that the defects in the visual and the hidden platform test were unrelated.

Discussion

Using the authentic promoter from the human *ACHE* gene in conjunction with the AChE-coding sequence, we created transgenic mice expressing human AChE in CNS neurons. The levels of overexpression were apparently sufficiently low to be compatible with life. The transgenic enzyme was processed normally and was detected preferentially in brain areas that normally express AChE, where it affected the responses of the transgenic animals to drugs causing hypothermia. Most importantly, there was a rapid decline in the spatial learning capacities of these transgenic animals, initiated in early adulthood and becoming progressively more severe, supporting the notion that subtle cholinergic imbalance can cause progressive learning deficiencies in mammals.

Our failure to obtain viable mice with high levels of AChE overexpression may imply that both the *Hp-ACHE* promoter, with its limited efficacy, and the low copy numbers of the transgene were important in allowing survival of the *ACHE*-transgenic mice. The expression pattern of the transgene excluded peripheral organs where the *ACHE* gene is normally expressed [30–32]; in particular, there was no expression in muscle, although MyoD-binding elements are included in the *Hp-ACHE* promoter. The restriction of expression to CNS neurons may occur because the promoter is incomplete, missing necessary enhancer elements. Alternatively, silencing elements in the promoter, similar to those reported in upstream sequences of the choline acetyltransferase gene [33], could prevent expression of this transgene in its normal target tissues. Finally, the insertion site within the host genome may affect expression. Additional studies will be required to distinguish between these possibilities.

The limited neuronal expression and low copy number of the transgene ensured that it could only cause a subtle cholinergic imbalance. The transgenic protein was processed and assembled normally, presumably due to the extremely high homology (95 %) between the human and the mouse enzymes [30–32]. It therefore accumulated in all of the relevant sites, with its highest excess

levels being found in the basal forebrain — the region most vulnerable to neuronal loss in Alzheimer's disease [1]. Interestingly, cholinergic synapses within the brains of the transgenic mice retained their normal length, unlike neuromuscular junctions from AChE-overexpressing *Xenopus* tadpoles. However, the *Xenopus* synapses also accumulated up to ten-fold more AChE [11,24]; in contrast, enzyme excess was limited to two-fold in the mouse synapses analyzed, perhaps reflecting an upper limit compatible with survival in mammals. The question of whether cholinergic imbalance can cause progressive structural changes to other particular types of cholinergic synapses in the mammalian brain must await further examination.

The resistance of transgenic mice to the induction of hypothermia by different agents demonstrated that the functioning of cholinergic synapses was modified by the overexpression of human AChE. Resistance to paraoxon was to be expected, as the amount of its target protein, AChE, was significantly increased in the brains of these mice. However, the resistance to muscarinic, nicotinic and serotonergic agonists reflected secondary changes affecting both cholinergic and serotonergic synapses, or perhaps only cholinergic ones — a recent report demonstrates that 8-OH-DPAT affects nicotinic receptors directly [34]. These changes were caused, either directly or indirectly, by the transgenic enzyme. However, no general alterations occurred in the network of neurons controlling thermoregulation, as the transgenic mice retained normal responses to noradrenergic agents and to cold exposure. This suggests a loss of specific synapses and/or receptor desensitization as possible causes, and indicates the use of cholinergic and serotonergic agonists for the early diagnosis of imbalanced cholinergic neurotransmission in human patients.

From their young adulthood onward, and also at a time when their spatial learning performance with a hidden platform was indistinguishable from that of controls, our transgenic mice failed to respond to short-distance visible cues. This could reflect a particular avoidance behaviour or could be due to the inability of these mice to focus their eyesight on a nearby target. The latter possibility is reminiscent of the differential response of Alzheimer's disease patients to tropicamide [35]. It is possible that autonomic control over pupil constriction and eyesight-focusing muscles requires precisely balanced cholinergic neurotransmission. It will be intriguing to examine whether Alzheimer's disease patients have more difficulties in focusing on nearby targets than unaffected, similarly-aged patients.

Of particular interest are the gradual spatial memory deficits displayed by the AChE-overexpressing transgenic mice in the hidden platform water maze, as opposed to their normal open field behaviour. The onset of these impairments in early adulthood suggests that the cholinergic balance essential for spatial memory can be sustained in younger transgenic mice, perhaps by a feedback mechanism that adjusts other key elements in cholinergic synapses. This intricate process resembles the increase in α-bungarotoxin binding levels in *Xenopus* embryos that overexpress AChE, and the reciprocal AChE accumulation in neuromuscular junctions of tadpoles expressing the mouse nicotinic ACh receptor [11]. Further to these observations, we now learn that, in mammals, this adjustment of the cholinergic balance can only be maintained for a limited time.

Several mechanisms of various levels have been implicated in the control of CNS cholinergic balance. Various ACh receptor genes have been shown to share common promoter elements [36,37], thus ensuring co-regulation by *trans*-acting factors. Furthermore, a single *cis*-acting promoter controls the production of both the vesicular ACh transporter and choline acetyltransferase [38,39]. A gradual failure to maintain either or both of these mechanisms, or others, may be involved in the progressive changes observed in our mice. The appearance of memory perturbation in the early stages of Alzheimer's disease may similarly signal the onset of failure to sustain cholinergic balance at the precise levels required for memory. The increase in brain AChE activity under stress [40] and the heterogeneous genomic origin of Alzheimer's disease in the vast majority of patients [2] may indicate that failure to maintain cholinergic balance can be due to variable causes.

The possibility exists that the overexpression of AChE may have effects that relate to the potential non-catalytic function(s) of this intriguing protein. Although the phenotypic differences observed in the transgenic mice are most probably correlated with acetylcholine hydrolysis, further experiments should be performed to explore any correlation with the potential functions of AChE in cell-to-cell interactions [41,42]. Indeed, evidence accumulated from patients suggests that AChE *per se* is closely linked to Alzheimer's disease: in patients, the brain ratio between AChE monomers and tetramers is significantly modified [43]; in the adrenal gland, selective AChE depletion has been observed [44]; and in the cerebrospinal fluid, a catalytically active AChE form with an anomalous isoelectric point has been detected [45]. These observations indicate that a functional excess of AChE might, independent of the catalytic site, be subsequently exerting new and possibly dangerous roles.

In either case, the gradual impairment of learning and memory due to AChE overexpression is consistent with the temporary partial improvement seen when anti-AChE drugs are administered to Alzheimer's disease patients [8,9]. Moreover, preliminary differential PCR displays [46,47] of mRNA from dissected brain regions of our transgenic mice have revealed age-dependent transcriptional changes, which await characterization. This approach may unravel the target genes being affected by the transgene. Testing the effects of drug treatments on the progressive transcriptional changes that occur in the brain of these mice might thereafter lead to

the development of novel strategies for prophylactic treatment of neurodegenerative disorders associated with cholinergic imbalance.

Finally, although AChE-overexpressing mice provide a model for behavioural, physiological and molecular aspects of cholinergic imbalance in mammals, they also demonstrate a dissociation between this imbalance and the β-amyloid deposits that occur in Alzheimer's disease. The possibility remains that cholinergic neurons are particularly sensitive to the neurotoxicity attributed to the β-amyloid peptides [12,13], in which case β-amyloid transgenic mice should develop cholinergic deficiencies with time. Alternatively, or in addition, cholinergic imbalance may lead to abnormal β-amyloid expression, in which case the AChE transgenic mice should develop β-amyloid deposits with time. A third possibility is that the linkage between the pathophysiological and the cognitive manifestations in Alzheimer's disease is unique to *Homo sapiens*.

Conclusions

Expression of human AChE in CNS neurons of transgenic mice creates impairments in spatial learning and memory which appear shortly after early adulthood and become progressively more severe. From early adulthood, these mice also show a marked, yet stable, decrease in performance in a visible water maze test. The open-field behaviour of the transgenic animals remains normal, although their responses to hypothermia-inducing drugs are decreased. These findings suggest that subtle alterations in cholinergic balance may cause physiologically observable changes and contribute to memory deterioration in at least some patients with sporadic Alzheimer's disease.

Materials and methods

Production of transgenic mice

DNA constructs were injected into fertilized eggs of FZB/N mice as described [19,20]. PCR amplification and Southern blot hybridization of tail DNA samples verified integration of variable copy numbers of the transgene into the genomes of founder mice and their progeny.

RNA extraction and PCR amplification

These were performed as detailed [20], except that the annealing temperature was 69 °C. Species-specific PCR primers were designed for human *ACHE* mRNA at nucleotides 1522(+) and 1797(–) in exons 3 and 4 [24], and for mouse at nucleotides 375(+) and 1160(–) in exons 2 and 3 [21]. Resultant PCR products (276 and 786 bp, respectively) were electrophoresed on agarose gels.

In situ *hybridization*

Wholemount *in situ* hybridizations were performed at 65 °C on 50 μm-thick, 4 % paraformaldehyde/1 % glutaraldehyde-fixed sections of transgenic and control brains with digoxigenin-labelled complementary human *ACHE* cRNA. Detection was with alkaline-phosphatase-conjugated anti-digoxigenin antibody (Boehringer/Mannheim).

AChE activity measurements

Acetylthiocholine hydrolysis levels were determined, following sucrose gradient centrifugation of tissue homogenates, prior to or following adhesion to human-selective anti-AChE monoclonal antibodies, essentially as detailed [24,32].

AChE cytochemical staining

Whole-mount cytochemical staining of AChE activity was performed on 50 μm-thick, paraformaldehyde–glutaraldehyde-fixed sections of brains as detailed [24], except that incubation was for 2 h. Electron microscopy was thereafter performed on 80 nm sections of paraformaldehyde-glutaraldehyde-fixed brain [24]. Control experiments with no acetylthiocholine verified that these electron-dense deposits were indeed reaction products of *in situ* AChE catalysis.

Hypothermic response measurements

Core body temperature was measured rectally in mice, using a thermocoupled element of 1 mm diameter and 10 mm length, at the noted times after intraperitoneal injections of paraoxon, oxotremorine, nicotine, tetralin (8-OH-DPAT) or clonidine.

Morris water maze tests

Mice were tested in a 60 × 60 × 15 cm water maze filled with 1.5 mg l^{-1} powdered milk, with a submerged hidden platform in a fixed location 1 cm below water level. Four trials of up to 2 min were performed per day for four days, each initiated randomly in a different corner of the maze. For the visual platform test, the water level was lowered by 2 cm, and a 10 cm high striped flag and a 7 cm high black cone were positioned on top of the now visible platform. Mean escape latencies per day (four sessions) were calculated for transgenic and sex- and age-matched controls, and statistically significant reductions of latencies were searched for as compared with the first day values in each section (one-way ANOVA, followed by Neuman Keuls test).

Open field test

Mice were placed in one corner of a 60 × 60 cm Plexiglass box with 30 cm high walls and the floor divided into 144 squares of 5 × 5 cm each. Using these squares, the motion path of the animals was manually traced for 5 min, which enabled measurements of walking distance and explored area. Grooming behaviour and incidence of defecations were also noted.

Acknowledgements: We thank T. Bartfai (Stockholm), J. Crawley (Washington, DC), A. Ungerer (Strasbourg) and H. Zakut (Tel Aviv) for helpful discussions and B. Norgaard-Pedersen (Copenhagen) for antibodies. This work was supported by USARMRDC grant 17-94-C-4031 and the Israel Academy of Sciences and Humanities (to H.S.). C.A. was a recipient of an INSERM, France fellowship, and an INSERM-NCRD exchange fellowship with the Israel Ministry of Science and Arts. The behavioural experiments were performed in the Smith Foundation Institute for Psychobiology at the Life Sciences Institute in the Hebrew University.

References

1. Katzman R: **Alzheimer's disease.** *N Engl J Med* 1986, **314**:962–973.
2. Ashall F, Goate AM: **Role of the β-amyloid precursor protein in Alzheimer's disease.** *Trends Biochem Sci* 1994, **19**:42–46.
3. Yankner BA, Mesulam MM: **Seminars in medicine of the Beth Israel Hospital, Boston. Beta-amyloid and the pathogenesis of Alzheimer's disease.** *N Engl J Med* 1991, **325**:1849–1857.

4. DeKosky ST, Scheff SW: **Synapse loss in frontal cortex biopsies in Alzheimer's disease: correlation with cognitive severity.** *Ann Neurol* 1990, **27:**457–464.
5. Mash DC, Flynn DD, Potter LT: **Loss of M2 muscarinic receptors in the cerebral cortex in Alzheimer's disease and experimental cholinergic denervation.** *Science* 1985, **228:**1115–1117.
6. Davies P, Maloney AJ: **Selective loss of central cholinergic neurons in Alzheimer's disease.** *Lancet* 1976, **2:**1403.
7. Coyle JT, Price DL, DeLong MR: **Alzheimer's disease: a disorder of cortical cholinergic innervation.** *Science* 1983, **219:**1186–1189.
8. Davis RE, Emmerling MR, Jaen JC, Moos WH, Spiegel K: **Therapeutic intervention in dementia.** *Clin Rev Neurobiol* 1993, **7:**41–83.
9. Knapp MJ, Knopman DS, Solomon PR, Pendlebury WW, Davis CS, Gracon SI: **A 30-week randomized controlled trial of high-dose tacrine in patients with Alzheimer's disease.** *J Am Med Assoc* 1994, **271:**985–991.
10. Ben Aziz-Aloya R, Seidman S, Timberg R, Sternfeld M, Zakut H, Soreq H: **Expression of a human acetylcholinesterase promoter-reporter construct in developing neuromuscular junctions of *Xenopus* embryos.** *Proc Natl Acad Sci USA* 1993, **90:**2471–2475.
11. Shapira M, Seidman S, Sternfeld M, Timberg R, Kaufer D, Patrick J, *et al.*: **Transgenic engineering of neuromuscular junctions in *Xenopus laevis* embryos transiently overexpressing key cholinergic proteins.** *Proc Natl Acad Sci USA* 1994, **91:**9072–9076.
12. LaFerla FM, Tinkle BT, Bieberich CJ, Haudenschield CC, Jay G: **The Alzheimer's Aβ peptide induces neurodegeneration and apoptotic cell death in transgenic mice.** *Nature Genet* 1995, **9:**21–31.
13. Games D, Adams D, Alessandrini R, Barbour R, Berthelette P, Blackwell C, *et al.*: **Alzheimer-type neuropathology in transgenic mice overexpressing V717F β-amyloid precursor protein.** *Nature* 1995, **373:**523–527.
14. Conquet F, Bashir ZI, Davies CH, Daniel H, Ferraguti F, Bordi F, *et al.*: **Motor deficit and impairment of synaptic plasticity in mice lacking mGluR1.** *Nature* 1994, **372:**237–243.
15. Grant SGN, O'Dell TJ, Karl KA, Stein PL, Soriano P, Kandel ER: **Impaired long-term potentiation, spatial learning, and hippocampal development in *fyn* mutant mice.** *Science* 1992, **258:**1903–1909.
16. Silva AJ, Paylor R, Wehner JM, Tonegawa S: **Impaired spatial learning in α-calcium-calmodulin kinase II mutant mice.** *Science* 1992, **257:**206–211.
17. Picciotto MR, Zoli M, Léna C, Bessis A, Lallemand Y, LeNovère N, *et al.*: **Abnormal avoidance learning in mice lacking functional high-affinity nicotine receptor in the brain.** *Nature* 1995, **374:**65–67.
18. Schmitt EV, Christoph G, Zeller R, Leder P: **The cytomegalovirus enhancer: a pan-active control element in transgenic mice.** *Mol Cell Biol* 1990, **10:**4406–4411.
19. Shani M: **Tissue-specific expression of rat myosin light-chain 2 gene in transgenic mice.** *Nature* 1985, **314:**283–286.
20. Beeri R, Gnatt A, Lapidot-Lifson Y, Ginzberg D, Shani M, Soreq H, Zakut H: **Testicular amplification and impaired transmission of human butyrylcholinesterase cDNA in transgenic mice.** *Hum Reprod* 1994, **9:**284–292.
21. Rachinsky TL, Camp S, Li Y, Ekström TJ, Newton M, Taylor P: **Molecular cloning of mouse acetylcholinesterase: tissue distribution of alternatively spliced mRNA species.** *Neuron* 1990, **5:**317–327.
22. Landwehrmeyer B, Probst A, Palacios JM, Mengod G: **Expression of acetylcholinesterase messenger RNA in human brain: an *in situ* hybridization study.** *Neuroscience* 1993, **57:**615–634.
23. Hammond P, Rao R, Koenigsberger C, Brimijoin S: **Regional variation in expression of acetylcholinesterase mRNA in adult rat brain analyzed by *in situ* hybridization.** *Proc Natl Acad Sci USA* 1994, **91:**10933–10937.
24. Seidman S, Sternfeld M, Ben Aziz-Aloya R, Timberg R, Kaufer-Nachum D, Soreq H: **Synaptic and epidermal accumulations of human acetylcholinesterase are encoded by alternative 3'-terminal exons.** *Mol Cell Biol* 1995, **14:**459–473.
25. Kitt CA, Höhmann C, Coyle JT, Price DL: **Cholinergic innervation of mouse brain structures.** *J Comp Neurol* 1994, **341:**117–129.
26. Yu J, Thomson R, Huestis PW, Bjelajac VM, Crinella FM: **Learning ability in young rats with single and double lesions to the 'general learning system'.** *Physiol Behav* 1989, **45:**133–144.
27. Eichenbaum H, Steward C, Morris RGM: **Hippocampal representation in place learning.** *J Neurosci* 1990, **10:**3531–3542.
28. Simpson CV, Ruwe WD, Myers RD: **Prostaglandins and hypothalamic neurotransmitter receptors involved in hypothermia: a critical evaluation.** *Neurosci Behav Rev* 1994, **18:**1–20.
29. Morris RGM, Garrud P, Rawlins JNP, O'Keefe J: **Place navigation impaired in rats with hippocampal lesions.** *Nature* 1981, **297:**681–682.
30. Massoulié J, Pezzementi L, Bon S, Krejci E, Valette FM: **Molecular and cellular biology of cholinesterases.** *Prog Neurobiol* 1993, **41:**31–91.
31. Taylor P, Radic Z: **The cholinesterases: from genes to proteins.** *Annu Rev Pharmacol Toxicol* 1994, **34:**281–320.
32. Soreq H, Zakut H: *Human Cholinesterases and Anticholinesterases.* San Diego: Academic Press, 1993.
33. Li YP, Baskin F, Davis R, Hersch L: **Cholinergic neuron-specific expression of the human choline acetyltransferase gene is controlled by silencer elements.** *J Neurochem* 1993, **61:**748–751.
34. Garcia-Colunga J, Miledi R: **Effects of serotonergic agents on neuronal nicotinic acetylcholine receptors.** *Proc Natl Acad Sci USA* 1995, **92:**2919–2923.
35. Scinto LFM, Daffner KR, Dressler D, Ransil BI, Rentz D, Weintraub S *et al.*: **A potential noninvasive neurobiological test for Alzheimer's disease.** *Science* 1994, **266:**1051–1054.
36. Jia HT, Tsay HJ, Schmitt J: **Analysis of binding and activating functions of the chick muscle acetylcholine receptor γ-subunit upstream sequence.** *Cell Mol Neurobiol* 1992, **12:**241–258.
37. Laufer R, Changeux JP: **Activity-dependent regulation of gene expression in muscle and neuronal cells.** *Mol Neurobiol* 1989, **3:**1–53.
38. Erickson JD, Varoqui H, Schäfer MKH, Modi W, Diebler MF, Weihe E, *et al.*: **Functional identification of a vesicular acetylcholine transporter and its expression from a 'cholinergic' gene locus.** *J Biol Chem* 1994, **269:**21929–21932.
39. Bejanin S, Cervini R, Mallet J, Berrard S: **A unique gene organization for two cholinergic markers, choline acetyltransferase and a putative vesicular transporter of acetylcholine.** *J Biol Chem* 1994, **269:**21944–21947.
40. Tsakiris S, Kontopoulos AN: **Time changes in Na^+, K^+-ATPase, Mg^{2+}-ATPase, and acetylcholinesterase activities in the rat cerebrum and cerebellum caused by stress.** *Pharmacol Biochem Behav* 1993, **44:**339–342.
41. Layer PG, Weikert T, Alber R: **Cholinesterases regulate neurite growth of chick nerve cells *in vitro* by means of a non-enzymatic mechanism.** *Cell Tissue Res* 1993, **273:**219–226.
42. Small DH, Reed G, Whitefield B, Nurcombe V: **Cholinergic regulation of neurite outgrowth from isolated chick sympathetic neurons in culture.** *J Neurosci* 1995, **15:**144–151.
43. Arendt T, Bruckner MK, Lange M, Bigl V: **Changes in acetylcholinesterase and butyrylcholinesterase in Alzheimer's disease resemble embryonic development — a study of molecular forms.** *Neurochem Int* 1992, **21:**381–396.
44. Appleyard ME, McDonald B: **Reduced adrenal gland acetylcholinesterase activity in Alzheimer's disease.** *Lancet* 1991, **338:**1085–1086.
45. Navaratnam DS, Priddle JD, McDonald B, Esiri MM, Robinson JR, Smith AD: **Anomalous molecular form of acetylcholinesterase in cerebrospinal fluid in histologically diagnosed Alzheimer's disease.** *Lancet* 1991, **337:**447–450.
46. Liang P, Pardee AB: **Differential display of eukaryotic messenger RNA by means of the polymerase chain reaction.** *Science* 1992, **257:**967–971.
47. Lev-Lehman E, El-Tamer A, Yaron A, Grifman M, Ginzberg D, Hanin I, *et al.*: **Cholinotoxic effects on acetylcholinesterase gene expression are associated with brain-region specific alterations in GC-rich transcripts.** *Brain Res* 1994, **661:**75–82.

Received: **11 May 1995**; revised: **28 June 1995.**
Accepted: **28 June 1995.**

THE CHOLINOTOXIN AF64A DIFFERENTIALLY ATTENUATES IN VITRO TRANSCRIPTION OF THE HUMAN CHOLINESTERASE GENES

I. Hanin,[1] A. Yaron, D. Ginzberg[2] and H. Soreq[2]

[1]Department of Pharmacology
Loyola University Chicago
Stritch School of Medicine
Maywood, Illinois 60153 USA
[2]The Department of Biological Chemistry
The Life Sciences Institute
Hebrew University
Jerusalem 91904, Israel

INTRODUCTION

Numerous reports in the literature have now demonstrated that ethylcholine aziridinium (AF64A) exerts selective cholinotoxicity, in vivo, in a number of animal species.[1,2] These effects are dose- and time-dependent and reversible, when low concentrations of AF64A (e.g. ≤ 2 nmol/lateral ventricle in the rat) are used.[3] The dose range for cholinoselectivity of AF64A needs to be established accurately with each specific application, since there is an upper dose limit at which AF64A begins to exert nonspecific degenerative effects.[1]

While the phenomenon of AF64A-induced cholinotoxicity has been well documented, the mechanism by which AF64A exerts its effect at the cholinergic nerve terminal has yet to be definitively established. The close structural similarity of AF64A to choline, its strong affinity for the high affinity choline transport (HAChT) system, and the protection afforded against AF64A induced cholinotoxicity in the presence of high doses of choline or hemicholinium-3,[4-9] all indicate that AF64A utilizes the HAChT mechanism to achieve its effect. We cannot rule out the possibility that some of the damage induced at cholinergic nerve cells may be via alkylation of proteins at the cholinergic nerve terminal by the aziridinium moiety of AF64A, inducing irreversible inhibition of the HAChT transporter site, ultimately resulting in depletion of nerve terminal choline which is essential for acetylcholine synthesis and hence destruction of the neuro.[10] However, there also is clear evidence that AF64A interacts directly with choline utilizing enzymes [e.g. acetylcholinesterase (AChE), choline acetyltransferase (ChAT) and choline kinase], and that could be another possible mechanism of AF64A-induced cholinotoxicity.[11-13] Moreover, the long-term effects of AF64A point to yet another possible mechanism for AF64A-induced cholinotoxicity. This third route might operate at the level of the nucleus, via interaction with the genes encoding for choline-binding proteins.[14] This paper describes our *in vitro* studies on the latter two possibilities.

Alzheimer's and Parkinson's Diseases
Edited by I. Hanin *et al.*, Plenum Press, New York, 1995

METHODS

Direct Effect of AF64A on AChE and BuChE activities in vitro was measured using the spectrophotometric method described by Neville et al. (1992).[15] This method is based on the ability of AChE to hydrolyze acetylthiocholine and of BuChE to hydrolyze butyrylthiocholine (obtained from Sigma). AF64A was prepared according to the procedure described elsewhere.[6] Following hydrolysis, exposure of the reaction product to dithio-bis-nitrobenzoate (DTNB) generates 5-thio-nitrobenzoate, which is bright yellow in color and can be monitored quantitatively at 405nm by spectrophotometry. The reaction is linear and highly reproducible. Human AChE was purified from erythrocyte membranes according to Liao et al.(1992).[16] Purified BuChE was obtained from Sigma. The enzymes were incubated in Ellman's reagent (0.1M phosphate buffer, pH 7.2, 0.5 mM DTNB) with different concentrations of AF64A (1 to 1000 μM) for 45 min at room temperature and at 37°C. Acetyl- or butyrylthiocholine were then added at final concentrations of 2 and 10mM, respectively, and substrate hydrolysis was monitored at 10 min intervals using a computer controlled microtiter plate reader (Vmax Kinetic Microplate Reader - Molecular Devices, California, USA) equipped with a Soft Max program.

Effect of AF64A on in vitro transcription of ACHE and BCHE DNAs was conducted as described by Futscher et al. (1992).[14] Briefly, we used three different transcription plasmids containing cDNAs encoding for human cholinesterases: 1) pSP64 (Promega Corporation, Madison, Wisconsin) containing an sp6 RNA polymerase binding site and BCHE coding sequence; 2) pGEM-ZF(+) (Promega Corporation, Madison, Wisconsin) containing a T7 RNA polymerase binding site and ACHE coding sequence; and 3) Bluescript SK(+) (Stratagene, La Jolla, California) containing a T3 RNA polymerase binding site and human BCHE DNA (for the purpose of comparing AF64A's effects on transcription of a single DNA primed by different RNA polymerases). Plasmid DNAs were linearized by enzymatic restriction with Hind III [pGEM-ZF(+), Bluescript SK(+)] or Sac I (pSP64) and purified by phenol/chloroform extraction and ethanol precipitation. Transcription was performed using an Amersham #RPN 2006 kit. Each 50 μl of transcription reaction included transcription buffer (40mM Tris-HCl pH 7.5, 6mM $MgCl_2$, 2mM spermidine, 0.01% bovine serum albumin), 0.01M dithiothreitol, 1 U/μl of human placenta RNase inhibitor, 500 μM of each NTP, 10 μCi of (α-^{32} P) (800 Ci/mmol), 5μg of control or drug treated DNA, and 20 units each of T7, SP6, or T3 polymerase, respectively. Reactions were allowed to continue for 60 min at 37°C, after which they were stopped by adding half the volume of stop-buffer (0.3% SDS, 60mM EDTA). Samples were stored at -20°C until subsequent analysis, at which time they were thawed, denatured by addition of four volumes of RNA loading dye (95% formamide, 0.2% bromophenol blue, 0.2% xylene cyanol), heated at 90°C for 10 min and chilled on ice before loading. Electrophoresis was either in 1% agarose gels or on denaturing gels consisting of 5% polyacrylamide, 7M urea, and 0.5 X TBE (0.089 Tris, 0.089M boric acid, 0.001M EDTA). Gels were electrophoresed at 400 volts for 3 hours. Autoradiography was conducted with Kodak film, and quantification of the transcription products was performed using a Soft Laser Scanning Densitometer model SL-TRFF (Biomed Instruments, CA, U.S.A.).

RESULTS

Effect of AF64A on the conditions of the spectrophotometric assay

Prior to conducting this assay on AChE and BuChE samples, we tested the reliability of the spectrophotometric assay in the presence of varying concentrations of AF64A. We

added AF64A at final concentrations of 1, 5, and 10 mM, respectively, to the reaction mixture to be used subsequently for the cholinergic enzymes assay, and allowed the reaction to occur for up to 60 min at room temp. while monitoring optical density at 405nm. AF64A addition resulted in a concentration and time-dependent decrease in $O.D._{405}$ (Figure 1). This indicated production of AF64A/5-thio-nitrobenzoate complexes above 5mM AF64A, resulting in quenched optical density. However, no color reduction occurred at an AF64A concentration of 1mM, indicating that AF64A doses below 1mM can safely be used for analysis of AChE and BuChE activities; the interaction of released thiocholine with DTNB, and the reduction in color reaction under these experimental conditions could only be due to enzyme inhibition by AF64A.

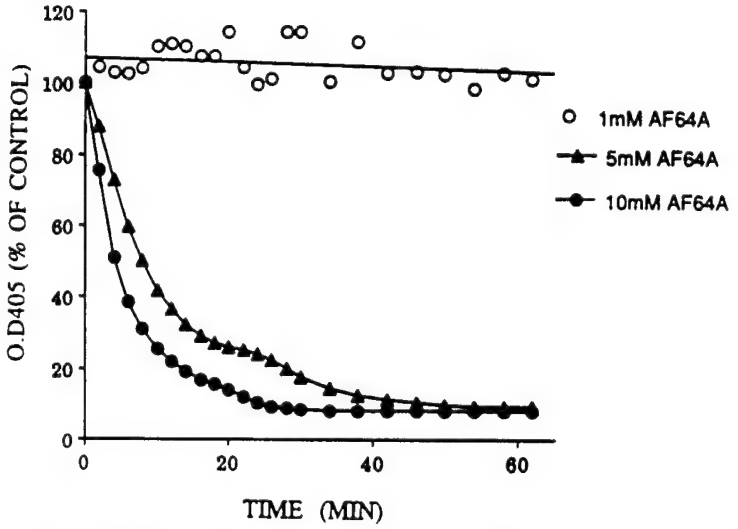

Figure 1: AF64A interaction with 5-thio-nitrobenzoate. A_{405} values were measured at different time points following the addition of AF64A to a reaction mixture including 5-thio-nitrobenzoate. Note that only concentrations above 1mM AF64A interact with 5-thio-nitrobenzoate to reduce optical density.

Effect of AF64A on AChE and BuChE Activities in vitro

AChE and BuChE were incubated for 60 min with AF64A, in the concentration range of 10^{-7}M-10^{-3}M. Results obtained are shown in Table 1, and reflect studies conducted at room temperature. Similar results were obtained when incubations were conducted for 60 min at 37°C (data not shown). Both AChE and BuChE were inhibited by AF64A, in a differential manner. Discernible inhibition of BuChE activity could only be observed above $5X10^{-4}$M of AF64A, and was limited to 32.63% at 10^{-3}M AF64A. In contrast, AChE activity was sensitive to as low as 10^{-5}M AF64A, and was inhibited by 59.63% in the presence of 10^{-3}M AF64A. Thus, AChE was more sensitive than BuChE to the effect of AF64A. However, the concentration of AF64A required to induce cholino-selective toxicity *in vivo*[17] is considerably less than the doses shown above to inhibit either AChE or BuChE *in vitro*. Assuming that ventricular volume is 160 μl,[18] the highest cholino-selective dose of AF64A (2 nmol/ventricle) would not exceed $1.25X\ 10^{-5}$M. Thus, neither AChE nor BuChE should be inhibited directly to any significant extent *in vivo*, at doses of AF64A shown to induce selective cholinotoxicity *in vivo* unless selective uptake exists which would concentrate the drug in cholinergic and/or cholinoceptive cells.

Table 1

AF64A ENZYME	10^{-3}M	$5x10^{-4}$M	10^{-4}M	10^{-5}M	10^{-6}M	10^{-7}M
AChE (RCG)	59.63% (n=6)	36.36% (n=4)	27.38% (n=6)	7.38% (n=6)	0.00% (n=6)	1.25% (n=4)
BuChE (serum)	32.63% (n=3)	15.05% (n=3)	1.71% (n=3)	3.68% (n=3)	0.71% (n=3)	---

Percent inhibition of catalytic activity of AChE and BuChE was determined as detailed in the Methods section. Note the differential sensitivity of the AChE protein to AF64A-induced damage. RCG: red cell ghosts.

Effect of AF64A on in vitro transcription of different transcription vectors carrying BCHE DNA

Plasmid DNAs carrying cholinesterase coding sequences were subjected to *in vitro* transcription following preincubation with concentrations of 0 - 100 μM AF64A. To ascertain that the observed effects reflected interaction with the coding sequences and did not depend on the transcription vectors and their viral polymerase binding sites, two different vectors carrying BCHE DNA were incubated with increasing concentrations of AF64A and their transcriptional activities tested. As seen in Figure 2, different promoters did not have an impact on the transcriptional changes induced by AF64A.

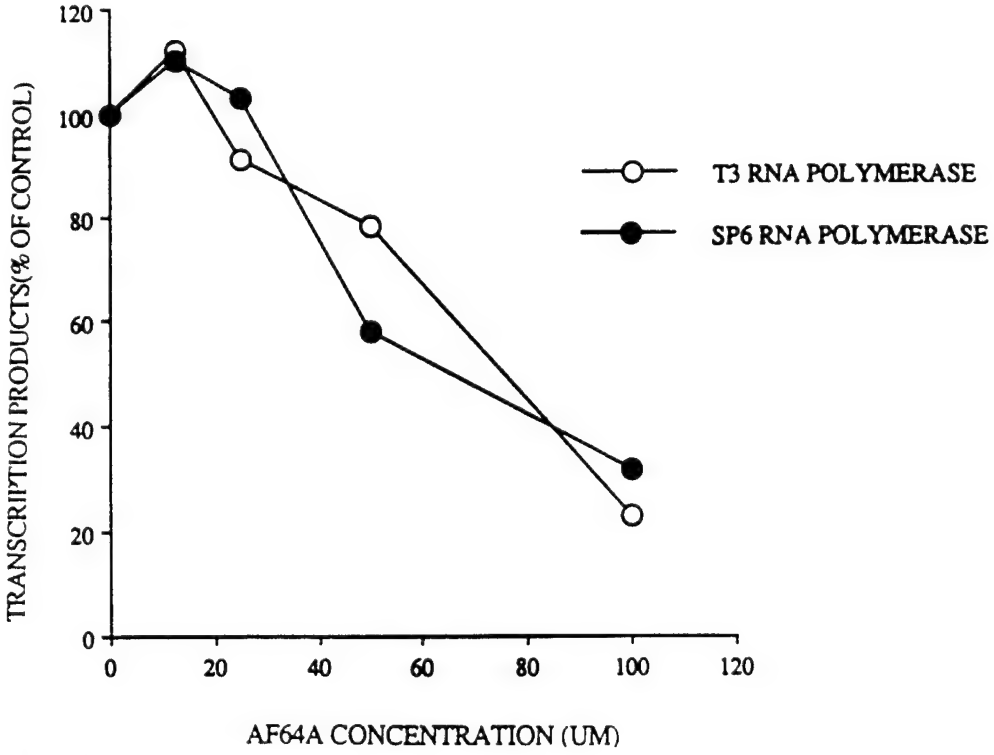

Figure 2: AF64A-induced transcriptional damage does not depend on the promoter employed. Plasmids carrying the human BCHE cDNA sequence under regulation of the T3 or the SP6 promoters were incubated separately with the noted concentrations of AF64A. Incorporation of [^{32}P] into RNA products was taken as a measure of transcription efficiency. Note the comparable decreases in these values for both plasmids.

Effect of AF64A on in vitro transcription of ACHE and BCHE DNAs

When ACHE and BCHE transcription vectors were incubated with AF64A for 60 min at 37°C, at concentrations of 12.5 - 100 μM, significant reductions were observed, in a dose-dependent fashion, in yields of [^{32}P]-labelled RNA transcripts (Figure 3). The magnitude of this effect differed, depending on the substrate. Inhibition of ACHE transcription was already significantly evident at 12.5 μM AF64A (-24%), and product levels continued to drop with increasing concentrations of the cholinotoxin. BCHE transcription was also inhibited by AF64A. However, a similar reduction only was evident at a concentration of 50 μM AF64A. Interestingly, AF64A's effect on the ACHE construct resulted in total reduction of ACHEmRNA levels, reflecting efficient attenuation of transcription. In contrast, AF64A's effect on the BCHE construct yielded concentration-dependent accumulation of short transcripts, perhaps reflecting early terminations. Thus the ACHE and the BCHE genes, both susceptible to AF64A's action, show a differential sensitivity. This difference also is reflected in the effect of AF64A on the transcriptional activities of these two genes in cholinergic neurons *in vivo* (Lev-Lehman et al., this book, 1994).

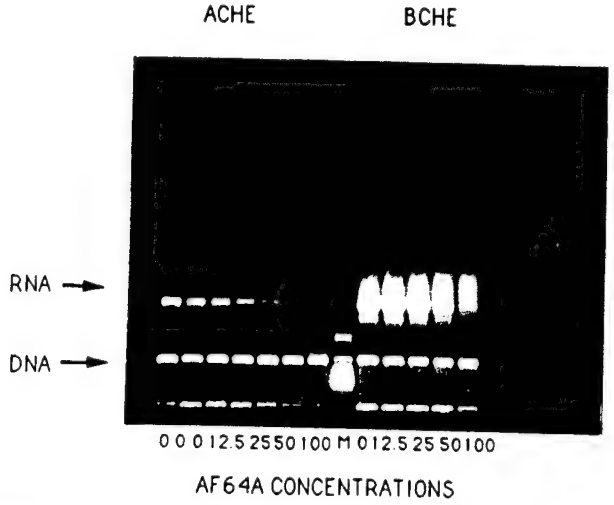

Figure 3: Differential sensitivity of ACHE and BCHE coding sequences for transcriptional damage induced by AF64A. Equal amounts of the two plasmids were incubated with the noted concentrations of AF64A followed by agarose gel electrophoresis of the reaction products. Note the relative resistance to AF64A of BCHE as compared with ACHE transcription.

DISCUSSION

Two mechanisms by which AF64A might affect AChE and BuChE activities *in vivo* were examined, using *in vitro* approaches: a) as an irreversible inhibitor of the enzyme proteins; and b) as an attenuator of transcription. At the protein level, AChE activity was more sensitive to AF64A than was that of BuChE. However, in the case of both enzymes, activities remained practically unchanged at physiologically relevant concentrations. Thus, reduction of AChE and/or BuChE activities following AF64A treatment *in vivo* could not be explained by a direct inhibition of enzyme activities except, conceivably, under conditions in which cholinergic or cholinoceptive cells accumulate this toxin in far higher concentrations than those administered.

ACHE and BCHE DNAs were both found to be sensitive to AF64A and displayed significant reductions in their ability to be transcribed *in vitro* in the presence of AF64A. ACHE DNA was more sensitive to AF64A than was BCHE DNA, probably because of the

difference in their base composition. ACHE DNA is G,C-rich;[19,20] AF64A has a strong affinity toward the N-7 position in guanines.[14] These two phenomena may predispose the ACHE gene toward AF64A, over the BCHE gene, which is A,T-rich.[20] AF64A should interact more effectively with G,C-rich genes in general, particularly with those amenable to transcription and hence made more vulnerable. G,C-rich genes tend to perform house-keeping functions[21] which could be another cause for AF64A-induced cytotoxicity. Also, AF64A may cause cytotoxicity through other mechanisms, for example by inhibiting guanine nucleotide - dependent processes.[14] Thus, the *in vivo* reductions reported for both AChE and BuChE activities following AF64A treatment can therefore be accounted for, at least in part, by DNA damage, with the ACHE gene being more susceptible to such damage possibly because it is G,C-rich in content.

In summary, the direct sensitivity of the cholinesterase proteins to AF64A toxicity could not account for the reductions in the cholinergic enzyme activities observed following AF64A treatment in the concentrations employed *in vivo*.[3] On the other hand, our findings indicate that AF64A interaction with cellular DNA may lead to differential reduction in CHEmRNA transcripts and, through that mechanism, to a reduction in cholinesterase activities *in vivo*. DNA repair mechanisms could eventually correct the damage, which would lead to a transient cytotoxicity. This implies that selective, yet transient reductions in the level of ACHE mRNA transcripts should be observed under AF64A treatment *in vivo*. Studies examining this question are already in progress.[17,22]

Acknowledgements

This study was supported by the Lady Davis Foundation and the Charles Smith Psychobiology fund (to IH) and by the U.S. Army Medical Research and Development Command (to H.S.).

REFERENCES

1. I. Hanin, AF64A-induced cholinergic hypofunction, in: *"Cholinergic Neurotransmission: Functional and Clinical Aspects,"* S.-M. Aquilonius and P.-G. Gillberg, eds., Elsevier Science Publishers, B.V., Amsterdam (1990).
2. I. Hanin, A. Fisher, H. Hortnagl, S.M. Leventer, P.E. Potter, and T.J. Walsh, in: *"Psychopharmacology: The Third Generation Of Progress,"* H.Y. Meltzer, ed., Raven Press, New York (1987).
3. A. El Tamer, J. Corey, E. Wulfert, and I. Hanin, Reversible cholinergic changes induced by AF64A in rat hippocampus and possible septal compensatory effect, *Neuropharmacology* 31:397 (1992).
4. C.R. Mantione, A. Fisher, and I. Hanin, The AF64A-treated mouse: possible model for central cholinergic hypofunction, *Science* 213:579 (1981).
5. Z. Pittel, A. Fisher, and E. Heldman, Reversible and irreversible inhibition of high affinity choline transport caused by ethylcholine aziridinium ion, *J. Neurochem.* 49:468 (1987).
6. A. Fisher, C.R. Mantione, D.J. Abraham, and I. Hanin, Long-term central cholinergic hypofunction induced in mice by ethylcholine aziridinium ion (AF64A) in vivo,. *J. Pharmacol. Exp. Therap.* 222:140 (1982).
7. D.L. Davies, N. Sakellaridis, T. Valcana, and A. Vernadakis, Cholinergic neurotoxicity induced by ethylcholine mustard aziridinium (AF64A) in neuron-enriched cultures, *Brain Res.* 378:251 (1986).
8. A. Amir, Z. Pittel, A. Shahar, A. Fisher, and E. Heldman, Cholinotoxicity of the ethylcholine aziridinium ion in primary cultures from rat central nervous system, *Brain Res.* 454:298 (1988).
9. L.R. Santiago, R.A. Kroes, L.C. Erickson, and I. Hanin, Choline (Ch) and hemicholinium-3 (HC-3) protect against AF64A-induced changes in N-myc expression in the human neuroblastoma cell line (LA-N-2), *Neurosci. Abstr.* 19:1747 (1993).
10. R.J. Rylett, and S.A. Walters, Uptake and metabolism of [^{3}H]choline mustard by cholinergic nerve terminals from rat brain, *Neuroscience* 36:483 (1990).
11. R.J. Rylett, Synaptosomal 'membrane-bound' choline acetyltransferase is most sensitive to inhibition by choline mustard, *J. Neurochem.* 52:869 (1989).

12. R.J. Rylett, and E.H. Colhoun, Carrier-mediated inhibition of choline acetyltransferase, *Life Sci.* 26:909 (1980).
13. K. Sandberg, R.L. Schnaar, M. McKinney, I. Hanin, A. Fisher, and J.T. Coyle, AF64A: an active site directed irreversible inhibitor of choline acetyltransferase, *J. Neurochem.* 44:439 (1985).
14. B.W. Futscher, R.O. Pieper, D.M. Barnes, I. Hanin, and L.C. Erickson, DNA-damaging and transcription-terminating lesions induced by AF64A *in vitro*, *J. Neurochem.* 58:1504 (1992).
15. L.F. Neville, A. Gnatt, Y. Loewenstein, S. Seidman, G. Ehrlich, and H. Soreq, Intramolecular relationships in cholinesterases revealed by oocyte expression of site-directed and natural variants of human BCHE, *EMBO. J.* 11:1641 (1992).
16. J. Liao, H. Heider, M.-C. Sun, and U. Brodbeck, Different glycosylation in acetylcholinesterase from mammalian brain and erythrocytes, *J. Neurochem.* 58:1230 (1992).
17. E. Lev-Lehman, A. El Tamer, D. Ginzberg, I. Hanin, and H. Soreq, Transient alterations in the *in vivo* levels of cholinesterase mRNAs suggest differential adjustment to cholinotoxic stimuli, in: *This Book*.
18. R. Hebel and M.W. Stromberg. "Anatomy of the Laboratory Rat," The Williams and Wilkins Company, Waverly Press, Inc., Baltimore (1976).
19. H. Soreq, R. Ben-Aziz. C. Prody, S. Seidman, A. Gnatt, L. Neville, J. Lieman-Hurwitz, E. Lev-Lehman, D. Ginzburg, Y. Lapidot-Lifson, and H. Zakut, Molecular cloning and construction of the coding region for human acetylcholinesterase reveals a G+C rich attenuating structure, *Proc. Natl. Acad. Sci. USA* 87:9688 (1990).
20. H. Soreq and H. Zakut, "Human Cholinesterases and Anticholinesterases," Academic Press, S.D. (1993).
21. G.P. Holmquist, Evolution of chromosome bands: Molecular ecology of noncoding DNA, *J. Mol. Evol.* 28:469 (1989).
22. E. Lev-Lehman, A. El Tamer, A. Yaron, M. Grifman, D. Ginzburg, I. Hanin, and H. Soreq, Cholinotoxic effects on acetylcholinesterase gene expression are associated with brain region specific alterations in G,C-rich transcripts, *Mol. Brain Res.* Submitted.

ELSEVIER

Brain Research 661 (1994) 75–82

BRAIN RESEARCH

Research report

Cholinotoxic effects on acetylcholinesterase gene expression are associated with brain-region specific alterations in G,C-rich transcripts

Efrat Lev-Lehman [a], Ahmed El-Tamer [b], Avraham Yaron [a], Mirta Grifman [a], Dalia Ginzberg [a], Israel Hanin [b], Hermona Soreq [a,*]

[a] *Department of Biological Chemistry, The Life Sciences Institute, the Hebrew University, Jerusalem 91904, Israel*
[b] *Department of Pharmacology, Loyola University Chicago, Stritch School of Medicine, Maywood, IL 60153, USA*

Accepted 19 July 1994

Abstract

To study the mechanisms underlying cholinotoxic brain damage, we examined ethylcholine aziridinium (AF64A) effects on cholinesterase genes. In vitro, AF64A hardly affected cholinesterase activities yet inhibited transcription of the G,C-rich AChE DNA encoding acetylcholinesterase (AChE) more than the A,T-rich butyrylcholinesterase (BChE) DNA. In vivo, intracerebroventricular injection of 2 nmol of AF64A decreased AChE mRNA in striatum and septum by 3- and 25-fold by day 7, with no change in BChE mRNA or AChE activity. In contrast, hippocampal AChE mRNA increased 10-fold by day 7 and BChE mRNA and AChE activity decreased 2-fold. By day 60 post-treatment, both AChE mRNA and AChE levels returned to normal in all regions except hippocampus, where AChE activity and BChE mRNA were decreased by 2-fold. Moreover, differential PCR displays revealed persistent induction, specific to the hippocampus of treated rats, of several unidentified G,C-rich transcripts, suggesting particular responsiveness of hippocampal G,C-rich genes to cholinotoxicity.

Keywords: Acetylcholinesterase; AF64A; Butyrylcholinesterase; Differential PCR display; Hippocampus; RT-PCR; Septum

1. Introduction

Cholinergic deficits have been associated with several neurodegenerative disorders such as Alzheimer and Huntington's diseases [33], suggesting that finely balanced cholinergic metabolism contributes to the maintenance of central nervous system circuits. Therefore, understanding the molecular and neurochemical changes underlying cholinergic signalling can assist in deciphering the causes for such diseases.

An animal model in which a selective cholinergic deficit has been induced is the ethylcholine aziridinium (AF64A) treated rat [6]. AF64A is structurally similar to choline, with the distinction that it possesses an ethyl moiety and an aziridinium ion. It is taken up by cholinergic neurons via the high affinity choline transport system [20] and causes a specific and long lasting reduction in the concentration and the activity of cholinergic pre-synaptic biochemical markers [21,28]. These markers include the neurotransmitter acetylcholine (ACh), the ACh hydrolysing enzyme acetylcholinesterase (AChE), the ACh synthesizing enzyme choline acetyltransferase (ChAT) [16], and the high affinity transport system for choline, which is the rate limiting step in ACh synthesis [22]. In addition, rats treated with AF64A also show behavioral cognitive deficits, suggesting that loss of synapses has occurred [2].

Referring to the analogy between AF64A and choline, and the presence of the highly reactive aziridinium ion which is susceptible to nucleophilic attack [12], it was suggested that AF64A serves as a potent inhibitor of enzymes that have affinity for choline, such as ChAT and AChE [29]. However, like other aziridinium compounds, AF64A was also found to react with DNA, to induce DNA damage and to cause premature termination of RNA transcription in vitro in a dose-dependent fashion. This probably occurs through direct interaction with the N-7 position in guanines in the DNA molecule [7]. Thus, the cholinotoxic effects of AF64A could be attributed to its in-

* Corresponding author. Fax: (972) (2) 520-258.

SSDI 0006-8993(94)00897-3

hibitory action on cholinergic enzyme activities, to interference with the synthesis of such enzymes, to its DNA damaging activity on G,C-rich genes or to all of these actions together.

AChE and the closely related acetylcholine hydrolyzing enzyme, butyrylcholinesterase (BChE) are highly similar in their amino acid sequence (50% identity in humans) [31], and in their computer modelled three dimensional structure [10], yet vary in their substrate specificity and in their interaction with inhibitors [19,27]. In addition, the rat AChE gene is G,C-rich (59%) [14] like its human homolog [30], with high predicted sensitivity to guanine binding agents, whereas the BChE gene is A,T-rich (67%) [26] and may be expected to be less sensitive to such agents. This difference made the two cholinesterase genes appropriate models for the in vitro studies described in this report on the effectiveness of AF64A on cholinergic gene expression and/or enzymatic activities. In parallel, we further examined the effects of intracerebroventricular (i.c.v.) administration of AF64A on cholinergic enzyme activities and determined the in vivo effect of AF64A on cholinesterase mRNA levels by reverse transcription coupled with DNA amplification (RT-PCR) in different rat brain areas. To compare the pattern of expression of G,C-rich genes in brains from AF64A treated and control rats, differential PCR-displays [18] were prepared with an arbitrary G,C-rich primer [32]. Our findings suggest a consistent correlation between the cholinotoxic effects of AF64A on G,C-rich sequences in vitro and in vivo and suggest the use of this approach for identifying the target genes to cholinotoxic agents.

2. Materials and methods

2.1. Stereotactic surgery and i.c.v. AF64A infusion

Male Sprague–Dawley rats (Zivic Miller Laboratories, Allison Park, PA) weighing between 250 and 350 g were housed in groups of 2/cage, in a room that was maintained on a 12-h dark–light cycle. Animals had free access to water and food ad libitum. AF64A was prepared as previously described [6]. An aqueous solution of acetylethylcholine mustard HCl (1.0 nmol/l) was adjusted to pH 11.5 with NaOH and stirred at room temperature for 20 min, after which pH was brought to 7.3 with HCl, and the solution stirred at room temperature for another 60 min. This solution was prepared freshly prior to each experiment, and subsequent to these procedures the solution was kept on ice during the time required for surgery (up to 6 h).

Animals were anesthetized with chloral hydrate (350 mg/kg) and positioned in a Kopf small animal stereotactic frame. Two needles (26 gauge) were passed through parallel drilled holes in the skull and positioned bilaterally in the ventricles at the following stereotaxic coordinates from the bregma: posterior 0.8 mm, lateral ± 1.5 mm, and ventral 3.6 mm. AF64A (2.0 nmol/1.5 μl) or an equal volume of vehicle, was infused bilaterally at a flow rate of 0.5 μl/min. The needles were left in place for 5 min after completion of the infusion; after which they were slowly pulled out.

2.2. Tissue preparation

At each predetermined time point post-AF64A administration the rat was decapitated, and its brain was removed and placed on an ice-cold surface. Specific brain regions were dissected out and frozen as soon as possible on dry-ice, then stored at -70°C until biochemical and molecular analyses could be carried out. Before the enzyme assay, tissues were thawed and homogenized in ice-cold sodium phosphate buffer (75 mM, pH 7.4, 1/20 w/v).

2.3. Cholinergic enzyme activity assays

ChAT activity assays were performed according to El-Tamer et al. [5]. Briefly, homogenate (10 μl) was added to 10 μl of buffer substrate mixture containing: sodium phosphate 75 mM (pH 7.4), NaCl 600 mM, $MgCl_2$ 40 mM, Eserine 2.0 mM, bovine serum albumin 0.05%, choline-iodide 10 mM, and [^{3}H]acetyl-coenzyme A 0.87 mM (18.6 mCi/mmol). After 30 min of incubation at 37°C, the tubes were placed on ice and 150 μl of sodium tetraphenylboron solution (75 mg/ml in 3-heptanone) was added to each tube in order to extract the newly synthesized radiolabeled ACh. Tubes were then vortexed, and after centrifugation 100 μl of the top organic layer were taken to measure the amount of [^{3}H]ACh extracted from the buffer, using liquid scintillation spectrometry. The amount of radioactivity extracted from buffer incubated in parallel, without tissue, was subtracted as blank.

2.4. Cholinesterase activities

Cholinesterase activities in brain tissues were measured according to the procedure adapted and described by Leventer et al. [15]. Alternatively, for the in vitro studies, AChE and BChE activities were measured spectrophotometrically as detailed elsewhere [24].

2.5. Statistical analysis

Statistical analysis of the data was performed by the one-way analysis of variance (ANOVA) and Ducan's Multiple-Range tests. Differences were considered significant if they had a P value of 0.05 or less.

2.6. In vitro transcription of AChE and BChE mRNAs in the presence of AF64A

Three transcription plasmids containing the cDNAs encoding for human cholinesterases were used: pSP64 BChE (Promega Corporation, Madison, WI) which contains the sp6 RNA polymerase binding site and hBChE coding sequence [24]; pGEM-ZF(+) (Promega Corporation, Madison, WI), which contains the T7 RNA polymerase binding site and the hAChE coding sequence [30,4] and a Bluescript SK(+) from Stratagene (La Jolla, CA) with T3 RNA polymerase binding site and the human BChE cDNA [24]. This latter plasmid was used to compare AF64A effects on transcription of a single cDNA primed by different RNA polymerases. Plasmid DNAs were incubated with different concentrations of AF64A for 60 min at 37°C. DNA was then purified by two ethanol precipitations. Transcription was performed using the transcription kit RPN #2006 from Amersham International (Buckinghamshire, England) on linearized transcription plasmids according to manufacturer's instructions and using the appropriate RNA polymerase. RNA molecules were radiolabeled by adding to the reaction mixture 10 μCi of [^{32}P]UTP (800 Ci/mmol) for each 5 μg of control or AF64A-treated DNA. Radiolabeled transcription products were denatured, electrophoresed on polyacrylamide gels (5%) containing 7 M urea and exposed to Kodak film autoradiography. Quantification of the transcription products

was performed by densitometric analysis of the film using the Soft Laser Scanning Densitometer Model SL-TRFF (Biomed Instruments, CA, USA) as detailed previously [13].

2.7. RT-PCR analysis of cholinesterase mRNA transcripts in different rat brain regions

Frozen brain regions were extracted by the RNAzol B (Cinna/Biotex Laboratories, Inc, Houston, TX) to yield total RNA according to manufacturer's instructions. Purified RNA samples were kept at −70°C. 100 ng of each RNA sample were subjected to reverse transcription using reverse transcriptase (Gibco BRL Life Technologies Inc. Gaithersburg, MD) followed by specific primer annealing and PCR conditions essentially as described elsewhere [17] with aliquots taken out every 4 cycles starting at cycle 26. PCR primers used in this experiment were 1522(+)/2003(−) and 271 (+)/457(−) for the human AChE and BChE genes, respectively, and 822(+)/996(−) for the rat β-actin, all as described elsewhere [17].

Quantification of the RT-PCR data was based on comparing the accumulation rate of PCR fragments deriving from the total RNA extraction to that resulting from in vitro transcribed specific RNA as detailed elsewhere [17].

2.8. Differential PCR display

The PCR display was essentially as described [32] except that 1 μg total RNA was used for each reaction and that the arbitrary primer used included 60% G,C residues: 5′-CCTCCGCGAGATCATCT-3′. Also, 25 mM of each dNTP was included and the annealing temperature for the high stringency cycles was 55°C. Exposure was for 1 day at room temperature.

3. Results

3.1. AF64A modulates cholinergic enzyme activities in vivo

AF64A effects on different cholinergic markers in vivo were first measured in a time-dependence study. To address the cholinergic deficits following i.c.v. administration of 2 nmol AF64A, we determined the enzymatic activities of AChE and ChAT in different brain regions. Septal AChE showed a slight but significant reduction (25%) which occurred late, at 60 days post-injection, while striatal AChE activity remained apparently unchanged until day 60. In contrast, AChE activity in hippocampus was reduced to 50–60% of control at day 7 through 60 post-AF64A administration (Fig. 1). The enzymatic activity of ChAT showed a different pattern: septal ChAT activity was significantly increased by 35% ($P < 0.01$) on day 7, returned to normal level by day 14 and decreased by 20% by day 60 post-AF64A treatment. In the striatum, ChAT activities remained normal after 0.5, 1.0 and 2 nmol/side AF64A at all of these time points (Fig. 1, and El-Tamer et al., unpublished data). However, hippocampal ChAT activity was significantly decreased to 40–50% of control level at day 7 through 60, corroborating previous observations [5]. The biochemical measurements thus revealed a particular long-term vulnerability to AF64A effects for cholinergic enzyme activities in the hippocampus.

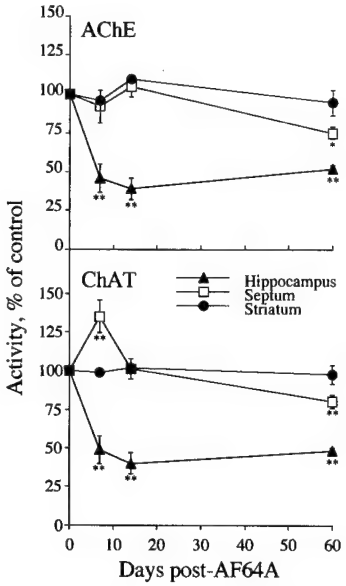

Fig. 1. In vivo effects of AF64A on cholinergic markers. Time-dependent effects of AF64A (2.0 nmol/side) on AChE and ChAT activities are presented for septum, hippocampus and striatum. Animals were sacrificed by decapitation at the indicated time after i.c.v. injection of AF64A. Enzymatic assays were performed in duplicate on tissue homogenates, all as detailed under Experimental Procedures. Data represent the average (mean ± S.E.M., $n = 3$ rats per group) of enzymatic activity expressed as percent of control. AChE activity in control group: mean ± S.E.M., 3476 ± 228, 9214 ± 281 and 20876 ± 474 nmol/mg/h in hippocampus, septum and striatum, respectively. ChAT activity in control group: mean ± S.E.M., 42.1 ± 3.5, 66.5 ± 5.2 and 209.7 ± 7.54 nmol/mg/h in hippocampus, septum and striatum, respectively. * $P < 0.05$; ** $P < 0.01$, compared to vehicle treated group.

3.2. Differential in vitro inhibition of cholinesterases by AF64A

In order to directly test the sensitivity of AChE and BChE to AF64A, we performed a kinetic spectrophotometric analysis of enzymatic activity following pre-incubation of AF64A in a concentration range of 1 to 1000 μM, with the tested enzymes. In this range of AF64A concentration our measurements fully reflected the interaction of the released thiocholine product with DTNB [24], and the color reduction under these experimental conditions was due to enzyme inhibition alone [9]. Following 45 min incubation of AChE and BChE with AF64A at room temperature, a dose-dependent reduction of the catalytic activity of these enzymes was observed (Fig. 2, Top). A significant inhibition of BChE was only detected at concentrations higher than 500 μM of the inhibitor and was limited to 32% inhibition at 1 mM AF64A. In contrast, AChE activity was sensi-

tive to concentrations of AF64A as low as 100 μM and 60% inhibition was caused in the presence of 1 mM AF64A (Fig. 2, Top). Similar results were obtained following incubation at a physiological temperature (37°C; results not shown). At the high concentration of AF64A used in vitro, one would expect susceptability to nucleophilic attack by cholinesterase activities. Moreover, at the physiologically effective average AF 64A concentration of 5–20 μM (based on administration of 2 nmol AF64A to approximately 160 ml CSF per ventricle, after Hebel and Stromberg [11]), neither of the enzymes should be inhibited. Therefore, we next focused our investigation on measurements at the mRNA level.

3.3. Pretreatment of cholinesterase cDNAs with AF64A causes differential damage to in vitro transcription

To compare the sensitivity of the AChE and BChE genes to AF64A, plasmid DNAs carrying each of these cholinesterase coding sequences were subjected to in vitro transcription following pre-incubation with 12.5–100 μM of AF64A. Significant reductions were observed in the yields of ^{32}P-labeled RNA transcripts from both AChE and BChE cDNA in a dose-dependent manner, however, to different extents. While yields of AChE mRNA transcripts were reduced to 76% of control following pre-incubation with as low as 12.5 μM of AF64A, 50 μM of this toxin were required to reduce BChE mRNA transcription to the same extent (Fig. 2, Bottom). The AChE gene therefore displayed differential sensitivity over that of the BChE gene toward AF64A toxicity in vitro, which predicted that physiologically effective concentrations of this cholinotoxin may modulate transcriptional activities of the corresponding genes in cholinergic and/or cholinoceptive cells.

3.4. AF64A administration modulates cholinesterase mRNA levels in vivo

To assess the in vivo levels of CHE mRNAs, total RNA extracts from septum, hippocampus and striatum from AF64A-treated and control rats were subjected to reverse transcription followed by kinetic followup of PCR amplification using primers specific to each of the cholinesterase genes (RT-PCR). As a control for the integrity of the examined mRNAs we followed the accumulation of β-actin mRNA. This analysis revealed that the amounts of septal and striatal AChE mRNA were reduced 25- and 3-fold at 7 days post-AF64A injection, respectively, and returned to 80 and 130% of control levels by day 60 (Fig. 3 and unshown data), while BChE mRNA levels remained unchanged (not shown). In contrast, hippocampal AChE mRNA was 10 times higher in treated rats at day 7 post-injection and returned to apparently normal levels (110%) at day 60. In this same region, BChE mRNA was reduced by 70% on day 7 and remained as low as 50% of control on day 60 (Fig. 3). Beta-actin mRNA products appeared in the RT-PCR tests 8 cycles before those of the cholinesterases, reflecting considerably higher levels than those of CHE mRNAs, and remained unchanged in septum and striatum after AF64A administration, demonstrating the specificity of the effects observed for CHE mRNAs. A 2-fold increase in β-actin mRNA was detected in the hippocampus, 7 days post AF64A administration (not shown), probably reflecting somewhat enhanced levels of general transcription in this cholinoceptive region. Although AChE activity was significantly reduced in the hippocampus, the RT-PCR analysis revealed a concomitant and pronounced increase in AChE mRNA, unique to this brain region.

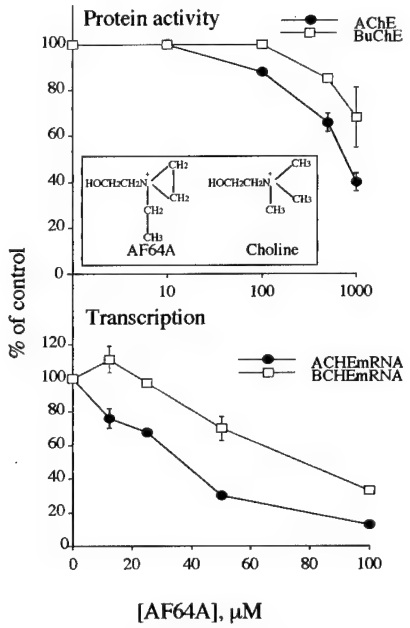

Fig. 2. In vitro effects of AF64A on mammalian CHE genes and their enzyme products. Top: direct AF64A induced inhibition of cholinesterase activities. Inhibition was measured following incubation with increasing concentrations of AF64A by determining remaining activities of AChE and BChE, all as detailed under methods. Inset: chemical structures of the cholinotoxin AF64A (a) and the native choline molecule (b), after Fisher et al. [6]. Bottom: differential sensitivity of the AChE and BChE genes for transcriptional damage induced by AF64A. Equal amounts of the noted plasmids incubated with the noted concentrations of AF64A were used for in vitro transcription in the presence of [^{32}P] nucleotides followed by agarose gel electrophoresis and autoradiogrephy of the ^{32}P-labeled reaction products. Note the relative resistance to AF64A of BChE – as compared with AChEcDNA. The same results were obtained for BChE mRNA transcribed from two transcription plasmids containing the human BChE coding sequences with two distinct RNA polymerases (not shown), demonstrating that the AF64A effects were due to the cDNA seqence and not to the type of RNA polymerase.

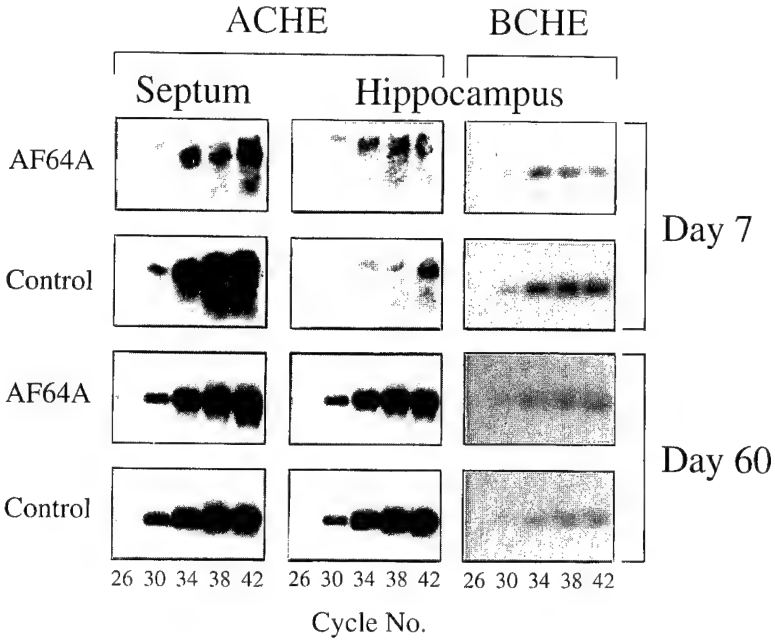

Fig. 3. In vivo modifications in cholinesterase mRNA levels following AF64A treatment. RNA was extracted from septum, hippocampus and striatum of 3 pooled animals 7 and 60 days post AF64A treatment and was subjected to RT-PCR procedure [17]. PCR products were detected as dark bands after hybridization followed by autoradiography.

3.5. AF64A induces region-specific alterations in the differential PCR display of G,C-rich transcripts

To examine whether the increased levels of AChE mRNA in 7 days treated hippocampus reflected a general change in transcription of G,C-rich genes, we employed the approach of differential PCR display [18,32]. To this end, we first examined whether this approach was sensitive enough to detect region-specific differences in G,C-rich transcripts. Amplification conditions were thus adapted so that differentially expressed transcripts were detected in the hippocampus, striatum and septum of control rats with an arbitrary G,C-rich primer. At least 50 conspicuous DNA products were detected after subjecting total RNA from each of these regions (pooled from three rats in each case) to first and second strand synthesis under low stringency annealing conditions, followed by PCR amplification (Fig. 4). A large part of the observed products was common to all regions, however, we also observed different PCR products which were dominant in specific regions (see Fig. 4 for striatum-specific products). Differential PCR displays from the same brain regions of individual animals confirmed that these bands were both dominant in specific regions and reproducible (data not shown).

The general pattern of displayed products did not change in the AF64A treated rats as compared to control rats (Fig. 4). While no AF64A-dependent

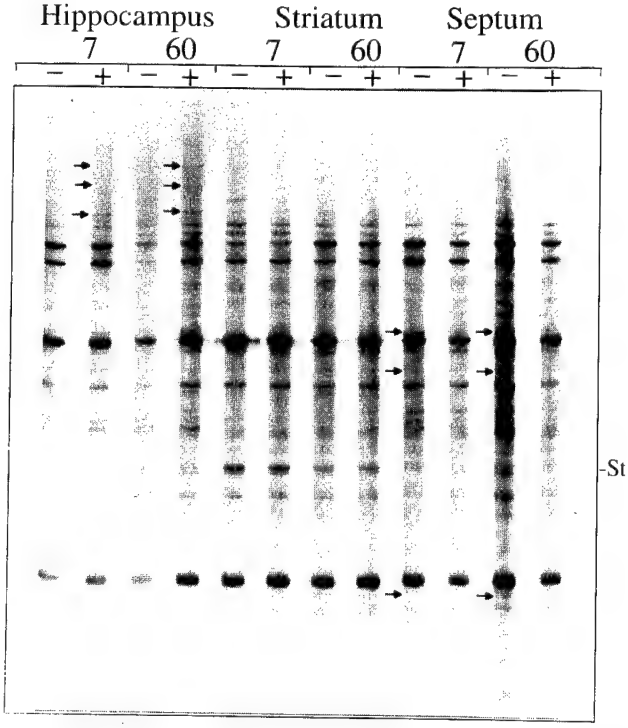

Fig. 4. PCR display. Differential PCR display of 1 μg total RNA extracted from hippocampus, striatum and septum pooled regions (from 3 animals/sample) of saline (−) and AF64A (+) injected rat brains, 7 and 60 days post treatment. Exposure was for 1 day at room temperature, for 10% of reaction mixture per lane. PCR fragments size was between 200 and 400 bp. Altogether most of the PCR products were common to the different brain regions; some were specific for either striatum (St) or hippocampus (not shown in this part of the gel). Arrows indicate PCR products whose intensity changed following AF64A injection.

changes could be observed in striatal mRNA, we were able to detect several quantitative changes in PCR products displayed from hippocampus and septum following AF64A administration. In the septum the levels of 3 transcripts were decreased on day 7 and remained low at day 60 (Fig. 4). At least 3 other PCR fragments appeared to be stronger in the treated as compared with non-treated hippocampus 60 days post AF64A. A less conspicuous but clear increase was also observed in these transcripts at day 7. Assuming that the PCR displays reflect the expression of over 30,000 distinct mRNA species in each brain region [23], this implies that the increase of AChE mRNA in the hippocampus was consistent with an increase in multiple G,C-rich transcripts which was particular to this cholinoceptive brain region.

4. Discussion

We found differential changes in activities of cholinergic marker proteins and in the levels of the corresponding mRNAs in the cholinoceptive hippocampus and the cholinergic septum and striatum of rats following i.c.v. administration of the cholinotoxin, AF64A. ChAT and AChE activities were conspicuously decreased in the hippocampus, reflecting damage to both processes and cell bodies. However, AChE mRNA and other unidentified G,C-rich mRNA transcripts were increased within hippocampal cell bodies, demonstrating a new and previously unforseen level of response to this cholinotoxic damage.

The in vivo experiments were complemented by a series of in vitro tests. In vitro inhibition of transcription of G,C-rich AChEcDNA was achieved at concentrations of AF64A that were 2 times lower than those required to inhibit the A,T-rich BChEcDNA, attributing at least part of the in vivo changes in AChE gene expression to its G,C-rich composition. In vitro studies further revealed that AChE activity was more sensitive to this alkylating agent than that of BChE, and that this inhibition required higher AF64A concentrations than those generally administered i.c.v. Moreover, access of such compounds to intracellular enzymes in the CNS parenchyma in the in vivo situation is very limited. Therefore, our in vitro tests suggest that to achieve direct inhibition of enzyme activities, the intracellular concentration of AF64A should be higher than those present in the CSF. The in vivo inhibition of AChE activity thus suggested that i.c.v.-administered AF64A actively accumulated in cholinergic synapses and entered into cholinergic and/or cholinoceptive cell bodies, where it could reach higher local concentrations. Our findings therefore support the theory of active uptake into cholinergic cell bodies via the choline transport system, which was previously suggested as a mechanism of action for AF64A [20,29]. Once in these cell bodies, AF64A is likely to interact with G,C-rich genes such as AChE and interfere with their transcription [7]. Moreover, the theory of active uptake further explains the apparent direct reduction of protein activities. Altogether, these findings imply that penetration of this alkylating agent into the brain can induce a multileveled cholinergic damage. This includes mechanisms of nucleophilic attack and blocking of guanines in the DNA at cholinergic cell bodies on the one hand, and interference with specific protein subsets at cell bodies and nerve terminals on the other hand. The damage caused by AF64A to DNA probably occurs through direct interaction with the N-7 position in guanines [7].

At the level of mRNA, the main damage induced in vivo by AF64A appeared to be region-specific and partially transient. That the transient decrease in AChE mRNA levels which was observed in cholinergic regions was probably limited to cholinergic cells was indicated from the observation that the average levels of the more ubiquitously expressed β-actin mRNA remained unchanged in spite of its equally high G,C-content (55%) [25]. At the protein level we could discriminate between the vulnerable hippocampus and the more resistant septum and striatum. Injection of 2 nmol AF64A/ventricle did not affect the activities of cholinergic markers measured in the striatum, which was previously found to be sensitive to higher doses of this cholinotoxin [28]. In contrast, the mRNA levels of both AChE, β-actin and other unidentified G,C-rich genes were significantly increased in the hippocampus by 7 days post AF64A administration. This indicated that the in vivo decrease in AChE activities in the hippocampus was secondary to the reduction in AChE mRNA in the septum, projecting to the hippocampus, and that this change caused a feedback increase of transcription of several genes, including AChE and β-actin, in this cholinoceptive and vulnerable area.

The hippocampus receives its main cholinergic innervation from medial-septal nuclei. Therefore, cholinoceptive cell bodies in this region should be sensitive to damage occurring to cholinergic neurons in the medial-septal nuclei. Cell bodies rich in AChE mRNA were indeed located by in situ hybridization to the CA1–3 regions and the dentate gyrus in rodent hippocampus (Lev-Lehman et al., unpublished data).

To evaluate the general transcriptional damage caused by AF64A, we adopted the recent approach of differential PCR display [18]. This strategy involves presentation of partial cDNA sequences, amplified from subsets of mRNAs by reverse transcription coupled to PCR using arbitrary primers [32]. Differentially expressed mRNAs were indeed observed in septum, striatum and hippocampus, and some of those particular to the hippocampus were modulated following

AF64A administration. The long term changes in gene expression detected by the PCR display suggest the use of this approach to clone and identify the modulated transcripts. That both the protein activities and the PCR display changes were long term can further indicate damage to the machinery of mRNA translation. This would reduce AChE activities even under conditions where AChE mRNA levels returned to normal, as was the case by day 60 post AF64A treatment.

The transcriptional changes in AF64A treated hippocampus are in line with the behavioral effects induced by this cholinotoxin. Moreover, prenatal administration of another alkylating agent, methylazoxymethanol (MAM) to pregnant rats at gestational day 14 or 15 resulted in a massive reduction in intrinsic cortical neurons and interneurons of hippocampus and striatum [3]. The enhanced transcription of β-actin and several other G,C-rich unidentified genes, in the AF64A treated hippocampus, therefore adds this cholinotoxin to the list of plasticity inducing agents, which calls for histological experiments to search for AF64A induced morphometric changes in the hippocampus.

Specific choline analogs can exert differential damage to cholinergic neurons through different mechanisms, such as selective block of receptors or interference with the functioning of genes encoding these protein products [1]. The fact that most of the cholinergic changes, on the mRNA level, were back to normal by 60 days post AF64A treatment supports the notion that cholinergic cells damaged by AF64A can largely recover and return to normal function. This reversibility can suggest the existence of intra-regional bypass machinery which responds to changes in the cholinergic balance by secondary regulation of gene transcription. Therefore, our present findings suggest the use of AF64A treated rats as a model for the cholinergic deficits occuring in Alzheimer's and Huntington's patients through characterization of the mRNA transcripts whose levels are modified in the septum and hippocampus after a single dose AF64A injection. The use of the sensitive PCR display method to decipher changes in gene expression can introduce a novel approach to the research of cholinergic deficits that will enable to pinpoint and characterize genes whose functioning is perturbed under conditions of cholinergic deficit.

Acknowledgements

This study was supported by the U.S. Army Medical Research and Development Command (to H.S.) and by the Lady Davis Foundation and the Charles Smith Psychobiology fund (to I.H. and H.S). E.L.-L. is an incumbent of a Golda Meir Pre-doctoral fellowship.

References

[1] Carmichael, W.W., The toxins of cyanobacteria, *Sci. Am.*, 270 (1994) 64–72.

[2] Chrobak, J.J., Hanin, I., Schmechel, D.E. and Walsh, T.J., AF64A-induced working memory impairment: behavioral, neurochemical and histological correlates, *Brain Res.*, 463 (1988) 107–117.

[3] Di-Luca, M., Merazzi, F., Cimino, M., Gispen, W.H., de Graan, P.N.E. and Cattabeni, E., Prenatally induced brain lesions, cognitive impairment and ptrotein-kinase C-dependent phosphorylation. In G. Racagni et al. (Eds.), *Biological Psychiatry*, Vol. 2, Elsevier, Amsterdam, 1991, pp. 188–191.

[4] Ehrlich, G., Ginzberg, D., Loewenstein, Y., Glick, D., Kerem, B., Ben-Ari, S., Zakut, H. and Soreq, H., Population diversity and distinct haplotype frequencies associated with AChE and BChE genes of Israeli Jews from Trans-Caucasian Georgia and from Europe, *Genomics*, in press.

[5] El-Tamer, A., Corey, J., Wulfert, E. and Hanin, I., Reversible cholinergic changes induced by AF64A in rat hippocampus and possible septal compensatory effect, *Neuropharmacology*, 31 (1992) 397–402.

[6] Fisher, A., Mantione, C.R., Abraham, D.J. and Hanin, I., Long term central cholinergic hypofunction induced in mice by ethylcholine aziridinium ion (AF64A) in vivo, *J. Pharm. Exp. Ther.*, 222 (1982) 140–145.

[7] Futscher, B.W., Pieper, O., Barnes, D.M., Hanin, I. and Erickson, L.C., DNA damaging and transcription-terminating lesions induced by AF64A in vitro, *J. Neurochem.*, 58 (1992) 1504–1509.

[8] Gall, C., Murray, K. and Isackson, P.J., Kainic acid-induced seizures stimulate increased expression of nerve growth factor mRNA in rat hippocampus, *Mol. Brain Res.*, 9 (1991) 113–123.

[9] Hanin, I., Yaron, A., Ginzberg, D. and Soreq, H., AF64A attenuates human acetylcholinesterase (AChE) and butyrylcholinesterase (BChE) gene transcription in vitro. In I. Hanin, A. Fisher and M. Yoshida, (Eds.), *Alzheimer's and Parkinson's Diseases: Recent Advances*, Plenum, NY, 1994, in press.

[10] Harel, M., Sussman, J.L., Krejci, E., Bon, S., Chanal, P., Massoulie, J. and Silman I., Conversion of acetylcholinesterase to butyrylcholinesterase: modeling and mutagenesis, *Proc. Natl. Acad. Sci. USA*, 89 (1992) 10827–10831.

[11] Hebel, R. and Stromberg, M.W. (Eds.), *Anatomy of the Laboratory Rat*, The Williams and Wilkins Company, Baltimore, Waverly Press, 1976, pp. 124–125.

[12] Hortnagl, H., Potter, P.E., Happe, K., Goldstein, S., Leventer, S., Wulfert, E. and Hanin, I., Role of aziridinium moiety in the in vivo cholinotoxicity of ethylcholine aziridinium ion (AF64A), *J. Neurosci. Methods*, 23 (1988) 101–105.

[13] Lapidot-Lifson, Y., Prody, C.A., Ginzberg, D., Meytes, D., Zakut, H. and Soreq, H., Coamplification of human acetylcholinesterase and butyrylcholinesterase genes in blood cells: Correlation with various leukemias and abnormal megakaryocytopoiesis, *Proc. Natl. Acad. Sci. USA*, 86 (1989) 4715–4719.

[14] Legay, C., Bon, S., Vernier, P., Coussens, F. and Massoulie, J., Cloning and expression of a rat acetylcholinesterase subunit: generation of multiple molecular forms and complementarity with a *Torpedo* collagenic subunit, *J. Neurochem.*, 60 (1993) 337–346.

[15] Leventer, S.M., McKeag, D., Clancy, M., Wulfert, E. and Hanin, I., Intracerebroventricular administration of ethylcholine mustard aziridinium ion (AF64A) reduces release of acetylcholine from hippocampal slices, *Neuropharmacology*, 24 (1985) 453–459.

[16] Leventer, S.M., Wulfert, E. and Hanin, I., Time course of ethylcholine aziridinium ion (AF64A)-induced cholinotoxicity in vivo, *Neuropharmacology*, 26 (1987) 361–365.

[17] Lev-Lehman, E., Hornreich, G., Ginzberg, D., Gnatt, A., Meshorer, A., Eckstein, F., Soreq, H. and Zakut, H., Antisense inhibition of acetylcholinesterase gene expression causes transient hematopoietic alterations in vivo, *Gene Therapy*, 1 (1994) 127–135.

[18] Liang, P. and Pardee, A.B., Differential display of eukaryotic messenger RNA by means of polymerase chain reaction, *Science*, 257 (1992) 967–971.

[19] Loewenstein, Y., Gnatt, A., Neville, L.F. and Soreq, H., Chimeric human cholinesterase: identification of reaction sites responsible for recognition of acetyl- or butyrylcholinesterase – specific ligands, *J. Mol. Biol.*, 234 (1993) 289–296.

[20] Mantione, C.R., Fisher, A. and Hanin, I., The AF64A-treated mouse: possible model for cholinergic hypofunction, *Science*, 213 (1981) 579–580.

[21] Mantione, C.R., Zigmond, M.J., Fisher, A. and Hanin, I., Selective presynaptic cholinergic neurotoxicity following intrahippocampal AF64A injection in rats, *J. Neurochem.*, 41 (1983) 251–255.

[22] Murrin, L.C., High-affinity transport of choline in neural tissue, *Pharmacology*, 21 (1980) 132–140.

[23] Nedivi, E., Hevroni, D., Naot, D., Israeli, D. and Citri, Y., Numerous candidate plasticity-related genes revealed by differential cDNA cloning, *Nature*, 363 (1993) 718–722.

[24] Neville, L.F., Gnatt, A., Loewenstein, Y., Seidman, S., Ehrlich, G. and Soreq, H., Intramolecular relationships in cholinesterases revealed by oocyte expression of site-directed and natural variants of human BChE, *EMBO. J.*, 11 (1992) 1641–1649.

[25] Nudel, U., Zakut, R., Shani, M., Neuman, S., Levi, Z. and Yaffe, D., The nucleotide sequence of the rat cytoplasmic beta-actin gene, *Nucl. Acids Res.*, 11 (1983) 1759–1771.

[26] Prody, C.A., Zevin-Sonkin, D., Gnatt, A., Goldberg, O. and Soreq, H., Isolation and characterization of full-length cDNA clones for cholinesterase from fetal human tissues, *Proc. Natl. Acad. Sci. USA*, 84 (1987) 3555–3559.

[27] Quinn, D., Acetylcholinesterase: enzyme structure, reaction dynamics and virtual transion states, *Chem. Rev.*, 87 (1987) 955–979.

[28] Sandberg, K., Hanin, I., Fisher, A. and Coyle, J.T., Selective cholinergic neurotoxin: AF64A's effects in rat striatum, *Brain Res.*, 293 (1984) 49–55.

[29] Sandberg, K., Schnaar, R.L., Hanin, I. and Coyle, J.T., AF64A: an active site directed irreversible inhibitor of choline acetyltransferase, *J. Neurochem.*, 44 (1985) 439–445.

[30] Soreq, H., Ben-Aziz, R., Prody, C., Seidman, S., Gnatt, A., Neville, L., Lieman-Hurwitz, J., Lev-Lehman, E., Ginzberg, D., Lapidot-Lifson, Y. and Zakut, H., Molecular cloning and construction of the coding region for human acetylcholinesterase reveals a G+C rich attenuating structure, *Proc. Natl. Acad. Sci. USA*, 87 (1990) 9688–9692.

[31] Soreq, H. and Zakut, H., *Human Cholinesterases and Anticholinesterases*, Academic Press, NY, 1993. pp. 1–314.

[32] Welsh, J., Chada, K., Dalal, S., Cheng, R., Ralph, D. and McClelland, M., Arbitrary primed PCR fingerprints of RNA, *Nuc. Acid Res.*, 20 (1992) 4965–4970.

[33] Wurtman, R.J., Choline metabolism as a basis for the selective vulnerability of cholinergic neurons, *Trends Neurosci.*, 15 (1992) 117–122.

Overlapping Drug Interaction Sites of Human Butyrylcholinesterase Dissected by Site-Directed Mutagenesis

YAEL LOEWENSTEIN-LICHTENSTEIN, DAVID GLICK, NELLY GLUZMAN, MEIRA STERNFELD, HAIM ZAKUT, and HERMONA SOREQ

Department of Biological Chemistry, The Institute of Life Sciences, The Hebrew University of Jerusalem, 91904 Israel (Y.L-L, D.G., N.G., M.S., H.S.); and Department of Obstetrics and Gynecology, The Edith Wolfson Medical Center and Sackler School of Medicine of Tel-Aviv University, Holon, Israel (H.Z.).

running title: Butyrylcholinesterase-Drug Interaction Sites

This work was supported by grants to H.S. and H.Z. from the U.S. Army Medical Research and Development Command (17-94-C-4031), the Israel Academy of Sciences and the Chief Scientist of the Israel Ministry of Health.

Summary

Butyrylcholinesterase (acylcholine acyl hydrolase, BuChE, EC 3.1.1.8) limits the access of drugs, including tacrine, to other proteins. The "atypical" BuChE variant, in which aspartate 70 at the rim of the active site gorge is substituted by glycine, displayed a more drastically weakened interaction with tacrine than with cocaine, dibucaine, succinylcholine, BW284c51 (1,5-bis(4-allyldimethylammoniumphenyl)pentan-3-one dibromide) or α-solanine. To delineate the protein domains that are responsible for this phenomenon, we mutated residues within the rim of the active site gorge, the region parallel to the peripheral site in the homologous enzyme acetylcholinesterase (acetylcholine acetyl hydrolase, AChE, EC 3.1.1.7), the oxyanion hole and the choline-binding site. When expressed in microinjected *Xenopus* oocytes, all mutant DNAs yielded comparable amounts of immunoreactive protein products. Most mutants retained catalytic activity close to that of wild-type BuChE and were capable of binding ligands. However, certain modifications in and around the oxyanion hole caused dramatic loss in activity. The affinities for tacrine were reduced more dramatically than for all other ligands, including cocaine, in both oxyanion hole and choline-binding site mutants. Modified ligand affinities further demonstrated a peripheral site in residues homologous with those of acetylcholinesterase. BuChE mutations which prevented tacrine interactions also hampered its ability to bind other drugs and inhibitors, which suggests a partial overlap of the binding sites. This predicts that in addition to their genetic predisposition to adverse responses to tacrine, homozygous carriers of "atypical" BuChE will be overly sensitive to additional anti-cholinesterases, and especially so when exposed to several anti-cholinesterases in combination.

ABBREVIATIONS AChE, acetylcholinesterase; BTCh, butyrylthiocholine; BuChE, butyrylcholinesterase; ChE, cholinesterase; DFP, diisopropylfluorophosphonate. The residue numbers in the text are those of human BuChE (1). For these, the corresponding *Torpedo* AChE residue number is given in parentheses: N68 (Y70), D70 (D72), W82 (W84), G115 (G117), G116 (G118), Q119 (Y121), T120 (T122), V127 (V129), S198 (S200), and A199 (A201).

Introduction

The pharmacokinetics of the cholinesterase (ChE) inhibitor Alzheimer's disease drug tacrine is significantly influenced by blood ChEs because when tacrine enters the circulation, it first encounters and reacts with serum BuChE and AChE on the surface of erythrocytes. Only those tacrine molecules that escape this screen can subsequently cause a physiological response by inhibiting brain AChE. Of the two ChEs in the blood, BuChE is quantitatively at least as important as AChE (1). Moreover, it is undoubtedly replaced in the blood faster than is AChE. Although it does not degrade tacrine, 20% of the circulating BuChE can sequester 40% of the total tacrine in the blood of patients (2). This, and the large number of natural BuChE variants (3,4) raises the question of what are the BuChE residues that interact with tacrine and how tacrine might modify the response of patients to other drugs or they, the response to tacrine.

The structure of AChE and the mode of binding of tacrine to it are known, thanks to X-ray crystallography work (5-7), but tacrine's interaction with BuChE must be different due to differences of amino acid residues at the homologous binding site (Fig. 1). In particular, the common "atypical" genetic variant of BuChE is predicted to differ in its tacrine interactions. The mutated residue D70, although far from the catalytic site, was first shown to affect ligand specificity when its natural mutation to a glycine residue was identified as the basis of the variant's failure to hydrolyze succinylcholine (8,9). It has been suggested that D70 is positioned in such a way that its free carboxylate group faces outward, which allows it to attract positively-charged inhibitors to the opening of the active site gorge (10,11). More recently, we observed that "atypical" BuChE interacts with tacrine with a 100-fold weaker affinity than does the normal enzyme (2). This raised the question of which additional BuChE residues are crucial for interactions with tacrine and what are the other drugs that interact poorly with "atypical" BuChE.

The X-ray crystallography of AChE (5), combined with site directed mutagenesis has detailed AChE's interaction sites with drugs and inhibitors (reviewed in 12,13). These include attraction of the substrate to a peripheral binding site and into a 20 Å-deep gorge and its binding to both the acyl- and choline-binding sites (Fig. 2). In the transition state the acyl and alkoxy substrate moieties, the incoming hydroxyl group of the enzyme's active site serine residue, and

the carbonyl oxygen create a tetrahedral array around the substrate carbonyl carbon atom. The carbonyl oxygen, now bearing a negative charge, is protected by the enzyme's oxyanion hole. The transition state collapses to the acyl-enzyme, and free choline leaves the active site (12). In an earlier study we had replaced the entire region of human BuChE, residues 55 to 138 which includes all these sites, with the homologous region from human AChE. The resulting chimera had catalytic and liganding properties intermediate between the two parent proteins (14). In order to further characterize sites of BuChE-drug interaction, we have now created a series of point mutations within this region to compare BuChE to its "atypical" variant and to AChE.

Four key regions in BuChE were addressed in the present study by site-directed mutagenesis:

(A) The oxyanion hole is lined in *Torpedo* AChE by the amide groups of the peptide bonds of residues homologous with BuChE G116, G117 and A199 (12), of which we mutated G116 and G117 and the adjacent G115.

(B) The choline-binding site was associated with the residue W82 by photoaffinity labeling (15,16), site directed mutagenesis (17-19), and diffusing quarternary ammonium inhibitors into *Torpedo* AChE crystals (6).

(C) A peripheral anionic site which accounted for the allosteric inhibition of AChE by BW284c51 and propidium (20) was identified with Y70 and Y121 (6,7,18-23). Mutagenesis experiments that replaced the two AChE residues, Y70 and Y72, in various combinations, demonstrated decreased affinity to AChE-typical ligands (24).

(D) The back door which was proposed by Gilson et al. (25) to allow direct exit of choline through a polypeptide flap has, as a major feature, residue V127. We have used this knowledge of AChE to predict key regions of interaction between BuChE and tacrine and selected additional anti-ChEs.

We now report that substitution of the relevant BuChE residues (Fig. 2) reveals partially overlapping binding sites for tacrine and other ligands. This predicts a genetic predisposition to adverse responses to several anti-ChE drugs in patients with the "atypical" BuChE phenotype and implicates other regions around BuChE residue D70 in such ligand interactions.

Materials and Methods

BW284c51, α-solanine, dibucaine hydrochloride, succinyldicholine dichloride and tacrine hydrochloride were purchased from Sigma Chemical Co. (St. Louis, MO). Cocaine hydrochloride was from E. Merck (Darmstadt, Germany). Human AChE and BuChE were from microinjected *Xenopus* oocytes.

Restriction enzymes, T4 polynucleotide kinase and T4 DNA ligase were from Boehringer Mannheim (Mannheim, Germany). Mutagenic primer oligonucleotides, supplied by Microsynth (Windisch, Switzerland), were: pTCT TGC TGT CAG GCC ATA GAT CAA AG-OH (N68A), pCT TGC TGT CAG GAC ATA GAT CAA A-OH (N68D), pT TGC TGT CAG AAG ATA GAT CAA AG-OH (N68K), pTCT TGC TGT CAG CGC ATA GAT CAA AG-OH (N68R), pCT TGC TGT CAG TAC ATA GAT CAA A-OH (N68Y), pGA TCA GAG ATG TTC AAC CCA AAC ACT-OH (W82F), pGA TCA GAG ATG TAC AAC CCA AAC ACT-OH (W82Y), pA TGG ATT TAT GCT GGT GGT TTT CA-OH (G115A), pTA TGG ATT TAT TGT GGT GGT TTT C-OH (G115C), pA TGG ATT TAT GAT GGT GGT TTT CA-OH (G115D), pTA TGG ATT TAT GAG GGT GGT TTT CAA-OH (G115E), pGG ATT TAT GGT GAG GGT TTT CAA ACT-OH (G116E), pT TAT GGT GGT GAT TTT CAA ACT GG-OH (G117D), pTT TAT GGT GGT TGT TTT CAA ACT G-OH (G117C), pTT TAT GGT GGT GAG TTT CAA ACT GGA-OH (G117E), pGGT GGT GGT TTT GCA ACT GGA ACA TC-OH (Q119A), pGT GGT GGT TTT GAA ACT GGA ACA T-OH (Q119E), pGGT GGT GGT TTT GGA ACT GGA ACA TC-OH (Q119G), pGGT GGT TTT CAC ACT GGA ACA TCA-OH (Q119H), pGT GGT GGT TTT AAA ACT GGA ACA T-OH (Q119K), pT GGT GGT TTT CGA ACT GGA ACA TC-OH (Q119R), pGGT GGT GGT TTT TAC ACT GGA ACA TC-OH (Q119Y), pGGT GGT TTT CAA GAG GGA ACA TCA TCT T-OH (T120E), pGGT GGT TTT CAA GGT GGA ACA TCA TC-OH (T120G), pGGT GGT TTT CAA CAT GGA ACA TCA TC-OH (T120H), pGT GGT TTT CAA AAG GGA ACA TCA TCT-OH (T120K), pCA TCT TTA CAT GAT TAT GAT GGC A-OH (V127D), pTA TGG ATT TAT GGT GCT GAT TTT CAA ACT GGA AC-OH (G116A/G117D).

Bases that are mismatched to wild-type BuChEcDNA (1) are underlined, and the substituted amino acids are shown in parentheses. The homologous (-) strands were also synthesized for use as mutagenic primers.

External primers for PCR mutagenesis were pCAT ACT GAA GAT GAC ATC ATA-OH (+154 to +174) and pAGC CAA CTG TTG ATC AAA TAA-OH (-701 to -681) for use with *Nco*I and *Ava*I in the mutagenesis of G115, G116, G117, G116/G117, Q119 and T120; pCAT ACT GAA GAT GAC ATC ATA-OH (+154 to +174) and pAGC CAA CTG TTG ATC AAA TAA-OH (-701 to -681) for use with *Acc*I and *Ava*I in the mutagenesis of N68 and W82; pCAT ACT GAA GAT GAC ATC ATA-OH (+154 to +174) and pTC AGT CTC ATT CTC TCT AG-OH (-953 to -935) for use with *Nco*I and *BamH*I in the mutagenesis of V127. *In vitro* transcription kits were from Promega (Madison, WI).

Following mutagenesis, the modified regions in each of these plasmids were sequenced for verification of structure. *In vitro* transcription, microinjection into *Xenopus* oocytes and expression of BuChEmRNA were all as described by Gnatt et al. (26). BuChE activity measurements and K_m and IC_{50} determinations in multiwell plates were as in Neville et al. (10). Immobilization of BuChE in the multiwell plates via adsorbed antibodies further enabled ELISA determination of BuChE (24). Ki values were calculated according to Hobbiger and Peck (27), $K_i = IC_{50}(1 + S/K_m)$. Despite the fact that steady-state hydrolysis of BTCh by BuChE probably does not obey the assumptions of Michaelis-Menten kinetics, as others do, and so that our data will be comparable with theirs, we use the K_m, Ki and k_{cat} values derived from the experimental data on the assumption that they are close enough to justify this analysis.

In order to test the integrity of the active site in oxyanion hole mutants that showed no catalytic activity (G117E, C and D), we incubated 100 ml of 1:10 (w/v) oocyte homogenate for 5 min at 21 °C in phosphate-buffered saline with 2 mCi of [^{3}H]-DFP (DuPont NEN, Bad Homburg, Germany), electrophoresed the product with commercial BuChE as a mobility standard and autoradiographed the gel for 2 months under an intensifying screen.

Results

Compared to normal BuChE, the affinity of the "atypical" BuChE variant for tacrine was reduced 100-fold, but for cocaine, succinylcholine, BW284c51, α-solanine and dibucaine, only 30-fold. Moreover, "atypical" BuChE frequently displayed lower affinity than AChE for many of these drugs (Table 1). Therefore, the properties of D70 alone could not explain the ligand-binding differences between "atypical" and normal BuChE. The involvement of additional residues was expected since D70 is conserved in AChE and BuChE, yet their drug interactions are drastically different. We had previously examined the chimeric ChE formed by replacement of residues 55-138 of BuChE by the corresponding peptide from AChE and found its affinities for other anti-ChEs to be generally intermediate between those of BuChE and AChE (14). In order to more precisely locate interaction sites, we have now prepared a series of point mutations at selected residues of the binding sites included in the chimeric peptide from BuChE (Fig. 2).

To evaluate changes that occurred in their catalytic properties, V_{max} and K_m values for BTCh were compared for oocyte-produced mutant BuChEs, "atypical" and normal BuChE and AChE. All mutants were detectable by the antibody to native human BuChE . Comparison with an ELISA standard curve constructed with BuChE from human serum allowed evaluation of the amount of enzyme being assayed, and enabled the determination of several k_{cat} values of key oxyanion hole mutants (Table 2). The ELISA assay also revealed that nearly equal amounts of each mutant human BuChE were produced in the *Xenopus* oocytes, regardless of its intrinsic activity, suggesting that none of these mutations hampered appropriate protein folding.

Inhibition of BTCh hydrolysis was observed over a wide range of inhibitor concentrations (Fig. 3). Succinylcholine, cocaine and dibucaine are substrates of BuChE, and as such compete with BTCh, yet have no sulfhydryl moiety that may be detected in the colorimetric assay we use. Whatever hydrolysis may have occurred did not materially change their concentrations, as the enzymatic rates we determined were linear over the course of the 20 to 30 min for which the average rate of BTCh hydrolysis was calculated. In many cases a mutation was innocuous (Table 1); in other cases inhibition of the mutants fell into one of only a few patterns, of which representative inhibition curves are shown (Fig. 3). It is evident from the figure and from

additional such curves (not shown) that the inhibition profile of tacrine was largely similar to that of α-solanine, while cocaine and dibucaine constituted another group. In spite of the low affinity of mutant BuChEs for succinylcholine, it may also fit this latter group. From curves such as those in Fig. 3 and the Km values, Ki values for each mutation were also calculated (Table 1). To assist visualization of the results, we calculated the ratios between the Ki values of each of the mutants to the corresponding Ki value for the normal enzyme (Fig. 4). There was no mutation with any detectable activity that had decreased affinity for all ligands, further excluding the possibility that a generalized failure prevented folding into an active conformation. Even the T120K mutation, which had very much lower affinity for all the inhibitors, had a normal Km value (Table 1, Figs. 3, 4).

The changes observed in inhibition parameters indicated involvement of several sites in ligand-BuChE interactions, yet excluded other sites from being involved. Thus, both choline-binding site mutations W82Y and F caused a significant increase in Km and Ki values for the set of inhibitors (>100-fold for tacrine, greater than for any other inhibitor) (Table 1, Fig. 4). This implied that the interaction between the substrate's quaternary ammonium moiety and the indol groups of the tryptophan residue are quite specific because other aromatic groups, the phenyl of phenylalanine (W82F) or hydroxyphenyl of tyrosine (W82Y), conferred lower affinity. However, mutating V127 into D resulted in no dramatic change in Km or Ki values for the examined substrate and inhibitors, which excludes the involvement of this back door residue with ligand interactions of BuChE.

Of the oxyanion hole mutations, the glycine residues at positions 115, 116, 117 have drawn special attention because they are conserved throughout the ChE family and are also found in the sequence of related α/β hydrolase-fold proteins (28). These glycine residues were suggested by Sussman et al. (5) to participate in the formation of the oxyanion hole. Several mutations were introduced in these residues: G115C, D, E, A and S, G116E, G117D and E and the double mutation G116A/G117D, all of which resulted in a significant reduction in activity but not in the level of protein expression, in complete agreement with others' predictions (5). The most significant influence of the substitution was noted for mutations G115D, G116E and G116A/G117D, all of which displayed no detectable catalytic activity. However, G115C

BuChE reacted with [^{3}H]-DFP, although it had lost almost all its activity (e.g. Fig. 5). Covalent labeling with [^{3}H]-DFP, like measures of enzymatic activity, relies on the structural integrity of catalytic site elements, but unlike enzymatic tests, the labeling is unrelated to substrate turnover rate. Thus, an oxyanion hole mutant might still react, even if very slowly, with DFP; labeling by DFP would therefore indicate that the protein has folded properly, but that there may be poor substrate binding or product release, which destroys its catalytic efficiency. As the covalent reaction of this OP agent with the active site serine of normal ChEs is quite fast, this is a very sensitive test for the integrity of the active site conformation. Slightly higher catalytic activity could be detected for mutants G115A and S, but k_{cat} and k_{cat}/K_m values were considerably lower than that of normal BuChE (Table 2). In contrast, a milder reduction of no more than 10-fold was found for k_{cat} values of G115A and S. Introduction of a glutamate at position 117 was yet better tolerated: only a minor decrease of about 5-fold was noted in k_{cat}. Moreover, K_m was not altered in oxyanion hole mutants in which moderate activities could be detected. When interactions with the group of reversible inhibitors were examined for these mutations, significant decreases in the interactions with tacrine, α-solanine and succinylcholine were found for G115A, by up to a 100-fold as compared with normal BuChE. Thus the oxyanion hole participates in both substrate and inhibitor interactions of BuChE.

To further identify sites that determine the specificity of BuChE, we created several mutants in the region homologous with the AChE peripheral site: N68D, K, R, Y and A, and Q119G, H, E, R, K, Y and A. All of these mutants were catalytically active, and displayed no significant change in their k_{cat} or K_m values as compared to normal BuChE (Tables 1 and 2). The inhibitor interactions of the various peripheral site mutant BuChEs were examined using tacrine and a group of other reversible inhibitors. None of the mutations in N68 displayed any significant alteration in inhibition toward the set of reversible inhibitors (Table 1, Fig. 4). However, mutations in Q119 caused changes in sensitivity to inhibitors, the greatest when basic residues replaced the glutamine. Significant loss of sensitivity to dibucaine and succinylcholine, but not for other ligands such as tacrine, α-solanine and cocaine, was found for Q119R and K.

Interestingly, when inhibition by the AChE-specific inhibitor BW284c51 was examined, a significant increase in sensitivity was noted for most of the peripheral site mutants, except when basic residues were introduced. The highest increase in sensitivity was found when acidic residues (glutamate and aspartate) replaced Q119 and N68 respectively, but increases were seen also when tyrosine residues, as in AChE, were introduced (Table 1, Fig. 4). Peripheral site interactions thus seemed to depend primarily on charge.

T120, which is adjacent to Q119 of the peripheral site, is conserved in BuChE from several organisms, yet differs from AChE, in which a serine residue occupies this position. It was important, therefore, to examine whether this residue plays a role in inhibitor interactions. The following changes were introduced: T120G, H, N and K, none of which displayed any significant change in k_{cat} or K_m value, as compared to normal BuChE. When their inhibition properties were examined for the set of reversible inhibitors, a striking loss of sensitivity was observed when a basic residue was introduced (T120K). This mutant was practically insensitive to all of the inhibitors examined, although its K_m value for BTCh remained unaltered. Introduction of a positive charge has therefore confirmed that this particular region in BuChE is important for charge-dependent ligand interactions. Alternatively or additionally, the effect of this mutation may be due to structural changes. Thus, of all the examined regions, it was in choline-binding site and oxyanion hole mutants, but not in peripheral site, that affinity for tacrine was reduced.

When the logarithms of the tacrine K_i values were plotted against the logarithms of each of the other K_i values (logarithms were used to more evenly distribute points and give appropriate weight to all mutations) and a linear regression analysis was performed, there was a positive correlation with each of the other inhibitors. Representative plots are shown in Fig. 6. The correlation coefficients were: tacrine/succinylcholine, $r = 0.66$; tacrine/dibucaine, $r = 0.58$; tacrine/α-solanine, $r = 0.90$; tacrine/BW284c51, $r = 0.57$; tacrine/cocaine, $r = 0.81$. In all cases, for the samples sizes, these correlation coefficients were higher than those for the 95% confidence limit (29). This indicates overlaps between the tacrine-binding site and the binding site of each of the other inhibitors.

Discussion

We have used site-directed mutagenesis and *Xenopus* oocyte expression of resultant human BuChE variants to demonstrate the involvement of the peripheral and choline-binding sites as well as the oxyanion hole in the binding of tacrine to human BuChE. Comparison of novel mutants with AChE and the natural "atypical" BuChE variant revealed that normal serum BuChE, but not mutants in the choline-binding site or oxyanion hole or the "atypical" enzyme, can effectively compete with AChE in binding of tacrine and several other drugs. Moreover, our findings predict that BuChE-tacrine interactions compete with BuChE's interaction with other drugs such as the muscle relaxant succinylcholine and dibucaine-like local anesthetics. Paralleling its wide substrate specificity, BuChE mutations generally caused only minor changes in liganding properties, sometimes even increasing affinity. This emphasizes the plasticity of the enzyme, a property well-suited to its role as a scavenger. Our current findings thus demonstrate that the scavenging capacity of BuChE extends across a wide array of ligands, suggesting that tacrine treatment in patients exposed to other anti-ChEs may result in a different effective dose. An important corollary of this finding is that the actions of other anti-ChEs, those for instance that are used therapeutically, will be differentially affected by the presence of tacrine, depending on blood BuChE concentration and properties. Another possibility is that mutations at the tacrine site effected changes in the binding site of another inhibitor or vice versa. An example of such transmission of an effect through the protein molecule seems to be the allosteric effect of binding of fasciculin to the peripheral anionic site of AChE (30), which lowers but does not abolish the activity of the enzyme.

X-ray crystallography locates tacrine at the bottom of the active site gorge of AChE that extends to the choline binding site, about 5 Å from D70 (6). Not surprisingly, therefore, inhibitors that stretch from the catalytic site to the peripheral site, such as succinylcholine and BW284c51 overlap with tacrine and show roughly the same pattern of inhibition of the mutant BuChEs as does tacrine. As the aglycone of α-solanine, solanidine also inhibits ChEs, it is presumably the shared bulky steroidal alkaloid moiety that blocks the entrance to the active site; the bulkiness of α-solanine with its three glycoside residues requires it inevitably to overlap the

tacrine-binding site. Although the atomic details of their binding to BuChE are unknown, cocaine and dibucaine have binding sites that overlap that of tacrine.

In BuChE, the residues homologous with glutamine and asparagine of AChE's peripheral anionic site are N68 and Q119 (2,13). Mutagenesis of N68 and Q119 in BuChE was performed in order to examine whether in BuChE these residues participate in interactions with AChE-specific inhibitors or with less specific ligands. Neither of these mutations caused any significant change in K_m value or k_{cat}, which indicates that this region does not participate directly in substrate interactions. We examined the inhibition of these mutants by the set of reversible inhibitors. Mutation of N68 did not cause any significant change in the sensitivity of BuChE to any of these inhibitors. In contrast, mutation of residue 119 resulted in changes of sensitivity which were most striking when a basic residue was introduced. Interestingly, significant reduction in sensitivity was also found for inhibition by succinylcholine and dibucaine, but not by tacrine, cocaine or α-solanine.

Our current mutagenesis studies demonstrate that peripheral site residue Q119 but not N68 participates in the primary interactions with some reversible inhibitors. The fact that these interactions were more drastically altered when a basic residue was introduced, further strengthens the conclusion that these primary interactions involve the positive charge on the inhibitor, and are disrupted due to electrostatic repulsion between the inhibitor and the peripheral site. These findings extend the findings of Masson et al. (31) that the peripheral site is not unique to AChE but exists also in BuChE, in which it plays a role in interactions with reversible inhibitors. The increase in sensitivity to the AChE-specific inhibitor BW284c51 which was seen when the AChE-conserved tyrosine residue was introduced in either positions 68 or 119 of BuChE is in accord with reciprocal experiments which were performed in AChE (19,32). Interestingly, an increase in sensitivity to BW284c51 was also found when acidic residues were introduced at positions 68 or 119. This might be explained by stabilizing electrostatic interactions which occurred between these negatively charged residues and the positively charged inhibitor. The relatively low affinity of the peripheral site makes it unlikely that scavenging of drugs by serum BuChE will act via this site.

Mutagenesis of T120, adjacent to Q119, further emphasizes the importance of this region in ligand binding also in BuChE. While mutations in this residue caused no change in the catalytic properties, a significant decrease in the sensitivity toward the examined reversible inhibitors was detected. A striking decrease of sensitivity toward all inhibitors, including tacrine was found upon substitution of a basic residue. This prominent change may be due to a combination of structural alteration and the introduction of charge. As the spectrum of inhibitors we have chosen includes representative natural anti-ChEs to which humans are exposed, the peripheral site of normal BuChE appears well-adapted to a role of attracting these xenobiotics to high-affinity binding sites on the protein.

When W82 was replaced at the choline-binding site with two smaller but still aromatic residues, tyrosine and phenylalanine, a significant reduction occurred in both K_m and k_{cat} values and led to significant increases in Ki values for the set of reversible inhibitors. This extended to BuChE the importance of the tryptophan residues at the choline-binding site and indicated the importance of this site for the binding of various other ligands. That the observed changes were similar to those found in parallel human AChE mutations (33), demonstrates the conservation between AChE and BuChE active sites.

Mutations of oxyanion hole glycine residues 116 and 117 and the adjacent 115 in BuChE caused quite dramatic reductions in catalytic activity. In some cases, BTCh-hydrolyzing activity was so low that only by resorting to DFP-reaction was any residual enzyme function detectable. The loss of catalytic activity may be attributed to distortions in the fine structure of this region, caused by introduction of residues larger than glycine, which prevent the formation of the oxyanion hole and stabilization of the catalytic transition state. Another possible reason could be the introduction of a charge which might have disturbed the formation of a stabilizing hydrogen bond. The fact that changes in G115 led to activity loss further implies that the effect of mutagenesis in this case was due to a structural impairment. Also, introduction of alanine at position 115 was tolerated better than when a larger residue was introduced. Interestingly, the mutation which was best tolerated was an introduction of a glutamate residue in position 117, which led to only a small reduction in the catalytic activity, while the introduction of an aspartate at residue 115 caused a total loss of detectable BTCh-hydrolyzing activity.

Substitution of histidine for G117 is also reported to have little effect on catalytic rate (34). When the inhibition properties of the catalytically active mutants were examined, it was reassuring to find that the mutations affected not only catalysis, but also caused a decrease in sensitivity to several reversible inhibitors which, like substrates, interact with this region of BuChE. Taken together, these findings provide experimental evidence for the importance of the putative oxyanion hole region to catalytic functioning and ligand interactions of BuChE.

The mutation of V127 into an aspartate residue resulted in little change in k_{cat} (data not shown) or K_m, complimenting the work of Kronman et al. (35) who had mutated this residue of AChE to alanine and arginine and had also found no major effect on catalysis. Thus, neither an acidic, a neutral nor a basic residue at this position affects catalysis. These data make the back door theory less appealing, despite its elegance. It therefore remains to be proven whether the choline moiety is regurgitated back through the gorge of BuChE and against the direction of the electrostatic field, or by an alternative pathway, and what mechanism accounts for the extremely high turnover rate for both ChEs.

All of the tested inhibitors were also shown to interact in BuChE with D70, which when mutated to a glycine residue in "atypical" BuChE exhibited a significant reduction in sensitivity. Based on recent reports, this situation may make the hepatic multidrug-resistance (MDR) system most vulnerable. The MDR system is an ATP-dependent mechanism for excretion of xenobiotics (36-38). It acts via *Mdr*1 in epithelial cells (36) and *Mdr*2 as a lipid transporter (37), essential for the integrity of hepatocytes (38). A parallel system with a widely-overlapping specificity is the vesicular monoamine transporter (VMAT), which sequesters positively charged aromatics by an exchange for protons. The K_d of the VMAT system for tacrine is on the order of 0.5 to 10 mM (39), intermediate between that of normal and "atypical" BuChE. When the BuChE is the "atypical" variant, or when the levels of free BuChE are low due to concurrent use of other drugs, tacrine is bound by the higher-affinity vesicular transporter. Sequestered in the vesicles, it can increase turnover of and damage membrane phospholipids, leading to hepatotoxicity. To test whether this is the case, the binding of tacrine to plasma proteins should be tested in patients with "atypical" BuChE. That the effective dose of tacrine may be significantly higher in carriers of "atypical" BuChE, may provide for the first

time a molecular explanation for tacrine's hepatotoxicity. As it is the liver that synthesizes and secretes BuChE (3,4), malfunction of this organ by any cause, even in non-carriers of the BuChE variant, may be exacerbated by the administration of tacrine. Our current observations may therefore carry important implications for tacrine's use by 100,000 Alzheimer's disease patients in the US where it is already an approved therapy (40) and in other countries where approval is pending. A full understanding of tacrine's mode of action and genotype-based dose instructions for normal and "atypical" BuChE carriers should guide to the development of the next generation of anti-ChEs.

References

1. Prody, C. A., D. Zevin-Sonkin, A. Gnat, O. Goldberg and H. Soreq. Isolation and characterization of full-length cDNA clones coding for cholinesterase from fetal human tissues. *Proc. Natl. Acad. Sci. USA* **84**:3555-3559 (1987).
2. Loewenstein-Lichtenstein, Y., M. Schwarz, D. Glick, B. Nørgaard-Pedersen, H. Zakut and H. Soreq. Genetic predisposition to adverse consequences of anti-cholinesterases in "atypical" BCHE carriers. *Nature Medicine* **1**:1082-1085 (1995).
3. Whittaker, M. *Cholinesterases*. Karger, Basel (1986).
4. Soreq, H. and H. Zakut. *Cholinesterases and Anticholinesterases*. Academic Press, San Diego (1993).
5. Sussman, J. L., M. Harel, F. Frolow, C. Oefner, A. Goldman, L. Toker and I. Silman. Atomic structure of acetylcholinesterase from *Torpedo californica*: A prototypic acetylcholine-binding protein. *Science* **253**:872-879 (1991).
6. Harel, M., I. Schalk, L. Ehret-Sabatier, F. Bouet, M. Goeldner, C. Hirth, P. Axelson, I. Silman and J. L. Sussman. Quarternary Ligand binding to aromatic residues in the active-site gorge of acetylcholinesterase. *Proc. Natl. Acad. Sci. USA* **90**:9031-9035 (1993).
7. Harel, M., J. L. Sussman, E. Krejci, S. Bon, P. Chanal, J. Massoulie and I. Silman. Conversion of acetylcholinesterase to butyrylcholinesterase: modeling and mutagenesis. *Proc. Natl. Acad. Sci. USA* **89**:10827-10831 (1992).
8. McGuire, M. C., C. P. Noguiera, C. P. Bartels, H. Lightstone, A. Hajra, A. F. L. van der Spek, O. Lockridge and B. N. La Du. Identification of the structural mutation responsible for the dibucaine-resistant (atypical) variant of human serum cholinesterase. *Proc. Natl. Acad. Sci. USA* **86**:953-957 (1989).
9. Neville, L. F., A. Gnatt, R. Padan, S. Seidman and H. Soreq. Anionic site interactions in human butyrylcholinesterase disrupted by two adjacent single point mutations. *J. Biol. Chem.* **265**:20735-20739 (1990).

10. Neville, L. F., A. Gnatt, Y. Loewenstein, S. Seidman, G. Ehrlich and H. Soreq. Intramolecular relationships in cholinesterases revealed by oocyte expression of site-directed and natural variants of human BCHE. *EMBO J.* **11**:1641-1649 (1992).

11. Soreq, H., A. Gnatt, Y. Loewenstein and L. F. Neville, Excavations into the active-site gorge of cholinesterases. *Trends Biochem. Sci.* **17**, 353-358 (1992).

12. Taylor, P. and Z. Radic. The cholinesterases: from genes to proteins. *Annu. Rev. Pharmacol. Toxicol.* **34**:281-320 (1994).

13. Schwarz, M., D. Glick, Y. Loewenstein and H. Soreq. Engineering of human cholinesterases explains and predicts diverse consequences of administration of various drugs and poisons. *Pharmacol. Therap.* **67**:283-322 (1995).

14. Loewenstein, Y., A. Gnatt, L. F. Neville and H. Soreq. A chimeric human cholinesterase: Identification of interaction sites responsible for sensitivity to acetyl- or butyrylcholinesterase-specific ligands. *J. Mol. Biol.* **234**:289-296 (1993).

15. Kieffer, B., M. Goeldner, C. Hirth, R. Aebersold and J.-Y. Chang. Sequence determination of a peptide fragment from electric eel acetylcholinesterase, involved in the binding of quarternary ammonium. *FEBS Lett.* **202**:91-96 (1986).

16. Kreienkamp, H.-J., C. Weise, R. Raba, A. Aaviksaar and F. Hucho. Anionic subsites of the catalytic center of acetylcholinesterase from *Torpedo* and from cobra venom. *Proc. Natl. Acad. Sci. USA* **88**:6117-6121 (1991).

17. Shafferman, A., C. Kronman, Y. Flashner, M. Leitner, A. Ordentlich, Y. Gozes, S. Cohen, N. Ariel, D. Barak, M. Harel, I. Silman, J. L. Sussman and B. Velan. Mutagenesis of human acetylcholinesterase, identification of residues involved in catalytic activity and in polypeptide folding. *J. Biol. Chem.* **267**:17640-17648 (1992).

18. Ordentlich, A., D. Barak, C. Kronman, Y. Flashner, M. Leitner, N. Ariel, S. Cohen, B. Velan and A. Shafferman. Dissection of the human acetylcholinesterase active center determinants of substrate specificity. Identification of residues constituting the anionic site, the hydrophobic site, and the acyl pocket. *J. Biol. Chem.* **268**:17083-17095 (1993).

19. Barak, D., C. Kronman, A. Ordentlich, N. Ariel, A. Bromberg, D. Marcus, A. Lazar, B. Velan and A. Shafferman. Acetylcholinesterase peripheral anionic site degeneracy conferred by amino acid arrays sharing a common core. *J. Biol. Chem.* **264**:6296-6305 (1994).

20. Taylor, P and S. Lappi. Interaction of fluorescent probes with acetylcholinesterase: the site and specificity of propidium binding. *Biochemistry* **14**:1989-1997 (1975).

21. Shafferman, A., B. Velan, A. Ordentlich, C. Kronman, H. Grosfeld, M. Leitner, Y. Flashner, S. Cohen, D. Barak and N. Ariel. Substrate inhibition of acetylcholinesterase: Residues affecting signal transduction from the surface to the catalytic center. *EMBO J.* **11**:3651-3658 (1992).

22. Radic, Z., R. Duran, D. C. Vellom, Y. Li, C. Cervenansky and P. Taylor. Site of fasciculin interactions with acetylcholinesterase. *J. Biol. Chem.* **269**:11233-11239 (1994).

23. Shafferman, A., A. Ordentlich, D. Barak, C. Kronman, N. Ariel, M. Leitner, Y. Segall, A. Bromberg, S. Reuveny, D. Marcus, T. Bino, A. Lazar, S. Cohen and B. Velan. Molecular aspects of catalysis and of allosteric regulation of acetylcholinesterases, in: *Enzymes of the Cholinesterase Family* (Quinn, D. M., A. S. Balasubramanian, B. P. Doctor and P. Taylor, eds.). Plenum Press, New York, pp. 189-196 (1995).

24. Schwarz, M., Y. Loewenstein-Lichtenstein, D. Glick, J. Liao, B. Norgaard-Pedersen and H. Soreq. Successive organophosphate inactivation and oxime reactivation reveals distinct responses of recombinant human cholinesterase variants. *Mol. Brain Res.* **31**:101-110 (1995).

25. Gilson, J. K., T. P. Straatsma, J. A. McCammon, D. R. Ripoll, C. H. Faerman, P. H. Axelsen, I. Silman and J. L. Sussman. Open "back door" in a molecular dynamics simulation of acetylcholinesterase. *Science* **263**:1276-1278 (1994).

26. Gnatt, A., Y. Loewenstein, A. Yaron, M. Schwarz and H. Soreq. Site-directed mutagenesis of active site residues reveals plasticity of human butyrylcholinesterase in substrate and inhibitor interactions. *J. Neurochem.* **62**:749-755 (1994).

27. Hobbiger, R. and A. W. Peck. Hydrolysis of suxamethonium by different types of plasma. *Br. J. Pharmacol.* **37**:258-271(1969).

28. Ollis, D. L., E. Cheah, M. Cygler, B. Dijkstra, F. Frolow, S. M. Franken, M. Harel, S. J. Remington, I. Silman, J. Shrag, J. L. Sussman, K. H. G. Verschueren and A. Goldman. The α/β hydrolase fold. *Prot. Engineer.* **5**:197-211 (1992).

29. Fry, P. C. *Biological Data Analysis. A Practical Approach.* Oxford University Press, Oxford (1993).

30. Bourne, Y., P. Taylor and P. Marchot. Acetylcholinesterase inhibition by fasciculin: crystal structure of the complex. *Cell* **83**:503-512 (1995).

31. Masson, P., M. T. Froment, C. Bartels and O. Lockridge. Peripheral anionic site of wild-type and mutant human butyrylcholinesterase, in *Enzymes of the Cholinesterase Family* (Quinn, D. M., A. S. Balasubramanian, B. P. Doctor and P. Taylor, eds.). Plenum Press, New York, pp. 230-231 (1995).

32. Radic, Z., N. A. Pickering, D. C. Vellom, S. Camp and P. Taylor. Three distinct domains in the cholinesterase molecule confer selectivity for acetyl- and butyrylcholinesterase inhibitors. *Biochemistry* **32**:12074-12084 (1993).

33. Ordentlich, A., D. Barak, C. Kronman, N. Ariel, Y . Segall, B. Velan and A. Shafferman. Contribution of aromatic moieties of tyrosine 133 and of anionic subsite tryptophan 86 to catalytic efficiency and allosteric modulation of acetylcholinesterase. *J. Biol. Chem.* **270**:2083-2091(1995).

34. Millard, C. B., O. Lockridge and C. A. Broomfield. Design and expression of organophosphorus acid anhydride hydrolase activity in human butyrylcholinesterase. *Biochemistry* **34**:15925-15933 (1995).

35. Kronman, C., A. Ordentlich, D. Barak, B. Velan and A. Shafferman. The "back door" hypothesis for product clearance in acetylcholinesterase challenged by site-directed mutagenesis. *J. Biol. Chem.* **269**:27819-27822 (1994).

36. Schinkel, A. H., J. J. M. Smit, O. van Tellingen, J. H. Beijnen, E. Wagenaar, L. van Deemter, C. A. A. M. Mol, M. A. van der Valk, E. C. Robanus-Maandag, H. J. P. J. te

Riele, A. J. M. Berns and P. P. Borst. Disruption of the mouse mdr1a P-glycoprotein gene leads to a deficiency in the blood-brain barrier and to increased sensitivity to drugs. *Cell* **77**:491-502 (1994).

37. Ruetz, S. and P. Gros. Phosphatidylcholine translocase: a physiological role for the *mdr*2 gene. *Cell* **77**:1071-1081 (1994).

38. Smit, J. J. M., A. H. Schnikel, R. P. J. Oude Elferink, A. K. Groen, E. Wagenaar, L. van Deemter, C. A. A. M. Mol, R. Ottenhoff, N. M. T. van der Lugt, M. A. van Roon, M. A. van der Valk, G. J. A. Offerhaus, A. J. M. Berns and P. Borst. Homozygous disruption of the murine *mdr*2 P-glycoprotein gene leads to a complete absence of phospolipid from bile and to liver disease. *Cell* **75**:451-462 (1993).

39. Yelin, R. and S. Schuldiner. The pharmacological profile of the vesicular monoamine transporter resembles that of the multidrug transporter. *FEBS Lett.* **377**: 201-207 (1995).

40. Winker, M. A. Tacrine for Alzheimer's disease: which patient, what dose? *J. Am. Med. Assn.* **271**:1023-1024 (1994).

Send correspondence to: Hermona Soreq, Ph. D., Department of Biological Chemistry, The Hebrew University of Jerusalem, 91904 Israel; fax 972-2-652-0258, tel. 972-2-658-5109, soreq@shum.huji.ac.il.

Table 1. Kinetic properties of variant butyrylcholinesterases: Km and Ki values[a]

variant/mutation		Km (mM)	Ki tacrine (μM)	Ki succinylcholine (mM)	Ki dibucaine (μM)	Ki α-solanine (μM)	Ki BW284c51 (μM)	Ki cocaine (mM)
normal	BuChE	2.8± 0.7	0.06± 0.03	4.0 ± 2.6	6.9± 4.6	3.3 ± 2.8	480 ± 110	0.39± 0.03
"atypical"	D70G	3.8± 0.4	9.1 ± 2.4	52 ± 13	182 ± 100	78.0 ± 2.5	2540	3.2 ± 0.1
peripheral site	N68D	1.1± 0.4	0.03± 0.01	0.26± 0.05	10.0± 0.2	1.26± 0.05	18	n.d.
	" K	2.5± 1.1	0.01± 0.005	4.3 ± 0.6	17 ± 6	3.7 ± 1.3	>700	0.43± 0.0
	" R	4.6± 1.	0.06± 0.03	11.2 ± 0.7	4.3± 0.9	6.5 ± 3.3	>800	0.20± 0.07
	" Y	3.4± 2.	0.04± 0.02	2.9 ± 0.9	39 ± 2	0.5 ± 0.3	112 ± 50	n.d.
	" A	1.1± 0.6	0.04± 0.03	0.7 ± 0.3	10 ± 6	0.7 ± 0.2	179 ± 91	n.d.
	Q119A	1.2± 0.6	0.02± 0.01	0.6 ± 0.2	20 ± 9	0.4 ± 0.1	68 ± 10	n.d.
	" E	0.6± 0.2	0.03± 0.03	0.12± 0.06	28.5± 5.0	0.28± 0.11	25.9± 4.6	n.d.
	" G	1. ± 0.1	0.04± 0.03	0.7 ± 0.3	26.2± 2.3	0.23± 0.18	95 ± 16	n.d.
	" H	0.7± 0.1	0.01± 0.003	0.5 ± 0.1	11.5± 4.7	0.3 ± 0.1	65	n.d.
	" K	0.8± 0.1	0.02± 0.004	30 ± 5.6	54.6± 5.7	9.0 ± 7.1	>450	0.20± 0.08
	" R	1.5± 0.6	0.05± 0.006	42 ± 16	115 ± 6	6.5 ± 3.7	>600	0.24± 0.16
	" Y	5.9± 0.6	0.09± 0.01	5.1 ± 0.3	107 ± 12	1.8 ± 0.9	78 ± 5	n.d.
	T120E	2.2± 0.4	0.12± 0.07	1.5 ± 0.1	1.1± 0.8	5.6 ± 1.3	128 ± 49	n.d.
	" G	2.6± 0.6	0.15± 0.08	4.6 ± 1.6	32 ± 5	0.65± 0.0	>400	n.d.
	" H	2.6± 0.3	1.20± 0.05	19 ± 3	80 ± 46	17 ± 6	>700	n.d.
	" K	6.1± 1.1	>85	78 ± 24	>900	>200	>800	12.6
choline site	W82Y	76 ± 28	3.2 ± 3.	61 ± 14	140 ± 6	78 ± 37	>1000	3.6 ± 0.1
	" F	31 ± 20	1.7 ± 1.1	86 ± 4	149 ± 39	77 ± 18	>1000	1.7 ± 1.3
oxyanion hole	G115A	1.7± 0.6	9.5 ± 1.6	33 ± 10	33 ± 9	157	460	0.9 ± 0.1
	" S	0.9± 0.1	0.83	24.3	74 ± 36	27	>500	1.1
	G117E	1.5± 0.3	0.2 ± 0.2	0.09± 0.05	19 ± 3	12.3 ± 9.9	330 ± 140	8.7 ± 5.3
back door	V127D	4.9± 1.	0.06± 0.03	2.5 ± 0.8	18 ± 5	4.6 ± 0.7	644 ± 32	n.d.
acetylcholinesterase		2.5	0.21	1.0	710	n.d.	0.13	3.9

Legend to Table 1

[a]The first column identifies the natural or site-directed mutant. Assays were performed in 0.1 to 25 mM BTCh (in the case of AChE, acetylthiocholine), pH 7.4, and K_m values were extracted using GraFit 3.0 (Erithacus Software Ltd., Staines, UK). Note that the assays were all conducted at 22 °C, which may account for differences in the kinetic constants from data collected by other laboratories. IC_{50} values were determined in 1 mM substrate over the indicated range of inhibitor concentrations (GraFit), and from them Ki values were calculated (27). Standard deviations are shown for 2 or 3 determinations; where no standard deviation is shown, only one determination was performed. The "atypical" natural BuChE mutant is also included. Mutants G115 D, G116E, G116A/G117D, G117C and D and G118E and D are not included in the Table because they had no detectable activity. n.d., not determined.

Table 2. Catalytic properties of variant butyrylcholinesterases: kcat and kcat/Km values[a]

variant/mutation		$k_{cat} \times 10^{-3}$ (min^{-1})	$k_{cat}/Km \times 10^{6}$ ($M^{-1}min^{-1}$)
normal BuChE		98± 33	35
"atypical"	D70G	~30	~8
oxyanion hole	G115A	3	2
	" S	2	2
	" C	0.71	n.d.
	" D	0.094	n.d.
	" E	0	n.d.
	G116E	0	n.d.
	G117E	17± 2	11
	" D	0.016	n.d.
	G116A/G117D	0	n.d.
AChE		70	28

[a]kcat values were calculated from activity measurements against BTCh and enzyme determinations by ELISA assays; Km values were taken from Table 1. n.d., not determined.

Legends for Figures

Fig. 1. Tacrine binding at the active site.

The 3-dimensional structure of *Torpedo* AChE crystals soaked with tacrine (right), is compared to the modeled homologous residues of human BuChE (left). The representation of human BuChE without tacrine was drawn after Harel et al. (7) and of AChE with tacrine after Harel et al. (6), using Insight II (Biosym Technologies).

Fig. 2. Sites of mutagenesis of human BuChE.

Ribbon diagrams are shown of (left) the polypeptide backbone of a cut-away view of human BuChE, showing the mutated sites on the polypeptide backbone of residues 55 to 138, and (right) the entire enzyme. The enzyme is viewed from above the opening of the active site gorge, toward the catalytic site. Labeled on the left, and indicated at similar angles on the right, are the peripheral binding site (N68, Q119 and T120), the oxyanion hole (G115 and G117), the choline-binding site (W82) and the "back door" (V127). Also shown are the site of natural variance (D70) and (right) the catalytic site serine (S198). The model of human BuChE (7) based on the 3-dimensional structure of *Torpedo* AChE (7) was analyzed using the Insight II program (Biosym Technologies, San Diego CA) on a Silicon Graphics computer.

Fig. 3. Representative inhibition profiles of variant BuChEs.

Inhibition profiles for a series of ChE inhibitors are shown for three peripheral site mutants (N68R, Q119K and T120K), a choline-binding site mutant (W82Y), and an oxyanion hole mutant (G115A) as compared with the inhibition profile of normal BuChE for each inhibitor. Note the different concentration units for each inhibitor.

Fig. 4. Relative inhibition constants of BuChE mutants.

The Ki values of inhibitors for the mutant enzymes (from Table 1) are shown relative to normal BuChE for mutations of three residues at the peripheral site (N68, Q119 and T120), the choline-binding site (W82), two at the oxyanion hole (G115 and G117) and the

"atypical" variant (D70G). Where only a minimum value is known, that value has been used in calculating the relative constant.

Fig. 5. Examples of [^{3}H]-DFP binding to inactive BuChE mutations. Oocyte homogenates (100 µl) were reacted with 2 mCi of [^{3}H]-DFP, product separated by polyacrylamide gel electrophoresis and autoradiographed 2 months. Lane 1, normal BuChE; lane 2, uninjected oocyte homogenate; lane 3, G117E; lane 4, G115C, lane 5, G115D and lane 6, G116A/G117D. The arrow marks the somewhat lower position of commercial human BuChE (9).

Fig. 6. Correlation of tacrine's affinity for BuChE variants with affinities for cocaine and α-solanine.

(Upper panel) A plot of the logarithms of the dissociation constants for tacrine vs. those for cocaine and the least squares line. (Lower panel) The corresponding plot for tacrine vs. α-solanine. The data are taken from Table 1, and the identification of the mutations is as in the Table, lacking only the sequence number of each residue.

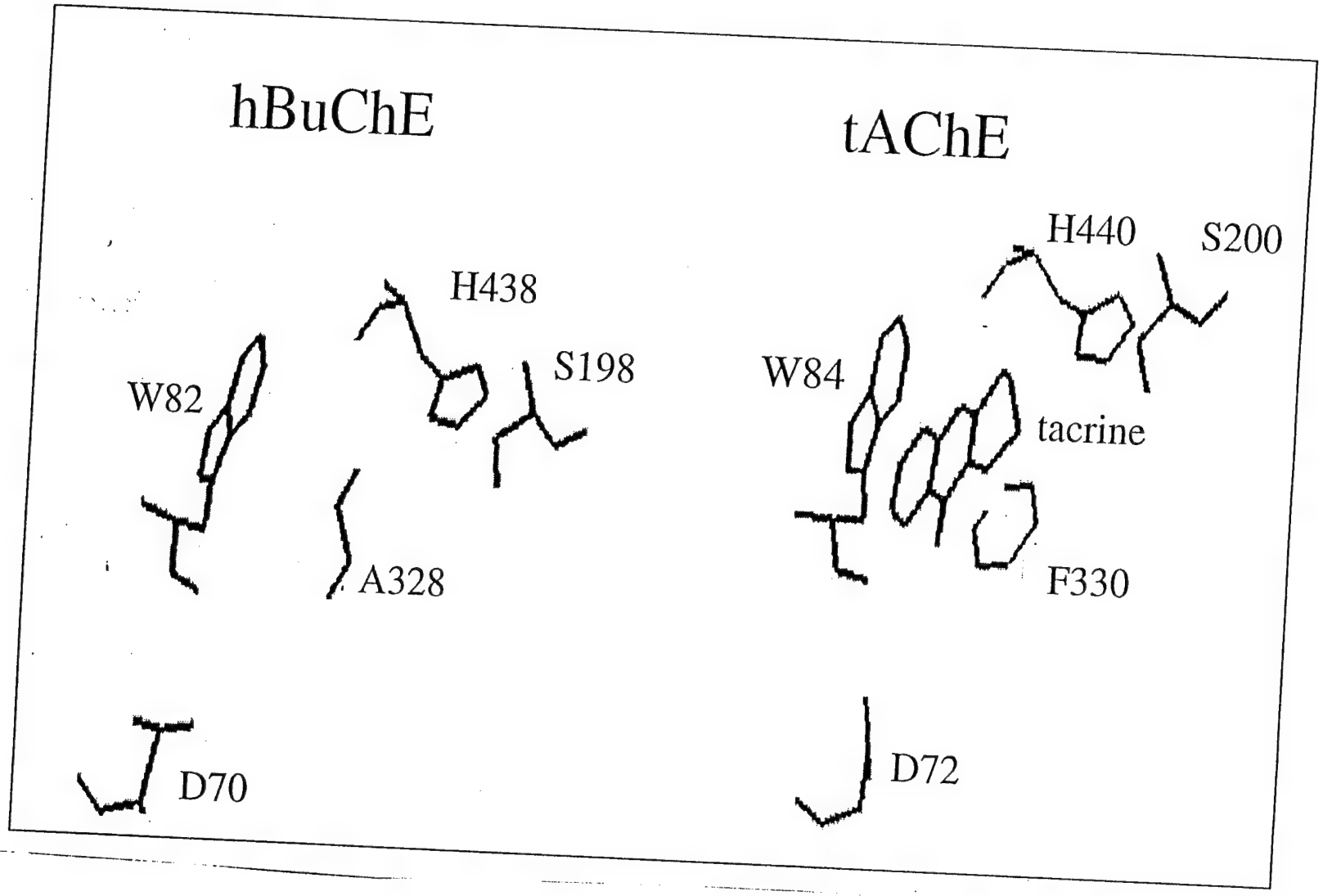
hBuChE
H438
S198
W82
A328
D70
tAChE
H440
S200
W84
tacrine
F330
D72

Figure 1

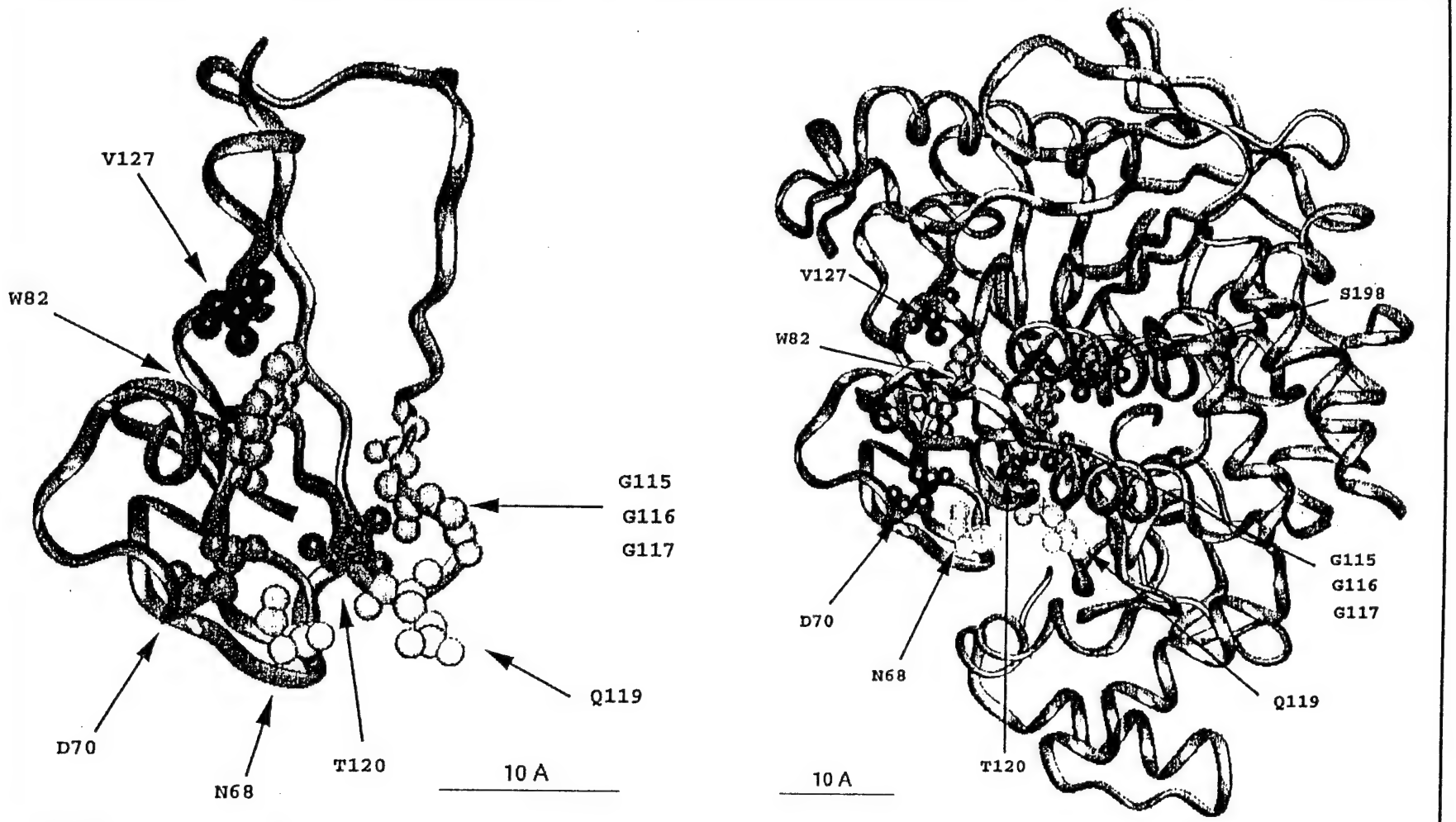
V127
W82
G115
G116
G117
Q119
D70
N68
T120
10 A
V127
S198
W82
G115
G116
G117
D70
N68
Q119
T120
10 A

Figure 2

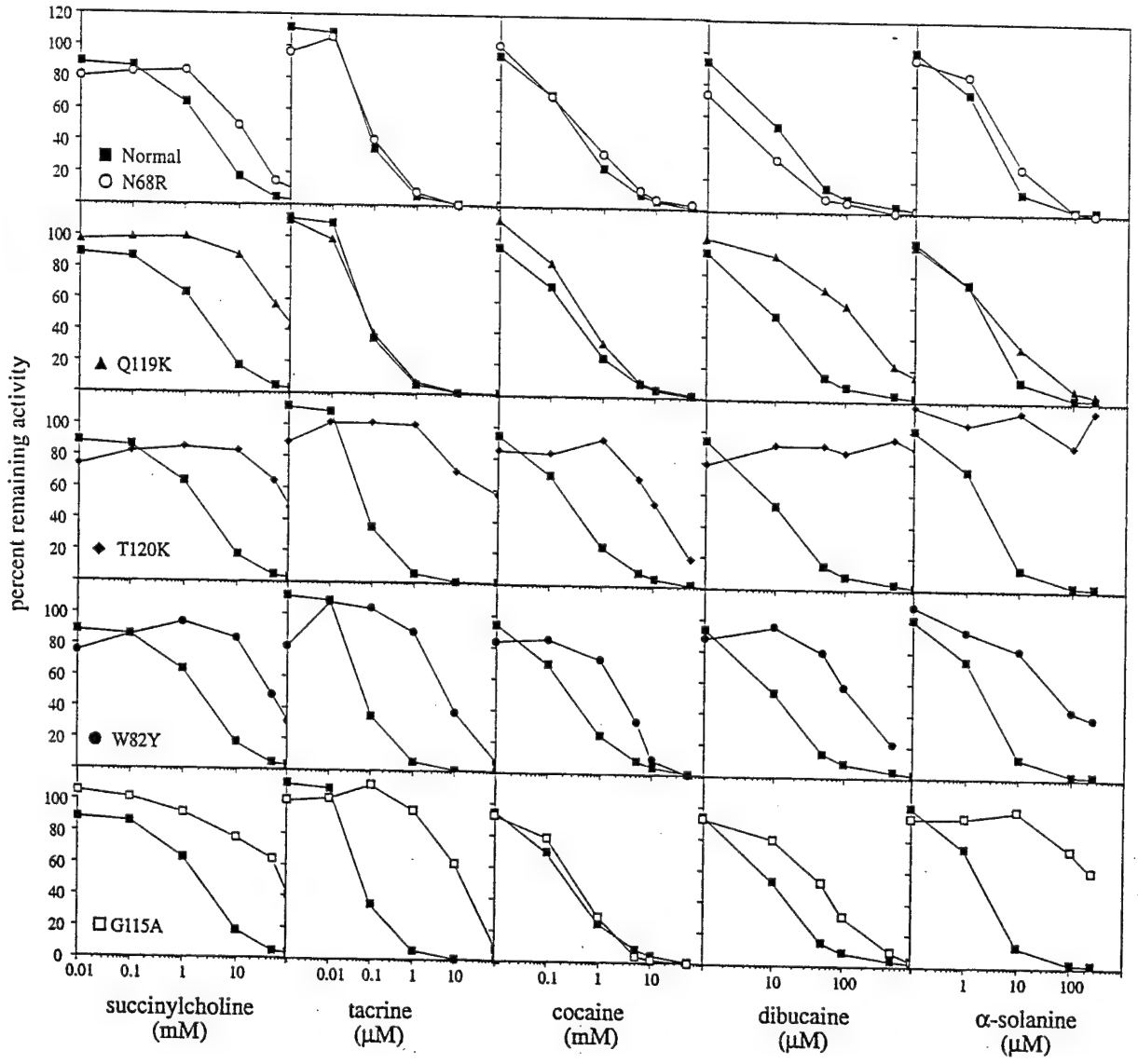
percent remaining activity
Normal
N68R
Q119K
T120K
W82Y
G115A
succinylcholine (mM)
tacrine (μM)
cocaine (mM)
dibucaine (μM)
α-solanine (μM)

Figure 3

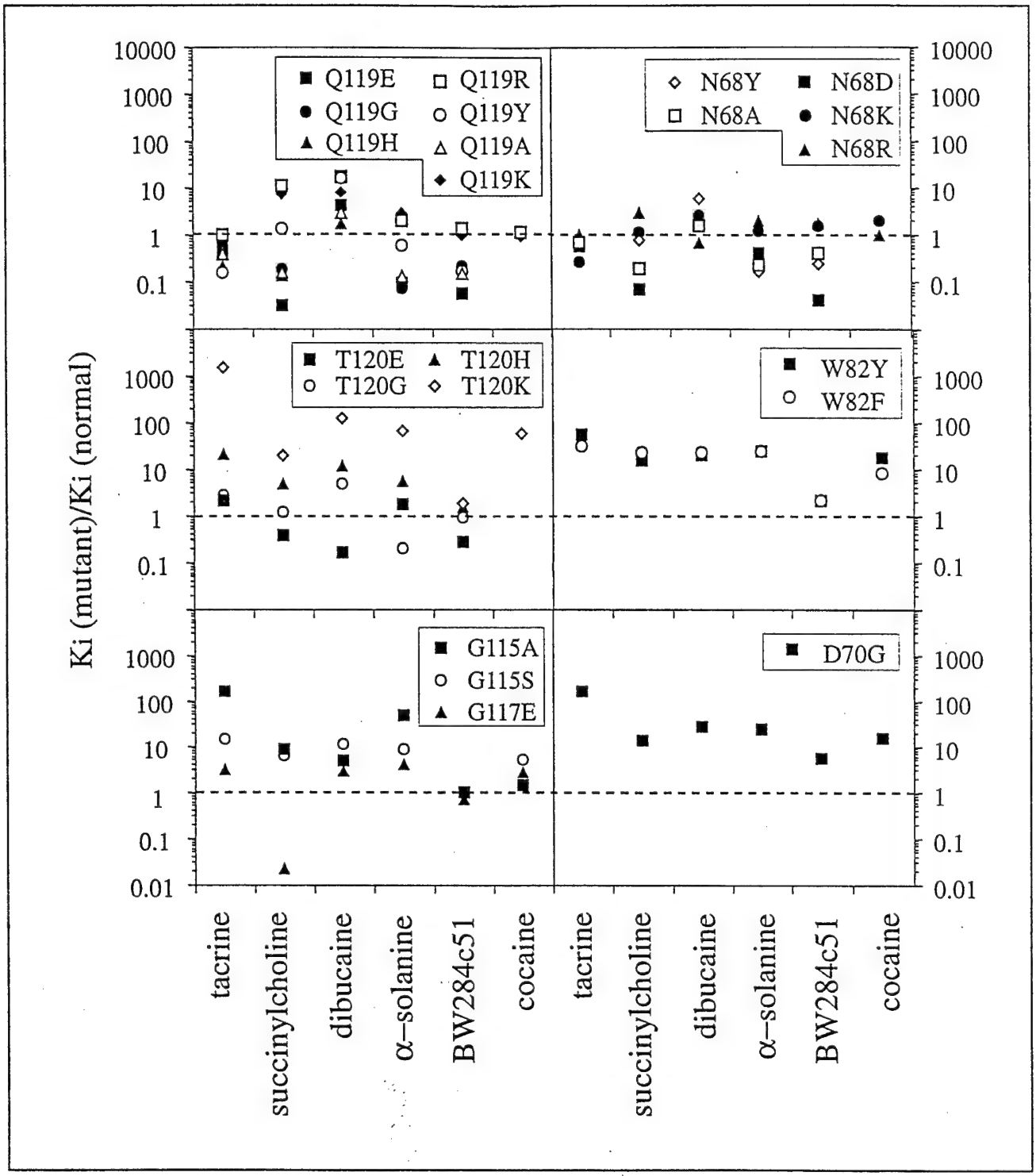
Ki (mutant)/Ki (normal)
10000
1000
100
10
1
0.1
0.01
Q119E
Q119G
Q119H
Q119R
Q119Y
Q119A
Q119K
N68Y
N68A
N68D
N68K
N68R
T120E
T120G
T120H
T120K
W82Y
W82F
G115A
G115S
G117E
D70G
tacrine
succinylcholine
dibucaine
α−solanine
BW284c51
cocaine

Figure 4

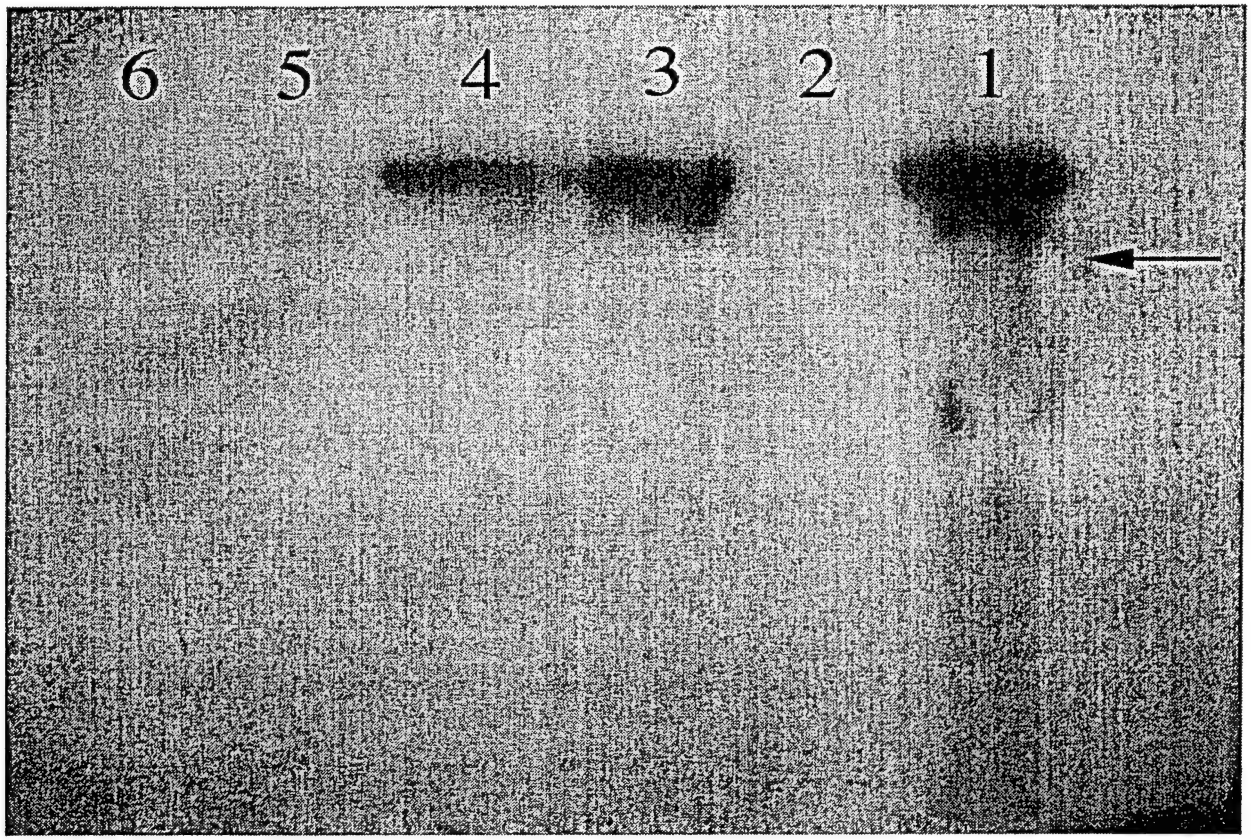

Figure 5

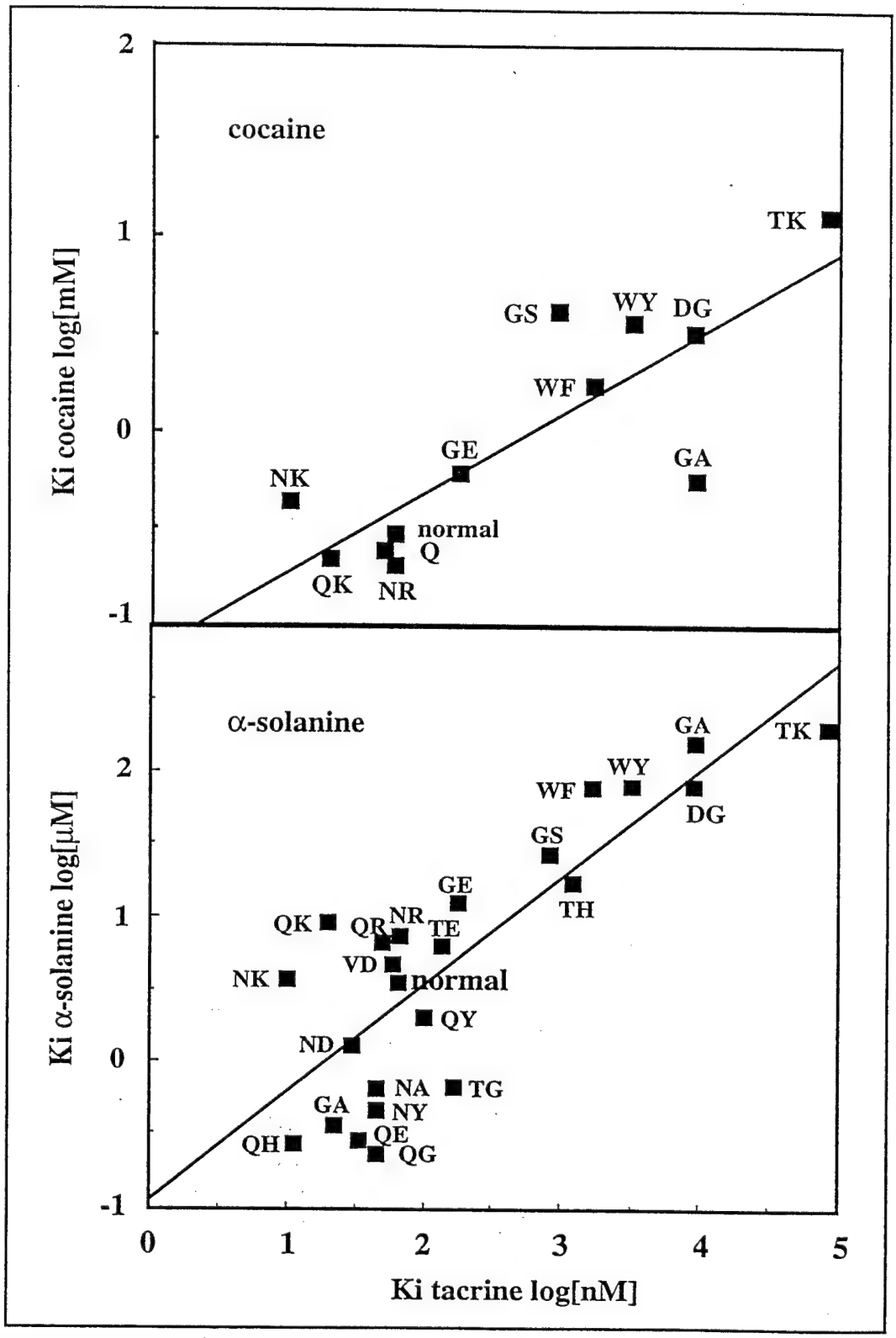
cocaine
Ki cocaine log[mM]
TK
GS
WY
DG
WF
GE
GA
NK
normal
Q
QK
NR
α-solanine
Ki α-solanine log[μM]
GA
TK
WY
WF
DG
GS
GE
TH
QK
QR
NR
TE
VD
NK
normal
QY
ND
NA
TG
GA
NY
QE
QH
QG
Ki tacrine log[nM]
2
1
0
-1
0
1
2
3
4
5

Figure 6

Genetic predisposition to adverse consequences of anti-cholinesterases in 'atypical' BCHE carriers

YAEL LOEWENSTEIN-LICHTENSTEIN[1], MIKAEL SCHWARZ[1], DAVID GLICK[1], BENT NØRGAARD-PEDERSEN[2], HAIM ZAKUT[3] & HERMONA SOREQ[1]

[1]*Department of Biological Chemistry, The Life Sciences Institute, The Hebrew University of Jerusalem, 91904 Israel*
[2]*Department of Clinical Biochemistry, Statens Serum Institut, Division of Biotechnology, DK-2300 Copenhagen S, Denmark*
[3]*Department of Obstetrics and Gynecology, The Sackler Faculty of Medicine of Tel Aviv University and The Edith Wolfson Medical Center, Holon, 58100 Israel*
Y.L.-L. present address: Department of Biochemistry and Biophysics, University of California at San Francisco, San Francisco, California 94143-0534, USA
Correspondence should be addressed to H.S.

Normal butyrylcholinesterase (BuChE)[1], but not several of its common genetic variants[2], serves as a scavenger for certain anti-cholinesterases (anti-ChEs). Consideration of this phenomenon becomes urgent in view of the large-scale prophylactic use of the anti-ChE, pyridostigmine, during the 1991 Persian Gulf War, in anticipation of nerve gas attack[3] and of the anti-ChE, tacrine, for improving residual cholinergic neurotransmission in Alzheimer's disease patients[4]. Adverse symptoms were reported for subjects in both groups, but have not been attributed to specific causes[4,5]. Here, we report on an Israeli soldier, homozygous for 'atypical' BuChE, who suffered severe symptoms following pyridostigmine prophylaxis during the Persian Gulf War. His serum BuChE and recombinant 'atypical' BuChE (ref. 6) were far less sensitive than normal BuChE to inhibition by pyridostigmine and several other carbamate anti-ChEs. Moreover, atypical BuChE demonstrated 1/200th the affinity for tacrine of normal BuChE or the related enzyme acetylcholinesterase (AChE). Genetic differences among BuChE variants may thus explain at least some of the adverse responses to anti-ChE therapies.

Atypical BCHE is the most common allele of the BCHE gene that causes a variant phenotype. Because of substitution of aspartate at position 70 by glycine[6,7], the atypical enzyme is incapable of hydrolysing succinylcholine administered at surgery[8,9], and is much less sensitive than the normal enzyme to several inhibitors[6-9]. Homozygous carriers of this variant allele (under 0.04% in Europe but up to 0.6% in certain subpopulations[10]) suffer post-anaesthesia apnea[9] and hypersensitivity to the anti-ChE insecticide parathion[11]. Recently, we learned of an individual, A.B., who had experienced succinylcholine-induced apnea and, during the Persian Gulf War under treatment with pyridostigmine, cholinergic symptoms. Therefore, we initiated a study of the interaction of ChE inhibitors in clinical use or testing[1] with serum ChEs from members of this subject's family, as compared with the enzyme from normal serum and with variant ChEs recombinantly produced in microinjected *Xenopus* oocytes[6].

Butyrylcholinesterase from sera of A.B. and his father, previously identified as homozygous and heterozygous carriers of the atypical BCHE allele, respectively[10], were compared with BuChE from individuals homozygous for the normal BCHE allele. To analyse inhibitors that covalently interact with ChEs, we immobilized native human BuChEs through monoclonal antibodies to multiwell microtitre plates[12]. Recombinant variant ChEs, including normal and atypical BuChEs (ref. 6) and the brain- and blood cell-characteristic alternative splicing variants of AChE, which differ in their C-terminal sequences and mode of membrane anchoring[13], were also subjected to inactivation by anti-ChEs and to subsequent spontaneous reactivation[12].

Normal BuChE hydrolysed 81 ± 23 nmol butyrylthiocholine (BTCh) per hour per microlitre serum (assayed at 2 mM substrate, an average from 20 individuals). The activity of atypical BuChE in A.B.'s serum, prepared in 1994, was found to be about one-third that of normal individuals. This serum contained a normal amount of enzyme protein (~2 ng μl^{-1}), within the range reported for normal serum[14]. Reduced specific activity of BuChE protein was seen also for the recombinant atypical enzyme, as compared with the normal enzyme[6]. Heterozygotes presented intermediate specific activities, 60–70% of the values determined for normal homozygotes (average of three genotyped individuals). Of this residual amount, one-fourth represents the allelic contribution of atypical BuChE, and three-fourths of it is contributed by the normal allele. Measurement of pseudo-first-order inactivation rates demonstrated that atypical BuChE reacts much more slowly than does its normal counterpart with four carbamates, pyridostigmine[3], physostigmine[15], heptyl physostigmine[16] and SDZ-ENA 713 (ref. 17) (Fig. 1*a* and Table 1(*a*)). Moreover, inactivation rate differences were also evident between the enzymes of homozygous normal and heterozygous sera (Fig. 1*a*). The loss and rate of loss of BuChE activity, thus, depend significantly on the individual's genotype, and reveal drastically lower scavenging capacities for each of the tested drugs in sera of individuals with the atypical as compared with the normal allele.

Dose-dependent inhibition by the reversible Alzheimer's disease drug tacrine was examined for native and recombinant normal and atypical BuChE (Table 1(*b*)). To mimic the heterozygous state, we tested 1:1 mixtures of oocyte homogenates, expressing recombinant normal and atypical enzyme (approximately equal amounts of the ChEs) (Fig. 1*b*). In both cases, we observed a drastic reduction in the capacity of atypical BuChE, as compared with the normal enzyme, to interact with tacrine. The sera of heterozygotes showed the expected intermediary inhibition curves (Fig. 1*b*). As the oocyte-produced enzyme remains primarily monomeric[11], the different scavenging capacities of BuChE variants depend exclusively upon the genotype of the individual; multisubunit assembly or competition between the normal and atypical subunits, does not occur in oocytes and therefore could not affect tacrine interactions. Consideration of the relevant site in the tacrine-enzyme complex three-dimensional structure[18,19], further revealed that the tacrine anilinic nitrogen is directed toward aspartate 70, making it a potential site of interaction. This protein-drug interaction is removed in atypical BuChE, reflected in a two orders of magnitude increase in tacrine's 50% inhibitory concentration (IC_{50}).

The data we report, as rates of inactivation of BuChE by carbamate inhibitors and degree of inhibition by tacrine, are relevant to clinical medicine because these rates contribute to the rate of metabolism of the carbamates in the first case, and in the second, binding to BuChE measures the sequestration of tacrine. However,

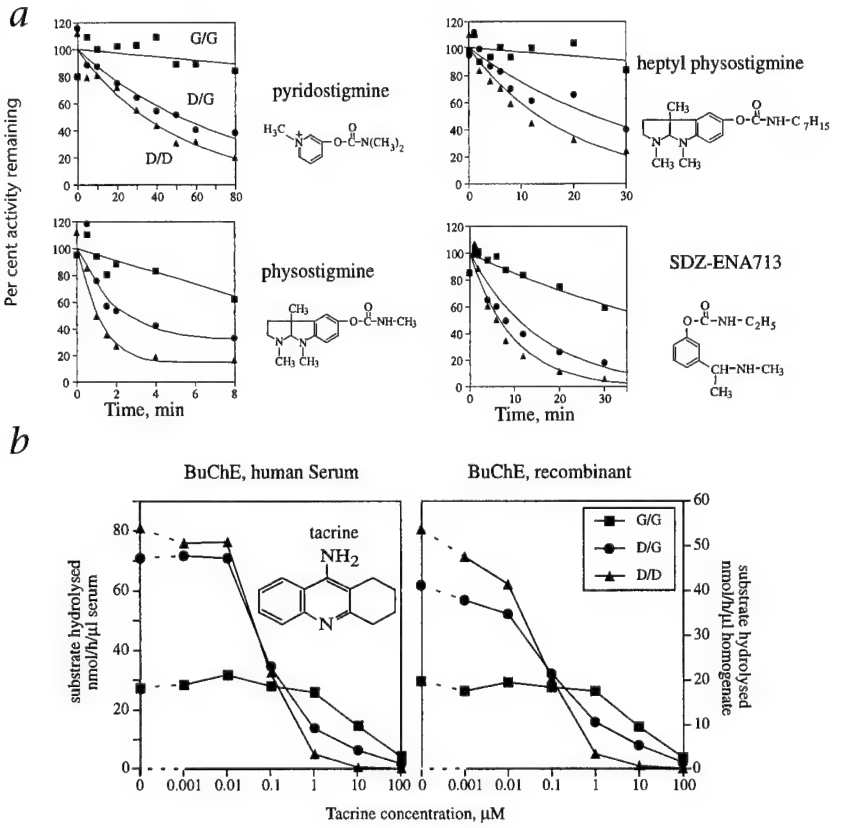

Fig. 1 Inhibition of BuChE variants by anti-ChEs. *a*, Differential inactivation kinetics of variant human sera BuChEs with carbamate inhibitors. Percent original activity as a function of time of exposure to four carbamates is presented for a representative experiment. Activities of immobilized ChEs were determined in 10 mM BTCh following incubation for the noted times with the covalent inhibitors pyridostigmine (10 µM), physostigmine (1 µM), heptyl physostigmine (0.01 µM), and SDZ-ENA 713 (10 µM). The lines are best fits of the data to pseudo-first-order conditions. ▲, normal, Asp70, BuChE homozygote (D/D); ■, atypical, Gly70, homozygote (G/G); ●, BuChE heterozygote (G/D). Lines are drawn for the inactivation by pyridostigmine using the pseudo-first-order rate constants 0.0014 min^{-1} (G/G), 0.0135 min^{-1} (G/D) and 0.0205 min^{-1} (D/D). *b*, Inhibition of serum and recombinant BuChE by tacrine. In the left panel, data for 3 representative serum types inhibited by tacrine: serum of the propositus, A.B., a homozygote for the atypical, Gly70, BuChE variant (G/G); of his father, a heterozygote for this variant (G/D); and of a normal homozygote with Asp70 (D/D). In the right panel, tacrine inhibition is observed on equivalent total amounts of recombinant normal (D/D) and atypical (G/G) enzymes produced in microinjected *Xenopus* oocytes[6].

in addition to inactivation rates and to general haemodynamic parameters, the dynamic level of drug concentration in a patient's serum may depend on the rate of reactivation of enzyme from drug-enzyme complexes. The reactivation rates of AChE and BuChE differed for several drugs, with the decreasing order SDZ-ENA 713, heptyl physostigmine, pyridostigmine and physostigmine (Table 1(*c*)). This is in agreement with the short therapeutic half-life of physostigmine[15] and the long half-life of SDZ-ENA 713 (ref. 17). However, for no drug was there a dramatic difference between the blood and brain forms of AChE or between normal and atypical BuChE (Table 1 (*c*)). This indicates that the reactivation step does not involve the C-terminal sequences. Moreover, it demonstrates that the weak response of atypical BuChE to these drugs does not extend to the reactivation step, and therefore can be explained only by a difference in the initial scavenging step.

The possibility that anti-ChE therapies may cause adverse reactions in individuals with variant BCHE genotypes, inferred by Valentino *et al.* in their studies of charged anti-ChEs (ref. 20), becomes a pertinent issue in view of the administration of pyridostigmine bromide to over 400,000 Persian Gulf War soldiers. This was probably the largest scale use ever of an investigational drug, approved because of the feared exposure of those soldiers to nerve agents[3]. Clinical studies with pyridostigmine showed no adverse effects in volunteers, yet had been limited to small numbers of healthy males and to only several days' exposure[5]. Also, war conditions included concurrent exposure to insecticides, chiefly organophosphorus anti-ChEs (ref. 21), which further decreased the level of ChEs in these soldiers to an unknown extent. In homozygotes and possibly in heterozygous carriers of the atypical BCHE allele, the lower capacity of blood BuChE to interact with and detoxify some of the drug probably resulted in larger effective doses reaching neuromuscular junctions. Atypical homozygotes with much lower protective capacity would be the most vulnerable to AChE inhibition under treatment by any anti-ChE drug.

Several Alzheimer's disease drugs emerged in this study as much faster inactivators of BuChE than of AChE, suggesting that when administered to patients, these drugs will interact initially with plasma BuChE. Significant differences are to be expected in those homozygous for the atypical BCHE allele and less so in heterozygotes, because of the greater than tenfold differences in the inactivation rates by these drugs of normal and atypical BuChE. Even in the case of pyridostigmine, which reacts faster with AChE than BuChE, an initial reduction in blood pyridostigmine by reaction with AChE leaves the level of the remaining drug very dependent upon the nature of the BuChE.

In order to determine whether there are enough binding sites to effect a significant depletion in the level of the reversible inhibitor, tacrine, seen by the cholinergic system, we have calculated the levels of ChE sites in the blood. The concentration of ChE in blood is approximately 50 nM, 75% due to soluble BuChE (ref. 14), 25% due to erythrocyte membrane AChE (ref. 22). This may be compared with plasma tacrine levels of 21 nM in patients under therapy[23]. Dissociation constants of 40 nM for normal BuChE (ref. 24) and 8,000 nM for atypical BuChE, calculated from the data of Table 1, indicate that about 40% of plasma tacrine is bound to BuChE in individuals with the normal allele. In contrast, only 1% is bound to BuChE in atypical homozygotes, with heterozygotes falling in between. The clinically effective dose reaching the central nervous system depends heavily, therefore, on the BCHE genotype. Even without the complication of BCHE polymorphism, BuChE levels can vary with the general state of health[11]. Since Alzheimer's disease patients are far from being as healthy as the pyridostigmine-treated soldiers, they may present yet more drastic symptoms in response to inappropriate dosage of anti-ChEs. The reported high percentage of cholinergic symptoms under tacrine treatment (up to 15%)[4] may reflect BCHE heterozygotes and also patients with liver

malfunctions and consequently with low serum BuChE levels.

Other than short-term effects, our findings also anticipate long-term adverse consequences of treatment with either type of anti-ChE in carriers of the atypical BCHE allele. Such consequences may be associated with the collection of symptoms popularly known as the Gulf War syndrome on one hand[21] or with tacrine's hepatotoxicity on the other[4]. These predictions add the BCHE alleles to the list of genes recognized as conferring differences in drug responses[25], and can be tested by genotype/phenotype analyses for atypical BCHE/BuChE (refs 2, 6, 10). If, indeed, the genotype of patients determines their response to anti-ChEs, as we predict based on the reported experiments, the incidence of the atypical BCHE allele will be significantly higher among Alzheimer's disease patients with adverse short- and/or long-term reactions to tacrine and among veterans who experienced cholinergic effects and those who suffer from other unexplained long-term ailments. Should this be the case, dosage of these drugs might be adjusted to match specific genotypes, for the purpose of avoiding these adverse responses.

Table 1 Deficient interaction of 'atypical' butyrylcholinesterase with various inhibitors

	BuChE		*AChE*	
	Normal	Atypical	Brain-type (E6)	Blood cell-type (E5)
(*a*) second order inactivation rate constants[a] (M^{-1} min^{-1}) × 10^{-3}				
Pyridostigmine (10^{-5} M)	1.4 ± 0.5	0.2 ± 0.3	22 ± 9	25 ± 7
Physostigmine (10^{-6} M)	380 ± 160	26 ± 9	ND	ND
Heptyl physostigmine (10^{-8} M)	11000 ± 3000	770 ± 440	1600 ± 700	1400 ± 400
SDZ-ENA 713 (10^{-5} M)	14 ± 3	0.47 ± 0.46	4.3 ± 1.8	3.3 ± 0.6
(*b*) IC_{50} values[b] (μM)				
Tacrine (recombinant)	0.054 ± 0.036	11.4 ± 1.4	0.15 ± 0.08	0.15 ± 0.04
Tacrine (serum)	0.082 ± 0.009	8.9 ± 2.5	–	–
(*c*) Time dependent reactivation[c] (percent original activity after 30 min)				
Pyridostigmine	9	8	32	24
Physostigmine	17	12	67	54
Heptyl physostigmine	13	13	3	3
SDZ-ENA 713	2	1	8	4

[a]Pseudo-first-order rate constants were extracted from data such as those in Fig. 1, but for the recombinant enzymes, and with the reagent concentrations indicated in parentheses, and were fit to a first-order decay model using the least-squares approach. Averages and standard deviations of at least four determinations are presented. ND, not determined because of the exceedingly high reactivation rates.

[b]IC_{50} values of tacrine were measured for recombinant human ChEs and for sera in the presence of 1 mM BTCh for BuChE or 1 mM acetylthiocholine for AChE. Values are calculated by GraFit 3.0 (Erithacus Software, Staines, UK). The data shown are averages and standard deviations of two serum samples or three recombinant enzyme samples.

[c]Spontaneous reactivation of recombinant human ChEs was examined after complete inhibition of the immobilized enzymes, followed by removal of unreacted inhibitor. Values of percent regained activity after 30 min are shown (average of two experiments).

Methods

All procedures followed were in accord with the Helsinki Declaration as revised in 1983 and with local institutional guidelines for the care and use of laboratory animals.

Patient and methods. A.B. (name and details in hospital medical records), born in 1970, suffered an incident of post-anaesthesia apnea in 1989. Anaesthesia was induced by Na pentothal (250 mg), and succinylcholine (75 mg), benzodiazepam (5 mg), petidine (50 mg), beatryl (0.1 mg) and atropine (0.5 mg) were administered. Mechanical respiration was continued for 5 h because of failure to breathe spontaneously after 30 min of surgery (closed reduction of bilateral tibial fractures). During this period the electrocardiogram and pulse remained normal, mean blood pressure was 130:80 and blood glucose, urea, Na and K values were normal. Haemoglobin count was 12 g dl^{-1}, with slight leukocytosis before surgery (14,000 cells per decilitre), yet with normal temperature. One day after surgery, the BuChE dibucaine number[9] was determined to be 23% of normal. A.B. was released following 9 days of uneventful hospitalization. We then found his serum BuChE to have approximately 30% of normal capacity for BTCh hydrolysis and no inhibition by succinylcholine, suggesting that he had the atypical enzyme[6,7]. A.B. was confirmed as being homozygous for the atypical allele, but not a carrier of other frequent point mutations of BuChE by PCR amplification, *Sau*IIIA restriction and direct sequencing of the corresponding region from the BCHE gene isolated from his venous blood DNA by established techniques[10]. The same methods revealed that both his parents and his sister were heterozygous carriers of the atypical BCHE allele. The patient was advised to avoid anti-ChE drugs and insecticides. A.B. served in the Israel Defense Forces in 1991, during the period of the Persian Gulf War and, with others, thrice daily received 30-mg prophylactic doses of pyridostigmine. He developed nausea, insomnia, weight loss, and general fatigue, which worsened consistently, and a deep depression. Following discontinuation of pyridostigmine, his condition improved gradually over the following weeks. A.B. is currently without symptoms.

Variant enzymes. Serum BuChE activity against BTCh was measured spectrophotometrically as detailed previously[6]. Recombinant normal and atypical BuChEs were produced in *Xenopus* oocytes microinjected with *in vitro* transcribed BCHE mRNAs prepared from the corresponding cDNA types[6]. Alternative recombinant AChEs were produced in ACHEDNA-injected oocytes under control of the cytomegalovirus promoter, using either the brain-characteristic 3'-exon 6 (ref. 13) or the blood cell-expressed domain composed of the fourth pseudo-intron and the 3'-exon 5 (ref. 13).

Inhibitors. Tacrine and physostigmine were purchased from Sigma Chemical Co. SDZ-ENA 713 and heptyl physostigmine were gifts of Sandoz (Berne, Switzerland) and Merck Sharp & Dohme (Harlow, UK), respectively. Pyridostigmine bromide was from Research Biochemicals International (Natik, Massachusetts).

Antibody immobilizations. Monoclonal mouse anti-human serum BuChE (no. 53-4) or anti-human AChE (no. 101–1) antibodies, 4 μg ml^{-1}, were adsorbed to multiwell microtitre plates overnight at 4 °C in carbonate buffer[12]. Free binding sites were blocked with PBS-T buffer (144 mM Na chloride, 20 mM Na phosphate, pH 7.4, 0.05% Tween 20, and 0.01% thimerosal) for 60 to 80 min at 37 °C. Homogenates of microinjected oocytes or serum samples were diluted 1:20 to 1:40 in

PBS-T to achieve similar activity levels and were incubated in the antibody-coated wells for 4 h at room temperature with agitation, and overnight at 4 °C. Plates were washed three times with PBS-T before use.

Inactivation and reactivation measurements. IC_{50} values were determined essentially as described[6], assaying soluble enzyme in the presence of tacrine against 1 mM acetylthiocholine. For inactivation by carbamates and reactivation, antibody-immobilized enzymes were exposed to the tested anti-ChEs in PBS-T buffer for varying times (0.5 to 80 min) at room temperature following an initial determination of catalytic activities. At the noted times, plates were washed three times with PBS-T and remaining substrate hydrolysis rates were determined[12]. Spontaneous reactivation at room temperature was measured for immobilized recombinant ChEs following complete inhibition, three washes with PBS-T, subsequent incubation and activity determination at 30 min.

Specific activity. These values were determined as detailed elsewhere[12].

Acknowledgements

The authors are grateful to J. Patrick (Houston) for useful discussions, to G. Ehrlich (Jerusalem) for help with experiments, to Marta Weinstock-Rosin (Jerusalem) and P.L. Herrling, and P. Neumann of Sandoz Research Institute (Berne) for supplying SDZ-ENA 713, and to L. Iversen, Merck Sharp & Dohme Research Laboratories (Harlow), for supplying heptyl physostigmine. Supported by the U.S. Army Medical Research and Development Command (DAMD 17-94-C-4031, to H.S. and H.Z.), by the Chief Scientist of the Israel Ministry of Health (900-19, to H.Z. and H.S.), by the U.S.–Israel Binational Science Foundation (to H.S.) and by a Levi Eshkol Post-Doctoral Fellowship from the Israel Ministry of Science (to M.S). Y.L.-L. is the recipient of the Landau Pre-Doctoral Research Prize.

RECEIVED 30 MAY; ACCEPTED 28 AUGUST 1995

1. Schwarz, M., Glick, D., Loewenstein, Y. & Soreq, H. Engineering of human cholinesterases explains and predicts diverse consequences of administration of various drugs and poisons. *Pharmacol. Ther.* (in the press).
2. La Du, B.N. *et al.* Phenotypic and molecular biological analysis of human butyrylcholinesterase variants. *Clin. Biochem.* **23**, 423–431 (1990).
3. Keeler, J.R., Hurst, C.G. & Dunn, M.A. Pyridostigmine used as a nerve agent pretreatment under wartime conditions. *JAMA* **266**, 693–695 (1991).
4. Winker, M.A. Tacrine for Alzheimer's disease; which patient, what dose? *JAMA* **271**, 1023–1024 (1994).
5. Sharabi, Y. *et al.* Survey of symptoms following intake of pyridostigmine during the Persian Gulf War. *Isr. J. med. Sci.* **27**, 656–658 (1991).
6. Neville, L.F. *et al.* Intramolecular relationships in cholinesterases revealed by oocyte expression of site-directed and natural variants of human BCHE. *EMBO J.* **11**, 1641–1649 (1992).
7. McGuire, M.C. *et al.* Identification of the structural mutation responsible for the dibucaine-resistant (atypical) variant form of human serum cholinesterase. *Proc. natn. Acad. Sci. U.S.A.* **86**, 953–957 (1989).
8. Kalow, W. & Davis, R.O. The activity of various esterase inhibitors towards atypical human serum cholinesterase. *Biochem. Pharmacol.* **1**, 183–192 (1958).
9. Lockridge, O. Genetic variants of serum cholinesterase influence metabolism of the muscle relaxant succinylcholine. *Pharmacol. Ther.* **47**, 35–60 (1990).
10. Ehrlich, G. *et al.* Population diversity and distinct haplotype frequencies associated with ACHE and BCHE genes of Israeli Jews from Transcaucasian Georgia and from Europe. *Genomics* **22**, 288–295 (1994).
11. Soreq, H. & Zakut, H. *Human Cholinesterases and Anticholinesterases* (Academic Press, San Diego, California, 1993).
12. Schwarz, M. *et al.* Successive organophosphate inhibition and oxime reactivation reveals distinct responses of recombinant human cholinesterase variants. *Molec. Brain Res.* **31**, 101–110 (1995).
13. Seidman, S. *et al.* Synaptic and epidermal accumulations of human acetylcholinesterase are encoded by alternative 3'-terminal exons. *Molec. cell. Biol.* **15**, 2993–3002 (1995).
14. Chatonnet, A. & Lockridge, O. Comparison of butyrylcholinesterase and acetylcholinesterase. *Biochem. J.* **260**, 625–634 (1989).
15. Giacobini, E. The second generation of cholinesterase inhibitors: Pharmacological aspects. in *Cholinergic Basis for Alzheimer Therapy* (eds Becker, R. & Giacobini, E.) 247–262 (Birkhauser, Boston, 1991).
16. Iversen, L.L. Approaches to cholinergic therapy in Alzheimer's disease. *Prog. Brain. Res.* **98**, 423–426 (1993).
17. Enz, A., Amstutz, R., Boddeke, H., Gmelin, G. & Malonowski, J. Brain selective inhibition of acetylcholinesterase: A novel approach to therapy for Alzheimer's disease. *Prog. Brain Res.* **98**, 431–437 (1993).
18. Harel, M. *et al.* Quaternary ligand binding to aromatic residues in the active-site gorge of acetylcholinesterase. *Proc. natn. Acad. Sci. U.S.A.* **90**, 9031–9035 (1993).
19. Harel, M. *et al.* Conversion of acetylcholinesterase to butyrylcholinesterase: Modeling and mutagenesis. *Proc. natn. Acad. Sci. U.S.A.* **89**, 10827–10831 (1992).
20. Valentino, R.J., Lockridge, O., Eckerson, H.W. & La Du, B.N. Prediction of drug sensitivity in individuals with atypical serum cholinesterase based on *in vitro* biochemical studies. *Biochem. Pharmacol.* **30**, 1643–1649 (1981).
21. Gavageran, H. NIH panel rejects Persian Gulf syndrome. *Nature* **369**, 8 (1994).
22. Ott, P. Lustig, A., Brodbeck, U. & Rosenbusch, J.P. Acetylcholinesterase from human erythrocyte membranes: Dimers as functional units. *FEBS Lett.* **138**, 187–189 (1982).
23. Johansson, I.M. & Nordberg, A. Pharmacokinetic studies of cholinesterase inhibitors. *Acta neurol. scand. Suppl.* **149**, 22–25 (1993).
24. Berman, H.A. & Leonard, K. Interaction of tetrahydroaminoacridine with acetylcholinesterase and butyrylcholinesterase. *Molec. Pharmacol.* **41**, 412–418 (1992).
25. May, D.G. Genetic differences in drug disposition. *J. clin. Pharmacol.* **34**, 881–897 (1994).

Pergamon

0163-7258(95)00019-4

Pharmac. Ther. Vol. 67, No. 2, pp. 283–322, 1995

0163-7258/95 $29.00

Associate Editor: P. K. CHIANG

ENGINEERING OF HUMAN CHOLINESTERASES EXPLAINS AND PREDICTS DIVERSE CONSEQUENCES OF ADMINISTRATION OF VARIOUS DRUGS AND POISONS

MIKAEL SCHWARZ, DAVID GLICK, YAEL LOEWENSTEIN, and HERMONA SOREQ*

Department of Biological Chemistry, The Institute of Life Sciences, The Hebrew University of Jerusalem, 91904 Israel

Abstract—The acetylcholine hydrolyzing enzyme, acetylcholinesterase, primarily functions in nerve conduction, yet it appears in several guises, due to tissue-specific expression, alternative mRNA splicing and variable aggregation modes. The closely related enzyme, butyrylcholinesterase, most likely serves as a scavenger of toxins to protect acetylcholine binding proteins. One or both of the cholinesterases probably also plays a non-catalytic role(s) as a surface element on cells to direct intercellular interactions. The two enzymes are subject to inhibition by a wide variety of synthetic (e.g., organophosphorus and carbamate insecticides) and natural (e.g., glycoalkaloids) anticholinesterases that can compromise these functions. Butyrylcholinesterase may function, as well, to degrade several drugs of interest, notably aspirin, cocaine and cocaine-like local anesthetics. The widespread occurrence of butyrylcholinesterase mutants with modified activity further complicates this picture, in ways that are only now being dissected through the use of site-directed mutagenesis and heterologous expression of recombinant cholinesterases.

Keywords—Cholinesterase, alternative mRNA splicing, site-directed mutagenesis, organophosphorus, insecticide, anticholinesterase.

CONTENTS

1. Introduction 284
2. Protein Chemistry and Enzymology 284
3. The Human Cholinesterase Genes 300
   3.1. Structure of the gene 300
   3.2. Chromosomal location 301
   3.3. Control elements 301
   3.4. Coordination of expression with other cholinergic factors 301
   3.5. Alternative splicing 302
   3.6. Polymorphism of molecular forms 302

*Corresponding author.

Abbreviations and nomenclature—ACh, acetylcholine; AChE, acetylcholinesterase enzyme; *ACHE*, acetylcholinesterase gene; AChR, acetylcholine receptor; AD, Alzheimer's disease; ASG, active site gorge; ATCh, acetylthiocholine; BuChE, butyrylcholinesterase enzyme; *BCHE*, butyrylcholinesterase gene; BTCh, butyrylthiocholine; BW 284C51, 1,5-bis(4-allyldimethylammonium phenyl)pentan-3-1 dibromide; CBS, choline-binding site; ChAT, choline acetyltransferase; ChE, cholinesterase enzyme; *CHE*, cholinesterase gene; DFP, diisopropylfluorophosphonate; G1, G2, etc., monomeric, dimeric, etc., globular forms of a cholinesterase; GPI, glycophosphatidyl inositol; iso-OMPA, tetraisopropyl pyrophosphoramide; nAChR, nicotinic acetylcholine receptor; OP, organophosphates; 2-PAM, 2-pyridine aldoxime methiodide; PAS, peripheral anionic site; PD, Parkinson's disease; THA, 1,2,3,4,-tetrahydro-9 aminoacridine (tacrine).

For identification of amino acid residues, the sequence position in a particular ChE is given, followed in parentheses by the identity and position number of the homologous residue in *Torpedo* AChE.

4. Inhibition of Cholinesterases: Mechanisms and Consequences 303
4.1. Organophosphates as anticholinesterases 305
4.2. Treatment of organophosphate poisoning 305
4.3. Natural cholinesterase poisons 307
4.4. Potential strategies for improved protection against organophosphates 307
5. Drugs that are Hydrolyzed or Scavenged by Cholinesterases 308
6. Neurodegenerative Diseases Related to Cholinergic Malfunction 308
6.1. Alzheimer's disease 308
6.2. Parkinson's disease 310
6.3. Huntington's disease 310
6.4. Amyotrophic lateral sclerosis 310
6.5. Myasthenia gravis 310
6.6. Hematological diseases 310
7. Non-Central Nervous System Excitatory Roles of Cholinesterases 311
8. Human Cholinesterase Variants Predict a Genetic Predisposition to Differential Responses to Cholinergic Drugs 312
Acknowledgements 314
References 315

1. INTRODUCTION

Acetylcholinesterase (E.C. 3.1.1.7, AChE) and butyrylcholinesterase (E.C. 3.1.1.8, BuChE) are two closely homologous proteins. Both are present in all vertebrates, and both are capable of hydrolyzing the neurotransmitter acetylcholine (ACh). Several earlier reviews, by Taylor (1991), Massoulie *et al.* (1993) and Soreq and Zakut (1993) and one quite recent one by Taylor and Radic (1994) may be consulted for specialized information on subtopics, especially on cholinesterases (ChEs) of non-human species and on the cell biology aspects of these enzymes. In the present review, we focus on the human genes and their natural and engineered mutations, and the impact of these mutations on the responses of the encoded enzymes to drugs and poisons.

The most obvious and best studied function of AChE is the hydrolysis of ACh to terminate neurotransmission at neuromuscular junctions, nicotinic or muscarinic synapses and secretory organs. Figure 1A outlines this catalytic process and presents the analogy between it and the interaction of ChEs with organophosphate (OP) inhibitors. AChE is characterized by a narrow specificity for ACh and certain inhibitors and by substrate inhibition. The role of BuChE, beyond hydrolyzing ACh at concentrations that would cause inhibition of AChE (Augustinsson, 1948), has not been identified with certainty, but as it has a wider substrate specificity and interacts with a broader range of inhibitors, it has been proposed that it scavenges anti-ChE agents, protecting synaptic AChE from inhibition and the multitude of ACh receptors from blockade (Soreq *et al.*, 1992).

2. PROTEIN CHEMISTRY AND ENZYMOLOGY

Functionally and structurally, the ChEs belong to the class of proteins known as the lipase/esterase family. The two subclasses of this family hydrolyze vastly different substrates, the first, in a homogeneous aqueous phase, the second, at lipid-water interfaces. Still, substantial sequence homology between its members has been recognized, predominantly in the N-terminal half of the molecules. However, comparison of the three-dimensional structure of *Geotrichum candidum* lipase and *Torpedo* AChE revealed a strikingly similar topology that extends through the entire length of the polypeptide chain. This common topological fold, named the α/β-hydrolase fold, has been identified in all members of the lipase/esterase family and in a number of other unrelated hydrolases with no sequence similarity to the ChEs or to each other (Ollis *et al.*, 1992). Comparison of structurally conserved (Greer, 1990) and variable regions of the different proteins suggests that invariant residues are placed in key internal positions to ensure correct folding and that the majority of low-variability positions are in the core of the protein. In contrast, residues facing the surface are much less conserved. A large β-sheet and crossover helices form the conserved scaffold, whereas loops covering the scaffold and surrounding the active site determine substrate specificity and consequently are unique to each enzyme (Cygler *et al.*, 1993).

(A) **Catalysis**

$$ChO\text{-}OCR + EnzOH \longrightarrow EnzO\text{-}OCR + ChOH$$

$$EnzO\text{-}OCR + OH^- \longrightarrow {}^-OOCR + EnzOH$$

Phosphorylation and reactivation

$$XPO(OR')_2 + EnzOH \longrightarrow EnzOPO(OR')_2 + HX$$

$$EnzOPO(OR')_2 + B: \longrightarrow B\text{-}PO(OR')_2 + EnzOH$$

(B)

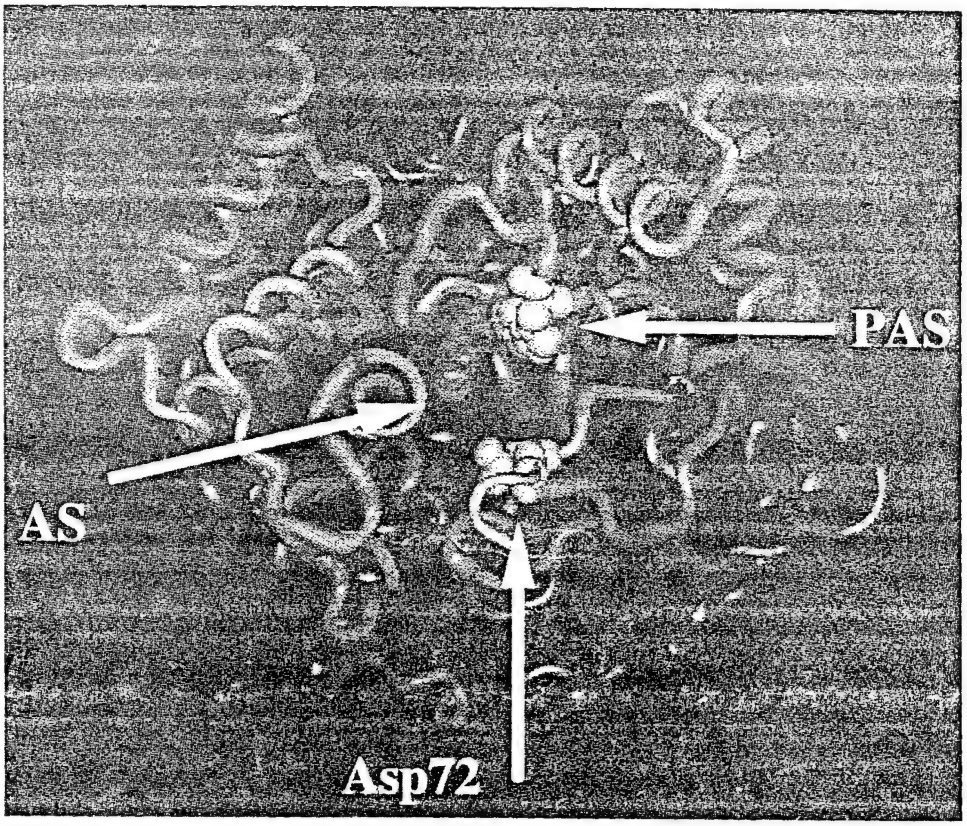

Fig. 1. Cholinesterases and the catalytic process. (A): Catalytic hydrolysis by ChEs the analogous phosphorylation and reactivation processes. Hydrolysis of an acyl-choline substrate (ChO-OCR) by a ChE (EnzOH) proceeds by two steps and involves the production of an acyl-enzyme intermediate (EnzO-OCR). An organophosphorus compound, $XPO(OR')_2$, interacts with these enzymes in a parallel fashion and may be displaced from the active site serine (S200) by strong nucleophiles (e.g., an oxime, represented as B:), releasing a reactivated enzyme. (B): Protein structure and the main active site domains. A ribbon model of *Torpedo* AChE is presented (after Sussman *et al.*, 1991). Space filling representations of serine 200 (S200) at the active (catalytic) site (AS), aspartate 70 (D70) at the entrance to the active site gorge (ASG) and tryptophan 279 (W279), part of the peripheral anionic site (PAS) are noted.

More specifically, the three-dimensional structure of AChE is becoming impressively detailed, thanks to data acquired from X-ray crystallography, combined with the use of specific ligands and site-directed mutants. The emerging feature is a globular protein that features an active center buried within its interior. A deep and narrow gorge extending from the surface of the protein down to the active center is the entry to the active site (Sussman *et al.*, 1991). The ChEs are notable for their catalytic rates, which approach the rate of diffusion, the theoretical limit for catalysis by any enzyme. An interesting mechanism has been proposed (Ripoll *et al.*, 1993) to explain this exceptionally high catalytic rate. Computer modeling of the distribution of charges in AChE suggests that the protein is a very strong dipole, with field lines that attract the positively charged ACh into the gorge and down to the active site where the lowest electrostatic potential lies. Further, the same field will accelerate expulsion of the final product, the acetate ion. It has also been proposed that a mobile flap, a "back

door," allows exit of choline from the catalytic site directly to the exterior of the protein without having to travel up the gorge, thus avoiding a potential traffic problem and accelerating catalytic turnover (Gilson *et al.*, 1994). This ingenious proposal awaits experimental verification.

Substrate inhibition studies of AChE suggested that there exists a peripheral anionic site (PAS) (Changeux, 1966). Further evidence for the PAS came from its interaction with the reversible inhibitor, propidium, which did not prevent the simultaneous binding of other inhibitors to the catalytic site (Taylor and Lappi, 1975). Analysis of the amino acid sequences and three-dimensional models of AChE has led to further identification of more residues potentially important in PAS involvement in the catalytic activity and inhibitor interaction of AChE. One example is W279 positioned at the entrance to the gorge on *Torpedo* AChE (Fig. 1B). When substituted by alanine, inhibition by the PAS-specific ligand, propidium, was strongly reduced as compared with wild-type *Torpedo* AChE, while action of the catalytic site-specific inhibitor edrophonium was unaffected (Harel *et al.*, 1992). This suggested that W279 is associated with the PAS. Further studies on human AChE confirmed this and also placed at the PAS residues Y72 (Y70) and Y124 (Y121) (see Abbreviations and Nomenclature). Together, these residues close to the entrance to the active site gorge (ASG) comprise several overlapping binding sites that all share residues W286 (W279) and D74 (D72) (Barak *et al.*, 1994). The information that the PAS is occupied is thought to be communicated to the active center from D74 (D72) near the surface, on to Y341 (Y334), with which it is hydrogen bonded, and relayed to Y337 (F330) at the hydrophobic subsite of the active center, which may rotate into the active site and block access of potential ligands (Ordentlich *et al.*, 1993a; Shafferman *et al.*, 1992b). Support for the role of D74 (D72) comes from its unique capacity to influence events taking place both at the PAS and the active center (Barak *et al.*, 1994). It was further shown for AChE that W286 (W279) is coupled to W86 in the active center. It was suggested that a "crosstalk" between these two tryptophan residues results in reorientation of W86 (W84), which may interfere with stabilization of enzyme-substrate complexes (Ordentlich *et al.*, 1993a). However, whether or not W286 (W279) is implicated in the well-known phenomenon of substrate inhibition of AChE (Shafferman *et al.*, 1992b; Harel *et al.*, 1992) is controversial. There is no such evidence for a PAS in BuChE, although its substrate activation by acetylthiocholine (ATCh) (Cauet *et al.*, 1987) and substrate inhibition by benzoylcholine (Augistinsson, 1948) suggest that one may exist.

Studies on a mutant human BuChE, the "atypical" variant, identified another residue that affects inhibitor interactions of the ChEs. The variation was identified as a point mutation of aspartate 70, which was replaced by a glycine residue (D70G) (McTiernan *et al.*, 1987; Lockridge, 1987, 1990; Neville *et al.*, 1990b), and the variant was demonstrated to display decreased interactions with inhibitors (Gnatt *et al.*, 1990; Neville *et al.*, 1990a; McGuire *et al.*, 1989) and a 4-fold lower specific activity than the wild-type BuChE (Neville *et al.*, 1992). This natural mutation and the many others discovered after it (reviewed by Soreq and Zakut, 1993) are presented in Table 1. The finding of this mutation led to intense work on the homologous residue of AChE (see below).

In the gorge lining, six aromatic residues are different in BuChEs. Two of them, F288 and F290, positioned at the acyl-binding pocket at the bottom of the AChE gorge, were replaced with their counterparts in BuChE, leucine and valine, respectively. The resultant double mutant hydrolysed butyrylthiocholine (BTCh) almost as well as ATCh (Harel *et al.*, 1992). It was also inhibited by the BuChE-specific inhibitor tetraisopropyl pyrophosphoramide (iso-OMPA) at a rate considerably faster than AChE. Thus, the bulky phenylalanyl residues at the gorge lining in AChE seem to prevent entrance of BTCh and iso-OMPA into the acyl-binding pocket. Parallel studies were performed on mouse AChE (Vellom *et al.*, 1993), with similar results. Table 2 summarizes briefly the many site-directed mutagenesis studies on variable ChEs and their biochemical implications.

A chimeric protein was created by exchanging a polypeptide sequence that includes the rim of the gorge (including D70) with the corresponding sequence from human AChE. It includes part of the conserved gorge lining and oxyanion hole and the choline binding site of human BuChE (residues 58–133 of the BuChE sequence). Therefore, its properties help explain the roles of these sites in catalysis and inhibitor interactions (Loewenstein *et al.*, 1993a). The catalytic properties of the chimera, in general, were identical to those of BuChE, sharing with BuChE recognition of succinylcholine as a substrate and physostigmine (eserine) as an inhibitor. However, the chimera acquired the AChE-like sensitivity to inhibition by echothiophate and iso-OMPA and displayed a pattern of inhibition, more similar to that of AChE than of BuChE, toward the anti-asthma drug bambuterol, the local anesthetic dibucaine and the AChE-specific inhibitor 1,5-bis(4-allyldimethylammonium phenyl)pentan-3-1

Table 1. *Naturally Occurring Variants of Human Cholinesterases*

Altered amino acid	Mutated nucleotide(s)	Comments	Source of mutated cDNA or enzyme and reference
Acetylcholinesterase			
WT	None	Normal	Brain, Soreq *et al.*, 1990
H322N	CAC → AAC	Causes Yt^b blood group	Blood, Lockridge *et al.*, 1992[1]; Bartels *et al.*, 1993
Butyrylcholinesterase			
WT	None	Normal	Brain, Prody *et al.*, 1987; Lockridge *et al.*, 1987
I6 → termination (frameshift)	ATT → TT	Silent. No enzyme activity and no detectable immunoreactive protein.	Blood, Primo-Parmo *et al.*, 1992[2]
P37S	CCT → TCT	Silent. No enzyme activity and no detectable immunoreactive protein.	Blood, Primo-Parmo *et al.*, 1992[2]
D70G	GAT → GGT	Located close to rim of ASG. Most common of variants. Level of mutant enzyme in blood is 30% of WT enzyme. K_m to BTCh unchanged, K_i to succinylcholine increased 30-fold and sensitivity to other ligands decreased up to 500-fold. See also double and triple mutants. Often linked on one allele with A539T.	Blood, Eckerson *et al.*, 1983; Bartels *et al.*, 1992b Glioblastoma expressed in XO, Gnatt *et al.*, 1990; Neville *et al.*, 1990a, 1992; Soreq *et al.*, 1992; Schwarz *et al.*, 1994
Y114H	TAT → CAT	No significant effect on catalytic properties. See also double and triple mutants.	Glioblastoma expressed in XO, Neville *et al.*, 1992; Soreq *et al.*, 1992; Schwarz *et al.*, 1994
D70G Y114H		K_m to BTCh increased 2-fold. K_i to succinylcholine increased 50-fold. Rate of reactivation by 2-PAM of DIP-BuChE decreased 10-fold.	Glioblastoma expressed in XO, Gnatt *et al.*, 1990; Neville *et al.*, 1992; Schwarz *et al.*, 1994
G117 → termination (frameshift)	GGT → GGAG	Silent. No enzyme activity and no detectable immunoreactive protein.	Blood, Noguiera *et al.*, 1990
V142M	GTG → ATG	H-variant, 10% specific activity of WT.	Blood, Lockridge, 1990
D170G	GAT → GGT	Silent. No enzyme activity and no detectable immunoreactive protein.	Blood, Primo-Parmo *et al.*, 1992[2]
S198G	AGT → GGT	Silent. No enzyme activity and no detectable immunoreactive protein.	Blood, Primo-Parmo *et al.*, 1992[2]
T243M	ACG → ATG	Fluoride-1, K_m-variant	Blood, Noguiera *et al.*, 1990
D301 → termination (frameshift)	Alu-insert (nucleotides 1062–1077)	Silent. No enzyme activity and no detectable immunoreactive protein.	Blood, Muratani *et al.*, 1991
T315 → termination (frameshift)	ACC → AACC	Silent. No enzyme activity and no detectable immunoreactive protein.	Blood, Primo-Parmo *et al.*, 1992[2]
G356R	GGA → CGA	Silent. No enzyme activity and no detectable immunoreactive protein.	Blood, Primo-Parmo *et al.*, 1992[2]

(*continued*)

Table 1. (*continued*)

Altered amino acid	Mutated nucleotide(s)	Comments	Source of mutated cDNA or enzyme and reference
G390V	GGT → GTT	Fluoride-2 variant. Up to 6-fold increase in K_m for ATCh and succinyldithiocholine at low substrate concentrations. K_i for tacrine and dibucaine increased 3- and 6-fold, respectively.	Blood expressed in CHO, Masson *et al.*, 1993
S425P	TCC → CCC	No significant effect on catalytic properties. See also double and triple mutants.	Glioblastoma expressed in XO, Gnatt *et al.*, 1990; Neville *et al.*, 1990, 1992; Schwarz *et al.*, 1994
D70G S425P		Full resistance to succinylcholine and dibucaine (K_is>1 M). Both rate of inactivation by DFP and reactivation by 2-PAM of DIP-BuChE decreased 10-fold.	Glioblastoma expressed in XO, Gnatt *et al.*, 1990; Neville *et al.*, 1990b, 1992; Schwarz *et al.*, 1994
D70G Y114H S425P		K_i to succinylcholine increased 80-fold. Rate of reactivation by 2-PAM of DIP-BuChE decreased 40-fold.	Glioblastoma expressed in XO, Neville *et al.*, 1992; Schwarz *et al.*, 1994
W471R	TGG → CGG	Silent. No enzyme activity and no detectable immunoreactive protein.	Blood, Primo-Parmo *et al.*, 1992[2]
Y500 → termination (frameshift)	TAT → TAA	Silent. No enzyme activity and no detectable immunoreactive protein.	Blood, Primo-Parmo *et al.*, 1992[2]
Q508L	CAA → CTA	Silent. No enzyme activity and no detectable immunoreactive protein.	Blood, Primo-Parmo *et al.*, 1992[2]
A539T	GCA → ACA	K-variant. 70% specific activity of WT. Genetically linked to D70G.	Blood, Bartels *et al.*, 1992b
E497V A539T	GAA → GTA GCA → ACA	J-variant. 33% specific activity of WT. E497V has not been identified without A539T.	Blood, Bartels *et al.*, 1992a
W471R	TGG → CGG	Silent. No enzyme activity and no detectable immunoreactive protein.	Blood, Primo-Parmo *et al.*, 1992[2]
F561Y	TTT → TAT	No significant effect on catalytic properties.	Glioblastoma expressed in XO, Gnatt *et al.*, 1990; Neville *et al.*, 1992; Soreq *et al.*, 1992
D70G F561Y		K_i to succinylcholine increased 40-fold.	Glioblastoma expressed in XO, Gnatt *et al.*, 1990; Neville *et al.*, 1992
D70G Y114H F561Y		K_i to succinylcholine increased 25-fold.	Glioblastoma expressed in XO, Neville *et al.*, 1992

Abbreviations: CHO, Chinese hamster ovary; WT, wide-type; XO, *Xenopus* oocytes.

[1] Lockridge, O., Bartels, C. F., Zelinski, T., Jbilo, O. and Kris, M. (1992) Part 1: Genetic variant of human acetylcholinesterase. Part 2: SV-40 transformed cell lines, for example COS-1, but not parental untransformed cell lines, express butyrylcholinesterase (*BCHE*). In: Multidisciplinary Approaches to Cholinesterase Functions, Proceedings of the Thirty-Sixth Oholo Conference on Multidisciplinary Approaches to Cholinesterase Functions, Eilat, Israel, 6–10 April 1992, pp. 53–59, Shafferman, A. and Velan, B. (eds.) Plenum Press, New York.

[2] Primo-Parmo, S. L., Bartels, C. F., Lightstone, H., van der Spek, A. F. L. and La Du, B. N. (1992) Heterogeneity of the silent phenotype of human butyrylcholinesterase – identification of eight new mutations. In: Multidisciplinary Approaches to Cholinesterase Functions, Proceedings of the Thirty-Sixth Oholo Conference on Multidisciplinary Approaches to Cholinesterase Functions, Eilat, Israel, 6–10 April 1992, pp. 61–64, Shafferman, A, and Velan, B. (eds.) Plenum Press, New York.

Table 2. *Site-Directed Mutants of Cholinesterases and their Properties*[1]

Torpedo AChE residue	Mutation	Organism enzyme[2]	Conserved residue[3] and three-dimensional location[4]	Comments	Expression system[5] and reference
Y70	Y72A	hAChE	A, B ASG rim, part of PAS	Small effect on K_m and k_{cat}. Up to 4-fold increase in K_i to PAS-specific ligands, as compared with WT. D72 is hydrogen bonded with Y443. See also double mutations.	HEK293, Barak *et al.*, 1994
Y70	Y72N	mAChE	A, B ASG rim, part of PAS	Contributes to the stabilization energy for PAS and AS specific ligand complexes. K_i for these ligands increased up to 9-fold. See also double, triple and quadruple mutants.	HEK293, Radic *et al.*, 1993
D72	D74E	hAChE	A, B Core of PAS	"Atypical" phenotype in hBuChE. Essential element in intramolecular communication down the gorge. Influence events both at the PAS and the AS through conformational changes at these sites, as seen by interactions with PAS- and AS-specific inhibitors. K_i for PAS- and AS-specific inhibitors increased 10-fold. Displays shifted substrate inhibition profile.	XO, Neville *et al.*, 1990a,b, 1992 HEK293, Shafferman *et al.*, 1992b
D72	D74N	hAChE	A, B Core of PAS	Decreased sensitivity to succinylcholine and dibucaine. IC_{50}-values for PAS- and AS-specific bisquaternary compounds increased up to 113-fold.	HEK293, Shafferman *et al.*, 1992[6]; Shafferman *et al.*, 1992a,b; Barak *et al.*, 1994
D72	D74G	hAChE	A, B Core of PAS	IC_{50} values for PAS- and AS-specific bisquaternary compounds increased up to 100-fold. No substrate inhibition.	Shafferman *et al.*, 1992a,b
D72	D74K	hAChE	A, B Core of PAS	IC_{50} values for PAS- and AS-specific bisquaternary compounds increased up to 1280-fold; for propidium, 36-fold. No substrate inhibition.	Shafferman *et al.*, 1992b
D72	Y109G	dChE	A, B except in *Drosophila* ASG rim	Y109 is not directly involved in catalysis, but contributes to the AS conformation. Mutations in Y109 produce allosteric effects. Less stable than WT at high temperature. Decreased activity at pH 10. K_m for ATCh increased 8-fold.	XO, Mutero *et al.*, 1992; Fournier *et al.*, 1992[7]
D72	Y109D	dChE	A, B except in *Drosophila* ASG rim	K_m unchanged. K_i for propidium increased 3-fold. Inhibition rate constant for dichlorovos and neostigmine increased 2.5-fold and decreased 6-fold, respectively.	XO, Mutero *et al.*, 1992; Fournier *et al.*, 1992[7]
D72	Y109K	dChE	A, B except in *Drosophila* ASG rim	Slight changes in inhibition rate constants for OPs and carbamates. More stable than WT at high temperature. K_m for ATCh and BTCh increased 128-fold and 27-fold, respectively. K_i for propidium increased 205-fold. Inhibition rate constants for paraoxon and dichlorovos decreased 6-fold and increased 4-fold, respectively.	XO, Mutero *et al.*, 1992; Fournier *et al.*, 1992[7]
D72	D74N	mAChE	A, B except in *Drosophila* ASG rim	K_m and K_is for ATCh increased 28-fold and 35-fold, respectively. Dramatic effect on stabilization of BW284C51 and decamethonium complexes, and 680-fold and 240-fold increases in K_i for these compounds, respectively.	HEK293, Radic *et al.*, 1993

(*continued*)

Table 2. (*Continued*)

Torpedo AChE residue	Mutation	Organism enzyme[2]	Conserved residue[3] and three-dimensional location[4]	Comments	Expression system[5] and reference
E82	E84Q	hAChE	A, B Surface	No effect on catalytic properties.	Shafferman *et al.*, 1992[6]; Shafferman *et al.*, 1992a
W84	W86A	hAChE	A, B CBS	Element of the hydrophobic subsite and classical anionic site. Methyl group of quaternary ammonium is positioned 4 Å from Trp indol plane. Involved in stabilization of choline moiety in the enzyme-substrate or inhibitor-complex. Has a major role in hydrolysis. Motion of residue suggested to be involved in accommodation of ligands. K_m increased 775-fold and k_{cat}/K_m decreased 3890-fold. K_i for propidium and decamethonium increased 621-fold and 15,000-fold, respectively. Involvement in anionic site identified also in photoaffinity labeling.	HEK293, Barak *et al*, 1994; Shafferman *et al.*, 1992[6]; Shafferman *et al.*, 1992b; Ordentlich *et al.*, 1993a
W84	W86E	hAChE	A, B CBS	No detectable catalytic activity. See W86A.	Shafferman *et al.*, 1992b
E89	N126D	dChE	A, B (±)	Glycosylation site on 18 kDa subunit.	XO, Mutero and Fournier 1992; Fournier *et al.*, 1992[7]
E92	E92Q	tAChE	A, B	Salt bridge between E92 and R44 (both conserved) stabilizing the protein conformation; 1% catalytic activity as compared with WT.	COS1, Bucht *et al.*, 1992[8]
E92	E92L	tAChE	A, B	Salt bridge between E92 and R44 (both conserved) stabilizing the protein conformation. 1% catalytic activity as compared with WT.	COS1, Bucht *et al.*, 1992[8]
D93	D93N	tAChE	A, B Surface	Hydrogen bond between D93 and Y96; 20% catalytic activity as compared with WT.	COS1, Bucht *et al.*, 1992[8] HEK293, Shafferman *et al.*, 1992[6]
D93	D95N	hAChE	A, B Surface	Low production. May be involved in targetting to secretion vesicles. No effect on catalysis.	HEK293, Shafferman *et al.*, 1992[6]; Shafferman *et al.*, 1992a
D93	D130N	dChE	A, B Surface	No effect.	XO, Fournier *et al.*, 1992[7]
Y121	Y124A	hAChE	A, B ASG rim	Part of PAS. Small or no effect on K_m, k_{cat} and propidium binding.	HEK293, Barak *et al.*, 1994
Y121	Y124Q	mAChE	A, B ASG rim	See hAChE Y124A and mAChE Y72N. K_i for PAS- and AS-specific ligands increased up to 7-fold.	HEK293, Radic *et al.*, 1993
Y70 Y121	Y72A + Y124A	hAChE	A, B ASG rim	See single mutations. K_i for propidium and BW284c51 increased 5-fold and 35-fold, respectively.	HEK293, Barak *et al.*, 1994
Y70 Y121	Y72N Y124Q	mAChE	A, B ASG rim	Summation of stabilization energies (ΔΔG) of single mutations suggests lack of appreciable interaction between the loci. K_i for PAS- and AS-specific ligands increased up to 100-fold. See also mouse chimera.	HEK293, Radic *et al.*, 1993

(*continued*)

Table 2. (*Continued*)

Torpedo AChE residue	Mutation	Organism enzyme[2]	Conserved residue[3] and three-dimensional location[4]	Comments	Expression system[5] and reference
D128	D131N	hAChE	Surface	No effect on activity.	Shafferman *et al.*, 1992[6]
D172	D175N	hAChE	A, B Part of α-helix C	Salt bridge with conserved R152. Mutant protein inactive and not secreted due to misfolding.	Shafferman *et al.*, 1992[6]
–	N174S	dChE	Glycosylation site	No homologous residue in other ChEs.	XO, Mutero and Fournier, 1992; Fournier *et al.*, 1992[7]
D172	D248N	dChE	A, B	See mutation in hAChE.	XO, Mutero and Fournier, 1992; Fournier *et al.*, 1992[7]
E199	E202Q	hAChE	A, B AS	Critical residue in AS conformation. Only charged residue at bottom. Stabilizes protonated His447 imidazolium, facilitating proton transfer from S203 and formation of acyl-enzyme intermediate. Hydrogen bond with E450. Mutant is less effective in acylation/deacylation steps. k_{cat} reduced 7-fold. IC_{50} to bisquaternary compounds increased up to 40-fold. Inactivation rate constant reduced 50-fold. Substrate inhibition affected. Confers resistance to aging.	HEK293, Shafferman *et al.*, 1992[6]; Shafferman *et al.*, 1992b; Ordentlich *et al.*, 1993b
E199	E202D	hAChE	A, B AS	See 202Q. k_{cat} reduced 25-fold. IC_{50} to edrophonium and bisquaternary compounds increased 25-fold and up to 80-fold, respectively.	Shafferman *et al.*, 1992b
E199	E202A	hAChE	A, B AS	See 202Q. k_{cat} reduced 37-fold. IC_{50} to edrophonium and bisquaternary compounds increased 80-fold and up to 800-fold, respectively.	Shafferman *et al.*, 1992b
E199	E199Q	tAChE	A, B AS	May interact with E443 and S226 through an entrapped water molecule. Affects interaction with PAS-specific inhibitors, suggesting allosteric coupling between the sites. K_m increased 14-fold. k_{cat}/K_m is 2% of that for WT enzyme. Shift in substrate inhibition profile. Mutant protein largely resistant to aging.	COS1, Gibney *et al.*, 1990; Radic *et al.*, 1992; Saxena *et al.*, 1993
E199	E199D	tAChE	A, B AS	Use of carbamoylating substrates demonstrates predominant influence of E199 on acylation rather than deacylation step. K_{cat} decreased 5-fold. K_m for ATCh unchanged. No substrate inhibition.	COS1, Gibney *et al.*, 1990; Radic *et al.*, 1992; Saxena *et al.*, 1993
E199	E199H	tAChE	A, B AS	Almost complete loss of catalytic activity.	COS1, Gibney *et al.*, 1990
S200	S200V	tAChE	A, B AS	Triad member. No detectable catalytic activity.	COS1, Gibney *et al.*, 1990
S200	S200C	tAChE	A, B AS	0.3% catalytic activity of WT enzyme.	COS1, Gibney *et al.*, 1990
S200	S203A	hAChE	A, B AS	No detectable catalytic activity. Normally secreted.	Shafferman *et al.*, 1992[6]; Shafferman *et al.*, 1992a

(*continued*)

Table 2. (*Continued*)

Torpedo AChE residue	Mutation	Organism enzyme[2]	Conserved residue[3] and three-dimensional location[4]	Comments	Expression system[5] and reference
S200	S203C	hAChE	A, B AS	No detectable catalytic activity. Normally secreted.	Shafferman *et al.*, 1992[6]; Shafferman *et al.*, 1992a
S200	S203T	hAChE	A, B AS	No detectable catalytic activity. Normally secreted.	Shafferman *et al.*, 1992[6]; Shafferman *et al.*, 1992a
S200	S198C	hBuChE	A, B AS	1% catalytic activity of WT enzyme.	XO, Gnatt *et al.*, 1992[9], 1994; Soreq *et al.*, 1992
S200	S198T	hBuChE	A, B AS	No detectable catalytic activity.	XO, Gnatt *et al.*, 1992[9], 1994; Soreq *et al.*, 1992
S200	S198D	hBuChE	A, B AS	No detectable catalytic activity.	XO, Gnatt *et al.*, 1992[9], 1994; Soreq *et al.*, 1992
S200	S198H	hBuChE	A, B AS	No detectable catalytic activity.	XO, Gnatt *et al.*, 1992[9], 1994; Soreq *et al.*, 1992
S200	S198Q	hBuChE	A, B AS	No detectable catalytic activity.	XO, Gnatt *et al.*, 1992[9], 1994; Soreq *et al.*, 1992
L252	C328V	dChE	a, b	No effect on molecular weight. Not involved in intrachain S-S bonds.	XO, Fournier *et al.*, 1992[7]; Mutero and Fournier, 1992
(−)	N331D	dChE	(−)	Glycosylation site on 55 kDa subunit.	XO, Fournier *et al.*, 1992[7]; Mutero and Fournier, 1992
E278	E285A	hAChE	A, B except dChE Rim of ASG	Only charged residue in PAS. Up to 6-fold increase in K_i for PAS- and AS-specific ligands.	HEK293, Barak *et al.*, 1994
E278	Y72A + E285A	hAChE	A, B except dChE Rim of ASG	K_i for propidium increased 10-fold.	HEK293, Barak *et al.*, 1994
W279	W286A	hAChE	A, b Rim of ASG Core of PAS	Essential element in intramolecular communication down the gorge; moves upon edrophonium and tacrine binding. K_i for PAS- and AS-specific ligands increased up to 13-fold.	Shafferman *et al.*, 1992b; Barak *et al.*, 1994; Ordentlich *et al.*, 1993a
W279	W286R	mAChE	A, b Rim of ASG Core of PAS	Contributes to the stabilization energy for PAS- and AS-specific ligand complexes. K_i for these ligands increased up to 110-fold. See also double, triple and quadruple mutants.	HEK293, Radic *et al.*, 1993
Y70 W279	Y72A + W286A	hAChE	A, b Rim of ASG Core of PAS	Synergistic effect of single mutations. IC_{50} for PAS- and AS-specific ligands increased up to 130-fold.	Barak *et al.*, 1994
Y70 W279	Y72N W286R	mAChE	A, b Rim of ASG Core of PAS	Summation of stabilization energies ($\Delta\Delta G$) of BW284C51 and decamethonium complexes of single mutations, suggests lack of appreciable interaction between the loci. K_m (ATCh) and K_i for PAS- and AS-specific ligands increased 15-fold and up to 570-fold, respectively.	HEK293, Radic *et al.*, 1993

(*continued*)

Table 2. (*Continued*)

Torpedo AChE residue	Mutation	Organism enzyme[2]	Conserved residue[3] and three-dimensional location[4]	Comments	Expression system[5] and reference
Y121 W279	Y124Q W286R	mAChE	A, b Rim of ASG Core of PAS	K_m (ATCh) and K_i for PAS- and AS-specific ligands increased 15-fold and up to 2500-fold, respectively. See mouse double mutant above.	HEK293, Radic *et al.*, 1993
Y121 W279	E285A + W286A	hAChE	A, b Rim of ASG Core of PAS	Synergistic effect of single mutations. IC_{50} for PAS- and AS-specific ligands increased up to 222-fold.	Barak *et al.*, 1994
Y121 W279	Y72A + E285A + W286A	hAChE	A, b Rim of ASG Core of PAS	Synergistic effect of single mutations. IC_{50} for PAS- and AS-specific ligands increased up to 387-fold.	Barak *et al.*, 1994
Y121 W279	Y124A + E285A + W286A	hAChE	A, b Rim of ASG Core of PAS	Synergistic effect of single mutations. IC_{50} for PAS- and AS-specific ligands increased up to 350-fold.	Barak *et al.*, 1994
Y70 Y121 W279	Y72N Y124Q W286R	mAChE	A, b Rim of ASG Core of PAS	Summation of stabilization energies ($\Delta\Delta G$) of BW284C51 and decamethonium complexes of single mutations, suggests lack of appreciable interaction between the loci. K_m (ATCh) and K_i for PAS- and AS-specific ligands increased 18-fold and up to 5,700-fold, respectively. K_i of mutant protein for BW284C51 close to that of BuChE. However, affinity for decamethonium is far lower, indicating that BuChE may use different residues than AChE to stabilize this compound.	HEK293, Radic *et al.*, 1993
Y70 Y121 W279	Y72N Y124Q W286A	mAChE	A, b Rim of ASG Core of PAS	K_m (ATCh) and K_i for PAS- and AS-specific ligands increased 5-fold and up to 1500-fold, respectively. See also mouse triple mutant above.	HEK293, Radic *et al.*, 1993
Y70 D72 Y121 W279	Y72N D74N Y124Q W286R	mAChE	A, b Rim of ASG Core of PAS	The influence of D74 on the stabilization energies ($\Delta\Delta G$) of BW284C51 and decamethonium complexes is not additive to the triple mutants. K_m (ATCh) and K_i for PAS- and AS-specific ligands increased 133-fold and up to 280,000-fold, respectively.	HEK293, Radic *et al.*, 1993
Y70 D72 Y121 W279	Y72N D74N Y124Q W286A	mAChE	A, b Rim of ASG Core of PAS	K_m (ATCh) and K_i for PAS- and AS-specific ligands increased 46-fold and up to 60,000-fold, respectively. See quadruple mutant above.	HEK293, Radic *et al.*, 1993
Y70 D72 Y121 W279	W279A	tAChE	A, b Rim of ASG Core of PAS	See hAChE. Conformational changes upon binding of tacrine, edrophonium. 10-fold decrease in sensitivity to propidium. No change in binding of edrophonium. Slightly less inhibited by high substrate concentrations.	Harel *et al.*, 1992
F288	F295L	hAChE	A, B ASG bottom; part of the ABS	Important in determining specificity to acyl moiety of substrate. Improved interaction with BTCh in the mutants. Increased affinity to iso-OMPA due to substitution with smaller residue. K_m for BTCh 10-fold reduced. K_m for ATCh unchanged.	HEK293, Ordentlich *et al.*, 1993a

(*continued*)

Table 2. (*Continued*)

Torpedo AChE residue	Mutation	Organism enzyme[2]	Conserved residue[3] and three-dimensional location[4]	Comments	Expression system[5] and reference
F288	F295A	hAChE	A, B ASG bottom; part of the ABS	K_m for BTCh 30-fold reduced. K_i for BW284C51 3-fold reduced.	Barak *et al.*, 1994; Ordentlich *et al.*, 1993a
F288	F295L	mAChE	A, B ASG bottom. part of the ABS	Reduced k_{cat} for ATCh. Enhanced k_{cat} and reduced K_m for BTCh.	HEK293, Vellom *et al.*, 1993; Radic *et al.*, 1993
F288	F295Y	mAChE	A, B ASG bottom; part of the ABS	K_m (ATCh) and k_{cat} decreased 2.5-fold and 25-fold, respectively.	HEK293, Radic *et al.*, 1993
F288	L286D	hBuChE	A, B ASG bottom; part of the ABS	Catalytic activity significantly affected. K_m increased 4-fold. Reduced sensitivity to a variety of OPs. IC_{50} for echothiophate increased 9-fold.	XO, Gnatt *et al.*, 1994; Schwarz *et al.*, 1994
F288	L286Q	hBuChE	A, B ASG bottom; part of the ABS	K_m increased 10-fold.	XO, Gnatt *et al.*, 1994; Schwarz *et al.*, 1994
F288	L286R	hBuChE	A, B ASG bottom; part of the ABS	K_m increased 5-fold.	XO, Gnatt *et al.*, 1994; Schwarz *et al.*, 1994
F288	L286K	hBuChE	A, B ASG bottom; part of the ABS	K_m increased 10-fold. IC_{50} for echothiophate increased more than 1000-fold. Reactivation rate of DIP-BuChE by 2-PAM decreased 40-fold.	XO, Gnatt *et al.*, 1994; Schwarz *et al.*, 1994
F288	F288L + F290V	tAChE	ABS	Removal of bulky phenyl rings appears to permit BTCh to enter the active site, and allows space for the entrance of bulky OPs such as iso-OMPA. Specific activity with ATCh as substrate is 10% of WT enzyme. BTCh hydrolyzed at same rate as ATCh.	COS 7, Harel *et al.*, 1992
R289	R296S	mAChE	A, B	No major change in catalytic parameters. Slight decrease in K_m for BTCh due to reduced steric hindrance.	HEK293, Vellom *et al.*, 1993; Radic *et al.*, 1993
F290	F297V	hAChE	A, B (±) ASG bottom; part of ABS	Secondary to F295 in determining specificity to aryl moiety of substrate. Contributes to AS plasticity. K_m for ATCh increased 9-fold.	HEK293, Ordentlich *et al.*, 1993a
F290	F297A	hAChE	A, B (±) ASG bottom; part of ABS	See F297V. Affinity to BW284C51 increased 2-fold. K_i for decamethonium increased 10-fold. K_m for ATCh increased 4-fold.	Barak *et al.*, 1994; Ordentlich *et al.*, 1993a
F290	F297I	mAChE	A, B (±) ASG bottom; part of ABS	Eliminates substrate inhibition and confers substrate activation. Role in orienting substrate to maximize catalysis. Reduced k_{cat} for ATCh, but increased k_{cat} for BTCh. K_m for ATCh increased 9-fold, but K_m for BTCh unchanged.	HEK293, Vellom *et al.*, 1993; Radic *et al.*, 1993

(*continued*)

Table 2. (*Continued*)

Torpedo AChE residue	Mutation	Organism enzyme[2]	Conserved residue[3] and three-dimensional location[4]	Comments	Expression system[5] and reference
F290	F297Y	mAChE	A, B (±) ASG bottom; part of ABS	K_m for ATCh unchanged.	HEK293, Radic *et al.*, 1993
F290	F295L + F297V	hAChE	A, B (±) ASG bottom; part of ABS	See single mutations.	Ordentlich *et al.*, 1993a
F290	F295L + F297I	hAChE	A, B (±) ASG bottom; part of ABS	See F297.	HEK293, Vellom *et al.*, 1993; Radic *et al.*, 1993
F290	F295L + R296S + F297I	hAChE	A, B (±) ASG bottom; part of ABS	Lower k_{cat} for ATCh as compared with single mutations; 5% activity of WT enzyme.	HEK293, Vellom *et al.*, 1993
V293	V300G	mAChE	A, B Near ABS	See R296S.	HEK293, Vellom *et al.*, 1993; Radic *et al.*, 1993
D326	D333N	hAChE	A, B ASG bottom	Charged moiety pointing away from triad. No effect on catalysis, but secretion reduced.	Shafferman *et al.*, 1992[6]; Shafferman *et al.*, 1992a
E327	E334Q	hAChE	A, B AS	Triad member. No detectable activity.	Shafferman *et al.*, 1992[6]; Shafferman *et al.*, 1992a
E327	E334A	hAChE	A, B AS	Triad member. No detectable activity.	Shafferman *et al.*, 1992[6]; Shafferman *et al.*, 1992a
E327	E334D	hAChE	A, B AS	Triad member. No detectable activity.	Shafferman *et al.*, 1992[6]; Shafferman *et al.*, 1992a
F330	Y337F	hAChE	A (±), B AS	Element of hydrophobic subsite. Minimal contribution to phosphorylation and dealkylation of OP-enzyme conjugate. Signal received from Y341 induces conformational changes (observed rotation of aryl moiety into gorge cavity upon edrophonium/tacrine binding), interfering/ preventing formation of ACh-enzyme complex causes substrate inhibition. Substrate inhibition not affected by mutation. IC_{50} for PAS- and AS-specific ligands increased up to 15-fold.	Shafferman *et al.*, 1992b; Barak *et al.*, 1994; Ordentlich *et al.*, 1993a
F330	Y337A	hAChE	A (±), B AS	No substrate inhibition due to substitution with small residue. K_i to edrophonium increased 8- to 30-fold. K_i to BW284C51 increased 50-fold. K_i to decamethonium decreased 7-fold.	Ordentlich *et al.*, 1993a,b; Shafferman *et al.*, 1992[6]; Shafferman *et al.*, 1992b; Barak *et al.*, 1994
F330	Y337A	mAChE	A (±), B AS	K_i for substituted phenothiazines is up to 1800-fold higher in AChE than BuChE. This difference is due primarily to Y337A substitution. Affinity for tacrine increased 7-fold, but decreased 19-fold for edrophonium, suggesting a role for this residue in stabilizing the latter, but not the former ligand.	HEK293, Radic *et al.*, 1993

(*continued*)

Table 2. (*Continued*)

Torpedo AChE residue	Mutation	Organism enzyme[2]	Conserved residue[3] and three-dimensional location[4]	Comments	Expression system[5] and reference
F330	Y337F	mAChE	A (±), B AS	Little influence on K_i for substituted phenothiazines. Affinity for tacrine decreased 3-fold.	HEK293, Radic *et al.*, 1993
F331	F338A	hAChE	A, B Near AS	Element of the hydrophobic subsite. Contributes to AS plasticity. K_i to decamethonium increased 3-fold.	Ordentlich *et al.*, 1993a; Shafferman *et al.*, 1992[6]; Shafferman *et al.*, 1992b; Barak *et al.*, 1994
F331	F338G	mAChE	A, B Near AS	Little influence on K_i for substituted phenothiazines.	HEK293, Radic *et al.*, 1993
F331	F329Q	hBuChE	A, B Near AS	See above. K_m unchanged. Changes in interaction with OPs depending on nature of both OP and residue substituted. IC_{50} to iso-OMPA decreased 10-fold.	XO, Gnatt *et al.*, 1994; Schwarz *et al.*, 1994; Soreq *et al.*, 1992
F331	F329L	hBuChE	A, B Near AS	IC_{50} to iso-OMPA and echothiophate increased 10-fold and 14-fold, respectively.	XO, Gnatt *et al.*, 1994; Schwarz *et al.*, 1994; Soreq *et al.*, 1992
F331	F329C	hBuChE	A, B Near AS	See F329L. Reactivation rate of DIP-BuChE by 2-PAM decreased 10-fold.	XO, Gnatt *et al.*, 1994; Schwarz *et al.*, 1994; Soreq *et al.*, 1992
F331	F329D	hBuChE	A, B Near AS	See F329L. Reactivation rate of DIP-BuChE by 2-PAM decreased 19-fold.	XO, Gnatt *et al.*, 1994; Schwarz *et al.*, 1994; Soreq *et al.*, 1992
Y334	Y341A	hAChE	A, B ASG rim (close to D74)	Relays signal from D74 to Y337. Can form hydrogen bond with D74. Effect on the stability of the enzyme complex with BW284C51 and decamethonium. K_i for PAS- and AS-specific inhibitors increased up to 34-fold. Substrate inhibition affected.	HEK293, Shafferman *et al.*, 1992b; Barak *et al.*, 1994
D342	D349N	hAChE	A, B Surface	No effect on catalysis, but secretion reduced.	Shafferman *et al.*, 1992[6]; Shafferman *et al.*, 1992a
D397	D404N	hAChE	A, B Salt bridge	Forms hydrogen bond with Y382 and salt bridge with R525. Crucial stabilizing role bringing together C409 and C382 (S-S loop). No detectable activity and no secretion.	Shafferman *et al.*, 1992[6]; Shafferman *et al.*, 1992a
H425	H425Q	tAChE	A, B Near AS	50% activity of WT enzyme. Mutation proved this residue is not a triad member.	COS 1, Gibney *et al.*, 1990
H425	H432A	hAChE	A, B Near AS	Secretion reduced.	HEK293, Shafferman *et al.*, 1992[6]; Shafferman *et al.*, 1992a
I439	M437D	hBuChE	A (±), B Near AS	No detectable activity suggests structural role.	XO, Gnatt *et al.*, 19929, 1994; Soreq *et al.*, 1992

(*continued*)

Table 2. (*Continued*)

Torpedo AChE residue	Mutation	Organism enzyme[2]	Conserved residue[3] and three-dimensional location[4]	Comments	Expression system[5] and reference
H440	H440Q	tAChE	A, B AS	Triad member. No detectable activity.	COS 1, Gibney *et al.*, 1990
H440	H425Q H440Q	tAChE	A, B AS	No detectable activity.	COS 1, Gibney *et al.*, 1990
H440	H447A	hAChE	A, B AS	No detectable activity.	HEK293, Shafferman *et al.*, 1992[6]; Shafferman *et al.*, 1992a
Y442	Y440D	hBuChE	A, B except dChE	Normal activity. Moderately decreased OP-binding.	XO, Neville *et al.*, 1992; Gnatt *et al.*, 1992[9], 1994; Soreq *et al.*, 1992
E443	E450A	hAChE	A, B Near AS	Hydrogen bonded with E202. Effect of mutation interactions with DFP, soman and substrates are similar to those of E202Q, due to hydrogen bond between these residues. Inactivation rate constant for DFP decreased 100-fold. Mutant protein shows marked resistance to aging.	HEK293, Ordentlich *et al.*, 1993b
E443 E445	E441G E443Q	hBuChE	A, B Near AS	3% catalytic activity of WT enzyme. Defective substrate H_2O binding.	XO, Neville *et al.*, 1992; Soreq *et al.*, 1992
V453	N531D	dChE	A (±), B (±)	Glycosylation site on 55 kDa subunit.	Fournier *et al.*, 1992[7]; Mutero and Fournier, 1992
L495	N569S	dChE	A, B	Glycosylation site on 55 kDa subunit.	Mutero and Fournier, 1992
I537	C615R	dChE	a, b	Not involved in intrachain S-S bonds. Involved in intersubunit S-S bond. Smaller protein migrating as a monomer (75 kDa).	Fournier *et al.*, 1992[7]; Mutero and Fournier, 1992
C572	C580A	hAChE	A, B	Causes secretion as monomer, suggesting that subunit assembly is not coupled to transport. No change in catalytic properties.	HEK293, Velan *et al.*, 1991
C572	C580S	hAChE	A, B	20- to 40-fold increase in specific activity, but no change in catalytic properties. Mutation facilitates correct folding.	*E. coli.*, Fischer *et al.*, 1993
Chimeras and deletions					
mBuCHE 5–174 in mAChE.				Increased binding to ethropropazine and AChE-like binding to iso-OMPA suggests that domains 175–487 dictate selectivity to these agents is accounted for within 5–174, as seen from major increase in K_i to BW284C51 and similar value of stabilization energy of BW284C51 complexed with the chimera and the double mutant Y72N, Y124Q, suggests that residues 5–174 and primarily Y72 and Y124, account for BW284C51 selectivity.	HEK293, Vellom *et al.*, 1993

(*continued*)

Table 2. (*Continued*)

Torpedo AChE residue	Mutation	Organism enzyme[2]	Conserved residue[3] and three-dimensional location[4]	Comments	Expression system[5] and reference
mBuCHE 5–174 and 488–575 in mAChE.				See mouse chimera above.	HEK293, Vellom *et al.*, 1993
hAChE 62–138 in hBuChE. Rim of ASG, conserved CBS and oxyanion hole.				K_m (BTCh) and inhibition by succinylcholine and physotigmine similar to WT BuChE. Sensitivity to iso-OMPA and echothiophate is AChE-like. Pattern of interaction with bambuterol, dibucaine and BW284C51 is intermediate of AChE and BuChE. Loss of substrate activation. No substrate inhibition.	XO, Loewenstein *et al.*, 1993a
Deletion of residues 148–166 in dChE. Cleavage site.				Partial effect on cleavage of protein into two subunits.	Fournier *et al.*, 1992[7]
Deletion of residues 167–180 in dChE. Cleavage site.				Partial effect on cleavage of protein into two subunits.	Fournier *et al.*, 1992[7]
Deletion of residues 148–180 in dChE. Cleavage site.				Prevents cleavage.	Fournier *et al.*, 1992[7]

[1] As is conventional (Massoulie *et al.*, 1993), the sequence number of each mutated residue is referred to as the homologous residue in *Torpedo* AChE.

[2] The prefixes d, h, m and t refer to *Drosophila*, human, mouse and *Torpedo*, respectively, for the corresponding AChE and BuChE proteins.

[3] A, B, conserved residue in AChE and BuChE, respectively; a, b, non-conserved residue; A (±), B (±), conserved residue in ChEs of some, but not all, species reported.

[4] Three-dimensional location is classified into active site (AS), active site gorge (ASG), acyl binding site (ABS), choline binding site (CBS), peripheral anionic site (PAS) and protein surface, specific helices in the hydrolase structure (following Cygler *et al.*, 1993), glycosylation sites and salt bridge associations.

[5] HEK293, human embryonic kidney cell line 293; COS1, monkey kidney cell line; XO, *Xenopus* oocytes; *E. coli.*, bacterial expression.

[6] Shafferman, A., Velan, B., Ordentlich, A., Kronman, C., Grosfeld, H., Leitner, M., Flashner, Y., Cohen, S., Barak, D. and Ariel, N. (1992c) Acetylcholinesterase catalysis—protein engineering studies. In: Multidisciplinary Approaches to Cholinesterase Functions, Proceedings of the Thirty-Sixth Oholo Conference on Multidisciplinary Approaches to Cholinesterase Functions, Eilat, Israel, 6–10 April 1992, pp. 165–1754, Shafferman, A. and Velan, B. (eds) Plenum Press, New York.

[7] Fournier, D., Mutero, A., Pralavorio, M. and Bride, J. M. (1992) Drosophila acetylcholinesterase: analysis of structure and sensitivity to insecticides by in vitro mutagenesis and expression. In: Multidisciplinary Approaches to Cholinesterase Functions, Proceedings of the Thirty-Sixth Oholo Conference on Multidisciplinary Approaches to Cholinesterase Functions, Eilat, Israel, 6–10 April 1992, pp. 75–81, Shafferman, A. and Velan, B. (eds.) Plenum Press, New York.

[8] Bucht, G., Artursson, E., Haggstrom, B., Osterman, A. and Hjalmarsson, K. (1992) Structurally important residues in the region ser91 to asn98 of Torpedo acetylcholinesterase. In: Multidisciplinary Approaches to Cholinesterase Functions, Proceedings of the Thirty-Sixth Oholo Conference on Multidisciplinary Approaches to Cholinesterase Functions, Eilat, Israel, 6–10 April 1992, pp. 185–188, Shafferman, A. and Velan, B. (eds.) Plenum Press, New York.

[9] Gnatt, A., Loewenstein, Y. and Soreq, H. (1992) Molecular dissection of functional domains in human cholinesterases expressed in microinjected Xenopus oocytes. In: Multidisciplinary Approaches to Cholinesterase Functions, Proceedings of the Thirty-Sixth Oholo Conference on Multidisciplinary Approaches to Cholinesterase Functions, Eilat, Israel, 6–10 April 1992, pp. 157–164, Shafferman, A. and Velan, B. (eds.) Plenum Press, New York.

dibromide (BW 284C51). It was concluded that the replacement residues interact with inhibitors, but not substrates. A similar chimera, but of the mouse ChEs, was a substitution of the amino-terminal 174 residues of AChE, which probably constitute the lip of the ASG, with the cognate residues of BuChE. This chimera showed considerably less inhibition by BW 284C51 than the parent AChE (Vellom *et al.*, 1993). Additional support for the role of this region in inhibitor interactions comes from kinetic studies of diisopropylfluorophosphonate (DFP) inhibition of human ChEs. BuChE was inhibited at a 160-fold faster rate than AChE, and the human BuChE/AChE chimera, which differs from BuChE by only 15 non-conserved residues, was inhibited at a rate similar to that of AChE (Schwarz *et al.*, 1994). In contrast, substitutions at the acyl-binding pocket resulted in a 2- to 5-fold reduction in rate. Also, changes at the carboxyl terminus of AChE had no effect on the inactivation rate, reemphasizing the importance of inhibitor interactions at the same region as was exchanged in the human ChE chimera.

Figure 2 presents the diverse mutations introduced into ChEs from various species. At the active center of *Torpedo* AChE, site-directed mutagenesis was employed to identify S200, H440 and E327

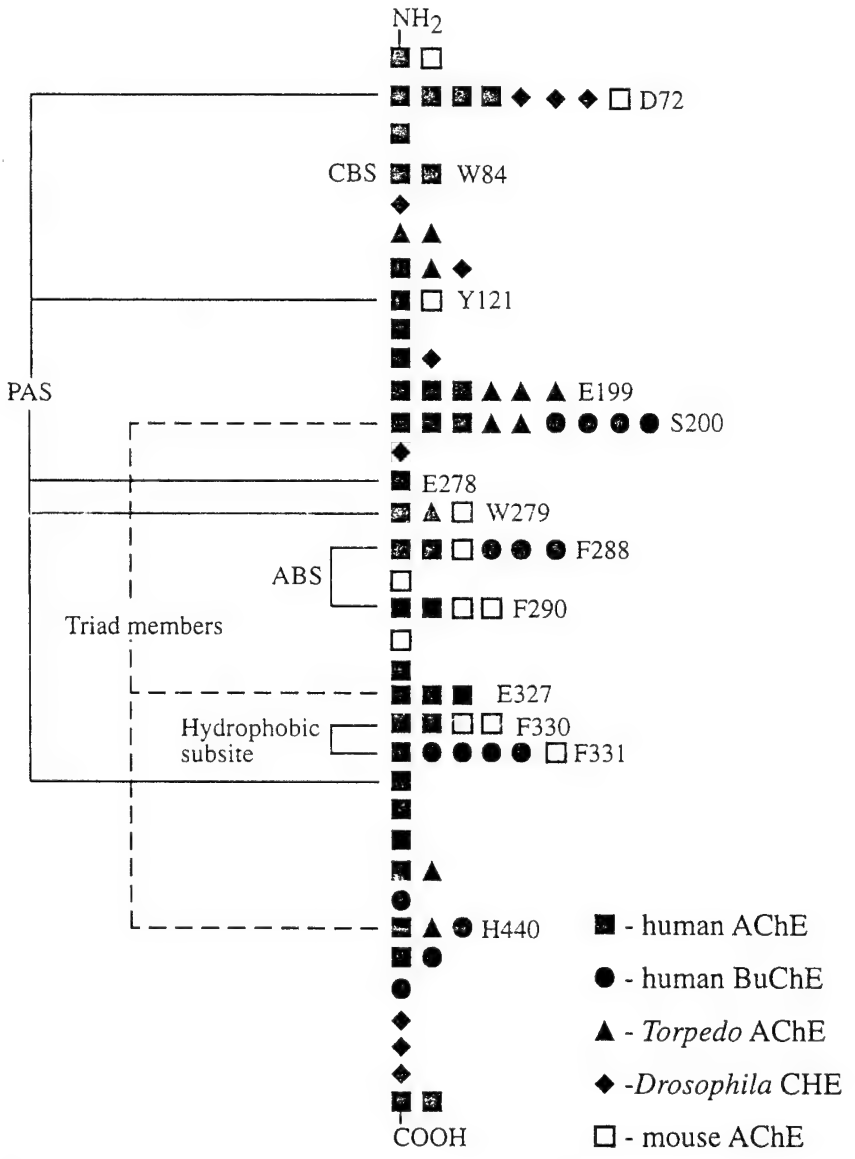

Fig. 2. Site-directed amino acid residue substitutions in ChEs from various species. Schematic view of site-directed mutations introduced into ChEs from different species (human, *Torpedo*, *Drosophila* and mouse) is shown in a linear scale marked by symbols specific to each enzyme and species. Important residues are noted by numbers and their association with the catalytic triad, hydrophobic subsite, peripheral anionic site (PAS), choline binding site (CBS) and acyl binding site (ABS) is outlined. Note that the *Drosophila* N174S and N331D mutations have no counterpart in the vertebrate enzymes and, therefore, do not appear in the figure.

as the catalytic triad. This is the first serine hydrolase found with glutamate as opposed to aspartate in its charge relay system (Sussman *et al.*, 1991; Gibney *et al.*, 1990; Shafferman *et al.*, 1992a). Subsequently, other members of the lipase/esterase family were found to display similar S-H-E triads. Substitution of active-site human W86 (W84) with alanine caused a 660-fold decrease in the affinity for ATCh, but had no effect on the affinity for an uncharged isosteric substrate, 3,3-dimethylbutyl thioacetate. Diminished inhibition by PAS-specific agents was also observed. This identified W86 (W84) as the classical "anionic" subsite of the active center that binds the cationic quaternary ammonium group of choline and active site inhibitors such as edrophonium (Ordentlich *et al.*, 1993a). In fact, the "anionic" site is a tryptophan residue, the π electrons of which interact with the quaternary ammonium group (Harel *et al.*, 1993). It also reinforces the suggested involvement of this residue in communicating to the active center the effect of occupancy of the PAS by a ligand (Shafferman *et al.*, 1992b). At the active site of BuChE, alterations at F329 (F331), L286 (F288) and Y440 (Y442) had marked effects on inhibitor interactions. In the case of F329 (F331) and Y440 (Y442), this was achieved without significantly changing K_m, demonstrating distinct requirements for inhibition and substrate interactions at the acyl- and choline-binding pocket (Gnatt *et al.*, 1994).

Mutation of G199 in *Torpedo* (Gibney *et al.*, 1990) or F297 (F290) in mouse AChE (Vellom *et al.*, 1993) eliminates substrate inhibition, suggesting, again, that the mutations interrupt intramolecular information transfer between the surface and the interior of the protein.

3. THE HUMAN CHOLINESTERASE GENES

3.1. Structure of the Gene

In humans, the two functionally distinct ChEs, AChE and BuChE, which share a high degree of amino acid sequence identity (>50%), are encoded by two separate genes, *ACHE* and *BCHE*, respectively (Soreq *et al.*, 1990; Fig. 3). The two genes have similar exon-intron organization (see below), but radically different nucleotide composition, *ACHE* being G,C-rich, while *BCHE* is A,T-rich. The electric eel, *Torpedo marmorata*, has both an *ACHE* and a *BCHE* gene (Toutant *et al.*, 1985), but in insects, a single gene encodes one ChE protein with mixed AChE and BuChE properties (Hall and Malcolm, 1991; Taylor and Radic, 1994). Gene duplication and divergence into separate AChE and BuChE enzymes apparently occurred before the evolution of the first vertebrates (Soreq and Zakut, 1990; Taylor, 1991). The presence of two distinct *CHE* genes in all vertebrates studied to date indicates that both protein products are biologically required in these species and, presumably, that they have distinct roles.

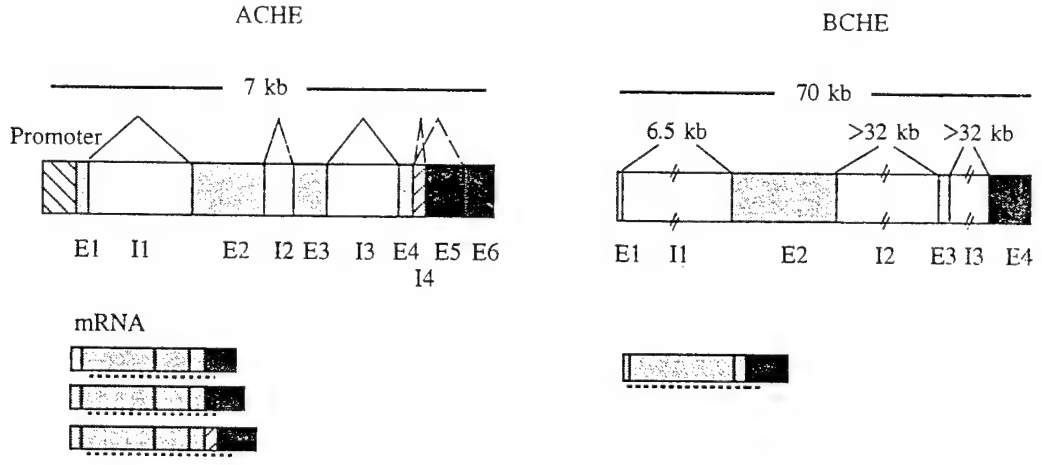

Fig. 3. The human *CHE* genes and their mRNA transcripts and protein products. Schematic drawings of the two human genes encoding ChEs is presented. Exons (E) are shaded, introns (I) are white, the ACHE promoter is cross-hatched and the alternative AChE exon, E5, is black. Open reading frames are marked by dashed underlining, alternative splicing options by triangles over the excised sequences and constant splicing sites by solid triangles over the excised sequences.

The human *ACHE* gene spans about 7 kb and includes 6 characterized exons and 4 introns. Through alternative splicing, it can give rise to several different mRNA transcripts (Sikorav *et al.*, 1988; Maulet *et al.*, 1990) (see Section 3.5). The *BCHE* gene is much larger than *ACHE*, spanning 70 kb, and consists of 4 exons, the first of which is non-translatable, but contains two potential translation initiation sites, and the second of which contains 83% of the coding sequence (Arpagaus *et al.*, 1990; Gnatt *et al.*, 1991). Only one *BCHE* mRNA transcript has been identified to date.

3.2. Chromosomal Location

Mapping of the human *BCHE* gene to its defined chromosomal location, 3q26-ter, was first performed by *in situ* hybridization to lymphocyte chromosomes and by blot hybridization to DNA of hybrid somatic cells (Gnatt *et al.*, 1990). Direct polymerase chain reaction amplification of human *BCHE*-specific DNA fragments from somatic cell hybrids and chromosome sorted libraries later confirmed this mapping of the *BCHE* gene to chromosome 3q26-ter (Gnatt *et al.*, 1991). When using *ACHE* specific primers, a prominent polymerase chain reaction product was observed with DNA from two different cell lines and from one chromosome-sorted library, all containing DNA from human chromosome 7. The use of fluorescent *in situ* hybridization with biotinylated *ACHE* DNA mapped the refined position of the *ACHE* gene to chromosome 7q22 (Ehrlich *et al.*, 1992; Getman *et al.*, 1992). These findings confirmed predictions that the two closely related *CHE* genes are not genetically linked in the human genome (Gnatt *et al.*, 1991). They further revealed that these two apparently unrelated genes are both located at chromosomal sites subject to frequent breakage in leukemias (Ehrlich *et al.*, 1994).

3.3. Control Elements

In humans, AChE is produced in muscle and nerve, in hemopoietic cells (Patinkin *et al.*, 1990; Lev-Lehman *et al.*, 1994; Soreq *et al.*, 1994), embryonic tissues (Zakut *et al.*, 1985, 1990), several tumors (Lapidot-Lifson *et al.*, 1989) and germ cells (Malinger *et al.*, 1989). Since the gene encoding AChE exists as a single copy, the regulatory elements controlling its activity are expected to respond to activating factors specific for these tissues and cell types. Indeed, a 596 bp fragment upstream of the initiation site for transcription contains numerous consensus motifs characteristic of binding sites for various transcription factors (Ben Aziz-Aloya *et al.*, 1993). The observed sequences include several types of nerve-specific motifs: the Egr-1 sequence, characteristic of brain-specific signal transduction pathways, the CBEB motif, which predicts cAMP responsiveness, and the AP2 signal, which is unique to genes expressed in neuronal crest cells. In addition, several MyoD motifs, associated with muscle-specific gene expression and the E-box motif found in the hematopoietically expressed heavy chain immunoglobulin genes are present. The GAGA, Zeste and USF motifs, known as recognition sites for genes induced during embryonic development, were also observed (Ben Aziz-Aloya *et al.*, 1993). Thus, the tightly regulated, yet pleiotropic, expression of *ACHE* in humans, at least in part could stem from the activity of the regulatory elements present in this short sequence. However, the promoter sequence alone cannot explain the intricate pattern of tissue-specific expression shown by the *ACHE* gene, as is evident from the observation that in transgenic mice carrying this promoter sequence and the human AChE coding sequence, AChE production was found to be limited to the CNS (Andres *et al.*, 1994). This suggests that additional control elements, upstream from the sequenced promoter, which were not included in the sequence incorporated into the genome of the transgenic mice, are involved in regulating AChE production.

3.4. Coordination of Expression with Other Cholinergic Factors

Several mechanisms ensure that there is an appropriate balance of the proteins that function at the cholinergic synapse. The ACh transporter is encoded by an intronless sequence embedded in the choline acetyltransferase (ChAT) gene, so expression of the two is coordinated (Erickson *et al.*, 1994). Expression of the ACh receptor (AChR), too, is coordinated with that of AChE (Kristt and Kasper, 1983), in spite of the fact that it is the product of several genes located on different chromosomes. The molecular mechanism of this coordination is unknown, but increasing the amount of AChE

expressed at the synapse by injection of *ACHE* DNA into fertilized *Xenopus* eggs causes morphological changes in neuromuscular junctions within the resultant embryos (Seidman *et al.*, 1994). These are particularly conspicuous in electron micrographs of myotomes, where the synapse covers a larger surface area and the cleft is wider, seemingly coordinated with the increased amount of the nicotinic AChR (nAChR) (Shapira *et al.*, 1994).

3.5. Alternative Splicing

Yet another level of control over expression of the *ACHE* gene is that of alternative splicing, a process involving the precise excision of intronic sequences from the precursor nuclear mRNA. All AChE mRNA forms include exons 1–4, and alternative splicing may occur both at their 5′ and 3′ ends. In the major mRNA form, found mainly in brain and muscle, the E4 exon is directly continued with E6, the connecting sequence, including I4 and E5, being spliced out (Fig. 3). Two alternatively spliced forms encode a protein with the potential to be anchored through a glycophosphoinositide (GPI) residue to the cell surface of hematopoietic cells; these two alternative transcripts are also expressed in several different tumor cell lines (Karpel *et al.*, 1994a). In one of these mRNA forms, the transcript continues through I4, E5 and E6; in the other, I4 is spliced out. An open reading frame continues through E4 and a small part of E6, or through E4 and part of E5, which encodes a 29 residue hydrophobic polypeptide sequence, typical of sequences that can be enzymatically exchanged for a GPI membrane anchor (Turner, 1994). The third form includes an open reading frame through E4 and part of I4, with no possibility for GPI anchoring. Therefore, at least three forms of human AChE mRNA are predicted, differing in the 3′-ends of their coding sequences. The major brain and muscle form contains E6, whereas those encoding the two alternative proteins include the open reading frames of I4 or E5 (Karpel *et al.*, 1994a). The alternative splicing patterns at the 5′-end of human *ACHE* mRNA have not yet been fully characterized; however, it is clear that they do not change the coding sequence.

3.6. Polymorphism of Molecular Forms

For AChE, several post-translational modifications, including palmitoylation (Roberts *et al.*, 1988a), oligomeric assembly, association with noncatalytic subunits (Roberts *et al.*, 1988b), glycosylation and the attachment of phospholipids, have been discovered, some of which affect the quaternary structure of the enzyme or direct it to its correct subcellular localization (Massoulie *et al.*, 1993).

The ChEs are largely extracellular, being either soluble or attached to the external surfaces of cells. Monomers of the AChE molecule may associate to form dimers and higher levels of organization through inter-monomer disulfide bonds and disulfide bonds to a non-catalytic polymer. These forms are referred to as G1 (globular, monomeric), G2 (disulfide-linked dimers of G1) and G4 (noncovalently associated dimers of G2). G4s may be linked in mammalian brain to a 20 kDa polymer of undefined nature (Inestrosa *et al.*, 1987; Fuentes *et al.*, 1988) or to a GPI that is anchored in the plasma membrane of cells, notably erythrocytes and cells of the *Torpedo* electric organ (Futerman *et al.**; Futerman *et al.*, 1985; Silman and Futerman, 1987; Taylor, 1991). However, in rat brain, a hydrophobic region of AChE has been identified through which the enzyme can bind directly to membranes, and no 20 kDa protein associated with AChE was observed in this study (Andres *et al.*, 1990, 1992). One to three G4s may be linked to ends of the three strands of a collagen-like protein, achieving yet higher levels of assembly (Hall, 1973). There is good evidence that the forms associated with the collagen-like tail are bound to heparan sulfate proteoglycans of the basal lamina of neuromuscular junctions and muscle endplates (McMahan *et al.*, 1978). The carbohydrate composition of membrane-bound forms of AChE from brain and erythrocytes varies, as seen by interactions with lectins, suggesting an additional level of complexity of ChE polymorphism (Meflah *et al.*, 1984). AChE also appears in a soluble form in serum, and hybrids of AChE and BuChE have also been reported (Tsim *et al.*, 1988).

*Futerman, A. H., Barton, P. L., Fiorini, R. M., Low, M. G., Sherman, W. R. and Silman, I. (1985) The involvement of phosphatidylinositol in the anchoring of hydrophobic forms of acetylcholinesterase to the plasma membrane. In: Molecular Basis of Nerve Activity, Proceedings of the International Symposium in Memory of David Nachmansohn (1899–1983), Berlin, (West) Germany, 11–13 October 1984, pp. 635–650. Changeux, J.-P., Hucho, F., Maelicke, A. and Neumann, E. (eds.) Walter de Gruyter, Berlin.

BuChE appears in many of the same forms (G1, G2, G4) as AChE. G1 is also disulfide-linked lbumin and another unidentified protein.* Further experimental work will be required to clarify molecular basis of the differences between salt-soluble (hydrophilic) and detergent-soluble drophobic) forms of ChEs, the nature of the 20 kDa mammalian polymer and its collagen-like unterpart in neuromuscular junctions and the cellular site at which these assemblies are made lassoulie *et al.*, 1993). Further information is likely to come from investigations into the heritable lure to link G4 AChE with its collagen-like tail and the consequent absence of AChE activity motor endplates (see Section 8).

That the oligomeric assembly of BuChE is regulated by tissue specifically expressed proteins s suggested by several lines of evidence. When microinjected alone into *Xenopus* oocytes, *in vitro* nscribed BuChE mRNA induced the formation primarily of dimeric BuChE. However, tissue-racted mRNA induced higher levels of subunit assembly, as seen when synthetic BuChE mRNA s complemented with muscle poly(A)$^+$ RNA. This resulted in a quantitative distribution of BuChE ong several forms that resembled the distribution of muscle AChE (Dreyfus *et al.*, 1989; Soreq *al.*, 1989). More recently, it was shown that human AChE cannot assemble into multimeric forms transiently transgenic *Xenopus* embryos (Seidman *et al.*, 1994), although it assembles correctly en expressed in brain neurons of a stably transgenic mouse pedigree (Andres *et al.*, 1994). These dings suggest that the yet unidentified factors required for AChE assembly direct aggregation in tissue- or species-specific manner.

Evidence for the importance of glycosylation for the intracellular transport of ChEs, but not for eir catalytic activity, comes from experiments in which glycosylation of human BuChE was inhibited tunicamycin (Dreyfus *et al.*, 1989; Soreq *et al.*, 1989) and in which the glycosylation sites of man AChE at N265, N350 and N464 were mutated (Velan *et al.*, 1993). Similarly, active non-ycosylated recombinant AChE can be produced in bacteria (Fischer *et al.*, 1993).

4. INHIBITION OF CHOLINESTERASES: MECHANISM AND CONSEQUENCES

Inhibition of ChE can be achieved by several different mechanisms. Simple competitive inhibition caused by such quaternary compounds as edrophonium, which binds selectively to the active site here it is stabilized by interaction of its quaternary nitrogen with the choline-binding pocket and hydrogen bonding (Sussman *et al.*, 1992†; Harel *et al.*, 1993). In contrast to edrophonium, carbamyl ers serve as hemi-substrates. During catalysis, a carbamoyl enzyme intermediate is formed, which far more stable than the acetyl-ChE intermediate. The very slow hydrolysis of the intermediate fectively sequesters ChE for several hours. Neostigmine (Fig. 4), one of many physostigmine rivatives, has increased stability and potency equal to or greater than physostigmine. Demecarium, o neostigmine molecules linked by a 10-carbon chain, has even greater affinity, since it interacts t only with the active site, but also with the PAS at the entrance of the ASG. As an ACh analog, ostigmine can also block nAChRs (Shaw *et al.*, 1985; Coleman *et al.*, 1987). In fact, quaternary monium anti-ChE compounds have additional direct actions at cholinergic sites, either as agonists antagonists. For example, neostigmine affects the spinal cord and the neuromuscular junction, th by inhibition of AChE activity and by stimulation of cholinergic receptors.

ACh is released from motor neurons in fairly well-defined quanta of about 10,000 molecules in onse to closely timed, discrete nerve impulses. Once released, ACh causes a localized depolarization e muscle fiber membrane, initiating an action potential that is propagated along its length. Normally,

*Masson, P. (1991) Molecular heterogeneity of human plasma cholinesterase. In: Cholinesterases, Structure, nction, Mechanism, Genetics, and Cell Biology, Proceedings of the Third International Meeting on olinesterases, La Grande Motte, France, 12–16 May 1990, pp. 42–46. Massoulie, J., Bacou, F., Barnard, , Chatonnet, A., Doctor, B. P. and Quinn, D. M. (eds) American Chemical Society, Washington.

†Sussman, J. L., Harel, M. and Silman, I. (1992) Three dimensional structure of acetylcholinesterase. In: ltidisciplinary Approaches to Cholinesterase Functions, Proceedings of the Thirty-Sixth Oholo Conference Multidisciplinary Approaches to Cholinesterase Functions, Eilat, Israel, 6–10 April 1992, pp. 95–108, fferman, A. and Velan, B. (eds.) Plenum Press, New York.

6.2. Parkinson's Disease

Parkinson's disease (PD) is a common type of adult-onset, chronic degenerative disorder of the CNS. Since PD is associated mainly with the dopaminergic, and not with the cholinergic system, few characterizations of AChE in PD have been performed. However, AChE activity has been observed in dopaminergic brain areas, and decreased AChE activity and molecular form changes that parallel those found in AD have been observed in up to 30% of PD. Therefore, cholinergic signaling may be connected with neurodegenerative processes in general or more specifically, with the pathophysiology of PD (Ruberg *et al.*, 1986). PD patients are usually treated with tricyclic antidepressants. The anti-ChE side effect of these drugs may be the basis of some of the benefit shown by this treatment of PD patients. Similarly, there is evidence of worsening of the symptoms in a PD patient receiving the anti-ChE, THA (Ott and Lannon, 1992).

6.3. Huntington's Disease

Huntington's disease is a dominant inherited autosomal neurodegenerative disorder with symptoms usually evident at the age of 30–40, and is associated with genetically programmed cell death in the CNS. The disease, progressing over a 10–20 year period, eventually destroys all motor function. In most cases of Huntington's disease, progressive dementia is a feature when cholinergic neurons of the brain stem are affected. AChE activity is diminished only in selective bundles of the affected area, known for their rich AChE activity, and ChAT activity is decreased in these same areas.

6.4. Amyotrophic Lateral Sclerosis

Amyotrophic lateral sclerosis, or motor neuron disease, is characterized by motor neuron degeneration and progressive failure of neuromuscular transmission. Both upper and lower motor neurons are affected. In neuromuscular endplates significant decreases of all forms of AChE are observed. The defect is thought to be related to disassembly of the synapses and neuromuscular endplates due to an excitotoxin, a failure of a trophic factor or a failure to detoxify a xenobiotic, the consequent decrease in nerve signaling, causing a defect in AChE excretion (Goonetilleke *et al.*, 1994). The connection between the recent finding that a mutant human superoxide dismutase introduced into test animals can cause the symptoms of amyotrophic lateral sclerosis (Gurney, *et al.*, 1994) and the observed neural defects has yet to be found.

6.5. Myasthenia Gravis

Myostigmine, a synthetic physostigmine derivative, is commonly used to treat patients with myasthenia gravis, a neuromuscular disease of an autoimmune nature, characterized by muscle weakness due to autoimmune anti-nAChR antibodies. Edrophonium induces an immediate, but brief, relief of the characteristic symptoms, due to reversible binding to the active site, terminated by rapid excretion of the drug by the kidneys.

There has been noted a considerable individual variation in the dosages of anti-ChE agents required to control the disorder. This may be due to individual levels of the autoantibodies or may be due to genetic differences in the BuChEs (see Section 8).

6.6. Hematological Diseases

There is ample evidence for perturbations in cholinergic functions being associated with hematological disorders. The increased risk of leukemia following exposure to OP agents has been mentioned in Section 4.1. Down's syndrome, like certain forms of familial AD, linked to chromosome 21 (Percy *et al.*, 1993), is associated with AChE deficiencies, and affected individuals have a high incidence of leukemia. Paroxysmal nocturnal hemoglobinuria, also associated with an elevated risk of leukemia, is characterized by a failure of the post-translational glycosylation of AChE. This prevents transport to and interaction of the enzyme with the erythrocyte membrane (Turner, 1994). Several other

hematological disorders associated with the cholinergic system were described by Soreq and Zakut (1993). Recently, antisense inhibition of *ACHE* gene expression, using phosphorothioate oligodeoxynucleotides, has been shown to induce massive proliferation of myeloid cells in bone marrow cultures, an *ex vivo* mimic of a leukemic syndrome (Soreq *et al.*, 1994). This is a warning that supreme caution must be used in the development and use of anti-ChE drugs or insecticides.

7. NON-CENTRAL NERVOUS SYSTEM EXCITATORY ROLES

Cytochemical staining has been used extensively to search for specific ChE activities in different tissues during development. AChE expression has been visualized by immunocytochemical or activity-dependent histological methods, and more recently by *in situ* hybridization. This revealed an association of AChE with numerous regions of the brain corresponding with the spatial distribution of different components of both cholinergic and non-cholinergic brain regions (Landwehrmeyer *et al.*, 1994). Transient AChE staining was also shown in the medosomal nucleus of the thalamus and its connection in the developing rodent, human and monkey brains (Kostovic and Goldman-Rakic, 1983; Kristt, 1983; Robertson and Yu, 1993). Other distinct neurons in these same areas were positively stained for BuChE, but not AChE or ChAT, activities (Graybiel and Ragsdale, 1982). Thus, several lines of evidence suggest a non-cholinergic role of ChEs, possibly related to morphogenesis.

In the peripheral nervous system, cholinergic signaling has been implicated in pancreatic function, as shown by the decreased AChE activity in the intrapancreatic ganglia of rats subjected to celiac and superior mesenteric ganglionectomy (Anglade, 1987). In fact, it was the investigation of the turnover of pancreatic phospholipids accompanying cholinergic stimulation of amylase secretion (Hokin and Hokin, 1953), which led eventually to the discovery of the phosphatidylinositol-derived second messengers of neurotransmitter/hormone action.

ChEs can be found in a wide range of tissues and cell types of clinical significance other than muscles and neurons, such as erythrocytes (Silver, 1974), erythroleukemia cell lines (Ajmar *et al.*, 1983; Bianchi Searra *et al.*, 1986; Karpel *et al.*, 1994a), adrenal medulla (Massoulie and Bon, 1982), ovarian follicles (Karnovsky and Roots, 1964), megakaryocytes (Burstein *et al.*, 1980; Patinkin *et al.*, 1990, 1994) and chorionic villi (Zakut *et al.*, 1991). In addition, ChE activity has been reported in a number of embryonic tissues derived from ectoderm, mesoderm and endoderm, as well as in various neoplastic tissues, such as ovarian carcinomas (Drews, 1975; Zakut *et al.*, 1990) and brain tumors (Ord and Thompson, 1952; Razon *et al.*, 1984). Interestingly, human oocytes were shown to express BuChE mRNA in a developmentally regulated fashion (Soreq *et al.*, 1987), although the enzyme activity that was evident in ovary homogenates was almost entirely AChE (Malinger *et al.*, 1989). Cholinergic signaling has also been implicated in chorionic villi, which express the *BCHE* gene (Zakut *et al.*, 1991) and in sperm motility, as suggested by the presence of ACh, AChE and ChAT (Bishop *et al.*, 1975, 1976), as well as BuChE in the mammalian sperm. Transgenic mice carrying the human *BCHE* gene displayed testicular amplification of this transgene and reduced fertility (Beeri *et al.*, 1994). Further, 1 μM of the ChAT inhibitor, 2-benzoyl methyl trimethyl ammonium, depressed sperm motility by 95% (Rama Sastry *et al.*, 1981), while ACh may either augment or impede sperm mobility (Sanyal and Khanna, 1971; Beeri *et al.*, 1994).

In most cases, reports of peptidase activity accompanying purified AChE or BuChE have been shown to be due to co-purification with other proteins. However, Balasubramanian and Bhanumathy (1993) reported evidence of an intrinsic peptidase activity. This activity co-precipitates with a monoclonal antibody directed against BuChE. They point out that the tetrapeptide sequence, HXXE, separated by over 100 residues from another histidine residue in Zn metallopeptidases, appears in human ChEs as $HGYE(X)_{107}H$ (BuChE residues 438–548 and AChE residues 440–550).

The effect of AChE, or the lack of the protein, in the hematopoietic system is difficult to reconcile with our understanding of AChE as the terminator of ACh action, as is the presence of AChE in the erythrocyte membrane. The sequence homology of AChE with the *Drosophila* adhesion proteins glutactin and neurotactin had also been noted (De La Escalera *et al.*, 1990; Cygler *et al.*, 1993). This homology had been attributed to the evolutionary diversion of a protein featuring the α/β-hydrolase into contemporary serine α/β-hydrolases and other proteins without catalytic function, such as

neurotactin and thyroglobulin (Taylor and Radic, 1994). A recent report (Layer *et al.*, 1993) on the G4 form of AChE in chick embryo tectal cell cultures, however, finds a direct quantitative relationship between inhibition of neurite growth and amount of an added anti-G4 antibody. This effect on neurite growth was not affected by at least one anti-ChE agent, echothiophate. Parallel morphological studies on retinal explants indicated that BW 284C51, which inhibits both AChE catalysis and neurite growth, visibly disrupted cell adhesion (Layer *et al.*, 1993). We note, also, that like AChE, notably the erythrocyte membrane form, other GPI-anchored proteins have been proposed to have roles in cell–cell signalling (Turner, 1994). Also, there has been a recent report of glioma cells in culture that when microinjected or transfected with DNA constructs expressing human AChE, showed dramatic morphological changes and rapid process extension (Karpel *et al.*, 1994b). These reports not only open a new arena of ChE studies, but breach the barrier to consideration of other non-enzymatic roles of ChEs, for instance in hematopoiesis, and in time may lead us to an understanding of the roles of several alternatively spliced forms of AChE.

A recent study supports the idea of a developmental role for AChE. The destiny of hematopoietic stem cells was altered by the addition of antisense phosphorothioate oligonucleotides in a manner that indicated that AChE normally diverts stem cells to apoptosis (Soreq *et al.*, 1994). The blockage of this effect, by OP agents, for instance, may be the basis of the uncontrolled proliferation of the stem cells seen in leukemia (Brown *et al.*, 1990). A developmental role has also been suggested for BuChE and AChE in *ex vivo* developing chick motor axons based on the use of selective inhibitors (Layer, 1991; Layer *et al.*, 1988a,b, 1993). Thus, there is accumulative evidence for a developmental role for ChEs that is not obviously related to their catalytic activity. Further experiments will be needed to determine whether this function is related to the presumed cell adhesion properties of these enzymes.

8. HUMAN CHOLINESTERASE VARIANTS PREDICT A GENETIC PREDISPOSITION TO DIFFERENTIAL RESPONSES TO CHOLINERGIC DRUGS

Over several decades, large-scale population surveys of BuChE phenotypes were carried out. Tens of thousands of individuals have been screened from different continents and ethnic origins (Whittaker, 1986). Since the *BCHE* gene was cloned in 1986, more than 20 different naturally occurring mutations have been documented (Table 1), with the great majority of the variant phenotype individuals carrying the D70G substitution. These mutated proteins result in a variety of phenotypes, including the complete absence of any BuChE protein due to a premature termination of protein synthesis (the "silent" mutations of Table 1). In at least one area of the brain, BuChE has been demonstrated in cells other than those that have AChE, suggesting a unique function (Graybiel *et al.*, 1981; Graybiel and Ragsdale, 1982). It would be interesting to know if the distribution of AChE among brain cells is different in individuals with silent BuChE. The mere existence of a "silent" phenotype, where individuals do well in spite of having no BuChE activity, has been used to argue that BuChE has no important function. However, natural selection operates on the level of species, not individuals. What may be tolerated in an isolated individual, over time and numbers, may be disadvantageous to a community. Also, since "knock-out" experiments have sometimes found no phenotypes for damaged genes, it would be reckless to conclude, therefore, that all such genes have no important biological role. With the exception of two polymorphisms at the 5′ and 3′ non-translated sequence, no mutation in *BCHE* cDNA has been found yet that will not lead to alteration in the protein sequence. Together, the catalytically silent mutations comprise 0.001% of homozygotes, which is far less than the catalytically active variants (Whittaker, 1986). Even in the absence of a well-understood physiological role for BuChE, this in itself suggests a selection advantage for carriers of various genes coding for active proteins, as compared with "silent" gene carriers.

Interestingly, the largest and main coding exon, E2, has 15 of the known mutations found on the *BCHE* gene. Thus, the average incidence of mutability in the coding domain (approximately 1:100 nucleotides) is exceedingly high. In most cases, the different *BCHE* variants were identified by the analysis of sequences originating from individuals expressing a variant phenotype and not by a random screening of the population. Several of the variants (e.g., D70G) were discovered in two continents simultaneously, while many others were detected only once, as "orphan" alleles.

One major physiological role of BuChE is thought to be as a scavenger of anti-ChE agents, thus protecting from inactivation the AChE of neuromuscular junctions and other cholinergic sites (Neville *et al.*, 1990a,b). This is deduced from the fact that BuChE interacts with a wider range of anti-ChE agents (Soreq *et al.*, 1992), and in certain cases (e.g., DFP and many carbamates), the rate of inactivation is considerably faster than that of AChE (Loewenstein *et al.*, 1994; Schwarz *et al.*, 1994). Accordingly, there must be an evolutionary pressure that accounts for the need for a scavenger of anti-ChE agents. There are many natural ChE inhibitors in the environment, including glycoalkaloids present in solanaceous plants (Gnatt *et al.*, 1994), fungal antibiotics like puromycin (Hersh, 1981) and its analogs, cocaine derivatives (Gatley, 1991), poisons from several species such as oysters (Abramson *et al.*, 1989), OPs from cyanobacteria (Carmichael, 1994) and polypeptides from snakes (fasciculin; Karlsson *et al.*, 1985), metals (aluminum, scandium and yttrium; Marquis and Lerrick, 1982) and the carbamate of calabar beans, physostigmine (Taylor, 1990b). Some of these ChE inhibitors are extremely poisonous. Several snake venoms contain peptides of 51–59 amino acid residues (e.g., fasciculin) that bind to AChE with K_d values as low as 10^{-10} M (Cervenansky *et al.*, 1990; Marchot *et al.*, 1993). However, it is significant, perhaps, that it is only the glycoalkaloids of the solanaceous food plants (tomato, potato, eggplant) that are inhibitors of both AChE and BuChE. Also, the uneven natural geographic distribution of these food plants must be seen alongside the large series of naturally occurring BuChE variants, also unevenly distributed among different populations – the "atypical" BuChE mutation, D70G (heterozygote frequency <5% among Europeans and Americans and up to 11% of other groups; Whittaker, 1986; Ehrlich *et al.*, 1994) – with variable affinities for them. Of all the classes of natural inhibitors of the ChEs, it seems that BuChE may be imagined to have adapted as a scavenger only for the glycoalkaloids.

The "atypical" mutation also confers resistance to inhibitors of pharmacological interest. It is clinically characterized by the inability of the affected enzyme to hydrolyze succinylcholine and dibucaine, and, compared with the wild-type BuChE, displays a specific activity of 25% of the wild-type enzyme, and at least 10-fold higher IC_{50} and K_i values for bambuterol, physostigmine and echothiophate. The affinity toward ACh is drastically reduced, although the K_m for BTCh is unchanged (Neville *et al.*, 1990a,b). If the mutant BuChE cannot scavenge anti-ChEs and reduce their serum levels, it will not protect synaptic AChE from their effects. The genetic variability of BuChE may well be the basis of the observed variability in the extent and intensity of responses to anti-ChE drugs. In fact, BuChE is reported to hydrolyze heroin (Fig. 4), which has a 4-fold higher K_m for the "atypical" variant than for the usual enzyme (Lockridge *et al.*, 1980). Clearly, this has the potential for explaining variations in responses to this narcotic. As noted in Section 5, BuChE hydrolyzes the methyl ester bond of cocaine and its derivatives. The local anesthetic procaine is hydrolyzed by BuChE, but it has a 15-fold higher K_m with the atypical variant than with the usual enzyme. Carriers of the atypical allele may not react substantially differently from carriers of the usual enzyme when receiving procaine i.m. as it would be exposed only minimally to BuChE. However, aspirin has a nearly 4-fold higher K_m with "atypical" BuChE (Valentino *et al.*, 1981). It acts after entering the blood stream where it is exposed to BuChE. This illustrates a potential for significant variations in response to pharmacological agents, arising from natural variations in this drug-processing enzyme. Just how variant BuChEs may function in detoxifying cocaine and its derivatives is an important issue that simply has not been addressed yet. Furthermore, it was found that the oxime 2-PAM reactivates DFP-inactivated D70G BuChE at a 5-fold lower rate than does wild-type BuChE. Variants having this mutation in tandem with one or two additional natural mutations (Y114H and S425P) display a rate of reactivation as much as 40-fold lower. Thus, the well-established therapy of OP-intoxicated patients with 2-PAM, intended to regenerate active ChE, may well be less efficient in the case of carriers of variant BuChE (Schwarz *et al.*, 1994). Indeed, it has been reported that the response of OP-poisoned patients to 2-PAM therapy varies widely (Willems *et al.*, 1993).

The most frequent variant, "atypical" BuChE, was compared with the common human BuChE and AChE in its inhibition rate with several anti-ChEs of pharmacological interest (Loewenstein *et al.*, 1994). With common BuChE, the carbamates physostigmine, heptyl-physostigmine (Modulanum®) and SDZ ENA 713 had inactivation rates higher than or equal to AChE, but "atypical" BuChE had considerably lower rates. This suggests that BuChE usually reacts with the drugs in preference to AChE. However, heterozygous, and especially homozygous, individuals carrying

the "atypical" gene may well show increased sensitivity to the drugs. Moreover, the reversible inhibitor, THA, had a 300-fold higher IC_{50} value with "atypical" BuChE than with common BuChE. These findings may help explain the variations in response to anti-ChE therapy that have been noted.

In contrast to the multitude of point mutations on the *BCHE* gene, only one single-point mutation has been observed in the *ACHE* gene. Its identity was discovered in several steps. The human *ACHE* gene was first demonstrated to present two codominant alleles at a single genetic locus (Coates and Simpson, 1972). Two decades later, replacement of His322 with asparagine was reported to be a common polymorphism.* The substituted amino-acid residue is positioned at the surface of the AChE protein, apparently modifying one or more immunogenic epitopes in erythrocyte membrane AChE. Thus, this allele was identified as causative of the uncommon Yt^b blood (Bartels *et al.*, 1993) group, for which an incidence of 5% has been determined in the Caucasian population (Lewis *et al.*, 1987) and a considerably higher incidence in Israel (Levene *et al.*, 1987), recently confirmed by molecular genetic means (Ehrlich *et al.*, 1994).

With the two codominant alleles of the *ACHE* gene, a situation exists where homozygotes with either of these alleles will recognize the product of the other allele as a non-self antigen, analogous to the Rh blood group phenomenon. Therefore, Yt^b homozygotes may develop an immunological response to transfused blood from either hetero- or homozygotes of the common Yt^a phenotype. The result is hemolysis of the foreign erythrocytes, a condition that was well recognized before its molecular basis was discovered.

The plethora of mutations in the *BCHE* gene may be taken as further support for the idea that the major role of BuChE is to function as a scavenger, as the selection of proteins with modified properties will confer better resistance to specific cholinergic poisons. It may also be that the role of scavenger can conflict with another role for BuChE, for instance, as a cell membrane element involved in development. In that case, a *decreased* affinity for an inhibitor in the environment may confer a selection advantage (Ehrlich *et al.*, 1994).

The very infrequent mutability of the *ACHE* gene, and the complete absence of any mutant with impaired function, had been taken as evidence that AChE is just too sensitive an enzyme to tolerate any mutation. However, several developments challenge this interpretation. Although there are no known natural mutations that affect the catalytic function of AChE, there are mutations in the enzymatic system that forms the G4 form by addition of a non-catalytic tail to the enzyme (Hutchinson *et al.*, 1993). This results in a deficiency of AChE in motor endplates, with a subsequent loss of motor function. It also raises the question of *why* there are no mutations of AChE that affect its function. If defective processing of the G4 form is compatible with life, even if with diminished motor function, are there no other possible AChE mutations that would preserve catalytic function? In fact, there are laboratory-produced site-directed mutations that have almost complete catalytic function. That similar natural mutations are not observed may suggest that the gene is unusually protected from mutation, perhaps by binding proteins, or that the selection pressures against establishment of mutants in the population are based on features besides catalysis.

In conclusion, the biological roles of human ChEs and their multiple variants are far from being fully understood. Rather, the era of genetic engineering has provided novel tools with which to explore these as yet unknown functions and their implications for the field of therapeutics, an exciting endeavor.

Acknowledgements—This research was supported by the U.S. Army Medical Research and Development Command (Contract No. 17-94-C-4031, to H.S.). M.S. was a recipient of a Levi Eshkol Post-Doctoral Fellowship and Y.L., a recipient of the Landau Pre-Doctoral Research Prize.

*Lockridge, O., Bartels, C. F., Zelinski, T., Jbilo, O. and Kris, M. (1992) Part 1: Genetic variant of human acetylcholinesterase. Part 2: SV-40 transformed cell lines, for example COS-1, but not parental untransformed cell lines, express butyrylcholinesterase (*BCHE*). In: Multidisciplinary Approaches to Cholinesterase Functions. Proceedings of the Thirty-Sixth Oholo Conference on Multidisciplinary Approaches to Cholinesterase Functions, Eilat, Israel, 6–10 April 1992, pp. 53–59. Shafferman, A. and Velan, B. (eds) Plenum Press, New York.

REFERENCES

Abramson, S. N., Radic, Z., Manker, D., Faulkner, D. J. and Taylor, P. (1989) Onchidal: a naturally occurring irreversible inhibitor of acetylcholinesterase with a novel mechanism of action. Mol. Pharmacol. 36: 349–354.

Ajmar, F., Garre, C., Sessarego, M., Ravazzolo, R., Barresi, R., Bianchi Searra, G. and Lituania, M. (1983) Expression of erythroid acetylcholinesterase in the K-562 leukemia cell line. Cancer Res. 43: 5560–5563.

Aldridge, W. N. (1975) Survey of major points of interest about reactions of cholinesterases. Croatia Chim. Acta 47: 225–233.

Aldridge, W. N. and Reiner, E. (1972) Enzyme Inhibitors as Substrates. Interactions of Esterases with Esters of Organophosphorus and Carbamic Acids. North-Holland Publishing Company, Amsterdam.

Andres, C., El Mourabit, M., Stutz, C., Mark, J. and Waksman, A. (1990) Are soluble and membrane-bound rat brain acetylcholinesterase different? Neurochem. Res. 15: 1065–1072.

Andres, C., El Mourabit, M., Mark, J. and Waksman, A. (1992) A unique hydrophobic domain of rat brain globular acetylcholinesterase for binding to cell membranes. Neurochem. Res. 17: 1247–1253.

Andres, C., Beeri, R., Lev-Lehman, E., Timberg, R., Shani, M. and Soreq, H. (1994) Transgenic overexpression of human acetylcholinesterase in mouse brain. J. Neurochem. 62 (Suppl. 1): S32A.

Anglade, P. (1987) Ultrastructural study of acetylcholinesterase activity in the intrapancreatic ganglia of the rat. Cell. Mol. Biol. 33: 63–67.

Arpagaus, M., Kott, M., Vatsis, K. P., Bartels, C. F. and La Du, B. N. (1990) Structure of the gene for human butyrylcholinesterase: evidence for a single copy. Biochemistry 29: 124–131.

Ashani, Y., Shapira, S., Levy, D., Wolfe, A. D., Doctor, B. P. and Raveh, L. (1991) Butyrylcholinesterase and acetylcholinesterase prophylaxis against soman poisoning in mice. Biochem. Pharmacol. 41: 37–41.

Atack, J. R., Perry, E. K., Bonham, J. R., Perry, R. H., Tomlinson, B. E., Blessed, G. and Fairbairn, A. (1983) Molecular forms of acetylcholinesterase in senile dementia of Alzheimer type: selective loss of the intermediate (10S) form. Neurosci. Lett. 40: 199–204.

Atack, J. R., Perry, E. K., Bonham, J. R., Candy, J. M. and Perry, R. H. (1986) Molecular forms of acetylcholinesterase and butyrylcholinesterase in the aged human central nervous system. J. Neurochem. 47: 263–277.

Augustinsson, K. B. (1948) Acetylcholinesterase: a study in comparative enzymology. Acta Physiol. Scand. 15 (Suppl. 52): 1–182.

Balasubramanian, A. S. and Bhanumathy, C. D. (1993) Noncholinergic functions of cholinesterases. FASEB J. 7: 1354–1358.

Baldessarini, R. J. (1990) Drugs and the treatment of psychiatric disorders. In: Pharmacological Basis of Therapeutics, pp. 383–435, Gilman, A. G., Rall, T. W., Nies, A. S. and Taylor, P. (eds.) Pergamon Press, New York.

Barak, D., Kronman, C., Ordentlich, A., Ariel, N., Bromberg, A., Marcus, D., Lazar, A., Velan, B. and Shafferman, A. (1994) Acetylcholinesterase peripheral anionic site degeneracy conferred by amino acid arrays sharing a common core. J. Biol. Chem. 264: 6296–6305.

Bartels, C. F., James, K. and La Du, B. N. (1992a) DNA mutations associated with the human butyrylcholinesterase J-variant. Am. J. Hum. Genet. 50: 1104–1114.

Bartels, C. F., Jensen, F. S., Lockridge, O., van der Spek, A. F. L., Rubenstein, H. M. Lubrano, T. and La Du, B. N. (1992b) DNA mutation associated with the human butyrylcholinesterase K-variant and its linkage to the atypical variant mutation and other polymorphic sites. Am. J. Hum. Genet. 50: 1086–1103.

Bartels, C. F., Zelinski, T. and Lockridge, O. (1993) Mutation at codon 322 in the human acetylcholinesterase (ACHE) gene accounts for YT blood group polymorphism. Am. J. Hum. Genet. 52: 926–936.

Beeri, R., Gnatt, A., Lapidot-Lifson, Y., Ginzberg, D., Shani, M., Soreq, H. and Zakut, H. (1994) Testicular amplification and impaired transmission of human butyrylcholinesterase cDNA in transgenic mice. Hum. Reprod. 9: 284–292.

Ben Aziz-Aloya, R., Seidman, S., Timberg, R., Sternfeld, M., Zakut, H. and Soreq, H. (1993) Expression of a human acetylcholinesterase promoter-reporter construct in developing neuromuscular junctions of *Xenopus* embryos. Proc. Natl. Acad. Sci. USA 90: 2471–2475.

Bianchi Searra, G. L., Garre, C., Ravazzolo, R., Coviello, D. and Origoni, P. (1986) Coordinated expression of acetylcholinesterase and hemoglobin in K562 cells induced to terminal differentiation by cytosine arabinoside (ara-C). Cell Biol. Int. Rep. 10: 167.

Bishop, M. R., Rama Sastry, B. V., Schmidt, D. E. and Harbison, R. D. (1975) Spermic cholinergic system and occurrence of acetylcholine and other quaternary ammonium compounds in mammalian spermatozoa. Toxicol. Appl. Pharmacol. 33: 733–734.

Bishop, M. R., Rama Sastry, B. V., Schmidt, D. E. and Harbison, R. D. (1976) Occurrence of choline acetyltransferase and acetylcholine and other quaternary ammonium compounds in mammalian spermatozoa. Biochem. Pharmacol. 25: 1617–1622.

Brown, L. M., Blair, A., Gibson, R., Everett, G. D., Cantor, K. P., Schuman, L. M., Burmeister, L. F., Van Lier, S. F. and Dick, F. (1990) Pesticide exposures and other agricultural risk factors for leukemia among men in Iowa and Minnesota. Cancer Res. 50: 6585–6591.

Burstein, S. A., Adamson, J. W. and Harker, L. A. (1980) Megakaryocytopoiesis in culture: modulation by cholinergic mechanisms. J. Cell. Physiol. 103: 201–208.

Carmichael, W. W. (1994) The toxins of cyanobacteria. Sci. Am. 270: 64–72.

Cauet, G., Friboulet, A. and Thomas, D. (1987) Horse serum butyrylcholinesterase kinetics: a molecular mechanism based on inhibition studies with dansylaminoethyltrimethylammonium. Biochem. Cell Biol. 65: 529–535.

Cervenansky, C., Dajas, F., Harvey, A. L. and Karlsson, E. (1990) The fasciculins. In: Snake Toxins, pp. 303–321, Harvey, A. L. (ed.) Pergamon Press, New York.

Changeux, J.-P. (1966) Responses of acetylcholinesterase from *Torpedo marmorata* to salts and curarizing drugs. Mol. Pharmacol. 2: 369–392.

Clement, J. G. (1991) Hypothermia: limited tolerance to repeated soman administration and cross-tolerance to oxotremorine. Pharmacol. Biochem. Behav. 39: 305–312.

Coates, J. T. and Simpson, N. E. (1972) Genetic variation in human erythrocyte acetylcholinesterase. Science 175: 1466–1477.

Coleman, B. A., Michel, L. and Oswald, R. (1987) Interaction of a benzomorphan opiate with acetylcholinesterase and the nicotinic acetylcholine receptor. Mol. Pharmacol. 32: 456–462.

Coyle, J. T., Price, D. L. and DeLong, M. R. (1983) Alzheimer's disease: a disorder of cortical cholinergic innervation. Science 219: 1184–1190.

Cygler, M., Schrag, J. D., Sussman, J. L., Harel, M., Silman, I. and Doctor, B. P. (1993) Relationship between sequence conservation and three-dimensional structure in a large family of esterases, lipases, and related proteins. Protein Sci. 2: 366–382.

Davis, R. E., Emmerling, M. R., Jaen, J. C., Moos, W. H. and Spiegel, K. (1993) Therapeutic intervention in dementia. Crit. Rev. Neurobiol. 7: 41–83.

De Kosky, S. T. and Scheff, S. W. (1990) Synapse loss in frontal cortex biopsies in Alzheimer's disease: correlation with cognitive severity. Ann. Neurol. 27: 457–464.

De La Escalera, S., Bockamp, E.-O., Moya, F., Piovant, M. and Jimenez, F. (1990) Characterization and gene cloning of neurotactin, a *Drosophila* transmembrane protein related to cholinesterases. EMBO J. 9: 3593–3601.

Doctor, B. P., Raveh, L., Wolfe, A. D., Maxwell, D. M. and Ashani, Y. (1991) Enzymes as pretreatment drugs for organophosphate toxicity. Neurosci. Behav. Rev. 15: 123–128.

Doctor, B. P., Blick, D. W., Caranto, G., Castro, C. A., Gentry, M. K., Maxwell, D. M., Murphy, M. R., Schultz, M., Waibel, K. and Wolfe, A. D. (1993) Cholinesterases as scavengers for organophosphorus compounds: protection of primate performance against soman toxicity. Chem. Biol. Interac. 87: 285–294.

Dretchen, K. L., Singh, A., Bradley, R. M. and Lynch, T. J. (1992) Protection against cocaine toxicity by human butyrylcholinesterase (BCHE) in rats. FASEB J. 6: A1282.

Drews, U. (1975) Cholinesterase in Embryonic Development, Progress in Histochemistry and Cytochemistry, Vol. 7. Fischer, Stuttgart.

Dreyfus, P. A., Seidman, S., Pincon-Raymond, M., Murawsky, M., Rieger, F., Schejter, E., Zakut, H. and Soreq, H. (1989) Tissue-specific processing and polarized compartmentalization of clone-produced cholinesterase in microinjected *Xenopus* oocytes. Cell. Mol. Neurobiol. 9: 323–341.

Eckerson, H. W., Oseroff, A., Lockridge, O. and La Du, B. N. (1983) Immunological comparison of the usual and atypical human serum cholinesterase phenotypes. Biochem. Genet. 21: 93–108.

Ehrlich, G., Viegas-Pequignot, E., Ginzberg, D., Sindel, L., Soreq, H. and Zakut, H. (1992) Mapping the human acetylcholinesterase gene to chromosome 7q22 by fluorescent in situ hybridization coupled with selective PCR amplification from a somatic hybrid cell panel and chromosome-sorted DNA libraries. Genomics 13: 1192–1197.

Ehrlich, G., Ginzberg, D., Loewenstein, Y., Glick, D., Kerem, B., Ben-Ari, S., Zakut, H. and Soreq, H. (1994) Population diversity and distinct haplotype frequencies associated with ACHE and BCHE genes of Israeli Jews from trans-Caucasian Georgia and from Europe. Genomics 22: 288–295.

Enz, A., Boddeke, H., Gray, J. and Spiegel, R. (1991) Pharmacologic and clinicopharmacologic properties of SDZ ENA 713, a centrally selective acetylcholinesterase inhibitor. Ann. NY Acad. Sci. 640: 272–275.

Enz, A., Amstutz, R., Boddeke, H. Gmelin, G. and Malanowski, J. (1993) Brain selective inhibition of acetylcholinesterase: a novel approach to therapy for Alzheimer's disease. Prog. Brain Res. 98: 431–437.

Erickson, J. D., Varoqui, H., Schafer, M. K.-H., Modi, W., Diebler, M.-F., Weihe, E., Rand, J., Eiden, L. E., Bonner, T. I. and Usdin, T. B. (1994) Functional identification of a vesicular acetylcholine transporter and its expression from a "cholinergic" gene locus. J. Biol. Chem. 269: 21929–21932.

Fischer, M., Ittah, A., Liefer, I. and Gorecki, M. (1993) Expression and reconstitution of biologically active human acetylcholinesterase from *Escherichia coli*. Cell. Mol. Neurobiol. 13: 25–38.

Fishman, E. B., Siek, G. C., MacCallum, R. D., Bird, E. D., Volicer, L. and Marquis, J. K. (1986) Distribution of the molecular forms of acetylcholinesterase in human brain: alterations in dementia of the Alzheimer type. Ann. Neurol. 19: 246–252.

Foutz, A. S., Boudinot, E. and Denavit-Saubie, M. (1987) Central respiratory depression induced by acetylcholinesterase inhibition: involvement of anaesthesia. Eur. J. Pharmacol. 142: 207–213.

Fuentes, M. E., Rosenberry, T. L. and Inestrosa, N. C. (1988) A 13 kDa fragment is responsible for the hydrophobic aggregation of brain G4 acetylcholinesterase. Biochem. J. 256: 1047–1050.

Futerman, A. H., Low, M. G., Michaelson, D. M. and Silman, I. (1985) Solubilization of membrane-bound acetylcholinesterase by a phosphatidylinositol-specific phospholipase C. J. Neurochem. 45: 1487–1494.

Gatley, S. J. (1991) Activities of the enantiomers of cocaine and some related compounds as substrates and inhibitors of plasma butyrylcholinesterase. Biochem. Pharmacol. 41: 1249–1254.

Getman, D. K., Eubanks, J. H., Camp, S., Evans, G. A. and Taylor, P. (1992) The human gene encoding acetylcholinesterase is located on the long arm of chromosome 7. Am. J. Hum. Genet. 51: 170–177.

Gibney, G., Camp, S., Dionne, M., MacPhee-Quigley, K. and Taylor, P. (1990) Mutagenesis of essential functional residues in acetylcholinesterase. Proc. Natl. Acad. Sci. USA 87: 7546–7550.

Gilson, M. K., Straatsma, T. P., McCammon, J. A., Ripoll, D. R., Faerman, C. H., Axelsen, P. H., Silman, I. and Sussman, J. L. (1994) Open "back door" in a molecular dynamics simulation of acetylcholine. Science 263: 1276–1278.

Gnatt, A., Prody, C. A., Zamir, R., Lieman-Hurwitz, J., Zakut, H. and Soreq, H. (1990) Expression of alternatively terminated unusual human butyrylcholinesterase messenger RNA transcripts, mapping to chromosome 3q26-ter, in nervous system tumors. Cancer Res. 50: 1983–1987.

Gnatt, A., Ginzberg, D., Lieman-Hurwitz, J., Zamir, R., Zakut, H. and Soreq, H. (1991) Human acetylcholinesterase and butyrylcholinesterase are encoded by two distinct genes. Cell. Mol. Neurobiol. 11: 91–104.

Gnatt, A., Loewenstein, Y., Yaron, A., Schwarz, M. and Soreq, H. (1994) Site-directed mutagenesis of active site residues reveals plasticity of human butyrylcholinesterase in substrate and inhibitor interactions. J. Neurochem. 62: 749–755.

Goonetilleke, A., de Belleroche, J. and Guiloff, R. J. (1994) Motor neurone disease. Essays Biochem. 28: 27–45.

Graybiel, A. M. and Ragsdale, C. W., Jr (1982) Pseudocholinesterase staining in the primary visual pathway of the macaque monkey. Nature 299: 439–442.

Graybiel, A. M., Pickel, V. M., Joh, T. H., Reis, D. J. and Ragsdale, C. W., Jr (1981) Direct demonstration of a correspondence between the dopamine islands and acetylcholinesterase patches in the developing striatum. Proc. Natl. Acad. Sci. USA 78: 5871–5875.

Greer, J. (1990) Comparative modeling methods: application to the family of the mammalian seine proteases. Proteins Struct. Funct. Genet. 7: 317–334.

Gregor, V. E., Emmerling, M. R., Lee, C. and Moore, C. J. (1992) The synthesis and *in vitro* acetylcholinesterase and butyrylcholinesterase inhibitory activity of tacrine (Cognex®) derivatives. Bioorgan. Med. Chem. Lett. 8: 861–864.

Gurney, M. E., Pu, H., Chiu, A. Y., Dal Canto, M. C., Polchow, C. Y., Alexander, D. D., Caliendo, J., Hentati, A., Kwon, Y. W., Deng, H.-X., Chen, W., Zhai, P., Sufit, R. L. and Siddique, T. (1994) Motor neuron degeneration in mice that express a human Cu,Zn superoxide dismutase mutation. Science 264: 1772–1775.

Hall, L. M. and Malcolm C. A. (1991) The acetylcholinesterase gene of *Anopheles stephensi*. Cell. Mol. Neurobiol. 11: 131–141.

Hall, Z. W. (1973) Multiple forms of acetylcholinesterase and their distribution in endplate and non-endplate regions of rat diaphragm muscle. J. Neurobiol. 4: 343–361.

Harel, M., Sussman, J. L., Krejci, E., Bon, S., Chanal, P., Massoulie, J. and Silman, I. (1992) Conversion of acetylcholinesterase to butyrylcholinesterase: modeling and mutagenesis. Proc. Natl. Acad. Sci. USA 89: 10827–10831.

Harel, M., Schalk, I., Ehret-Sabatier, L., Bouet, F., Goeldner, M., Hirth, C., Axelsen, P. H., Silman, I. and Sussman, J. L. (1993) Quaternary ligand binding to aromatic residues in the active-site gorge of act acetylcholinesterase. Proc. Natl. Acad. Sci. USA 90: 9031–9035.

Hersh, L. B. (1981) Inhibition of aminopeptidase and acetylcholinesterase by puromycin and puromycin analogs. J. Neurochem. 36: 1594–1596.

Hokin, M. R. and Hokin, L. E. (1953) Enzyme secretion and the incorporation of P^{32} into phospholipids of pancreas slices. J. Biol. Chem. 203: 967–977.

Hutchinson, D. O., Walls, T. J., Nakano, S., Camp, S., Taylor, P., Harper, C. M., Groover, R. V., Peterson, H. A., Jamieson, D. G. and Engel, A. G. (1993) Congenital endplate acetylcholinesterase deficiency. Brain 116: 633–653.

Inestrosa, N. C., Roberts, W. L., Marshall, T. L. and Rosenberry, T. L. (1987) Acetylcholinesterase from bovine caudate nucleus is attached to membranes by a novel subunit distinct from those of acetylcholinesterases in other tissues. J. Biol. Chem. 262: 4441–4444.

Isenschmid, D. S., Levine, B. S. and Caplan, Y. H. (1989) A comprehensive study of the stability of cocaine and its metabolites. J. Anal. Toxicol. 13: 250–256.

Kambam, J. R., Naukam, R. and Berman, M. L. (1992) Inhibition of pseudocholinesterase activity protects from cocaine-induced cardiorespiratory toxicity in rats. J. Lab. Clin. Med. 119: 553–556.

Kambam, J., Mets, B., Hickman, R. M., Janicki, P., James, M. F. and Kirsch, R. E. (1993) The effects of inhibition of plasma cholinesterase and hepatic microsomal enzyme activity on cocaine, benzoylecgonine, ecgonine methyl ester, and norcocaine blood levels in pigs. J. Lab. Clin. Med. 120: 323–328.

Karlsson, E., Mbugua, P. M. and Rodriguez-Ithurralde, D. (1985) Anticholinesterase toxins. Pharmacol. Ther. 30: 259–276.

Karnovsky, M. J. and Roots, L. (1964) A "direct coloring" thiocholine method for cholinesterases. J. Histochem. Cytochem. 12: 219–221.

Karpel, R., Ben Aziz-Aloya, R., Sternfeld, M., Ehrlich, G., Ginzberg, D., Tarroni, P., Clementi, F., Zakut, H. and Soreq, H. (1994a) Expression of three alternative acetylcholinesterase messenger RNAs in human tumor cell lines of different tissue origins. Exp. Cell Res. 210: 268–277.

Karpel, R., Sternfeld, M., Ginzberg, D., Guhl, E., Graessmann, A. and Soreq, H. (1994b) Overexpression of acetylcholinesterase variants induces morphogenic changes in rat glioma cells. J. Neurochem. 63 (Suppl. 1): S63D.

Knapp, M. J., Knopman, D. S., Solomon, P. R., Pendlebury, W. W., David, C. S. and Gracon, S. I. (1994) A 30-week randomized controlled trial of high-dose tacrine in patients with Alzheimer's disease. JAMA 271: 985–991.

Kostovic, I. and Goldman-Rakic, P. S. (1983) Transient cholinesterase staining in the mediodorsal nucleus of the thalamus and its connections in the developing human and monkey brain. J. Comp. Neurol. 219: 431–447.

Kristt, D. A. (1983) Acetylcholinesterase in the ventrobasal thalamus: transience and patterning during ontogenesis. Neuroscience 10: 923–939.

Kristt, D. A. and Kasper, E. K. (1983) High density of cholinergic-muscarinic receptors accompanies high-intensity of acetylcholinesterase staining in layer-IV of infant rat somatosensory cortex. Dev. Brain Res. 8: 373–376.

Landwehrmeyer, B., Probst, A., Palacios, J. M. and Mengod, G. (1994) Expression of acetylcholinesterase messenger RNA in human brain: an *in situ* hybridization study. Neuroscience 57: 615–634.

Lapidot-Lifson, Y., Prody, C. A., Ginzberg, D., Meytes, D., Zakut, H. and Soreq, H. (1989) Coamplification of human acetylcholinesterase and butyrylcholinesterase genes in blood cells: correlation with various leukemias and abnormal megakaryocytopoiesis. Proc. Natl. Acad. Sci. USA 86: 4715–4717.

Layer, P. G. (1991) Cholinesterases during development of the avian nervous system. Cell. Mol. Neurobiol. 11: 7–33.

Layer, P. G., Alber, R. and Rathjen, F. G. (1988a) Sequential activation of butyrylcholinesterase in rostral half somites and acetylcholinesterase in motoneurons and myotomes preceding growth of motor axons. Development 102: 387–396.

Layer, P. G., Rommel, S., Bulthoff, H. and Hengstenberg, R. (1988b) Independent spatial waves of biochemical differentiation along the surface of chicken brain as revealed by the sequential expression of acetylcholinesterase. Cell Tissue Res. 251: 587–595.

Layer, P. G., Weikert, T. and Alber, R. (1993) Cholinesterases regulate neurite growth of chick nerve cells in vitro by means of a non-enzymatic mechanism. Cell Tissue Res. 273: 219–226.

Levene, C., Bar-Shany, S., Manny, N., Moulds, J. J. and Cohen, T. (1987) The Yt blood groups in Israeli Jews, Arabs, and Druse. Transfusion 27: 471–474.

Lev-Lehman, E., Ginzberg, D., Hornreich, G., Ehrlich, G., Meshorer, A., Eckstein, A., Soreq, H. and Zakut, H. (1994) Antisense inhibition of acetylcholinesterase gene expression causes transient hematopoietic alterations *in vivo*. Gene Therapy 1: 127–135.

Lewis, M., Kaita, H., Philipps, S., McAlpine, P. J., Wong, P., Giblett, E. R. and Anderson, J. (1987) The Yt blood group system (ISBT No.011). Vox Sang. 53: 52–56.

Lockridge, O. (1990) Genetic variants of human serum cholinesterase influence metabolism of the muscle relaxant succinylcholine. Pharmacol. Ther. 47: 35–60.

Lockridge, O., Mottershaw-Jackson, N., Eckerson, H. W. and La Du, B. N. (1980) Hydrolysis of diacetylmorphine (heroin) by human serum cholinesterase. J. Pharmacol. Exp. Ther. 215: 1–8.

Lockridge, O., Bartels, C. F., Vaughan, T. A., Wong, C. K., Norton, S. E. and Johnson, L. (1987) Complete amino acid sequence of human serum cholinesterase. J. Biol. Chem. 262: 549–557.

Loewenstein, Y., Gnatt, A., Neville, L. F. and Soreq, H. (1993a) A chimeric human cholinesterase: identification of interaction sites responsible for sensitivity to acetyl- or butyrylcholinesterase-specific ligands. J. Mol. Biol. 234: 289–296.

Loewenstein, Y., Gnatt, A., Neville, L. F., Zakut, H. and Soreq, H. (1993b) Structure-function relationship studies in human cholinesterases reveal genomic origins for individual variations in cholinergic drug responses. Prog. Neuropsychophamacol. Biol. Psychiat. 17: 905–926.

Loewenstein, Y., Liao, J., Norgaard-Pedersen, B., Zakut, H. and Soreq, H. (1994) Faster inhibition rates of normal BuChE as compared with AChE and the D70G "atypical" BuChE mutant predict individual variabilities in response to anticholinesterase therapy. J. Neurochem. 63 (Suppl. 1): S6D.

Malinger, G., Zakut, H. and Soreq, H. (1989) Cholinoceptive properties of human primordial, preantral, and antral oocytes: in situ hybridization and biochemical evidence for expression of cholinesterase genes. J. Mol. Neurosci. 1: 77–84.

Marchot, P., Khelif, A., Ji, Y.-H., Mansuelle, P. and Bougis, P. E. (1993) Binding of ^{125}I-fasciculin to rat brain acetylcholinesterase: the complex still binds diisopropyl fluorophosphate. J. Biol. Chem. 268: 12458–12567.

Marquis, J. K. and Fishman, E. B. (1985) Presynaptic acetylcholinesterase. Trends Pharmacol. Sci. 6: 387–388.

Marquis, J. K. and Lerrick, A. J. (1982) Noncompetitive inhibition by aluminum, scandium, and yttrium of acetylcholinesterase from *Electrophorus electricus*. Biochem. Pharmacol. 31: 1437–1440.

Marrs, T. C. (1993) Organophosphate poisoning. Pharmacol. Ther. 58: 51–66.

Masson, P., Adkins, S., Gouet, P. and Lockridge, O. (1993) Recombinant human butyrylcholinesterase G390V, the fluoride-2 variant, expressed in Chinese hamster ovary cells, is a low affinity variant. J. Biol. Chem. 268: 14329–14341.

Massoulie, J. and Bon, S. (1982) The molecular forms of cholinesterase and acetylcholinesterase in vertebrates. Annu. Rev. Neurosci. 5: 57–106.

Massoulie, J., Pezzementi, L., Bon, S., Krejci, E. and Vallette, F. M. (1993) Molecular and cellular biology of the cholinesterases. Prog. Neurobiol. 41: 31–91.

Maulet, Y., Camp, S., Gibney, G., Rachinsky, T. L., Ekstrom, T. J. and Taylor, P. (1990) Single gene encodes glycophospholipid-anchored and asymmetric acetylcholinesterase forms: alternative coding exons contain inverted repeat sequences. Neuron 4: 289–301.

Maxwell, D. M., Castro, C. A., De La Hoz, D. M., Gentry, M. K., Gold, M. B., Solana, R. P., Wolfe, A. D. and Doctor, B. P. (1992) Protection of rhesus monkeys against soman and prevention of performance decrement by pretreatment with acetylcholinesterase. Toxicol. Appl. Pharmacol. 115: 44–49.

McGuire, M. C., Nogueira, C. P., Bartels, C. F., Lightstone, H., Hajra, A., van der Spek, A. F. L., Lockridge, O. and La Du, B. N. (1989) Identification of the structural mutation responsible for the dibucaine-resistant (atypical) variant form of human serum cholinesterase. Proc. Natl. Acad. Sci. USA 86: 953–957.

McMahan, U. J., Sanes, J. R. and Marshall, L. M. (1978) Cholinesterase is associated with the basal lamina at the neuromuscular junction. Nature 271: 172–174.

McTiernan, C., Adkins, S., Chatonnet, A., Vaughan, T. A., Bartels, C. F., Kott, M., Rosenberry, T. L., La Du, B. N. and Lockridge, O. (1987) Brain cDNA clone for human cholinesterase. Proc. Natl. Acad. Sci. USA 84: 6682–6686.

Meflah, K., Bernard, S. and Massoulie, J. (1984) Interaction with lectins indicates differences in the carbohydrate composition of the membrane-enzymes acetylcholinesterase and 5′-nucleotidase in different cell types. Biochimie 66: 59–69.

Minthon, L., Gustafson, L., Dalfelt, G., Hagberg, B., Nilsson, K., Risberg, J., Rosen, I., Seiving, B. and Wendt, P. E. (1993) Oral tetrahydroaminoacridine treatment of Alzheimer's disease evaluated clinically and by regional cerebral blood flow and EEG. Dementia 4: 32–42.

Mullan, M. and Crawford, F. (1993) Genetic and molecular advances in Alzhiemer's disease. Trends Neurosci. 16: 398–403.

Muratani, P., Hada, T., Yamamoto, Y., Kaneko, Y., Shigero, Y., Ohue, T., Furuyama, J. and Higashino, K. (1991) Inactivation of the cholinesterase gene by *Alu* insertion: possible mechanism for human gene transposition. Proc. Natl. Acad. Sci. USA 88: 11315–11319.

Mutero, A. and Fournier, D. (1992) Post-translational modifications of *Drosophila* acetylcholinesterase; in vitro expression in *Xenopus* oocytes. J. Biol. Chem. 267: 1695–1700.

Mutero, A., Pralavorio, M., Simeon, V. and Fournier, D. (1992) Catalytic properties of cholinesterases: importance of tyrosine 109 in *Drosophila* protein. NeuroReport 3: 39–42.

Neville, L. F., Gnatt, A., Loewenstein, Y. and Soreq, H. (1990a) Aspartate-70 to glycine substitution confers resistance to naturally occurring and synthetic anionic-site ligands on in-ovo produced human butyrylcholinesterase. J. Neurosci. Res. 27: 452–460.

Neville, L. F., Gnatt, A., Padan, R., Seidman, S. and Soreq, H. (1990b) Anionic site interactions in human butyrylcholinesterase disrupted by two single point mutations. J. Biol. Chem. 265: 20735–20738.

Neville, L. F., Gnatt, A., Loewenstein, Y., Seidman, S., Ehrlich, G. and Soreq, H. (1992) Intramolecular relationships in cholinesterase revealed by oocyte expression of site-directed and natural variants of human BCHE. EMBO J. 11: 1641–1649.

Nogueira, C. P., McGuire, M. C., Graeser, C., Bartels, C. F., Arpagaus, M., Lightstone, H., Lockridge, O. and La Du, B. N. (1990) Identification of a frameshift mutation responsible for the silent phenotype of human serum cholinesterase, Gly 117(GGT → GGAG). Am. J. Hum. Genet. 46: 934–942.

Olianas, M. C., Onali, P., Schwartz, J. P., Neff, N. H. and Costa, E. (1984) The muscarinic receptor adenylate cyclase complex of rat striatum: desensitization following chronic inhibition of acetylcholinesterase activity. J. Neurochem. 42: 1439–1443.

Ollis, D. L., Cheah, E., Cygler, M., Dijkstra, B., Frolow, F., Franken, S. M., Harel, M., Remington, S. J., Silman, I., Schrag, J. D., Sussman, J. L., Versschveren, K. H. G. and Goldman, A. (1992) The α/β hydrolase fold. Protein Eng. 5: 197–211.

Ord, M. G. and Thompson, R. H. (1952) Pseudocholinesterase activity in the central nervous system. Biochem. J. 51: 245–251.

Ordentlich, A., Barak, D., Kronman, C., Flashner, Y., Leitner, M., Ariel, N., Cohen, S., Velan, B. and Shafferman, A. (1993a) Dissection of the human acetylcholinesterase active center determinants of substrate specificity. Identification of residues constituting the anionic site, the hydrophobic site, and the acyl pocket. J. Biol. Chem. 268: 17083–17095.

Ordentlich, A., Kronman, C., Barak, D., Stein, D., Ariel, N., Marcus, D., Velan, B. and Shafferman, A. (1993b) Engineering resistance to "aging" of phosphylated human acetylcholinesterase: role of hydrogen bond network in the active center. FEBS Lett. 334: 215–220.

Ott, B. R. and Lannon, M. C. (1992) Exacerbation of parkinsonism by tacrine. Clin. Neuropharmacol. 15: 322–325.

Patinkin, D., Seidman, S., Eckstein, F., Benseler, F., Zakut, H. and Soreq, H. (1990) Manipulations of cholinesterase gene expression modulate murine megakaryocytopoiesis in vitro. Mol. Cell. Biol. 10: 6046–6050.

Patinkin, D., Lev-Lehman, E., Zakut, H., Eckstein, F. and Soreq, H. (1994) Antisense inhibition of butyrylcholinesterase gene expression predicts adverse hematopoietic consequences to cholinergic inhibitors. Cell. Mol. Neurobiol 14: 459–473.

Percy, M. E., Markovic, V. D., Dalton, A. J., McLachlan, D. R. C, Berg, J. M., Rusk, A. C. M., Somerville, M. J., Chodakowski, B. and Andrews, D. F. (1993) Age-associated chromosome 21 loss in Down syndrome: possible relevance to mosaicism and Alzheimer disease. Am. J. Med. Genet. 45: 584–588.

Perry, E. K., Tomlinson, B. E., Blessed, G., Bergmann, K., Gibson, P. H. and Perry, R. H. (1978) Correlation of cholinergic abnormalities with senile plaques and mental test scores in senile dementia. Br. Med. J. 2: 1457–1459.

Prody, C. A., Gnatt, A., Zevin-Sonkin, D., Gnatt, A., Goldberg, O. and Soreq, H. (1987) Isolation and characterization of full-length cDNA clones coding for cholinesterase from fetal human tissues. Proc. Natl. Acad. Sci. USA 84: 3555–3559.

Prody, C. A., Dreyfus, P., Zamir, R., Zakut, H. and Soreq, H. (1989) De novo amplification within a "silent" human cholinesterase gene in a family subjected to prolonged exposure to organophosphorous insecticides. Proc. Natl. Acad. Sci. USA 86: 690–694.

Radic, Z., Gibney, G., Kawamoto, S., MacPhee-Quigley, K., Bongiorno, C. and Taylor, P. (1992) Expression of recombinant acetylcholinesterase in a baculovirus system: kinetic properties of glutamate 199 mutants. Biochemistry 31: 9760–9767.

Radic, Z., Pickering, N. A., Vellom, D. C., Camp, S. and Taylor, P. (1993) Three distinct domains in the cholinesterase molecule confer selectivity for acetyl- and butyrylcholinesterase inhibitors. Biochemistry 32: 12074–12084.

Radic, Z., Duran, R., Vellom, D. C., Li, Y., Cervenansky, C. and Taylor, P. (1994) Site of fasciculin interactions with acetylcholinesterase. J. Biol. Chem. 269: 11233–11239.

Rakonczay, Z. and Brimijoin, S. (1988) Biochemistry and pathophysiology of the molecular forms of cholinesterases. In: Subcellular Biochemistry, Vol. 12, Immunological Aspects, pp. 335–378, Harris, J. R. (ed.) Plenum Press, New York.

Rama Sastry, B. V., Janson, V. E. and Chaturverdi, A. K. (1981) Inhibition of human sperm motility by inhibitors of choline acetyltransferase. J. Pharmacol. Exp. Ther. 216: 378–384.

Ratner, D., Oren, B. and Vigder, K. (1983) Chronic dietary anticholinesterase poisoning. Isr. J. Med. Sci. 19: 810–814.

Raveh, L., Ashani, Y., Levy, D., De La Hoz, D., Wolfe, A. D. and Doctor, B. P. (1989) Acetylcholinesterase prophylaxis against organophosphate poisoning; quantitative correlation between protection and blood-enzyme level in mice. Biochem. Pharmacol. 38: 529–534.

Raveh, L., Grunwald, J., Marcus, D., Papier, Y., Cohen, E. and Ashani, Y. (1993) Human butyrylcholinesterase as a general prophylactic antidote for nerve agent toxicity; *in vitro* and *in vivo* quantitative characterization. Biochem. Pharmacol. 45: 2465–2474.

Razon, N., Soreq, H., Roth, E., Bartal, A. and Silman, I. (1984) Characterization of activities and forms of cholinesterases in human primary brain tumors. Exp. Neurol. 84: 681–695.

Ripoll, D. R., Faerman, C. H., Axelsen, P. H., Silman, I. and Sussman, J. L. (1993) An electrostatic mechanism for substrate guidance down the aromatic gorge of acetylcholinesterase. Proc. Natl. Acad. Sci. USA 90: 5128–5132.

Roberts, W. L., Myher, J. J., Kuksis, A., Low, M. G. and Rosenberry, T. L. (1988a) Lipid analysis of the glycoinositol phospholipid membrane anchor of human erythrocyte acetylcholinesterase; palmitoylation of inositol results in resistance to phosphoinositol-specific phospholipase C. J. Biol. Chem. 263: 18766–18775.

Roberts, W. L., Santikarn, S., Reinhold, V. N. and Rosenberry, T. L. (1988b) Structural characterization of the glycoinositol phospholipid membrane anchor of human erythrocyte acetylcholinesterase by fast atom bombardment mass spectronomy. J. Biol. Chem. 263: 18776–18784.

Robertson, R. T. and Yu, J. (1993) Acetylcholinesterase and neural development: new tricks for an old dog? News Physiol. Sci. 8: 266–272.

Ruberg, M., Rieger, F., Villageois, A., Bonnet, A. M. and Agid, Y. (1986) Acetylcholinesterase and butyrylcholinesterase in frontal cortex and cerebrospinal fluid of demented and non-demented patients with Parkinson's Disease. Brain Res. 362: 83–91.

Salte, R., Syvertsen, C., Kjonnoy, M. and Fonnum, F. (1987) Fatal acetylcholinesterase inhibition in salmonids subjected to a routine organophosphate treatment. Aquaculture 61: 173–179.

Sanyal, R. K. and Khanna, S. K. (1971) Action of cholinergic drugs on motility of spermatozoa. Fertil. Steril. 22: 356–359.

Saxena, A., Doctor, B. P., Maxwell, D. M., Lenz, D. E., Radic, Z. and Taylor, P. (1993) The role of glutamate-199 in the aging of cholinesterase. Biochem. Biophys. Res. Commun. 197: 343–349.

Schwarz, M., Loewenstein, Y., Glick, D., Liao, J., Norgaard-Pedersen, B. and Soreq, H. (1994) Dissection of successive organophosphorus inhibition and oxime reactivation by human cholinesterase variants. J. Neurochem. 63 (Suppl. 1): S80D.

Seidman, S., Ben Aziz-Aloya, R., Timberg, R., Loewenstein, Y., Velan, B., Shafferman, A., Liao, J., Norgaard-Pedersen, B., Brodbeck, U. and Soreq, H. (1994) Overexpressed monomeric human acetylcholinesterase induces subtle ultrastructural modifications in developing neuromuscular junctions of *Xenopus laevis* embryos. J. Neurochem. 62: 1670–1681.

Shafferman, A., Kronman, C., Flashner, Y., Leitner, M., Grosfeld, H., Ordentlich, A., Gozes, Y., Cohen, S., Ariel, N., Barak, D., Harel, M., Silman, I., Sussman, J. L. and Velan, B. (1992a) Mutagenesis of human acetylcholinesterase: identification of residues involved in catalytic activity and in polypeptide folding. J. Biol. Chem. 267: 17640–17648.

Shafferman, A., Velan, B., Ordentlich, A., Kronman, C., Grosfeld, H., Leitner, M., Flashner, Y., Cohen, S., Barak, D. and Ariel, N. (1992b) Substrate inhibition of acetylcholinesterase: residues affecting signal transduction from the surface to the catalytic center. EMBO J. 11: 3561–3568.

Shapira, M., Seidman, S., Sternfeld, M., Timberg, R., Kaufer, D., Patrick, J. and Soreq, H. (1994) Transgenic engineering of neuromuscular junctions in *Xenopus laevis* embryos transiently overexpressing key cholinergic proteins. Proc. Natl. Acad. Sci. USA 91: 9072–9076.

Shaw, K. P., Aracava, Y., Akaike, A., Daly, J. W., Rickett, D. L. and Albuquerque, E. X. (1985) The reversible cholinesterase inhibitor physostigmine has channel-blocking and agonist effects on the acetylcholine receptor-ion channel complex. Mol. Pharmacol. 28: 527–538.

Sikorav, J.-L., Duval, N., Anselmet, A., Bon, S., Krejci, E., Legay, C., Osterlund, M., Riemund, B. and Massoulie, J. (1988) Complex alternative splicing of acetylcholinesterase transcripts in *Torpedo* electric organ; primary structure of the precursor of the glycolipid-anchored dimeric form. EMBO J. 7: 2983–2993.

Silman, I. and Futerman, A. H. (1987) Modes of attachment of acetylcholinesterase to the surface membrane. Eur. J. Biochem. 170: 11–22.

Silver, A. (1974) The Biology of Cholinesterases. North-Holland Publishing Company, Amsterdam.

Soreq, H. and Zakut, H. (1990) Cholinestera e Genes: Multilevelled Regulation. Karger, Basel.

Soreq, H. and Zakut, H. (1993) Human Cholinesterases and Anticholinesterases. Academic Press, San Diego.

Soreq, H., Malinger, G. and Zakut, H. (1987) Expression of cholinesterase genes in human oocytes revealed by in-situ hybridization. Human Reproduct. 2: 689–693.

Soreq, H., Seidman, S., Dreyfus, P. A., Zevin-Sonkin, D. and Zakut, H. (1989) Expression and tissue-specific assembly of human butyrylcholinesterase in microinjected *Xenopus* oocytes. J. Biol. Chem. 264: 10608–10613.

Soreq, H., Ben Aziz, R., Prody, C. A., Seidman, S., Gnatt, A., Neville, L., Lieman-Hurwitz, J., Lev-Lehman, E., Ginzberg, D., Lapidot-Lifson, Y. and Zakut, H. (1990) Molecular cloning and construction of the coding region for human acetylcholinesterase reveals a G+C-rich attenuating structure. Proc. Natl. Acad. Sci. USA 87: 9688–9692.

Soreq, H., Gnatt, A., Loewenstein, Y. and Neville, L. F. (1992) Excavations into the active-site gorge of cholinesterases. Trends Biochem. Sci. 17: 353–358.

Soreq, H., Patinkin, D., Lev-Lehman, E., Grifman, M., Ginzberg, D., Eckstein, F. and Zakut, H. (1994) Antisense oligonucleotide inhibition of acetylcholinesterase gene expression induces progenitor cell expansion and suppresses hematopoietic apoptosis *ex vivo*. Proc. Natl. Acad. Sci. USA 91: 7907–7911.

Sussman, J. L., Harel, M., Frolow, F., Oefner, C., Goldman, A., Toker, L. and Silman, I. (1991) Atomic structure of acetylcholinesterase from *Torpedo californica*: a prototypic acetylcholine-binding protein. Science 253: 872–879.

Taylor, P. (1990a) Cholinergic agonists. In: Pharmacological Basis of Therapeutics, pp. 122–130, Gilman, A. G., Rall, T. W., Nies, A. S. and Taylor, P. (eds.) Pergamon Press, New York.

Taylor, P. (1990b) Anticholinesterase agents. In: Pharmacological Basis of Therapeutics, pp. 131–149, Gilman, A. G., Rall, T. W., Nies, A. S. and Taylor, P. (eds.) Pergamon Press, New York.

Taylor, P. (1991) The cholinesterases. J. Biol. Chem. 266: 4025–4028.

Taylor, P. and Lappi, S. (1975) Interaction of fluorescence probes with acetylcholinesterase: the site and specificity of propidium binding. Biochemistry 145: 1989–1997.

Taylor, P. and Radic, Z. (1994) The cholinesterases: from genes to proteins. Annu. Rev. Pharmacol. Toxicol. 34: 281–320.

Toutant, J. P., Massoulie, J. and Bon, S. (1985) Polymorphism of pseudocholinesterase in *Torpedo marmorata* tissues: comparative study of the catalytic and molecular properties of this enzyme with acetylcholinesterase. J. Neurochem. 44: 580–592.

Tsim, K. W. K., Randall, W. R. and Barnard, E. A. (1988) An asymmetric form of muscle acetylcholinesterase contains three subunit types and two enzymic activities in one molecule. Proc. Natl. Acad. Sci. USA 85: 1262–1266.

Turner, A. J. (1994) PIG-tailed membrane proteins. Essays Biochem. 28: 113–127.

United Nations Security Council (1984) Report of specialist appointed by the Secretary General. Paper S/16433.

Valentino, R. J., Lockridge, O., Eckerson, H. W. and La Du, B. N. (1981) Prediction of drug sensitivity in individuals with atypical serum cholinesterase based on *in vitro* biochemical studies. Biochem. Pharmacol. 30: 1643–1649.

Velan, B., Grosfeld, H., Kronman, C., Leitner, M., Gozes, Y., Lazar, A., Flashner, Y., Marcus, D., Cohen, S. and Shafferman, A. (1991) The effect of elimination of intersubunit disulfide bonds on the activity, assembly, and secretion of recombinant human acetylcholinesterase: expression of acetylcholinesterase cys-580 → ala mutant. J. Biol. Chem. 266: 23977–23984.

Velan, B., Kronman, C., Ordentlich, A., Flashner, Y., Leitner M., Cohen, S. and Shafferman, A. (1993) N-Glycosylation of human acetylcholinesterase: effects on enzyme activity, stability and biosynthesis. Biochem. J. 296: 649–656.

Vellom, D. C., Radic, Z., Li, Y., Pickering, N. A., Camp, S. and Taylor, P. (1993) Amino acid residues controlling acetylcholinesterase and butyrylcholinesterase specificity. Biochemistry 32: 12–17.

Watkins, P. B., Zimmerman, H. J., Knapp, M. J., Gracon, S. I. and Lewis, K. W. (1994) Hepatoxic effects of tacrine administration in patients with Alzheimer's disease. J. Am. Med. Assn. 271: 992–998.

Wecker, L., Kiauta, T. and Dettbarn, W.-D. (1978) Relationship between acetylcholinesterase inhibition and the development of a myopathy. J. Pharmacol. Exp. Ther. 206: 97–104.

Whittaker, M. (1986) *Cholinesterase*. Karger, Basel.

WHO (1986a) Organophosphorus Insecticides: A General Introduction. Environmental Health Criteria 63, World Health Organization, Geneva.

WHO (1986b) Carbamate Pesticides: A General Introduction. Environmental Health Criteria 64, World Health Organization, Geneva.

Willems, J. L., DeBisschop, H. C., Verstraete, A. G., Declerck, C., Christiaens, Y., Vanscheeuwyck, P., Buylaert, W. A., Vogelaers, D. and Colardyn, F. (1993) Cholinesterase reactivation in organophosphorus poisoned patients depends on the plasma concentrations of the oxime pralidoxime methylsulphate and of the organophosphate. Arch. Toxicol. 67: 79–84.

Wills, J. H. (1970) Toxicity of anticholinesterases and treatment of poisoning. In: Anticholinesterase Agents, International Encyclopedia of Pharmacology and Therapeutics Section 13, pp. 357–369, Karczmar, A. G. (ed.) Pergamon Press, Oxford.

Winker, M. A. (1994) Tacrine for Alzheimer's disease; which patient, what dose? JAMA 271: 1023–1024.

Wolfe, A. D., Blick, D. W., Murphy, M. R., Miller, S. A., Gentry, M. K., Hartgraves, S. L. and Doctor, B. P. (1995) Use of cholinesterases as pretreatment drugs for the protection of rhesus monkeys against soman toxicity. Toxicol. Appl. Pharmacol., in press.

Wright, C. I., Guela, C. and Mesulam, M. M. (1993) Protease inhibitors and indoleamines selectively inhibit cholinesterases in the histopathologic structures of Alzheimer disease. Proc. Natl. Acad. Sci. USA 90: 683–686.

Zakut, H., Matzkel, A., Schejter, E., Avni, A. and Soreq, H. (1985) Polymorphism of acetylcholinesterase in discrete regions of the developing human fetal brain. J. Neurochem. 45: 382–389.

Zakut, H., Ehrlich, G., Ayalon, A., Prody, C. A., Malinger, G., Seidman, S., Ginzberg, D., Kehlenbach, R. and Soreq, H. (1990) Acetylcholinesterase and butyrylcholinesterase genes coamplify in primary ovarian carcinomas. J. Clin. Invest. 86: 900–908.

Zakut, H., Lieman-Hurwitz, J., Zamir, R., Sindell, L., Ginsberg, D. and Soreq, H. (1991) Chorionic villi cDNA library displays expression of butyrylcholinesterase: putative genetic disposition for ecological danger. Prenat. Diag. 11: 597–607.

ELSEVIER

Molecular Brain Research 31 (1995) 101–110

MOLECULAR BRAIN RESEARCH

Research report

Successive organophosphate inhibition and oxime reactivation reveals distinct responses of recombinant human cholinesterase variants

Mikael Schwarz [a,1], Yael Loewenstein-Lichtenstein [a], David Glick [a], Jian Liao [a,2], Bent Norgaard-Pedersen [b], Hermona Soreq [a,*]

[a] *Department of Biological Chemistry, The Life Sciences Institute, The Hebrew University of Jerusalem, 91904 Jerusalem, Israel*
[b] *Statens Seruminstitut, 2300 Copenhagen, Denmark*

Accepted 7 February 1995

Abstract

To explore the molecular basis of the biochemical differences among acetylcholinesterase (AChE), butyrylcholinesterase (BuChE) and their alternative splicing and allelic variants, we investigated the acylation phase of cholinesterase catalysis, using phosphorylation as an analogous reaction. Rate constants for organophosphate (DFP) inactivation, as well as for oxime (PAM)-promoted reactivation, were calculated for antibody-immobilized human cholinesterases produced in *Xenopus* oocytes from natural and site-directed variants of the corresponding DNA constructs. BuChE displayed inactivation and reactivation rates 200- and 25-fold higher than either product of 3′-variable AChE DNAs, consistent with a putative in vivo function for BuChE as a detoxifier that protects AChE from inactivation. Chimeric substitution of active site gorge-lining residues in BuChE with the more anionic and aromatic residues of AChE, reduced inactivation 60-fold but reactivation only 4-fold, and the rate-limiting step of its catalysis appeared to be deacylation. In contrast, a positive charge at the acyl-binding site of BuChE decreased inactivation 8-fold and reactivation 30-fold. Finally, substitution of Asp70 by glycine, as in the natural 'atypical' BuChE variant, did not change the inactivation rate yet reduced reactivation 4-fold. Thus, a combination of electrostatic active site charges with aromatic residue differences at the gorge lining can explain the biochemical distinction between AChE and BuChE. Also, gorge-lining residues, including Asp70, appear to affect the deacylation step of catalysis by BuChE. Individuals carrying the 'atypical' BuChE allele may hence be unresponsive to oxime reactivation therapy following organophosphate poisoning.

Keywords: Organophosphate; Oxime reaction; Acetylcholinesterase; Butyrylcholinesterase; Diisopropylfluorophosphonate; Pyridine-2-aldoxime methiodide

1. Introduction

In spite of access to the 3-dimensional structure [6,29] and ample experimental [3–6,12–19,31] and theoretical [3,15,20,22–28] work, the biological implications of the complex catalytic process of cholinesterases (ChEs) are far from being fully understood. There are two human ChE genes, ACHE and BCHE, both of which have been cloned and expressed (reviewed by Soreq and Zakut [28]). These encode the homologous acetylcholinesterase (AChE, EC 3.1.1.7) and butyrylcholinesterase (BuChE, EC 3.1.1.8) proteins. The active site in both enzymes is positioned at the bottom of a deep gorge lined with hydrophobic residues [6,29]. However, although both these enzymes hydrolyze their substrates at exceptionally fast rates [20,22], they display clear differences in substrate specificity and in-

Abbreviations and nomenclature: ABS, acyl-binding site; AChE, acetylcholinesterase; BBS, butyryl binding site; BChE, butyrylcholinesterase; BTCh, butyrylthiocholine; CBS, choline-binding site; ChE, cholinesterase; DFP, diisopropylfluorophosphonate; DIP, diisopropylphosphoryl; ELISA, enzyme-linked immunosorbant assay; E5, the product of the mRNA encoding exons 2, 3, 4, intron 4 and exon 5; E6, the product of the mRNA encoding exons 2, 3, 4, and 6; OP, organophosphorus agent; PAM, pyridine-2-aldoxime methiodide; tAChE, *Torpedo* AChE. Numbering of human BuChE residues is according to its published sequence [28]. Point mutations are indicated by the wild-type residue, the position in the sequence, and the mutant residue; thus, $L^{286}K$ is the replacement of leucine 286 by arginine.

* Corresponding author. Fax: (972) (2) 652-0258.
[1] Present address: Department of Cell Biology, Stanford University School of Medicine, Stanford, CA 94305, USA.
[2] Present address: Division of Gastroenterology, Stanford University School of Medicine, Stanford, CA 94305, USA.

SSDI 0169-328X(95)00040-2

hibitor interactions [6,27,31]. In the case of BuChE, the relatively less aromatic gorge is lined with fewer aryl groups and more alkyl residues [6,29]. The catalytic triad, its adjacent choline- and acyl-binding sites and the surrounding residues determine the characteristic specificities of these enzymes to substrates and inhibitors [6,18,20,31]. An appreciation of the molecular basis of the differences between AChE and BuChE, therefore, requires a consideration of the contributions of specific residues both in the gorge lining and in the active site regions of the two enzymes.

ChE catalysis is a multi-step process, which includes attraction of the substrate into the deep gorge, formation of an acyl-enzyme intermediate by displacement of the choline alkoxy group by the hydroxyl oxygen of the enzyme's active site serine, exchange of water for the choline molecule, and hydrolysis of the acyl-enzyme (Figs. 1 and 2A). Detailed dissection of catalysis by any natural or recombinant ChE variant [18,19,28,31] should attempt to discriminate among effects on one or another of these stages of catalysis. As the slowest of these stages has a half-time in the order of 100 μs [3,20,22], we have recruited the inactivation of ChEs by an organophosphorus agent (OP) [30] as an analogous reaction in order to study in isolation the first of these two stages of catalysis (Fig. 1A). OP phosphorylation of the active site serine [19] is just as specific for S^{198} (sequence numbers for human BuChE [28]; S^{198} of human BuChE is homologous to S^{200} of *Torpedo* AChE [23]) as is the acylation stage of catalysis. Furthermore, it also has a pH/rate profile shaped by dependence on a conjugate base of pK_a near 7.2 and a conjugate acid of pK_a near 9.3 [35]. Thus, the same features of AChE that promote its acylation should facilitate its phosphorylation.

Cleavage of the phosphoryl-ChE bond is extremely slow, making OPs hemi-substrate inhibitors, but the rate of dephosphorylation can be enhanced by rationally designed nucleophiles, such as pyridine-2-aldoxime methiodide (PAM, Fig. 1B) [35]. PAM is a rigid zwitterionic molecule that juxtaposes its nucleophilic group precisely against the phosphoryl bond, which it displaces. That PAM acts from the choline binding site is indicated by choline being a competitive inhibitor [22], and by natural substrates competing with PAM in the reactivation reaction [12]. Moreover, the order of effectiveness of non-assisted hydrolysis of the spectrum of dialkylphosphoryl-ChEs formed by OP agents (dimethyl > diethyl > diisopropyl) is maintained in the PAM-assisted reactivations [30]. In spite of the obvious steric and electronic differences between PAM and a water molecule, PAM-promoted reactivation thus shares mechanistic characteristics with the deacylation step of catalysis.

Because BuChE is prevalent in serum, it can react easily with anti-ChEs before they have a chance to inactivate AChE at brain synapses and neuromuscular junctions. However, in addition to the differences between AChE and BuChE, several allelic variants of BuChE differ in their interactions with natural (e.g. glyco-alkaloids of the *Solanaceae*) and man-made anti-ChEs (e.g. OP and carbamate pesticides) [28]. Succinyl-

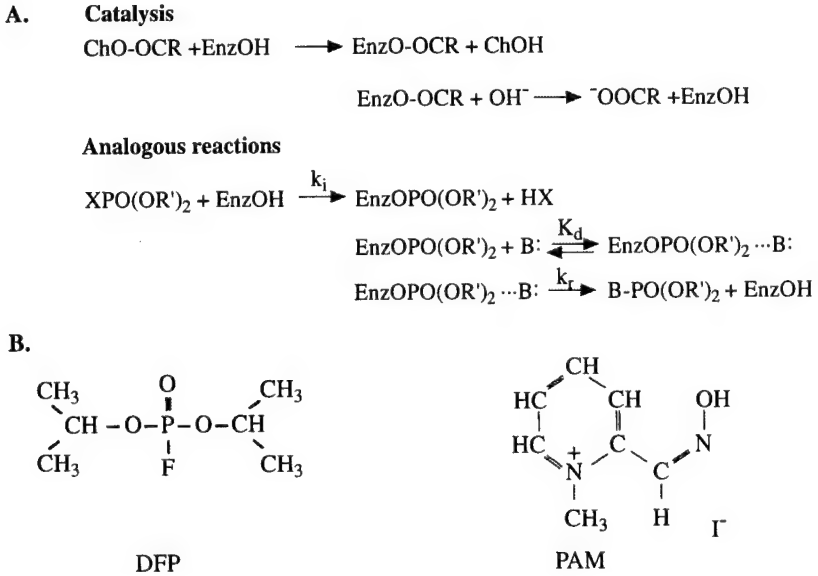

Fig. 1. The experimental paradigm. A: catalysis and analogous reactions. In the catalytic cycle the enzyme's active site serine (Enz-OH) displaces the choline moiety of the substrate, forming an acyl-enzyme (covalent) intermediate. The OP agents, being hemi-substrates, act analogously: serine displaces the leaving group (X), forming a dialkylphosphoryl-enzyme [30]. Catalysis continues with the hydrolysis of the acyl enzyme, whereas hydrolysis of the phosphoryl-ChE bond is extremely slow. The reactivation rate, however, can be enhanced by nucleophiles (B) such as choline and PAM, which actively displace the phosphoryl group. B: structure of DFP and PAM.

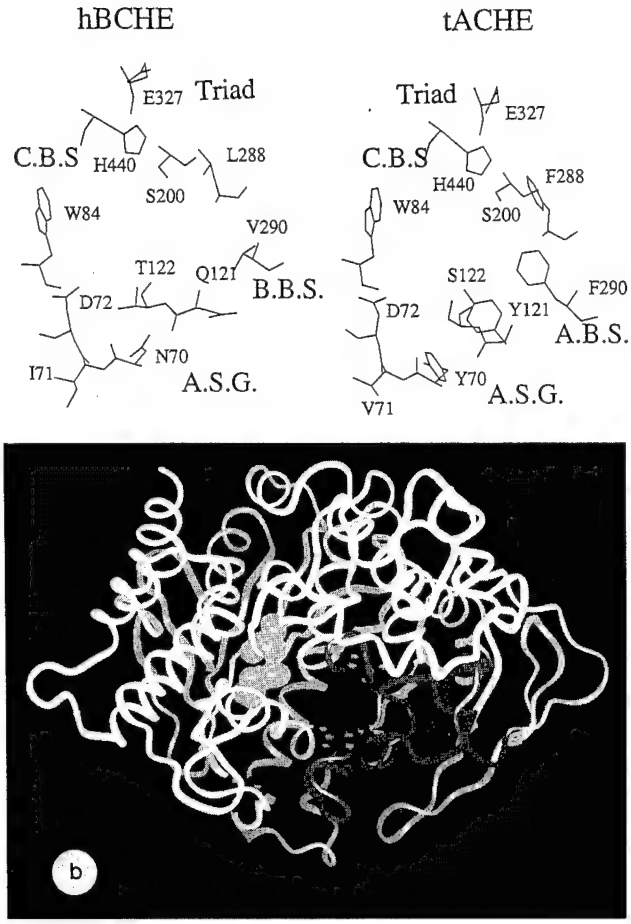

Fig. 2. The analyzed regions. A: active site environment in AChE and BuChE. Active site residues in *Torpedo* AChE (right, tACHE) and human BuChE (left, hBCHE) are shown following the existing structure and numbering of residues in *Torpedo* AChE [29] and the computer model of human BuChE6 [5]. Note differences in the acyl-binding site (ABS) and the butyryl binding site (BBS), and in the number of aromatic residues, and the similarity in the choline-binding site (CBS) and the catalytic triad (BuChE residues S^{198}, H^{438} and E^{327}). L^{288} in *Torpedo* is equivalent to L^{286} in human BuChE. Numbering of AChE residues is as for the *Torpedo* enzyme [28,29]. B: positioning of the replaced regions: The ribbon model of human BuChE was drawn after Harel et al. [6] and as detailed elsewhere [13,27]. The active site gorge lies in the plane of the figure, with its opening at the bottom. The substituted chimeric peptide [13] is shown in dark gray; site-directed (brightest balls) and natural (dark balls) mutations were introduced in positions indicated as space-filling models, counterclockwise: S^{425} (bottom left), D^{70} (center), Y^{114} (top), L^{286} (upper) and F^{329} (lower). Natural point mutations included D^{70} on the rim of the gorge, Y^{114} in the chimeric region, and S^{425}.

choline, which is used as a muscle relaxant prior to anesthesia, is slowly hydrolyzed by normal BuChE, but the fairly common $D^{70}G$ ('atypical') variant of BuChE does not hydrolyze it [2,16,17], resulting in post-operative apnea in individuals homozygous for this variant. This raises the question whether individuals with this and other variant BuChEs, when exposed to anti-ChEs, such as pesticides, pharmaceuticals, etc., will react differently than those with the common BuChE.

To analyze catalysis on a micro scale and to avoid interference with rate measurements by inactivating or reactivating reagents, we immobilized recombinant *Xenopus* oocyte-produced variant ChEs on selective monoclonal antibodies in multi-well plates and subjected the bound enzymes to successive OP inactivation and oxime-promoted reactivation. By this approach we measured major changes in rates of the reaction with diisopropylfluorophosphonate (DFP) and PAM (Fig. 1B) for a large series of human ChE variants differing within the gorge lining, the acyl-binding site or the C-terminus, always by comparison to the wild-type enzyme forms. Thus, we were able to implicate several regions of ChEs in particular stages of catalysis based on changes in rates of inactivation and reactivation, and predict anomalous responses to ChE inhibitors for individuals carrying the 'atypical' BuChE variant.

2. Materials and methods

2.1. Chemicals

Monoclonal mouse anti-human AChE and BuChE antibodies were purified as detailed [11]. Polyclonal rabbit anti-human BuChE was a product of Dako (Glostrup, Denmark). The horseradish peroxidase (HRP) conjugate of goat anti-rabbit immunoglobulin was from Jackson Laboratories (Bar Harbor, ME); DFP was a product of Aldrich Chemical Co. (Milwaukee, WI). All other chemicals were the highest quality available from Sigma Chemical Co. (St. Louis, MO).

2.2. Mutants of BuChE

Production of natural and site-directed variants of cholinesterases and their expression in *Xenopus* oocytes has been described [4,8,13,17,18]. The enzyme samples represent products of 3 independent microinjections of mRNA for BuChE and for each of its mutants, 2 microinjections of AChE (E6) DNA [24], 1 of AChE (E5) DNA [8], and 3 microinjections of mRNA of the BuChE/AChE chimera [13].

2.3. Immobilization of recombinant enzymes

Mouse anti-human serum BuChE or monoclonal anti-human AChE antibodies [11] were adsorbed to microtiter plates (Nunc, Roskilde, Denmark) at 0.5 μg/ml in 0.1 M carbonate buffer, pH 9.6, for at least 4 h at room temperature. Plates were then washed 3 times in PBS-T buffer (144 mM NaCl, 20 mM Na phosphate, pH 7.4, 0.05% Tween-20). Free binding

sites on the well surface of the microtiter plate were blocked with PBS-T for 1 h at 37° C. Microinjected oocyte homogenates containing the enzyme were then added at a dilution of 1:20 in PBS-T or at a concentration of 100 mIU/ml in PBS-T for at least 3 h at room temperature with agitation. Plates were washed 3 times with PBS-T before use.

2.4. Inactivation of immobilized enzymes

Inactivation, reactivation and assay were all performed at pH 7.4. Immobilized enzymes were exposed to DFP in PBS-T buffer for varying times. Activity was always measured at 30 mM butyrylthiocholine, which was at least 10 times the K_m value for BuChE and the natural mutants, and 1.5- to 5-times that of the site-directed mutants [4]. Activity of AChE (E6 and E5) was measured at 2 mM acetylthiocholine.

2.5. Reactivation of inactivated immobilized enzymes

Determination of rate constants for reactivation is complicated by ageing, the progressive refractoriness of OP-inhibited enzyme to reactivation [19,30]. Once hydrolysis of one of the two alkyl groups occurs, the product, monoalkyl phosphoryl-ChE, is resistant to reactivation. The aging process proceeds concurrently with reactivation. In order to minimize the extent of ageing, inactivations were performed at sufficiently high DFP concentrations to bring residual activities to below 2% of the uninhibited level within 10 min, and reactivations were begun as soon as possible, usually within 5 min. The wells containing diisopropylphosphoryl (DIP)-ChE were exposed to 1 mM PAM in PBS-T, 22° C for various times, then washed several times with PBS-T and assayed for enzyme activity.

2.6. Assay of immobilized cholinesterases

Spectrophotometric assessment of hydrolysis rate in 96-well microtiter plates was performed as described [4,17,18,24]. To each well were added 200 μl 30 mM butyrylthiocholine (or, in the case of AChE, 2 mM acetylthiocholine) in 0.5 mM 3,3′-dithiobis(6-nitrobenzoic acid) (DTNB), 100 mM Na phosphate, pH 7.4. Absorbance at 405 nm was automatically recorded on a Molecular Devices microtiter plate reader (Menlo Park, CA).

2.7. Calculation of rate constants

Rate constants for inactivation (k_i) were calculated by linear regression analysis of $\ln(A_t)$ vs. t, where t is the time of exposure to DFP, and A_t is the remaining activity at time t. The pseudo-first order rate constant for reactivation, k_r, was calculated by linear regression analysis of $\ln(A_\infty - A_i)/(A_\infty - A_t)$ vs. t, where t is the time of exposure to PAM, and A_∞ is the potential activity, A_t, the activity at time t, and A_i, the residual activity of the inhibited enzyme.

Table 1
Kinetic rate constants for DFP-inactivation, PAM-reactivation and catalysis of cholinesterases [a]

Variant	$k_i \times 10^{-4}$ (M^{-1} min^{-1})	$k'_r \times 10^3$ (min^{-1})	$k_{cat} 10^{-3}$ (min^{-1})
BuChE	1220 ± 4 (3)	150 ± 30 (11)	96 ± 22 (6)
Chimera	19 ± 8 (2)	40 ± 18 (6)	36 ± 14 (5)
AChE (E6)	7 ± 1 (4)	6 ± 2 (3)	7.5 [c]
AChE (E5)	5 (1)	8 ± 3 (2)	
$L^{286}D$	188 ± 24 (3)	120 ± 30 (3)	38 ± 15 (5)
$L^{286}Q$	166 ± 40 (3)	120 ± 20 (4)	42 ± 24 (5)
$L^{286}R$	268 ± 164 (3)	6 ± 3 (3)	13 ± 7 (5)
$L^{286}K$	138 ± 4 (3)	4 ± 1 (3)	13 ± 5 (4)
$F^{329}R$		43 (1)	
$F^{329}Q$	1398 ± 532 (3)	44 ± 15 (5)	
$F^{329}C$	552 ± 408 (2)	14 ± 2 (4)	
$F^{329}D$	442 ± 190 (3)	8 ± 1 (4)	
$S^{425}P$ [b]	1054 ± 408 (3)	134 ± 8 (4)	
$D^{70}G$ [b]	1008 ± 418 (3)	32 ± 4 (4)	
$D^{70}G + Y^{114}H$ [b]	2112 ± 1074 (3)	12 ± 5 (3)	
$D^{70}G + S^{425}P$ [b]	260 ± 12 (2)	11 (1)	
$D^{70}G + Y^{114}H + S^{425}P$ [b]	1598 ± 294 (3)	4 ± 1 (3)	

[a] Second order rate constants for inhibition (k_i) were calculated for each of the noted variants of human ChEs from rates observed between 1 nM and 1 μM DFP, as in Fig. 3A. Pseudo-first order rate constants for reactivation (k'_r) were calculated from rates observed at 1 mM PAM, as in Fig. 3B. k_{cat} values were calculated from the rates of reaction with 30 mM butyrylthiocholine and the quantity of enzyme evaluated by ELISA assay of the enzyme, using known amounts of human serum BuChE to construct a standard curve. Numbers of experiments, in parentheses, and standard deviations are shown.

[b] Natural variant of BuChE.

[c] Taken from Ordentlich et al. [19].

2.8. Quantification of immobilized cholinesterase

A rabbit anti-human BuChE polyclonal antibody was added to the immobilized ChE at 1:4,000 dilution in PBS-T for 1 h at 37° C. After washing with PBS-T, a goat anti-rabbit antibody conjugated to HRP was added at 1:10,000 dilution in PBS-T. HRP activity was assayed by using *o*-phenylenediamine dihydrochloride at 1 mg/ml in phosphate/citrate buffer, pH 9.6, and Na perborate as substrates. Purified human BuChE was used as a standard. The absorbance at 450 nm was recorded on a Molecular Devices microtiter plate reader.

3. Results

3.1. Spatiotemporal dissociation of catalytic steps

Since residues in the gorge lining and the acyl-binding site of human BuChE differ from those in AChE (Fig. 2A), we first focussed on the involvements of these regions in the catalytic process. To this end, we collected rate constants for each of the two recombinant human enzymes as produced in microinjected *Xenopus* oocytes from the corresponding cloned in vitro transcribed mRNA [18] or cDNA [24]. To further dissect the differences between human AChE and BuChE, we also examined a chimera in which the gorge rim, the gorge lining, the conserved oxyanion hole and the choline-binding site of BuChE were substituted with the homologous peptide of AChE [13]. The major difference in the chimeric enzyme was that its gorge lining was more aromatic than BuChE. To test whether variations in the C-terminus [28] would affect catalytic properties of isolated, immobilized ChEs, we used ACHE cDNA vectors. These included a vector encoding the major form of human AChE expressed in brain and muscle [26], and designated E6, and an alternative vector, differing in the 3′-terminus and representing the variant ACHE mRNA species expressed in hematopoietic and tumor cells (E5) [8].

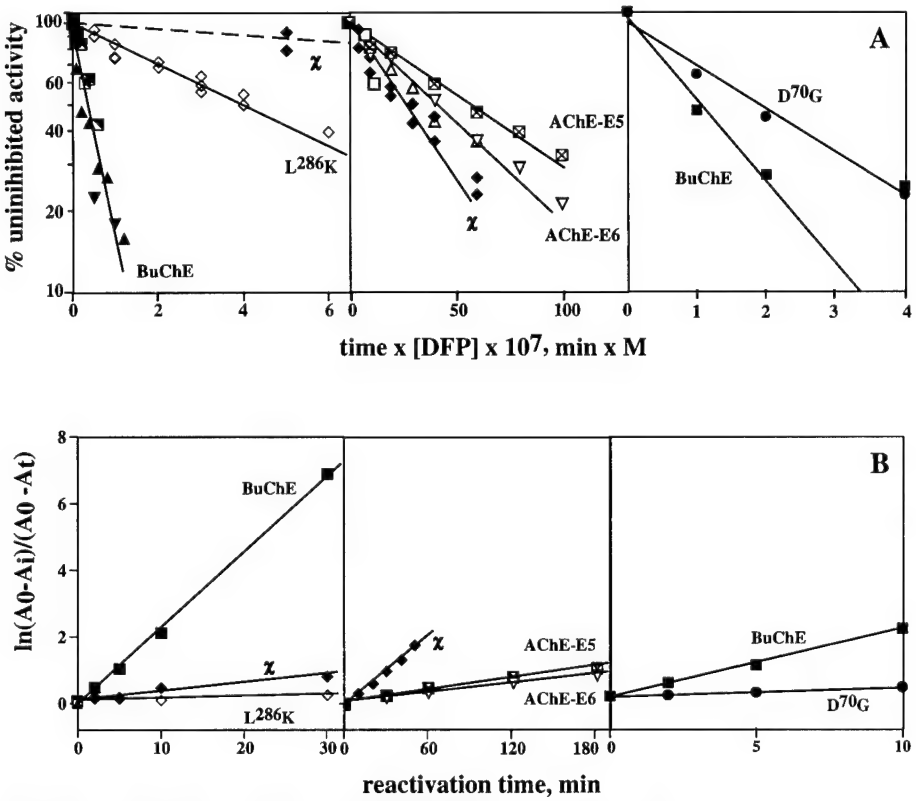

Fig. 3. Inactivation of ChEs and reactivation by PAM. A: data are presented as percent original activity vs. duration of exposure to DFP times the DFP concentration (k_i [DFP]). In the left panel, a comparison of BuChE and its $L^{286}K$ mutant and the BuChE/AChE chimera (χ). In the center panel, a comparison of the natural alternatives of AChE (E6) and AChE (E5), and the chimera. In the right panel, a comparison of representative data for the $D^{70}G$ variant and BuChE. The chimera is presented in the left panel and BuChE in the right panel to assist correlation of the rates of $L^{286}K$ and $D^{70}G$. BuChE inactivations: ■ 1 nM, ◥ 5 nM, ▲ 10 nM, ▼ 50 nM DFP. AChE (E6) inactivations: □ 0.1 μM, △ 0.5 μM, ▽ 1 μM DFP; AChE (E5) ⊠ 1 μM DFP. $L^{286}K$ BuChE inactivation: ◇ 50 nM DFP. $D^{70}G$ inactivation: ●, 5 nM DFP. B: a logarithmic function of the regain in activity vs. time is presented in the left panel for BuChE ■, the BuChE/AChE chimera ◆, and the $L^{286}K$ mutant ◇ in 1 mM PAM; in the center panel for AChE (E6) ▽, AChE (E5) ⊠, and the chimera ◆, in 0.6 mM; and in the right panel, representative data for BuChE, ●. and the $D^{70}G$ variant, ■, in 1 mM PAM.

Several natural and site-directed mutants of recombinant human BuChE completed this series. These included the 'atypical' $D^{70}G$ variant, alone or in combination with other natural mutations [17,18], and site-directed point mutations at the acyl-binding site [4]. Fig. 2B positions these changes on the ribbon model of human BuChE and Table 1 lists these alterations.

We next wished to examine the kinetic consequences that changing these defined regions in the enzyme would confer on the different steps of catalysis. To this end, each of the recombinant, immobilized enzyme variants was reacted with DFP, followed by regeneration of activity by PAM. DFP and PAM concentrations were chosen to yield phosphorylation and reactivation half-times measured in minutes. The *Xenopus* oocyte-produced enzymes were enriched by adsorption onto an immobilized antibody [11,24]. ELISA measurements provided determinations of the amounts of recombinant proteins for evaluation of k_{cat} values and confirmed that all of the examined proteins were produced in quantities of the same order of magnitude.

3.2. The gorge lining contributes to enzyme phosphorylation

Rates of DFP inactivation were determined for normal BuChE, $L^{286}K$ BuChE and the chimera as compared with the two alternative forms of AChE (Fig. 3A). The second order rate constant for inactivation of AChE by DFP, 7×10^4 min^{-1} M^{-1} (Table 1), was found to be 160-fold lower than that of BuChE. This value was in good agreement with the value of 3×10^4 min^{-1} M^{-1} determined for native, purified human AChE [14] and was almost identical to the 9.1×10^4 min^{-1} M^{-1} value determined more recently for purified recombinant human AChE [19] and to the value of 9.5×10^4 min^{-1} M^{-1} determined by Jandorf et al. [7]. Introduction of a positive charge into the acyl-binding site of the $L^{286}K$ mutant slowed the inactivation rate of BuChE approximately 8-fold (Fig. 3A). In contrast, substitution of the gorge lining by the corresponding AChE peptide with its 27 amino acid replacements, including 12 non-conservative substitutions [13], reduced this rate 60-fold, down to the level displayed by the two AChE forms (Fig. 3A).

In general, inactivation rates of natural BuChE mutants were not severely affected. There was virtually no effect of $D^{70}G$ or $S^{425}P$ alone, but the $D^{70}G/S^{425}P$ double mutant displayed a lowered inactivation rate which was paradoxically restored in the $D^{70}G/S^{425}P/Y^{114}H$ natural triple mutant [4]. Most site-directed acyl-site mutants of L^{286} and F^{329} also displayed 2- to 7-fold moderately lower inactivation rates than native BuChE, with the exception of $F^{329}Q$, which remained unchanged.

Table 2
Constants for PAM reactivation of DIP-ChEs [a]

Variant	$k_r \times 10^3$ (min^{-1})	K_d (mM)
BuChE	220 ± 60 (4)	0.30 ± 0.08
Chimera	48 ± 20 (3)	0.34 ± 0.13
AChE (E6)	7 ± 3 (3)	0.27 ± 0.04
AChE (E5)	10 ± 5 (2)	0.19 ± 0.07
$L^{286}K$	35 ± 27 (3)	> 5

[a] True first order rate constants for reactivation (k_r) and dissociation constants for the DIP-enzyme/PAM complex (K_d) were evaluated from a plot of the reciprocals of the pseudo-first order rate constants vs. the reciprocals of PAM concentrations between 0.1 and 0.6 mM. Numbers of experiments, in parentheses, and standard deviations are shown.

3.3. Active site charges hamper reactivation

To study the dephosphorylation step of catalysis, the same series of enzymes that were inhibited by DFP were further assessed for rates of reactivation by PAM. The K_d for DIP-BuChE, 0.3 mM, was close to the value of 0.2 mM found for purified diethylphosphoryl-BuChE [32]. Incidentally, the serum PAM levels that are achieved during therapy for OP poisoning do not exceed 40 μM [33], well below this value.

The pseudo-first order rate constant for reactivation of DFP-inhibited BuChE (Table 1) was 25-fold higher than for either form of AChE (Fig. 3B and Table 1). The chimera displayed a reactivation constant only moderately (4-fold) lower than that of native BuChE, demonstrating that only a small part of the difference in reactivation between AChE and BuChE is attributable to gorge-lining residues. Moreover, the lower rate for AChE and the chimera was due to a lower true first-order rate constant (k_r), whereas the affinity for PAM, K_d, remained unchanged (Table 2). In contrast, the BuChE $L^{286}K$ mutant displayed a 40-fold reduction in the pseudo-first order rate constant for reactivation, reflecting a reduction in both reactivation rate and affinity for PAM, the latter probably influenced by electrostatic repulsion by the positive charge that was introduced. This emphasizes the importance of the acyl-binding site in the reactivation process. We further substituted an acidic (aspartate), a basic (arginine), a sulfhydryl (cysteine) and a polar (glutamine) group for F^{329}. Of these, only the sulfhydryl and acidic groups disrupted the reactivation by 10- to 20-fold (Table 1).

For the natural BuChE variants, effects of $D^{70}G$ and $Y^{144}H$ on reactivation were cumulative. The natural substitution of D^{70} by glycine [17] made the resulting variant reactivate at a rate 5-fold lower than that of the wild-type enzyme (Fig. 3B, right; Table 1). Addition of the $Y^{114}H$ or $S^{425}P$ mutation to the $D^{70}G$ mutation resulted in an even slower reactivating enzyme, and a combination of all three mutations in one variant caused the most severe decrease, 40-fold, in the

rate of reactivation (Table 1). Thus, reactivation rates, as compared to the parent enzyme, were seriously impaired in certain natural and site-directed mutants of BuChE, more than in the chimera.

3.4. C-terminal variations are innocuous in catalytic terms

Both alternative ACHE DNA forms led to enzymes with similar inactivation rates (Fig. 3A and Table 1), demonstrating that the natural variability in the C-terminus of AChE contributes to the inactivation rate far less than differences in the acyl-binding site and gorge lining of ChEs. Moreover, reactivation, as well, appeared to be unaffected by the natural C-terminus modifications in AChE (Fig. 3B and Table 1). Finally, the kinetic rate constants derived for DFP-inactivation and PAM reactivation of the AChE preparations encoded by the two 3′-variable ACHE DNAs were indistinguishable (Tables 1 and 2), demonstrating that the natural C-terminal variations in AChE are innocuous in catalytic terms.

3.5. Effects of variations on k_{cat}

To investigate the contribution of specific effects of the analogous reactions on catalysis, and thereby place effects on the analogous reactions in a practical context, the consequences of each variation were further evaluated by determining turnover numbers (k_{cat}, Table 1). The k_{cat} for human BuChE as determined by us, 96,000 min^{-1}, was in good agreement with that reported for recombinant mouse BuChE [31]. Effects on k_{cat} in the various mutants were not cumulations of effects on k_i and k'_r, nor are they expected to be, as only the slowest step will be reflected in the catalytic rate. Thus, substitution of L^{286} with a basic residue reduced reactivation 40-fold but led to only a 5-fold reduction in k_{cat} (Table 1). Other replacements at this position, and substitution of the gorge lining in the chimera, had considerably smaller effects on this value. Thus, modest changes in the catalytic rate may mask large variations in the rates of specific steps in the catalytic process of both native and mutant ChEs.

4. Discussion

In order to more fully understand the biological consequences of the diversity of ChEs, we dissected the effects of specific modifications in these enzymes on distinct steps in catalysis. To this end, we employed successive OP phosphorylation and oxime-induced dephosphorylation as steps analogous to the acylation and possibly deacylation reactions of substrate hydrolysis. Adsorption of the recombinant ChEs onto immobilized selective monoclonal antibodies enriched the enzymes, separated the catalytic steps and prevented OP-induced ageing and oxime-dependent acceleration of substrate hydrolysis. The rate constants thus obtained were similar to those published for the purified proteins in solution. This, in turn, suggests wider use of our method for partial purification by adsorption onto antibody-coated wells of microtiter plates and subsequent activity assay. For example, protein phosphorylation and dephosphorylation by kinases and phosphatases, or other transient covalent modifications modulating protein properties, should be readily available for sequential dissection by this technique.

We chose to focus on three peptide regions within the human ChE molecules. These were (a) the gorge lining, known to differ in hydrophobicity between AChE and BuChE [6,29], (b) the acyl-binding site, known to be critical for the substrate specificities of AChE and BuChE [6,31] and (c) the C-terminal peptide in AChE, which is subject to natural variations due to alternative splicing [8,10]. DFP was chosen for comparative inactivation of these ChEs because of the mechanistic similarities of inactivation by DFP to the acylation stage of catalysis. Moreover, being a symmetric compound, DFP can have no inactive stereoisomer. Set against this is the fact that the phosphorus atom has 4 substituents, unlike the carbonyl carbon of substrates, which has 3, so that the substituents inevitably interact with ChEs somewhat differently than does a substrate. In any event, we found the reactivity of AChE toward DFP to be remarkably lower than that of BuChE, in spite of the close similarity of these two enzymes, a phenomenon noted 40 years ago by Jandorf et al. in the compparison of human AChE and equine BuChE [7]; our use of the 'atypical' and the chimeric enzyme suggested that aromatic gorge-lining residues, especially residues Y^{72} and Y^{124}, which participate in the peripheral anionic site [25], contribute significantly toward this difference. Interestingly, even OP agents that are, unlike DFP, designed as anti-AChE poisons, inactivate BuChE and AChE at similar rates [21], suggesting a special vulnerability of BuChE to OPs. Even in the case of those anti-AChEs, BuChE, with a larger binding site, acts as a scavenger to protect AChE [21]. In contrast, the natural alterations of the C-terminus in AChE did not affect its catalytic properties. This further emphasizes the dramatic effects of modifications in the gorge lining and acyl-binding site, regions much more important for interactions with ligands.

To draw conclusions about the effect of mutations on the first phase of catalysis by the chimera, L^{286} mutants and the AChE variants, we compared the changes in their k_i values to those observed in k_{cat}. If acylation by a mutant is rate limiting for catalysis, and if phosphorylation is perfectly analogous to acylation, we would expect a decrease in k_{cat} in the same propor-

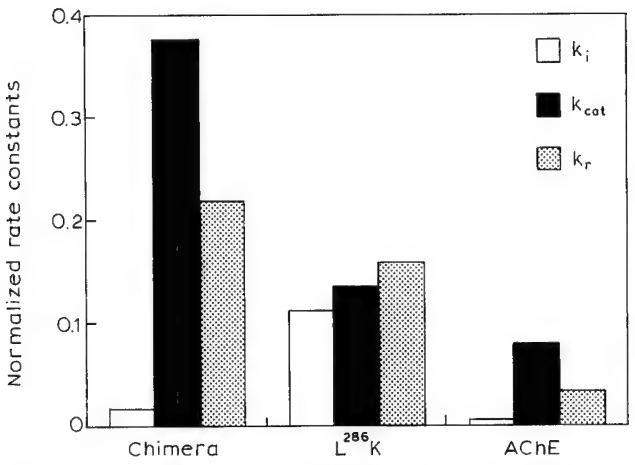

Fig. 4. Tests for the rate-limiting step. Normalized k_i, k_i(mutant)/k_i(BuChE), normalized k_r, k_r(mutant)/k_r(BuChE) and normalized k_{cat}, k_{cat}(mutant)/k_{cat}(BuChE) are presented for each protein. Bar heights for the variants are shown in comparison to the reference enzyme, BuChE.

tion as in k_i. Thus, k_i(mutant)/k_i(BuChE), called normalized k_i, would be equal to normalized k_{cat}, k_{cat}(mutant)/k_{cat}(BuChE), for any mutant for which acylation is the rate-limiting step. If, however, acylation is not rate limiting for a mutant, there is no coupling of the values of the rate constants. In such cases, the rate-limiting step of catalysis may be seriously impaired while inactivation rate remains high (normalized $k_i \gg$ normalized k_{cat}), or catalysis can remain unaffected while inactivation is impaired (normalized $k_i \ll$ normalized k_{cat}). Fig. 4 presents these normalized values in a bar graph. We find that for the $L^{286}K$ mutant (Fig. 4) acylation appears to be rate limiting (the height of the normalized k_i bar is approximately that for the normalized k_{cat} bar), but for the chimera, normalized k_i is very different from normalized k_{cat}.

In the same way, we can calculate a normalized k_r, k_r(mutant)/k_r(BuChE), to test whether, given the reservations we have noted, reactivation can be a reliable model for deacylation, i.e. whether this parameter gives information that is consistent with findings for the acylation step. For the chimera, the height of the normalized k_r bar was close to that for the normalized k_{cat} bar. Therefore, by the same criterion we use for inactivation/acylation, we can tentatively conclude that for the chimera, deacylation is rate limiting (Fig. 4). This analysis indicates that for the $L^{286}K$ mutant deacylation is also rate limiting (Fig. 4). Thus, for the chimera we find a single rate-limiting step, whereas this analysis for the $L^{286}K$ mutant is in apparent contradiction to our finding regarding acylation. Nevertheless, for the mutant both acylation and deacylation may proceed at closely similar rates, a conclusion previously reached by Quinn on the basis of his mechanistic studies on AChE [20]. Our observation that there are ChEs for which either phase of reaction seems to be rate limiting, apparently indicates the two rates are similar, and that small modification in structure can make either step decisively rate limiting. Finally, the normalized k_r and k_{cat} bars for AChE are approximately equal, implying that for AChE acting on the poor substrate, butyrylthiocholine, deacylation seems to be rate limiting.

The strikingly lower inactivation rate of the chimera than that of BuChE may be attributable to its having its active site gorge narrowed by numerous aromatic residues. (The chimera's acyl binding site is unchanged.) Nevertheless, it appears (Fig. 4) that for the chimera deacylation is the rate-limiting step. This could be due to subtle realignments of functional residues at the catalytic site. For the $L^{286}K$ mutation, both inactivation and reactivation are affected. Introduction of a positive charge at the acyl biding site, and possibly also tightly bound water molecules, may disrupt both phases of the reaction. The capacity of AChE to hydrolyze the disfavored substrate, butyrylthiocholine, is reduced to 1/30th the rate of BuChE. This may indicate that even with a narrower gorge and tighter acyl-binding site, deacylation is rate limiting. With the optimal substrate, we suspect the acylation phase for AChE to be even faster, with deacylation remaining the rate-limiting step.

The accessibility of BuChE as a serum enzyme raises the possibility that PAM acts by regenerating BuChE and allowing it to react with more of the OP before the OP has a chance to inactivate neuromuscular AChE, in effect turning serum BuChE into an OPase. A finding with important consequences for dealing with OP poisoning is that $D^{70}G$, by far the most common of the phenotypically different BuChE variants [34] reacts with DFP as fast as the normal enzyme, but is reactivated by PAM at only one-fifth the rate. Since $D^{70}G$ also has a 4-fold lower specific activity, than the wild type enzyme (ref. [17] and unpublished observations), $D^{70}G$ BuChE will have less detoxifying capacity to protect OP-poisoned individuals than its normal counterpart. Moveover, when intravenous PAM administration, in conjunction with other therapies, is used to treat OP intoxication [30], carriers of $D^{70}G$ BuChE will have a genetic predisposition to poor responses to such therapy. This applies to 'atypical' homozygotes, as well as heterozygotes, who together compose up to 7.5% of some populations [2]. Thus, the recently reported variable efficacy of PAM treatment [33] may be due to genetic diversity in the treated patients. Individual differences may further be expected in the sensitivity to poisoning by therapeutic anti-ChEs, such as those used in Alzheimer's disease [9]. Natural anti-ChEs, such as glyco-alkaloids in *Solanum* plants [18] and neurotoxins excreted by cyanobacteria [1] may also have diverse effects on these individuals. From an evolutionary point of view, the existence in all vertebrates of two distinct ChEs with specific catalytic properties may be of vital

importance as a survival advantage. Moreover, the emergence of genetically polymorphic alleles of BuChE can be advantageous to all higher animal species, which must be able to defend themselves against threats characteristic of the environment to which they have adapted. The biological effects of natural and synthesized anti-ChE agents, depending as they do upon an initial encounter with BuChE, will thus be greatly influenced by just which BuChE allele an individual carries.

Acknowledgements

This study was supported by a grant from the Medical Research and Development Command of the U.S. Army (to H.S.). M.S. was a recipient of a Levi Eshkol Post-Doctoral Fellowship, D.G. received support from the Israel Ministry of Immigrant Absorption, and J.L. was a recipient of an EMBO Fellowship.

References

[1] Carmichael, W.W., The toxins of cyanobacteria, *Scientific Am.*, 270 (1994) 64–72.

[2] Ehrlich, G., Ginzberg, D., Loewenstein, Y., Glick, D., Kerem, B., Ben-Ari, S., Zakut, H. and Soreq, H., Population diversity and distinct hapotype frequencies associated with ACHE and BCHE genes of Israeli Jews from transcaucasian Georgia and from Europe, *Genomics,* 22 (1994) 288–295.

[3] Gilson, J.K., Straatsma, T.P., McCammon, J.A., Ripoll, D.R., Faerman, C.H., Axelsen, P.H., Silman, I. and Sussman, J.L, Open 'back door' in a molecular dynamics simulation of acetylcholinesterase, *Science,* 263 (1994) 1276–1278.

[4] Gnatt, A., Loewenstein, Y., Yaron, A., Schwarz, M. and Soreq, H., Site-directed mutagenesis of active site residues reveals plasticity of human butyrylcholinesterase in substrate and inhibitor interactions, *J. Neurochem.*, 62 (1994) 749–755.

[5] Hackley Jr., B.E., Plapinger, R., Stolberg, M. and Wagner-Jauregg, T., Acceleration of the hydrolysis of organic fluorophosphates and fluorophosphonates with hydroxamic acids, *J. Am. Chem. Soc.*, 77 (1955) 3651–3653.

[6] Harel, M., Sussman, J.L., Krejci, E., Bon, S., Chanal, P., Massoulie, J. and Silman, I., Conversion of acetylcholinesterase to butyrylcholinesterase: modeling and mutagenesis, *Proc. Natl. Acad. Sci. USA,* 89 (1992) 10827–10831.

[7] Jandorf, B.J., Michel, H.O., Schaffer, N.K., Egan, R. and Summerson, W.H., The mechanism of reaction between esterases and phosphorus-containing anti-esterases, *Disc. Faraday Soc.*, 20 (1955) 134–142.

[8] Karpel, R., Ben Aziz-Aloya, R., Sternfeld, M., Ehrlich, G., Ginzberg, D., Tarroni, P., Clementi, F., Zakut, H. and Soreq, H., Expression of three alternative acetylcholinesterase messenger RNAs in human tumor cell lines of different tissue origins, *Exp. Cell Res.*, 210 (1994) 268–277.

[9] Knapp, M.J., Knopman, D.S., Solomon, P.R., Pendlebury, W.W., Davis, C.S. and Gracon, S.I., A 30-week randomized controlled trial of high-dose tacrine in patients with Alzheimer's disease, *J. Am. Med. Assn.*, 271 (1994) 985–991.

[10] Li, Y., Camp, S. and Taylor, P., Tissue-specific expression and alternative mRNA processing of the mammalian acetylcholinesterase gene, *J. Biol. Chem.*, 268 (1993) 5790–5797.

[11] Liao, J., Mortensen, V., Norgaard-Pedersen, B., Koch, C. and Brodbeck, U., Monoclonal antibodies against brain acetylcholinesterases which recognize the subunits bearing the hydrophobic anchor, *Eur. J. Biochem.*, 215 (1993) 333–340.

[12] Liu, W., Zhao, K.-Y. and Tsou, C.-L., Reactivation kinetics of diethylphosphoryl acetylcholine esterase, *Eur. J. Biochem.*, 151 (1985) 525–529.

[13] Loewenstein, Y., Gnatt, A., Neville, L.F. and Soreq, H., Chimeric human cholinesterase: identification of interaction sites responsible for recognition of acetyl- or butyrylcholinesterase-specific ligands, *J. Mol. Biol.*, 234 (1993) 289–296.

[14] Main, A.R. and Iverson, F., Measurement of the affinity and phosphorylation constants governing irreversible inhibition of cholinesterases by di-isopropyl phosphofluoridate, *Biochem. J.*, 100 (1966) 525–531.

[15] Massoulie, J., Pezzementi, L., Bon, S., Krejci, E. and Vallette, F.M., Molecular and cellular biology of cholinesterases, *Prog. Neurobiol.*, 41 (1993) 31–91.

[16] McGuire M.C., Nogueira, C.P., Bartels, C.P., Lightstone, H., Hajra, A., van der Spek, A.F.L., Lockridge, O. and La Du, B.N., Identification of the structural mutation responsible for the dicbucaine-resistant (atypical) variant form of human serum cholinesterase, *Proc. Natl. Acad. Sci. USA*, 86 (1989) 953–957.

[17] Neville, L.F., Gnatt, A., Padan, R., Seidman, S. and Soreq, H., Anionic site interactions in human butyrylcholinesterase disrupted by two single point mutations, *J. Biol. Chem.*, 265 (1990) 20735–20738.

[18] Neville, L.F., Gnatt, A., Loewenstein, Y., Seidman, S., Ehrlich, G. and Soreq, H., Intramolecular relationships in cholinesterases revealed by oocyte expression of site-directed and natural variants of human BCHE, *EMBO J.*, 11 (1992) 1641–1649.

[19] Ordentlich, A., Kronman, C., Barak, D., Stein, D., Ariel, N., Marcus, D., Velan, B. and Shafferman, A., Engineering resistance to aging of phosphylated human acetylcholinesterase. Role of hydrogen bond network in the active center, *FEBS Lett.*, 334 (1993) 215–220.

[20] Quinn, D.M., Acetylcholinesterase: enzyme structure, reaction dynamics, and virtual transition states, *Chem. Rev.*, 87 (1987) 955–979.

[21] Raveh, L., Grunwald, J., Marcus, D., Papier, Y., Cohen, E. and Ashani, Y., Human butyrylcholinesterase as a general prophylactic antidote for nerve agent toxicity, *Biochem. Pharmacol.*, 45 (1993) 2465–2474.

[22] Rosenberry, T.L., Acetylcholinesterase, *Adv. Enzymol.*, 43 (1975) 104–210.

[23] Schumacher, M., Camp, S., Maulet, Y., Newton, M., MacPhee-Quigley, K., Taylor, S.S., Friedmann, T. and Taylor, P., Primary structure of *Torpedo californica* acetylcholinesterase deduced from its cDNA sequence, *Nature*, 319 (1986) 407–409.

[24] Seidman, S., Ben Aziz-Aloya, R., Timberg, R., Loewenstein, Y., Velan, B., Shafferman, A., Liao, J., Norgaard-Pedersen, B., Brodbeck, U. and Soreq, H., Overexpressed monomeric human acetylcholinesterase induces subtle ultrastructural modifications in developing neuromuscular junctions of *Xenopus laevis* embryos, *J. Neurochem.*, 62 (1994) 1670–1681.

[25] Shafferman, S., Velan, B., Ordentlich, A., Kronman, C., Grosfeld, H., Leitner, M., Flashner, Y., Cohen, S., Barak, D. and Ariel, N., Substrate inhibition of acetylcholinesterase: residues affecting signal transduction from the surface to the catalytic center, *EMBO J.*, 11 (1992) 3651–3658.

[26] Soreq, H., Ben-Aziz, R., Prody, C.A., Seidman, S., Gnatt, A., Neville, L., Lieman-Hurwitz, J., Lev-Lehman, E., Ginsberg, D., Lapidot-Lifson, Y. and Zakut, H., Molecular cloning and construction of the coding region of human acetylcholinesterase

reveals a G,C-rich attenuating structure, *Proc. Natl. Acad. Sci. USA*, 87 (1990) 9688–9692.

[27] Soreq, H., Gnatt, A., Loewenstein, Y. and Neville, L.F., Excavations into the active site gorge of cholinesterases, *Trends Biochem. Sci.*, 17 (1992) 353–358.

[28] Soreq, H. and Zakut, H., *Human Cholinesterases and Anticholinesterases*, Academic Press, San Diego, 1993.

[29] Sussman, J.L., Harel, M., Frolow, F., Oefner, C., Goldman, A., Toker, L. and Silman, I., Atomic structure of acetylcholinesterase from *Torpedo californica*: a prototypic acetylcholine-binding protein, *Science*, 253 (1991) 872–879.

[30] Taylor, P., Cholinergic agonists, Anticholinesterase agents. In A.G. Gilman, L.S. Goodman, T.W. Rall, A.S. Nies and P. Taylor (Eds.), *The Pharmacological Basis of Therapeutics*, 8th Ed., Pergamon Press, New York, 1990, pp. 122–147.

[31] Vellom, D.C., Radic, Z., Li, Y., Pickering, N.A., Camp, S. and Taylor, P., Amino acid residues controlling acetylcholinesterase and butyrylcholinesterase specificity, *Biochemistry*, 32 (1993) 12–17.

[32] Wang, E.I.C. and Braid, P.E., Oxime reactivation of diethylphosphoryl human serum cholinesterase, *J. Biol. Chem.*, 242 (1967) 2683–2687.

[33] Willems, J.L., DeBisschop, H.C., Verstraete, A.G., Declerck, C., Christiaens, Y., Vanscheeuwyck, P., Buylaert, W.A., Vogelaers, D. and Colardyn, F., Cholinesterase reactivation in organophosphorus poisoned patients depends on the plasma concentrations of the oxime pralidoxime methylsulphate and of the organophosphate, *Arch. Toxicol.*, 67 (1993) 79–84.

[34] Whittaker, M., *Cholinesterase*, Karger, Basel, 1986.

[35] Wilson, I.B., The mechanism of enzyme hydrolysis studied with acetylcholinesterase. In W.D. McElroy and B. Glass (Eds.), *The Mechanism of Enzyme Catalysis*, The Johns Hopkins Press, Baltimore, 1954, pp. 642–657.

Journal of Neurochemistry
Raven Press, Ltd., New York

Overexpressed Monomeric Human Acetylcholinesterase Induces Subtle Ultrastructural Modifications in Developing Neuromuscular Junctions of *Xenopus laevis* Embryos

Shlomo Seidman, Revital Ben Aziz-Aloya, Rina Timberg, Yael Loewenstein, *Baruch Velan, *Avigdor Shafferman, †Jian Liao, ‡Bent Norgaard-Pedersen, †Urs Brodbeck, and Hermona Soreq

*Department of Biological Chemistry, Hebrew University of Jerusalem, Jerusalem; *Department of Biochemistry, Israel Institute for Biological Research, Ness-Ziona, Israel; †Institute of Biochemistry and Molecular Biology, University of Bern, Bern, Switzerland; and ‡Statens Seruminstitut, Copenhagen, Denmark*

Abstract: Formation of a functional neuromuscular junction (NMJ) involves the biosynthesis and transport of numerous muscle-specific proteins, among them the acetylcholine-hydrolyzing enzyme acetylcholinesterase (AChE). To study the mechanisms underlying this process, we have expressed DNA encoding human AChE downstream of the cytomegalovirus promoter in oocytes and developing embryos of *Xenopus laevis*. Recombinant human AChE (rHAChE) produced in *Xenopus* was biochemically and immunochemically indistinguishable from native human AChE but clearly distinguished from the endogenous frog enzyme. In microinjected embryos, high levels of catalytically active rHAChE induced a transient state of overexpression that persisted for at least 4 days postfertilization. rHAChE appeared exclusively as nonassembled monomers in embryos at times when endogenous *Xenopus* AChE displayed complex oligomeric assembly. Nonetheless, cell-associated rHAChE accumulated in myotomes of 2- and 3-day-old embryos within the same subcellular compartments as native *Xenopus* AChE. NMJs from 3-day-old DNA-injected embryos displayed fourfold or greater overexpression of AChE, a 30% increase in postsynaptic membrane length, and increased folding of the postsynaptic membrane. These findings indicate that an evolutionarily conserved property directs the intracellular trafficking and synaptic targeting of AChE in muscle and support a role for AChE in vertebrate synaptogenesis.
Key Words: Neuromuscular junction—*Xenopus laevis* embryos—Human acetylcholinesterase—Muscle.
J. Neurochem. **62,** 1670–1681 (1994).

Formation of a functional neuromuscular junction (NMJ) requires the targeted deposition of synaptic proteins at the nerve–muscle interface (Flucher and Daniels, 1989; Froehner, 1991; Ohlendieck et al., 1991). Among these proteins is the acetylcholine-hydrolyzing enzyme acetylcholinesterase (AChE), responsible for terminating cholinergic neurotransmission across the NMJ (Hall, 1973). It is not yet clear how the selective accumulation of synapse-specific proteins at the NMJ is accomplished. One mechanism for achieving synaptic localization of AChE is probably the compartmentalized transcription and translation of AChE mRNA (Rotundo, 1990; Rossi and Rotundo, 1992). Aggregation and anchoring of AChE at the postsynaptic cell surface are mediated by evolutionarily conserved components of the synaptic basal lamina, such as heparan sulfate proteoglycans (Brandan et al., 1985) and agrin (McMahan, 1990). Similar mechanisms appear to be involved in the biosynthesis of the nicotinic acetylcholine receptor (AChR) (Changeux, 1991; Phillips et al., 1991; Wallace, 1991) and may represent a general solution to the problem of localizing junctional proteins in muscle cells (Pavlath et al., 1989; Ralston and Hall, 1989). However, the molecular determinants controlling the intracellular transport of AChE and the elements specifying its synaptic localization in muscle remain to be elucidated.

In the developing *Xenopus laevis* embryo, muscle differentiation, primitive neuromuscular contacts, and spontaneous synaptic activity are observed within 1 day postfertilization (PF) (Kullberg et al., 1977). During the ensuing 24 h, ultrastructural specializations characterizing synaptic differentiation are observed, followed by the acquisition of spontaneous

Received July 14, 1993; revised manuscript received September 16, 1993; accepted September 16, 1993.

Address correspondence and reprint requests to Dr. H. Soreq at Department of Biological Chemistry, Hebrew University of Jerusalem, Jerusalem, 91904, Israel.

Abbreviations used: AChE, acetylcholinesterase; ACHE, acetylcholinesterase gene; AChR, acetylcholine receptor; CMV, cytomegalovirus; CMVACHE, acetylcholinesterase cDNA downstream of the cytomegalovirus promoter–enhancer element; mAb, monoclonal antibody; NMJ, neuromuscular junction; PF, postfertilization; rHAChE, recombinant human acetylcholinesterase.

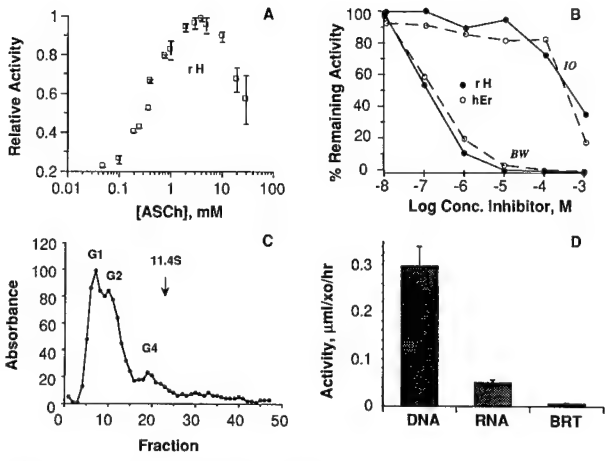

FIG. 1. *Xenopus* oocytes express catalytically active rHAChE. **A:** Inhibition by excess substrate. Mature *Xenopus* oocytes were injected with 5 ng of in vitro-transcribed AChE mRNA (Soreq et al., 1990) and incubated overnight at 17°C. Homogenates corresponding to one-third oocyte were assayed for AChE activity in the presence of various concentrations of acetylthiocholine (ASCh) substrate [average of three experiments ± SEM (bars)]. **B:** Sensitivity to selective inhibitors. Oocyte homogenates were preincubated for 30 min in assay buffer containing the AChE-specific, reversible inhibitor 1,5-bis(4-allyldimethylammoniumphenyl)-pentan-3-one dibromide [BW284C51 (BW)] or the butyrylcholinesterase-specific inhibitor tetraisopropylpyrophosphoramide (IO) at the indicated concentrations and assayed for remaining activity following addition of 2 m*M* ASCh. Data are averages of duplicate assays from two independent microinjection experiments. AChE extracted from human erythrocytes (hEr) served as control. rH, rHAChE. **C:** Oligomeric assembly. Homogenates from ACHE mRNA-injected oocytes were subjected to sucrose density centrifugation as described in Materials and Methods. Data are averages of three experiments. Note that in addition to the free monomer (3.2S; G1), the oocyte appears to generate dimers (5.6S; G2) and to a lesser extent tetramers (10.2S; G4) of human AChE. Endogenous oocyte AChE activity is undetectable under these conditions. The arrow marks the position of bovine liver catalase (11.4S). **D:** Expression of ACHE DNA in *Xenopus*. Oocytes were injected with 5 ng of synthetic ACHE mRNA or CMVACHE (Velan et al., 1991*a*) and incubated for 1 (RNA) to 3 (DNA) days. Oocytes injected with incubation medium (BRT) or uninjected oocytes served as control. Activity is expressed as micromoles of substrate hydrolyzed per hour per oocyte, in mean ± SEM (bars) values for three independent microinjection experiments.

motor activity and hatching (Cohen, 1980). Fervent embryonic development and ultrastructural maturation of the neuromuscular system continue, giving rise to a free swimming tadpole within 4–5 days. From day 2 PF, a steady increase in AChE activity is observed (Gindi and Knowland, 1979), concomitant with a developmentally regulated decrease in the time course of the synaptic potential in *Xenopus* myotomes (Kullberg et al., 1980). The rapid development of the neuromuscular system in *Xenopus* thus makes it an excellent in vivo model for the study of vertebrate myogenesis and synaptogenesis.

We have cloned a DNA sequence encoding human AChE and used it to express catalytically active AChE in microinjected *Xenopus* oocytes (Soreq et al., 1990) and cultured human cells (Velan et al., 1991*a*). Placed downstream of either the native human AChE gene (ACHE) promoter or the cytomegalovirus (CMV) enhancer–promoter and introduced into fertilized *Xenopus* eggs, this DNA led to overexpression of AChE in NMJs of 2-day-old embryos (Ben Aziz-Aloya et al., 1993). Here, we present a biochemical and histochemical characterization of this recombinant human AChE (rHAChE) as expressed in *Xenopus*. Moreover, we demonstrate the persistence of overexpressed enzyme in NMJs to at least day 3 of embryonic development and offer evidence indicating subtle alterations in the ultrastructure of NMJs from embryos overexpressing rHAChE. Our findings indicate the assignment of catalytically active monomeric rHAChE to subcellular compartments common to those occupied by native, multimeric *Xenopus* AChE in embryonic myotomes and suggest a morphogenetic role for AChE in vertebrate synaptogenesis.

MATERIALS AND METHODS

In vitro fertilization and microinjections

DNA microinjections into *X. laevis* oocytes and fertilized eggs were essentially as previously described (Ben Aziz-

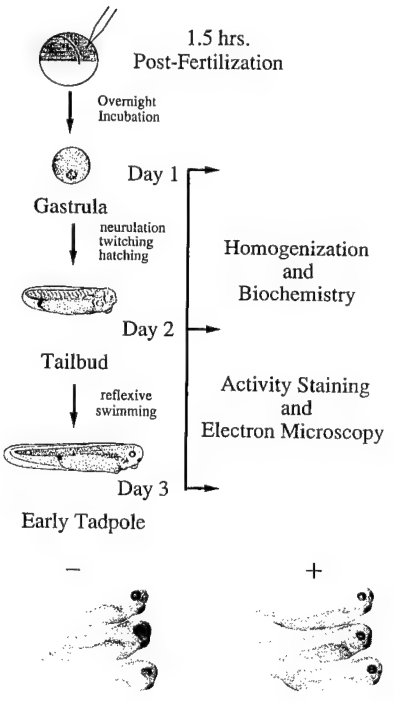

FIG. 2. Normal development of CMVACHE-injected embryos. A schematic representation of a microinjection experiment depicting the principal developmental stages and analytical approaches used in this work is shown together with photographs displaying the normal gross development of unstained microinjected embryos (+) compared with control uninjected embryos (−) 3 days PF. In vitro fertilized eggs of *Xenopus laevis* were injected with 1 ng of CMVACHE and cultured for 1–4 days as described in Materials and Methods. Sketches are modeled after those of Deuchar (1966).

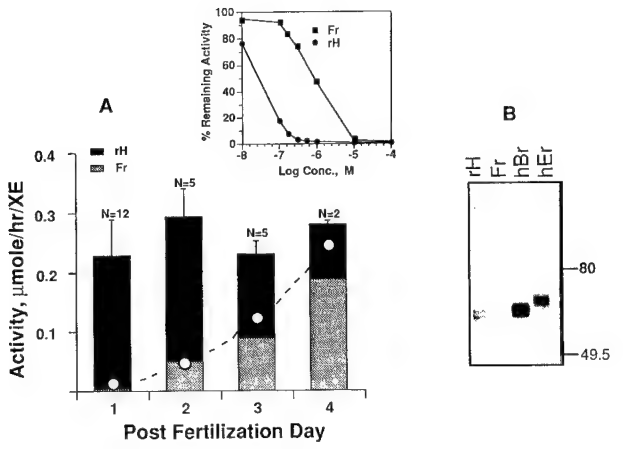

FIG. 3. CMVACHE-injected *Xenopus* embryos express and maintain biochemically distinct heterologous human AChE for at least 4 days. **A:** Overexpression of rHAChE in developing embryos. High-salt/detergent extracts of CMVACHE-injected and uninjected embryos were prepared and assayed for AChE activity in the presence and absence of the selective inhibitor echothiophate (3.3×10^{-7} *M*; **inset**). Endogenous AChE activity was calculated according to an algorithm assuming 90% inhibition of rHAChE and 20% inhibition of frog AChE at this concentration of inhibitor. The bar graph represents the total AChE activity measured per microinjected embryo at various time points following microinjection and the calculated activities attributable to rHAChE (dark shading) and endogenous frog AChE (light shading). The total AChE activity measured in uninjected control embryos at the same time points is indicated by open circles. Data represent average ± SEM (bars) values from four to six embryos from the indicated number (N) of independent microinjection experiments. Inset: Selective inhibition of rHAChE by echothiophate. Homogenates representing endogenous frog (Fr) or recombinant human (rH) AChE were assayed for activity following a 40-min preincubation with the indicated concentrations of echothiophate. Data are averages of three experiments. **B:** Immunochemical discrimination between rHAChE and embryonic *Xenopus* AChE. Affinity-purified AChE from CMVACHE-injected *Xenopus* embryos (rH), control uninjected embryos (Fr), human brain (hBr), and erythrocytes (hEr) was subjected to denaturing gel electrophoresis and protein blot analysis as described in Materials and Methods. Each lane represents ~20 ng of protein, except rH, which contained only 6 ng. Note the complete absence of immunoreactivity with embryonic *Xenopus* AChE, although silver staining of a parallel gel demonstrated detectable protein at the corresponding position (data not shown). The faint upper bands (140–160 kDa) in the lanes displaying native human AChEs represent dimeric forms resulting from incomplete reduction of the intersubunit disulfide bonds (see Liao et al., 1992). Prestained molecular weight markers indicated on the right were from Bio-Rad, U.S.A..

Aloya et al., 1993). Fertilized eggs were dejellied with 2% cysteine and injected within the first two cleavage cycles in medium containing 5% Ficoll in 0.3× Mark's modified Ringer (MMR). Several hours after microinjection, embryos were transferred into 0.3× MMR and cultured overnight at 17–19°C. One-day-old embryos were transferred to either 0.1× MMR or aged tap water and cultured for an additional 1–3 days.

Activity assays

Embryos were harvested in groups of three to five apparently normal individuals and stored frozen until used. Homogenates were prepared in a high-salt/detergent buffer [0.01 *M* Tris, 1.0 *M* NaCl, 1% Triton X-100, and 1 m*M* EGTA (pH 7.4); 150 μl per embryo] and assayed for enzymatic activity as detailed elsewhere (Neville et al., 1992). For subcellular fractionations, groups of three embryos were homogenized in low-salt buffer [0.02 *M* Tris-HCl (pH 7.5), 0.01 *M* $MgCl_2$, and 0.05 *M* NaCl; 100 μl per embryo] and centrifuged at 100,000 rpm for 10 min in a Beckman model TL100 tabletop ultracentrifuge. The supernatant was collected and considered the low-salt-soluble fraction. The pellet was resuspended in low-salt/detergent buffer [0.01 *M* phosphate buffer (pH 7.4) and 1% Triton X-100], incubated on ice for 1 h, and centrifuged as above for 5 min to generate the detergent-soluble fraction. The remaining pellet was resuspended in high-salt buffer [0.01 *M* phosphate buffer (pH 7.4), 1.0 *M* NaCl, and 1 m*M* EGTA] to release the high-salt-soluble AChE fraction.

Protein blot analyses

rHAChE was purified by affinity chromatography from ~180 "day 1" embryos injected with plasmid DNA carrying AChE cDNA downstream of the CMV promoter–enhancer element (CMVACHE) using a modified procedure for the purification of native human AChE (Gennari and Brodbeck, 1985). In brief, AChE from embryos homogenized in low-salt/detergent buffer was bound to Sepharose beads carrying *N*-(1-amino-hexyl)-3-dimethylethylaminobenzoic amide by shaking overnight at room temperature. Elution was with 0.02 *M* edrophonium chloride (Tensilon; Hoffmann-La Roche, Basel, Switzerland). Embryonic *Xenopus* AChE was similarly purified from 1-week-old tadpoles but had to be eluted by boiling in 0.1% sodium dodecyl sulfate. Denaturing sodium dodecyl sulfate–polyacrylamide gel electrophoresis and blotting were essentially as described elsewhere (Liao et al., 1992) using a pool of monoclonal antibodies (mAbs; 132-1,2,3; 6 μg/ml each) raised against denatured human brain AChE (Brodbeck and Liao, 1992).

Sucrose gradient analysis of AChE subunit assembly

Freshly prepared, high-salt/detergent extracts from one or two embryos or five to 10 oocytes were applied to 12-ml 5–20% linear sucrose density gradients and centrifuged overnight at 4°C. Fractions were collected into 96-well mi-

TABLE 1. *Subcellular fractionation of rHAChE in CMVACHE-injected* Xenopus *embryos*

	rH			
Fraction	Day 1	Day 2	Day 3	Fr (day 3)
LSS	57 ± 2	60 ± 4	53 ± 3	36 ± 5
DS	37 ± 2	34 ± 4	36 ± 3	31 ± 4
HSS	6 ± 2	5 ± 1	10 ± 1	33 ± 7

Fertilized *Xenopus* eggs were microinjected with 1 ng of CMVACHE DNA, cultured for 1–3 days, and subjected to homogenization and subcellular fractionation as described in Materials and Methods. rHAChE in each fraction (rH) was detected by enzyme–antigen immunoassay (Liao et al., 1992) using a specific mAb (101-1) raised against bovine brain AChE. Endogenous AChE activity in uninjected tadpoles (Fr) was determined by the standard colorimetric assay described in Materials and Methods. Percent enzyme activity in each fraction (average ± SEM) is shown for three to five groups of three embryos from a single microinjection experiment. LS, low-salt soluble; DS, detergent soluble; HSS, high-salt soluble.

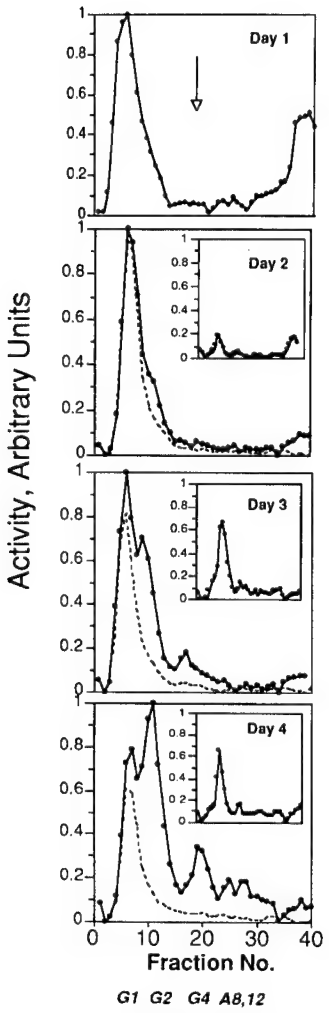

FIG. 4. rHAChE in microinjected *Xenopus* embryos remains monomeric. High-salt/detergent extracts representing two embryos were subjected to sucrose density centrifugation as described in Materials and Methods. Shown are total AChE (solid line) and immunoreactive rHAChE (dotted line) from CMVACHE-injected embryos 1–4 days PF. rHAChE appeared exclusively as a peak representing monomeric AChE (~3.2S) at all time points. The arrow marks the position of bovine liver catalase (11.4S). **Insets:** AChE molecular forms in control uninjected embryos scaled to the total activity levels observed in DNA-injected embryos (see Fig. 2). Peak analysis demonstrated that the distribution of oligomeric forms was identical to that observed in CMVACHE-injected embryos. Note that monomeric AChE is essentially undetectable in control embryos. G1, G2, and G4 indicate the expected positions of the globular monomer, dimer, and tetramer in the gradient; A8 and 12 indicate the positions of "tailed" asymmetric forms. Fraction 0 represents the top of the gradient.

crotiter plates and assayed for total AChE activity as previously described (Soreq et al., 1989). To distinguish between rHAChE and endogenous *Xenopus* AChE in gradient fractions, 100-μl aliquots were transferred to a Maxisorp immunoplate (Nunc, Copenhagen, Denmark) coated with an mAb (mAb 101-1) recognizing human but not frog AChE and diluted 1:1 with double distilled water. Following overnight incubation, the plates were washed three times with phosphate-buffered saline containing 0.05% Tween 20, and each well was assayed for catalytically active AChE.

Cytochemical AChE staining and electron microscopy

Embryos were fixed, cytochemically stained for AChE, and prepared for electron microscopy as previously described (Ben Aziz-Aloya et al., 1993). Cytochemical staining (Karnovsky, 1964) was carried out in acetate buffer (pH 6.1) for 15–20 min at 4°C within 3 days of fixation.

RESULTS

Xenopus-expressed AChE is biochemically indistinguishable from native human AChE

Microinjected into mature *X. laevis* oocytes, 5 ng of in vitro-transcribed AChE mRNA directed the production of catalytically active AChE displaying substrate and inhibitor interactions characteristic of the native human enzyme (Fig. 1A and B). The apparent K_m calculated for rHAChE toward acetylthiocholine was 0.3 m*M*, essentially identical to that displayed by rHAChE expressed in cell lines (Velan et al., 1991*a*) and native human erythrocyte AChE (data not shown). In sucrose density centrifugation rHAChE sedimented primarily as monomers and dimers, although a discernible peak apparently representing globular tetrameric AChE was also observed (Fig. 1C). When CMVACHE (Velan et al., 1991*a*) was microinjected into oocytes, active AChE in yields 10–20-fold higher than that observed following RNA injections was obtained (Fig. 1D), demonstrating efficient transcription from this promoter in *Xenopus*.

Transient expression of CMVACHE in *Xenopus* embryos

Microinjected into cleaving *Xenopus* embryos, CMVACHE directed the biosynthesis of rHAChE at levels similar to those observed in DNA-injected oocytes. Yet, the gross morphology and development of CMVACHE-injected embryos appeared completely normal (Fig. 2). Moreover, gross motor function of microinjected embryos, as evaluated by twitching and hatching on day 2, reflexive swimming on day 3, and free swimming on later days, was unimpaired compared with normal, uninjected controls. Microinjected tadpoles survived up to 4 weeks, showing no overt developmental handicaps (data not shown). Following overnight incubation, at which time embryos had reached the late gastrula stage, endogenous AChE levels were negligible, and rHAChE activity represented a 50–100-fold excess over normal (Fig. 3A). From day 2 PF, detectable endogenous AChE activities increased steadily. Using the irreversible AChE inhibitor echothiophate (Neville et al., 1992) to distinguish between endogenous frog AChE and rHAChE (Fig. 3A, inset), we observed the persistence of receding levels of rHAChE for at least 4 days PF. For the first 3 days rHAChE accounted for >50% of the total measured AChE activity in microinjected embryos and resulted in a state of general overexpression com-

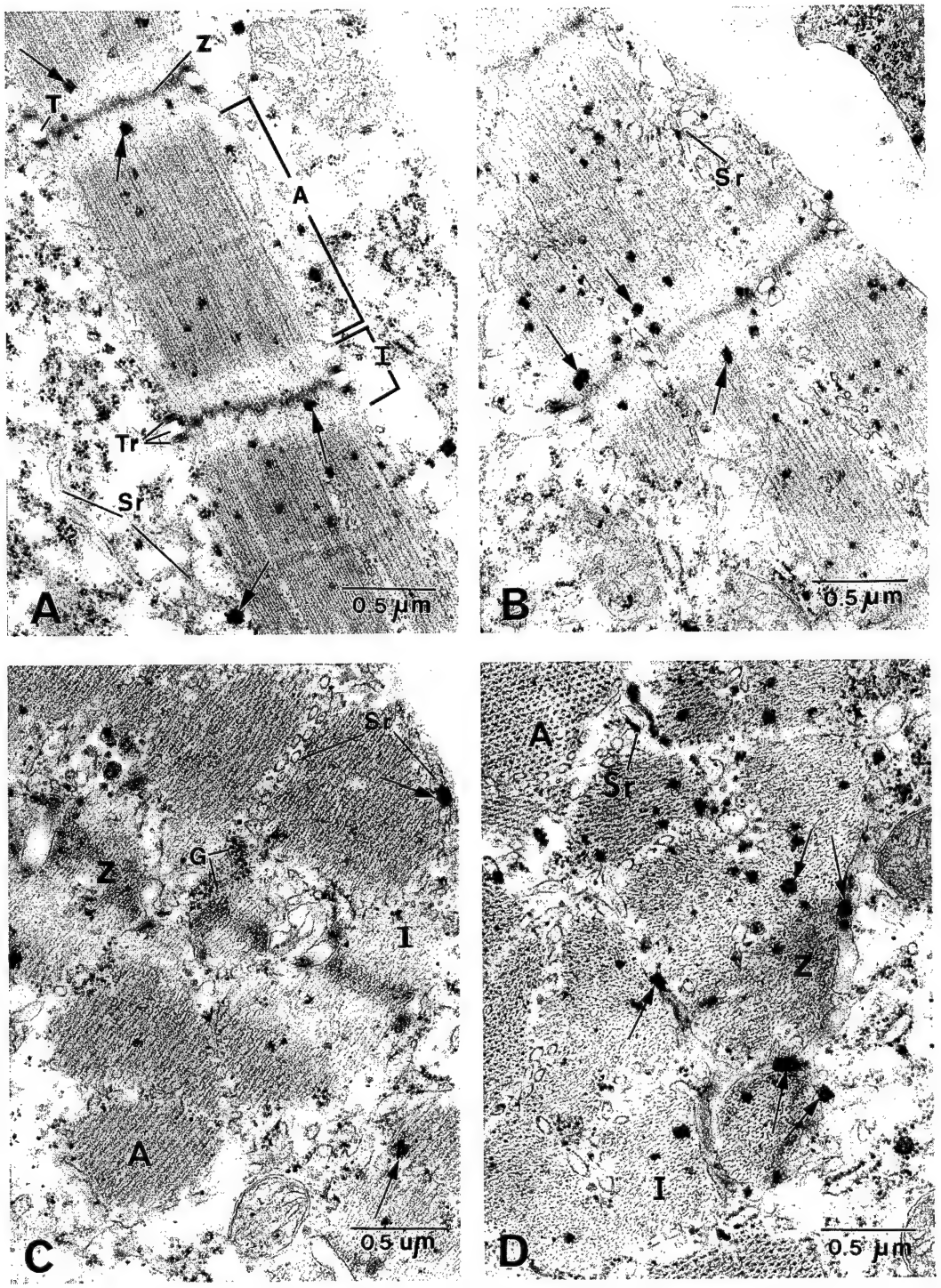

FIG. 5. Disposition of rHAChE in myotomes from 2-day-old microinjected *Xenopus* embryos. Fertilized *Xenopus* eggs were microinjected with 1 ng of CMVACHE, incubated for 2 days at 17°C, fixed, stained, and prepared for electron microscopy as described in Materials and Methods. Uninjected embryos from the same fertilization served as controls and were similarly treated. Arrows mark accumulations of reaction product indicating sites of catalytically active AChE. **A:** Uninjected control myotome in longitudinal section following activity staining for AChE. **B:** Myotome section from CMVACHE-injected embryo. **C:** Uninjected control myotome in transverse section. **D:** Transverse section from CMVACHE-injected embryo. Note the increased intensity of staining in sections from injected embryos versus uninjected controls within the same subcellular compartments, especially within the sarcoplasmic reticulum (Sr). A, A band; I, I band; Z, Z disc; Tr, triad; T, T tubules; G, glycogen particles. Bar = 0.5 μm.

pared with uninjected controls. By day 6 PF, no heterologous enzyme could be detected in homogenates (data not shown). At all time points examined, the level of frog AChE in CMVACHE-injected tadpoles appeared less than that observed in uninjected embryos.

In immunoblot analysis following denaturing gel electrophoresis, rHAChE was observed to comigrate with native human brain AChE, yielding a clearly visible doublet band at ~68 kDa (Fig. 3B). rHAChE was selectively recognized by a pool of mAbs raised against denatured human brain AChE, and no cross-immunoreactivity with embryonic *Xenopus* AChE was observed (Fig. 3B). The doublet band observed may reflect differences in glycosylation (Kronman et al., 1992). Sequential extractions with low-salt, detergent, and high-salt buffers revealed that ~35% of rHAChE synthesized in transiently transgenic embryos was associated with membranes, requiring detergent for solubilization (Table 1). Whereas up to 33% of the endogenous enzyme in day 3 uninjected tadpoles appeared in the high-salt-extractable fraction, salt-soluble rHAChE remained primarily in the low-salt fraction at all days examined (Table 1). Enzyme-antigen immunoassay with a species-specific mAb (mAb 101-1) was used to differentiate between human and frog enzyme in the fractions.

rHAChE remains monomeric in *Xenopus* embryos

To examine the possibility that heterologous human AChE could undergo homomeric oligomeric assembly or interact with either catalytic or noncatalytic subunits of *Xenopus* AChE to produce hybrid oligomers, sucrose density centrifugation and enzyme–antigen immunoassay were performed. At all time points examined, we observed rHAChE exclusively as nonassembled monomers sedimenting at ~3.2S, despite the concomitant accumulation of various multimeric forms of the endogenous frog enzyme (Fig. 4). When oligomeric AChE purified from CMVACHE-transfected cell cultures (Velan et al., 1991*b*) or from human brain (Liao et al., 1992) was preincubated with extracts of day 3 uninjected embryos and similarly analyzed, monomers, dimers, and tetramers were detected, and the distribution of oligomeric forms observed was identical to that in control samples (data not shown). Thus, mAb 101-1 detects all the globular configurations of rHAChE, and proteolytic activity does not appear to degrade stable oligomeric AChE in embryo extracts. Endogenous *Xenopus* AChE appeared primarily as a dimer on day 2 PF with globular tetrameric and asymmetric tailed forms appearing and increasing in content from day 3 onward (Fig. 4, insets). Superposition of the gradients from control and CMVACHE-injected embryos demonstrated that the normal developmental progression of *Xenopus* AChE oligomeric assembly was conserved in CMVACHE-injected embryos despite the high excess of rHAChE monomers (Fig. 4 and data not shown).

Subcellular disposition of rHAChE in myotomes of CMVACHE-injected embryos

Whole-mount cytochemical staining of CMVACHE-injected embryos indicated accumulation of AChE in myotomes 2 days PF (data not shown). We therefore undertook an ultrastructural analysis, at the electron microscope level, of myotomes from 2- and 3-day-old embryos microinjected with CMVACHE as compared with normal uninjected controls. Longitudinal and transverse sections from rostral trunk somites revealed clearly discernible myofibers 2 days PF in both injected and uninjected embryos (Fig. 5). By day 3 PF, both groups displayed significant increases in their numbers of myofibrillar elements and in maturation of the sarcoplasmic reticulum (Fig. 6). To examine the subcellular localization of nascent AChE in transgenic and control embryos, we used cytochemical activity staining (Karnovsky, 1964). In both the experimental and control groups, crystalline deposits of electron-dense reaction product were observed primarily in association with myofibrils, among the myofilaments, and within the sarcoplasmic reticulum (Figs. 5 and 6). Various organelles, including the nuclear membrane, free and bound polyribosomes, Golgi, and sometimes mitochondria, were also stained (Figs. 5 and 6 and data not shown).

At day 2 PF, staining in CMVACHE-injected embryos was conspicuously more pronounced than that observed in uninjected controls, in both the quantity and intensity of reaction product (Fig. 5). However, variability was observed between tissue blocks, probably reflecting mosaic expression of the injected DNA and/or variability in the efficiency of expression between embryos (S.S. and H.S., unpublished data). In longitudinal sections from CMVACHE-injected embryos, staining appeared to be concentrated at the I band of myofibers, particularly around the triad marking the intersection of the sarcoplasmic reticulum and T-tubule systems. In contrast, the sparse staining observed in control sections appeared randomly distributed. By day 3 PF, the general staining intensity in both groups had significantly increased, whereas observable differences between the groups were less dramatic. Cross sections revealed especially prominent staining within the sarcoplasmic reticulum (Fig. 6A and B). Strong staining was now observed at both the A and I bands and, for the first time, within the T-tubules (Fig. 6C and D). Overall, day 2 CMVACHE-injected myotomes resembled day 3 uninjected control myotomes in staining incidence and intensity (Figs. 5A and C and 6B and D).

Ultrastructural consequences of overexpressed AChE in *Xenopus* NMJs

We have previously demonstrated up to 10-fold overexpression of catalytically active AChE in NMJs of CMVACHE-injected embryos 2 days PF (Ben

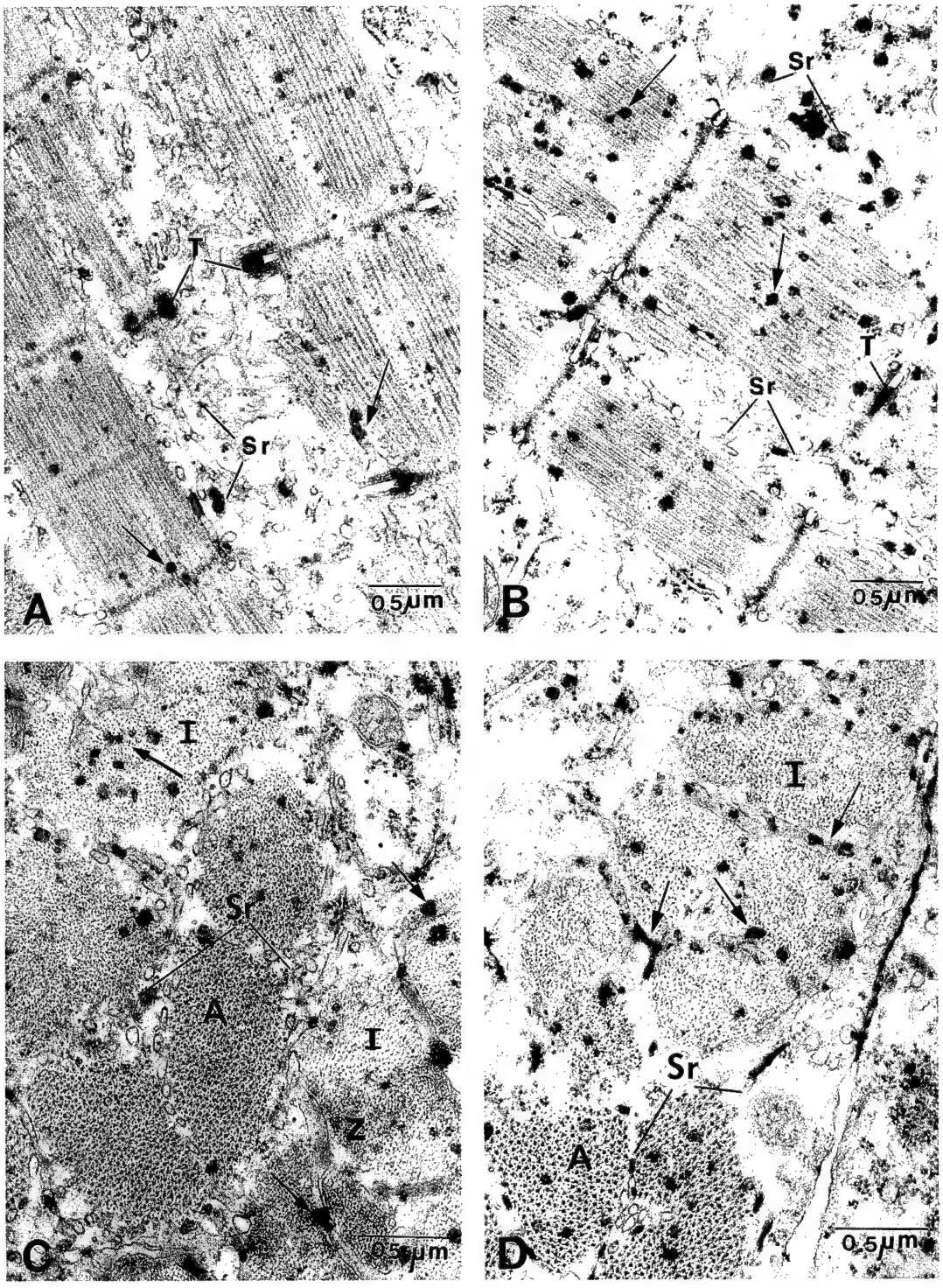

FIG. 6. Overexpression of AChE in myotomes of CMVACHE-injected embryos persists to day 3. Analyses were as in Fig. 5 except that embryos were analyzed after incubation for 3 days. Note the developmental increases in myotomal AChE in both control uninjected (**A** and **C**) and CMVACHE-injected sections (**B** and **D**), especially within the sarcoplasmic reticulum (Sr) and T-tubules (T). Bar = 0.5 μm.

Aziz-Aloya et al., 1993). To examine the persistence of this state and its implications for synaptic ultrastructure, we studied both cytochemically stained and closely appositioned unstained NMJs from 3-day-old injected and control embryos (Fig. 7 and Table 2). In the injected group, 72% of the postsynaptic membrane length (Table 2) was stained, on average, for active AChE. In contrast, only 22% of the postsynaptic length was stained in controls. Moreover, the total area covered by reaction product was approximately

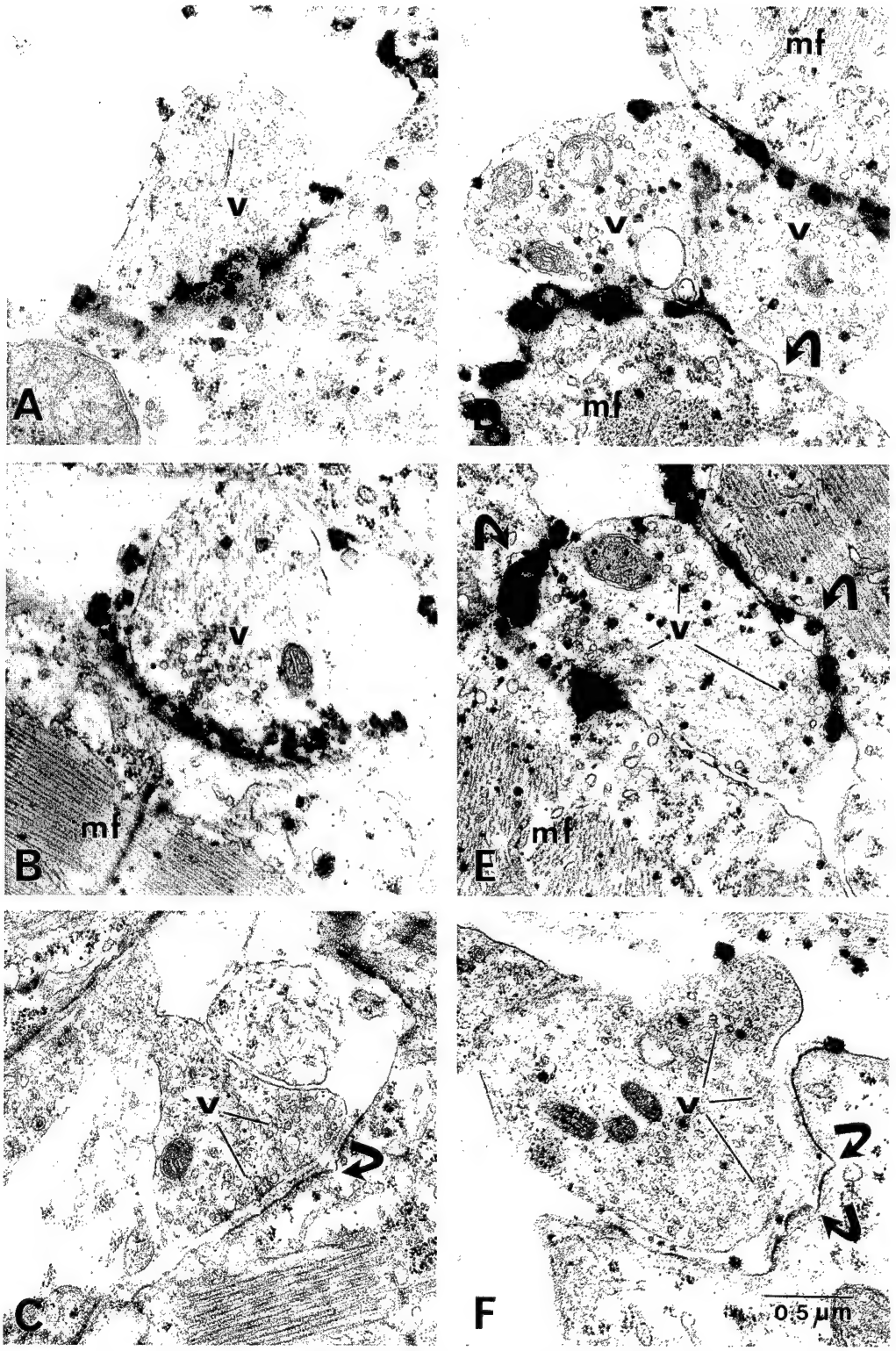

FIG. 7. Structural features in NMJs of 3-day-old CMVACHE-injected *Xenopus* embryos overexpressing AChE. *Xenopus* embryos were cultured for 3 days, fixed, stained for AChE catalytic activity, and examined by transmission electron microscopy as described in Materials and Methods. Two cytochemically stained synapses are presented from uninjected control (**A** and **B**) and CMVACHE-injected (**D** and **E**) embryos. Note the particularly high-density staining in areas directly opposite nerve terminal zones enriched in presynaptic neurotransmitter vesicles (v). **C** and **F:** Representative unstained NMJs from a control and a CMVACHE-injected embryo, respectively. The synapse shown in B represents the highest degree of staining observed in a control section. mf, myofibril. Arrows indicate postsynaptic folds.

TABLE 2. *Overexpression of AChE in NMJs of 3-day-old CMVACHE-injected* Xenopus *embryos*

Experiment	PSL (μm)	SL (μm)	SL/PSL ratio	SA (μm²)
Uninjected	2.57	0.79	0.004	0.156
	3.95	0.79	0.200	0.126
	1.54	0.80	0.060	0.080
	2.35	0.73	0.310	0.082
	1.17	0.44	0.085	0.063
	1.60	0.29	0.180	0.056
	1.02	0.29	0.280	0.040
	0.88	0.58	0.650	0.075
Average ± SD	1.88 ± 0.93	0.58 ± 0.22	0.22 ± 0.19	0.084 ± 0.038
+ CMVACHE	1.76	1.17	0.660	0.284
	2.50	2.05	0.820	0.331
	2.64	1.91	0.720	0.285
	2.50	2.40	0.960	0.476
	3.50	2.03	0.580	0.396
	1.85	1.66	0.900	0.333
	3.10	1.85	0.600	0.535
	3.23	1.76	0.540	0.289
Average ± SD	2.64 ± 0.58	1.85 ± 0.33	0.72 ± 0.15	0.37 ± 0.09
p	<0.01	<0.002	<0.002	<0.002

Eight representative synapses from CMVACHE-injected or control uninjected embryos were assessed for postsynaptic membrane length (PSL), the sum total length covered by reaction product (SL), the fraction of nerve–muscle contact distance displaying reaction product (SL/PSL), and the total stained area (SA). Average ± SD values are given. Measurements were performed on electron micrographs using a hand-held mapping device.

fourfold greater in NMJs from CMVACHE-injected embryos than those from controls (Table 2). In addition, the staining observed in NMJs from injected embryos was considerably more intense than that displayed by control NMJs, forming large black accumulations of reaction product as opposed to the lighter, more diffuse staining observed in controls (Fig. 7A, B, D, and E).

Ultrastructural features of NMJs from injected and uninjected embryos were best discerned in unstained synapses. NMJs from control embryos generally appeared smooth and relatively undeveloped, with up to two secondary folds of the postsynaptic membrane and a single nerve–muscle contact (Fig. 7C). In contrast, NMJs from CMVACHE-injected embryos displayed an average of three secondary folds and one to three discrete contacts between pre- and postsynaptic membranes (Fig. 7F). Furthermore, the average postsynaptic membrane length in NMJs from CMVACHE-injected embryos was 30% larger and considerably less variable than that measured in control embryos (SL; Table 2). Yet, the distance across the synaptic cleft was both larger and more variable in injected embryos than in controls (129 ± 72 vs. 94 ± 23 nm; n = 14). NMJs overexpressing rHAChE thus appeared more developed in their structural buildup than controls.

DISCUSSION

Numerous important nervous system proteins have been expressed in DNA- and RNA-injected oocytes of *X. laevis* (reviewed by Soreq and Seidman, 1992). To study the role and regulation of specific gene products in embryonic development (Vize et al., 1991) and myogenesis (Hopwood et al., 1991), microinjected *Xenopus* embryos have been used. Here, we used microinjected oocytes to demonstrate the efficacy of the CMV promoter in *Xenopus,* observing five- to 10-fold higher levels of heterologous enzyme than that induced by microinjection of in vitro-transcribed mRNA. Although no direct interactions between rHAChE and endogenous *Xenopus* AChE catalytic or structural subunits were observed, calculations of *Xenopus* AChE levels in microinjected embryos indicated that some feedback regulation may be operative in repressing endogenous AChE biosynthesis under conditions of overexpression. Feedback regulation of AChE has been previously demonstrated in chicken retinospheroids (Willbold and Layer, 1992).

Ectopic gene expression/overexpression often results in gross morphogenic aberrations (Harvey and Melton, 1988; McMahon and Moon, 1989; Sokol et al., 1991). Yet, we found that *Xenopus* embryos can tolerate large excesses of catalytically active heterologous AChE without suffering gross morphological or developmental abnormalities. This observation is especially interesting in light of evidence implicating AChE in the early embryonic development of noncholinergic tissues (Drews, 1975) and with developmental processes such as gastrulation and cell migration (Drews, 1975; Fitzpatrick-McElligot and Stent, 1981), nerve outgrowth and differentiation (Layer,

1991), and proliferation and differentiation of hematopoietic cells (Lapidot-Lifson et al., 1989, 1992; Patinkin et al., 1990). As neither the overall rate of development nor general morphology of CMVACHE-injected embryos was altered by 50–100-fold excesses of the active enzyme at the gastrula stage, our findings do not support a role for rHAChE in modulating cell growth, proliferation, or movement in very early *Xenopus* embryogenesis. However, because these biological activities may be unassociated with acetylcholine hydrolysis, they may demonstrate species specificity and remain undetected in our system.

Despite their lack of MyoD elements, some constructs carrying the pan-active CMV promoter (Schmidt et al., 1990) were shown to be expressed in myotomes of transgenic mouse embryos (Kothary et al., 1991). Therefore, the characteristic subcellular segregation of overexpressed rHAChE in muscle may reflect either tissue-specific biosynthesis or posttranslational processing of nascent enzyme present in myotomal progenitor cells at the onset of myogenesis. The high levels of rHAChE present in gastrula-stage embryos may argue for the latter possibility. In that case, the cytochemical data indicate the existence of an intrinsic, evolutionarily conserved property directing the subcellular trafficking of AChE in muscle and thus explain the accumulation of rHAChE in NMJs of ACHE DNA-injected embryos. Furthermore, these results may imply that cotranslational processes are not required for the correct compartmentalization of AChE in muscle cells. In a similar vein, purified recombinant synapsin was shown to be incorporated into synaptic nerve terminals of cultured myotomes following microinjection into fertilized *Xenopus* eggs (Lu et al., 1992).

The general state of myotomal overexpression induced by microinjection of CMVACHE persisted at least 3 days. The area covered by reaction product in cytochemically stained NMJs from day 3, CMVACHE-injected embryos was four- to fivefold over that observed in controls. This figure represents a twofold lower excess than that measured in day 2 NMJs (Ben Aziz-Aloya et al., 1993) yet is slightly greater than the ratio of rHAChE to frog AChE as determined in homogenates at day 3 (Fig. 3A). This apparent reduction in the level of synaptic overexpression from day 2 to day 3 PF may reflect the overall decline in total rHAChE activity observed during this period. However, because this calculation does not consider the higher-density staining observed in NMJs from CMVACHE-injected embryos, it represents an underestimate of the actual synaptic AChE content. Therefore, our data indicate enhanced stability of rHAChE at the NMJ compared with the total pool, a conclusion consistent with the observation that extracellular matrix-associated AChE persists in situ long after denervation of adult frog skeletal muscle (Anglister and McMahan, 1985).

Mammalian cells cotransfected with cDNAs encoding catalytic and noncatalytic AChE subunits (Krejci et al., 1991) produce multimeric globular and asymmetric AChEs, indicating that spatial coexistence may normally be the only requirement for multimeric assembly. Human cell lines transfected with various CMVACHE constructs similarly express and secrete homooligomers (Velan et al., 1991*a*; Kronman et al., 1992). rHAChE displayed oligomeric assembly in microinjected *Xenopus* oocytes but not in developing embryos, where only monomeric rHAChE was detected. Nonetheless, rHAChE was found to accumulate in its natural subcellular compartments and was correctly transported to the NMJ of transiently transfected tadpoles. These findings are puzzling in light of the demonstration that secretion appears linked to oligomerization in transfected human 293 cells (Velan et al., 1991*b*; Kerem et al., 1993). Furthermore, the lack of demonstrable oligomeric assembly leaves the mode of association of rHAChE with the extracellular surface unexplained. It is noteworthy, however, that DNA constructs encoding the parallel AChE form from *Torpedo* (Duval et al., 1992) and the rat (Legay et al., 1993) also gave rise to globular amphiphilic AChE forms in transfected mammalian cells, including type II amphiphilic monomers.

In humans, ultrastructural and physiological alterations of the NMJ have been associated with congenital AChE and AChR deficiencies (Wokke et al., 1989; Jennekens et al., 1992) and may be associated with changes in the balance between these two molecules at the synapse. In one of these syndromes, patients presented, in addition to AChE/AChR deficits, NMJs displaying decreased miniature end-plate potentials, reduced postsynaptic membrane lengths, and severely impaired postsynaptic secondary folding (Smit et al., 1988)—opposite features to those observed in our NMJs overexpressing AChE. It is yet unclear whether the reduced expression of synaptic AChE and/or AChR represents a cause or an outcome of the ultrastructural aberrations observed in these patients. Our current observations suggest that disturbed regulation of AChE may, indeed, carry ultrastructural consequences for synaptic development. It will thus be interesting to assess the impact of AChE overexpression on the expression and organization of AChR and other key synaptic proteins in these transiently transgenic tadpoles.

Acknowledgment: We are grateful to Dr. J. Yisraeli, Hadassah Medical School, Jerusalem, Israel, for guidance in the embryo microinjections. This research was supported by the U.S. Army Medical Research and Development Command (grant DAMD 17-90-Z0038), the United States–Israel Binational Science Foundation (grant 89-00205), and the Israel Science Foundation administered by the Israel Academy of Sciences and Humanities (to H.S.). J.L. was a recipient of a short-term EMBO fellowship.

REFERENCES

Anglister L. and McMahan U. J. (1985) Basal lamina directs acetylcholinesterase accumulation at synaptic sites in regenerating muscle. *J. Cell Biol.* **101,** 735–743.

Ben Aziz-Aloya R., Seidman S., Timberg R., Sternfeld M., Zakut H., and Soreq H. (1993) Expression of a human acetylcholinesterase promoter–reporter construct in developing neuromuscular junctions of *Xenopus* embryos. *Proc. Natl. Acad. Sci. USA* **90,** 2471–2475.

Brandan E., Maldonado M., Garrido J., and Inestrosa N. C. (1985) Anchorage of collagen-tailed acetylcholinesterase is mediated by heparan sulfate proteoglycans. *J. Cell Biol.* **101,** 985–992.

Brodbeck U. and Liao J. (1992) Subunit assembly and glycosylation of acetylcholinesterase from mammalian brain, in *Multidisciplinary Approaches to Cholinesterase Functions* (Shafferman A. and Velan B., eds), pp. 33–38. Plenum Press, New York.

Changeux J. P. (1991) Compartmentalized transcription of acetylcholine receptor genes during motor endplate epigenesis. *New Biol.* **3,** 413–429.

Cohen M. W. (1980) Development of an amphibian neuromuscular junction *in vivo* and in culture. *J. Exp. Biol.* **89,** 43–56.

Deuchar E. M. (1966) *Biochemical Aspects of Amphibian Development.* Methuen and Co. Ltd., London.

Drews U. (1975) Cholinesterase in embryonic development. *Prog. Histochem. Cytochem.* **7,** 1–52.

Duval N., Massoulie J., and Bon S. (1992) H and T subunits of acetylcholinesterase from *Torpedo,* expressed in COS cells, generate all types of molecular forms. *J. Cell Biol.* **118,** 641–653.

Fitzpatrick-McElligot S. and Stent G. S. (1981) Appearance and localization of acetylcholinesterase in embryos of the leech *Helodbella triserialis. J. Neurosci.* **1,** 901–907.

Flucher B. E. and Daniels M. D. (1989) Distribution of Na^+ channels and ankyrin in neuromuscular junctions is complementary to that of acetylcholine receptors and the 43 Kd protein. *Neuron* **3,** 163–175.

Froehner S. C. (1991) The submembrane machinery for nicotinic acetylcholine receptor clustering. *J. Cell Biol.* **114,** 1–7.

Gennari K. and Brodbeck U. (1985) Molecular forms of acetylcholinesterase from human caudate nucleus: comparison of salt-soluble and detergent-soluble tetrameric enzyme species. *J. Neurochem.* **44,** 697–704.

Gindi T. and Knowland J. (1979) The activity of cholinesterases during the development of *Xenopus laevis. J. Embryol. Exp. Morphol.* **51,** 209–215.

Hall Z. W. (1973) Multiple forms of acetylcholinesterase and their distribution in endplate and non-endplate regions of rat diaphragm muscle. *J. Neurobiol.* **4,** 343–361.

Harvey R. P. and Melton D. A. (1988) Microinjection of synthetic Xhox-1A homeobox mRNA disrupts somite formation in developing *Xenopus* embryos. *Cell* **53,** 687–697.

Hopwood N. D., Pluck A., and Gurdon J. B. (1991) *Xenopus* Myf-5 marks early muscle cells and can activate muscle genes ectopically. *Development* **111,** 551–560.

Jennekens F. G. I., Hesselmans L. F. G. M., Veldman H., Jansen E. N. H., Spaans F., and Molenaar P. C. (1992) Deficiency of acetylcholine receptors in a case of end-plate acetylcholinesterase deficiency: a histochemical investigation. *Muscle Nerve* **15,** 63–72.

Karnovsky M. J. (1964) The localization of cholinesterase activity in rat cardiac muscle by electron microscope. *J. Cell Biol.* **23,** 217–232.

Kerem A., Kronman C., Bar-Nun S., Shafferman A., and Velan B. (1993) Interaction between assembly and secretion of recombinant human acetylcholinesterase. *J. Biol. Chem.* **268,** 180–184.

Kothary R., Barton S. C., Franz T., Norris M. L., Hettle S., and Surani A. M. H. (1991) Unusual cell specific expression of a major human cytomegalovirus immediate early gene promoter–lacZ hybrid gene in transgenic mouse embryos. *Mech. Dev.* **35,** 25–31.

Krejci E., Coussen F., Duval N., Chatel J.-M., Legay C., Puype M., Vandekerckhove J., Cartaud J., Bon S., and Massoulie J. (1991) Primary structure of a collagenic tail peptide of *Torpedo* acetylcholinesterase: co-expression with catalytic subunit induces the production of collagen-tailed forms in transfected cells. *EMBO J.* **10,** 1285–1293.

Kronman C., Velan B., Gozes Y., Leitner M., Flashner Y., Lazar A., Marcus D., Sery T., Papier A., Grosfeld H., Cohen S., and Shafferman A. (1992) Production and secretion of high levels of recombinant human acetylcholinesterase in cultured cell lines: microheterogeneity of the catalytic subunit. *Gene* **121,** 295–304.

Kullberg R. W., Lentz T. L., and Cohen M. W. (1977) Development of the myotomal neuromuscular junction in *Xenopus laevis:* an electrophysiological and fine-structural study. *Dev. Biol.* **60,** 101–129.

Kullberg R. W., Mikelberg F. S., and Cohen M. W. (1980) Contribution of cholinesterase to developmental decreases in the time course of synaptic potentials at an amphibian neuromuscular junction. *Dev. Biol.* **75,** 255–267.

Lapidot-Lifson Y., Prody C. A., Ginzberg D., Meytes D., Zakut H., and Soreq H. (1989) Co-amplification of human acetylcholinesterase and butyrylcholinesterase in blood cells: correlation with various leukemias and abnormal megakaryocytopoiesis. *Proc. Natl. Acad. Sci. USA* **86,** 4715–4717.

Lapidot-Lifson Y., Patinkin D., Prody C., Ehrlich G., Seidman S., Ben-Aziz R., Eckstein F., Benseler F., Zakut H., and Soreq H. (1992) Cloning and antisense oligodeoxynucleotide inhibition of a human homolog of cdc2 required in hematopoiesis. *Proc. Natl. Acad. Sci. USA* **89,** 579–583.

Layer P. (1991) Cholinesterases during avian development. *Cell. Mol. Neurobiol.* **11,** 7–34.

Legay C., Bon S., Vernier P., Coussen F., and Massoulié J. (1993) Cloning and expression of a rat acetylcholinesterase subunit: generation of multiple molecular forms, complementarity with a *Torpedo* collagenic subunit. *J. Neurochem.* **60,** 337–346.

Liao J., Heider H., Sun M.-C., and Brodbeck U. (1992) Different glycosylation in acetylcholinesterases from mammalian brain and erythrocytes. *J. Neurochem.* **58,** 1230–1238.

Lu B., Greengard P., and Poo M. (1992) Exogenous synapsin I promotes functional maturation of developing neuromuscular synapses. *Neuron* **8,** 521–529.

McMahan U. J. (1990) The agrin hypothesis. *Cold Spring Harb. Symp. Quant. Biol.* **55,** 407–418.

McMahon A. P. and Moon R. T. (1989) Ectopic expression of the proto-oncogene int-1 in *Xenopus* embryos leads to duplication of the embryonic axis. *Cell* **58,** 1075–1084.

Neville L. F., Gnatt A., Loewenstein Y., Seidman S., Ehrlich G., and Soreq H. (1992) Intra-molecular relationships in cholinesterases revealed by oocyte expression of site-directed and natural variants of human BCHE. *EMBO J.* **11,** 1641–1649.

Ohlendieck K., Ervasti J. M., Matsumura K., Kahl S. D., Levelille C. J., and Campbell K. P. (1991) Dystrophin-related protein is localized to neuromuscular junctions of adult skeletal muscle. *Neuron* **7,** 499–508.

Patinkin D., Seidman S., Eckstein F., Benseler F., Zakut H., and Soreq H. (1990) Manipulations of cholinesterase gene expression modulate murine megakaryocytopoiesis *in vitro. Mol. Cell. Biol.* **10,** 6046–6050.

Pavlath G. K., Rich K., Webster S. G., and Blau H. M. (1989) Localization of muscle gene products in nuclear domains. *Nature* **337,** 570–573.

Phillips W. D., Kopta C., Blount P., Gardner P. D., Steinbach J. H., and Merlie J. P. (1991) ACh receptor-rich membrane domains organized in fibroblasts by recombinant 43 kilodalton protein. *Nature* **251,** 568–570.

Ralston E. and Hall Z. W. (1989) Transfer of a protein encoded by a single nucleus to nearby nuclei in multinucleated myotubes. *Nature* **244,** 1066–1069.

Rossi S. G. and Rotundo R. L. (1992) Cell surface acetylcholinesterase molecules on multinucleated myotubes are clustered over the nucleus of origin. *J. Cell Biol.* **119,** 1657–1667.

Rotundo R. L. (1990) Nucleus-specific translation and assembly of

acetylcholinesterase in multinucleated muscle cells. *J. Cell Biol.* **110**, 715–719.

Schmidt E. V., Christoph G., Zeller R., and Leder P. (1990) The cytomegalovirus enhancer: a Pan-active control element in transgenic mice. *Mol. Cell. Biol.* **10**, 4406–4411.

Smit L. M. E., Hageman G., Veldman H., Molenaar P. C., Oen B. S., and Jennekens F. G. I. (1988) A myasthenic syndrome with congenital paucity of secondary clefts: CPSC syndrome. *Muscle Nerve* **11**, 337–348.

Sokol S., Christian J. L., Moon R. T., and Melton D. A. (1991) Injected Wnt RNA induces a complete body axis in *Xenopus* embryos. *Cell* **67**, 741–752.

Soreq H. and Seidman S. (1992) *Xenopus* oocyte microinjection: from gene to protein, in *Methods in Enzymology* (B. Rudy and L. Iversen, eds), pp. 225–265. Academic Press, San Diego.

Soreq H., Seidman S., Dreyfus P. A., Zevin-Sonkin D., and Zakut H. (1989) Expression and tissue specific assembly of cloned human butyrylcholine esterase in microinjected *Xenopus laevis* oocytes. *J. Biol. Chem.* **264**, 10608–10613.

Soreq H., Ben-Aziz R., Prody C., Seidman S., Gnatt A., Neville L., Lieman-Hurwitz J., Lev-Lehman E., Ginzberg D., Lapidot-Lifson Y., and Zakut H. (1990) Molecular cloning and construction of the coding region for human acetylcholinesterase reveals a G,C rich attenuating structure. *Proc. Natl. Acad. Sci. USA* **87**, 9688–9692.

Velan B., Kronman C., Grosfeld H., Leitner M., Gozes Y., Flashner Y., Sery T., Cohen S., Ben-Aziz R., Seidman S., Shafferman A., and Soreq H. (1991*a*) Recombinant human acetylcholinesterase is secreted from transiently transfected 293 cells as a soluble globular enzyme. *Cell. Mol. Neurobiol.* **11**, 143–156.

Velan B., Grosfeld H., Kronman C., Leitner M., Gozes Y., Lazar A., Flashner Y., Marcus D., Cohen S., and Shafferman A. (1991*b*) The effect of elimination of intersubunit disulfide bonds on the activity, assembly, and secretion of recombinant human acetylcholinesterase. *J. Biol. Chem.* **266**, 23977–23984.

Vize P. D., Melton D. A., Hemmati-Brivanlou A., and Harland R. M. (1991) Assays for gene function in developing *Xenopus* embryos, in *Methods in Cell Biology* (Kay B. K. and Peng H. B., eds), pp. 367–387. Academic Press, San Diego.

Wallace B. G. (1991) The mechanisms of agrin-induced acetylcholine receptor aggregation. *Philos. Trans. R. Soc. Lond. Biol.* **331**, 272–280.

Willbold E. and Layer P. (1992) Formation of neuroblastic layers in chicken retinospheroids: the fibre layer of Chievitz secludes AChE positive cells from mitotic cells. *Cell Tissue Res.* **268**, 401–408.

Wokke J. H. J., Jennekens F. G. I., Molenaar P. C., Van den Oord C. J. M., Oen B. S., and Busch H. F. M. (1989) Congenital paucity of secondary synaptic clefts (CPSC) syndrome in 2 adult siblings. *Neurology* **38**, 648–654.

MOLECULAR AND CELLULAR BIOLOGY, June 1995, p. 2993–3002
0270-7306/95/$04.00+0

Vol. 15, No. 6

Synaptic and Epidermal Accumulations of Human Acetylcholinesterase Are Encoded by Alternative 3′-Terminal Exons

SHLOMO SEIDMAN, MEIRA STERNFELD, REVITAL BEN AZIZ-ALOYA,† RINA TIMBERG, DANIELA KAUFER-NACHUM, AND HERMONA SOREQ*

Department of Biological Chemistry, The Life Sciences Institute, The Hebrew University of Jerusalem, Jerusalem, Israel

Received 27 September 1994/Returned for modification 18 January 1995/Accepted 7 February 1995

Tissue-specific heterogeneity among mammalian acetylcholinesterases (AChE) has been associated with 3′ alternative splicing of the primary AChE gene transcript. We have previously demonstrated that human AChE DNA encoding the brain and muscle AChE form and bearing the 3′ exon E6 (ACHE-E6) induces accumulation of catalytically active AChE in myotomes and neuromuscular junctions (NMJs) of 2- and 3-day-old *Xenopus* embryos. Here, we explore the possibility that the 3′-terminal exons of two alternative human AChE cDNA constructs include evolutionarily conserved tissue-recognizable elements. To this end, DNAs encoding alternative human AChE mRNAs were microinjected into cleaving embryos of *Xenopus laevis*. In contrast to the myotomal expression demonstrated by ACHE-E6, DNA carrying intron I4 and alternative exon E5 (ACHE-I4/E5) promoted punctuated staining of epidermal cells and secretion of AChE into the external medium. Moreover, ACHE-E6-injected embryos displayed enhanced NMJ development, whereas ACHE-I4/E5-derived enzyme was conspicuously absent from muscles and NMJs and its expression in embryos had no apparent effect on NMJ development. In addition, cell-associated AChE from embryos injected with ACHE-I4/E5 DNA was biochemically distinct from that encoded by the muscle-expressible ACHE-E6, displaying higher electrophoretic mobility and greater solubility in low-salt buffer. These findings suggest that alternative 3′-terminal exons dictate tissue-specific accumulation and a particular biological role(s) of AChE, associate the 3′ exon E6 with NMJ development, and indicate the existence of a putative secretory AChE form derived from the alternative I4/E5 AChE mRNA.

Acetylcholinesterase (AChE) is accumulated at neuromuscular junctions (NMJs) (25), where it serves a vital function in modulating cholinergic neurotransmission (reviewed in reference 31). The molecular mechanisms by which AChE and other synaptic proteins accumulate in the NMJ are poorly understood. Compartmentalized transcription and translation in and around the junctional nuclei probably contribute to the NMJ localization of AChE (9). However, the high concentration of AChE at NMJs suggests that an additional step(s) may be required to actively accumulate this molecule in its ultimate synaptic destination. In that case, it is possible to postulate the existence of a unique molecular tag identifying some AChE forms as NMJ bound. We have previously offered evidence that an evolutionarily conserved NMJ-recognizable signal is embedded within the primary amino acid sequence of the major brain and muscle (brain-muscle) form of AChE (1). In the present report, we trace this signal as derived from an alternative 3′ exon in the human AChE gene.

In addition to its synaptic location, AChE is known to exist in several nonneuronal cell types, including epidermal and hematopoietic cells (31). Recent studies have correlated this particular tissue distribution of AChE with the 3′ alternative splicing patterns of the mRNA transcripts encoding the AChE protein. The dominant brain-muscle AChE form found in NMJs (AChE-T) was shown to be encoded by an mRNA carrying exon E1 and the invariant coding exons E2, E3, and E4, spliced to alternative exon E6 (1, 15). AChE mRNA bearing exons E1 through E4 and alternative exon E5 encodes the glycolipid phosphatidylinositol (GPI)-linked form of AChE characteristic of vertebrate erythrocytes (AChE-H) (13, 16). An additional readthrough mRNA species retaining the intronic sequence I4 located immediately 3′ to exon E4 was previously observed in rodent bone marrow and erythroleukemic cells (13, 16) and in various tumor cell lines of human origin (11). The tissue-specific posttranscriptional and post-translational management of AChE mRNA and its polypeptide products raised the question of whether alternative 3′ exons and/or C-terminal peptides play a role in mediating the accumulation of AChE in NMJs as opposed to other tissues expressing this enzyme.

To examine the molecular mechanisms underlying the tissue-specific accumulation patterns of AChE, we established an in vivo model for the expression of alternative human AChEs in transiently transgenic embryos of *Xenopus laevis*. Placed downstream of the cytomegalovirus (CMV) promoter-enhancer unit (32) and microinjected into fertilized eggs of *X. laevis*, DNA carrying the invariant coding exons and alternative exon E6 (ACHE-E6) directed the production of catalytically active AChE which accumulated in muscle cells, nerve terminals, and NMJs of 2- and 3-day-old embryos (1, 27). Here, we have constructed an additional CMV ACHE plasmid (ACHE-I4/E5), potentially encoding the remaining two alternative AChE mRNAs, and compared its expression pattern in microinjected *Xenopus* embryos with that of ACHE-E6. Our findings indicate that tissue-specific accumulation of AChE may be dictated by alternative splicing of AChE mRNAs, that the 3′-terminal exon E6 plays an essential role in accumulation of AChE in NMJs, where it enhances NMJ development, and that the readthrough AChE mRNA may engender a unique secre-

* Corresponding author. Phone: 972-2-585109. Fax: 972-2-520258.
† Present address: Department of Molecular Genetics and Virology, The Weizmann Institute of Science, Rehovot 76100, Israel.

tory form of human AChE accumulated in epithelial cells, which is excluded from NMJs.

MATERIALS AND METHODS

Vectors. The plasmid referred to here as ACHE-E6 and employed to express the major brain-muscle form of AChE has been described in detail (CMV ACHE) (32). This plasmid contains the AChE-encoding exons E2, E3, E4, and E6 (30) downstream of the CMV promoter and is followed by the simian virus 40 polyadenylation site. ACHE-E6 was used to construct ACHE-I4/E5 by exchanging the cDNA restriction fragment *Not*I-*Hpa*I with the genomic fragment *Not*I-*Hin*dII (see Fig. 1). ACHE-I4/E5 potentially encodes both the GPI-linked erythrocyte AChE form generated by splicing of I4 and/or the readthrough AChE form (11). Repeated DNA sequencing of this plasmid DNA, using a Hot Tub PCR cycle sequencing kit (Amersham, Amersham, United Kingdom) confirmed that the I4 domain includes a stop codon, correcting previous erroneous sequencing (11).

***Xenopus* embryo microinjections.** In vitro fertilization and microinjection of mature *Xenopus* eggs were performed as described elsewhere (27), except that embryos were raised at 19 to 21°C.

RT-PCR procedure and primers. Total RNA was extracted from *Xenopus* embryos 1 day after injection by the RNAsol-B method (Cinna/Biotecx), according to the protocol supplied by the manufacturer, and was treated with DNase (Promega) as previously described (1). Reverse transcription followed by PCR (RT-PCR) analyses were performed as detailed elsewhere (11), using a Perkin-Elmer Cetus thermal controller. Amplification was for 1 min at 94°C [first cycle, 3 min], 1 min at 65°C, and 1 min at 72°C [last cycle, 6 min], performed with the following primer pairs: pair 1, E3/1522+ (5′-CGGGTCTACGCCTACGTCTTT GAACACCGTGCTTC-3′) and E6/2003− (5′-CACAGGTCTGAGCAGCGAT CCTGCTTGCTG-3′); pair 2, E3/1522+ and E5/1917− (5′-ATGGGTGAAGC CTGGGCAGGTG-3′); pair 3, E3/1522+ and I4/1939− (5′-GGTTACACTGGC GGGCTCC-3′); pair 4, E3/1522+ and E4/1797− (5′-CAGGTCCAGACTAAC GTACTGCTGAGCCCCCGCCG-3′). The primers were named according to their position in the human AChE alternative coding sequences (11, 30) and designated upstream (+) or downstream (−) per their orientation. Amplification products (20%) were electrophoresed on a 2% agarose gel and UV photographed (320 nm).

AChE activity assays and subcellular fractionations. AChE activities were determined with a standard colorimetric assay adapted to a 96-well microtiter plate (20, 27). Assays were performed in 0.1 M phosphate buffer (pH 7.4)–0.5 mM dithio-bis-nitrobenzoic acid–1 mM acetylthiocholine substrate at room temperature. Optical density at 405 nm was monitored for 20 min at 3- to 5-min intervals.

Subcellular fractionation of 1-day-old embryos into low-salt (0.01 M Tris-HCl [pH 7.4], 0.05 M $MgCl_2$, 144 mM NaCl), low-salt–detergent (1% Triton X-100 in 0.01 M Na phosphate [pH 7.4]), and high-salt (1 M NaCl in 0.01 M Na phosphate [pH 7.4]) buffers was performed as previously described (27).

Nondenaturing gel electrophoresis. Electrophoresis was performed in 6% polyacrylamide gels (32). Wherever noted, 0.5% Triton X-100 was included. The gels were run in the cold for 2 to 4 h, rinsed two to three times with double-distilled water, and stained for several hours or overnight for catalytically active AChE by the thiocholine method for histochemical staining of AChE developed by Karnovsky and Roots (10) and detailed below.

Whole-mount cytochemical staining. Two-day-old *Xenopus* embryos were fixed for 20 min in 4% paraformaldehyde (in 0.6× phosphate-buffered saline [PBS]), rinsed three times with PBS, and transferred to a clean glass vial. Fixed embryos were incubated in staining solution (0.67 mM acetylthiocholine, 5 mM sodium citrate, 3 mM cupric sulfate, 0.5 mM potassium ferricyanide in 0.1 M acetate buffer [pH 5.9]) overnight at room temperature with gentle rotation, rinsed several times with PBS, and postfixed with 2.5% glutaraldehyde for 1 h. The embryos were then dehydrated by successive transfers through 30, 50, 70, and 100% methanol, mounted in Murray's clearing solution (benzyl alcohol-benzyl benzoate, 1:2), and viewed under low magnification with a Zeiss stereomicroscope. Clearing permitted visualization of internal structures and improved with time up to 18 to 24 h.

Electron microscopy and morphometric analyses. Histochemical staining and transmission electron microscopy were performed as previously described in detail (1, 27). Morphometric analyses of NMJs from 2-day-old embryos raised at 21°C were performed with the SigmaScan software (Jandel Co., Berkeley, Calif.) and an IBM-compatible personal computer.

RESULTS

Alternative mRNAs dictate specific accumulation of AChE in muscle or epidermis. To examine the ability of alternative splicing to account for tissue-specific accretion of AChE, in vitro-fertilized *Xenopus* eggs were microinjected with 1 ng of ACHE-E6 or ACHE-I4/E5 DNA (Fig. 1). The resultant embryos were raised for 2 to 3 days, fixed, and stained for catalytically active enzyme. Following injection of ACHE-E6, encoding the brain-muscle form of AChE, 2-day-old tailbud embryos displayed conspicuous overexpression of AChE in the developing myotomes (Fig. 2, top panels). Myotomal overexpression was primarily observed as pronounced longitudinal staining along the plane of the muscle fibers between the vertical bands representing natural intersomitic accumulations of AChE. With the exception of brain tissues, no other tissues displayed consistently or prominently enhanced staining. However, myotomal overexpression of AChE was clearly mosaic, varying in intensity within and between individual somites. Uninjected control embryos displayed the characteristic transverse staining along the junctions between somites but only faint staining within the myotomes (Fig. 2, top panels).

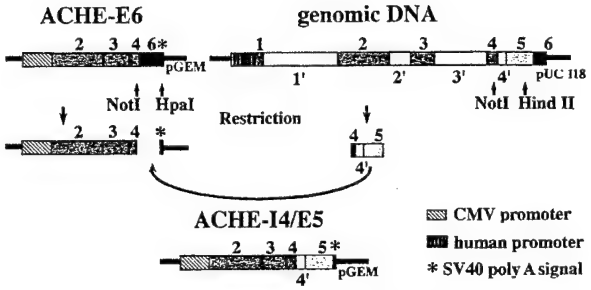

FIG. 1. DNA constructs. The DNA constructs employed in this study are presented. See Materials and Methods for details. SV40, simian virus 40.

In contrast to the striking accumulation of ACHE-E6-derived AChE in myotomes, we did not observe any enhancement of staining in myotomes of embryos injected with ACHE-I4/E5. Rather, we noted pronounced punctuated staining of the epidermis which was never seen in uninjected embryos (Fig. 2, bottom panels). These differential staining patterns were probably not due to variable levels of AChE mRNA, as whole-mount in situ hybridization (9) revealed similar ubiquitous distributions of both transcripts (data not shown). Epidermal staining could be observed over the entire body along both the rostral-caudal and dorsal-ventral axes. Intersomitic staining was unaffected by overexpression of ACHE-I4/E5. Although limited epidermal staining was occasionally observed in ACHE-E6-injected embryos, this phenomenon appeared restricted to sites of particularly high myotomal expression and was considerably less well defined (Fig. 2, bottom panels). These observations indicated that AChE derived from ACHE-E6 DNA was specifically accumulated in muscle, whereas AChE derived from ACHE-I4/E5 was accumulated in the epidermis.

ACHE-I4/E5 is excluded from the NMJ localization characteristic of ACHE-E6 and plays no role in NMJ development. Electron microscopic analysis of myotomes stained for catalytically active AChE revealed conspicuous overexpression of enzyme in NMJs of ACHE-E6-injected embryos and correlated overexpression with alterations in synaptic ultrastructure (27). To finely examine the potential for ACHE-I4/E5-derived AChE to be similarly localized, we performed morphometric analyses of cross sections from a series of stained NMJs from DNA-injected or control uninjected embryos (Fig. 3A through C). The average AChE-stained cross-sectional area of NMJs from ACHE-E6-injected embryos reached three or four times that observed in NMJs from uninjected embryos (0.33 ± 0.29 μm^2 versus 0.08 ± 0.09 μm^2). In contrast, the average stained area of NMJs from embryos injected with ACHE-I4/E5 (0.14 ± 0.03 μm^2) displayed only a minor increase compared with

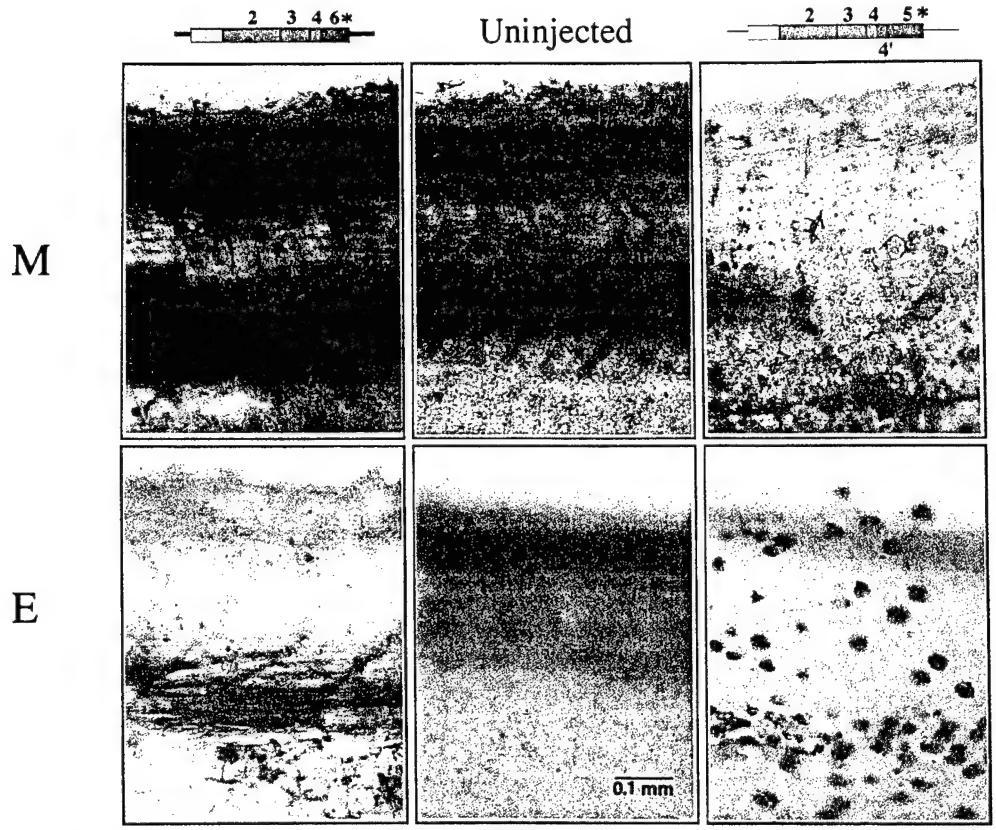

FIG. 2. Alternative AChE mRNAs dictate tissue-specific accumulation of AChE. DNA-injected or control uninjected *Xenopus* embryos were raised for 2 days at 19°C, fixed, stained for catalytically active AChE, and examined in whole mount as described in Materials and Methods. Schematic representations of the microinjected DNAs which gave rise to the staining pattern exhibited in each micrograph are shown (see Fig. 1). (M) Micrographs taken at the inner focal depth of muscle; (E) micrographs taken at the higher focal depth of epidermis. (M [left]) Midtrunk myotomes from ACHE-I4/E5-injected embryo. Note, in addition to the natural intersomitic vertical bands of brown stain indicating sites of AChE activity, dark—almost black—horizontal bands of staining parallel to the plane of the myotomal muscle fibers. This type of longitudinal staining, although variable in intensity along the body and between embryos, was observed exclusively in ACHE-E6-expressing embryos and served as an unequivocal marker for overexpression from this plasmid. (M [center]) Midbody view of uninjected control embryo. Note the accumulation of reaction product at the junctions flanking the individual somites and the very light staining along the horizontal plane of the muscle fibers. (M [right]) Faintly stained myotomes from ACHE-I4/E5-injected embryo. Note that staining is considerably lighter than in control, uninjected embryos. (E [left]) Unlabeled epidermis of ACHE-E6-injected embryo. When photographed at the higher focal depth of the epidermis, ACHE-E6 embryos displayed faint reflections of the deeper muscle stain whereas no stainable enzyme could be detected in epidermis. (E [center]) Unlabeled epidermis of control embryo. Focusing on epidermis, uninjected control embryos revealed no epidermal stain. Faint staining of myotomes below could be observed. (E [right]) ACHE-I4/E5-expressing embryo displaying punctuated epidermal staining. The plane of focus is slightly higher than that in the upper panels. Note the irregular spotted appearance of the skin resulting from ACHE-I4/E5 overexpression and the complete absence of enhanced staining in the myotomes.

that for the controls. Transverse sections of myofibers displayed a parallel pattern of highly intensified staining in myotomes of ACHE-E6-injected embryos compared with both ACHE-I4/E5-injected and uninjected controls (Fig. 3D through F). A twofold increase in mean postsynaptic membrane length was associated with ACHE-E6-mediated overexpression compared with that for the controls (3.8 ± 2.1 μm versus 2.2 ± 1.3 μm). In contrast, the average postsynaptic length observed in ACHE-I4/E5-injected embryos (1.9 ± 0.2 μm) was approximately the same as that for the controls.

At least 40% of NMJs from uninjected and ACHE-I4/E5-injected embryos displayed postsynaptic lengths less than 3 μm. In contrast, these small synapses were not observed in ACHE-E6-injected embryos (Fig. 4). Rather, a class of large NMJs (>4 μm) rarely observed in control or ACHE-I4/E5-injected embryos dominated in those transgenic for ACHE-E6. When the AChE-stained area was calculated as a function of postsynaptic length, ACHE-I4/E5-injected and control uninjected embryos displayed a similar, constant relationship between these parameters, whereas ACHE-E6-injected embryos displayed a higher ratio for all length categories (Fig. 4). Thus, there appeared to be a causal correlation between AChE overexpression in muscle and enhanced postsynaptic length in individual synapses, confirmed by the lack of effect by ACHE-I4/E5. Together, these observations imply a specific role for the E6 exon in localizing AChE to NMJs and demonstrate that the effects of AChE overexpression on NMJ biogenesis are dependent on the muscle localization of the enzyme.

The I4/E5 domain directs AChE accumulation in ciliated epidermal cells and its excretion. To study the cellular and subcellular distribution of overexpressed AChE in epidermal cells from embryos injected with ACHE-I4/E5, we examined epidermis from cytochemically stained embryos by electron microscopy. Two types of cells were labelled by the electron-dense crystals of the AChE reaction product: (i) ciliated cells derived from the inner, sensorial, epidermal layer and (ii) mucus-discharging secretory cells (Fig. 5) (2). There were many fewer ciliated cells than secretory cells. Yet, the inci-

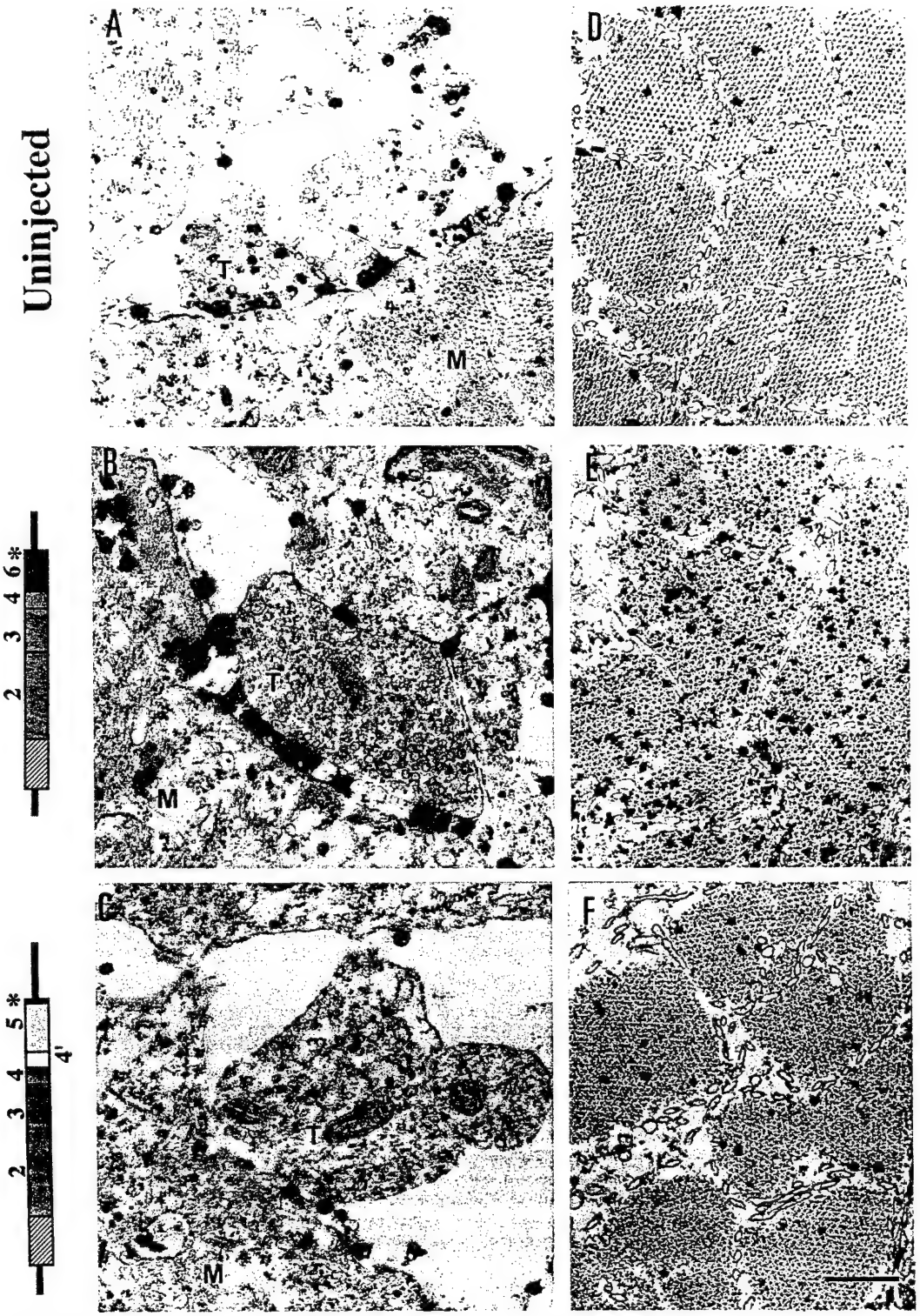

FIG. 3. I4/E5-derived AChE, unlike ACHE-E6, is excluded from NMJs. Two-day-old DNA-injected and control uninjected *Xenopus* embryos raised at 19°C were cytochemically stained for catalytically active AChE and examined by electron microscopy as described in Materials and Methods. Note the significantly enhanced staining, observed as dark electron-dense deposits, and increased size displayed by NMJs from ACHE-E6-injected embryos (B) as compared with those from control (A) and ACHE-I4/E5-injected (C) embryos. Shown are transverse sections of myofibers from control (D), ACHE-E6-injected (E), and ACHE-I4/E5-injected (F) embryos; note the correlation between myotomal and synaptic levels of expression. T, nerve terminal; M, muscle cell. For an explanation of the schematic diagrams, see Fig. 1. Bar = 1 μm.

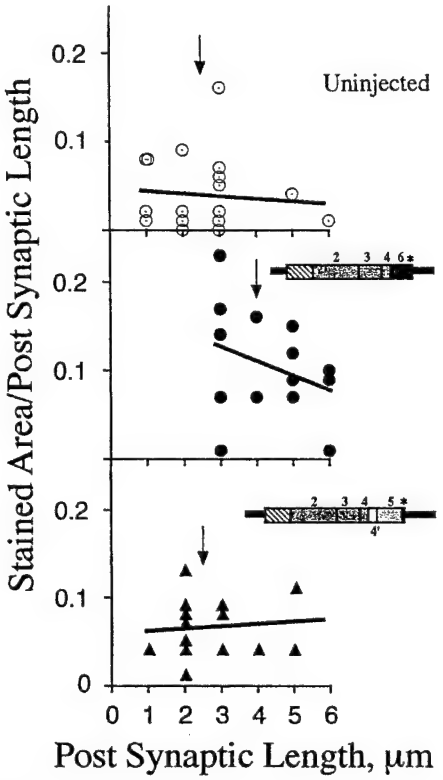

FIG. 4. ACHE-E6 but not ACHE-I4/E5 promotes NMJ maturation. Ratios of AChE-stained area to postsynaptic length as a function of length are presented for cross sections from at least 14 individual NMJs from embryos injected with ACHE-E6 (middle panel) or ACHE-I4/E5 (lower panel) and raised for 2 days at 21°C as compared with controls (upper panel). The solid line represents the best-fit line through the datum points, and the arrows designate the mean postsynaptic length for each microinjection group. Note the rightward shift toward larger NMJs in embryos injected with ACHE-E6 compared with those found in ACHE-I4/E5-injected and control embryos. For an explanation of the schematic diagrams, see Fig. 1.

dence and intensity of staining were higher among the ciliated cells, with some displaying massive apical accumulations of reaction product (Fig. 5). This irregular mosaic of heavily stained cells corresponded well to the punctuated array of stained cells observed in whole-mount embryos (Fig. 2). In uninjected control and ACHE-E6-injected embryos, both types of epidermal cells displayed scant staining, if any (Fig. 5B, D, and F and data not shown).

Ciliated cells were characterized, in addition to their cilia, by their dense cytoplasm, rich accumulation of mitochondria, and the presence of numerous small vesicles, most of which were filled with reaction product in stained cells (Fig. 5). Crystals of reaction product were also observed, however, in the cytoplasm and increased in size and density in a graded fashion toward the apex. In contrast, secretory cells were identified on the basis of their large, distinctive, chondroitin-laden secretory vesicles (Fig. 5) (21), some of which appeared to be fused to the plasma membrane (data not shown). In labelled secretory cells from ACHE-I4/E5-injected embryos, up to 20% of the vesicles stained positively for AChE. However, only an occasional crystal of reaction product could be observed in vesicles from uninjected or ACHE-E6-injected embryos (Fig. 5 and data not shown). No gross morphological features distinguished stained cells or vesicles in ACHE-I4/E5-injected embryos from unstained ones or from those observed in control or ACHE-E6-injected embryos.

The observation that mature secretory vesicles in epidermis of ACHE-I4/E5-injected embryos stained positively for AChE suggested that this enzyme form may be secreted along with the mucus naturally contained within these vesicles. To determine whether AChE was being excreted from the body, healthy neurula-stage embryos either injected with vector or uninjected were incubated overnight and the AChE activity found in the medium was compared with that measured in total homogenates. Only incubation medium from embryos injected with ACHE-I4/E5 DNA displayed significant AChE activity, representing up to 40% of the total measured activity (Fig. 6). Together, these observations indicated that a property or properties intrinsic to the I4/E5-terminal exon confer(s) a signal for epidermal accumulation, polarized subcellular transport, and excretion of AChE. Transfection studies with cultured glioma cells later revealed that secretion of the ACHE-I4/E5 product is a general phenomenon (11a).

Epidermal excretion is associated with readthrough AChE mRNA. Microinjected *Xenopus* embryos have been shown to correctly splice intron I1 from a human AChE promoter-reporter construct to produce catalytically active AChE (1). ACHE-I4/E5 potentially leads to both the mRNA encoding the erythrocyte GPI-linked AChE, by splicing out of intron I4, and/or the complete readthrough mRNA in which the invariant exons continue directly from exon E4 into intron I4 and through it into exon E5 (11) (Fig. 7A). To determine which AChE mRNA(s) was produced in our *Xenopus* embryos, we subjected total RNA extracted from 1-day-old ACHE-E6- or ACHE-I4/E5-injected embryos to RT-PCR with E4-, I4-, E5-, or E6-specific primers (Fig. 7A and see Materials and Methods). When an E6-specific primer pair was employed to analyze RNA from ACHE-E6-injected gastrulae, the expected 482-bp fragment representing full-length ACHE-E6 mRNA was reproducibly observed (Fig. 7B). When RNA from ACHE-I4/E5-injected embryos was subjected to RT-PCR, both the invariant exon E4 and the intronic sequence I4 were detected. However, the E5-specific primer pair repeatedly failed to generate either the 479-bp fragment representing the full-length readthrough mRNA or the 399-bp fragment representing spliced E5-bearing mRNA (Fig. 7B). A parallel reaction using control plasmid DNA and the identical E5-specific primers did yield the 479-bp band, however, validating the efficacy of this primer pair (Fig. 7B). Moreover, this same primer pair has been successfully utilized to detect native E5-carrying mRNAs in human tissues and transfected mammalian cells (11, 11a). These data therefore indicated that the recombinant human AChE activity induced by ACHE-E6 reflected the complete brain-muscle form of AChE, whereas heterologous AChE activity produced in *Xenopus* embryos from ACHE-I4/E5 was derived from a readthrough AChE mRNA which was, at least partially, truncated. This, together with the stop codon included in I4, implied that the polypeptide encoded by ACHE-I4/E5-derived mRNA in *Xenopus* embryos could display biochemical characteristics distinct from both brain-muscle and erythrocyte AChEs.

Unique properties of ACHE-I4/E5-derived AChE. Microinjection of 1 ng of ACHE-E6 DNA induces transiently high levels of catalytically active recombinant human AChE in *Xenopus* embryos (27). When ACHE-I4/E5 was introduced into 1- to 2-cell cleaving embryos, equivalent levels and a similarly transient pattern of heterologous overexpression were observed, peaking at days 1 to 2 postfertilization and receding at day 4 or 5 (Fig. 8A). Overall, development of injected embryos appeared normal through gastrulation, neurulation, hatching,

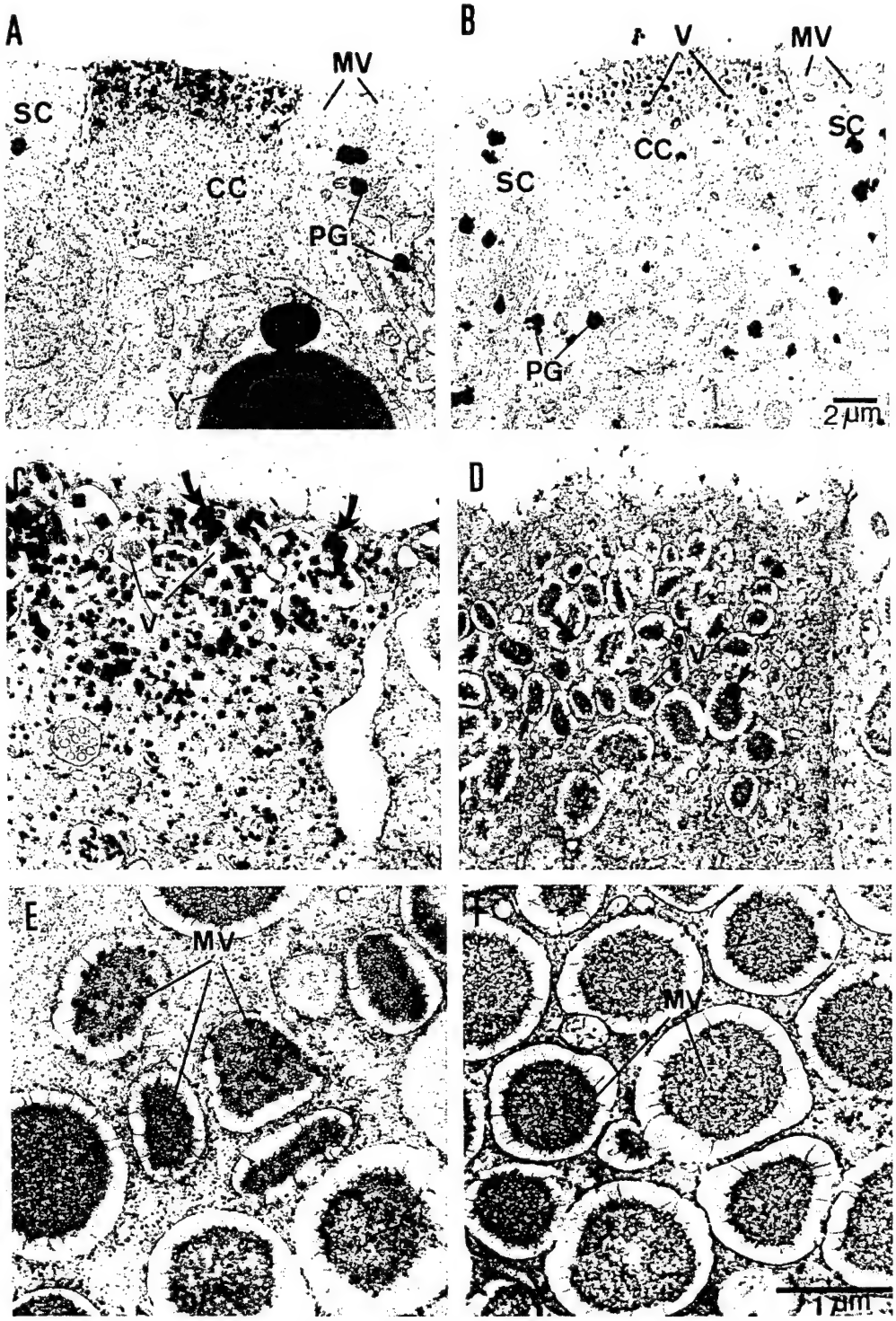

FIG. 5. ACHE-I4/E5-induced AChE accumulates in epidermal cells. Three-day-old DNA-injected and control uninjected *Xenopus* embryos raised at 19°C were fixed and stained for catalytically active AChE as described in Materials and Methods, except that the electron micrographs shown in panels A through D were taken after extending the staining reaction for 2 h. (A and B) Low-magnification image of ciliated (CC) and secretory (SC) cells of *Xenopus* epidermis from ACHE-I4/E5-injected (A) and control (B) embryos. Note the massive accumulation of crystalline electron-dense reaction product at the apex of the CC from an ACHE-I4/E5-injected embryo. Cilia are not visible at this depth. MV, secretory mucous vesicles; PG, pigment granules; V, vesicles; Y, yolk. (C and D) High-magnification image of the apical ridge of a ciliated epidermal cell from ACHE-I4/E5-injected (C) and control, uninjected (D) embryos. Note the appearance of crystals both within V (arrows) and within the cytoplasm of the injected embryo. (E and F) High-magnification image of MV from ACHE-I4/E5-injected (E) and control, uninjected (F) embryos. Note that only MV from the ACHE-I4/E5-injected embryo demonstrate accumulation of reaction product in exocytotic vesicles adjacent to the external cell membrane.

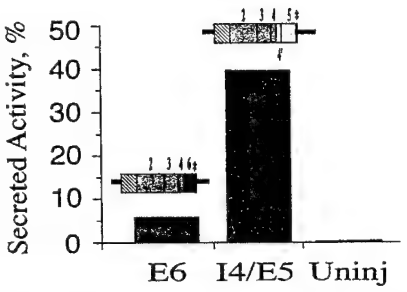

FIG. 6. ACHE-I4/E5 but not ACHE-E6 is excreted into the external medium. Fractions of total recovered AChE activity (medium plus whole-cell extract) in the external growth medium are presented for 20 DNA-injected (E6 and I4/E5) or control (Uninj) embryos following incubation of neurula-stage embryos overnight (day 1→day 2) in fresh buffer. Note that only embryos expressing ACHE-I4/E5 DNA displayed significant secretion of AChE into the surrounding medium. For an explanation of the schematic diagrams, see Fig. 1.

and the acquisition of motor function. Although mock injections indicated that microinjection may slightly retard growth and the accumulation of endogenous AChE (data not shown), quantitative RT-PCR performed with primers specific for XmyoD (8) and *Xenopus* GATA-2 (34) indicated that no global changes occurred in the levels of endogenous RNAs encoding these myogenesis- and hematopoiesis-promoting proteins in AChE DNA-injected embryos (data not shown).

To compare the hydrodynamic properties of the recombinant human enzymes, we performed sequential extractions of gastrula-stage embryos into low-salt, low-salt–detergent, and high-salt buffers. AChE activity from embryos injected with ACHE-E6 DNA consistently partitioned into both the low-salt (55%) and low-salt–detergent (35%) fractions. In contrast, activity from embryos injected with ACHE-I4/E5 was 85 to 90% solubilized in the low-salt step (Fig. 8B). In sucrose density gradient centrifugation, a single peak between 3 and 4 S was observed for the ACHE-E6- and ACHE-I4/E5-derived enzymes, both of which cosedimented with the clearly monomeric recombinant enzyme produced in bacteria (reference 27 and data not shown). This is consistent with a monomeric configuration for the cell-associated recombinant molecules. However, by nondenaturing polyacrylamide gel electrophoresis, catalytically active AChE from ACHE-I4/E5-injected embryos migrated significantly faster than the bands representing either recombinant human AChE from ACHE-E6-injected embryos or native AChE from human brain or erythrocytes (Fig. 8C). When electrophoresis was performed in the absence of detergent, no significant shift in the migration of ACHE-I4/E5-derived bands was observed, suggesting that this molecule represented a nonhydrophobic AChE species (Fig. 8C).

DISCUSSION

In transiently transgenic *X. laevis* embryos, AChE mRNA bearing the alternative 3′ exon E6 induced specific accumulation of human AChE in muscle and NMJs and enhanced NMJ development. Replacement of E6 with an in-frame pseudointronic sequence of similar size directed production of equal amounts of a soluble enzyme species that was amassed in epidermal cells and excreted into the external culture medium and which was not incorporated into muscle or NMJs and did not affect their development. These observations suggest that the 3′-terminal exons encoding the various AChE subtypes played indispensable roles in their NMJ or epidermal localization.

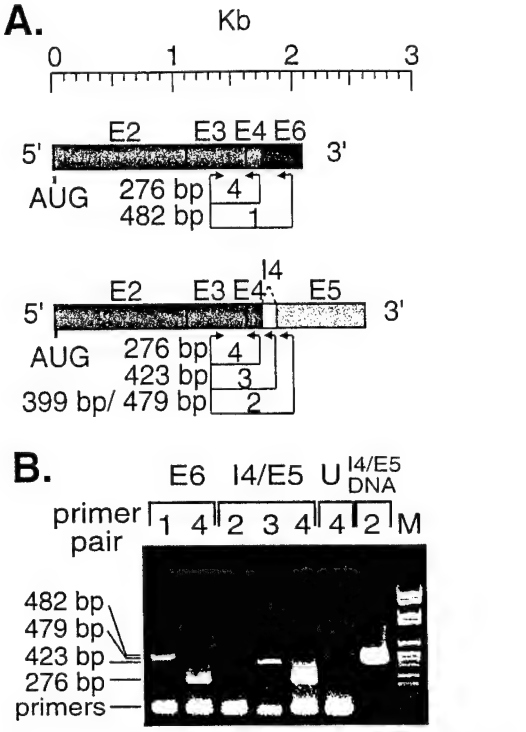

FIG. 7. Epidermal expression of ACHE-I4/E5 is associated with presence of a 3′-truncated readthrough mRNA. (A) Schematic representation of possible AChE mRNA products. Schemes present ACHE-E6 (upper) and ACHE-I4/E5 (lower) mRNA; I4 (indicated by dashed triangle) may be spliced out of the primary ACHE-I4/E5 transcript or retained in the mature mRNA. The expected product lengths of PCR primer pairs 1 through 4 (see Materials and Methods) are indicated to the left of the arrows. (B) RT-PCR. RT-PCR was performed on total RNA from 1-day-old *Xenopus* embryos injected with the ACHE-E6 (E6) or ACHE-I4/E5 (I4/E5) DNA constructs. Uninjected embryos (U) served as the control. PCR products were electrophoresed as previously described (1), and their lengths were evaluated by markers (M) of known size. PCR analysis of DNA performed with the ACHE-I4/E5 DNA construct (I4/E5 DNA) confirmed the ability of primer pair no. 2 to yield a PCR product. Control reactions, without RT, did not yield amplification products, proving the absence of contaminating DNA sequences (data not shown).

Differential posttranscriptional management of alternative AChE forms. The native human AChE promoter includes consensus recognition sites for transcription factors indicative of tissue-specific regulation of transcription (1). However, the CMV promoter used to direct the expression of AChE in *X. laevis* is pan-active (26), and our in situ hybridization suggests that it is expressed in the embryos in a nonspecific manner relatively early in development. This would explain the high levels of heterologous enzyme observed at the gastrula stage (day 1). Thus, the tissue-specific accumulation of alternative heterologous AChEs reflects differential posttranscriptional or posttranslational management of their respective RNA and/or protein products. Stabilization of AChE mRNA was recently shown to account for the increased AChE activity accompanying differentiation of cultured myoblasts (7). Our present observations add differential stability of alternative AChE polypeptides as a potential factor in the tissue-specific accumulation of these AChE forms.

In vivo, AChE is subject to tissue-specific and developmentally regulated posttranscriptional and posttranslational processing, which gives rise to a complex array of molecular forms varying in their extents of oligomeric assembly, association

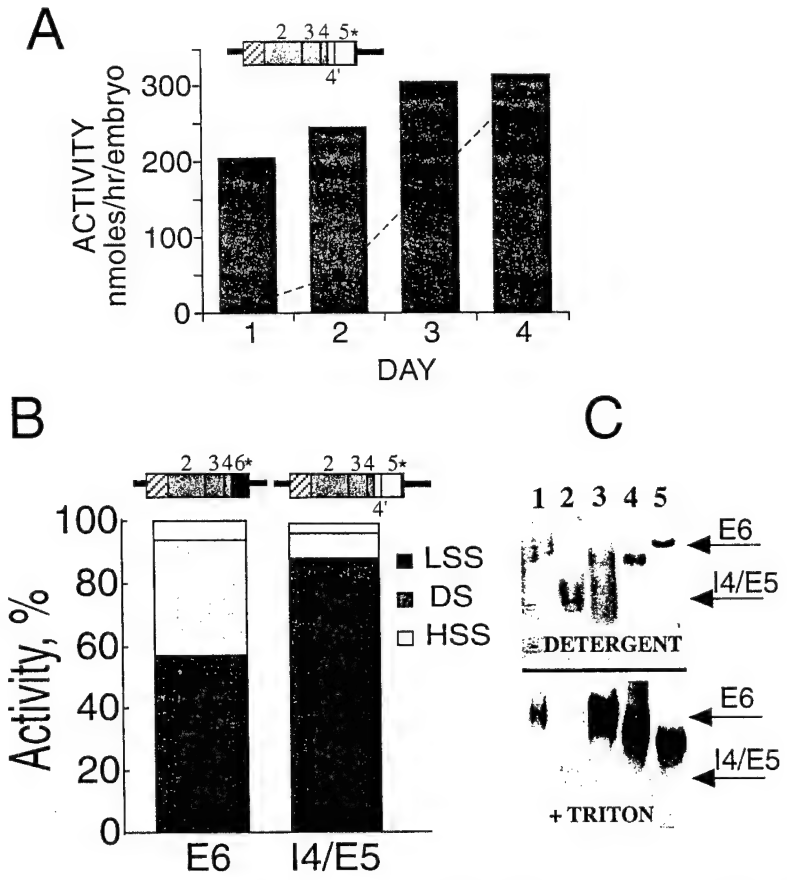

FIG. 8. ACHE-I4/E5 expression yields a soluble, hydrophilic enzyme with fast electrophoretic mobility. (A) Transient expression. Cleaving embryos (1 to 2 cells) injected with approximately 1 ng of ACHE-I4/E5 DNA under control of the CMV promoter were grown for 1 to 4 days at 20°C. Homogenates were assayed for acetylthiocholine hydrolyzing activity. The columns represent total AChE activity measured in DNA-injected embryos. The squares (▣) represent endogenous AChE activity measured in age-matched control uninjected embryos. Note the developmentally regulated increase in endogenous AChE levels and the concomitant decline in the relative extent of overexpression from days 1 to 4. The data represent averages of three separate groups of four embryos from a single microinjection experiment. (B) Differential solubility. Sequential extractions of 10 1-day-old DNA-injected embryos into low-salt-soluble (LSS), low-salt–detergent-soluble (DS), and high-salt-soluble (HSS) fractions were performed as described in Materials and Methods. The columns represent the relative fractions of the total summed activities extracted at each step for a single representative experiment. Endogenous *Xenopus* AChE activities were considered negligible and were ignored. Note the predominantly low-salt-soluble nature of the ACHE-I4/E5 (I4/E5) product(s) as compared with that of the recombinant human AChE as encoded by ACHE-E6 (E6). (C) Distinct electrophoretic mobility of alternative AChEs. Nondenaturing gel electrophoresis was performed as described in Materials and Methods in the presence or absence of 0.5% Triton X-100. Lanes 1 and 2, ACHE-E6- and ACHE-I4/E5-derived products, respectively, as expressed in *Xenopus* embryos (1 day postfertilization); lane 3, purified human erythrocyte AChE; lanes 4 and 5, recombinant human AChE-E6 (E6) as expressed in human 293 cells and *E. coli*, respectively. Note that the ACHE-I4/E5 (I4/E5) product(s) migrates significantly faster than all the other AChE forms both in the presence and in the absence of detergent. No band representing endogenous *Xenopus* AChE could be detected at this time point. The smearing of activity in lane 3 of the no-detergent (−) gels probably represents aggregation of the hydrophobic GPI-linked AChE erythrocyte dimer in the absence of Triton X-100. For an explanation of the schematic diagrams in panels A and B, see Fig. 1.

with noncatalytic subunits, hydrodynamic properties, and sites of subcellular localization (17). One level at which this diversity is controlled appears to be alternative splicing of 3′ exons (11, 15, 28). Transfections of AChE-coding sequences into mammalian cells indicated that alternative splicing alone could account for these multiple molecular forms of AChE (5, 12, 14, 16). Our results extend these conclusions by demonstrating that alternative splicing may dictate the final complement of specific AChE catalytic subunits available to particular cell types through selective management of specific AChE mRNAs and AChE polypeptides. Translated or nontranslated AChE mRNA, stable or unstable AChE mRNA, or polypeptides may dictate the final complement of specific AChE catalytic subunits expressed in particular cell types.

3′ exon E6 defines an indispensable motif for synaptic accumulation of AChE. Compartmentalized biosynthesis of the nicotinic acetylcholine receptor (reference 18 and reviewed in reference 4) as well as other NMJ proteins (22, 24) suggests that an intricate network of factors are at work to produce and localize NMJ proteins around junctional regions prior to their active accumulation at the NMJ. This network could potentially include *cis*-acting elements intrinsic to the mRNA or primary amino acid sequences of NMJ-targeted proteins as well as *trans*-acting cellular components capable of anchoring or translocating these molecules within the muscle. An example of a *trans*-acting factor controlling the translocation and subcellular anchoring of specific mRNAs is the 69-kDa protein associated with the developmentally regulated accumulation of two vegetal mRNAs in *Xenopus* oocytes (23). Our present findings demonstrate that the transiently transgenic embryos of *X. laevis* can be further employed to search for *cis*- and *trans*-acting factors controlling the management of proteins from

heterologous species. Recent work demonstrating the spatially restricted biosynthesis of AChE in avian muscle predicts the existence of localized cellular factors recognizing AChE and/or its encoding mRNA (9). In the present study, we observed that exon E6 and/or its encoded peptide participate in forming a recognition signal(s) through which such putative cellular elements might mediate accumulation and subcellular localization of AChE. Search of the Genetics Computer Group data bank did not reveal significant homologies between the E6-encoded peptide and any protein except the related acetylcholine-hydrolyzing enzyme butyrylcholinesterase. However, it is interesting that this enzyme, which has high homology (56%) to AChE in the corresponding C-terminal domain, also accumulated in NMJs of microinjected *Xenopus* embryos (reference 29 and unpublished observations). Moreover, both these enzymes are also found in brain nerve-nerve synapses (29). Thus, our findings suggest that exon E6 defines a conserved motif for muscle accumulation and trafficking of cholinesterases into synapses but not necessarily a general signal for targeting proteins to NMJs. Further experiments will be required to determine whether E6 is sufficient to direct synaptic accumulation of unrelated proteins to the NMJ as well.

A novel I4/E5-derived readthrough form of human AChE. An mRNA representing the I4 readthrough transcript in mouse tissues was reported but is considered absent in human cells. This difference was attributed to an inherent property of the human AChE nucleotide sequence (16). Nonetheless, we have recently observed, using RT-PCR and I4-specific primers, mRNA carrying the retained I4 sequence, in addition to E5 and E6, in several tumor cell lines of human origin (11) as well as in numerous mouse tissues (data not shown). That study did not, however, reveal whether this mRNA species is translated into protein and what the properties of the putative human readthrough AChE might be. In the present work, RT-PCR indicated the presence of a potentially truncated readthrough mRNA derived from ACHE-I4/E5 in microinjected *Xenopus* embryos. The protein translated from this readthrough RNA would lack the cleavable hydrophobic E5 stretch, precluding GPI linkage and leaving the relatively hydrophilic I4-encoded peptide. This could explain the high solubility of catalytically active AChE derived from ACHE-I4/E5 DNA.

When DNA encoding the mouse readthrough mRNA, where a nonsense codon appears 40 nucleotides downstream of the E4/I4 boundary, was expressed in COS cells, 97% of the total activity was soluble and secreted into the culture medium (16). The present study suggests that a truncated human readthrough AChE mRNA might also be translatable, giving rise to a catalytically active, nonmuscle, secretory form of AChE in *X. laevis*. However, the overall timing and levels of ACHE-I4/E5 expression in the embryos as assessed in total homogenates indicate generally similar stability of its mRNA and protein product as compared with those derived from ACHE-E6. Therefore, these observations may offer the first indications for the existence of yet another stable human AChE subtype representing the common exons E2, E3, and E4 and the pseudointron I4.

The human readthrough AChE mRNA (11) carries a 9-nucleotide sequence (5′-ACCTGCCCA-3′) beginning 18 nucleotides downstream of the I4/E5 boundary that is identical (in 8 of 9 bp) to that contained within a 19-bp consensus mRNA-destabilizing site (3). This sequence mediates endonucleolytic cleavage of RNA in *X. laevis* and *Drosophila melanogaster* and could explain the appearance of a truncated RNA. Indeed, when DNA encoding GPI-linked *Drosophila* AChE was expressed in microinjected *Xenopus* oocytes, a hydrophobic, but nonglypiated, membrane-associated enzyme was obtained. However, deletion of the sequence encoding the 27-amino-acid hydrophobic C-terminal peptide yielded a soluble, secreted AChE (6). Experiments to determine the precise 3′ and/or C-terminal limit of ACHE-I4/I5-derived mRNA and its polypeptide product are currently in progress.

Secretory AChE-I4/E5 may reflect an in vivo entity. It is yet uncertain whether generation of the unusual ACHE-I4/E5-derived protein and its accumulation in epidermis reflect natural events in the biosynthesis of human AChE or an anomalous expression pattern for this AChE in *X. laevis*. However, the putative AChE generated from ACHE-I4/E5 in *X. laevis* is catalytically indistinguishable from the ACHE-E6-derived enzyme (26a) and should be very close in size to the 583-amino-acid brain-muscle form. Therefore, the presence of such a discrete molecule in native human tissues would be difficult to detect and might easily go unnoticed. Moreover, a soluble AChE form with a distinct migration profile in isoelectric focussing was observed in the cerebrospinal fluid of patients with Alzheimer's disease (19), and soluble AChE monomers were reported in the serum of patients with carcinomas (33). Thus, the distinct migration of the short readthrough AChE derived from ACHE-I4/E5 in nondenaturing gel electrophoresis may provide a tool to search for a naturally occurring form of this enzyme species in humans.

In conclusion, we have used microinjected *Xenopus* embryos for transgenic overexpression of DNA constructs encoding variable C-terminal alternative forms of AChE. We established an NMJ-accumulating role for the 3′ exon E6 and observed epidermal expression and active secretion for human AChE encoded by a construct carrying the alternative 3′ region, I4/E5. ACHE-I4/E5 displayed hydrophilic properties and fast electrophoretic migration, reminiscent of a human AChE form reported in Alzheimer's disease. It was further excluded from muscle and NMJ structures and, in contrast with ACHE-E6, did not enhance NMJ development. These findings demonstrate that alternative 3′ exons in the AChE gene specify distinct tissue-recognizable signals and suggest the use of transiently transgenic *Xenopus* embryos for disclosing cell type specificities and biological roles of gene products from heterologous species.

ACKNOWLEDGMENTS

We thank R. Harland, Berkeley, Calif., for advice in whole-mount procedures; A. Shafferman, Ness-Ziona, Israel, for recombinant human AChE expressed in 293 cells; M. Gorecki, Rehovot, Israel, for recombinant human AChE expressed in *Escherichia coli*; J. Liao, Bern, Switzerland, for purified human AChEs; Christian Andres for helpful discussions; and Frank Goldberg for help with some of the experiments.

This research was supported by the Israel Basic Research Fund and the U.S. Army Medical Research and Development Command.

REFERENCES

1. **Ben Aziz-Aloya, R., S. Seidman, R. Timberg, M. Sternfeld, H. Zakut, and H. Soreq.** 1993. Expression of a human acetylcholinesterase promoter-reporter construct in developing neuromuscular junctions of *Xenopus* embryos. Proc. Natl. Acad. Sci. USA **90**:2471–2475.
2. **Billett, F. S., and R. P. Gould.** 1971. Fine ultrastructural changes in the differentiating epidermis of *Xenopus laevis* embryos. J. Anat. **108**:465–480.
3. **Brown, B. D., H. D. Zipkin, and R. Harland.** 1993. Sequence-specific endonucleolytic cleavage and protection of mRNA in *Xenopus* and *Drosophila*. Genes Dev. **7**:1620–1631.
4. **Changeux, J. P.** 1991. Compartmentalized transcription of acetylcholine receptor genes during motor endplate epigenesis. New Biol. **3**:413–429.
5. **Duval, N., J. Massoulie, and S. Bon.** 1992. H and T subunits of acetylcholinesterase from *Torpedo*, expressed in COS cells, generate all types of molecular forms. J. Cell. Biol. **118**:641–653.
6. **Fournier, D., A. Mutero, and D. Rungger.** 1992. *Drosophila* acetylcholinesterase: expression of a functional precursor in *Xenopus* oocytes. Eur. J. Biochem. **203**:513–519.

7. **Fuentes, M. E., and P. Taylor.** 1993. Control of acetylcholinesterase gene expression during myogenesis. Neuron **10:**379–387.
8. **Hopwood, N. D., A. Pluck, and J. B. Gurdon.** 1989. MyoD expression in the forming somites is an early response to mesoderm induction in *Xenopus* embryos. EMBO J. **8:**3409–3417.
9. **Jasmin, B. J., R. K. Lee, and R. L. Rotundo.** 1993. Compartmentalization of acetylcholinesterase mRNA and enzyme at the vertebrate neuromuscular junction. Neuron **11:**467–477.
10. **Karnovsky, M. J., and L. Roots.** 1964. A direct coloring method for cholinesterases. J. Histochem. Cytochem. **12:**219–221.
11. **Karpel, R., R. Ben Aziz-Aloya, M. Sternfeld, G. Ehrlich, D. Ginzberg, P. Tarroni, F. Clementi, H. Zakut, and H. Soreq.** 1994. Expression of three alternative acetylcholinesterase messenger RNAs in human tumor cell lines of different tissue origins. Exp. Cell Res. **210:**268–277.

11a. **Karpel, R., et al.** Submitted for publication.

12. **Krejci, E., F. Coussen, N. Duval, J.-M. Chatel, C. Legay, M. Puype, J. Vandekerckhove, J. Cartaud, S. Bon, and J. Massoulie.** 1991. Primary structure of a collagenic tail peptide of *Torpedo* acetylcholinesterase: co-expression with catalytic subunit induces the production of collagen-tailed forms in transfected cells. EMBO J. **10:**1285–1293.
13. **Legay, C., S. Bon, and J. Massoulie.** 1993. Expression of a cDNA encoding the glycolipid-anchored form of rat acetylcholinesterase. FEBS Lett. **315:** 163–166.
14. **Legay, C., S. Bon, P. Vernier, F. Coussen, and J. Massoulie.** 1993. Cloning and expression of a rat acetylcholinesterase subunit: generation of multiple molecular forms, complementarity with a Torpedo collagenic subunit. J. Neurochem. **60:**337–346.
15. **Li, Y., S. Camp, T. L. Rachinsky, D. Getman, and P. Taylor.** 1991. Gene structure of mammalian acetylcholinesterase. Alternative exons dictate tissue-specific expression. J. Biol. Chem. **266:**23083–23090.
16. **Li, Y., S. Camp, and P. Taylor.** 1993. Tissue-specific expression and alternative messenger RNA processing of the mammalian acetylcholinesterase gene. J. Biol. Chem. **268:**5790–5797.
17. **Massoulie, J., L. Pezzementi, S. Bon, E. Krejci, and F. M. Vallette.** 1993. Molecular and cellular biology of cholinesterases. Prog. Neurobiol. **41:**31–91.
18. **Merlie, J., and J. R. Sanes.** 1985. Concentration of acetylcholine receptor mRNA in synaptic regions of adult muscle fibers. Nature (London) **317:**66–68.
19. **Navaratnam, D. S., J. D. Priddle, B. McDonald, M. M. Esiri, J. R. Robinson, and A. D. Smith.** 1991. Anomalous molecular form of acetylcholinesterase in cerebrospinal fluid in histologically diagnosed Alzheimer's disease. Lancet **337:**447–450.
20. **Neville, L. F., A. Gnatt, Y. Loewenstein, S. Seideman, G. Ehrlich, and H. Soreq.** 1992. Intramolecular relationships in cholinesterases revealed by oocyte expression of site-directed and natural variants of human BCHE. EMBO J. **11:**1641–1649.
21. **Nishikawa, S., and F. Sasaki.** 1993. Secretion of chondroitin sulfate from embryonic epidermal cells in *Xenopus laevis*. J. Histochem. Cytochem. **9:**1373–1381.
22. **Pavlath, G. K., K. Rich, S. G. Webster, and H. M. Blau.** 1989. Localization of muscle gene products in nuclear domains. Nature (London) **337:**570–573.
23. **Pressman-Schwartz, S., L. Aisenthal, Z. Elisha, F. Oberman, and J. K. Yisraeli.** 1992. A 69-kDa RNA-binding protein from *Xenopus* oocytes recognizes a common motif in two vegetally localized maternal mRNAs. Proc. Natl. Acad. Sci. USA **89:**11895–11899.
24. **Ralston, E., and Z. W. Hall.** 1989. Transfer of a protein encoded by a single nucleus to nearby nuclei in multinucleated myotubes. Nature (London) **244:**1066–1069.
25. **Salpeter, M.** 1967. Electron microscope radioautography as a quantitative tool in enzyme cytochemistry. I. The distribution of acetylcholinesterase at motor endplates of a vertebrate twitch muscle. J. Cell Biol. **32:**379–389.
26. **Schmidt, E. V., G. Christoph, R. Zeller, and P. Leder.** 1990. The cytomegalovirus enhancer: a pan-active control element in transgenic mice. Mol. Cell. Biol. **10:**4406–4411.

26a. **Schwarz, M., Y. Loewenstein-Lichtenstein, D. Glick, J. Liao, B. Norgaard-Pedersen, and H. Soreq.** Catalysis by human cholinesterase variants dissected by successive organophosphorus inhibition and oxime reactivation. Mol. Brain Res., in press.

27. **Seidman, S., R. Ben Aziz-Aloya, R. Timberg, Y. Loewenstein, B. Velan, A. Shafferman, J. Liao, B. Norgaard-Pedersen, U. Brodbeck, and H. Soreq.** 1994. Overexpressed monomeric human acetylcholinesterase induces subtle ultrastructural modifications in developing neuromuscular junctions of *Xenopus laevis* embryos. J. Neurochem. **62:**1670–1681.
28. **Sikorav, J. L., N. Duval, A. Anselmet, S. Bon, E. Krejci, C. Legay, M. Osterlund, B. Reimund, and J. Massoulie.** 1988. Complex alternative splicing of acetylcholinesterase transcripts in *Torpedo* electric organ: primary structure of the precursor of the glycolipid-anchored dimeric form. EMBO J. **7:**2983–2993.
29. **Soreq, H., R. Beeri, S. Seidman, R. Timberg, Y. Loewenstein, M. Sternfeld, and C. Andres.** 1994. Modulating cholinergic neurotransmission through transgenic overexpression of human cholinesterases, p. 84–87. *In* R. E. Becker and E. Giacobini (ed.), Pharmacological basis of cholinergic therapy in Alzheimer's disease. Birkhauser, Boston.
30. **Soreq, H., R. Ben-Aziz, C. Prody, S. Seidman, A. Gnatt, L. Neville, J. Lieman-Hurwitz, E. Lev-Lehman, D. Ginzberg, Y. Lapidot-Lifson, and H. Zakut.** 1990. Molecular cloning and construction of the coding region for human acetylcholinesterase reveals a G,C rich attenuating structure. Proc. Natl. Acad. Sci. USA **87:**9688–9692.
31. **Soreq, H., and H. Zakut.** 1993. Human cholinesterases and anticholinesterases. Academic Press, San Diego, Calif.
32. **Velan, B., C. Kronman, H. Grosfeld, M. Leitner, Y. Gozes, Y. Flashner, T. Sery, S. Cohen, R. Ben-Aziz, S. Seidman, A. Shafferman, and H. Soreq.** 1991. Recombinant human acetylcholinesterase is secreted from transiently transfected 293 cells as a soluble globular enzyme. Cell. Mol. Neurobiol. **11:**143–156.
33. **Zakut, H., L. Even, S. Birkenfeld, G. Malinger, R. Zisling, and H. Soreq.** 1988. Modified properties of serum cholinesterases in primary carcinomas. Cancer **61:**727–737.
34. **Zon, L. I., C. Mather, S. Burgess, M. E. Bolce, R. M. Harland, and S. H. Orkin.** 1991. Expression of GATA-binding proteins during embryonic development in *Xenopus laevis*. Proc. Natl. Acad. Sci. USA **88:**10642–10646.

Biomed & Pharmacother (1994) 48, 253-259

Mutations and impaired expression in the ACHE and BCHE genes: neurological implications

H Soreq[1], G Ehrlich[1], M Schwarz[1], Y Loewenstein[1], D Glick[1], H Zakut[2]

[1]*Department of Biological Chemistry, The Life Sciences Institute, The Hebrew University, Jerusalem 91904;*
[2]*Department of Obstetrics and Gynecology, The Sackler Faculty of Medicine, Tel-Aviv University, The Edith Wolfson Medical Center, Holon 58100, Israel*

Summary – The acetylcholine hydrolysing cholinesterases control the termination of cholinergic signalling in multiple tissues and are targets for a variety of drugs, natural and man-made poisons and common insecticides. Molecular cloning and gene mapping studies revealed the primary structure of human acetyl- and butyrylcholinesterase and localized the corresponding ACHE and BCHE genes to the chromosomal positions 3q26-ter and 7q22, respectively. Several different point mutations in the coding region of BCHE were found to be particularly abundant in the Israeli population. Analytical expression studies in microinjected *Xenopus* oocytes have demonstrated that the biochemical properties of cholinesterases may be modified by rationalized site-directed mutagenesis and in chimeric ACHE/BCHE constructs. These properties are differently altered in the various allelic BCHE variants, conferring resistance to several anti-cholinesterases, which may explain the evolutionary emergence of these multiple alleles. At the clinical level, abnormal expression of both ACHE and BCHE and the *in vivo* amplification of the ACHE and BCHE genes has been variously associated with abnormal megakaryocytopoiesis, leukemias and brain and ovarian tumors. Moreover, antisense oligonucleotides blocking the expression of these genes were shown to interfere with hemocytopoiesis in culture, implicating these genes in cholinergic influence on cell growth and proliferation.

ACHE / BCHE / mutations / neurological diseases

Introduction

Two single-copy genes, designated ACHE and BCHE, encode the acetylcholine-hydrolysing enzymes acetyl- and butyrylcholinesterase (AChE and BuChE, respectively). The clinical role of AChE needs no introduction to neurologists; however, the role of BuChE is less obvious. In addition to hydrolyzing acetylcholine, though at a considerably slower pace than AChE [47], BuChE acts as a scavenger of poisons targeted at acetylcholine binding proteins. These include, in particular, AChE and the various acetylcholine receptors [47]. The human ACHE and BCHE genes were both molecularly cloned [42, 48] and mapped to the chromosomal positions 7q22 [20, 22] and 3q26 [5, 23], respectively. Because of the physiological role of the enzymes, mutations in both of the cholinesterase genes (CHEs) are physiologically important, as indicated by the fact that reduced cholinesterase (ChE) enzyme activity due to natural or man-produced inhibitors has severe neurological consequences. In the following, we discuss the current state of information regarding the basis for these consequences.

BuChE mutations: causes for congenital susceptibility to altered drug responses

Twenty-two different mutations in the coding region of the human BCHE gene have been identified in the human population since the gene was cloned [41]. Some of these alter various amino acids and introduce different phenotypic changes in the resultant enzyme [37]. Other mutations introduce stop signals into the mRNA transcript, producing incomplete, "silent" (inactive), BuChE [40]. The active variants are far more abundant in the population than the silent ones, all of which together are only 0.0001% of homozygotes [55], which suggests that the frequent phenotypically-effective variants confer a selection advantage for

development. The presumption is, that random mutation would produce more silent mutations, and, as these are rare, they must be selected against.

Cholinesterase genes were analyzed by molecular cloning, library screening and polymerase chain reactions (PCR) amplification, all as detailed elsewhere [20, 23, 42, 48]. Positions of substituted amino acid residues within the mature AChE protein were determined by superimposing the primary amino acid sequence of human AChE [48] onto the crystal structure of *Torpedo* AChE [52], using the Insight program (Biosym) on a Silicon Graphics computer as detailed in [49]. For BuChE mutations, we employed the recent computer model of human BuChE [25].

The currently available data on mutations in the coding region of the human BCHE gene and their phenotypic consequences are presented in table I and figure 1 and the different mutations causing "silent" BuChE phenotypes are superimposed in figure 2 on the ribbon model of the BuChE protein [25]. It is interesting to note that several of these BuChE variants (*eg* Asp70 → Gly) were simultaneously discovered on two continents, while many others have been detected only once. The search for new variants was not random; mutations in BCHEcDNA or BCHE genes were sought in DNA samples taken from individuals who expressed the variant phenotypes [38, 40, 43] or from tumors presenting biochemical alterations in the BuChE protein [23, 37].

Several of the variant BuChE proteins display an inability to hydrolyze the muscle relaxant succinylcholine [37, 55]. Consequently, patients with such variant BuChEs may suffer prolonged apnea when given standard doses of succinylcholine during anesthesia [26]. The low serum levels of BuChE activity characteristic of several of these variants also implies that tissue types to which ChE activity is essential will be subject to severe stress under exposure of individuals carrying these variants to organophosphorous (OP) insecticides designed to block ChE activities, or by naturally occurring ChE inhibitors.

A single point mutation in the ACHE gene: immunogenic implications

In contrast to the multitude of point mutations in the BCHE gene, records of phenotypically effective variants in the ACHE gene are so far limited to a single point mutation. This was discovered in several steps. The human ACHE gene was first demonstrated to present two co-dominant alleles in a single genetic locus [13]. Recently, a common polymorphism was reported in the ACHE gene, in which His322 is replaced by asparagine due to a C → A substitution [31]. Furthermore, this allele has been identified as the basis of the Yt^b blood group [50], for which an incidence of 5% has been determined in the general Caucasian population [29] and a considerably higher incidence in Israel [28].

The genomic position of the Yt mutation is shown in figure 1. In view of the complete agreement between the original observation of phenotypic diversity and the recent findings on the Yt mutation, it appears that the ACHE gene is much less susceptible to mutation than the related BCHE gene.

Discussion

The plethora and frequency of BuChE variants as compared with the genetic stability of AChE undoubtedly reflects the different levels of importance of these two enzymes. Thus, the essential function of AChE in the termination of neurotransmission precludes mutations that compromise the activity of AChE, as these are undoubtedly lethal. In contrast, the scavenging role, which has been proposed for BuChE, may even lead to a positive selection pressure for proteins with modified properties when these confer resistance to specific cholinergic poisons. However, we posit two caveats: the extreme rarity of the silent BuChE mutations strongly suggests a role for BuChE that perhaps has not yet been identified, and selection does not necessarily render BuChE variants advantageous when faced with man-made ChE inhibitors.

The body's first line of defence against anti-ChEs is plasma BuChE, which scavenges the agent. Congenital variations of BuChE, however, may impair this protective property. Excess ChE inhibitors that have not been eliminated by the BuChE screen, upon reaching neuromuscular junctions (NMJs) may block diaphragm muscles, with a lethal effect [14]. Neurological implications of BuChE mutations, include congenital susceptibility to cholinergic drugs and poisons. Such poisons include primarily OP insecticides, the inhibition by which causes a very specific re-

Table I. Human butyrycholinesterase variants and their phenotypes.

No[a]	*Mutated nucleotide*	*Altered amino acids*	*Phenotype*	*Reference*
1	Wildtype	None	Normal	Prody *et al* (1987) Lockridge *et al* (1987)
2	ATT TT	I6-ter	Silent (frameshift)	Primo-Parmo *et al* (1992)
3	CCT TCT	P37S	Silent	Primo-Parmo *et al* (1992)
4	GAT GGT	D70G	Resistance to succinyl choline and other ligands	Gnatt *et al* (1990) Neville *et al* (1990b)
5	TAT CAT	Y114H	No significant effect, when alone	Neville *et al* (1992)
6	GGT GAT	G115D	Silent	Primo-Parmo *et al* (1992)
7	GGT GGAG	G117-ter	Silent (frameshift)	Noguiera *et al* (1990)
8	GTG ATG	V142M	H-variant (10% specific activity)	Lockridge (1990)
9	GAT GGT	D170G	Silent	Primo-Parmo *et al* (1992)
10	AGT GGT	S198G	Silent	Primo-Parmo *et al* (1992)
11	ACG ATG	T243M	Fluoride-1 (Km variant)	Nogueira *et al* (1992)
12	Alu insert (nt 1062-1077)	D301-ter	Silent (frameshift)	Soreq and Zakut (1993)
13	ACC AACC	T315-ter	Silent (frameshift)	Primo-Parmo *et al* (1992)
14	GGA CGA	G356R	Silent	Primo-Parmo *et al* (1992)
15	GGT GTT	G390V	Fluoride-2 (Km variant)	Bartels *et al* (1992a)
16	TCG CCC	S425P	When coupled with G70, full resistance to succinyl choline and dibucaine	Gnatt *et al* (1990)
17	TGG CGG	W471R	Silent	Primo-Parmo *et al* (1992)
18	GAA GTA	E497V	J variant (33% specific activity)	Bartels *et al* (1992a)
19	TAT TAA	Y500-ter	Silent	Primo-Parmo *et al* (1992)
20	CAA CTA	Q508L	Silent	Primo-Parmo *et al* (1992)
21	GCA ACA	A539T	K variant (70% specific activity)	Bartels *et al* (1992b)
22	TTT TAT	F561Y	No significant effect when alone	Gnatt *et al* (1990)

[a]Mutant number refers to figure 1.

action of the OP compound with the active site serine of ChEs [3]. Blocking of ChEs leads to acetylcholine (ACh) accumulation [2], synaptic excitation and subsequent paralysis. Delayed neurotoxicity includes damage to the peripheral nervous system [1], although the mechanism of this effect is unknown. Clinical symptoms of acute OP poisoning include, in the following

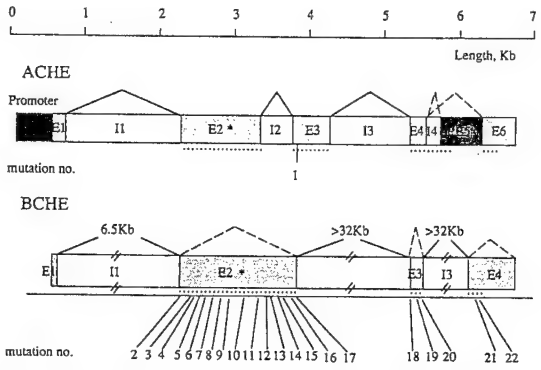

Fig 1. The organization of the ACHE (upper) and BCHE (lower) genes. Note the arrangement of exons (E) and introns (I) and the positions of the natural mutations, numbered as in table I. Above the bars representing the genes are constant (solid lines) and alternative (broken lines) sequences that are excised from the RNA transcripts prior to translation into a tissue- or subcellular component-specific enzyme form.

Fig 2. Locations of butyrylcholinesterase mutations. The 22 mutated amino acid residues or the residue corresponding to a mutated codon are shown as space-filling atoms superimposed on the backbone of the BuChE molecule. Note the distribution of the mutations over the entire protein molecule.

order: flushing, dry mouth, fasciculations, tremor, restlessness, agitation, ataxia [34] weakness, convulsions, coma and death [19]. Immediate treatment aimed at restoration of cholinergic function terminates all of these symptoms, although, paradoxically, the levels of plasma BuChE and red blood cell AChE remain low for up to 3 and 12 weeks, respectively [35]. This suggests a much faster regeneration of AChE at the NMJ, but this has not been documented.

Treatment of OP intoxication includes prophylactic and therapeutic use of derivatives of the reversible ChE inhibitor physostigmine (eserine) [56]. Reactivators of AChE and BuChE were designed to be attracted to the choline-binding site (like choline, they possess a permanent positive charge) and to have a reactive group (–C=NOH) that can promote hydrolysis of the phosphate that blocks the enzyme's reactive site. A successful reactivator is PAM (pyridinium-2 aldoxime methiodide) [57]. This reactivation process, though, is hampered by "ageing", which occurs after ChEs interact with certain OPs, such as sarin (isopropylmethylphosphonofluoridate), DFP (diisopropylphosphorofluoridate) and malathion (0,0-diethyldithiophosphate diethylmercaptosuccinate). This process is believed to involve dealkylation of the covalently bound OP group, rendering therapy by oximes ineffective [3, 32]. In addition to affecting the NMJ, OPs cause delayed damage to the central nervous system (CNS) [1], where the exact mechanism of their action is unknown. In all body tissues poisonous ChE inhibitors may be dealt with by plasma BuchE, which reacts with the agent, sparing the more vital AChE. Congenital variabilities in BuchE, however, may impair this protection property.

BuChE levels in serum of individuals with the common BCHE allele have been shown to vary with a standard deviation of 25% in the normal, non-exposed population [6]. In addition, increased or decreased BuChE activities have been attributed to some disease states. These include burn injuries, renal disease, or liver dysfunction, for decrement of BuChE levels, whereas increases have been observed in cases of obesity, asthma, and alcoholism [27, 45, 55, 58]. This, in turn, implies variable sensitivity of affected individuals to OP poisoning. It is therefore not surprising that long-term neurological and/or psychiatric effects of OP poisoning in man have been subject to dispute for many years. In rodents, the OP agent tri-*o*-cresyl phosphate was shown to induce chronic, progressive degeneration of lower motor neurons [10] suggesting that parallel effects may be anticipated in humans under occupational exposure. At least one such paralysis case has, indeed, been reported [17]. Subsequent reports of long-term neuropsychiatric disturbances in individuals who were subject to chronic OP poisoning [16, 21] were reinforced by observations of EMG abnormalities in occupationally exposed individuals [24]. In addition, acute pesti-

cide intoxication was reported to produce an abnormal EEG, similar to that detected in epileptic patients [11, 33] or other, less drastic yet long-term and persistent alterations [18, 51]. These conclusions are consistent with the hypothesis that cholinergic signaling is involved in memory [4] and calls for particular caution in the use of OP insecticides.

In contrast with these early and alarming studies, other investigators failed to observe long-term psychiatric [53] and/or neurological [12] changes following OP poisoning, either in man or in experimental animals. Neurobehavioral abnormalities were sought in workers chronically exposed to OP insecticides and no defects in performance could be observed in memory or language abilities [44]. A more recent epidemiological attempt to evaluate the latent neurological effects of OP pesticide poisoning was performed in Colorado and included 100 individuals with a history of previous acute OP pesticide poisoning, matched according to age and education with non-poisoned control individuals [46]. The study was performed several years after the exposures, and revealed no persistent alterations in audiometric, ophthalmic, EEG or blood ChE tests. However, neuropsychological abnormalities in memory, abstraction and mood as well as impaired motor reflexes were statistically significant in the OP-exposed individuals in the range characteristic of patients with cerebral damage or dysfunction. This study clearly demonstrates chronic neurological consequences of acute OP poisoning and explains the reasons for the previous disagreement between researchers, since it reveals sequelae too subtle to be detected by standard techniques.

A recent study further describes aggressive behavior following exposure to cholinesterase inhibitors [15]. This was reported in four different individuals with no previous history of violent behavior and appeared to be reversible, which adds unprovoked aggressive behavior to the list of neurotoxic effects of OP poisoning.

Thus, point mutations in the BCHE gene may cause congenital variability in the susceptibility of OP poisoning. Among the cholinergic drugs, ChE inhibitors used experimentally to treat senile patients, should be mentioned. They include mainly carbamates such as physostigmine and derivatives [54]. It is important to note that several of the variant BuChE subtypes drastically differ in their inhibition constants for carbamates [37]. In this case as well, phenotypic variabilities in the intensity and duration of response to cognitive drugs may be expected in individuals having the variant genotypes.

Acknowledgments

Supported by Grant DAMD 17-90-Z0038 from the US Army Medical Research and Development Command and from the EWH British Research Trust, London (to HS and HZ). MS is the recipient of a Levi Eshkol postdoctoral fellowship. DG received support from the Israel Ministry of Immigrant Absorption.

References

1 Abou-Donia MB, Lapadula DM. Mechanisms of organophosphorous ester-induced delayed neurotoxicity; type I and type II. *Ann Rev Pharmacol Toxicol* 1990;30:405-40
2 Akasu T, Ariyoshi M, Tokimasa T. Postsynaptic modulation of cholinergic transmission by endogenous substances. *Comp Biochem Physiol* 1988;91C:241-6
3 Aldridge WN, Reiner E. *Enzyme Inhibitors as Substrates.* Amsterdam: North-Holland, 1972
4 Allain H, Moran P, Bentue-Ferrer D, Martinet JP, Lieury A. Pharmacology of the memory process. *Arch Gerontol Geriatr* (Suppl) 1989;1:109-20
5 Allderdice PW, Gardner HA, Galutira D, Lockridge O, La Du BN, McAlpine PJ. The cloned butyrylcholinesterase (BCHE) gene maps to a single chromosome site. 3q26, *Genomics* 1991;11:452-4
6 Altland K, Goedde HW, Held K, Jensen M, Munsch H, Solem E. New biochemical and immunological data on quantitative and qualitative variability of human pseudocholinesterase. *Humangenetik* 1971;14:56-60
7 Arpagaus M, Chatonnet A, Rogers L, Venta P, La Du, BN Lockridge O. Genomic clones for human butyrylcholinesterase. *J Cell Biol* 1989;107:521
8 Bartels CF, Zelinski T, Lockridge O. Mutation at codon 322 in the human AChE gene accounts for YT blood group polymorphism. *Am J Hum Genet* 1993;52:928-36
9 Bartels CF, Jensen FS, Lockridge O, van der Spek AFL, Rubinstein HM, Lubrano T, La Du BN. DNA mutation associated with the human butyrylcholinesterase K-Variant and its linkage to the atypical variant mutation and other polymorphic sites. *Am J Hum Genet* 1992;50:1086-1103
10 Bidstrup PL, Bonnell J, Beckett AG. Paralysis following poisoning by a new organic phosphorous insecticide (Mipafox). *Br Med J* 1953;1:1068-72
11 Brown HW. Electroencephalographic changes and disturbance of brain function following human organophosphate exposure. *Northwest Med* 1971;70:845-6
12 Clark G. Organophosphate insecticides and behavior: a review. *Aerosp Med* 1971;42:735-40
13 Coates PM, Simpson NE. Genetic variation in human erythrocyte acetylcholinesterase. *Science* 1972;175:1466-7
14 Costa LG. Interactions of neurotoxicants with neurotransmitter systems. *Toxicology* 1988;49:359-66

15 Devinsky O, Kernan J, Bear DM. Aggressive behavior following exposure to cholinesterase inhibitors. *J Neuropsychiatry Clin Neurosci* 1992;4:189-94

16 Dille JR, Smith PW. Central nervous system effects of chronic exposure to organophosphate insecticides. *Aerosp Med* 1964;35:475- .

17 Drenth JH, Ensberg IFG, Roberts DV, Wilson A. Neuromuscular function in agricultural workers using pesticides. *Arch Environ Health* 1972;25:395-8

18 Duffy FH, Burchfield JL, Bartels PH, Gaon M, Sim VM. Long-term effects of an organophosphate upon the human electroencephalogram. *Toxicol Appl Pharmacol* 1979; 47:161-76

19 Durham WF, Hayes WJ Jr. Organic phosphorous poisoning and its therapy. *Arch Environ Health* 1962;5:21-47

20 Ehrlich G, Viegas-Pequignot V, Ginzberg D, Sindel L, Soreq H, Zakut H. Mapping the human acetylcholinesterase gene to chromosome 7q22 by fluorescent *in situ* hybridization coupled with selective PCR amplification from a somatic hybrid cell panel and chromosome-sorted DNA libraries. *Genomics* 1992;13:1192-7

21 Gershon S, Shaw FH. Psychiatric sequelae of chronic exposure to organophosphorous insecticides. *Lancet* 1961; i:1371-4

22 Getman DK, Eubanks JH, Camp S, Evans GA, Taylor P. The human gene encoding acetylcholinesterase is located on the long arm of chromosome 7. *Am J Hum Genet* 1992;51:170-177

23 Gnatt A, Prody CA, Zamir R, Lieman-Hurwitz J, Zakut H, Soreq H. Expression of alternatively terminated unusual human butyrylcholinesterase messenger RNA transcripts, mapping to chromosome 3q26-ter, in nervous system tumors. *Cancer Res* 1990;50:1983-7

24 Grob D, Harvey AM. The effects and treatment of nerve gas poisoning. *Am J Med* 1953;24:52-63

25 Harel M, Sussman JL, Krejci E, Bon S, Chanal P, Massoulie J, Silman I. Conversion of acetylcholinesterase to butyrylcholinesterase: modeling and mutagenesis. *Proc Natl Acad Sci USA* 1992;89:10827-31

26 Hodgkin WE, Giblett ER, Levine H, Bauer W, Motulsky AG. Complete pseudocholinesterase deficiency: genetic and immunologic characterization. *J Clin Invest* 1965; 44:486-97

27 Hunter D. *The Diseases of Occupations*. 5th Edn, London: English Universities Press, 1975:pp 368-77

28 Levene C, Bar-Shany S, Manny N, Moulds JJ, Cohen T. The Yt blood groups in Israeli Jews, Arabs, and Druse. *Transfusion* 1987;27:471-4

29 Lewis M, Kaita H, Philipps S, McAlpine PJ, Wong P, Giblett ER, Anderson J. The Yt blood group system (ISBT No. 011) Genetics studies. *Vox Sang* 1987;53:52-6

30 Lockridge O. Genetic variants of human serum cholinesterase influence metabolism of the muscle relaxant succinylcholine. *Pharmacol Ther* 1990;47:35-60

31 Lockridge O, Bartels CF, Vaughan TA, Won CK, Norton SE, Johnson LL. Complete amino acid sequence of human serum cholinesterase. *J Biol Chem* 1987;262:549-57

32 Loomis TA. Distribution and excretion of pyridine-2-aldoxime methiodide (PAM); atropine and PAM in sarin poisoning. *Toxicol Appl Pharmacol* 1963;5:489-99

33 Metcalf DR, Holmes JH. EEG, psychological, and neurological alteration in humans with organophosphorous exposure. *Ann NY Acad Sci* 1969;160:357-65

34 Michotte A, Van Dijck I, Maes V, D'Haenen H. Ataxia as the only delayed neurotoxic manifestation of organophosphate insecticide poisoning. *Eur Neurol* 1989;29:23-26

35 Murphy SD. Pesticides. *In:* Casarett LJ, Doull J, eds. *Toxicology – The Basic Science of Poisons*. New York: Macmillan, 1975

36 Neville LF, Gnatt A, Padan R, Seidman S, Soreq H. Anionic site interactions in human butyrylcholinesterase disrupted by two single point mutations. *J Biol Chem* 1990;265:20735-8

37 Neville LF, Gnatt A, Loewenstein Y, Seidman S, Ehrlich G, Soreq H. Intramolecular relationships in cholinesterases revealed by oocyte expression of site-directed and natural variants of human BCHE. *EMBO J* 1992;11:1641-9

38 Noguiera CP, McGuire MC, Graeser C *et al.* Identification of a frameshift mutation responsible for the silent phenotype of human serum cholinesterase, Gly 117 (GGT → GGAG). *Am J Hum Genet* 1990;46:934-42

39 Nogueira CP, Bartels CF, McGuire MC *et al.* Identification of two different point mutations associated with the fluoride-resistant phenotype for human butyrylcholinesterase. *Am J Hum Genet* 1992;51:821-8

40 Primo-Parmo SL, Bartels CF, Lightstone H, van der Spek AFL, La Du BN. Heterogeneity of the silent phenotype of human butyrylcholinesterase-identification of eight new mutations. *In:* Shaffeman A, Velan B, eds. *Multidisciplinary Approaches to Cholinesterase Functions*. New York: Plenum Press, 1992;pp 61-4

41 Prody C, Zevin-Sonkin D, Gnatt A, Koch R, Zisling R, Goldberg O, Soreq H. Use of synthetic oligodeoxynucleotide probes for the isolation of a human cholinesterase cDNA clone. *J Neurosci Res* 1986;16:25-35

42 Prody CA, Zevin-Sonkin D, Gnatt A, Goldberg O, Soreq H. Isolation and characterization of full-length clones coding for human cholinesterase from fetal human tissues. *Proc Natl Acad Sci USA* 1987;84:3555-9

43 Prody CA, Dreyfus PA, Zamir R, Zakut H, Soreq H. *De novo* amplification within a "silent" human cholinesterase gene in a family subjected to prolonged exposure to organophosphorous insecticides. *Proc Natl Acad Sci USA* 1989;86:690-4

44 Rodnitzky RL, Levin HS, Mick DL. Occupational exposure to organophosphate pesticides: neurobehavioral study. *Arch Environ Health* 1975;30:98-103

45 Rosalki SB. Genetic influences on diagnostic enzymes in plasma. *Enzyme* 1988;39:95-109

46 Savage EP, Keefe TJ, Mounce LM, Heaton RK, Lewis JA, Burcar PJ. Chronic neurological sequelase of acute organophosphate pesticide poisoning. *Arch Environ Health* 1988;43:38-45

47 Soreq H, Zakut H. *Human Cholinesterases and Anticholinesterases*. San Diego: Academic Press, 1993,324 pp

48 Soreq H, Ben-Aziz R, Prody CA *et al.* Molecular cloning and construction of the coding region for human acetylcholinesterase reveals a G+C-rich attenuating structure. *Proc Natl Acad Sci USA* 1990;87:9688-92

49 Soreq H, Gnatt A, Loewenstein Y, Neville LF. Excavations into the active-site gorge of cholinesterases. *Trends Biochem Sci* 1992;17:353-8

50 Spring FA, Anstee DJ. Evidence that the antigens of the Yt blood-group system are located on human erythrocyte acetylcholinesterase. *Blood* 1992;80:2136-41

51 Stoller A, Krupinski J, Christophers AJ, Blanks GK: Organophosphorous insecticides and major mental illness: an epidemological investigation. *Lancet* 1965;i:1387-8

52 Sussman JL, Harel M, Frolow F, Oefner C, Goldman A, Toker L, Silman I. Atomic structure of acetylcholinesterase from *Torpedo californica:* a prototypic acetylcholine-binding protein. *Science* 1991; 253:872-9

53 Tabershaw IR, Cooper WC. Sequelae of acute organic phosphate poisoning. *J Occup Med* 1966;8:5-20

54 Taylor P. Cholinergic agonists, Cholinergic antagonists, Agents acting at the neuromuscular junction and autonomic ganglia. *In:* Gilman AG, Rall TW, Nies AS, Taylor P, eds. *Goodman and Gilman's The Pharmacological Basis of Therapeutics.* 8th edition. New York: Pergamon Press, 1990;pp 122-130, 131-149, 166-186

55 Whittaker M. *Cholinesterase.* Basel:Karger, 1986

56 Wills JH. Toxicity of anticholinesterases and treatment of poisoning. *In: International Encyclopedia of Pharmacology and Therapeutics.* Vol. I, Oxford: Pergamon Press, 1970;pp 357-69

57 Wilson IB. Molecular complementarity and antidotes for alkylphosphate poisoning. *Fed Proc* 1959;18:752-8

58 Zakut H, Even L, Birkenfeld S, Malinger G, Zisling R, Soreq H. Modified properties of serum cholinesterases in primary carcinomas. *Cancer* 1988;61:727-37

TRANSGENIC ACHE INDUCES NEUROMUSCULAR DETERIORATION IN MICE

Christian Andres[1], Rachel Beeri[1], Alon Friedman[1], Efrat Lev-Lehman[1], Rina Timberg[1], Moshe Shani[2] and Hermona Soreq[1,3]

[1]Department of Biological Chemistry, The Hebrew University of Jerusalem, 91904 Israel

[2]Department of Genetic Engineering, ARO, The Volcani Center, Bet Dagan, 50250 Israel

[3]To whom correspondence should be addressed (Tel: 972 2 6585 109, Fax: 972 2 6520 258).

Running Title: Neuromuscular Defects in ACHE-Transgenic Mice

Abstract

The long-term contribution of balanced cholinergic neurotransmission toward neuromuscular properties was studied by expressing human acetylcholinesterase (hAChE) in motoneurons, but not muscle, of transgenic mice. Spinal cord cholinergic axodendritic synapses in transgenic mice were morphologically normal despite 7-fold higher cytochemical AChE activity as compared with control synapses. In contrast, although muscle extracts included only ca. 6% of hAChE of motoneuron origin, transgenic neuromuscular junctions were 60% larger than controls and displayed either exaggerated or shortened post-synaptic folds. Neuromuscular impairment was evident in grip tests at the age of 4 weeks, worsened with age and was accompanied by progressive amyotrophy and abnormal electrical motor response, reflecting enlarged motor units and junctional dysfunction. The vulnerability of vertebrate neuromuscular junctions to alterations in cholinergic neurotransmission, highlights the morphogenic role of AChE and outlines the cascade of NMJ transformations leading to neuromotor impairments.

Introduction

In addition to their structural complexity, vertebrate neuromuscular junctions (NMJ) are distinguished by continuous fluctuations in the mode, extent and duration of their functioning, dependent on physical activity (Jasmin and Gisiger, 1990; Greensmith and Vrbova, 1991, Dan and Poo, 1994). Unlike brain synapses, NMJs are not protected from the environment by the blood-brain barrier. Therefore, NMJs are frequently subject to insults by various endogenous and exogenous toxic compounds such as drugs, poisons and constituents of the circulation (i.e. antibodies) that impair the fine balance of nerve-muscle communication. This distinction, and the impressive knowledge of NMJs accumulated over many years of research (see Hall and Sanes, 1993, and Hall, 1995 for reviews) elicited great interest in evaluating the interconnections between well-balanced neuromuscular communication and the structural and functional integrity of vertebrate NMJs.

The *in vivo* contribution of several of the numerous muscle and nerve constituents defining neuromuscular properties and functions was approached by genomic disruption or overexpression of key NMJ proteins (i.e. CNTF, Masu et al., 1993, synapsin IIa, Schaeffer et al., 1994, laminin β2, Noakes et al., 1995, GAP-43, Aigner et al., 1995). The neuromuscular deformities resulting from the changes in these NMJ components appeared early in development and caused secondary changes in additional muscle proteins. Thus proteins with primary structural roles led to imbalanced neurotransmission and others, primarily involved in nerve-muscle communication, disrupted NMJ buildup. This indicated that NMJ infrastructure and imbalanced neuromuscular communication both contributed toward the final phenotypes. The involvement of other neuromuscular components in NMJ integrity and functioning was shown by their alteration in congenital or acquired muscle diseases. For example, the Eaton Lambert syndrome is associated with malfunctioning presynaptic calcium channels (Lambert and Elmqvist, 1971), whereas myasthenia gravis involves autoimmune blockage of the muscle nicotinic acetylcholine receptor (Engel and Santa, 1971), and muscular dystrophy is caused by mutations in the structural muscle protein dystrophin (Koenig et al., 1987). While each of these syndromes appears to have a single identified origin, their long term outcome clearly reflects accumulated damage due to the secondary and tertiary changes in additional nerve and/or muscle components. Therefore abnormal neuromuscular infrastructure and communication may both be involved also in these pathologies.

To dissociate the cumulative outcome of imbalanced neuromuscular communication from structural consequences of specific protein disruptions, structure-function analyses are required in animal models where elements essential for neuromuscular signaling are modulated in a more subtle manner than total knock-out. Since acetylcholine (ACh) modulates growth cone

development (Zheng et al., 1994), and because muscle electrical activity affects synapse maintenance and depends on activation of ACh receptors, altered ACh levels should also affect NMJ construction. This was in line with the changes of NMJ development which we observed in transiently transgenic *Xenopus* tadpoles overexpressing the ACh hydrolyzing enzyme acetylcholinesterase (AChE, acetylcholine acetyl hydrolase, EC 3.1.1.7.) (Shapira et al., 1994; Seidman et al., 1995). However, the universality of these findings remained unclear, as computer models predicted impressive breadth of the range of AChE that is compatible with appropriate neuromuscular functioning (Anglister et al., 1994). Moreover, it remained unknown whether the morphogenic effect of AChE in *Xenopus* was due to neuronal or muscle expression of the non-integrated transgene and the long-term physiological outcome of these human enzyme-induced changes in NMJ structure could not be investigated in the transiently transgenic *Xenopus* tadpoles.

To unravel the long-term morphogenic role of AChE in mammalian NMJs, we have now used transgenic mice stably expressing human AChE (hAChE) in motoneurons, but not in muscle (Beeri et al., 1995). We observed in NMJs from these mice structural deformities resembling the NMJ deterioration occurring in variable myasthenic syndromes, including considerable enlargement of the synaptic NMJ area coupled with electromyographic evidence for collateral innervation, decreased efficiency of muscle function and progressive amyotrophy. This sheds new light on the importance of well balanced nerve-muscle interactions toward NMJ integrity and offers a novel research tool for molecularly dissecting the contribution of such balance toward NMJ properties.

Results

Transgenic hAChE is expressed in spinal cord neurons but not muscle: Transgenic hACHE cDNA products were clearly detected in spinal cord, but not muscle of adult transgenic FVB/N mice carrying two copies of the human ACHE transgene (Beeri et al., 1995). This was done using species-specific PCR primers designed to distinguish between human and mouse ACHE mRNA and extended our previous analyses which indicated limitation of expression of this transgene, including 592bp from the ACHE promoter, to the central nervous system (Fig. 1, A,B and Beeri et al., 1995). Interestingly, direct muscle injection of plasmid DNA containing a larger 1.0Kb area from the parallel rat promoter induced transcription in muscle fibers (Chan and Jasmin, 1995). Further experiments will be required to investigate the precise requirements for muscle expression of AChE. Kinetic follow-up of the PCR amplification showed no apparent difference between mouse ACHEmRNA levels in the spinal cord of adult transgenic as compared with control mice (data not shown), suggesting that transcription of this transgene did not affect the expression of the corresponding host gene.

To identify specific ACHE-expressing cell types within the spinal cord, we employed a high resolution in situ hybridization technique. To this end, a 5'-biotinylated 50-mer ACHEcRNA probe was synthesized with 2-O-methyl chemical modification in the ribose moiety of all nucleosides. In addition to enabling immediate sensitive detection by streptavidin-alkaline phosphatase conjugates, this ensured tighter hybridization (Kawasaki et al., 1993), and thus better specificity than that provided by unmodified cRNA, as well as protection of our cRNA probe from nucleolytic degradation (Eckstein, 1985). Using this method, we detected ACHE mRNA transcripts spread throughout the perikarya and the apical end of processes in neuronal cell bodies within the anterior horn. ACHE mRNA transcripts appeared both in large (> 20μm diameter) polygonal neurons with the characteristic features of α motoneurons (Jones et al., 1993) and in smaller (< 10μm diameter) round cells resembling interneurons (Fig.1C-F). AChE mRNA levels and distribution in spinal cord sections from both transgenic and control mice were apparently similar (Fig.1C,D). Cytochemical staining further demonstrated conspicuous AChE expression in neuronal perikarya and processes within transgenic spinal cord, high above the level observed in control sections (data not shown). Parallel analyses of successive spinal cord sections demonstrated similar patterns of ACHE mRNA labeling in the cervical, lumbar and sacral regions of the spinal cord and revealed no labeling in cells with glial morphology, in agreement with observations of others (Hietanen et al., 1990) and with our own brain analyses in these transgenic mice (Beeri et al., 1995). Cresyl violet staining in 5 transgenic and 5 control animals confirmed that neuronal distribution, cell numbers and shape remained largely

unmodified (data not shown). suggesting that hAChE expression did not damage neuronal proliferation and/or survival.

Axo-dendritic cholinergic spinal cord synapses remain largely unmodified despite hAChE accumulation: Following cytochemical activity staining, axo-dendritic cholinergic synapses labeled by the electron dense crystals of the AChE reaction product revealed principally similar axon diameter, pre-synaptic length and numbers of adjacent mitochondria in transgenic and control animals (Table IA and data not shown). Synaptic areas occupied by AChE reaction products (Table IA and Fig. 2A) were 7-fold larger in transgenic spinal cord sections. However, the presynaptic area occupied by vesicles was only slightly smaller in transgenic synapses than in control terminals whereas vesicle density was slightly higher in transgenic synapses than in controls (Table IA). Also, no sign of neuronal degeneration was observed. Thus, transgenic AChE expression in spinal cord neurons was associated with increased synaptic AChE staining but did not substantially change morphometric parameters in cholinergic neurons and axo-dendritic synapses.

Globular human AChE tetramers are found in transgenic spinal cord and muscle: AChE activity in spinal cord extracts of transgenic animals, 255 nmol acetylthiocholine hydrolysed/min/mg protein, was ca. 25% higher than that of control animals. This was due to AChE of human origin, immunoreactive with species-specific antibodies (Seidman et al., 1995) that was evenly distributed between the low salt-soluble and the detergent soluble fractions. Linear sucrose gradient centrifugation followed by measurement of AChE activities in the resultant sucrose gradient fractions revealed that the detergent-soluble AChE in the spinal cord consisted mainly of globular tetramers (G4), with minor fractions of monomers (G1) and dimers (G2). The G4 enzyme peak in transgenic mice was considerably higher than in controls. Immobilization via monoclonal anti-human AChE antibodies demonstrated that this G4 fraction included ca. 18 % of the human enzyme (Fig. 2B).

Normal post-translational processing would transport part of the transgenic motoneuron AChE to NMJs, where it could contribute to the general pool of synaptic AChE activities. To characterize the biochemical properties of motoneuronal AChE in NMJ, we subjected detergent soluble muscle extracts to sucrose density centrifugation and identified the transgenic enzyme by antibody immobilization as above. No significant increment was observed in the total muscle AChE activities, which were considerably lower than those in the spinal cord (33.4 ± 6.9 nmol/min/mg protein in 6 control animals, and 35.9 ± 1.3 in 7 transgenics). However, whereas detergent-soluble muscle AChE in control animals was composed of approximately equal parts of G_1 and G_4 enzyme, the G_4:G_1 ratio was 2-fold higher in transgenics (Fig. 2B). Antibody immobilization further revealed both G4 tetramers and some monomers of human origin in this

detergent-soluble fraction, altogether 6% of total muscle AChE activity which was contributed by the motoneuron-expressed transgene. Considering the fact that NMJs represent less than 0.1% of the muscle surface (Hall, 1995) this increase could reflect a significant accumulation of the transgenic enzyme in the synaptic microenvironment.

Neuromuscular junctions of transgenic animals undergo dramatic morphological changes: Cytochemically stained areas of diaphragm endplates were 60% larger than control NMJs (Fig. 3 and Table IB). This increase reflected general structural changes, as it was also observed with the non-specific dye methylene blue, with over half of transgenic endplate areas but only 10% of controls being larger than 600 μm^2. In addition, 82% of 161 transgenic endplates lost the classical "pretzel" boundaries (Lyons and Slater, 1991) found in 82% of 172 control endplates (for 4 animals in each case). Rather, transgenic endplates acquired a simple elipsoid aspect (Figure 3). Also, muscle fiber diameters were 15% larger in transgenics compared to controls ($p< 0.005$, Student's t test) (Fig. 3 and Table IB). Similar morphological changes were also found in hindleg quadriceps endplates and in anterior tibialis muscles (not shown).

Electron microscope analyses of diaphragm preparations, stained with methylene blue for localization of the junctional regions, revealed highly variable NMJ infrastructure in the transgenic animals. Unlike the situation in spinal cord synapses, the density of pre-synaptic vesicles was significantly higher in transgenic as compared with control NMJs (Table IB). Another difference was observed in the post-synaptic folds. The average length of post-synaptic folds per μm synapse was determined for 16 transgenic and 14 control NMJs. While the general average for all these synapses was the same, detailed subclassification revealed clear differences between and within these two groups. Synapses with average length values per μm NMJ which deviated by more than 1 standard deviation unit from the corresponding value in normal mice were grouped separately. 11 out of 14 NMJs in control mice but only 7 out of 16 analyzed NMJs in transgenic mice possessed post-synaptic folds with an average length of 0.6±0.05 μm/μm synapse length, within this 1 SD rnage (Table IB). One fourth of the NMJs in transgenic mice as compared with only 7% of analyzed control NMJs presented highly exaggerated, branched and densely packed post-synaptic folds, similar to those occurring in the Eaton-Lambert syndrome (Lambert and Elmqvist, 1971) (average of 0.87 ± 0.16 μm). One third of the transgenic NMJs, but only 14% of control NMJs possessed short, ablated post-synaptic folds (0.30 ± 0.07 μm) resembling those of myasthenic patients (Engel and Santa, 1971). Similar changes of both types were reported in NMJs of aged humans (Wokke et al., 1990).

Decreased muscle volume and atrophy of muscle fibers in adult transgenic animals was first observed macroscopically in 4-month old mice. Electron microscopy subsequently indicated general loosening of intracellular structures in some muscle fibers. Cell space was

filled with large, structureless vacuoles. The distance between myofilaments and between myofibrils was enlarged. Triads of T-tubules and terminal cisternae appeared dissociated, mitochondria were no longer aligned with I-bands of the sarcolemma and were clearly swollen, with cristae no longer visible (Fig. 4). No NMJ could be observed in association with these damaged muscle regions. Post-synaptic abnormalities within the muscle tissue were therefore far more dramatic than those observed in the spinal cord itself, despite the lack of transgene expression in muscle.

Transgenic hAChE expression leads to electromyographic abnormalities: Direct recording from the gastrocnemius muscle with a tungsten electrode, revealed no spontaneous denervation activity. However, in response to stimulation of the common trunk of the sciatic nerve, the evoked potentials recorded from the gastrocnemius muscle fibers presented three main abnormalities. First, muscle potentials were of greater amplitudeand duration compared to those of age and sex-matched controls, with frequent multiwaved shapes (mainly three subpeaks), rarely seen in controls (Fig. 5A,B). Second, progressive increase of stimulation intensity led to more pronounced increases in response amplitude in transgenic as compared with control mice, These reflected increased number of muscle fibers recruited by the stimulated axons, which implied abnormal enlargement of the responding motor units (Fig. 5A,B). Finally, repetitive supramaximal stimulations at 1 Hz induced pathological late potentials (latency up to 40 msec) which appeared frequently in transgenic animals but very rarely in controls (Fig. 5B).In addition, in 2 of 4 cases, 3HZ stimulations following tetanization by 300 stimulations at 30 Hz resulted in myasthenia-like decreases (over 10%) in the intensity of responses in transgenic, but not in control animals (data not shown). However, the intensity of response recorded on the surface of the sciatic nerve did not differ between controls and transgenic mice, nerve conduction velocity remained normal and no late potentials were detected in these measurements. Electromyographic measurements thus confirmed and extended the morphological observations, pointing at generally unchanged neuronal properties coupled with neuromuscular abnormalities.

hAChE- induced progressive impairments in muscle functioning: Transgenic animals walked normally, with similar track width and pace length to those of controls (data not shown). Mean swimming speed was only slightly slower, 21.4 ± 4.0 m/min in 10 transgenics as compared to 24.9 ± 4.1 m/min in 10 controls. However, transgenic animals performed considerably worse than controls in a rope grip test (Fig. 6A). This deficiency was already significant ($P < 0.02$) at the age of 4 weeks but was worse ($P < 0.01$) at 4 months of age, concomitantly with amyotrophy. When hung on the rope with their front legs, transgenic mice acquired a loose posture (Fig. 6B); and 4 months old transgenics, but not control animals, fell off

the rope altogether (in 20% of 30 sessions with 10 animals), probably due to deficient capacity of their forelegs in addition to weakened trunk and hindlegs. This, in addition to diaphragm NMJ abnormalities, was perhaps the reason for the abnormal mortality rate in these transgenic mice (9 of 150 mice under 10 months as compared with no mortality at this age group among controls).

Discussion

Transgenic overexpression of human AChE in spinal cord neurons induced only moderate modifications in the morphology of cholinergic spinal cord synapses yet caused the appearance of enlarged, abnormally shaped NMJs and degenerating, wasting muscle fibers with abnormal electromyographic properties and progressively worsening neuromuscular impairments. Therefore, NMJs appear to respond to transgenic AChE overexpression differently from spinal cord cholinergic synapses.

Spinal cord cholinergic synapses appear resistant to hAChE overexpression: The 25% increase in spinal cord AChE activities did not alter the distribution or number of AChE-expressing neurons in the spinal cord of transgenic mice. This excludes AChE from being involved in neuronal survival, unlike other proteins such as CNTF (Masu et al., 1993). Cytochemical staining of axo-dendritic cholinergic synapses in the transgenic spinal cord revealed a 7-fold excess in synaptic AChE activities, close to the excess observed in NMJs of transiently transgenic *Xenopus* tadpoles expressing the same hAChE transgene (Ben Aziz et al., 1993, Shapira et al., 1994, Seidman et al., 1995). This suggests an upper limit for AChE excess compatible with synaptic infrastructure. Interestingly, characteristic morphometric parameters of spinal cord synapses such as axon diameter, pre-synaptic length, and mitochondria density remained grossly unchanged. The space occupied by pre-synaptic vesicles in these synapses was slightly reduced and vesicle density was reciprocally increased. This differed from the drastic changes occurring under β_2-laminin disruption (Noakes et al., 1995), which indicates that the changed AChE levels did not prevent maintenance of appropriate amounts of pre-synaptic vesicles.

NMJ vulnerability to hAChE overexpression is associated with muscle deformities: The morphological NMJ changes observed in hAChE-transgenic mice imply modulations in the downstream input of cholinergic signals into muscle, the ultimate target of the motor system. Whereas muscle is known to contribute the collagen-tailed synaptic AChE forms soluble in high salt (Massoulié et al., 1993), our present findings pinpoint a significant fraction of the detergent-soluble globular AChE tetramers in mammals as being of neuronal origin, similar to the situation in amphibia (Anglister, 1991). Exercise-induced increases were observed in muscle G4 AChE and were interpreted as reflecing muscle responses to the exercise (Jasmin and Gisiger, 1991). In view of our current findings, these changes could include motoneuron transcriptional response in addition to muscle overexpression.

Recent theoretical calculations, based on morphometric measurements in NMJs of adult lizard (Anglister et al., 1994) postulated that increasing synaptic AChE concentration by up to 2-fold should have no consequences on cholinergic signaling. Whether the clearly abnormal

phenotypes we observe are associated with a larger AChE excess in the synaptic microenvironment, with the long-term effect of this excess, with its embryonic appearance or with species-specific distinctions in all of these should be further investigated. In any event, our findings demonstrate that a moderate increase in the motoneuron expression of AChE is sufficient to alter not only NMJ function, but also its mode of development and its permanent structure; and that such changes further reach the muscle itself.

Mouse and *Xenopus* NMJs respond similarly to transgenic hACHE expression: The morphogenic effects of the ACHE transgene in the spinal cord sufficed to promote secondary muscle deterioration in adult animals, although this transgene was not expressed in muscle. Transgenic mice displayed generally regular motor behavior as long as no special muscle efforts were required of them, suggesting that basal level NMJ functioning was sustained, unlike that observed under changes in β2-laminin (Hall and Sanes, 1993). Alternatively, or in addition, brain-controlled feedback processes could compensate at least in young animals, for the intrinsic neuromotor impairments occurring in the transgenic mice. Yet, NMJ structures in the transgenic mice covered 60% larger areas than controls, lost their characteristic pretzel shape, assumed fading boundaries, and developed either highly exaggerated or drastically shortened post-synaptic folds. In *Xenopus* NMJs, hAChE overexpression increased the length and width of transgenic NMJs in a manner dependent on pre-synaptic expression of the human transgene (Shapira et al., 1994, Seidman et al., 1995). That hAChE-expressing NMJ areas were enlarged in these two evolutionarily distant species supports the notion that AChE is a morphogenic element of vertebrate NMJs. That the change was quantitatively similar in these two experimental models may reflect a limitation in the capacity of NMJs to be enlarged. Exaggeration of post-synaptic folds also occurs in the Eaton-Lambert syndrome (Lambert and Elmqvist, 1971), where the functioning of pre-synaptic Ca^{++} channels is impaired and hence ACh secretion and post-synaptic receptor activation are decreased. This suggests decreased activation of ACh receptors in certain nerve terminals of our transgenic mice. The yet more severe phenotype of degenerated post-synaptic folds appears in NMJs of myasthenia gravis patients, where post-synaptic ACh receptors are blocked by antibodies (Engel and Santa, 1971). Changes in the levels of activated ACh receptors thus occur in both syndromes with NMJ malformations which display similar phenotypic changes to those observed in our mice.

Electromyography analyses indicate abnormal NMJ functioning: Significant changes in neuronal AChE levels led to muscle weakening and amyotrophy in adult transgenic mice. That general resting motor behavior in these animals was apparently normal could reflect compensation for these abnormalities, for example by increasing endplate space and synaptic cleft volume. However, the dramatic increment in normalized muscle electrical activity in

response to increased stimulus intensities implies that larger numbers of muscle fibers were activated by the neurons excited in these single events. Since the nerve response apparently remained unchanged, this further indicates that each neuron extended more terminals to contact transgenic muscle fibers than under normal conditions. Similar abnormalities occur in neuromuscular diseases such as the Eaton-Lambert syndrome (Eaton and Lambert, 1957, Chaudry et al., 1991, Bertorini et al., 1994) or in prion diseases (Westaway et al., 1994).

The hAChE-induced phenotype progresses with age: The progressive loss of motor functions in our transgenic mice parallels their progressive deterioration of learning and memory (Beeri et al., 1995). Since muscle weakening is associated with the advanced stages of Alzheimer's disease (Thomas et al., 1982), of certain prion diseases (Westaway et al., 1994), of the Eaton-Lambert syndrome and of acquired and congenital myasthenias, we conclude that cholinergic imbalance per se can actively contribute to abnormalities in both cognitive and motor functions, with the resultant phenotypes worsening with age. The increase in synapse, muscle fiber and motor unit size, and even the unexplained mortality in these mice could all be due to NMJ imbalance. However, we cannot rule out the possibility that some of these abnormalities can be due to the expression of the AChE transgene in higher brain areas associated with motor function. That myasthenia gravis patients experience stable maintenance of muscle functioning under treatment with the AChE inhibitor pyridostigmine (Drachman et al., 1982) may therefore indicate that parallel therapeutic approaches can be beneficial also to patients with other neurodegenerative diseases associated with cholinergic imbalance.

hAChE overexpression may gradually change NMJ properties: Overexpressed AChE would inevitably reduce ACh levels in the synaptic cleft of transgenic NMJs. Unless compensated for (for example, by ACh overproduction), this should limit the activation of post-synaptic receptors. The outcome would be parallel to the situation occurring in the Eaton-Lambert syndrome because of limited ACh release due to malfunctioning pre-synaptic Ca^{++} channels. This postulates the appearance of seemingly functional NMJs with increased density of pre-synaptic vesicles and prolonged, exaggerated and over-branched post-synaptic folds. Furthermore, uncompensated, drastic reduction of ACh levels may totally prevent activation of post-synaptic ACh receptors, parallel to the autoimmune blockage of such receptors in myasthenia gravis. This should lead to degenerate NMJs, with characteristically small post-synaptic folds and diffuse ablated structures. Finally, muscle degeneration would cause the complete disappearance of NMJs. Although we saw both types of malformed NMJs in the transgenic mice, we have no way of concluding whether a single synapse can first acquire one of these structural phenotypes, then the second and finally disappear altogether. However, the progressive worsening of muscle functioning in these mice suggests that this may be the case.

Thus the damaging effects of transgenic hAChE would first be compensated for, allowing for apparently normal muscle function in spite of the initial reduction in ACh levels. Partial suppression of receptors' activation would hence lead to the NMJ abnormalities characteristic of the Eaton Lambert syndrome, which is still compatible with muscle fiber innervation. However, the potential for full compensation of this imbalanced cholinergic signaling probably declines with age, as is the case in several muscle diseases. Subsequent deterioration and receptor blockage should then cause the myasthenic NMJ phenotype accompanied by muscle fiber denervation, which should in turn, elicit reinnervation, motor unit enlargement and NMJs loss. Figure 7 presents this potential chain of events in a scheme.

The morphogenic effect of AChE may reflect non-catalytic function(s): At least some of the observed neuromotor effects in our transgenic mice may be unrelated to the catalytic function of AChE but rather reflect its homology to neurexin-binding elements like neurotactin (De la Escalera et al., 1990), gliotactin (Auld et al., 1995) , **neuroligin** (Ichtchenko et al., 1995) and be due to imbalanced activation of neurexins, their potential target receptors (Ushkariov et al., 1992). Further studies are required to disclose whether any change occurred in neurexins' turnover in these mice and thus shed new light on the function(s) of these intriguing receptors within the motor system.

In conclusion, the CNS hAChE-transgenic mice offer new opportunities in the study of nerve-muscle communication. Follow-up of their embryonic development will reveal the spatiotemporal parameters of their neuromuscular disease and narrow the time-span when these abnormalities might be initiated. Differential PCR display analyses (Liang and Pardee, 1992) should best show the mRNA transcripts whose altered expression levels precede these changes. Systemic treatment with anti-ChEs can prove whether these changes are preventable and/or reversible, whereas creation of transgenic mice overexpressing a mutation-inactivated hAChE should distinguish between contributions of the catalytic activity of the transgenic enzyme and those related with its structural properties. Finally, mating with other CNS hAChE-expressing lines with different AChE expression levels can demonstrate the time and dose-dependence of these neuromuscular defects on the transgene copy number, whereas mating with animal strains with other disrupted NMJ components can unravel multigenic contributions toward nerve-muscle contacts. Transgenic manipulations of cholinergic functions in vertebrates can hence mimic and therefore model pathological degeneration of neuromuscular junctions in humans.

Experimental Procedures

Testing transcriptional tissue specificity of the hAChE transgene: ACHE mRNA transcripts of human and mouse origin were pursued in spinal cord and muscle RNA extracts from apparently homozygous FVB/N mice carrying the hACHE transgene, as compared with control mice (Beeri et al., 1995). Species-specific PCR primers were designed at nucleotides 1522 (+) and 1797 (-) in exons 3 and 4 of the human transgene (Soreq et al., 1990) and at nucleotides 1361(+), 1896(-) in exons 3 and 6 of the mouse gene (Rachinsky et al., 1990). Resultant PCR products (276 and 536 bp, respectively) obtained from similar amounts of RNA were electrophoresed on agarose gels.

High resolution in situ hybridization: All procedures were carried out at room temp., unless stated otherwise. Cervical spinal cord sections (50 μm) from transgenic and control mice were fixed with 4% paraformaldehyde, 0.1% glutaraldehyde (2 hr) and were washed at 4°C (2x15 min) in PBT (100 mM phosphate buffer pH 7.4, 144 mM NaCl, 0.1% Tween-20). Following gradual dehydration in 25%, 50%, 75% and 100% methanol in PBT (5 min each step), sections were kept in 100% methanol at -20°C until use. Rehydration was with the same methanol/PBT series in reverse order, followed by washes (2x5 min./PBT). One hr clearing in 5% hydrogen peroxide was followed by washes (3x5 min./PBT) and 15 min incubation with 10 μg/ml proteinase K in PBT. Sections were then washed 20 min with 2 mg/ml glycine in PBT, and 2 x 5 min with PBT. Following 20 min refixation with 4% paraformaldehyde/ 0.2% glutaraldehyde in PBT, and 2 x 5 min washes with PBT, prehybridization solution was added for 1 hr at 52°C (50% formamide, 5 x SSC pH 4.5, 50 μg/ml yeast tRNA, 1% SDS, 50 μg/ml heparin). This was replaced by the same solution plus 10 μg/ml 50- mer 5' biotinylated 2-0-methyl ACHEcRNA probe (positions 1932-1981 in mouse exon 6; Microsynth, Windisch, Switzerland). Hybridization was for 16 hr at 52°C. Post-hybridization washes were 2 x 30 min, 56°C with solution 1 (50% formamide, 5 x SSC pH 4.5, 1% SDS), 1 x 10 min, 56°C with 1:1 solution 1:solution 2 (0.5 NaCl, 10 mM TrisHCl pH 7.5, 0.1% Tween-20), 3 x 5 min with solution 2 at room temp., 5 min with solution 2, 5 min at room temp. with solution 3 (50% formamide, 2 x SSC, pH 4.5), 2 x 30 min at 56°C with solution 3, 3 x 5 min with TBST (136 mM NaCl, 2.7 mM KCl, 25 mM Tris pH 7.5, 0.1% Tween 20, 2 mM Levamisol). To prevent non-specific binding and suppress endogenous alkaline phosphatase, 1% skim milk in TBST and 2 mM Levamizol were added for 1 hr. The ELF 6605 kit (Molecular Probes, Eugene, OR) was then employed at dilution 1:250 to stain for alkaline phosphatase - streptavidin conjugates.

Staining procedures: For structural NMJ analyses, mice were sacrificed by cervical dislocation, and diaphragm muscles were fixed in situ by squirting (5 min., room temp.) fresh 4% paraformaldehyde, 0.1% glutaraldehyde solution in phosphate buffered saline. Fixed diaphragm

was then dissected, refixed for 2 hr and kept at 4°C in PBS until used for cytochemical AChE staining (Beeri et al., 1995) or for staining with 0.1% methylene blue. Diaphragm regions rich in NMJs were dissected into rectangles of about 3 x 5 mm, immobilized on glass slides and photographed in a Zeiss Axioplan microscope at x 200 magnification. Sections of cervical spinal cord (50 μm thick, paraformaldehyde-glutaraldehyde fixed) were stained for 30 min and thiocholine precipitates observed by electron microscopy in 80 nm cut stained sections (Seidman et al., 1995). Control experiments on sections from transgenic spinal cord, with no acetylthiocholine verified that these electron-dense deposits were indeed reaction products of in situ AChE catalysis-mediated hydrolysis of the substrate. Morphometric measurements were performed as detailed previously (Seidman et al., 1995) using the Sigma Scan program (Jandel, Germany).

AChE activity measurements: Acetylthiocholine hydrolysis levels were determined spectrophotometrically in the presence of 1.10^{-5} M of the selective butyrylcholinesterase inhibitor iso-OMPA. Tissue homogenates were tested directly or following sucrose gradient centrifugation and adhesion to a human-selective anti-AChE monoclonal antibody (AC 101.1, Seidman et al., 1995) for 30 min.

Electromyography: After general anasthesia (with 60 mg/kg weight Nembutal, injected intraperitoneally) and resection of the hindleg, a tungsten bipolar stimulating electrode was positioned on the trunk of the sciatic nerve and evoked muscle fiber potentials recorded by a microelectrode placed on the gastrocnemius muscle. The nerve was stimulated by brief (0.1 msec) stimuli at increasing intensities (< 1 mAmp). Data were recorded through an AM Systems, AC-DC amplifier (Model 1800), digitized on line and analysed using Pclamp 6.0 (Axon Instruments Inc.). Muscle temperature, retained at 32 ± 1°C by a warming lamp, was continuously monitored. In each animal, about 10 different places were recorded.

Grip test: Mice were suspended with their forelegs on a 3 mm thick horizontal rope at 1 m height above bench level. The time in sec. it took them to grip at the rope with their hindlegs and escape this uncomfortable situation (performance time) was thrice measured in 1 min intervals for sex-matched mice with similar body weights. Performance time was recorded as 10 sec both for unsuccessful trials or for those trials which ended in animals falling off the rope.

Acknowledgments: We thank Drs. C. Kalcheim and S. Seidman (Jerusalem) for helpful discussions, Ms. Sivan Henis for help with experiments and Dr. B. Norgaard-Pedersen (Copenhagen) for antibodies. This work was supported by USARMRDC grant 17-94-C-4031, the Israel Academy of Sciences and Humanities and the U.S-Israel Binational Science Foundation (to H. S.). C. A. was a recipient of an INSERM (France)-NCRD exchange

fellowship with the Israel Ministry of Science and Arts, and A.F. received a research grant from the Smith Foundation for Psychobiology.

References

1. Aigner L., Arber, S., Kapfhammer, J.P., Laux, C.S., Botteri, F., Brenner, H-R, and Caroni, P. (1995) - Overexpression of the neural growth-associated protein GAP-43 induces nerve sprouting in the adult nervous system of transgenic mice. Cell **83**:269-278.
2. Anglister, L. (1991) - Acetylcholinesterase from the motor terminal accumulates in the synaptic basal lamina of the myofiber. Cell Biol., **115**: 755-764.
3. Anglister, L., Stiles J.R. and Salpeter M.M. (1994) - Acetylcholinesterase density and turnover number at frog neuromuscular junctions, with modeling of their role in synaptic function. Neuron, **12**:783-794.
4. Auld, V.J., Fetter, R.D., Broadie, K., and Goodman, C.S. (1995) - Gliotactin, a novel transmembrane protein on peripheral glia is required to form the blood-nerve barrier in Drosophila. Cell **81**:757-767.
5. Beeri, R., Andres, C., Lev-Lehman, E., Timberg, R., Huberman, T., Shani, M. and Soreq, H. (1995) - Transgenic expression of human acetylcholinesterase induces progressive cognitive deterioration in mice. Current Biology **5**:1063-1071.
6. Ben-Aziz-Aloya, R., Seidman, S., Timberg, R., Sternfeld, M., Zakut, H. and Soreq, H. (1993) - Expression of a human acetylcholinesterase promoter-reporter construct in developing neuromuscular junctions of *Xenopus* embryos. Proc. Natl. Acad. Sci. USA, **90**:2471-2475.
7. Bertorini, T.E., Stalberg, E., Yuson, C.P. and Engel, W.K. (1994) Single-fiber electromyography in neuromuscular disorders, correlation of muscle histochemistry, single-fiber electromyography and clinical findings. Muscle and Nerve **17**:345-53.
8. Burns, M.E. and Augustine, G.J. (1995) - Synaptic structure and function: Dynamic organization yields architectural precision. Cell **83**:187-194.
9. Chan, R.Y.Y. and Jasmin, B.J. (1995) Regulatory elements and transcription of the acetylcholinesterase gene in adult rat skeletal muscle fibers. Abst., Society for Neuroscience, San Diego, California. p.800.
10. Chaudhry, V, Watson, D.F., Bird, S.J. and Cornblath, D.R. (1991) Stimulated single-fiber electromyography in Lambert-Eaton myasthenic syndrom. Musle and Nerve **14**:1227-30.
11. Dan, Y. and Poo, M-m (1994) - Retrograde interactions during formation and elimination of neuromuscular synapses. Curr. Opin. in Neurobiol. **4**:95-100.
12. De Felipe, C., Pinnock, R.D. and Hunt, S.P. (1995) - Modulation of Chemotropism in the developing spinal cord by substance P. Science **267**:899-902.

13. Dela Escalera S., Bockamp, E.O., Hoya, F., Riovant, M. and Jimenez, F. (1990) - Characterization and gene cloning of neurotactin, a Drosophila transmembrane protein related to cholinesterases. EMBO J. **9 (11):**3593-3601.

14. Drachman, D.B., Adams, R.N. and Josifek, L.F. (1982) - Functional activity of autoantibodies to acetylcholine receptor and the clinical severity of myasthenia gravis. N. Eng. J. Med **307:** 769-775.

15. Eaton, L.M. and Lambert, E.H. (1957) - Electromyography and electric stimulation of nerves in diseases of motor unit: observations on the myasthenic syndrome associated with malignant tumors. J. Am. Med. Assoc. **163**:1117-1124.

16. Engel, A. G. and Santa, T. (1971) - Histometric analysis of the ultrastructure of the neuromuscular junction in myasthenia gravis and in the myasthenic syndrome. Ann. N. Y. Acad. Sci., **183**:46-63.

17. Eckstein, F. (1985) - Nucleotide phosphorothioates, Annu. Rev. Biochem. **54**: 367-402.

18. Funakoshi, H., Belluardo, N., Arenas, E., Yamamoto, Y., Casabona, A., Persson, H., and Ibánez, C.F. (1995) - Muscle-derived neutrotrophin-4 as an activity-dependent trophic signal for adult motor neurons. Science **268**:1495-1499.

19. Greensmith, L. and Vrbova, G. (1991) - Neuromuscular contacts in the developing rat soleus depend on muscle activity. Dev. Brain Res. **62**:121-129.

20. Hall, Z.W. (1995) - Laminin β2 (S-Laminin): A new player at the synapse. Science **269**:362-363.

21. Hall, Z.W. and Sanes, J.R. (1993) - Synaptic structure and development: the neuromuscular junction. Cell **10**:99-121.

22. Han, H-Q, Nichols, R.A., Rubin, M.R., Bähler and Greengard, P. (1991) - Induction of formation of presynaptic terminals in neuroblastoma cells by synapsin IIb. Nature **349**:697-700.

23. Hietanen, M., Pelto-Huikko, M. and Rechardt, L. (1990) - Immunocytochemical study of the relations of acetylcholinesterase, enkephalin-, substance P-, choline acetyltransferase- and calcitonin gene-related peptide-immunoreactive structures in the ventral horn of rat spinal cord. Histochem. **93**:473-477.

24. Hollingworth, S., Marshall, M.W. and Robson, E. (1990) - Excitation contraction coupling in normal and MDX mice. Muscle & Nerve **13**:16-20.

25. Ichtchenko, K., Hata, Y., Nguyen, T., Ullrich, B., Missler, M., Moomaw, C. and Sudhof, T.C. (1995) - Neuroligin 1: a splice site-specific ligand for beta-neurexins. Cell **81**:435-443.

26. Jasmin, B. and Gisiger, V. (1990) - Regulation by exercise of the pool of G_4 acetylcholinesterase characterizing fast muscles: opposite effect of running training in antagonist muscles. J. of Neurosci. **5**:1444-1454.

27. Jo, S.A., Zhu, X., Marchionni, M.A. and Burden, S.J. (1995) - Neuregulins are concentrated at nerve-muscle synapses and activate ACh-receptor gene expression. Nature, **373**:158-161.

28. Kawasaki, A.M., Casper, M.D., Freier, S.M., Lesnik, E.A., Zounes, M.C., Cummins, L.L., Gonzalez, C. and Dan Cook, P. (1993) - Uniformly modified 2'-Deoxy-2'-fluro-phosphorothioate oligonucleotides as nuclease resistant antisense compounds with high affinity and specificity for RNA targets, J. Med. Chem.**36**:831-841.

29. Koenig, M., Hoffman, E.P., Bertelson, C.J., Monaco, A.P., Feenex, C. and Kunkel, L.M. (1987) - Complete cloning of the Duchenne muscular dystrophy (DMD) cDNA and preliminary genomic organization of the DMD gene in normal and affected individuals. Cell **50**:509-517.

30. Lambert, E.H. and Elmqvist, D. (1971) - Quantal components of end plate potentials in the myasthenic syndrome. Ann. N.Y. Acad. Sci. 183-199.

31. Liang, P. and Pardee, A.B. (1992) - Differential display of eukaryotic messenger RNA by means of the polymerase chain reaction, Science **257**:967-971.

32. Lyons, P.R. and Slater, C.R. (1991) - Structure and function of the neuromuscular junction in young adult mdx mice. J. Neurocytol **20**:969-981.

33. Massoulié, J., Pezzementi, L., Bon, S., Krejci, E. and Vallette, F.M. (1993) - Molecular and cellular biology of cholinesterases, Prog. Neurobiol. **41**:31-91.

34. Masu, Y., Wolf, E., Holtmann, B. Sendtner, M., Gottfried, B. and Thoenen, H. (1993) - Disruption of the CNTF gene results in motor neuron degeneration. Nature **365**:27-32.

35. Navaratnam, V. and Lewis, P.R. (1970) - Cholinesterase-containing neurons in the spinal cord of the rat. Brain Res. **18**:411-425.

36. Noakes, P. G., Gautam, M., Mudd, J., Sanes, J. R. and Merlie, J. P. (1995) - Aberrant differentiation of neuromuscular junctions in mice lacking S-laminin/laminin β2. Nature. **374**: 258-262.

37. Rachinsky, T. L., Camp, S., Li, Y., Ekstrom, T. J., Newton, M. and Taylor, P. (1990) - Molecular cloning of mouse acetylcholinesterase: tissue distribution of alternatively spliced mRNA species. Neuron **5**: 317-327.

38. Schaeffer, E., Alder, J., Greengard, P. and Poo, M-m. (1994) - Synapsin IIa accelerates functional development of neuromuscular synapses. Proc. Natl. Acad. Sci. **91**:3882-3886.

39. Seidman, S., Sternfeld, M., Ben Aziz-Aloya, R., Timberg, R., Kaufer-Nachum, D. and Soreq, H. (1995) - Synaptic and epidermal accumulations of human acetylcholinesterase are encoded by alternative 3'-terminal exons. Mol Cell Biol. **14**: 459-473.

40. Shapira, M., Seidman, S., Sternfeld, M., Timberg, R., Kaufer, D., Patrick, J. and Soreq, H. (1994) - Transgenic engineering of neuromuscular junction in *Xenopus laevis* embryos transiently overexpressing key cholinergic proteins. Proc. Natl. Acad. Sci. USA **91**:9072-9076.

41. Smith, D.O. and Emmerling, M. (1988) - Biochemical and physiological consequences of an age-related increase in acetylcholinesterase activity at the rat neuromuscular junction. J. of Neurosci. **8**:3011-3017.

42. Soreq, H., Ben-Aziz, R., Prody, C.A., Gnatt, A., Neville, L., Lieman-Hurwitz, J., Lev-Lehman, E., Ginzberg, D., Seidman, S. Lapidot-Lifson, Y. and Zakut, H. (1990) - Molecular cloning and construction of the coding region for human acetylcholinesterase reveals a G,C-rich attenuating structure. Proc. Natl. Acad. Sci. USA **87**, 9688-9692.

43. Thomas, M., Ballantyne, J.P., Hansen, S., Weir, A.I. and Doyle, D. (1982) - Anterior horn cell dysfunction in Alzheimer's disease. J. Neurol. Neurosurg. and psychiatry **45**:378-381.

44. Van Essen, D.C., Gordon, H., Soha, J.M. and Fraser, S.E. (1990) - Synaptic dynamics at the neuromuscular junction: mechanisms and models. J. Neurobiol. 21:223-249

45. Westaway, D., DeArmond, S.J., Cayetano-Canlas, J., Groth, D., Foster, D., Yang, S-L., Torchia, M., Carlson, G.A. and Prusiner, S.B. (1994) - Degeneration of skeletal muscle, peripheral nerves, and the central nervous system in transgenic mice overexpressing wild-type prion proteins. Cell **76**:117-129.

46. Wokke, L.H.J., Jennekens, F.G.I., van den Oord, C.J.M., Veldman, H., Smith, L.M.E. and Leppink, G.J. (1990) - Morphological changes in the human end plate with age. J. Neurol. Sci. **95**:291-310.

47. Zheng, J. Q., Felder, M., Connor, J. A. and Poo, M-m. (1994) - Turning of nerve growth cones induced by neurotransmitters. Nature **368**: 140-144.

Table 1: Morphometric parameters of hAChE-expressing cholinergic synapses

Morphometric parameters were determined under visual or electron microscopy as detailed under Experimental Procedures for the numbers noted in parentheses of axo-dendritic cholinergic synapses from the anterior spinal cord of at least 5 adult control and transgenic mice (A) and of the noted numbers of NMJs (B1-3) or analysed folds (B4-6) from the gastronemius muscle of control and transgenic mice. Statistical significance (Student's test) is noted wherever relevant.

Figure 1: The hACHE DNA transgene is expressed in spinal cord neurons but not in muscle.

A: Scheme of the human ACHE transgene. Exons (E) are represented by boxes. I=Intron, Pr=Promoter. Open reading frame (dotted underline) initiates at exon 2. Because of species differences, it was possible to distinguish between human and mouse ACHEmRNA by RT-PCR. Species-specific primers between the regions noted by arrows yielded the following expected RT-PCR products: h, human-specific; m, mouse-specific. + and - signs denote primer orientations.

B: PCR products. RT-PCR products of the sizes expected for human (h) and mouse-specific (m) ACHEcDNA were obtained from spinal cord (left) and striated muscle (right) RNA and were electrophoresed on agarose gels. T = transgenic, C = control, M = molecular weight marker. P=primer type. Note that no expression of hACHE mRNA could be detected in muscle.

C-F: ACHE mRNA expression in both control and transgenic spinal cord is limited to neurons. Wholemount in situ hybridization was performed on sections of cervical spinal cords from transgenic and control animals, using a 5'-biotinylated 2-0-methylated 50-mer ACHEcRNA probe. Detection was with a fluorogenic substrate for streptavidin-conjugated alkaline phosphatase. Presented are low magnification micrographs of transgenic (C) and control (D) anterior cervical spinal cord sections, as well as high magnification of ACHEmRNA labeling in motorneurons (E) and smaller, presumably interneurons (F) from the spinal cord of control mice. Size bars equal 100 and 10 μm, respectively for C,D and E,F.

Figure 2: Transgenic AChE accumulates in spinal cord synapses and reaches muscle.

A: AChE overexpression in axo-dendritic synapses from anterior spinal cord of transgenic mice.

Electron micrographs are presented for 80 nm sections of paraformaldehyde-glutaraldehyde fixed spinal cord from transgenic (T) and control (C) mice. Acetylthiocholine hydrolysis

products appear as dark crystals, particularly conspicuous in the synaptic cleft between axons (A) and dendrites (D). Size bar equals 10μm.

B: Transgenic spinal cord human AChE is found in muscle homogenates. Detergent-soluble homogenates of spinal cord and muscle were fractionated by sucrose gradient centrifugation and AChE activity determined prior to (line) or after binding to a specific anti-human AChE monoclonal antibody (shaded area) (Seidman et al., 1995). Note the different activity scales for spinal cord and muscle. Arrows denote sedimentation of an internal marker, bovine catalase (11.4 S). Activity peaks reflecting globular monomers, dimers and tetramers are labeled G1, G2 and G4, respectively with the top of each tube at the left handside.

Figure 3: Enlargement and shape modifications in diaphragm neuromuscular junctions of transgenic animals.

Top: Synapse stainings. Wholemount cytochemical staining of AChE activity was performed on fixed diaphragms of 4 month old control (C) and transgenic (T) animals. Note weaker AChE staining and larger circumference and elipsoid, fading boundaries of transgenic NMJs as compared with the complex, sharp contours in controls. Two representative diaphragms out of 12 control and 12 transgenic ones.

Center: Similarly fixed diaphragms stained with 0.1% methylene blue to reveal protein density.

Bottom: Distribution analyses. Left: Area stained by AChE reaction product, in μm^2 (for 90 control, 100 transgenic terminals). Right: Muscle fiber diameter, in μm (for 69 control, 75 transgenic fibers). Note the upward shift in distribution of both parameters for transgenic as compared with control mice.

Figure 4: Variable NMJ deformities and amyotrophy in transgenic mice.

Electron microscopy of 80 nm sections of terminal diaphragm zones was performed following AChE activity staining for 10 min. Note the exaggerated post-synaptic folds (F, panels A,B) as well as the short, undeveloped folds marked by arrowheads (C) in transgenic NMJs as compared with controls (A). V = vesicles. Muscle fiber amyotrophy, loss of muscle fiber organization and swelling of mitochondria (Mt) at disrupted Z bands (Z) is shown for transgenic (E) as compared with control muscle (D).

Figure 5: Transgene-induced electromyographic abnormalities.

Electromyographic recordings were taken from the gastrocremius muscle in response to stimulation of the sciatic nerve.

A: Motor units enlargement. Evoked muscle fiber potentials following sciatic nerve stimulation were recorded by a microelectrode placed on the surface of the gastrocnemius muscle in 3 transgenic (filled squares) and 3 control (empty squares) mice. In control animals, a small increase in stimulus intensity induced small and gradual increases in the amplitude of the

muscle's compound action potential. Supramaximal response amplitudes were up to 10-fold greater than the threshold response. In transgenic animals, parallel increases in stimulus intensity triggered considerably larger jumps in the amplitude of the action potentials.

Inset. Superposition of responses evoked by increasing stimulus intensity up to 1.0 mA at 1Hz as in the enclosed scale. Saturation of response occurred only at high stimulus intensities and required more stimuli in transgenics than in controls. Note that in the transgenic muscle several negative peaks were observed in response to a single stimulus.

B: Latencies of evoked spikes. Delayed repetitive firing of action potentials was frequently recorded in 4 transgenic muscles but only rarely in 4 controls. Following 100 supramaximal stimulations at 1 Hz, abnormal late potentials (filled bars) appeared in transgenic animals for up to 40 msec post-stimulation as compared with a few signals in control animals (empty bars). Presented are numbers of response spikes as a function of latency time for 10^6 different measurements.

Figure 6: Motor function impairments appear early and worsen with age.

A: Muscle strength impairment. Rope-grip tests were performed thrice at 1 min intervals for groups of 4 week (top) and 4 month (bottom) old transgenic (T, n = 5 & 7 for top and bottom figures respectiveiy) and control (C, n = 5 & 10) mice. Noted are escape latency values in sec. ± SD. Note the slower performance of transgenics as compared with controls at both age groups and the worsening of this phenotype with age.

B: Trunk and hindlegs weakening. Mice were suspended with their forelegs on a 3 mm diameter rope and their ability to grip the rope with their hindlegs was noted. Presented are a 4 months old control mouse, 3 sec following test initiation (C), and a matched transgenic mouse (T), whose hindlegs, trunk and tail postures are clearly abnormal. This mouse fell off the rope 5 sec. after this photograph was taken.

Figure 7: Transgenic hAChE induces two distinct phenotypes in neuromuscular junctions: The putative course of events which results from AChE overexpression in motorneurons is presented schematically for a series of single muscle fibers (right-hand side) and a series of NMJs (left-hand side). Normal NMJs (top panel) should be pretzel-shaped, create a characteristic electromyographical pattern, presented in the top inset, and possess average size, non-branched post-synaptic folds. Abnormal NMJs with exaggerated folds, similar to those occurring in the Eaton-Lambert syndrome (second panel) as well as NMJs with degenerated folds, ressembling those characteristic of myasthenia gravis (third panel) appeared more frequently in transgenic than in control mice. The fractions (%) of analyzed NMJs which presented distinct types of post-synaptic folds in transgenic (T) and control (C) mice are shown

for each category. Reinnervation created the abnormal electromyographic response observed in transgenic mice (bottom inset). Finally, degeneration occurred.

TABLE I

Morphometric parameters of hAChE-expressing cholinergic synapses

A. Anterior spinal cord axo-dendritic synapses		
Parameter	Control	Transgenic
axon minimal diameter, μm	0.93 ± 0.34 (40)	0.74 ± 0.28 (44)
axonic mitochondria area, μm^2	0.23 ± 0.13 (37)	0.19 ± 0.1 (31)
dendrite minimal diameter, μm	2.44 ± 2.3 (20)	1.61 ± 0.9 (15)
dendritic mitochondria area, μm	0.52 ± 0.52 (19)	0.35 ± 0.21 (13)
AChE stained area, μm^2	0.05 ± 0.04 (43)	0.34 ± 0.90 (47) P<0.03
space occupied by vesicles, μm^2	0.47 ± 0.3 (37)	0.39 ± 0.29 (44)
vesicles No/μ^2	95.8 ± 33.9 (16)	107.9 ± 27.9 (16)

B. Neuromuscular junctions		
Parameter	Control	Transgenic
AChE stained area, μm^2	398 ± 136.4 (90)	625.6 ± 227.7 (100) P<0.001
End plate methylene blue stained area, μm^2	301 ± 92.1 (38)	723.7 ± 495.3 (33) P< 0.001
Vesicles No./μ^2	122.5±30.7 (12)	161.4±41.8 (9) P< 0.02
Mean length of post-synaptic folds/μm NMJ	0.56 ± 0.12 (14)	0.65 ± 0.37 (16)
Muscle fiber diameter, μ	30.8 ± 7.45 (69)	35.6 ± 5.17 (7.5)

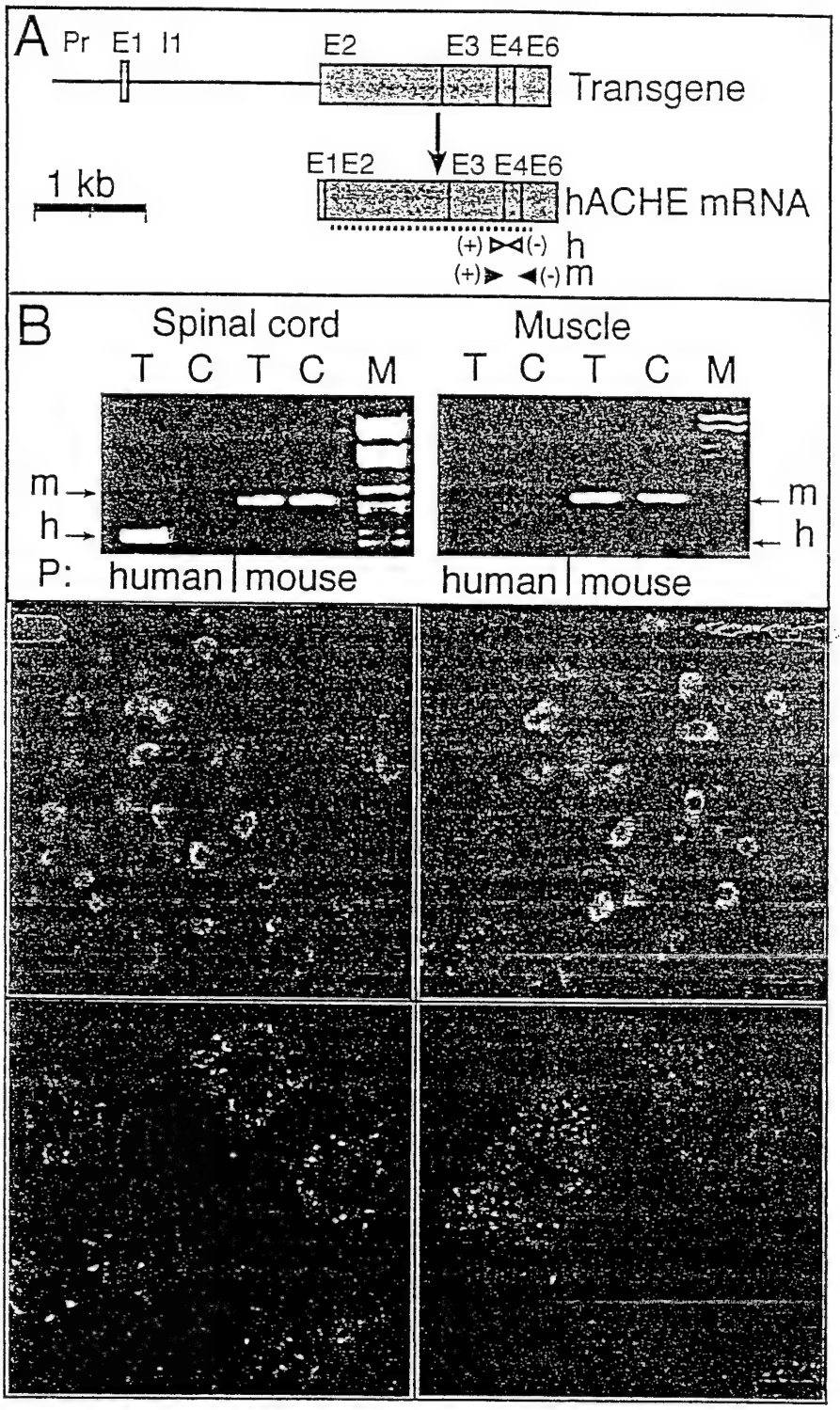
A
Pr E1 I1
E2
E3 E4E6
Transgene
1 kb
E1E2
E3 E4E6
hACHE mRNA
(+)⋈(-) h
(+)► ◄(-)m
B
Spinal cord
Muscle
T C T C M
T C T C M
m
h
m
h
P: human | mouse
human | mouse

Figure 1

Figure 2

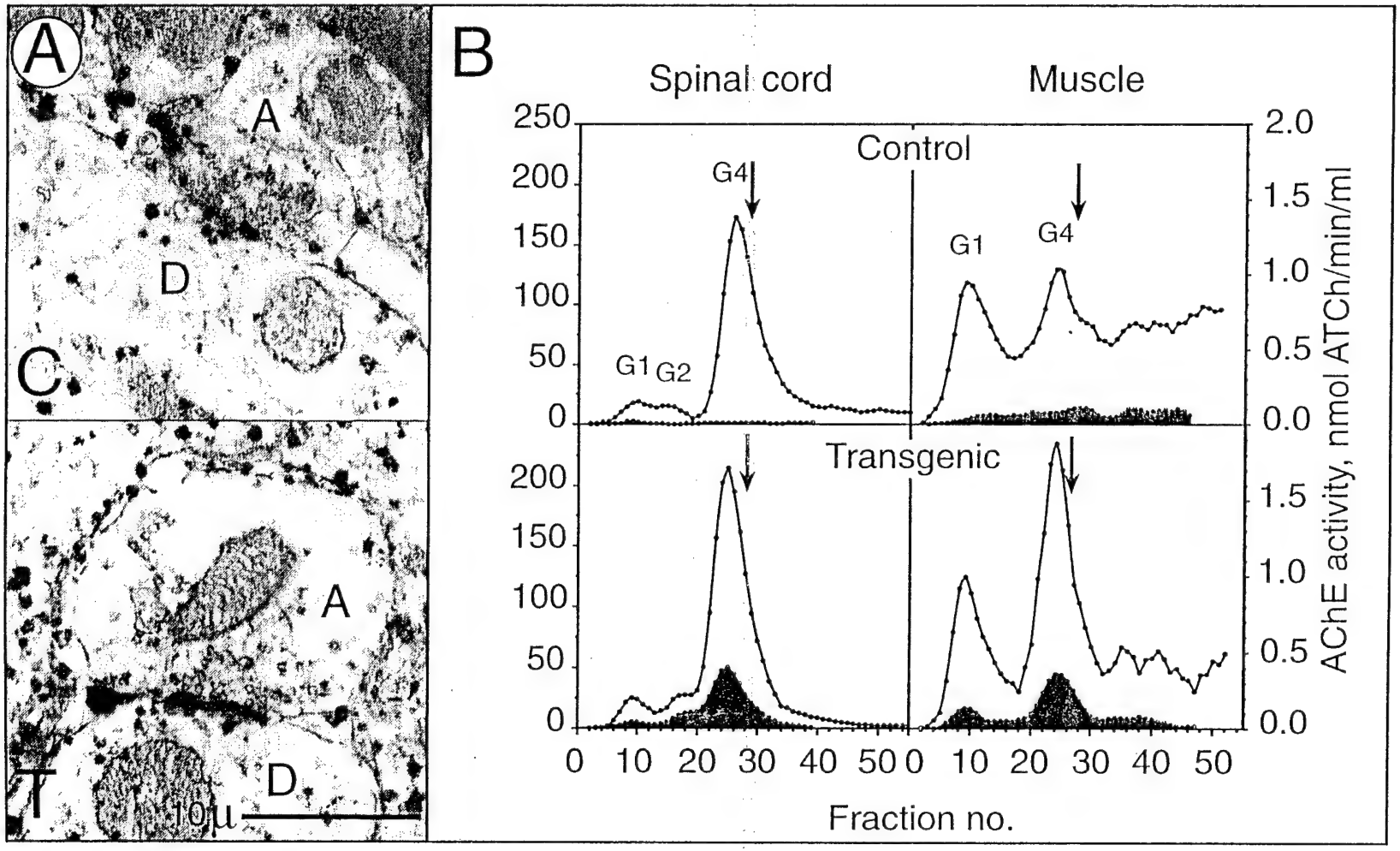
A
A
D
C
A
T
D
10μ
B
Spinal cord
Muscle
Control
Transgenic
G1
G2
G4
G1
G4
250
200
150
100
50
0
2.0
1.5
1.0
0.5
0.0
AChE activity, nmol ATCh/min/ml
0 10 20 30 40 50 0 10 20 30 40 50
Fraction no.

Figure 3

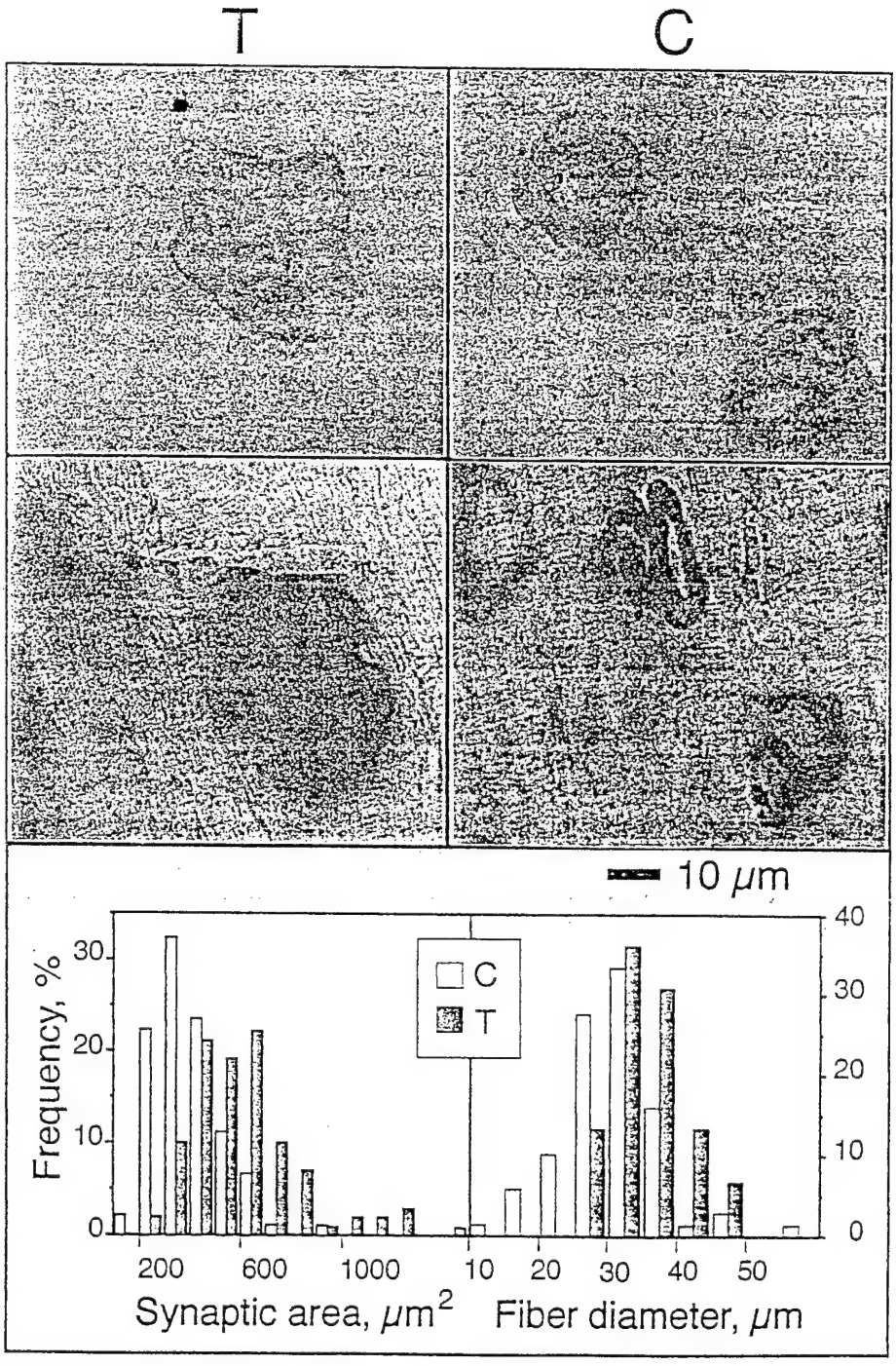
T
C
10 μm
Frequency, %
0
10
20
30
C
T
0
10
20
30
40
200
600
1000
10
20
30
40
50
Synaptic area, μm2
Fiber diameter, μm

Figure 4

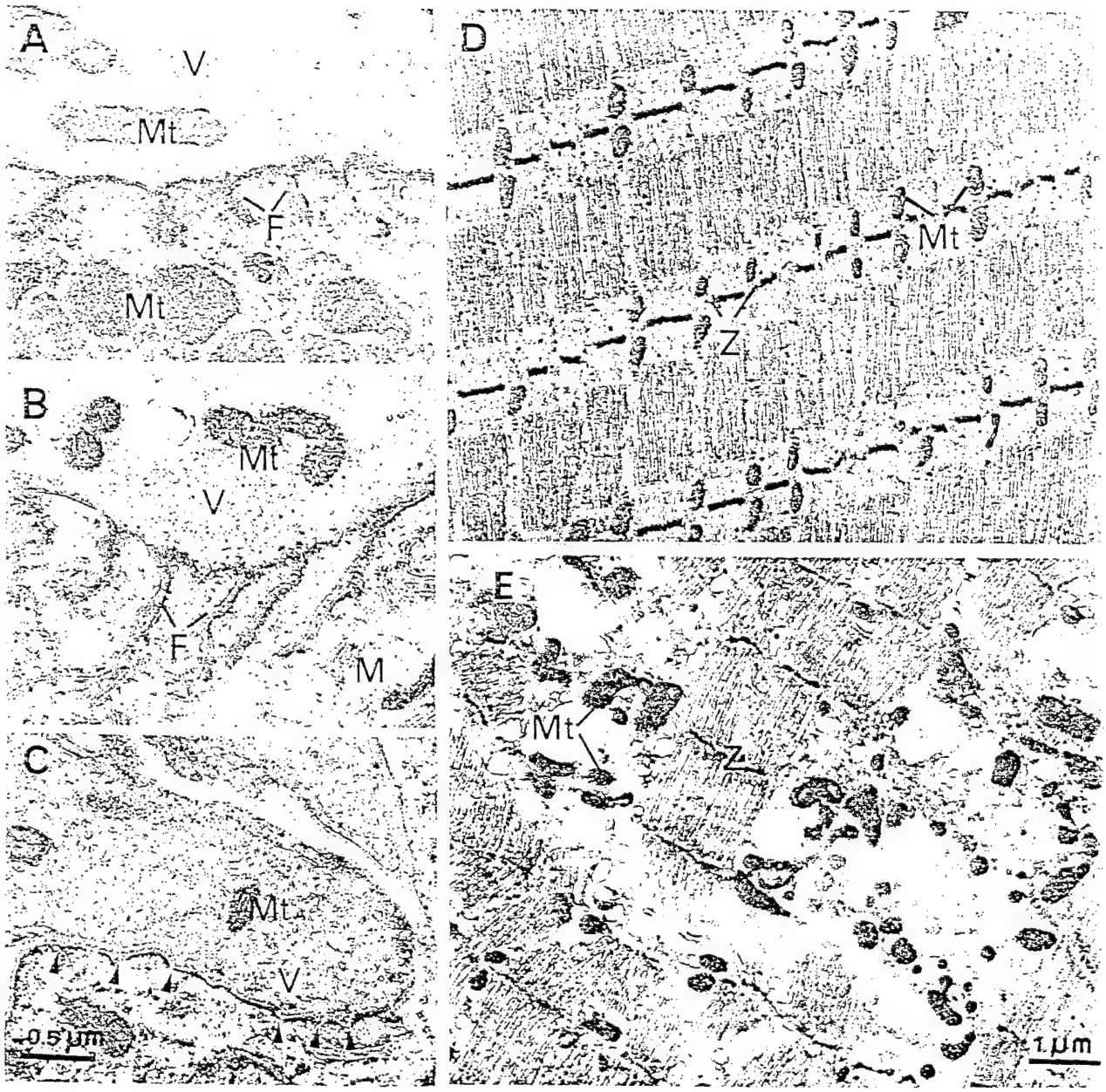

Figure 5

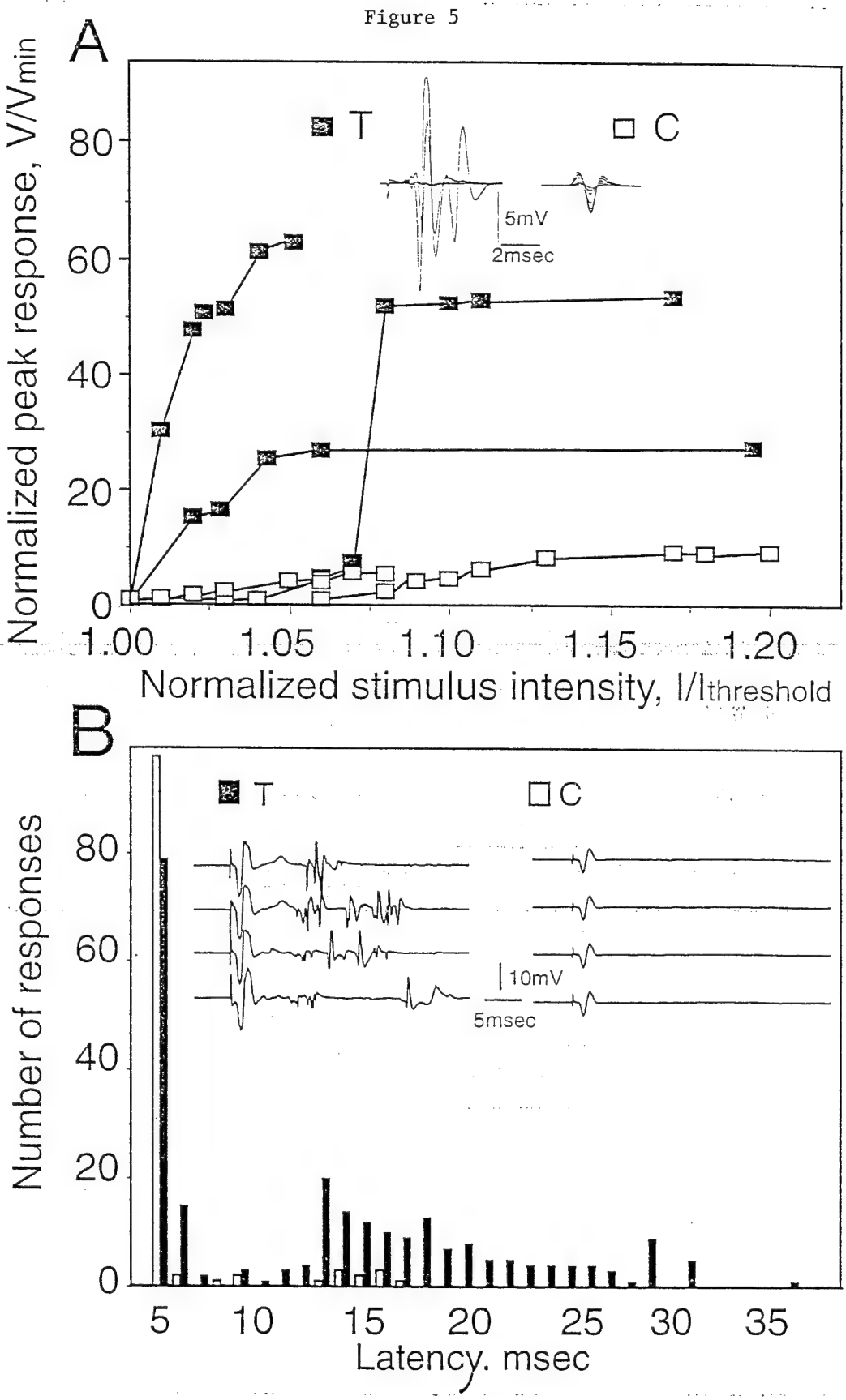
A
T
C
5mV
2msec
Normalized peak response, V/Vmin
0
20
40
60
80
1.00
1.05
1.10
1.15
1.20
Normalized stimulus intensity, I/Ithreshold
B
T
C
10mV
5msec
Number of responses
0
20
40
60
80
5
10
15
20
25
30
35
Latency. msec

Figure 6

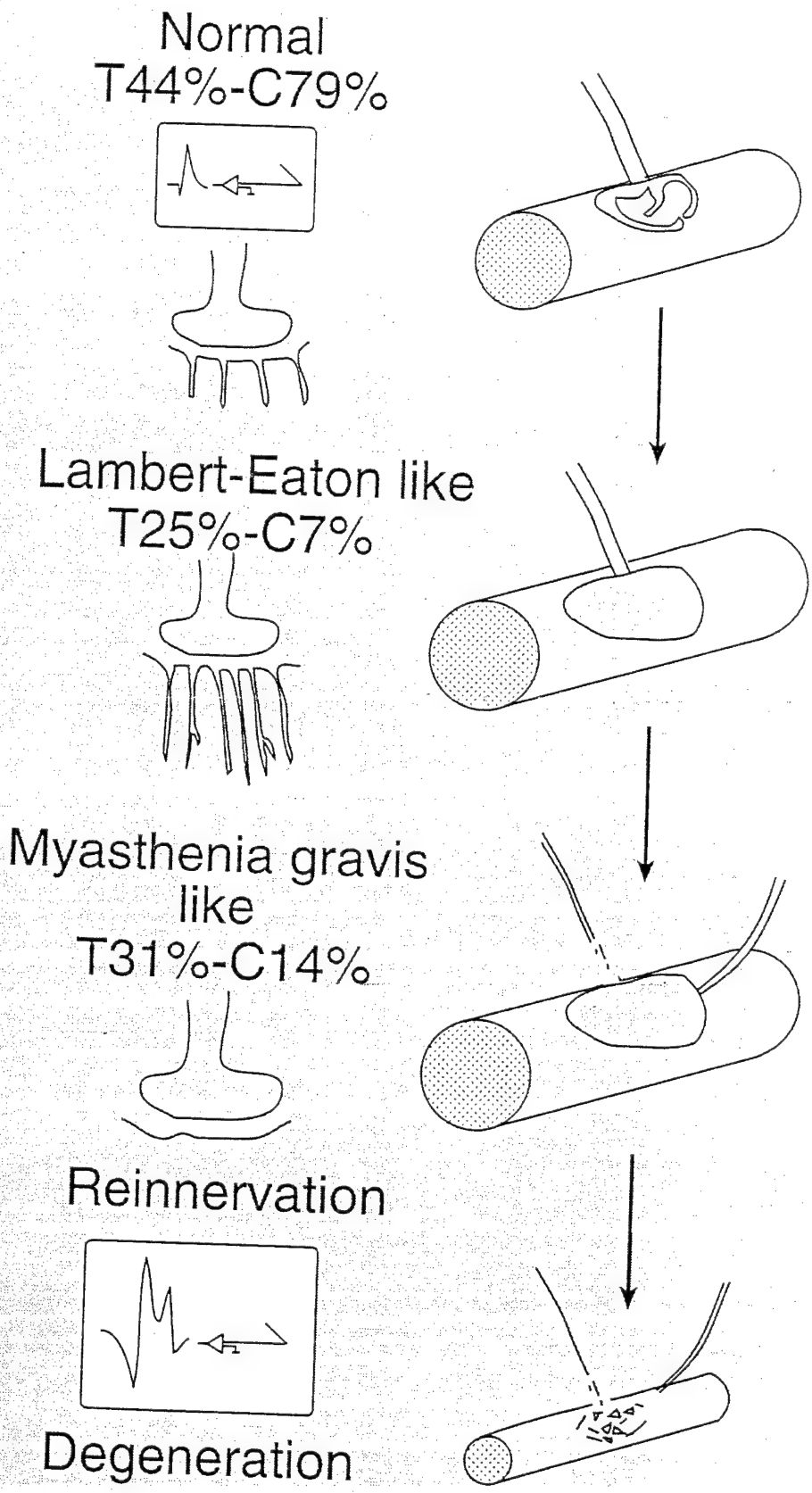
Normal
T44%-C79%
Lambert-Eaton like
T25%-C7%
Myasthenia gravis
like
T31%-C14%
Reinnervation
Degeneration

Figure 7

Pyridostigmine Brain Penetration Under Stress Enhances Neuronal Excitability and Induces Early Immediate Transcriptional Response

Alon Friedman, [*#], Daniela Kaufer-Nachum, [*], Joshua Shemer, ,[#&], Israel Hendler, [#&], Hermona Soreq,[*] and IlanTur-Kaspa, [#&$]

[*] Department of Biological Chemistry, The Life Sciences Institute, The Hebrew University, Jerusalem 91904, Israel.

[#] Medical Corps, Israel Defense Forces. P.O. Box 02419, Israel.

[&] Sheba Medical Center, Sackler school of Medicine, Tel-Aviv University, Tel-Hashomer 52621, Israel.

[$] The views expressed are those of the authors and are not to be construed as official policy of the Medical Corps, Israel Defense Forces.

Running Title: Stress and Pyridostigmine

Address for correspondence

Alon Friedman, MD, PhD

Department of Biological Chemistry,

The Life Sciences Institute,

The Hebrew University,

Jerusalem 91904, Israel.

Tel: 972-2-6585109 FAX: 972-2-6520258

email: alon@neuro.bgu.ac.il

Submitted on: 28/4/96

ABSTRACT

When prophylactically administered during the Gulf war under the threat of chemical warfare, use of the peripherally-acting acetylcholinesterase (AChE) inhibitor pyridostigmine was unexpectedly associated with central nervous system symptoms. Therefore, we examined pyridostigmine access to brain AChE under stress and investigated the outcome of such access. Here we report that stress-induced increase in blood-brain-barrier permeability reduces by >100 fold the pyridostigmine dose required to inhibit mouse brain AChE activity by 50%. Furthermore, pyridostigmine directly enhanced electrical excitability and induced transcription of the c-fos oncogene in hippocampal slices in vitro. These findings suggest that peripherally acting drugs administered under stress may reach the brain and directly affect centrally controlled functions.

Key Words: Acetylcholinesterase, Blood-Brain-Barrier, c-fos, Pyridostigmine, Stress

INTRODUCTION

Pyridostigmine, a carbamate acetylcholinesterase (AChE) inhibitor, is routinely employed in the treatment of the autoimmune disease myasthenia gravis[1]. Pyridostigmine is also recommended by most western armies for use as pretreatment under threat of chemical warfare, because of its protective effect against organophosphate poisoning[2,3]. Due to this drug's quaternary ammonium group, which prevents its penetration through the blood-brain-barrier (BBB), the symptoms associated with its routine use in patients as well as in healthy volunteers primarily reflect perturbations in peripheral nervous system (PNS) functions[1,4]. Unexpectedly, under similar regimen, pyridostigmine administration during the Gulf war resulted in a >3 fold increase in the frequency of reported central nervous system (CNS) symptoms[5]. This was not due do enhanced absorption (or decreased elimination) of the drug because the inhibition efficacy of serum cholinesterase was not modified[5]. Since previous animal studies have shown stress-induced disruption of the blood-brain-barrier (BBB)[6], an alternative possibility was that the stress situation associated with war allowed pyridostigmine penetration into the brain. To examine this possibility we treated adult mice with pyridostigmine following a forced swim protocol, shown by others to simulate stress[7]. To test whether pyridostigmine affects central cholinergic systems we determined brain AChE activity, c-fos oncogene mRNA levels and electrophysiological responses of hippocampal neurons. For comparison, we employed saline and the homologous CNS-accessible carbamate AChE inhibitor, physostigmine. Our findings demonstrate a drastic increase in the accessibility of pyridostigmine into brain under stress, with far reaching implications for the therapeutic use of variable peripherally acting drugs.

RESULTS

Pyridostigmine and physostigmine displayed similar efficacy in inhibiting AChE activity when added to brain homogenates (Fig 1A). Also, they were similarly effective in reducing serum BuChE activity when injected into non-stressed mice (16.7 ± 6.9% and 22.6 ± 5.4% reduction from normal levels respectively, 10 minutes following intraperitoneal injection of 0.1 mg/kg pyridostigmine or physostigmine into 3 animals in each group). However, brain AChE activity in homogenates prepared from the brains of non-stressed mice was considerably less inhibited by the injected pyridostigmine than by physostigmine (Fig 1B). Thus, pyridostigmine doses previously proven to be protective against organophosphates (0.1-0.5 mg/kg, 15-30% inhibition of serum BuChE activity)[2,3] did not reduce brain AChE levels, whereas similar doses of physostigmine inhibited more then 50% of brain AChE activity (Fig 1B). In contrast, AChE activity, measured in homogenates from the cerebral cortex of drug-injected stressed mice, was reduced by 0.1 mg/kg of either pyridostigmine or physostigmine to less then 50% of normal level (Fig. 1C). The stress treatment therefore reduced the pyridostigmine dose required to inhibit 50% of brain AChE from 1.50 to 0.01 mg/kg. This coincided with a >10-fold increase in brain penetration of the albumin-binding dye Evans-blue following stress (Fig 1D-F).

As the pyridostigmine doses that inhibited cortical AChE activity in non-stressed mice (>1mg/kg) were reported to perturb CNS functions in primates[8], we examined its effect on mRNA levels of the c-fos oncogene, an indirect marker for enhanced neuronal excitability[7], by reverse transcription followed by PCR amplification (RT-PCR). More than 100-fold increase in brain c-fos mRNA level was evident as soon as 10 min. following *i.p* injection of 2 mg/kg pyridostigmine in non-stressed animals (95% inhibition of cortical AChE) (Fig 2A).

To directly explore the effect of pyridostigmine on cholinergic brain circuits, we further adapted the use of brain slices[9] for combined electrophysiological and molecular neurobiology analyses. Direct application of 1mM pyridostigmine to hippocampal slices for 30 min. reduced AChE activity with similar efficacy to the <u>in vivo</u> situation and induced a

parallel 100-fold increase in c-fos mRNA levels. Control tests with primers for synaptophysin mRNA revealed no change either in vivo or in brain slices, demonstrating the selectivity of this response (data not shown). Moreover, electrophysiological recordings in such slices revealed a pyridostigmine-induced increase in the amplitude and rate of rise of evoked population spikes in the CA1 area of the hippocampus, in response to stimulation of the Schaffer Collaterals (Fig 2B). This enhancement in summated neuronal activity demonstrated directly the increased excitability of the local circuit following pyridostigmine application.

Double-blind human studies testing pyridostigmine effects on 35 young healthy volunteers ("peace time", ref. 10 and additional data, not reported previously) as compared to those observed in 213 treated soldiers during the Gulf war (extension of ref. 5) resemble our current rodent data. In both human studies each individual was asked to report on a yes/no questionnaire regarding symptoms related to the drug. During peace time, in agreement with previous reports[1,4], documented symptoms were mainly related to peripheral nervous system (PNS) functions (symptoms included: abdominal pain, diarrhea, frequent urination, increased salivation, rhinorrhea and excess sweating) with an average of 18.8%, (range: 5.5-38.9%), while only 8.3% (range: 0-16.6%) of participants reported on symptoms related to CNS functions (headaches, insomnia, drowsiness, nervousness, difficulties in focusing attention and impaired calculation capacities) (Fig. 3). In contrast, extension of the reported study performed during the Gulf war, revealed that 23.6% (range: 6.2-53.4%) of the 213 soldiers examined reported on CNS symptoms while only 11.4% (range: 6.1-20.4%) reported on PNS symptoms (Fig. 3). In parallel, in control mice injected with 0.1mg/kg pyridostigmine, serum BChE activity was inhibited similarly to that measured in humans at peace time (18.8±3.5% in humans and 20.4±5.5% in mice). Under these conditions, no inhibition of mouse brain AChE was measured (see also Fig. 1). Injection of similar doses of pyridostigmine to stressed mice caused a significant inhibition of mouse brain AChE, with a tendency toward limitation of BChE inhibition (Fig. 3). Thus, PNS effects were relatively suppressed and CNS effects-enhanced due to either the restrain stress in mice or the psychological stress associated with war in humans.

DISCUSSION

Our findings demonstrate significant correlations between stress and pyridostigmine-induced CNS effects. We confirmed the accepted notion that treating non-stressed mice with prophylactic doses of pyridostigmine does not inhibit CNS AChE, corresponding to unaffected CNS functions in non-stressed primates[8] or men at peace time[4]. Yet, similar treatment under stress conditions (in mice) was associated with increased BBB permeability, neuronal excitability, oncogene activation and drastic decreases in brain AChE activity.

Interestingly, we found that serum BChE inhibition is similarly suppressed under stress as the PNS-related symptoms caused by pyridostigmine. The 2-fold stress-induced suppression in PNS effects as per soldiers reports could be due to enhanced drug scavenging in peripheral tissues, for example by adrenaline induction of the p450 scavenging system[11]. Alternatively , or in addition, drug concentration in the periphery could be reduced due to the dilution effect caused by the stress-induced brain penetrance. Hormonal changes have been known to disrupt the integrity[12] of the intricate microglial connections blocking access of large molecules into the brain which may explain at least part of the observed changes under stress treatment. However, it is conceivable that AChE inhibition adds up on these hormonal effects on microglial connections, thus increasing BBB permeability. Further studies will be required to reveal whether AChE is expressed in microglia and examine their potential response to its inhibition.

In view of the reports of BBB disruption in Alzheimer's disease[13], our data may further explain the low doses of pyridostigmine which affected electroencephalograph (EEG) patterns, attention and short term memory in Alzheimer's patients[14] as well as reports on myasthenic patients who developed, under routine pyridostigmine doses, CNS symptoms which regressed following the drug withdrawal[15]. Susceptibility to CNS symptoms may particularly be expected when free drug levels are increased in the circulation due to reduced capacities for drug scavenging, for example, in carriers of the 'atypical' BCHE mutation[16]. Other potential reasons for such CNS effects include liver malfunctioning, for example under hepatitis, which is known to reduce BChE levels in the circulation[17] . Individuals subjected to

drugs of abuse (i.e. cocaine) should also be vulnerable to cholinesterase inhibitors, as BChE is the major cocaine scavenger in human blood[18].

That increased neuronal excitability and c-fos mRNA levels were observed following application of pyridostigmine both in vivo and in hippocampal slices maintained in-vitro, suggests that this was the direct outcome of pyridostigmine access to the brain. The early immediate transcriptional response following pyridostigmine application can be attributed to AChE inhibition, increasing acetylcholine levels, subsequent massive activation of muscarinic receptors[19] and corresponding induction of signal transduction processes. Since hippocampal neurotransmission systems are normally involved in stress responses[20], access of pyridostigmine to the brain can be expected to add yet more "stress like" symptoms above those associated with the war situation. That some of the associated stress effects[20] parallel those reported during the Gulf war[5] further strengthens this hypothesis.

While this study describes acute, short-term effects induced by pyridostigmine under stress, it does not yet address the intricate long-term consequences reported by Gulf war veterans[21] . However, the immediate early response observed in our study predicts the induction of secondary and tertiary processes with unknown consequences, depending on complex and variable elements. In addition, the CNS symptoms referred to pyridostigmine may shed new light on previously unforeseen complications attributable to various peripherally acting drugs. Thus, our study predicts that drugs considered to be limited to the periphery may become centrally active under stress conditions and as dependent on liver activities and general scavenging capacities.

METHODOLOGY

Stress Induction: Stress was induced in adult FVB/N mice by 2x4 min. forced swim with a 4 min. rest interval[7]. Ten min. following stress, animals were injected intra-peritoneally with either 0.9% NaCl (control), or with pyridostigmine (Research Biochemical International, Natik, MA) or physostigmine (Sigma, St Louis, MI) at the noted doses. Animals were decapitated 10 min. following injection, trunk blood was collected[7], cerebral cortex was quickly dissected and homogenized in solution D (10mM Tris-HCl, pH 7.4, 1M NaCl, 1% Triton-X100, 1mM EDTA, 1:10 weight/volume)[22].

AChE activity measurements: Acetylthiocholine (ATCh) hydrolysis levels were determined spectrophotometrically in nmol ATCh per min. per mg brain protein, as previously described[23]. Butyrylcholinesterase (BChE) activity in serum was measured using Butyrylthiocholine (BTCh) as substrate. In both cases, selective inhibitors were employed to suppress non-specific hydrolysis[22].

Determination of Blood-Brain-Barrier permeability: Anaesthetized animals (Nembutal, 60mg/kg), were injected intracardially with 0.1 ml of 2% of the albumin-binding dye Evan's-blue in 0.9% NaCl. Following perfusion with 0.9% NaCl, brains were removed, homogenized and dye concentration determined spectrophotometrically[24].

RT-PCR: Brain c-fos cDNA was amplified by RT-PCR[23] using as primers 1604(+): 5' TCTTATTCCGTTCCCTTCGGATTCTCCGTT - 3' and 2306(-): 5' TCTTATTCCGTTCCCTTCGGATTCTCCGTT - 3'. Nos. denote nucleotide positions in the Genebank c-fos sequence (accession no. V00727). Ten µl of each reaction mixture, removed at the noted cycles, were electrophoresed and ethidium-stained[23].

Electrophysiological Recordings: Extracellular potentials were recorded in hippocampal slices maintained in vitro[9]. Schaffer collateral fibers were stimulated with a bipolar tungsten stimulating electrode. Recording glass microelectrodes were located in the CA1 area.

Acknowledgements

We thank Z. Selinger and J. Yarom (Jerusalem) and E. Lev (I.D.F) for helpful discussions and for help with experiments. Supported in part by the U.S. Army Medical Research and Development Command (to H.S), and by a research grant from the Charles E. Smith Laboratory for collaborative research, The National Institute for Psychobiology in Israel (to A.F & H.S).

REFERENCES

1. Taylor, P. Cholinergic agonists, Anticholinesterase Agents. In: The Pharmacological Basis of Therapeutics. 8th Ed., (Eds: Gilman A.G., Rall T.W., Nies A.s. & Taylor P.), pp. 122-130, 131-147 (1990). Pergamon Press, New York.
2. Deyi, X., Linxiu, W., & Shuqiu, P. The inhibition and protection of cholinesterase by physostigmine and pyridostigmine against soman poisoning *in vivo*. Fundam. Appl. Toxicol. 1, 217-221 (1981).
3. Diruhumber, P., French, M.C., Green, D.M., Leadbeater, L., & Stratton, J.A. The protection of primates against soman poisoning by pretreatment with pyridostigmine. J. Pharmacol. 31, 295-299 (1979).
4. Borland, R.G., Breman, D.H. & Nicholson, A.N. Studies on the possible central and peripheral effects in man of a cholinesterase inhibitor (pyridostigmine). Hum. Toxicol. 4, 293-300 (1985).
5. Sharabi, Y. et al. Survey of symptoms following intake of pyridostigmine during the Persian gulf war. Isr. J. Med. Sci. 27, 656-658 (1991).
6. Sharma, H.S., Cervos-Navarro, J. & Dey, P.K. Increased blood-brain barrier permeability following acute short-term swimming exercise in conscious normotensive young rats. Neurosci. Res. 10, 211-221 (1991).
7. Melia, K.M. , Ryabinin, A.E. , Schroeder, R. , Bloom, F.E. & Wilson, M.C. Induction and habituation of immediate early gene expression in rat brain by acute and repeated restraint stress. J. Neurosci. 14, 5929-5938 (1994).
8. Blick, D.W. et al. Acute behavioral toxicity of pyridostigmine or soman in primates. Toxicol. Appl. Pharmacol. 126, 311-318 (1994).
9. Friedman, A.& Gutnick, M.J. Intracellular calcium and control of burst generation in neurons of guinea-pig neocortex in-vitro. Europ. J. Neurosci. 1, 374-381 (1989).

10. Glickson, M. et al. The influence of pyridostigmine on human neuromuscular functions - studies in healthy human subjects. Fund. Appl. Toxicol. 16, 288-298 (1991).

11. Ehrhart-Bornstein, M., Bornstein, S.R., Trzeclak, W.H., Usadel, H., Guse-Behling, H., Waterman, M.R. and Scherbaum, W.A. Adrenaline stimulates cholesterol side-chain cleavage cytochrome P450 mRNA accumulation in bovine adrenocortical cells. J. Endocrinol. 131, 5-8 (1991).

12. Brust, P. Blood-brain-barrier transport under different physiological and pathophysiological circumstances including ischemia. Exp.Pathol. 42, 213-219 (1991).

13. Harik, S.I. & Kalaria, R.N. Blood-brain-barrier abnormalities in Alzheimer's disease. Ann. New York Acad. of Sci. 640, 47-52 (1991).

14. Agnoli, A., Martucci, N., Manna, V., Conti, L. & Fioravanti, M. Effect of cholinergic and anticholinergic drugs on short term memory in Alzheimer's dementia. A neuropsychological and computerized electroencephalographic study. Clin. Neuropharmacol. 6, 311-323 (1983).

15. Iwasaki, Y., Wakata, N. & Sinoshita, M. Parkinsonism induced by pyridostigmine. Acta Neurol. Scand. 78, 236 (1988).

16. Loewenstein-Lichtenstein Y. et al. Genetic predisposition to adverse consequences of anti-cholinesterases in 'atypical' butyrylcholinesterase carriers. Nature/Medicine. 1, 1082-1085 (1995).

17. Whittaker, M. Cholinesterases. In: Monographs in Human Genetics. S.Krager AG, Basel. 65-85 (1986).

18. Schwarz, M., Glick, D., Loewenstein, Y. & Soreq, H. Engineering of human cholinesterases explains and predicts diverse consequences of administration of various drugs and poisons. Pharmac.Ther. 67, 283-321 (1995).

19. Brown, D.A. Slow cholinergic excitation - a mechanism for increasing neuronal excitability. Trends Neurosci. 6, 302-306 (1983).

20. McEwen, B.S. & Sapolsky, R.M. Stress and cognitive function. Curr. Opin. in Neurobiol. 5, 205-216 (1995).

21. Gavageran, H. NIH panel rejects Persian gulf syndrome. Nature. 369, 8 (1994).

22. Neville, L.F., Gnatt. A. Padam, R., Seidman, S. & Soreq, H. Anionic site interactions in human butyrylcholinesterase disrupted by two single point mutations. J. Biol. Chem. 265, 20735-20738 (1990).

23. Seidman, S. et al. Synaptic and epidermal accumulations of human acetylcholinesterase are encoded by alternative 3'-terminal exons. Mol. Cell. Biol. 15, 2993-3002 (1995).

24. Uyama, O. et al. Quantitative evaluation of vascular permeability in the gerbil brain after transient ischemia using Evans blue fluorescence. J. Cerebral Blood Flow and Metabolism, 8, 282-284 (1988).

Figure 1: Stress intensifies AChE inhibition by pyridostigmine due to increased BBB permeability. **A: AChE inhibition in brain homogenates**. Acetylthiocholine hydrolysis was measured following addition of increasing concentrations of pyridostigmine (filled squares) or physostigmine (empty circles) to brain homogenates from control animals. Presented are % remaining activities as compared with those of brain homogenates with no added drug. **B: Inhibiting brain AChE activity by drug injection**. Percent of normal specific cortical AChE activity was measured in brain homogenates prepared from non-stressed animals sacrificed 10 minutes following injection of the noted doses of physostigmine (n=9) or pyridostigmine (n=11) in non-stressed animals. Presented are % remaining activities as compared with those of brain homogenates from non-stressed, 0.9% NaCl injected animals (n=12). **C: Pyridostigmine inhibition of brain AChE following stress.** Swim forced test was followed 10 minutes later by injection of either 0.1 mg/kg pyridostigmine (n=8), or physostigmine (n=5). AChE activity measurments were as under B. Presented are % remaining activities as compared with those of brain homogenates from similarly stressed, 0.9% NaCl injected animals (n=6). **D-E: BBB permeability following stress.** shown are representative brains dissected from anaesthetized animals, 10 min following the intracardial injection of Evan's-blue. D: control animal, E: 10 min. following stress session. **F: Spectrophotometric evaluation of dye concentration in brain homogenates.** Methodology followed ref. 24.

Figure 2: Pyridostigmine enhances neuronal excitability and increases oncogene mRNA levels. **A: The kinetics of brain c-fos cDNA accumulation during RT-PCR amplification**. Total RNA from hippocampus dissected from mice was extracted using RNAclean (AGS,Heidelberg,Germany), its integrity verified by gel elctrophoresis (evaluation of 2.0 ratio between 28 S and 18 S ribosomal RNA) and its quantity and purity from proteins evaluated by a ratio of 1.8-2.0 between O.D absorbance at 260 and 280 nm. c-fos cDNA was amplified following reverse transcription of similar RNA samples from the brain of control or stressed animals. PCR product samples were withdrawn every 3rd cycle, which allows for 8-fold increases between samples. The earlier appearance in PCR cycle No., of amplified c-fos-cDNA 20 min. following injection of 2mg/kg pyridostigmine (+) as

compared to 0.9% NaCl (-) indicates >100-fold increases in the amount of c-fos mRNA under stress.

B: Extracellular evoked potentials. Cortico-hippocampal slices (400 μm thick) were cut using a vibratome (Vibroslice, Campden Instruments, Loughborough, UK.), and were placed in a humidified holding chamber, continuously perfused with oxygenated (95% O_2, 5% CO_2) artificial cerebrospinal fluid (aCSF)[9] . Schaffer collateral fibers were stimulated with a bipolar tungsten stimulating electrode and extracellular evoked potentials were recorded in the cell-body layer of the CA1 area of the hippocampus. Single response to supramaximal stimulus intensity (1.5 times stimulus the intensity of which caused maximal response) is drawn before (-) and 30 min. following (+) addition of pyridostigmine (1mM) to the perfusing solution.

Figure 3: Pyridostigmine effects in humans during peace and war time and in non-stressed and stressed rodents

Left panels (humans): Results of a double blind, placebo controlled study (extension of Glickson et al., 1991[10]) (dashed bars, "peace"). Pyridostigmine (n=18) or placebo (n=17) were administered to young healthy males volunteers. Symptoms were reported at the end of the study. Presented are ranges (%) of soldiers reporting pyridostigmine-induced symptoms related to CNS (top) or PNS (bottom panel). During the Gulf war 213 male soldiers aged 18-22 years were questioned, 24 hours after initiation of pyridostigmine treatment[5] (filled bars). Mean values for human data are marked by horizontal lines across the relevant bars.

Right panels (Rodents): summary of measured brain AChE inhibition (top) and serum BChE inhibition in mice (bottom) 10 minutes following injection of 0.1mg/kg pyridostigmine in non-stressed (control, n=4), and stressed (n=5) mice. Percent inhibition ± standard deviation was calculated in comparison to the average activity calculated in non-injected, not-stressed (n=12) and stressed (n=6) animals.

Figure 1

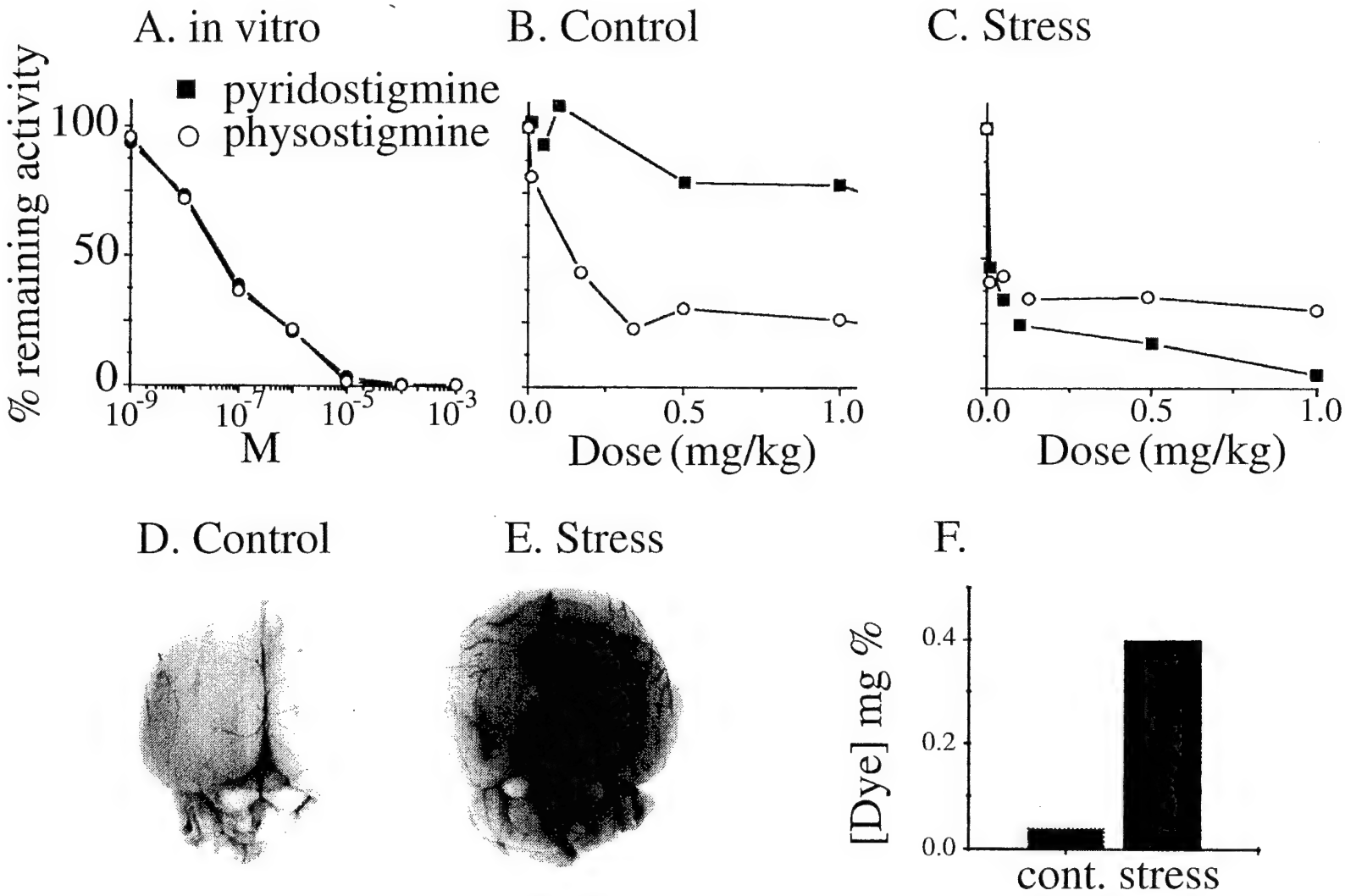
A. in vitro
B. Control
C. Stress
pyridostigmine
physostigmine
% remaining activity
100
50
0
10^{-9}
10^{-7}
10^{-5}
10^{-3}
M
0.0
0.5
1.0
Dose (mg/kg)
D. Control
E. Stress
F.
[Dye] mg %
0.4
0.2
0.0
cont.
stress

Figure 2

A. c-FOS cDNA, IN VIVO

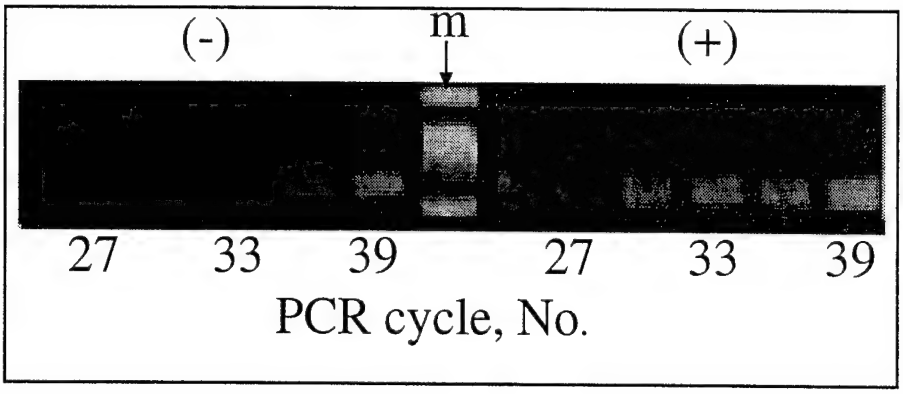

B. FIELD POTENTIALS, EX VIVO

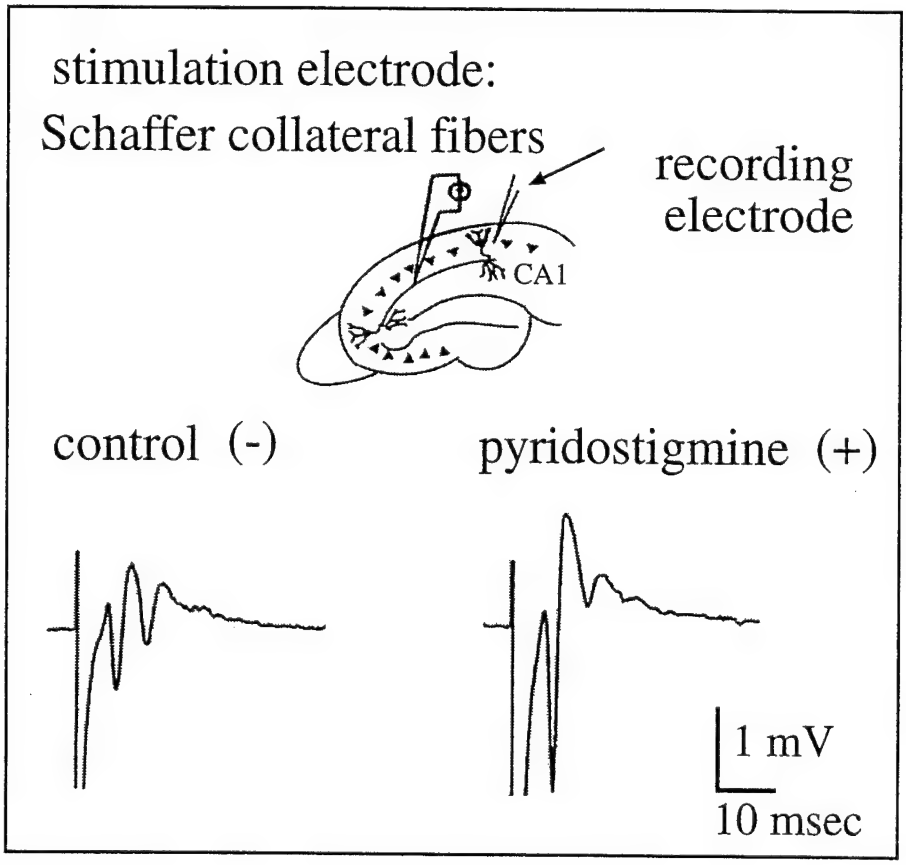

Figure 3

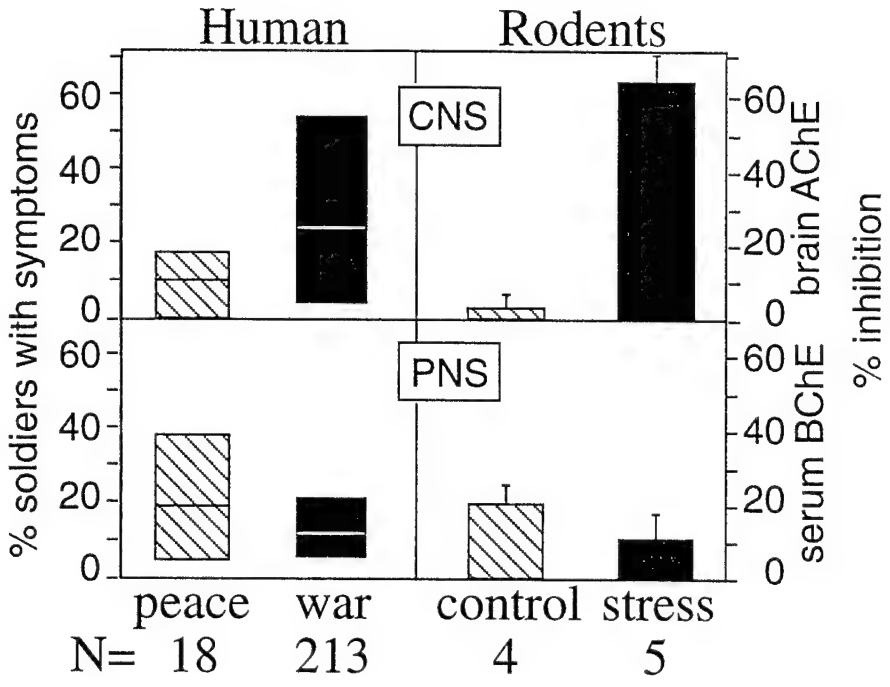
Human
Rodents
CNS
PNS
% soldiers with symptoms
brain AChE
serum BChE
% inhibition
0
20
40
60
peace
war
control
stress
N= 18
213
4
5

6/25/96 12:50

Acetylcholinesterase Phosphorylation at Non-Consensus Protein Kinase A Sites Enhances the Rate of Acetylcholine Hydrolysis.

Mirta Grifman[1], Ayelet Arbel[1], Dalia Ginzberg[1], David Glick[1], Sharona Elgavish[1, 2], Boaz Shaanan[1, 2] and Hermona Soreq[1, 3]

[1]Department of Biological Chemistry and [2]The Wolfson Center for Applied Structural Biology. The Institute of Life Sciences, The Hebrew University of Jerusalem, 91904 Israel.

[3]To whom correspondence should be addressed. (e-mail: soreq@shum.huji.ac.il)

running title: PKA phosphorylation activates AChE catalysis.

Summary

Here, we report that cAMP-dependent protein kinase (PKA) phosphorylates recombinant human acetylcholinesterase (acetylcholine acetyl hydrolase, EC 3.1.1.7, AChE) *in vitro*. Such treatment enhanced acetylthiocholine (ATCh) hydrolysis up to 10-fold as compared to untreated AChE, while leaving unaffected the enzyme's affinity for this substrate and for various active and peripheral site inhibitors. In addition, we found that alkaline phosphatase treatment enhanced the electrophoretic migration, under denaturing conditions, of AChE isolated from various sources. Moreover, alkaline phosphatase changed the isoelectric point of part of the treated AChE molecules to a higher one, indicating that AChE is phosphorylated *in vivo*. Enhancement of aceylthiocholine hydrolysis also occurred with *Torpedo* AChE, which has no consensus motif for PKA phosphorylation. Also, mutation of the single PKA site in human ACHE (threonine 249) did not prevent this enhancement, suggesting that in both cases it was due to phosphorylation at non-consensus sites. *In* vivo suppression of the acetylcholine hydrolysing activity of AChE and consequent impairment in cholinergic neurotransmission occur under exposure to multiple compounds. These include both natural and pharmacological agents, organophosphate and carbamate insecticides and chemical warfare agents. Based on our current findings, phosphorylation of AChE offers a rapid molecular feedback mechanism that can compensate for fluctuations in cholinergic neurotransmission, modulating the hydrolytic activity of this enzyme and enabling acetylcholine hydrolysis to proceed under such challenges.

key words: acetylcholinesterase; neurotransmission, cAMP-dependent protein kinase A; non-consensus sites; protein phosphorylation.

Introduction

Acetylcholinesterase (AChE) is a key component of cholinergic brain synapses and neuromuscular junctions, in which it hydrolyzes the neurotransmitter acetylcholine (Taylor, 1990, Soreq & Zakut, 1993). In addition to terminating cholinergic neurotransmission, it may have non-catalytic function(s) in cellular development (Greenfield, 1984, Layer and Willbold. 1995; Small et al., 1995; Karpel et al., 1996). This may explain its presence on the surface of erythrocytes and in embryonic tissues (Massoulié et al., 1993). The central role of AChE in cholinergic neurotransmission is demonstrated by the fact that it is the target of a variety of toxic compounds, both natural and man-made. For example, several natural compounds inhibit the catalytic activity of cholinesterases including glycoalkaloids, which are ubiquitous in solaneous food plant species such as potatoes (Neville et al., 1992), the snake venom protein inhibitor fasciculin (Bourne et al., 1995) and cyanobacteria toxins. Chemical warfare agents (e. g., sarin and tabun) and organophosphate insecticides (e. g. malathion and tetraethylpyrophosphate) also are designed to inhibit AChE (Taylor, 1990). In addition, AChE is a target of several pharmacological agents that attempt to enhance cholinergic neurotransmission in the treatment of disorders associated with cholinergic imbalance such as Alzheimer's disease and myasthenia gravis (Schwarz et al., 1995). The widespread presence of both natural and man-made anti-AChE compounds (Millard and Broomfield, 1995) suggests the existence of mechanisms to enable this enzyme to function under diverse conditions.

The crucial role of AChE in cholinergic neurotransmission implies that adjustments in its activity in response to fluctuating physiological conditions should occur within a very short time scale. This excludes regulation at the levels of gene expression, multimeric assembly and intracellular targeting, none of which offers a sufficiently rapid response to be physiologically relevant. AChE is present in various glycosylated forms (Meflah et al., 1984), but the carbohydrate moiety does not contribute to catalytic activity (Fischer et al., 1993). Allosteric modulation and substrate inhibition of AChE have also been reported (Changeux, 1966, Barak

et al., 1995), but no physiologically significant scheme for controlling AChE activity in response to changed conditions has been demonstrated. As phosphorylation is the most frequently seen post-translational mechanism of control of physiological processes, and since the human AChE amino acid sequence (Soreq and Zakut, 1993) reveals several consensus phosphorylation sites, we have investigated phosphorylation as a mechanism of control of AChE activity.

Results

AChE carries consensus phosphorylation sites: Known AChE amino acid sequences were searched for consensus phosphorylation sites with the aid of the three-dimensional model of *Torpedo* AChE (Sussman et al., 1991). This enabled the selection of serine or threonine residues at the surface of the protein, which are susceptible for enzyme phosphorylation. Five such sites were found in human AChE, for casein kinase II (S128, S355 and T466), protein kinase C (T11, A11 in mouse) and protein kinase A (T249), where numbers correspond to the human AChE sequence (Fig. 1A). Eleven more serine and threonine residues were found on the protein surface of *Torpedo* AChE, however, none of those was part of a known consensus motif for phosphorylation by any recognized kinase (Fig. 1B).

AChE can be phosphorylated *in vitro*. To determine which of the kinases identified in this search is in practice capable of phorphorylating human AChE, we used commercially available kinases and the highly purified human recombinant AChE produced in transfected 293 cells (Velan et al., 1991). Of casein kinase II, protein kinase C and protein kinase A (PKA) only the latter could incorporate ^{33}P-ATP into AChE. Moreover, this kinase also phosphorylated recombinant human AChE produced in *E. coli*, native human AChE from brain or blood sources and bovine erythrocyte AChE, all with apparently similar efficiency (Fig. 2). The intensity of kinase labeling of human and bovine AChE was lower than that obtained under the same conditions with H1 histone, suggesting relatively limited availability of AChE amino acid residues susceptible to phosphorylation. PKA completely failed to phosphorylate the closely related enzyme human butyrylcholinesterase (BuChE), even though it includes a consensus PKA site (Fig. 2).

Ex-vivo AChE is partially phosphorylated: When treated with alkaline phosphatase (AP), electrophoretically separated under denaturing conditions and subjected to immunodetection, a fraction of purified AChEs from different sources migrated faster than the non-treated enzyme (Fig. 3A). This indicated that certain portions of each of these AChE preparations had been

phosphorylated *in vivo*, that these enzyme molecules retained their phosphorylation throughout the purification process and that at least some of the phosphate groups associated with AChE *in vivo* could be removed *in vitro* by AP. This, in turn predicted that the AP treatment should reduce some of the negative charges associated with the treated enzyme molecules. To test this prediction, we performed isoelectric focusing under non-denaturing conditions followed by activity staining of the AP-treated enzyme. Interestingly, a new faint band representing a novel AChE subtype appeared on the isoelectric focusing gel. This enzyme displayed an isoelectric point of 5.9, higher than any of the isoelectric subtypes of the untreated enzyme (Fig. 3B). Its activity represented less than 3% of the total staining, a far smaller portion than that part of the immunochemically detected AP-treated enzyme which migrated faster in SDS-PAGE (compare Fig. 3A to 3B).

In contrast to the effect of AP on the electrophoretic migration of AChE, PKA phosphorylation did not modify the immunochemically detectable protein bands following electrophoresis under denaturing conditions (not shown). Furthermore, PKA treatment of hAChE followed by isoelectric focusing and activity staining revealed only activity bands that existed in the control enzyme preparation (Fig. 3B), in agreement with the results observed by immunochemical detection.

AChE phosphorylation enhances hydrolytic activity: PKA phosphorylation increased by up to 10-fold the rate of ATCh hydrolysis by the recombinant human enzyme from either *E. coli* or transfected cells. This also occurred with AChE purified from natural sources, such as human brain or erythrocytes or *Torpedo* electroplax (Table I). This latter increment was rather surprising as *Torpedo* AChE lacks the consensus T249 PKA site. Yet, the specificity of this reaction was demonstrated by the fact that activation of AChE by PKA was inhibited by 40% in the presence of the highly specific PKA inhibitor, PKI.

In contrast, PKA had no effect on butyrylthiocholine hydrolysis by human serum BuChE, although this enzyme does carry the PKA consensus motif (Table I). Thus, incorporation of ^{33}P and the enhancement in acetylthiocholine hydrolysis were clearly associated with each other.

Unlike the catalytic rate, the Km for ATCh of the treated AChE preparations remained unaffected at 0.05 mM. Moreover, IC_{50} and Ki values for several cholinesterase inhibitors

targeted either to the active or the peripheral site (Schwarz et al., 1995) were also unmodified. These included the carbamate physostigmine, the organophosphate echothiophate, the Alzheimer's disease drug tetrahydroamino acridine (tacrine, Cognex ™), the selective inhibitor BW284C51, which acts both at the active and the peripheral site and the snake venom protein inhibitor fasciculin (Table II).

To test the potential of AChE phosphorylation to enhance acetylcholine hydrolysis under exposure to various AChE inhibitors, we subjected identical amounts of recombinant human AChE produced in transfected 293 cells to PKA phosphorylation *in vitro* and then to increasing concentrations of several inhibitors. PKA-phosphorylated human AChE was as sensitive as the untreated enzyme to inhibition by tacrine (Fig. 4A). However, at therapeutic tacrine concentrations of $2x10^{-8}$M (Johansson and Nordberg, 1993, Knapp et al., 1994), phosphorylated AChE displayed considerably higher activities than the control enzyme (Fig. 4A). A parallel difference in remaining enzyme activity was observed in the presence of 10^{-8} to 10^{-10} M physostigmine (Fig. 4B), 10^{-8} to 10^{-11} M fasciculin (Fig. 4C), which blocks the entrance to the active site of AChE (Bourne et al., 1995) and 10^{-8} to 10^{-11} M of echothiophate (Fig. 4D). Thus, PKA phosphorylation provides the means to compensate for suppression of AChE activity by a wide range of concentrations of various inhibitors.

Evidence for phosphorylation at non-consensus sites: The only consensus site for PKA phosphorylation in the human AChE sequence is T249 (see Fig.1A) and it is conserved in all of the mammalian AChEs (Massoulié et al., 1993). Nevertheless, PKA was able to enhance the catalytic activity of *Torpedo* AChE (Table I), even though it does not contain the consensus site. This in turn, suggested that PKA phosphorylation occurs also in non-consensus sites in all of the examined AChE preparations, including those of human origin. In that case, substitution of T249 in the human enzyme should not prevent the capacity of PKA to phosphorylate this protein and increase its catalytic activity. To test this hypothesis we employed site-directed mutagenesis to substitute threonine 249, which resides on the protein surface close to the entrance to the active site gorge, by alanine. Non-purified T249A hAChE secreted from transfected COS cells hydrolyzed ATCh at a normal rate and was 2-fold activated by PKA, an efficiency similar to that observed for its non-mutated counterpart (Table I). Moreover, the

mutant unpurified enzyme displayed a similar Km to that of its normal counterpart and maintained unmodified IC_{50} and Ki values for several cholinesterase inhibitors (Table III). We conclude that PKA phosphorylation of AChE, like that of the cystic fibrosis trans-membrane receptor protein (CFTR)(Seibert et al., 1995), takes place also at non-consensus serine/threonine residues.

Discussion

We have shown that AChE can be phosphorylated *in vitro,* employed different methods to demonstrate that AChE exists *in vivo* in a phosphorylated state and showed that its phosphorylation can be physiologically relevant, particularly under exposure to various natural and man-made AChE inhibitors. That this phosphorylation is a general phenomenon was indicated by the fact that PKA was able to incorporate ^{33}P from ATP into purified AChE from different animal and tissue sources. Moreover, AP treatment of AChE modified the isoelectric focusing pattern of the active enzyme from various sources and enhanced the electrophoretic migration of a significant fraction of the treated enzyme under denaturing conditions, similarly to the effects on other *in vivo* phosphorylated proteins (e. g. Cdc25 (Gross et al., 1992)).

Phosphorylation of AChE is independent of either glycosylation or C-terminal variations in the enzyme, as it occurs with the non-glycosylated *E. coli*-produced enzyme as well as with the erythrocyte and brain-derived forms which differ in their 40 C-terminal amino acids and tissue specificity due to alternative splicing (Seidman et al., 1995, Karpel et al., 1996). However, the location where this *in vivo* phosphorylation takes place is still open. That it does not depend upon glycosylation implies that it may occur intracellularly, as is the case for most of the known PKA phosphorylations (Walsh and Van Patten, 1994). Yet, the alternative possibility of extracellular phosphorylation (Shaltiel et al., 1993, Volonte et al., 1994) cannot be excluded at present. At the physiological level, PKA phosphorylation at the immediate vicinity of the synaptic cleft may provide a yet more rapid response to reduced enzyme activity than that provided by intracellular phosphorylation.

Phosphorylation of many key elements of the nervous system demonstrates the importance of protein kinases for synaptic functioning. For example, PKA phosphorylation of synapsin down-regulates pre-synaptic release (Pieribone et al., 1995). Within the cholinergic synapse, PKA phosphorylation of choline acetyltransferase (Schmidt and Rylett, 1993) and of the

nicotinic acetylcholine receptor (Hoffman et al., 1994) take place *in vivo*. Receptor phosphorylation leads to channel desensitization and to a reduced sensitivity to acetylcholine (Léna and Changeux, 1993, Hoffman et al., 1994). Based on our current findings, this suppression in post-synaptic response is expected to be augmented by AChE phosphorylation, which will fasten acetylcholine hydrolysis. Conversely, specific phosphatases might enhance synaptic transmission in response to cholinergic cues by suppressing AChE's activity. Indeed, phosphatase inhibitors were shown to reinforce physiological properties associated with cholinergic circuits (e. g. long term potentiation, Muller et al., 1992).

The fact that AChE phosphorylation affects neither the Km of the enzyme for ATCh nor its affinity for active and peripheral site inhibitors, excludes the possibility that the attraction of ligands to the active site or intermediary complex were affected. Rather, these suggest that the activation may be due to a faster product release. Negative charges of phosphate groups on peripheral AChE sites could also affect the enzyme's dipole moment, which has been considered as an important contribution to AChE catalytic rate (Ripoll et al., 1993). Phosphorylation can further modulate enzyme activities under anti-cholinesterase therapies, with special importance for patients with genetic predisposition for adverse responses to such therapies (Loewenstein-Lichtenstein et al., 1995).

The existence of a consensus PKA motif was insufficient to ensure the examined cholinesterase phosphorylation, as was evident from the fact that BuChE failed to be phosphorylated. However, this could reflect a prior state of complete phosphorylation or steric hindrance due to the excessive glycosylation characteristic of BuChE (Soreq & Zakut, 1993). Subsequent experiments demonstrated that a consensus PKA site was not necessary for the observed effect: PKA was able to activate AChE *in vitro*, even when prepared from *Torpedo,* which lacks the consensus site or when the single T249 consensus PKA motif on human AChE was mutated. This suggested that PKA can phosphorylate AChE at non-consensus sites, as it does on the CFTR protein (Seibert et al., 1995).

The cerebrospinal fluid (CSF) of Alzheimer's disease patients, both *in vivo* and *postmortem*, showed an anomalous AChE band following isoelectric focusing and activity staining (Smith et al., 1991). If the hyperphosphorylation of Tau in the Alzheimer's disease brain (Trojanowski

and Lee, 1995) reflects a general state of excess kinase activity, it is possible that AChE is also hyperphosphorylated under these circumstances. This could explain the appearance of the new AChE species in the CSF of Alzheimer's disease patients. Phosphorylation-dependent activation of AChE could then contribute to the deficit in acetylcholine, which is one of the features of Alzheimer's disease. In addition, the levels of AChE catalytic activity remain unchanged in the Alzheimer's disease brain, in spite of the death of cholinergic neurons (Perry et al., 1985) which produce most of this enzyme. Hyperphosphorylation can explain this apparent enigma, as well. Further experiments would be required to find out if the phosphorylation state of AChE is modified in this and other diseases which involve cholinergic deficits.

Activation of AChE catalysis by phosphorylation adds up on the potential responses to cAMP stimuli that would result in enhancement of acetylcholine hydrolysis. The promoter of the human ACHE gene (Ben Aziz-Aloya et al., 1993) includes a cAMP-response element, and cAMP and its analogs indeed enhance AChE activities in cultured cells (Soreq et al., 1983). Our present findings imply that this response to cAMP may reflect both transcription from the ACHE gene and enhanced catalysis by its protein product.

Several lines of evidence (Greenfield, 1984, Layer et al., 1993, Small and Willbold 1995, Karpel et al., 1996, Inestrosa et al., 1996) demonstrate non-catalytic activities for AChE which may also be affected by its phosphorylation. The sequence homologies between AChE and the novel family of neurexin ligands including neuroligins-1, 2 and 3 (Ichtchenko et al., 1996) raise the possibility that the non-catalytic properties of AChE may be due to its capacity to interact with neurexins. Phosphorylation of surface amino acid residues is likely to be of primary importance to such protein-protein interactions, as is the case for cyclin interactions (Patriotis et al., 1994). Neurotactin, one of these non-catalytically active nervous system proteins with sequence homology to AChE is indeed phosphorylated *in vivo* (Barthalay et al., 1992). AChE phosphorylation is thus a key process with the potential to control numerous functions, both within cholinergic synapses and in the developing nervous system.

Materials and Methods

Computer analyses: The MOTIF program (version 8, Genetics Computer Group, University of Wisconsin, Madison, WI) was used to identify consensus phosphorylation motifs. The amino acid sequence numbers of human and *Torpedo* AChE sequences correspond to the m55040 and x05497 Genbank accession numbers, respectively. The three dimensional structure of AChE (Sussman et al., 1991) was plotted using the Insight II program (Biosym Technologies) on a Silicon Graphics computer (Indigo R4000). Surface residues were determined according to the proportion of exposed surface as compared to the relative exposure level of the same residue in Gly-X-Gly peptides (Miller et al., 1987).

Reagents: Purified recombinant human AChE preparations were gifts of Drs. A. Shafferman, Ness Tziona (for 293 cells preparations) and A. Fischer, Ness Tziona (for *E. coli* preparations). AChE, purified from human erythrocytes and brain and from bovine erythrocytes as well as monoclonal antibodies to human AChE were a gift of U. Brodbeck, Bern. H1 histone was a Boehringer (Mannheim, Germany) product. Echothiophate, pyridostigmine bromide and fasciculin were products of Ayerst Laboratories (Montreal, PQ, Canada), Research Biochemicals International (Natik, MA) and Alomone (Jerusalem, Israel), respectively. All other reagents were purchased from Sigma Chemical Co. (St. Louis, MO). All anticholinesterases were dissolved in double distilled water and kept at -20°C at 100-fold stock concentrations or were added directly to reaction mixtures.

Cell lines and transfections: COS-1 monkey kidney cells (a gift of Y. Gruenbaum, Jerusalem) were grown in Dulbecco modified Eagle medium (DMEM) containing 10% fetal calf serum (FCS) at 37 °C, 5% CO_2 , in a humidified chamber. COS-1 cells were transfected using Lipofectamine™ (GIBCOBRL, Bethesda, MA) according to the manufacturer's instructions and were incubated in DMEM containing 2% FCS for 3 days, at which stage medium was collected for AChE enzymatic analyses.

In vitro phosphorylation/dephosphorylation: Proteins were phosphorylated by 30 min incubation at 30 °C in 18 mM Mg acetate, 25 mM MES (pH 6.8), 50 mM EDTA, 0.2 mM ATP

(Boheringer), 1 µCi [γ -^{33}P]-ATP (1000-3000 Ci/mmol, Amersham Life Sciences, Aylesbury, UK) and 25 casein units of cAMP-dependent protein kinase catalytic subunit (PKA)(Promega, Madison, WI) in a final volume of 50 µl. For the enzymatic analysis of phosphorylated AChE, 100 casein units were used. To inhibit phosphorylation, 20 µg of cAMP-dependent protein kinase peptide inhibitor (PKI, Promega, Madison, WI) were added to the phosphorylation reaction mixture. For dephosphorylation, AChEs were incubated for 60 min at 37 °C in: 50 mM Tris-HCl (pH 8.5), 0.1 mM EDTA with 20 U calf intestine alkaline phosphatase (Boehringer) in a final volume of 20 µl.

Gel electrophoresis: SDS-PAGE was performed according to Laemmli (1970) using 8% polyacrylamide gels. For immunochemical detection, proteins from SDS-gels were electroblotted onto nitrocellulose membranes (Schleicher & Schuell, Dassel, Germany) in a semi-dry-blot system as described (Harlow and Lane, 1988). After transfer, membranes were washed in 20 mM Na phosphate (pH 7.4), 144 mM NaCl, 0.1% (v/v) Tween-20, at room temp. for 1 h, blocked in 5% (w/v) dried skim milk, then rinsed and incubated with anti-human AChE monoclonal antibodies 132-2 and 132-3 at 6 µg/ml each for 1 h. After 3 washes, as above, membranes were incubated with a 1:4000 dilution of a sheep anti-mouse Ig, horseradish peroxidase linked F(ab'$_2$) fragment (Amersham) for 1 h. Chemiluminescent detection was performed with Amersham's ECL kit as instructed.

Proteins were separated according to their isoelectric point on native polyacrylamide-ampholyte gels (pH 4-6) as described (Bolag and Edelstein, 1991). Gels were prefocused for 30 min at 100 mV and then run for an additional 2.5 h at 100 mV. After separation, gels were stained overnight for cholinesterase activity as detailed (Karpel et al., 1996) using 0.5 mM ATCh.

Colorimetric determination of cholinesterase activities: was performed as described elsewhere, using 1 mM ATCh (Neville et al., 1992). For Km determination ATCh in the range of 0.01 to 10 mM was used. Effects of inhibitors were determined over a concentration range of at least 5 orders of magnitude. Pre-incubations of the inhibitor with the enzyme for 20 min preceded the addition of substrate and activity measurements. Ki values for reversible inhibitors were calculated from experimental IC_{50} values according to the equation $Ki=IC_{50}/(1+S/Km)$, were S was the ATCh concentration, 1 mM.

PCR mutagenesis: T249A E6-ACHEDNA was produced from the CMV-E6 plasmid (Karpel et al., 1996) by PCR mutagenesis as described (Higuchi, 1990), using the following primers:
hACHEmut987 (+): 5'CAGGGCCGCGCAGCTGGCCCAC3';
hACHEmut 1008 (-): 5'GTGGGCCAGCTGCGCGGCCCTG3';
hACHE 823 (+): 5'GGTGACCCGACATCAGTGACGCTGTT3';
hACHE1855 (-): 5'GGAAGCGGTTCCAGAAGGCGCAGGC3', where the underlined base denotes the mutation, the primer numbering corresponds to the human ACHE sequence and (+) or (-) is the upstream or downstream orientation, respectively. The PCR program was 1 min at 94 °C (first cycle for 15 min), 1 min at 68 °C and 1 min at 72 °C (last cycle for 5 min). The amplified end product was restricted with *NotI* and *SphI* (New England Biolabs, Beverly, MA) and exchanged with the corresponding wild-type fragment. The accuracy of the T249A substitution was verified by automated sequencing (Applied Biosystems 377).

Acknowledgements

We thank Drs. G. Robinson (Urbana, Illinois) for critically reviewing this manuscript, A. Shafferman and A. Fischer (Ness Tziona, Israel) for the gifts of purified recombinant human AChE, U. Brodbeck (Bern, Switzerland) for purified native AChEs and monoclonal antibodies and Y. Gruenbaum (Jerusalem) for COS-1 cells. This study was supported by the U. S. Army Medical Research and Development Command (Grant DAMD 17-94-C-4031, to H. S.).

References:

Barak, D., Ordentlich, A., Bromberg, A., Kronman , C., Marcus, D., Lazar, A., Ariel, N., Velan, B. and Shafferman, A. (1995) Allosteric modulation of acetylcholinesterase activity by peripheral ligands involves a conformational transition of the anionic subsite. *Biochemistry* **34**, 15444-15452.

Barthalay, Y., Hipeau-Jacquotte, R., De La Escalera, S., Jimenez, F. and Piovant, M. (1990) *Drosophila* neurotactin mediates hrterophilic cell adhesion. *EMBO J.* **9**, 3603-3609.

Ben Aziz-Aloya, R., Seidman, S., Timberg, R., Sternfeld, M., Zakut H. and Soreq, H. (1993) Expression of a human acetylcholinesterase promoter-reporter construct in developing neuromuscular junctions of *Xenopus* embryos. *Proc. Natl. Acad. Sci. U.S.A.* **90**, 2471-2475.

Bolag, D.M. and Edelstein, S.J. (1991) Isoelectric Focusing. In *Protein Methods* (Wiley-Liss, eds.), pp. 161-174, New York.

Bourne, Y., Taylor, P. and Marchot, P. (1995) Acetylcholinesterase inhibition by fasciculin: crystal structure of the complex. *Cell* **83**, 503-512.

Changeux, J-P. (1966) Responses of acetylcholinesterase from *Torpedo marmorata to* salts and curarizing drugs. *Mol. Pharmacol.* **2**, 369-392.

Fischer, M., Ittah, A., Liefer, I. and Gorecki, M. (1993). Expression and reconstitution of biologically active human acetylcholinesterase from Escherichia coli. *Cell. Mol. Neurobiol.* **13**, 25-38.

Greenfield S. (1984) Acetylcholinesterase may have novel functions in the brain. *Trends Neurosci.* **7**, 364-368.

Gross, E., Goldberg, D. and Levitzki, A. (1992) Phosphorylation of S. cerevisiae Cdc25 in response to glucose results in its dissociation from Ras. *Nature* **360**, 762-765.

Harlow, E. and Lane, D. (1988) Immunobloting. In: *Antibodies: a Laboratory Manual.* (Cold Spring Harbor Laboratory Press, eds.), pp. 488-495, Cold Spring Harbor.

Higuchi, R. (1990) Recombinant PCR. In *PCR Protocols: A Guide to Methods and Applications* (Innis, M.A., Gelfand,D. H., Sninsky, J.J. and White T.J. eds.), pp. 177-183, San Diego.

Hoffman, P. W., Ravindran, A. and Huganir, R. L. (1994) Role of phosphorylation in desensitization of acetylcholine receptors expressed in *Xenopus* oocytes. J. Neursci. **14**, 4185-4195.

Ichtchenko, K., Nguyen, T. and Sudhof, T. C. (1996) Structures, alternative splicing and neurexin binding of multiple neuroligins. *J. Biol. Chem.* **271**, 2676-2682.

Inestrosa, N. C., Alvarez, A., Perez, C. A., Moreno, R. D., Vicente, M., Linker, C., Casanueva, O. I., Soto, C. and Garrido, J. (1996) Acetylcholinesterase accelerates assembly of amyloid-β-peptides into Alzheimer's fibrils: possible role of the peripheral site of the enzyme. *Neuron* **16**, 881-891.

Johansson, I. M. & Nordberg, A. (1993) Pharmacokinetic studies of cholinesterase inhibitors. *Acta neurol. scand. Suppl.* **149**, 22-25.

Karpel, R., Sternfeld, M., Ginzberg, D., Guhl, E., Graessmann, A. and Soreq, H. (1996) Overexpression of alternative human acetylcholinesterase forms modulates process extensions in cultured glioma cells. *J. Neurochem.* **66**, 114-123.

Knapp, M.J., Knopman, D.S., Solomon, P.R., Pendlebury, W.W., David, C.S. and Gracon, S.I. (1994) A 30-week randomized controlled trial of high-dose tacrine in patients with Alzheimer's disease. *J. Am. Med. Assn.* **271**, 985-991.

Laemmli, U.K. (1970) Cleavage of structural proteins during the assembly of the head of bacteriophage T4. *Nature* **227**, 680-683.

Layer. P. and Willbold, E. (1995) Novel functions of cholinesteases in development, physiology and disease. *Prog. Hisotchem. Cytochem.* **29**, 1-92.

Léna, C. and Changeux, J.-P. (1993) Allosteric modulation of the nicotinic acetylcholine receptor. *Trends Neurolog. Sci.* **16**, 181-186.

Loewenstein-Lichtenstein, Y., Schwarz, M., Glick, D., Nørgaard-Pedersen, B., Zakut, H. and Soreq, H. (1995) Genetic predisposition to adverse consequences of anti-cholinesterases in "atypical" BCHE carriers. *Nature Med.* **1**, 1082-1085.

Massoulié, J., Pezzementi, L., Bon, S., Krejci, E. and Vallette, F.M. (1993) Molecular and cellular biology of cholinesterases. *Prog. Neurobiol.* **41**, 31-91.

Meflah, K., Bernard, S. and Massoulié, J. (1984) Interaction with lectins indicates differences in the carbohydrate composition of the membrane-enzymes acetylcholinesterase and 5'-nucleotidase in different cell types. *Biochemie* **66**, 59-69.

Millard, C. B., and Broomfield, C. A. (1995) Anticholinesterases: Medical applications of neurochemical principles. *J. Neurochem.* **64**, 1909-1918.

Miller, S., Janin, J., Lisk, A. M. and Chothia, C. (1987) Interior and surface of monomeric proteins. *J. Mol. Biol.* **196**, 641-656.

Muller, W., Petrozzino, J. J., Griffith, L. C., Danho, W. and Connor, J. A. (1992) Specific involvement of Ca(2+)-calmodulin kinase II in cholinergic modulation of neuronal responsiveness. *J. Neurophysiol.* **68**, 2264-2269.

Neville, L. F., Gnatt, A., Loewenstein, Y., Seidman, S., Ehrlich, G. and Soreq, H. (1992) Intramolecular relationships in cholinesterases revealed by oocyte expression of site-directed and natural variants of human BCHE. *EMBO J.* **11**, 1641-1649.

Patriotis, C., Makris, A., Chernoff, J. and Tsichlis, P. N. (1994) Tpl-2 acts in concert with Ras and Raf-1 to activate mitogen-activated protein kinase. *Proc. Natl. Acad. Sci.* USA **91**, 9755-9759.

Perry, E. K., Tomlinson, B. E., Blessed, G., Bergman, K., Gibson, P. H. and Perry R. H. (1985) Cholinergic correlates of cognitive impairment in Parkinson's disease: comparison with Alzheimer's disease. *J. Neurol. Neurosurg. Psychiat.* **48**, 413-422.

Pieribone, V. A., Shupliakov, O., Brodin, L., Hifiker-Rothenfluh, S., Czernik, A. J. and Greengard, P. (1995) Distinct pools of synaptic vesicles in neurotransmitter release. *Nature* **375**, 493-497.

Ripoll, D.R., Faerman, C.H., Axelsen, P.H., Silman, I. and Sussman, J.L. (1993) An electrostatic mechanism for substrate guidance down the aromatic gorge of acetylcholinesterase. *Proc. Natl. Acad. Sci. USA* **90**, 5128-5132.

Schmidt, B.M. and Rylett, R.J. (1993) Phosphorylation of rat brain choline acetyltransferase and its relationship to enzyme activity. *J. Neurochem.* **61**, 1774-1781.

Schwarz, M., Glick, D., Loewenstein, Y. and Soreq, H. (1995) Engineering of human cholinesterases explains and predicts diverse consequences of administration of various drugs and poisons. Pharmacol. Therap. **67**, 283-322.

Seibert, F.S., Tabcharani, J.A., Chang, X.-B., Dulhanty, A. M., Mathews, C., Hanrahan, J.W. and Riordan, J.R. (1995) cAMP-dependent protein kinase-mediated phosphorylation of cystic fibrosis transmembrane conductance regulator residue Ser-753 and its role in channel activation. *J. Biol. Chem.* **270**, 2158-2162.

Seidman, S., Sternfeld, M., Ben Aziz-Aloya, R., Timberg, R., Kaufer, D. and Soreq, H. (1995) Synaptic versus epidermal accumulation of human acetylcholinesterase is encoded by alternative 3'-terminal exons. *Mol. Cell. Biol.* **14**, 459-473.

Shaltiel, S., Schwartz, I., Korc-Grodzicki, B. and Kreizman, T. (1993) Evidence for an extra-cellular function for protein kinase A. *Mol. Cell Biochem.* **127**, 283-291.

Small, D.H., Reed, G., Whitefield, B. and Nurcombe, V. (1995) Cholinergic regulation of neurite outgrowth from isolated chick sympathetic neurons in culture. *J. Neurosci.* **15**, 144-151.

Smith, A. D., Jobst, K. A., Navaratnam, D. S., Shen, Z. X., Priddle, J. D., McDonalds, B., King, E. and Esiri, M. M. Anomalous acetylcholinesterase in lumbar CSF in Alzheimer's disease. (1991) *Lancet* **338**, 1538.

Soreq, H., Miskin, R., Zutra, A. and Littauer, U. Z. (1983) Modulation in the levels and localization of plasminogen activator in differentiating neuroblastoma cells. *Dev. Brain. Res.* **7**, 257-259.

Soreq, H. and Zakut, H. (1993) *Human Cholinesterases and Anticholinesterases*, Academic Press, San Diego.

Sussman, J.L., Harel, M., Frolow, F., Oefner, C., Goldman, A., Toker, L. and Silman, I. (1991). Atomic structure of acetylcholinesterase from *Torpedo californica*: a prototypic acetylcholine-binding protein. *Science* **253**, 872-879.

Taylor, P. (1990) Cholinergic agonists, Anticholinesterase agents. In *Pharmacological Basis of Therapeutics*, Gilman, A.G., Rall, T.W., Nies, A.S. and Taylor, P. (eds), pp. 122-130, 131-149 , New York.

Trojanowski, J. Q. and Lee, V. M. (1995) Phosphorylation of paired helical tau filaments in Alzheimer's disease neurofibrillary lesions: focusing on phosphatases. *FASEB J.* **9**, 1570-1576.

Velan, B., Kronman,C., Grosfeld, H., Leitner, M., Gozes, Y., Flashner, Y., Sery, T., Cohen, S., Ben-Aziz, R., Seidman, S., Shafferman, A. and Soreq, H. (1991) Recombinant human acetylcholinesterase is secreted from transiently transfected 293 cells as a soluble globular enzyme. *Cell. Mol. Neurobiol.* **11**, 143-156.

Volonte, C., Merlo, D., Ciotti, M. T. and Calissano, P. Identification of an ecto-kinase activity in cerebellar granule primary neuronal cultures. (1994) *J. Neurochem.* **63**, 2028-2037.

Walsh, D. A. and Van Patten, S. M. (1994) Multiple pathway signal transduction by the cAMP-dependent protein kinase. *FASEB J.* **8**, 1227-1236.

Table I. Effect of protein kinase A on the activity of cholinesterases from various sources[a]

	catalytic activity (μmol/min/ml)		+kinase / -kinase	PKA consensus site[d]
	- kinase	+ kinase		
AChE				
recombinant human, from 293 cells	8.3	76.9	9.3	+
recombinant human, from *E. coli*	0.3	2.4	8.0	+
human erythrocyte	3.2	12.8	4.0	+
human brain	4.5	11.3	2.5	+
Torpedo electroplax[b]	4.2	17.7	4.2	-
COS cells transfected with normal E6-ACHEDNA[c]	0.9	1.8	2.0	+
COS cells transfected with T249A E6-ACHEDNA[c]	1.0	2.2	2.2	-
BuChE				
human serum	1.1	1.2	1.1	+

[a]The data shown represent one out of three reproducible experiments with standard deviations below 30%. For BuChE activity determinations, 5 mM butyrylthiocholine was used as a substrate. All enzyme preparations were highly purified except for [b] which was partially purified and for [c] which was tested in conditioned medium from transfected cells with no further purification. [d]The existence of a PKA consensus site on each of the examined sequences is noted.

Table II. Kinetic constants of human acetylcholinesterase purified from embryonic kidney 293 cells.[a]

	- kinase	+ kinase
Km (μM) [a]	50	50
Ki values (μM)		
tacrine	0.007	0.006
fasciculin 02	0.0002	0.0003
BW284c51	0.3	0.3
IC50 (μM)		
physostigmine	0.01	0.01
echothiophate	0.01	0.01

[a] Kinetic constants of recombinant AChE purified from 293 cells with no further treatment (-kinase) or treated with PKA (+kinase) were determined as detailed in Methods.

Table III. Abolition of the PKA consensus site does not modify AChE properties.

	E6-ACHEDNA-transfected[a]	T249A E6-ACHEDNA-transfected[b]
Ki values (μM)		
succinylcholine	290	290
dibucaine	720	730
BW284c51	0.007	0.007
tacrine	0.058	0.072
fasciculin 02	0.000,000,1	0.000,000,1
fasciculin 03	0.000,000,2	0.000,000,2
IC50 value (μM)		
pyridostigmine	0.50	0.55

[a] COS cells were tansfected with E6-ACHEDNA as detailed under Methods and the biochemical properties of AChE secreted into the medium were determined as in Tables I and II.

[b] Site-directed mutagenesis was employed to substitute T249 into A. Tests were similar to those under [a].

Legends to Tables and Figures:

Fig. 1: Serine and threonine residues on the three dimensional models of AChE.

A: Consensus motifs for kinases: Superimposition of *Torpedo* (yellow) and mouse (magenta) AChEs according to their C*a* atoms. Amino acid numbers are as in the human sequence. Active site serine (203) is displayed as a turquoise sphere, the PKA consensus site threonine (249) in violet, the casein kinase II consensus sites S128, S355 and T466 in grey and the protein kinase C consensus site T11 (A11 in mouse) in green.

B: Surface-exposed serine and threonine residues: Active site serine 203 is displayed as a turquoise sphere toghether with those serine and threonine residues which were calculated to be exposed at the surface of the *Torpedo* AChE protein (see Methods section).

Fig. 2: *In vitro* phosphorylation of AChEs.

Phosphorylation reactions were performed on 5 µg purified recombinant AChE expressed in 293 kidney cells (hAChE (293)), 2 µg purified recombinant AChE expressed in *E. coli* (h (E. coli)), 5, 3 and 5 µg of native AChE purified from human red blood cells (hRBC), human brain (hbrain) and bovine red blood cells (bRBC) respectively, 0.2 mU human BuChE (hBuChE) and 5 µg histone (H1). One fifth of each of the phosphorylation reactions, was separated by SDS-PAGE followed by either protein staining with Commassie brilliant blue (CBB) or by 48h autoradiography (^{33}P). A reaction without PKA served as a control (C). Note that all proteins except BuChE were phosphorylated by PKA. Numbers on both sides of the figure indicate molecular weight in kD.

Fig. 3: Dephosphorylation of AChE modifies its electrophoretic and isoelectric properties.

A. Alkaline phosphatase enhances the electrophoretic migration of AChE. Alkaline phosphatase (AP) treated and control untreated (C) recombinant human AChE from 293 cells (293, 3 µg), from human red blood cells (hRBC, 5 µg) or human AChE produced in *E. coli* (*E. coli*, 3 µg) were electrophoretically separated under denaturing conditions and immunochemically detected.

The arrow indicates the position of that fraction of these proteins that migrated faster after dephosphorylation.

B. Alkaline phosphatase induces the appearance of a novel AChE subtype with high isoelectric point. 3 μg hAChE (293) in a final volume of 20 μl was treated either with PKA or with AP and was subjected to isoelectric focusing gel electrophoresis followed by activity staining of the gels. Similarly treated AChEs served as a control (C). The arrow indicates an additional band at a higher isoelectric point, which could only be observed after dephosphorylation.

Figure 1

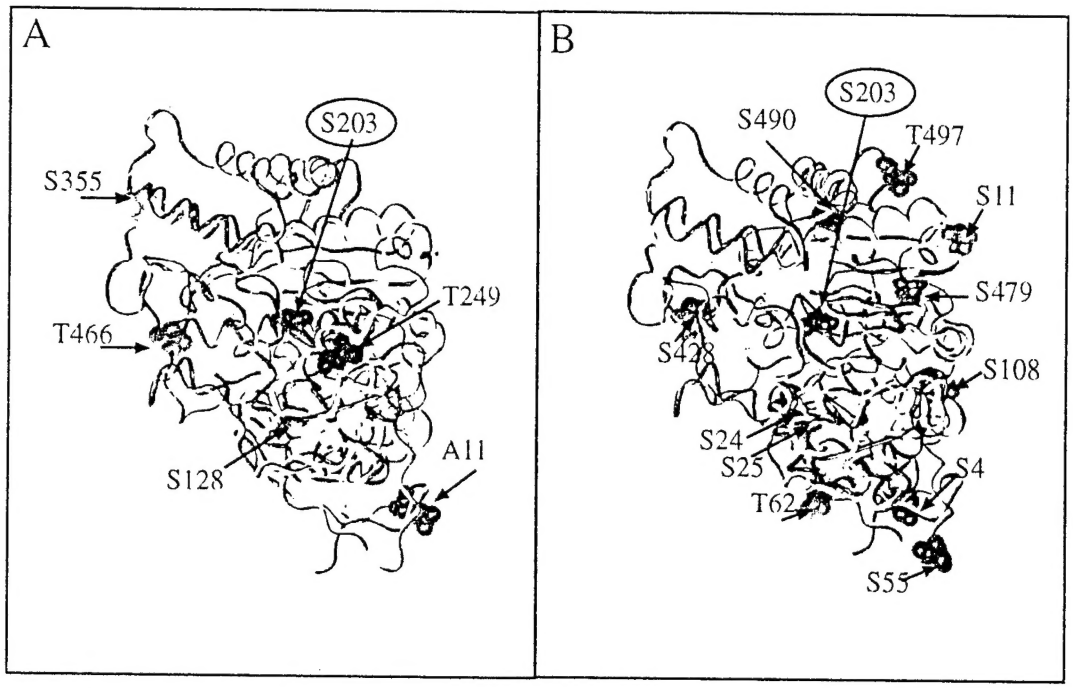
A
S203
S355
T249
T466
S128
A11
B
S203
S490
T497
S11
S479
S428
S108
S24
S25
S4
T62
S55

Figure 2

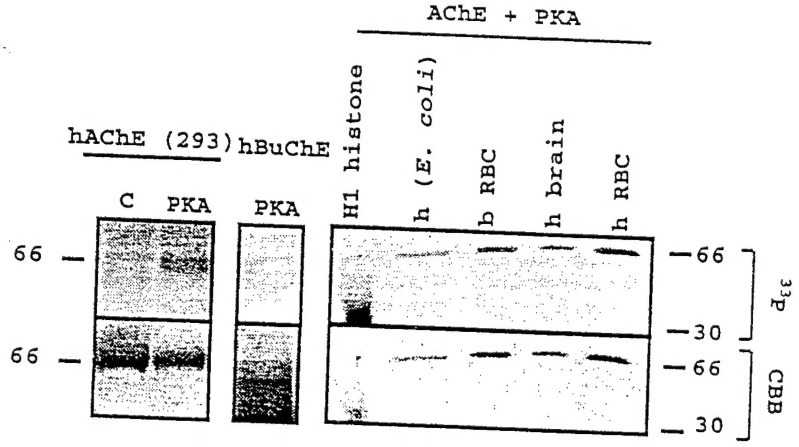
AChE + PKA
hAChE (293)
hBuChE
C
PKA
PKA
H1 histone
h (E. coli)
h RBC
h brain
h RBC
66
66
66
30
66
30
^{33}P
CBB

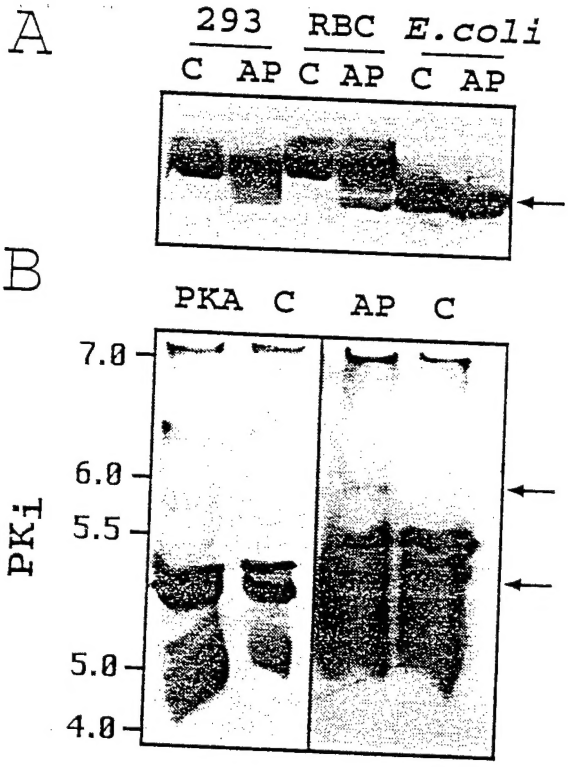

Figure 3